eCAM
Evidence-Based Complementary and Alternative Medicine

Medicinal Plants in the Prevention and Treatment of Chronic Diseases 2013

Guest Editors: Mohamed Eddouks, Debprasad Chattopadhyay, Vincenzo De Feo, and William Chi-shing Cho

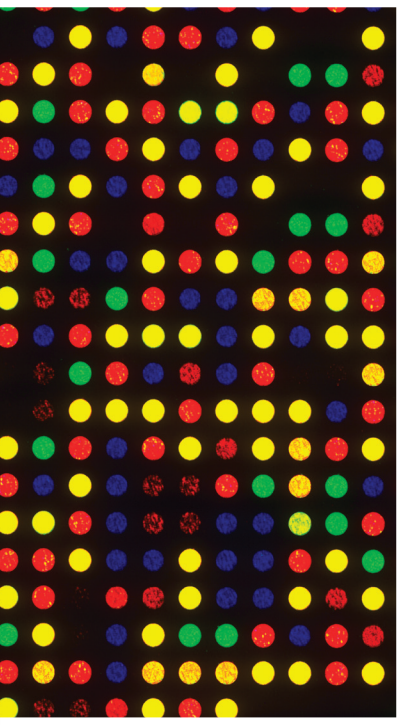

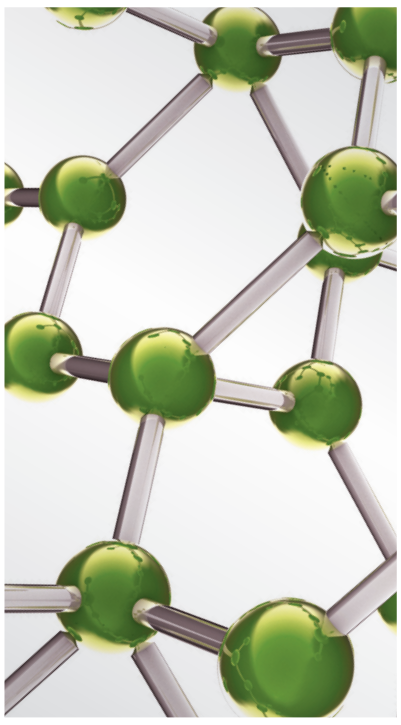


Medicinal Plants in the Prevention and Treatment of Chronic Diseases 2013

Evidence-Based Complementary and Alternative Medicine

Medicinal Plants in the Prevention and Treatment of Chronic Diseases 2013

Guest Editors: Mohamed Eddouks, Debprasad Chattopadhyay, Vincenzo De Feo, and William Chi-shing Cho

Editorial Board

Contents

Hindawi Publishing Corporation
Evidence-Based Complementary and Alternative Medicine
Volume 2014, Article ID 180981, 3 pages
http://dx.doi.org/10.1155/2014/180981

Editorial

Medicinal Plants in the Prevention and Treatment of Chronic Diseases 2013

Mohamed Eddouks,[1] Debprasad Chattopadhyay,[2] Vincenzo De Feo,[3] and William Chi-shing Cho[4]

[1] *Moulay Ismail University, FST Errachidia, BP 21, 52000 Errachidia, Morocco*
[2] *ICMR Virus Unit, Division of Ethnomedicine, ID & BG Hospital, General Block 4, 57 Dr. Suresh C. Banerjee Road, Kolkata 700 010, India*
[3] *Dipartimento di Farmacia, Università degli Studi di Salerno, Via Giovanni Paolo II 132, Fisciano, 84084 Salerno, Italy*
[4] *Department of Clinical Oncology, Queen Elizabeth Hospital, Kowloon, Hong Kong*

Correspondence should be addressed to Mohamed Eddouks; mohamed.eddouks@laposte.net

Received 18 January 2014; Accepted 18 January 2014; Published 26 March 2014

Since time immemorial, in search for rescue for their disease, people looked for drugs in nature. The traditional use of medicinal plants can lead to the discovery of new potent botanical agents in the treatment of several diseases. Some 7000 natural compounds are currently used in modern medicine; most of these had been used for centuries by traditional healers and the global market value of medicinal plant products exceeds $100 billion per annum. In spite of the development of pharmacological agents for the treatment of chronic diseases, the use of medicinal plants continues to flourish. Over the last century, the drastic changes of human life style and eating habits lead to the emergence of various chronic diseases. The decreasing efficacy of some synthetic drugs and the increasing contraindications of their usage make the usage of natural drugs topical again. Thus, the study of phytotherapy for chronic diseases treatment might yield an excellent return in potential sources of medicinal plants which play vital roles in disease prevention and their promotion and use fit into all existing prevention strategies. In this issue, we aim to present some recent advances in the use of medicinal plants for treating the chronic diseases such as diabetes, cancer, cardiovascular diseases, inflammation, and neurologic disorders.

In a clinical study, "Effect of eucalyptus oil inhalation on pain and inflammatory responses after total knee replacement: a randomized clinical trial," Y. S. Jun et al. demonstrate the beneficial effects of eucalyptus oil inhalation on pain and inflammatory responses after total knee replacement surgery. S. Zhang et al., "Skimmin, a coumarin from *Hydrangea paniculata*, slows down the progression of membranous glomerulonephritis by anti-inflammatory effects and inhibiting immune complex deposition," investigated the renoprotective activity of skimmin, one of the major pharmacologically active molecules present in *Hydrangea paniculata*. They studied also the underlying mechanisms of the observed renoprotective effects of skimmin in a rat model of membranous glomerulonephritis induced by cationic bovine serum albumin which may be the inhibition of IL1β and IL-6 expression. In another study "Traditional Chinese medicine Tang-Luo-Ning ameliorates sciatic nerve injuries in streptozotocin-induced diabetic rats," D.-W. Zou et al. describe the beneficial effect of Tang-Luo-Ning (TLN), an effective traditional Chinese medicine for the treatment of diabetic peripheral neuropathy (DPN). To illustrate the underlying neural protection mechanisms of TLN, the effect of TLN on electrophysiology and sciatic nerve morphology was investigated in a model of streptozotocin-induced DPN. G. Belcaro et al., "Grape seed procyanidins in pre- and mild hypertension: a registry study," studied the efficacy of a standardized grape seed procyanidins extract in decreasing blood pressure when associated with nondrug intervention (diet and lifestyle modification) in a controlled

registry study involving healthy prehypertensive and mildly hypertensive subjects. The authors supported that the effect on blood pressure adds to the beneficial effects of grape seed procyanidins on the cardiovascular disease phenotype associated with the oxidation of membrane lipids (endothelial disfunction, formation of oxidized LDL, and activation of phagocytic cells). A study titled ("Effect of *Nelumbo nucifera* petal extracts on lipase, adipogenesis, adipolysis, and central receptors of obesity") by C. C. Velusami et al. demonstrates that both methanol and successive water extracts of *Nelumbo nucifera* petals had an effect on inhibition of lipid storage in adipocytes and increasing lipolysis. In addition, methanol extract exhibited the concentration dependent inhibitory effect on lipase activity. Furthermore, *Nelumbo nucifera* petal extracts showed evident agonist and antagonist activity towards serotonin and cannabinoid receptors, respectively, while it showed no effects towards melanocyte concentrating hormone and melanocortin receptors. Another clinical study performed by G. Belcaro et al. "Greenselect Phytosome for borderline metabolic syndrome" demonstrates that Greenselect Phytosome, a proprietary lecithin formulation of a caffeine-free green tea catechin extract, was especially effective for weight/waist changes in a controlled registry study on asymptomatic subjects borderline for metabolic syndrome factors and with increased plasma oxidative stress. A. Hunyadi et al., "Metabolic effects of mulberry leaves: exploring potential benefits in type 2 diabetes and hyperuricemia," report a series of relevant *in vitro* and *in vivo* studies on the bioactivity of an extract of mulberry leaves and its fractions. *In vivo* antihyperglycemic and antihyperuricemic activity, plasma antioxidant status, *in vitro* glucose consumption by adipocytes in the presence or absence of insulin, xanthine oxidase inhibition, free radical scavenging activity, and inhibition of lipid peroxidation were analyzed.

In addition, known bioactive constituents of mulberry were identified and quantified. A study performed by H.-M. Zhao et al., "Si Shen Wan inhibits mRNA expression of apoptosis-related molecules in p38 MAPK signal pathway in mice with colitis," demonstrated that Si Shen Wan, a formula of traditional Chinese medicine used to treat ulcerative colitis, allergic colitis, and chronic colitis, effectively inhibited mRNA expression of apoptosis-related molecules in p38 MAPK signal pathway to downregulate colonic epithelial cells apoptosis in colonic mucosa from mice with colitis. In another study "Therapeutic potential of andrographolide isolated from the leaves of *Andrographis paniculata* nees for treating lung adenocarcinomas," Y.-T. Tung et al. have studied the antipulmonary cancer effects of andrographolide in a lung tumor mouse model induced by human vascular endothelial growth factor A165 (hVEGF-A165). The antiangiogenesis and chemotherapeutic potential of andrographolide may provide a cure for pulmonary tumors in the future. Z.-Z. Meng et al., "Effect of Xiaoyaosan decoction on learning and memory deficit in rats induced by chronic immobilization stress," observed the effect of Xiaoyaosan (XYS) decoction on chronic immobilization stress- (CIS-) induced learning and memory deficit in rats from behaviors and changes of proteins in hippocampus. The findings suggested that XYS decoction may be helpful in reversing CIS-induced learning and memory deficit by increasing the levels of postsynaptic density protein 95 and synaptophysin on the hippocampal nerve synapses and improving synaptic plasticity.

A review conducted by L. O. Chuah et al., "Updates on antiobesity effect of *Garcinia* origin (–)-HCA," summarizes the update of chemical constituents, significance of *in vivo*/clinical antiobesity effects, and the importance of the current market potential of *Garcinia*/hydroxycitric acid especially as a potential supplement for weight management and as antiobesity agent. A study realized by Y. Liang et al., "Effects of the Chinese traditional prescription Xiaoyaosan decoction on chronic immobilization stress-induced changes in behavior and ultrastructure in rat hippocampus," demonstrated the potential mechanism of Xiaoyaosan (XYS) decoction's antidepressant-like effect in α-amino-3-hydroxy-5-methyl-4-isoxazolepropionic acid (AMPA) receptors related to synaptic plasticity in the hippocampus rats induced by chronic immobilization stress. The study demonstrates that XYS decoction may produce an antidepressant-like effect, which appears to be involved with AMPA receptors related synaptic plasticity of hippocampus. In another study "*Citrus Bergamia* Risso elevates intracellular Ca^{2+} intracellular stores in human umbilical vein endothelial cells," G. H. Seol et al. demonstrate that Citrus Bergamia Risso mobilizes Ca^{2+} from primary intracellular stores via Ca^{2+}-induced and IP3-mediated Ca^{2+} release and affect promotion of Ca^{2+} influx, likely via an store-operated Ca^{2+} mechanism. This finding supports the potential roles of bergamottin in cardiovascular function. J. Hoscheid et al., "Inhibitory effect of the hexane fraction of the ethanolic extract of the fruits of *Pterodon pubescens* Benth in acute and chronic inflammation," confirm the anti-inflammatory activity of the hexane fraction of an ethanolic extract of *Pterodon pubescens* Benth. The anti-inflammatory activity was measured with increasing doses of the hexane fraction by using a carrageenan-induced rat model of pleurisy and a rat model of complete Freund's adjuvant-induced arthritis. The results of biochemical, hematological, and histological analyses indicated a significant decrease in glucose, cholesterol, and triglycerides levels and reduction in the number of total leukocytes and mononuclear cells. The study demonstrates also the absence of toxicity for the doses used. H. Park et al., "Ampelopsis Radix protects dopaminergic neurons against 1-methyl-4-phenylpyridinium/1-methyl-4-phenyl-1,2,3,6-tetrahydropyridine-induced toxicity in Parkinson's disease models *in vitro* and *in vivo*," have demonstrated that Ampelopsis Radix has neuroprotective effects with antioxidant mechanisms in Parkinson's disease models. The standardized extract of Ampelopsis Radix protected dopaminergic neurons by inhibiting reactive oxygen species generation *in vitro*, showed potent radical scavenging activities *in vitro*, and protected the dopaminergic neurons in the brain in the mouse Parkinson's disease model leading to motor improvements. Another paper by H. Ha et al., "Antiatopic dermatitis effect of *Artemisia iwayomogi* in dust mice extract-sensitized Nc/Nga mice," demonstrates the anti-inflammatory and antiatopic dermatitis effects of *Artemisia iwayomogi* both *in vitro* and *in vivo*. *Artemisia iwayomogi* inhibited the nitric oxide

and histamine productions in RAW264.7 and MC/9 cells. Furthermore, isochlorogenic acid A, chlorogenic acid, and scopoletin were demonstrated to be the major components of this plant. Additionally, in the mice, the topical application of *Artemisia iwayomogi* reduced the dermatitis scores in the dorsal skin and ears and reduced the plasma levels of IgE. E. Panzarini et al., "Administration dependent antioxidant effect of *Carica papaya* seeds water extract," demonstrate that *Carica papaya* seeds water extract is potentially useful for protection against oxidative stress. The authors have assessed the antioxidant activities of the *Carica papaya* seeds water extract against hydrogen peroxide oxidative stress in human skin Detroit 550 fibroblasts. An *in vivo* study by M.-H. Chen et al., "Antidiabetic and antihyperlipidemic effects of *Clitocybe nuda* on glucose transporter 4 and AMP-activated protein kinase phosphorylation in high-fat-fed mice," demonstrates that amelioration of diabetic and dyslipidemic state by *Clitocybe nuda* extract in high-fat-fed mice occurred by regulation of GLUT4, glucose-6-phosphatase, and AMP-activated protein kinase phosphorylation. The plant extract decreased hepatic glucose production in the liver and enhanced glucose uptake in skeletal muscle. This study presents a deep analysis of mechanisms of action involved in the antidiabetic and antihyperlipidemic activities of *Clitocybe nuda*.

After the first volume of this special issue published in 2012, we hope that this issue will present valuable information for scientists and clinicians.

Acknowledgments

We would like to thank all the authors for their contributions to this issue; 45 papers have been submitted and only 18 have been highly selected and finally approved for publication. We would like to thank all the editorial team of this special issue and all the reviewers for their appreciated effort and excellent expertise.

Mohamed Eddouks
Debprasad Chattopadhyay
Vincenzo De Feo
William Chi-shing Cho

Hindawi Publishing Corporation
Evidence-Based Complementary and Alternative Medicine
Volume 2014, Article ID 281508, 13 pages
http://dx.doi.org/10.1155/2014/281508

Research Article

Administration Dependent Antioxidant Effect of *Carica papaya* Seeds Water Extract

Elisa Panzarini, Majdi Dwikat, Stefania Mariano, Cristian Vergallo, and Luciana Dini

Department of Biological and Environmental Science and Technology (Di.S.Te.B.A.), University of Salento, Prov.le Lecce-Monteroni, 73100 Lecce, Italy

Correspondence should be addressed to Luciana Dini; luciana.dini@unisalento.it

Received 22 August 2013; Accepted 31 December 2013; Published 25 March 2014

Academic Editor: Mohamed Eddouks

Carica papaya is widely used in folk medicine as herbal remedy to prevent, protect against, and cure several diseases. These curative properties are based on the presence in different parts of the plant of phytochemical nutrients with antioxidant effect. Seeds are the less exploited part; thus this study is aimed at assessing the antioxidant activities of the *C. papaya* seeds water extract against hydrogen peroxide (H_2O_2) oxidative stress in human skin Detroit 550 fibroblasts. *C. papaya* seeds water extract is not toxic and acts as a potent free radical scavenger, providing protection to Detroit 550 fibroblasts that underwent H_2O_2 oxidative stress. Data show that (i) the maximum protective effect is achieved by the simultaneous administration of the extract with 1 mM H_2O_2; (ii) the extract in presence of an oxidative stress does not increase catalase activity and prevents the release of cytochrome C and the inner mitochondrial transmembrane potential ($\Delta\psi_m$) loss; (iii) the extract is more efficient than vitamin C to hamper the oxidative damage; (iv) the purified subfractions of the seeds water extract exert the same antioxidant effect of whole extract. In conclusion, *C. papaya* seeds water extract is potentially useful for protection against oxidative stress.

1. Introduction

Oxidative stress, based on imbalance between prooxidants production and antioxidant defences, is involved in aging process and in several human chronic diseases, for example, cancer, atherosclerosis, coronary heart disease, macular degeneration, Alzheimer's disease, inflammation, and emphysema [1]. Vitamins C and E, β-carotene, flavonoids, tannins, anthocyanins, and other phenolic compounds are plant derived compounds with antioxidant activities by scavenging free radicals and represent a special group of nutritional supplements. Food rich in these antioxidants plays a key role in the prevention of oxidative stress based diseases [2, 3].

Papaya (*Carica papaya*), a member of the family Caricaceae, is a tropical fruit rich in dietary antioxidants (vitamin C, tocopherols, total phenols, and β-carotene) [4] and bioactive phytochemicals with antioxidant activity (benzyl isothiocyanate) [5]. Different parts of *C. papaya* (leaves, barks, roots, latex, fruit, flowers, and seeds) are used in folk medication to treat a broad range of diseases [6]. Several scientific studies validate many of these traditional uses by demonstrating that *C. papaya* displays a wide range of therapeutic activities (i.e., antiprotozoal, antifungal, antibacterial, antiviral, anti-inflammatory, antihypertensive, hypoglycemic and hypolipidemic, wound healing, antitumor, neuroprotective, diuretic, abortifacient, and antifertility) [6, 7]. These properties mainly depend on the antioxidant activity of some secondary metabolites present in the *C. papaya* organs. The studies of the antioxidant nutrients in *C. papaya* have led to the identification of the main compounds that differ in the different organs. Whole fruit extract contains ferulic, p-coumaric, and caffeic acid, carotenoids, and vitamin C that collectively protect human cells from oxidative stresses [4] and promote wound healing and skin repair [8, 9]; leaves extract contains folic acid, vitamins B_{12}, A, and C, alkaloids, saponins, glycosides, tannins, and flavonoids [10] with anticancer activity [11, 12] and protection against the alcohol-induced oxidative damage to the gastric mucosa [13]; seeds extract contains different phenolic compounds, vanillic acid, and vitamin C with antioxidant [14–17] and anticancer [5] activities. Thus, *C. papaya* extracts may act as a synergistic

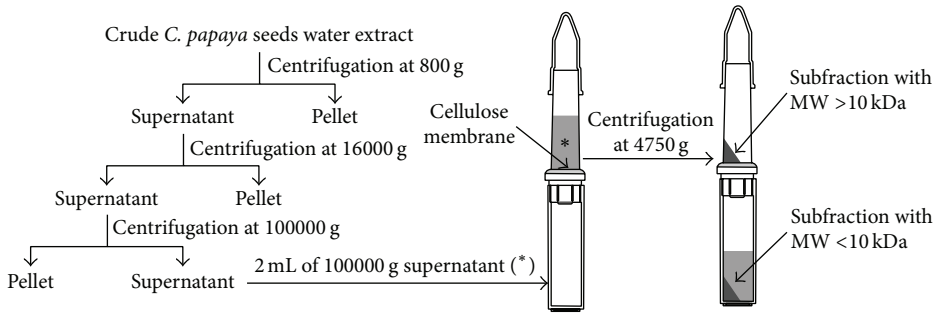

Figure 1: Differential centrifugation of crude *C. papaya* seeds water extract. The crude extract was subjected to a short run at 800 g by Centrifuge 4236 A (Beckman Coulter Inc., Brea, CA, USA) to obtain a first pellet and a supernatant that was further centrifuged at 16000 g to obtain a second pellet and supernatant. The second supernatant was centrifuged at 100000 g to obtain a third pellet and supernatant. This last supernatant was centrifuged at 4750 g by using a Centricon centrifugal filter device with an Ultracel YM-10 regenerated cellulose membrane that permits the ultrafiltration into the lower chamber of substances with molecular weight (MW) < 10 kDa, while substances with MW > 10 kDa are collected in the upper chamber (Merck Millipore, Billerica, MA, USA).

therapeutic dietary supplement in patients with oxidative stress related diseases or could be added to formulations to promote wound healing. Even if literature data reporting on papaya fruit protection against H_2O_2-induced oxidative damage are conspicuous, up to date, no researches have explored similar antioxidant activity of papaya seeds water extract. Indeed, water extract has the advantage to prevent the use of harmful chemical compounds. It is worth noting to mention that seeds represent the waste of the consumption of papaya fruits, not only as food but also as raw material for medical preparations. Therefore, the aim of this study was to investigate the antioxidant activity of *C. papaya* seeds water extract in human skin Detroit 550 fibroblasts in which the oxidative stress was induced by hydrogen peroxide (H_2O_2). Special attention was paid to the modality of administration and to evaluate if the highest antioxidant effect of *C. papaya* seeds water extract depends on the whole crude extract or on specific subfractions.

2. Materials and Methods

2.1. Chemicals. All chemicals were of analytical grade and provided by Sigma-Aldrich (St. Louis, MO, USA) unless otherwise indicated.

2.2. C. papaya Seeds Water Extract Preparation and Fractionation. Seeds were removed from mature *C. papaya* fruits, rinsed with water, and left to dry at room temperature (RT). 10 g of seeds were ground in a mortar, and the powder was left in infusion for 24 h (hours) in 500 mL of sterile distilled water at RT. The crude extract was subjected to a short run (800 g) to obtain a pellet representing the seeds wastes. Unless otherwise indicated, fibroblasts were treated for 1, 2, 4, 8, or 24 h with 1 or 2 mg/mL (w/v, in culture medium) of supernatant in the presence or absence of a prooxidant (1 mM H_2O_2) with or without a known antioxidant (50, 100, 150, 200, and 250 μM vitamin C).

To test also the efficacy of the extract subfractions, the crude whole extract was subjected to short runs by Centrifuge 4236 A (Beckman Coulter Inc., Brea, CA, USA). In particular, the last supernatant obtained at 100000 g was centrifuged at 4750 g by using a Centricon centrifugal filter device with an Ultracel YM-10 (Merck Millipore, Billerica, MA, USA) regenerated cellulose membrane that permits the ultrafiltration into the lower chamber of substances with molecular weight (MW) < 10 kDa, while substances with MW > 10 kDa are collected in the upper chamber. The pellet obtained was added to fibroblasts in order to obtain 1 mg/mL (w/v, in culture medium) final concentration. In Figure 1, the detailed fractioning procedure is illustrated.

2.3. Cell Cultures and Treatments. Human skin Detroit 550 fibroblasts were purchased from Centro Substrati Cellulari (Istituto Zooprofilattico Sperimentale, Brescia, Italy) and cultured in 75 cm^2 flasks (Iwaki, Tokyo, Japan) at a cell density of 10^6 fibroblasts/mL in Eagle's minimum essential medium (EMEM) with Earle's Balanced Salts (Cambrex Bio-Science, Verviers, Belgium), supplemented with 10% (v/v) heat-inactivated fetal calf serum (Cambrex), 2 mM L-glutamine (Cambrex), 100 IU/mL penicillin-streptomycin, and 10000 IU/mL nystatin (antimycotic solution) (Cambrex) in a humidified atmosphere with 5% CO_2 at 37°C. Culture medium was changed every 2 days.

The prooxidative stress was induced by incubating the fibroblasts with 1 mM H_2O_2 for 1 h at 37°C either alone or in combination with 1 or 2 mg/mL (w/v, in culture medium) of *C. papaya* seeds water extract or vitamin C (50, 100, 150, 200, and 250 μM). *C. papaya* extract or vitamin C was added to the culture medium simultaneously with H_2O_2 and/or during the recovery (1 h) in fresh medium at 37°C.

2.4. Cell Viability and Morphology

MTT Assay. Cell viability was determined by 3-(4,5-dimethylthiazol-2-yl)-2,5-diphenyltetrazolium bromide (MTT) dye mitochondria reduction in living fibroblasts according to Sladowski et al. [18]. Briefly, 5×10^5 fibroblasts were incubated with 1 mg/mL of MTT prepared in supplemented EMEM culture medium, for 2 h at 37°C and 5% CO_2; fibroblasts were washed three times with 0.2 M Phosphate Buffer Saline

(PBS) pH 7.4, and the reduced MTT formazan crystals were solubilised with DiMethyl SulfOxide (DMSO) (Carlo Erba, Milano, Italy). The optic density (OD) was read at the spectrophotometer (Ultrospec 4000 UV/Visible Spectrophotometer, Pharmacia Biotech, Stockholm, Sweden) at 570 nm.

Light Microscopy. Morphological changes of living fibroblasts were investigated with an inverted light microscope (LM) Eclipse TS100 (Nikon, Kawasaki, Kanagawa Prefecture, Japan). Fibroblasts, washed with 0.2 M PBS pH 7.4 and fixed with formalin 4% (v/v, in 0.2 M PBS pH 7.4), were rubber scraped and deposited on slides. Haematoxylin-eosin (H-E) staining slides were examined under a LM Eclipse 80i (Nikon) for the scoring of apoptosis, necrosis, or mitosis by counting at least 500 fibroblasts in 50–100 high-power microscopic fields (0.25 mm^2).

Electron Microscopy. Ultrastructure of cell was obtained by conventional transmission (TEM) and scanning electron microscopy (SEM). 10×10^6 fibroblasts washed with 0.2 M PBS pH 7.4 and rubber scraped were fixed with 2.5% glutaraldehyde (v/v, in 0.1 M cacodylate buffer pH 7.4) for 1 h at ice temperature. After an extensive washing, fibroblasts were postfixed with 1% OsO_4 (w/v, in 0.1 M cacodylate buffer pH 7.4) for 1 h at 4°C. Fibroblasts were dehydrated, embedded in Spurr's resin (TAAB Laboratories Equipment Ltd, Aldermaston, England), and examined under a CM12 TEM (Philips, Amsterdam, Netherlands) operating at 80 kV. An aliquot of 1% OsO_4 postfixed fibroblasts was dehydrated by using a Critical Point Dryer 020 (Balzer, Balzers, Liechtenstein), stub-mounted, and gold-coated by using a Balzer Sputter Coater 040 before observation under a XL20 SEM (Philips) operating at 15 kV.

2.5. Catalase Activity. For catalase (EC 1.11.1.6.; $2H_2O_2$ oxidoreductase) activity assay, fibroblasts were rinsed three times with 0.2 M PBS pH 7.4, rubber scraped, centrifuged at 450 g for 7–10 min at 4°C, and suspended in 1 mL of cold buffer (50 mM potassium phosphate pH 7, containing 1 mM EDTA). $3–5 \times 10^6$ fibroblasts were sonicated for four cycles on ice (40% of amplitude, 10 s of sonication, and 5 s of pause) (Sonoplus Ultrasonic homogenizer HD 2070, Bandelin electronic, Berlin, Germany) and then centrifuged at 10000 g for 15 min at 4°C. Catalase activity was determined in the supernatants by using the FR20 kit following the manufacturer's instructions (Oxford Biomedical research, Oxford, USA).

2.6. Induction of Apoptosis. Fibroblasts were induced to apoptosis with 10 μg/mL puromycin (PMC, in culture medium) for 6 h at 37°C in a 5% CO_2 humidified atmosphere or with 10^{-2} M cycloheximide (CHX, in culture medium) for 24 h followed by recovery in fresh medium for an additional 1 h at 37°C in a 5% CO_2 humidified atmosphere, in the absence or in the presence of 1 or 2 mg/mL (w/v, in culture medium) of *C. papaya* seeds water extract.

2.7. $[Ca^{2+}]$. 5×10^7 fibroblasts washed twice with loading buffer (10^7 mM NaCl, 5 mM KCl, 7 mM $NaHCO_3$, 3 mM $CaCl_2$, 1 mM $MgSO_4 \times 6H_2O$, 20 mM Hepes, 10 mM glucose, and 1% bovine serum albumin (BSA)) were incubated at the concentration of 10^6 fibroblasts/mL with 4 mM 1-(2-(4-carboxyphenyl)-6-amino-benzofuran-5-oxy)-2-(2′-amino-5′-methylphenoxy)ethane-N,N,N′,N′-tetraacetic acid (Fura-2) acetoxymethyl ester for 45 min at 37°C in a 5% CO_2 humidified atmosphere. After two washes with the loading buffer, fibroblasts were resuspended in the same freshly made buffer at a final concentration of 7×10^6 fibroblasts/mL and stored at RT until use. 2 mL of cell suspension, prewarmed at 37°C for 20 min and adjusted at a final concentration of 1.4×10^5 fibroblasts/mL, was placed in a glass cuvette for Fura-2 fluorescence measure with a FP-750 spectrofluorometer (Jasco Europe s.r.l., Lecco, Italy) equipped with an electronic stirring system and a thermostabilised (37°C) cuvette holder and monitored by a personal computer running the Jasco Spectra Manager software for Windows 95 (Jasco Europe s.r.l.). The excitation wavelengths were 340 and 380 nm and the emission wavelength was 510 nm; the slit widths were set to 10 nm. Fluorescence values were converted to $[Ca^{2+}]_i$ values according to Grynkiewicz et al. [19].

2.8. HSP-70. The inducible cytosolic Heat Shock Protein 70 (HSP-70) protein was detected by Western blot from the total cytosolic proteins of Detroit 550 fibroblasts. Proteins were separated by sodium dodecyl sulfate-polyacrylamide gel electrophoresis (SDS-PAGE) by using 12.5% acrylamide gels according to Laemmli [20] and then electrotransferred onto nitrocellulose paper sheets (Hybond-C extra, Amersham, UK) according to Towbin et al. [21]. Before electrophoresis, proteins (25 μg) were denaturized with 2% SDS, 10% glycerol, 5% β-mercaptoethanol, and 0.05% bromophenol blue in 62.5 mM Tris-HCl (pH 6.8) for 4 min at 95°C. After blockage with 25 mM Tris-HCl (pH 8.0) containing 3% BSA, 127 mM NaCl, and 2.7 mM KCl (TBS buffer) and washing with TBS containing 0.05% Tween 20, nitrocellulose sheets were incubated with monoclonal anti-HSP-70 (1 μg/mL) for 2 h at RT. Specific antibody binding was detected using goat anti-mouse immunoglobulin G (IgG) conjugated to biotin (1 μg/mL), streptavidin conjugated to peroxidase (1 : 1,500 dilution), and 3-3′diaminobenzidine (DAB) as a substrate. Biotinylated SDS molecular weight (MW) standards were run in parallel to samples and stained. β-actin Western blots were used as controls. Quantification was performed by using a GS-700 Imaging densitometer (Bio-Rad, Hercules, CA, USA).

2.9. Mitochondrial Transmembrane Potential. Changes in the inner mitochondrial transmembrane potential ($\Delta\psi_m$) were determined by incubating fibroblasts with the fluorescent probe 5,5′,6,6′-tetrachloro-1,1′,3,3′-tetraethylbenzimidazolylcarboc iodide (JC-1) (Cell Technology, JC-1 Kit, Mountain View, CA, USA) for 15 min at 37°C in the dark. JC-1 was dissolved in DMSO, stored, and used according to the manufacturer's instruction. The monomeric form of the lipophilic cation JC-1 remains in the cytoplasm and stains it in green, while the dimeric form enters the mitochondria with an intact membrane potential and stains them in red. The percentage of the organic solvent in the samples never

exceeded 1% (v/v). Fibroblasts grown on coverslips were rapidly washed with 0.2 M PBS pH 7.4, drained to prevent buffer salt crystals formation, and air-dried. Once completely dried, coverslips were mounted with Histovitrex mounting medium (Carlo Erba, Milan, Italy) and observed with an epifluorescence LM Eclipse 80i (Nikon, Kawasaki, Kanagawa Prefecture, Japan) equipped with a C-HGFIE Hg precentered fiber illuminator (130 W) and a digital camera DXM 1200F by setting a FITC or TRITC filter.

2.10. Cytochrome C Quantification. Quantitative determination of cytosolic and mitochondrial cytochrome C was performed with an Assay Designs' human cytochrome C TiterZyme Enzyme Immunometric Assay (EIA) kit (Assay Designs Inc., Ann Arbor, MI, USA). Fibroblasts rinsed twice with 0.2 M PBS pH 7.4 were suspended in digitonin cell permeabilization buffer (250 nM sucrose, 137 mM NaCl, 70 mM KCl, 1.3 mM Na_2HPO_4, 1.4 mM K_2HPO_4, 0.2 mg/mL digitonin, and 0.1% hydorol M) to obtain a cytosolic fraction of cytochrome C and then in a radio-immunoprecipitation assay (RIPA) cell lysis buffer (50 mM Tris HCl pH 7.4, 150 mM NaCl, 1 mM EDTA, 1 mM EGTA, 1% Triton X-100, 1% sodium deoxycholate, and 0.1% SDS) to obtain a mitochondrial fraction of cytochrome C. Both fractions were incubated with a biotinylated monoclonal antibody to cytochrome C immobilized on a microtiter plate for 1 h. The excess of antibody was washed out and streptavidin conjugated to alkaline phosphatase was added for 30 min before the addition of pNPP (p-nitrophenyl phosphate) substrate for additional 45 min. The colour generated by the reaction was read at 405 nm, using the ETI-SYSTEM Fast Reader (Sorin Biomedica, Vicenza, Italy). The values were expressed as pg of cytochrome C of μg total proteins. The protein concentration was measured by using a Bio-Rad Protein assay kit.

2.11. Statistical Analysis. Data were analysed by performing one-way analysis of variance (ANOVA) at the 95% confidence level. *P* values less than 0.05 were considered significant. Data are the means ± standard errors (SEs) of six independent experiments each done in duplicate.

3. Results

3.1. Cytotoxicity of C. papaya Seeds Water Extract. *C. papaya* seeds water extract was preliminary tested for cytotoxicity (Figure 2). The two concentrations of extract used in the present work (1 and 2 mg/mL) were never toxic at all incubation times. Indeed, 1 mg/mL extract increased cell viability of about 43% over the control value at 4 h of incubation ($P < 0.05$, Figure 2(a)). Likewise, H-E stained control (Figure 2(b), (A)) and 1 mg/mL extract 4 h treated Detroit 550 fibroblasts (Figure 2(b), (D)) exhibited the same spindle shape with a central large ovoid nucleus and many randomly distributed filopodia and microvilli that were better seen at SEM (Figure 2(b), (B)–(E)) and TEM (Figure 2(b), (C)–(F)) level. The TEM analysis allowed observing that these cytoplasmic protrusions were particularly abundant in fibroblasts incubated with 1 mg/mL of *C. papaya* seeds water extract (Figure 2(b), (C)–(F), insert). The percentages of apoptotic, necrotic, and mitotic cells were not modified between control *versus* treated fibroblasts during 8 h of culture (Figure 2(c)).

3.2. Antioxidant Activity of C. papaya Seeds Water Extract. The antioxidant activity of *C. papaya* seeds water extract was assayed on fibroblasts in which H_2O_2-mediated oxidative stress was induced. *C. papaya* seeds water extract protected fibroblasts from the oxidative stress only when added simultaneously with H_2O_2 (Figure 3(a)). In fact, cell viability was increased on extract-treated fibroblasts with respect to the fibroblasts incubated only with H_2O_2, thus suggesting an antioxidant activity. However, the extract was unable to protect fibroblasts when added during the recovery (Figure 3(a)). No differences in the antioxidant efficacy were found between the two extract concentrations.

The antioxidant activity of *C. papaya* seeds water extract was compared with a well-known antioxidant, vitamin C (Figure 3(b)). No toxic concentrations of vitamin C (50, 100, 150, 200, and 250 μM) were added to the culture medium simultaneously with H_2O_2 or during recovery. Antioxidant vitamin C effect was differently exerted than extract. In fact, vitamin C was more efficient to hamper the oxidative stress when added after oxidative stress ignition than simultaneously with H_2O_2 in a concentration dependent manner (Figure 3(b)). Interestingly, *C. papaya* seeds water extract was, in absolute, more efficient than vitamin C to protect Detroit 550 fibroblasts against the oxidative stress. In fact, cell viability increased about 9 times with 1 mg/mL *C. papaya* seeds water extract (added during 1 h H_2O_2 incubation) and about 3 times with the most efficient concentration of vitamin C (200 μM added during recovery) with respect to H_2O_2 treatment alone (please compare Figures 3(a) and 3(b)).

3.3. Catalase Activity. Catalase enzyme is one of the most efficient antioxidant molecules of eukaryotic living cells by hydrolysing H_2O_2 to water and oxygen. The H_2O_2-induced oxidative stress increased catalase activity of about 1.2-fold over the control ($P < 0.05$, Figure 3(c)). When the extract was added simultaneously to the oxidative stress, catalase enzyme activity was similar to the control value (Figure 3(c)). The reduction of the catalase activity was only partially observed (−10% than H_2O_2 treatment alone) when the extract was added during the recovery ($P < 0.05$, Figure 3(c)).

3.4. Antiapoptotic Activity of C. papaya Seeds Water Extract. H_2O_2 represents also an inducer of apoptosis through the production of reactive oxygen species (ROS) [22]; thus the ability of the *C. papaya* seeds water extract to reduce the percentage of apoptotic fibroblasts was assayed. Data are reported in Figure 3(d). Both concentrations of *C. papaya* seeds water extract very efficiently decreased the number of apoptotic fibroblasts of about 30% when added during the H_2O_2-mediated oxidative stress ($P < 0.05$, Figure 3(d)). In fact, cell viability was comparable to untreated ones (Figure 3(a)). Conversely, any antiapoptotic effect of both concentrations of *C. papaya* seeds water extract was observed when added during recovery, as indicated by the unchanged viability (Figure 3(a)) and apoptotic cells

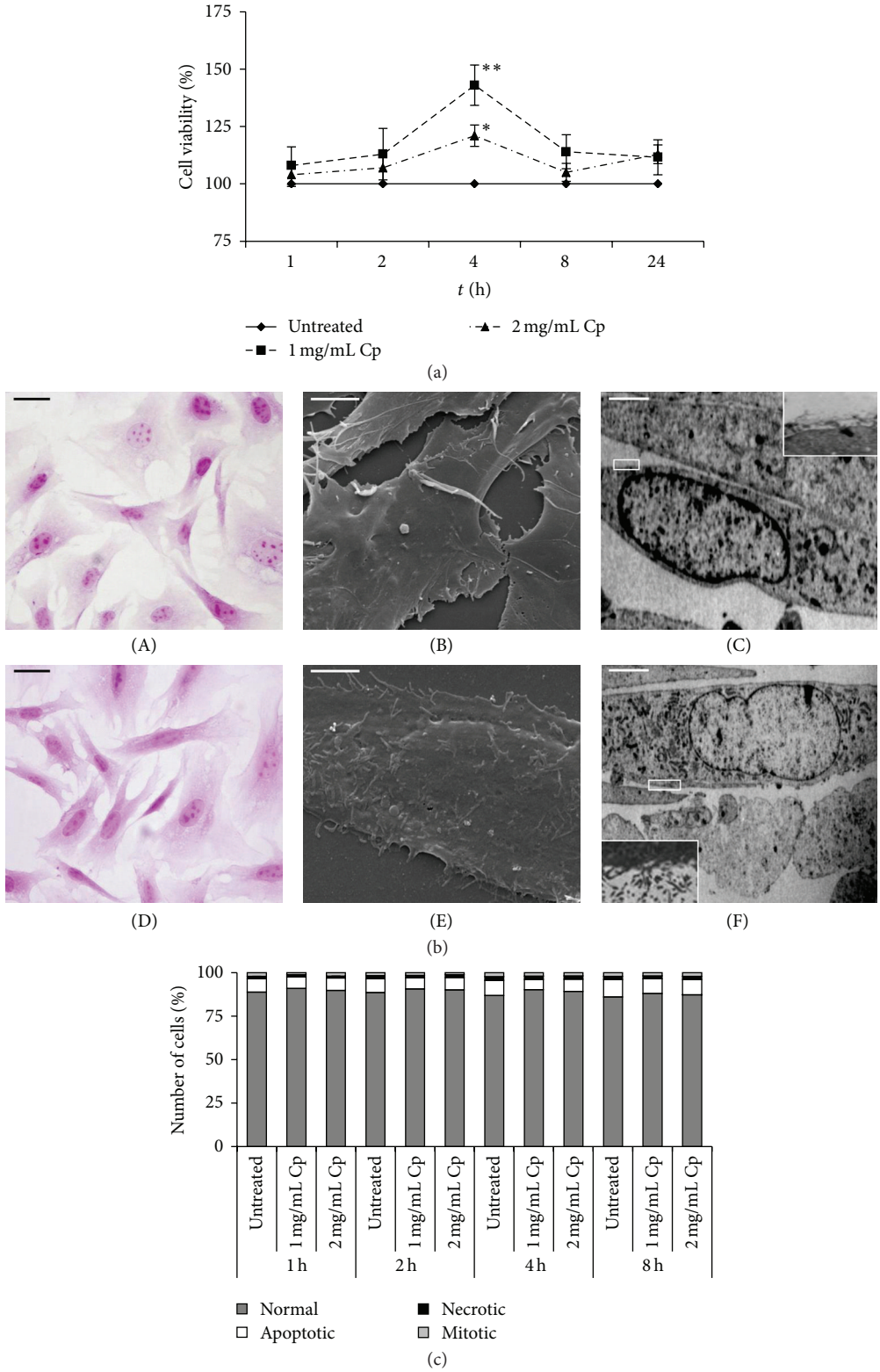

FIGURE 2: Viability and morphology of Detroit 550 fibroblasts treated with *C. papaya* seeds water extract. (a) Viability was assessed by MTT assay. Detroit 550 fibroblasts were treated with 1 or 2 mg/mL *C. papaya* (Cp) seeds water extract for 1, 2, 4, 8, and 24 hours (h). The values are reported as percentage of the control untreated fibroblasts considered as 100%. Each value represents the mean ± SE of six independent experiments, each done in duplicate. Single star indicates value significantly different from untreated control fibroblasts ($P < 0.05$). Two stars indicate value significantly different from the one star value ($P < 0.05$). (b) LM (A, D), SEM (B, E), and TEM (C, F) micrographs of Detroit 550 fibroblasts untreated (A–C) or treated with 1 mg/mL of *C. papaya* seeds water extract for 4 h (D–F). (A, D): H-E stained fibroblasts; bars = 20 μm. (B, E): bars = 5 μm. (C, F): the inset is a magnification showing microvilli; bars = 5 μm. (c) Percentages of normal, apoptotic, necrotic, and mitotic Detroit 550 fibroblasts after treatment with 1 or 2 mg/mL *C. papaya* (Cp) seeds water extract for 1, 2, 4, and 8 h. At least 500 fibroblasts for each treatment were scored on H-E stained slides.

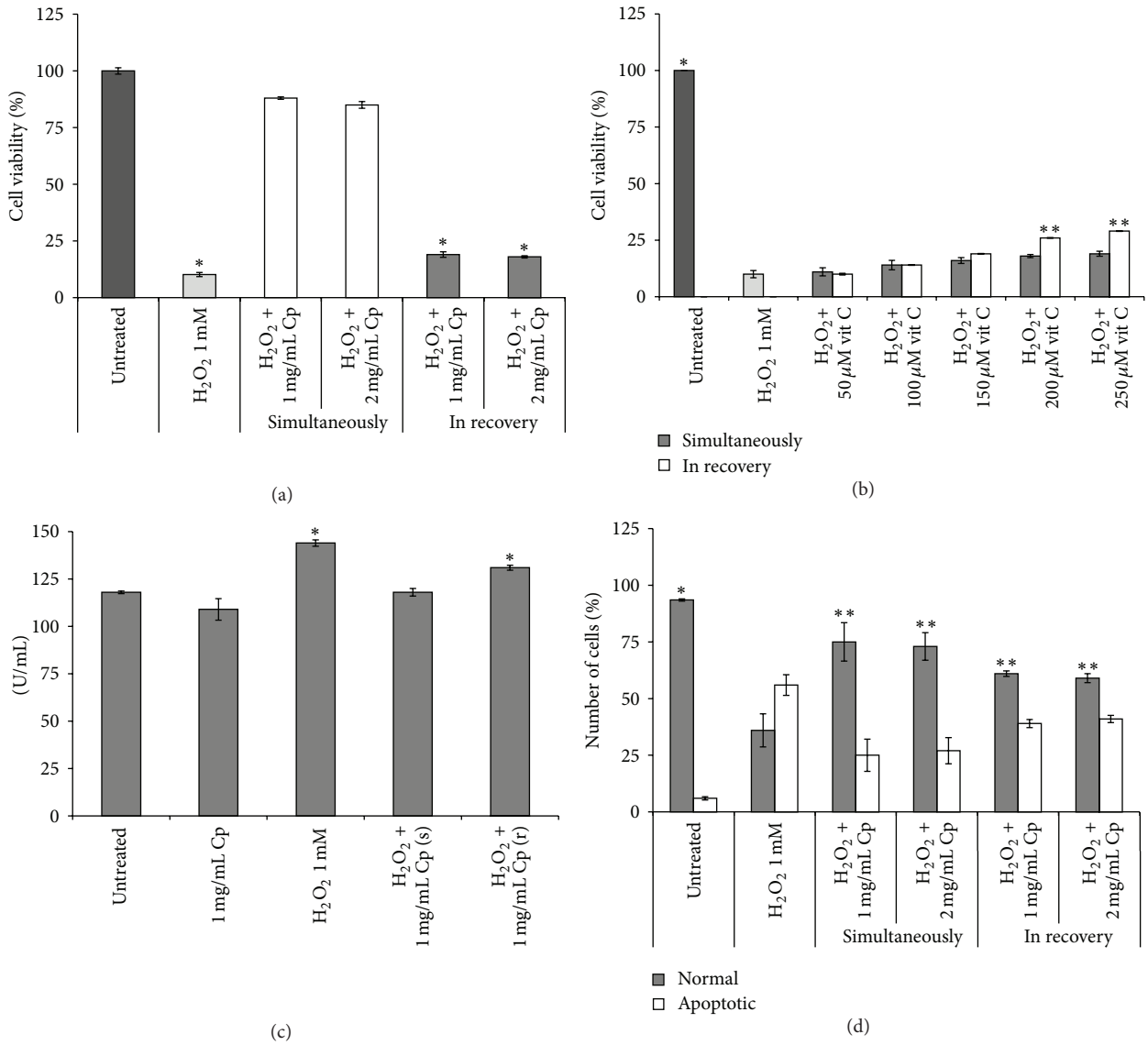

Figure 3: Antioxidant activity of *C. papaya* seeds water extract on Detroit 550 fibroblasts. (a-b) Viability was assessed by MTT assay. The values are reported as percentage of the control untreated fibroblasts considered as 100%. (a) Detroit 550 fibroblasts were treated with 1 or 2 mg/mL *C. papaya* (Cp) seeds water extract simultaneously with 1 mM H_2O_2 for 1 h or during the recovery. Single star indicates values significantly different from untreated control fibroblasts ($P < 0.05$). (b) Detroit 550 fibroblasts were treated with different concentrations of vitamin C (vit C) simultaneously with 1 mM H_2O_2 for 1 h or during the recovery. Single star indicates that the value is significantly different from all others ($P < 0.05$). Two stars indicate values significantly different from those marked with one star and from the simultaneous treatment value ($P < 0.05$). (c) Catalase enzyme activity (U/mL) measured in Detroit 550 fibroblasts treated with 1 mg/mL of Cp seeds water extract added simultaneously (s) with 1 mM H_2O_2 for 1 h or during recovery (r). Single star shows values significantly different from all others ($P < 0.05$). (d) Percentages of normal and apoptotic Detroit 550 fibroblasts after treatment with 1 mM H_2O_2 administrated either alone or in combination with 1 or 2 mg/mL of Cp extract or with Cp extract added during 1 h recovery. At least 500 fibroblasts for each treatment were scored on H-E stained slides. Single star shows a value significantly different from all others and from the corresponding apoptotic untreated control fibroblasts ($P < 0.05$). Two stars indicate values significantly different from the untreated control fibroblasts and from the corresponding apoptotic ones ($P < 0.05$). Each value represents the mean ± SE of six independent experiments, each done in duplicate.

values (Figure 3(b)) *versus* H_2O_2 treatment alone. To verify if *C. papaya* seeds water extract exerts protection from apoptosis induced through pathways different from oxidative stress, fibroblasts were incubated with CHX and PMC that are able to induce apoptosis by inhibiting protein synthesis. Data of Figure 4 show that induction of apoptosis was unaffected by the presence of *C. papaya* seeds water extract added simultaneously to CHX or PMC treatments (Figures 4(a) and 4(b)). Comparable results were obtained by biochemical and morphological analysis.

Altogether these data suggest that inhibition of H_2O_2-mediated apoptosis is not exerted on the apoptotic process

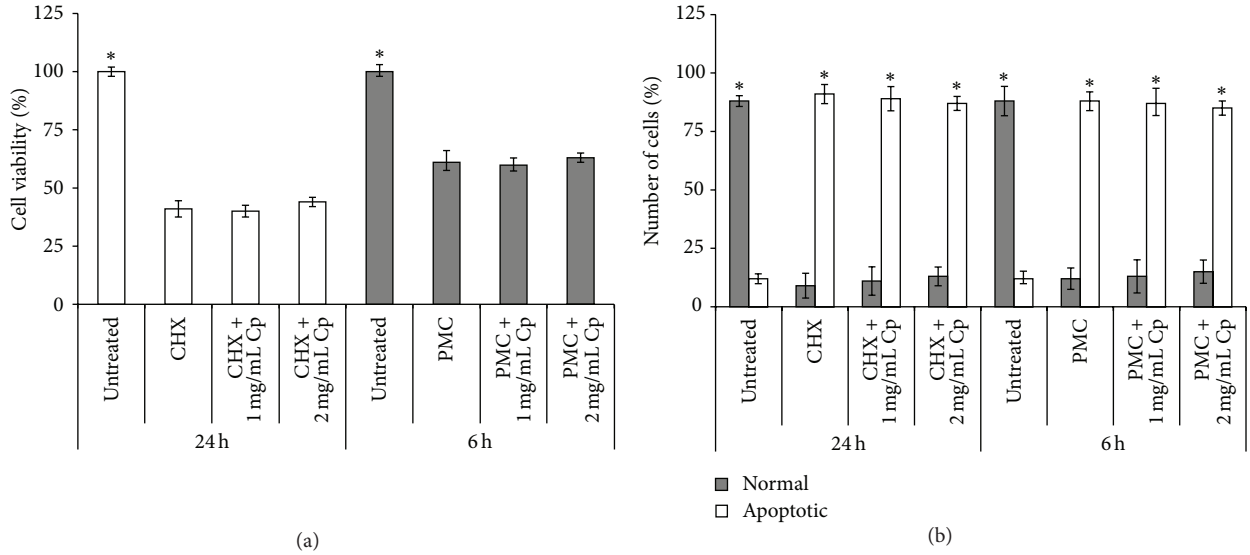

Figure 4: Antiapoptotic activity of *C. papaya* seeds water extract on Detroit 550 fibroblasts. Detroit 550 fibroblasts were treated with 10^{-2} M cycloheximide (CHX, in culture medium) or 10 μg/mL puromycin (PMC, in culture medium) either alone or in combination with 1 or 2 mg/mL of *C. papaya* (Cp) extract for 24 or 6 hours (h), respectively. (a) Viability was assessed by MTT assay. Stars show significant value with the corresponding 24 or 6 h values ($P < 0.05$). (b) Percentages of normal and apoptotic fibroblasts. At least 500 fibroblasts for each treatment were scored on H-E stained slides. Single star indicates values that differ significantly from the corresponding normal or apoptotic ones ($P < 0.05$). Each value represents the mean ± SE of six independent experiments, each done in duplicate.

itself but it is the result of the antioxidant activity of *C. papaya* seeds water extract. In fact, no inhibition of H_2O_2-mediated apoptosis was observed when the extract was added while oxidative stress is already ignited.

3.5. Mitochondrial $\Delta\psi_m$ and Cytochrome C. Oxidative stress induces the loss of $\Delta\psi_m$ and the release of cytochrome C into the cytoplasm. These two events trigger the onset of apoptosis *via* the intrinsic pathway. The $\Delta\psi_m$ was evaluated by the high sensitive fluorescent probe JC-1. The monomeric form of JC-1 labels the cytoplasm of fibroblasts in brilliant green, while the dimeric form can enter into mitochondria with a normal $\Delta\psi_m$ and stain them in red. Data are shown in Figures 5 and 6. JC-1 labelled fibroblasts treated with 1 mg/mL of *C. papaya* seeds water extract did not alter $\Delta\psi_m$ (Figures 5(e) and 5(f)), while 1 mM of H_2O_2 induced the loss of $\Delta\psi_m$, thus preventing the passage of JC-1 dimers into the mitochondria (Figures 5(g) and 5(h)). When 1 mg/mL of *C. papaya* seeds water extract was added simultaneously to the oxidative stress, it prevented the $\Delta\psi_m$ loss and, thus, mitochondria were red stained (Figures 5(i) and 5(j)). The extract was unable to hamper $\Delta\psi_m$ loss when added during recovery (Figures 5(k) and 5(l)).

Mitochondrial $\Delta\psi_m$ loss causes in turn changes in the permeability of the outer mitochondrial membrane and provokes the release of cytochrome C, a well-known apoptotic-inducing factor. The cytosolic concentration of cytochrome C increased 6-fold than the control value during oxidative stress, that is, 300 pg *versus* 50 pg, respectively ($P < 0.05$, Figure 6). The addition during the oxidative stress of 1 mg/mL *C. papaya* seeds water extract prevented the release of cytochrome C. No effect has been observed upon the administration of the extract after the oxidative stress induction, as indicated by the unchanged cytochrome C concentration values with respect to H_2O_2 damaged fibroblasts (Figure 6).

3.6. [Ca^{2+}] Ions. Oxidative stress induces Ca^{2+} ions influx into the cytoplasm, which in turn causes disruption of the normal physiological pathways and leads to cell death. Ca^{2+} ions influx into the cytoplasm was prevented by 1 mg/mL of *C. papaya* seeds water extract when added simultaneously to H_2O_2 (Figure 7). The same behaviour was observed with addition of 200 μM vitamin C either alone or simultaneously with 1 mM H_2O_2 added for 1 h. [Ca^{2+}] ions concentration was 160 nM in H_2O_2 treated fibroblasts and 100 nM in control and extract or vitamin C treated ones ($P < 0.05$, Figure 7).

3.7. HSP-70. HSPs protect cells against a plethora of stresses, including oxidative stress. A reduction of 7% of the amount of HSP-70 was observed when fibroblasts were treated for 1 h with 1 mg/mL *C. papaya* seeds water extract ($P < 0.05$, Figure 8(a)). Overexpression of HSP-70 protein was found upon 1 mM H_2O_2 incubation of Detroit 550 fibroblasts ($P < 0.05$, Figure 8(b)). *C. papaya* seeds water extract, added during the oxidative stress but not during the recovery, hampered the stress by decreasing the amount of HSP-70 to control value (Figure 8(b)).

3.8. Antioxidant Activity of C. papaya Seeds Water Extract Subfractions. The fractionation of *C. papaya* seeds water extract by differential centrifugation (Figure 1) allowed us to evaluate if the antioxidant effect of extract was an exclusive property of the whole crude extract or was mainly related to a specific class of compounds. Any of the different subfractions (1 mg/mL final concentration) was cytotoxic as shown with

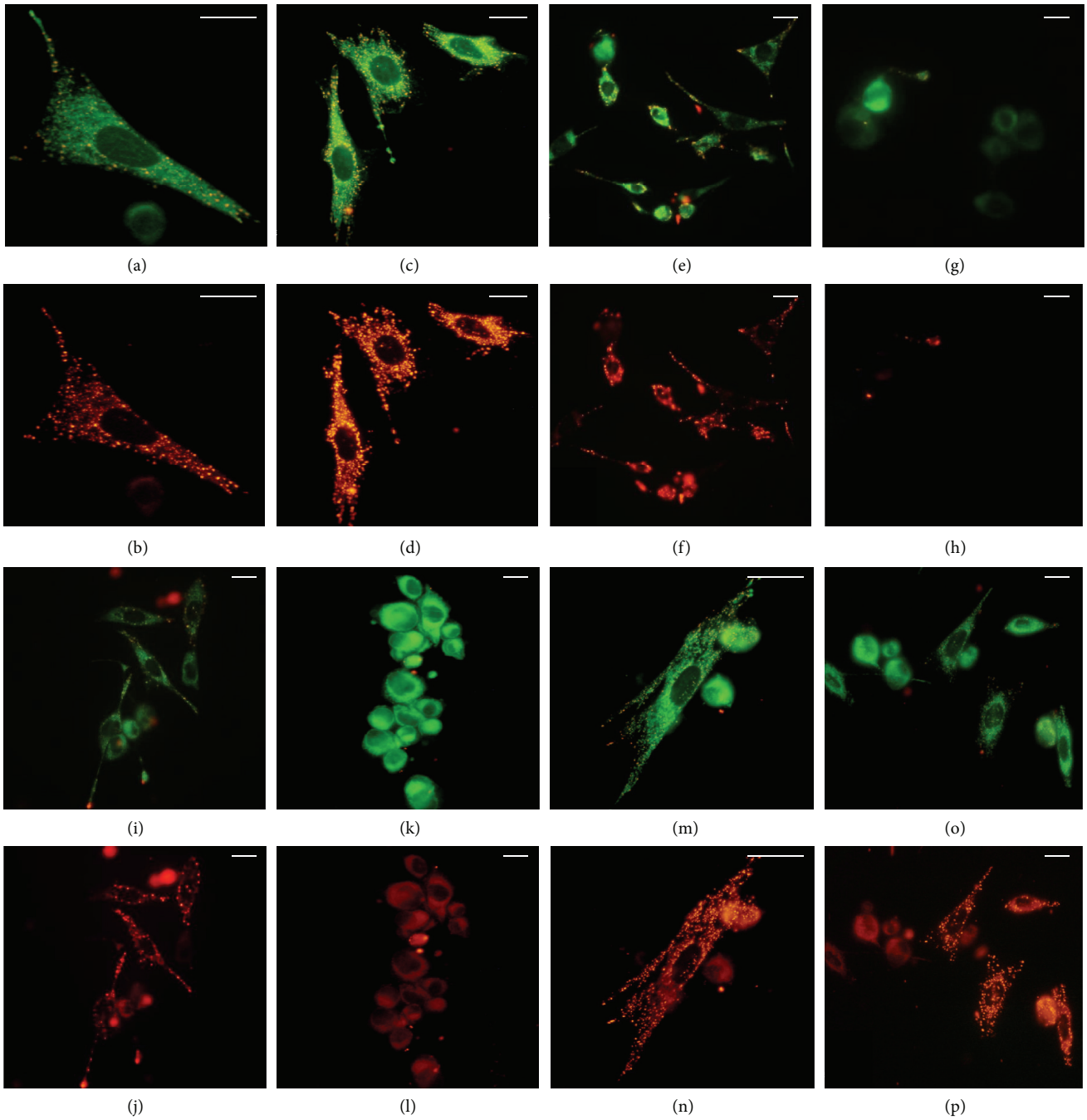

Figure 5: Detroit 550 fibroblasts labelled with the fluorescent probe JC-1 after the treatment with the *C. papaya* seeds water extract and/or with H_2O_2. Fibroblasts were labelled with JC-1 (1% v/v) and green or red fluorescence was observed with an epifluorescence LM by setting a FITC (a, c, e, g, i, k, m, and o) or TRITC filter (b, d, f, h, j, l, n, and p). (a)–(d): control untreated fibroblasts at T0 (a, b) and at 4 h (c-d); (e)-(f): fibroblasts treated with 1 mg/mL of *C. papaya* (Cp) extract for 4 h; (g)-(h): fibroblasts incubated with H_2O_2 1 mM for 1 h; ((i)-(j)): fibroblasts incubated with 1 mM H_2O_2 and 1 mg/mL of Cp simultaneously for 1 h; (k)-(l): fibroblasts incubated with 1 mM H_2O_2 for 1 h and with 1 mg/mL of Cp extract added during recovery; (m)-(n): cell treated with 1 mg/mL of the subfraction with MW > 10 kDa (see Figure 1); (o)-(p): fibroblasts simultaneously incubated with 1 mg/mL of the subfraction with MW > 10 kDa and 1 mM H_2O_2 for 1 h. Bars = 20 μm.

MTT assay and JC1 staining (Figures 9 and 5, resp.). Figure 5 shows red stained mitochondria of Detroit 550 fibroblasts treated with MW > 10 kDa subfraction alone (Figures 5 (m) and 5(n)) and simultaneously with H_2O_2 (Figures 5(o) and 5(p)). The subfractions increased viability of Detroit 550 fibroblasts: the maximum increment was measured with the supernatant obtained by 100000 g centrifugation of 16000 g supernatant ($P < 0.05$, Figure 9), especially with the subfraction containing substances with MW < 10 kDa (Figure 9). Regarding the antioxidant activity, the different subfractions

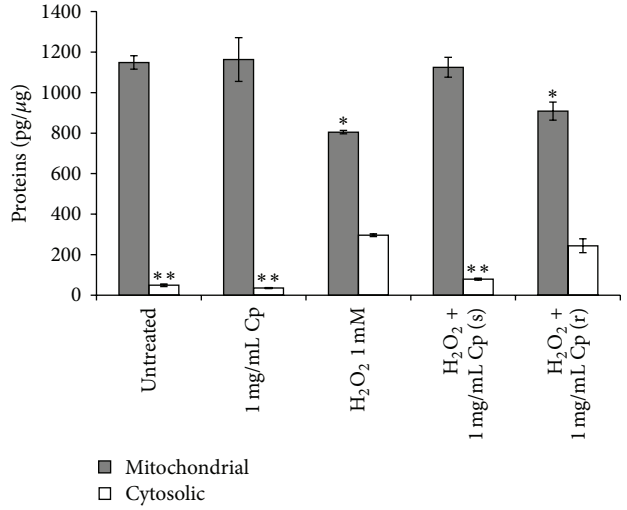

Figure 6: Cytoplasmic and mitochondrial cytochrome C levels. Detroit 550 fibroblasts incubated with 1 mM H_2O_2 for 1 h simultaneously (s) or during recovery (r) with 1 mg/mL of *C. papaya* (Cp) seeds water extract were harvested for the content of mitochondrial and cytosolic cytochrome C by ELISA assay. Concentrations are expressed as pg/μg of total proteins. Single star indicates a significant value *versus* the untreated control fibroblasts ($P < 0.05$); two stars indicate a significant value *versus* all the others values relative to the cytosolic cytochrome C ($P < 0.05$). Each value represents the mean ± SE of six independent experiments, each done in duplicate.

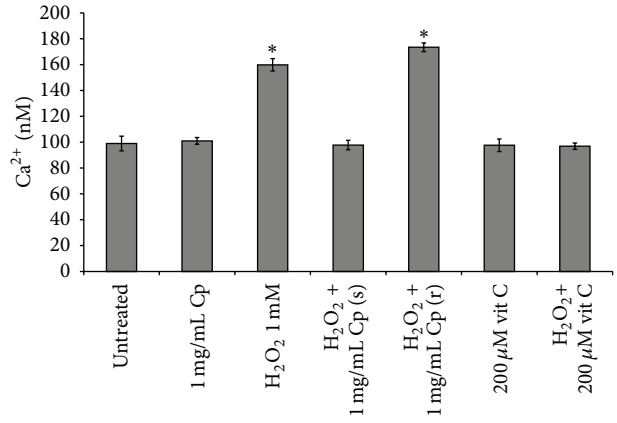

Figure 7: Ca^{2+} ions. Ca^{2+} ions concentration (nM) found after incubation of Detroit 550 fibroblasts with 1 mg/mL *C. papaya* (Cp) seeds water extract or with 200 μM vitamin C (vit C) added simultaneously (s) or during recovery (r) with 1 mM H_2O_2 either for 1 h. The values indicated with the single star differ significantly from all the others ($P < 0.05$). Each value represents the mean ± SE of six independent experiments, each done in duplicate.

were not significantly different than the whole extract when added simultaneously with the oxidative stress (Figure 9). Any of the subfractions could reduce the oxidative stress when added during recovery.

4. Discussion

The present study shows that *C. papaya* seeds water extract has a potent antioxidant activity in H_2O_2 oxidative stress-induced human skin Detroit 550 fibroblasts. Our results suggest that the extract is not toxic, decreases cell death, ensures Ca^{2+} homeostasis, and counteracts mitochondrial dysfunctionality in oxidative stress-damaged Detroit 550 fibroblasts. The best effect primarily depends on the modality of administration and to a lesser extent on the dose and composition, that is, whole extract *versus* subfractions. We found that (i) the protective effect was exerted when the extract was added concomitantly to the oxidative stress, suggesting that the bioactive compounds of *C. papaya* extract are not inactivated by H_2O_2 (as it is for vitamin C) but, conversely, can scavenge H_2O_2 but not free radical; (ii) the sufficient dose to induce antioxidant effect in our experimental design is 1 mg/mL, likely due to the concentration of the diverse bioactive molecules; (iii) the crude whole extract is effective as much as the subfractions.

Thus, our data strongly highlight the antioxidant role of the molecules contained in *C. papaya* seeds water extract, encouraging their exploitation. In fact, substances with antioxidant properties have recently received unprecedented attention as possible therapeutic and preventive agents in consideration of the role of ROS in health and diseases. In addition, due to the augmented recycling interest of the agrofood industry, the numbers of studies on residual sources in replacing synthetic antioxidants with natural ones are increasing. The wastes or byproducts from food processing such as seeds and peels contain higher source of potential antioxidant compounds than the edible portion [23]; conversely, byproduct-derived antioxidants successfully developed are very limited. Grape seed and olive waste extract in the European food processing industry represent these exceptions [24]. In this context, *C. papaya* seeds water extract could be a source to exploit. In fact, papaya seeds contain several molecules, like fatty acids, crude protein, crude fiber, papaya oil, carpaine, benzyl isothiocyanate, glucotropaeolin, benzyl thiourea, hentriacontane, β-sitosterol, caricin, and an enzyme myrosin [7] that confer vermifuge [25, 26], abortifacient [27, 28], antifertility [29–32], wound-healing [33], anticancer [34], antibacterial [35], and antifungal [36] properties as well as antioxidant activities for the presence of secondary metabolites, such as phenolic compounds, vanillic acid, flavonoids, α-tocopherol, and vitamin C. Despite the wide and historical use of *C. papaya* in the traditional management of many diseases [4], the scientific validation of the use of papaya seeds as antioxidant is scarce. Therefore, in the present work we tested *C. papaya* seeds water extract that conforms to the use in folk medicine and ensures no toxicity related to chemicals used during the preparation. In our hands, *C. papaya* seeds water extract is not toxic and, as a whole, it is more efficient than vitamin C to hamper the H_2O_2 oxidative damage.

The choice of the methodology for extract preparation is very important to preserve antioxidant activity [17, 37]. The antioxidant activity of seed extract could be further improved, taking into account that the comparison of five extract fractions, that is, ethanol, petroleum ether, ethyl acetate, n-butanol, and water, demonstrated the strongest

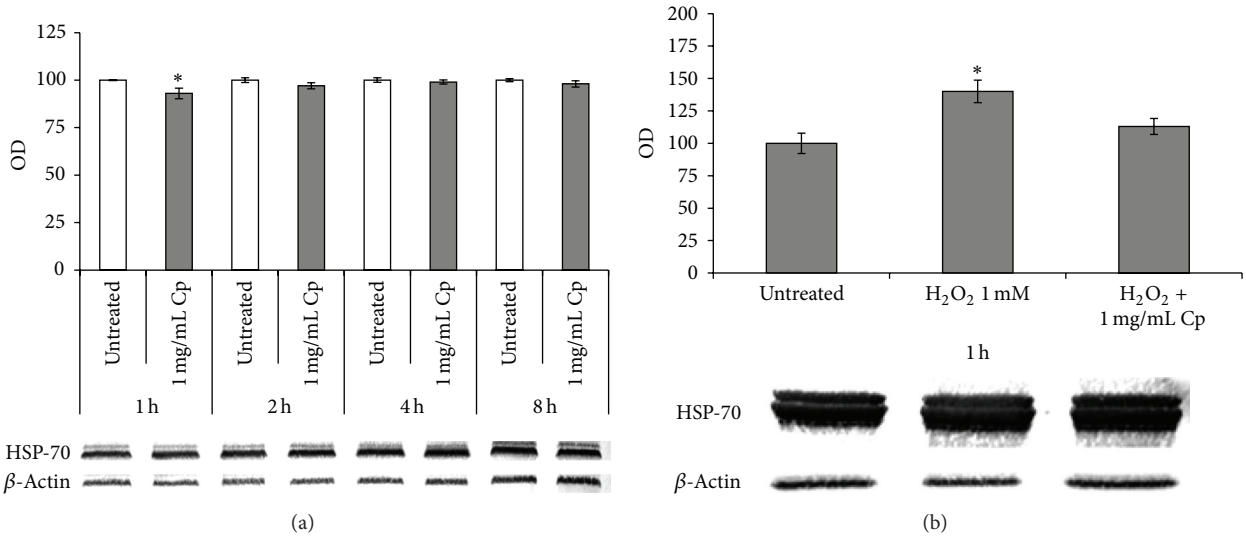

Figure 8: Western blot of HSP-70. (a) Western blots and optic densities (OD) of inducible cytosol HSP-70 of control untreated Detroit 550 fibroblasts or treated with 1 mg/mL of *C. papaya* (Cp) seeds water extract for 1, 2, 4, and 8 hours (h); (b) Western blots and OD of inducible cytosol HSP-70 of Detroit 550 fibroblasts incubated with 1 mM H_2O_2 for 1 h in absence or in presence of 1 mg/mL of Cp seeds water extract. Values are expressed as percentage of the control untreated fibroblasts value taken as 100%. The star shows a significant value with respect to all the others without star ($P < 0.05$). Each value represents the mean ± SE of six independent experiments, each one done in duplicate.

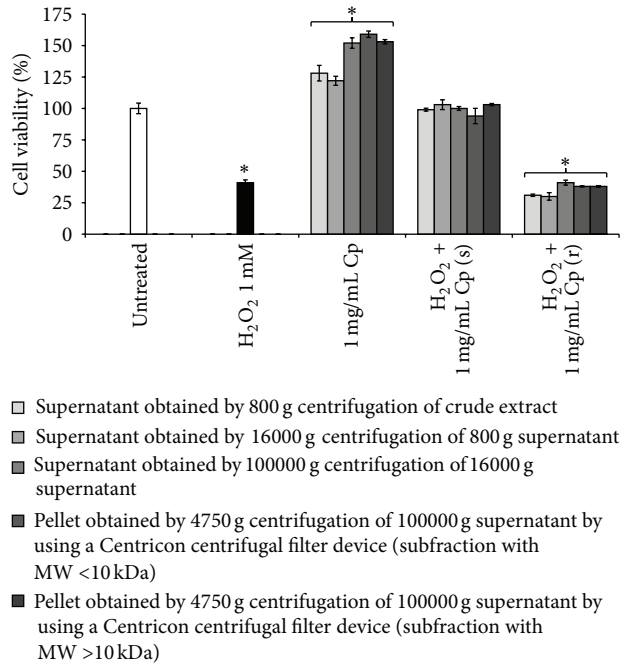

Figure 9: Viability of Detroit 550 fibroblasts treated with different subfractions of *C. papaya* seeds water extract. Viability of Detroit 550 fibroblasts treated with 1 mg/mL (w/v, in the culture medium) of different subfractions obtained from the *C. papaya* (Cp) extract (see Figure 1) administrated either alone or with 1 mM H_2O_2 added simultaneously (s) or during 1 h recovery (r) was evaluated by MTT test. One star indicates values significantly different from control untreated fibroblasts ($P < 0.05$). Each value represents the mean ± SE of six independent experiments done in duplicate. For the preparation of subfractions, see Figure 1 and Materials and Methods section.

antioxidant activity of the ethyl acetate and n-butanol fractions, whereas the water extract had always the weakest antioxidant activity [17]. Despite this data, we tested the water extract because it is edible, thus compatible with a putative human administration. Here, we also demonstrated that the modality of administration is crucial as well. Since experimental H_2O_2 oxidative stress is based on two-step procedure, that is, 1 mM H_2O_2 for 1 h followed by 1 h of recovery in fresh medium, we found that the best modality of papaya extract administration is when it is added simultaneously with the oxidative stress inducer. This suggests that the extract acts directly with H_2O_2. In addition, *C. papaya* seeds water extract was, as a whole, much more efficient than vitamin C, a well-known antioxidant agent. In fact, vitamin C had its highest antioxidant activity when added in the recovery. H_2O_2 must be firstly converted by fibroblasts to free radicals that can be then neutralized by vitamin C. In fact, ascorbic acid or vitamin C is a water soluble antioxidant that delays or inhibits cellular damage mainly through free radical scavenging. Vitamin C belongs to primary antioxidants group that are able to donate electrons to free radical, scavenging them to compounds more stable and not harmful to cells [38].

The robust antioxidant activity of *C. papaya* seed extract can protect from cell death. In fact, we showed the ability of the extract to prevent H_2O_2-induced apoptosis. However, the extract does not affect directly the apoptotic process but indirectly by hampering the oxidative stress-induced apoptosis. In fact, *C. papaya* extract has no efficacy against CHX- and PMC-induced apoptosis, inhibitors of protein synthesis. Therefore, the protection from the oxidative-stress-induced apoptosis is an indirect consequence of the ability of the extract to prevent the production or to block the activity of harmful metabolites, like free radicals.

Antioxidant function in biological systems is much more complicated than a simple free radical scavenging process. An antioxidant may affect biological system by (i) suppressing the formation of ROS and reactive nitrogen species (RNS); (ii) affecting enzyme activities [39]; (iii) inducing *de novo* biosynthesis of defence enzymes and thereby affecting other endogenous antioxidants [40]; (iv) preserving NO activity [41], or (v) sequestering transition metal ions. It is obvious that some compounds use more than one mechanism for their antioxidants effect on biological systems. Our data show that the antioxidant effect of *C. papaya* seeds water extract did not increase scavenging enzymes activity, as catalase. When added simultaneously to the oxidative stress, the extract reduces the catalase activity to normal level. This suggests that the antioxidant effects of the *C. papaya* seeds water extract are exerted not *via* modulation of catalase enzyme activity but by (i) scavenging and chelating the oxidative molecules (H_2O_2) or (ii) reestablishing or maintaining the reduction/oxidation balance inside the cell.

Oxidative stress causes mitochondrial dysfunction *via* loss of $\Delta\psi_m$, accumulation of mitochondrial DNA mutations, and increment of the level of oxidative damage to DNA, proteins, and lipids [1]. Yakes and Van Houten [42] demonstrated that H_2O_2 treatment affects mainly mitochondria rather than DNA in human cells. In our system, *C. papaya* seeds water extract prevents the $\Delta\psi_m$ loss and the consequent release of cytochrome C into the cytosol.

Cytochrome C is normally bound to the inner mitochondrial membrane by association with cardiolipin, whose peroxidation leads to cytochrome C and release through the outer mitochondrial membrane into the cytosol. Once in the cytoplasm, cytochrome C triggers the activation of caspase-9 that activates the intrinsic pathway of apoptosis [43]. Since *C. papaya* seeds water extract prevents oxidative-induced cell death by blocking the cytochrome C release from mitochondria to cytosol, by reducing the mitochondrial ROS and by inhibiting the mitochondrial permeability transition, we speculate that it is cell permeable and able to target mitochondria.

Oxidative stress burst can disrupt normal physiological pathways that, in turn, trigger the Ca^{2+} signaling dependent cell death. In fact, oxidative stress causes Ca^{2+} influx into the cytoplasm from the extracellular environment and from the endoplasmic reticulum (ER) through, respectively, cell membrane and ER channels [44]. *C. papaya* seeds water extract elicits antioxidant effect also by preventing the H_2O_2-induced alteration of Ca^{2+} homeostasis. The significant cytosolic HSP-70 induction occurred after exposure to H_2O_2 was decreased by *C. papaya* seeds water extract to normal level. These results point to the possible involvement of redox mechanisms in the heat shock signal transduction pathway, which may play an important regulatory role in the genetic mechanisms of tolerance to oxidative stress.

The antioxidant properties of five subfractions of the water crude extract obtained by differential centrifugation were tested in the same conditions of the whole extract. Each subfraction showed activities comparable to those tested for the whole extract, thus indicating that the antioxidant activity of the *C. papaya* seeds water extract is not entirely attributable to only one molecule or few association of molecules and that there is no synergistic activity of the bioactive compounds. It is worth noting that one of the five subfractions tested expressed a property that was not shown by the other subfractions. In fact, the subfraction with MW > 10 kDa was able to counteract the loss of $\Delta\psi_m$. The reason of such behavior needs further investigations.

Altogether our data are in favour of a beneficial effect of the exogenous supplementation of *C. papaya* seeds water extract (as whole or as MW > 10 kDa subfraction) representing an efficient tool to minimize free radical-induced damage.

5. Conclusions

In conclusion, this study indicates that also nonedible parts of *C. papaya,* in particular seeds water extract, may be a promising source of antioxidants, which may have therapeutic implications. In fact, we showed that *C. papaya* seeds protect fibroblasts from H_2O_2-induced stress due to the antioxidant activity of the water extract. All together our results gave indication on the benefits, on the modality of administration, and on the extraction of *C. papaya* seeds that are important for the extent of the antioxidant activity and open a new perspective in the biotechnological utilization of the *C. papaya*. Indeed, this aspect could be very important to recycle the waste of papaya fruit, playing an important role to improve the complete utilization of its nonedible byproducts.

Conflict of Interests

Elisa Panzarini, Majdi Dwikat, Stefania Mariano, Cristian Vergallo, and Luciana Dini have no conflict of interests regarding the publication of this paper.

References

[1] K. Brieger, S. Schiavone, F. J. Miller, and K. H. Krause, "Reactive oxygen species: from health to disease," *Swiss Medical Weekly*, vol. 142, pp. 1–14, 2012.

[2] S. A. Stanner, J. Hughes, C. N. Kelly, and J. Buttriss, "A review of the epidemiological evidence for the 'antioxidant hypothesis'," *Public Health Nutrition*, vol. 7, no. 3, pp. 407–422, 2004.

[3] J. Mursu, K. Robien, L. J. Harnack, K. Park, and D. R. Jacobs Jr., "Dietary supplements and mortality rate in older women: The Iowa Women's Health Study," *Archives of Internal Medicine*, vol. 171, no. 18, pp. 1625–1633, 2011.

[4] A. Ali, S. Devarajan, M. Waly, M. M. Essa, and M. S. Rahman, "Nutritional and medicinal value of papaya (Carica papaya L.)," in *Natural Products and Bioactive Compounds in Disease Prevention*, M. M. Essa, A. Manickavasagan, and E. Sukumar, Eds., pp. 34–42, Nova Science Publishers, New York, NY, USA, 2011.

[5] Y. Nakamura, M. Yoshimoto, Y. Murata et al., "Papaya seed represents a rich source of biologically active isothiocyanate," *Journal of Agricultural and Food Chemistry*, vol. 55, no. 11, pp. 4407–4413, 2007.

[6] P. Jaiswal, P. Kumar, V. K. Singh, and D. K. Singh, "Carica papaya Linn: a potential source for various health problems," *Journal of Pharmacy Research*, vol. 3, no. 5, pp. 998–1003, 2010.

[7] K. L. Krishna, M. Paridhavi, and J. A. Patel, "Review on nutritional, medicinal and pharmacological properties of Papaya (Carica papaya Linn.)," *Natural Product Radiance*, vol. 7, no. 4, pp. 364–373, 2008.

[8] N. S. Anuar, S. S. Zahari, I. A. Taib, and M. T. Rahman, "Effect of green and ripe Carica papaya epicarp extracts on wound healing and during pregnancy," *Food and Chemical Toxicology*, vol. 46, no. 7, pp. 2384–2389, 2008.

[9] S. A. S. H. Ajlia, F. A. A. Majid, A. Suvik, M. A. W. Effendy, and H. Serati Nouri, "Efficacy of papain-based wound cleanser in promoting wound regeneration," *Pakistan Journal of Biological Sciences*, vol. 13, no. 12, pp. 596–603, 2010.

[10] N. A. Imaga, G. O. Gbenle, V. I. Okochi et al., "Phytochemical and antioxidant nutrient constituents of Carica papaya and parquetina nigrescens extracts," *Scientific Research and Essays*, vol. 5, no. 16, pp. 2201–2205, 2010.

[11] C. Morimoto, N. H. Dang, and N. Dang, "Cancer prevention and treating composition for preventing, ameliorating, or treating solid cancers, e.g. lung, or blood cancers, e.g. lymphoma, comprises components extracted from brewing papaya," Patent WO2006004226-A1, EP1778262-A1, JP2008505887-W, US2008069907-A1, YS Therapeutic Co Ltd (YSTH-Non-standard) Toudai Tlo Ltd (TODNon- standard) Morimoto C (MORI-Individual) Dang NH (DANG-Individual), 2008.

[12] N. Otsuki, N. H. Dang, E. Kumagai, A. Kondo, S. Iwata, and C. Morimoto, "Aqueous extract of Carica papaya leaves exhibits anti-tumor activity and immunomodulatory effects," *Journal of Ethnopharmacology*, vol. 127, no. 3, pp. 760–767, 2010.

[13] M. Indran, A. A. Mahmood, and U. R. Kuppusamy, "Protective effect of Carica papaya L leaf extract against alcohol induced acute gastric damage and blood oxidative stress in rats," *West Indian Medical Journal*, vol. 57, no. 4, pp. 323–326, 2008.

[14] V. Kothari and S. Seshadri, "Antioxidant activity of seed extracts of Annona squamosa and Carica papaya," *Nutrition and Food Science*, vol. 40, no. 4, pp. 403–408, 2010.

[15] S. Norshazila, I. S. Zahir, K. M. Suleiman, M. R. Aisyah, and K. K. Rahim, "Antioxidant levels and activities of selected seeds of Malaysian tropical fruits," *Malaysian Journal of Nutrition*, vol. 16, no. 1, pp. 149–159, 2010.

[16] J. Contreras-Calderón, L. Calderón-Jaimes, E. Guerra-Hernández, and B. García-Villanova, "Antioxidant capacity, phenolic content and vitamin C in pulp, peel and seed from 24 exotic fruits from Colombia," *Food Research International*, vol. 44, no. 7, pp. 2047–2053, 2011.

[17] K. Zhou, H. Wang, W. Mei, X. Li, Y. Luo, and H. Dai, "Antioxidant activity of Papaya seed extracts," *Molecules*, vol. 16, no. 8, pp. 6179–6192, 2011.

[18] D. Sladowski, S. J. Steer, R. H. Clothier, and M. Balls, "An improved MTT assay," *Journal of Immunological Methods*, vol. 157, pp. 203–207, 1993.

[19] G. Grynkiewicz, M. Poenie, and R. J. Tsien, "A new generation of Ca^{2+} indicators with greatly improved fluorescence properties," *The Journal of Biological Chemistry*, vol. 260, no. 6, pp. 3440–3450, 1985.

[20] U. K. Laemmli, "Cleavage of structural proteins during the assembly of the head of the bacteriophage T4," *Nature*, vol. 227, no. 5259, pp. 680–685, 1970.

[21] H. Towbin, T. Staehelin, and J. Gordon, "Electrophoretic transfer of proteins from polyacrilamide gels to nitrocellulose sheets: procedure and some applications," *Proceedings of the National Academy of Sciences of the United States of America*, vol. 76, no. 9, pp. 4350–4354, 1979.

[22] P. Formichi, E. Radi, C. Battisti et al., "Human fibroblasts undergo oxidative stress-induced apoptosis without internucleosomal DNA fragmentation," *Journal of Cellular Physiology*, vol. 208, no. 2, pp. 289–297, 2006.

[23] S. Okonogi, C. Duangrat, S. Anuchpreeda, S. Tachakittirungrod, and S. Chowwanapoonpohn, "Comparison of antioxidant capacities and cytotoxicities of certain fruit peel," *Food Chemistry*, vol. 103, no. 3, pp. 839–846, 2007.

[24] W. Peschel, F. Sánchez-Rabaneda, W. Diekmann et al., "An industrial approach in the search of natural antioxidants from vegetable and fruit wastes," *Food Chemistry*, vol. 97, no. 1, pp. 137–150, 2006.

[25] J. A. O. Okeniyi, T. A. Ogunlesi, O. A. Oyelami, and L. A. Adeyemi, "Effectiveness of dried Carica papaya seeds against human intestinal parasitosis: a pilot study," *Journal of Medicinal Food*, vol. 10, no. 1, pp. 194–196, 2007.

[26] A. Sapaat, F. Satrija, H. H. Mahsol, and A. H. Ahmad, "Anthelmintic activity of papaya seeds on Hymenolepis diminuta infections in rats," *Tropical Biomedicine*, vol. 29, no. 4, pp. 508–512, 2012.

[27] O. Oderinde, C. Noronha, A. Oremosu, T. Kusemiju, and O. A. Okanlawon, "Abortifacient properties of aqueous extract of Carica papaya (Linn) seeds on female Sprague-Dawley rats," *The Nigerian Postgraduate Medical Journal*, vol. 9, no. 2, pp. 95–98, 2002.

[28] A. Adebiyi, P. G. Adaikan, and R. N. V. Prasad, "Tocolytic and toxic activity of papaya seed extract on isolated rat uterus," *Life Sciences*, vol. 74, no. 5, pp. 581–592, 2003.

[29] N. J. Chinoy, J. M. D'Souza, and P. Padman, "Effects of crude aqueous extract of Carica papaya seeds in male albino mice," *Reproductive Toxicology*, vol. 8, no. 1, pp. 75–79, 1994.

[30] N. K. Lohiya, R. B. Goyal, D. Jayaprakash, A. S. Ansari, and S. Sharma, "Antifertility effects of aqueous extract of Carica papaya seeds in male rats," *Planta Medica*, vol. 60, no. 5, pp. 400–404, 1994.

[31] P. Udoh, I. Essien, and F. Udoh, "Effects of Carica papaya (paw paw) seeds extract on the morphology of pituitary-gonadal axis of male Wistar rats," *Phytotherapy Research*, vol. 19, no. 12, pp. 1065–1068, 2005.

[32] A. Ortega-Pacheco, M. Jimenez-Coello, K. Y. Acosta-Viana et al., "Effects of papaya seeds extract on the sperm characteristics of dogs," *Animal Reproduction Science*, vol. 129, no. 1-2, pp. 82–88, 2011.

[33] B. S. Nayak, R. Ramdeen, A. Adogwa, A. Ramsubhag, and J. R. Marshall, "Wound-healing potential of an ethanol extract of Carica papaya (Caricaceae) seeds," *International Wound Journal*, vol. 9, no. 6, pp. 650–655, 2012.

[34] T. T. Nguyen, P. N. Shaw, M. O. Parat, and A. K. Hewavitharana, "Anticancer activity of Carica papaya: a review," *Molecular Nutrition & Food Research*, vol. 57, no. 1, pp. 153–164, 2013.

[35] G. Dawkins, H. H. Hewitt, Y. Wint, P. C. M. Obiefuna, and B. Wint, "Antibacterial effects of Carica papaya fruit on common wound organisms," *West Indian Medical Journal*, vol. 52, no. 4, pp. 290–292, 2003.

[36] P. Chávez-Quintal, T. González-Flores, I. Rodríguez-Buenfil, and S. Gallegos-Tintoré, "Antifungal activity in ethanolic extracts of Carica papaya L. cv. Maradol leaves and seeds," *Indian Journal of Microbiology*, vol. 51, no. 1, pp. 54–60, 2011.

[37] Y. K. Ang, W. C. M. Sia, H. E. Khoo, and H. S. Yim, "Antioxidant potential of Carica papaya peel and seed," *Focusing on Modern Food Industry*, vol. 1, no. 1, pp. 11–16, 2012.

[38] J. Vaya and M. Aviram M, "Nutritional antioxidants: mechanisms of action, analyses of activities and medical application," *Current Medicinal Chemistry—Immunology, Endocrine & Metabolic Agents*, vol. 1, no. 1, pp. 99–117, 2001.

[39] A. Tasinato, D. Boscoboinik, G.-M. Bartoli, P. Maroni, and A. Azzi, "d-α-tocopherol inhibition of vascular smooth muscle cell proliferation occurs at physiological concentrations, correlates with protein kinase C inhibition, and is independent of its antioxidant properties," *Proceedings of the National Academy of Sciences of the United States of America*, vol. 92, no. 26, pp. 12190–12194, 1995.

[40] K. Hensley, K. A. Robinson, S. P. Gabbita, S. Salsman, and R. A. Floyd, "Reactive oxygen species, cell signaling, and cell injury," *Free Radical Biology and Medicine*, vol. 28, no. 10, pp. 1456–1462, 2000.

[41] A. L. Stewart-Lee, L. A. Forster, J. Nourooz-Zadeh, G. A. A. Ferns, and E. E. Anggard, "Vitamin E protects against impairment of endothelium-mediated relaxations in cholesterol-fed rabbits," *Arteriosclerosis and Thrombosis*, vol. 14, no. 3, pp. 494–499, 1994.

[42] F. M. Yakes and B. Van Houten, "Mitochondrial DNA damage is more extensive and persists longer than nuclear DNA damage in human cells following oxidative stress," *Proceedings of the National Academy of Sciences of the United States of America*, vol. 94, no. 2, pp. 514–519, 1997.

[43] H. H. Szeto, "Cell-permeable, mitochondrial-targeted, peptide antioxidants," *The AAPS Journal*, vol. 8, no. 2, pp. E277–E283, 2006.

[44] G. Ermak and K. J. A. Davies, "Calcium and oxidative stress: from cell signaling to cell death," *Molecular Immunology*, vol. 38, no. 10, pp. 713–721, 2002.

Hindawi Publishing Corporation
Evidence-Based Complementary and Alternative Medicine
Volume 2014, Article ID 673286, 8 pages
http://dx.doi.org/10.1155/2014/673286

Research Article

Antiatopic Dermatitis Effect of *Artemisia iwayomogi* in Dust Mice Extract-Sensitized Nc/Nga Mice

Hyekyung Ha,[1] Hoyoung Lee,[1,2] Chang-Seob Seo,[1] Hye-Sun Lim,[1] Mee-Young Lee,[1] Jun Kyoung Lee,[1] and Hyeunkyoo Shin[1]

[1] *Herbal Medicine Formulation Research Group, Korea Institute of Oriental Medicine, 1672 Yuseongdae-ro, Yuseong-gu, Daejeon 305-811, Republic of Korea*
[2] *KM Health Technology Research Group, Korea Institute of Oriental Medicine, 1672 Yuseongdae-ro, Yuseong-gu, Daejeon 305-811, Republic of Korea*

Correspondence should be addressed to Hyeunkyoo Shin; hkshin@kiom.re.kr

Received 20 August 2013; Revised 9 January 2014; Accepted 9 January 2014; Published 23 February 2014

Academic Editor: Mohamed Eddouks

Aims. *Artemisia iwayomogi* (AI) has been used for fever reduction, diuresis, and hepatoprotection in Korea. The present study was performed to evaluate the anti-inflammatory and antiatopic dermatitis effects of AI using both *in vitro* and *in vivo* systems. *Methods*. The compositions in AI were analyzed by HPLC. To determine the anti-inflammatory effects of AI, the production of nitric oxide (NO) was measured in lipopolysaccharide treated RAW264.7 cells. Histamine levels were assayed to evaluate the antiallergic effects on MC/9 cells stimulated with phorbol-12 myristate 13-acetate and A23187. Finally, AI (10 mg/mouse/day) was topically applied onto the backs and ears of *Dermatophagoides farinae*-sensitized Nc/Nga mice for four weeks. *Results*. Isochlorogenic acid A (20.63 ± 0.26 mg/g), chlorogenic acid (9.04 ± 0.08 mg/g), and scopoletin (8.23 ± 0.01 mg/g) were among the major components of AI. AI inhibited the NO and histamine productions in RAW264.7 and MC/9 cells, respectively. In the mice, the topical application of AI reduced the dermatitis scores in the dorsal skin and ears and reduced the plasma levels of IgE. *Conclusions*. These results suggest that AI might be explored as a potential therapeutic agent to treat AD, and that the analytic method using HPLC will facilitate the development of quality control for AI.

1. Introduction

Traditionally, herbal medicine has been used to treat or prevent diseases. *Artemisia iwayomogi* (AI, Compositae) has been used in Korea to treat various diseases, including hepatic failure and inflammatory and immune-related diseases. AI has been known to inhibit hepatic fibrogenesis by reducing oxidative stress and lipid peroxidation [1] and preventing high fat diet- (HFD-) induced obesity and metabolic disorders through the downregulation of gene expressions related to adipogenesis and inflammation in visceral adipose tissues [2]. *A. capillaries* (AC, Compositae), one of the *Artemisia* herbs, has been traditionally used as an herbal medicine in East Asia and has been reported in pharmacopoeias in Korea, China, and Japan. However, AI is only mentioned in the Korean herbal pharmacopoeia. The efficacies of AI have been less reported than those of AC because AI is not traditionally used in other countries.

Atopic dermatitis (AD) is a common inflammatory, chronic or chronically relapsing, noncontagious, and pruritic skin disorder [3]. AD is often accompanied with allergic inflammation, which is initiated by the activation of the adaptive immune response. Immunoglobulin E (IgE) is produced in plasma cells and bound by mast cells in type I allergic reactions. The IgE-primed mast cells release chemical mediators, such as histamine, leukotrienes (LTs), and prostaglandin D_2 (PGD_2). These mediators lead to immediate phase reactions in the tissue, such as redness and itching, shortly after allergen-IgE binding. In the later phases of the disease, cytokines (IL-4 and IL-13) and chemokines are generated and released several hours after allergen-antibody cross-linking [4].

Topical corticosteroids (TCs) and nonpharmacological treatments, such as emollients, are first-line prescription therapies for AD. TCs are currently the most potent treatment

for AD. However, their chronic use can also be associated with significant adverse effects, such as the thinning of the skin, adrenal gland suppression, and treatment resistance [5, 6]. As a second-line therapy, topical calcineurin inhibitors (TCIs), such as tacrolimus and pimecrolimus, have been reported to be effective for atopic dermatitis. TCIs have been developed to suppress the results of immune responses during rejection in organ transplant recipients. However, concerns over systemic toxicity have limited their use. Topical tacrolimus ointment causes transient burning in ~60% of patients [7, 8]. Subsequently, the need to efficiently manage the AD response while reducing its side effects has led to the development of alternative remedies.

AI has been used to treat allergic diseases; the effects of AI on atopic dermatitis (AD), an inflammatory allergic disease, have not been established to date. The present study was conducted to analyze the contents of the ingredients in AI and to evaluate the anti-inflammatory and antiallergic effects of AI in lipopolysaccharide- (LPS-) treated RAW264.7 cells and phorbol-12 myristate 13-acetate (PMA) and A23187-treated MC/9 cells, respectively. In addition, AI was applied to analyze these treatments' effects on the AD response in Nc/Nga mice.

2. Materials and Methods

2.1. Chemicals and Reagents for HPLC Analysis. Chlorogenic acid and caffeic acid were purchased from Acros Organics (Pittsburgh, PA, USA). Scopoletin was purchased from Wako Pure Chemical Industries, Ltd. (Osaka, Japan). Isoquercitrin, isochlorogenic acid A, and isorhamnetin were from Biopurify Phytochemicals Ltd. (Chengdu, China). The purity of the six compounds was determined to be ≥98% by HPLC analysis. HPLC-grade reagents, methanol, acetonitrile, and water were obtained from J.T.Baker (Phillipsburg, NJ, USA). Glacial acetic acid was of analytical reagent grade and was procured from Junsei (Tokyo, Japan).

2.2. HPLC Conditions. HPLC analysis was performed using a Shimadzu LC-20A HPLC system (Shimadzu Co., Kyoto, Japan) consisting of an LC-20AT pump, DGU-20A_3 online degasser, SPD-M20A detector, SIL-20AC autosampler, and CTO-20A column oven. The data processor used was LC Solution software (version 1.24, Shimadzu Co., Kyoto, Japan). The column for separation used was a Gemini C_{18} (250 × 4.6 mm; particle size 5 μm, Phenomenex; Torrance, CA, USA). The mobile phases were composed of A (1.0% aqueous acetic acid, v/v) and B (acetonitrile with 1.0% acetic acid, v/v). The gradient flow was as follows: 0–5 min, 10–10% B; 5–30 min, 10–50% B; 30–35 min, 50–50% B; 35–40 min, 50–10% B. The temperature of the column oven was maintained at 40°C. The analysis was performed at a flow-rate of 1.0 mL/min with PDA detection at 254, 320, and 340 nm. The injection volume was 10 μL.

Standard stock solutions of six compounds, chlorogenic acid, caffeic acid, scopoletin, isoquercitrin, isochlorogenic acid A, and isorhamnetin (Figure 1) were dissolved in methanol at concentrations of 1.0 mg/mL and kept below 4°C. Working standard solutions were diluted to calibration curves in the concentration range of 0.78–50.00 μg/mL for chlorogenic acid and scopoletin, 0.16–10.00 μg/mL for caffeic acid, isoquercitrin, and isorhamnetin, and 2.34–150.00 μg/mL for isochlorogenic acid A, respectively.

2.3. Preparation of Water Extract and Sample Solution. The dried AI (2.5 kg) was extracted with water (25 L × 1 time) at 100°C for 2 h using an herb extractor (COSMOS-660, Kyungseo Machine Co., Inchon, Korea). AI was purchased from HMAX (Jecheon, Korea) in June 2008. These materials were confirmed taxonomically by Professor Je-Hyun Lee of Dongguk University, Korea. A voucher specimen (AI-2008-ST27) was deposited at the Herbal Medicine Formulation Research Group, Korea Institute of Oriental Medicine. The extract solution was filtered through filter paper and freeze-dried (359.51 g). The yield of extract was 14.38%. The lyophilized extract (20 mg) was dissolved in 70% ethanol (10 mL) and then filtered through a 0.2 μm membrane filter (Woongki Science, Seoul, Korea) before being injected into the HPLC for simultaneous determination.

2.4. Nitric Oxide (NO) and PGE_2 Productions in LPS-Stimulated RAW264.7 Cells. The murin macrophage cell line, RAW264.7, was obtained from the American Type Culture Collection (ATCC, Rockville, MD, USA) and cultured in Dulbecco's modified Eagle's medium (DMEM, Gibco BRL., NY, USA) containing 5.5% (v/v) heat-inactivated fetal bovine serum (FBS, Gibco BRL., NY, USA) and 100 U/mL penicillin and 100 μg/mL streptomycin (Gibco BRL, NY, US). The cells were seeded in 96-well plates (2.5×10^3 cells/well) for the cytotoxicity assay and then incubated with various concentrations of AI extract (10, 50, and 100 μg/mL) for 24 hr. The final volume of culture medium was 100 μL/well. The vehicle control was 1% DMSO. After treatment, 10 μL of Cell Counting Kit-8 reagent (CCK-8, Dojindo, Japan) was added to each well and the plates were incubated for 4 hr. The absorbance was measured at 450 nm using a microplate reader (Benchmark Plus, Bio-Rad Laboratories Inc., PA, USA), and the percentages of viable cells were calculated. Cytotoxicity did not occur on RAW264.7 cells after the treatment of the AI extract in the range of 10–100 μg/mL.

For the NO and PGE_2 assays, RAW264.7 cells were seeded at a density of 5×10^5 cells/well in the 48-well plates. After 16 hr, the cells were stimulated with 1 μg/mL of LPS in the absence or presence of AI (10–100 μg/mL) for 18 hr. N^G-methyl-L-arginine (NMMA; Sigma-Aldrich, Inc., MO, USA) and indomethacin (Sigma-Aldrich, Inc.) were used as the positive controls to inhibit NO and PGE_2 production, respectively. The final volume was 500 μL/well. The samples were treated with LPS on the cells at the same time. After incubation, the cell culture media were collected and used to measure the NO (A Griess reagent system, Promega., WI, USA) [9] and PGE_2(PGE_2ELISA kit, Cayman Chemical Co., MI, USA) levels according to the manufacturer's protocols.

2.5. Histamine Production in PMA and A23187-Stimulated MC/9 Cells. The rat mast cell line, MC/9, was obtained from ATCC and cultured in Iscove's modified Dulbecco's medium (Gibco BRL., NY, USA) before being supplemented

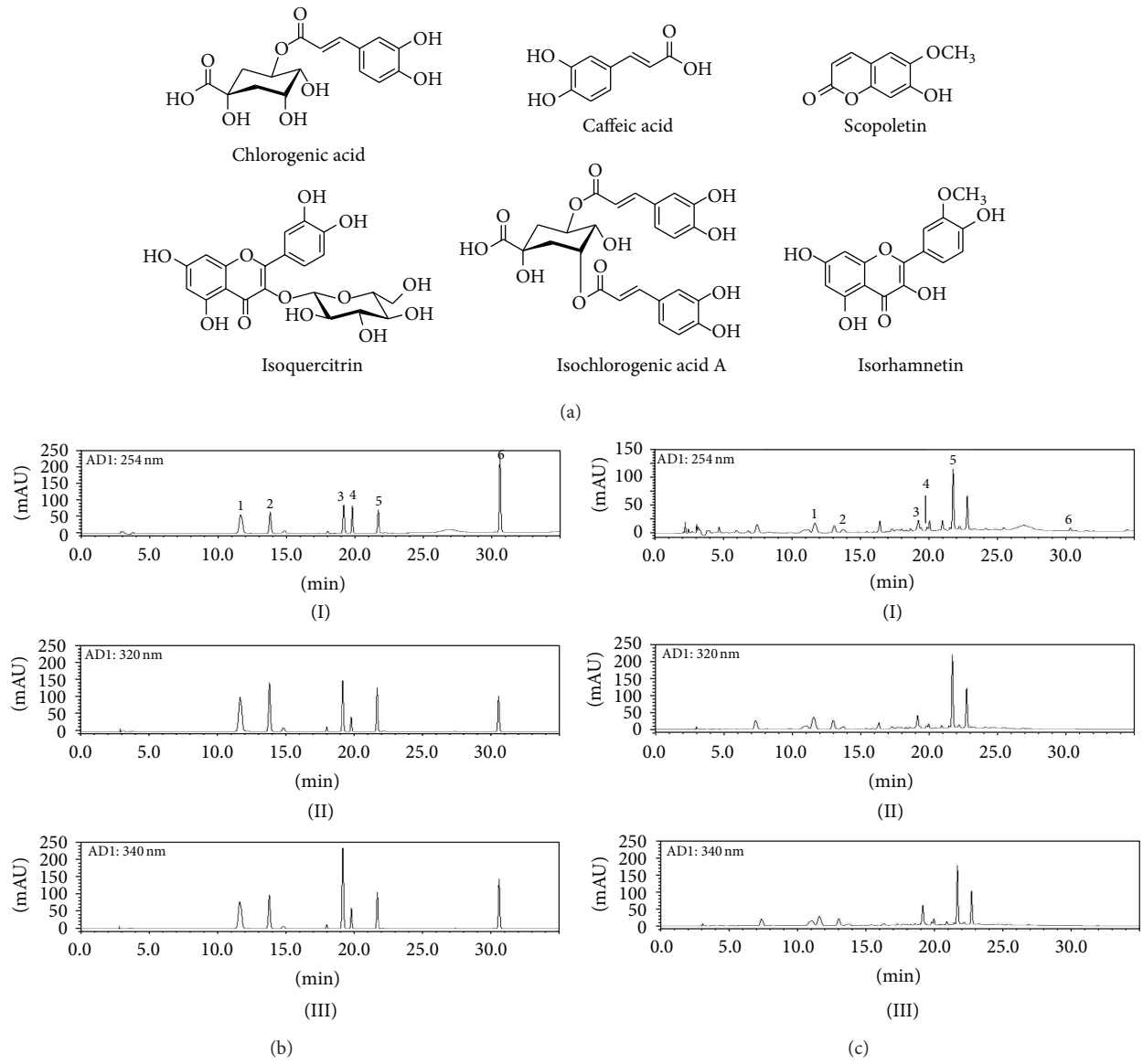

Figure 1: Chemical structures of the ingredients of *A. iwayomogi* (AI; A) and HPLC chromatograms of reference standards (b) and AI extracts (c). The detection wavelengths were 254 nm (I), 320 nm (II), and 340 nm (III). Chlorogenic acid (1), caffeic acid (2), scopoletin (3), isoquercitrin (4), isochlorogenic acid A (5), and isorhamnetin (6).

with 10% heat-inactivated FBS, penicillin (100 U/mL), and streptomycin (100 μg/mL) in a 5% CO_2 incubator at 37°C. The cytotoxicity for AI was assayed with the same method as in RAW264.7 cells. There was no cytotoxicity in the MC/9 cells after treatment with the AI extracts at concentrations below 50 μg/mL. For the histamine production assay, the cells were seeded in 48-well plates (2×10^5 cells/well) and cultured for 16 hr. After incubation, MC/9 cells were stimulated with phorbol 12-myristate 13-acetate (PMA, 50 nM, Sigma-Aldrich, St Louis, MO, USA) and A23187 (1 μM, calcium ionophore, Sigma-Aldrich) in the absence or presence of AI (25 and 50 μg/mL) for 24 h [10]. The final volume was 500 μL/well. The samples were treated with PMA and A23187 on the cells at the same time. The supernatants were collected, and histamine production was measured with an ELISA kit, according to the protocol provided by Oxford Biomedical Research (Oxford, MI, USA).

2.6. Animals and Sensitization. AD-like skin lesions were generated in male NC/Nga mice (Central Laboratory Animal Inc., Seoul, Korea) using *Dermatophagoides farinae* extract ointment (Biostir-AD, Biostir Co., Ltd., Kobe, Japan) [11]. The mice were housed individually in an air-conditioned room maintained at 24 ± 2°C with 55 ± 15% relative humidity. All procedures involving animals were conducted in accordance with the guidelines of the Institutional Animal Care and Use Committee of the Korea Institute of Oriental Medicine (approval number: #10-052).

Ten-week old mice were divided randomly into four groups with seven mice per group: the unsensitized (normal; 200 μL of 70% EtOH/mouse/day), *D. farinae*-sensitized (control; 200 μL of 70% EtOH/mouse/day), *D. farinae*-sensitized plus Protopic ointment-treated (Protopic; 50 mg/mouse/day), and *D. farinae*-sensitized plus AI extract-treated (AI; 10 mg/mouse/day) groups. For sensitization, 50 mg Biostir-AD was topically applied on the upper dorsal skin and the backs of the ears twice weekly for 4 weeks. The AI extract was dissolved in the vehicle solution (70% EtOH). The Protopic ointment was used as a positive control. The vehicle, AI extract, and positive control were applied on the upper dorsal skin and ears every day during the 4 weeks of sensitization.

2.7. Dermatitis Score. The dermatitis scores were assessed on the dorsal skin and ears once a week for 4 weeks. The Eczema Area and Severity Index (EASI) scoring system was applied to assess the severity of the dermatitis. This was defined as the sum of the scores for the erythema/hemorrhage, edema, excoriation/erosion, and scaling/dryness as follows: no symptoms, 0; mild, 1; moderate, 2; and severe, 3 [12].

2.8. Histological Analysis. After 4 weeks of treatment, the mice were anesthetized by i.p. injections of pentobarbital sodium (Entobar inj., Hanlim Pharm. Co., Ltd., Korea). Blood samples were collected from the inferior *vena cava* and then stored in the Microtainers (Becton, Dickinson and Company, NJ, USA) containing K_2-EDTA. Plasma samples were collected after centrifugation at 10000 rpm for 10 min and stored at −80°C. A complete gross observation was performed on all terminated animals. The dorsal skin and one ear of each mouse were taken and fixed in 10% (v/v) neutral buffered formalin for 24 hr. The tissues were embedded in paraffin and then sectioned at 4 μm thickness. The tissue sections were stained with hematoxylin and eosin (H and E) to estimate the epidermal inflammation (hypertrophy and infiltration by inflammatory cells). Mast cells of dermis were stained with toluidine blue and the sections were observed under the microscope. Average mast cell numbers were measured by counting 3 different areas in each slide of skin (×100), and the mean number of cells was calculated.

2.9. Plasma Levels of IGE and Histamine. The plasma levels of IgE (Bethyl Laboratories Inc., USA) and histamine (Oxford Biomedical Research, USA) were quantified using ELISA kits according to the manufacturer's instructions.

2.10. Statistical Analysis. The data were analyzed using a one-way ANOVA followed by the Bonferroni multiple comparison test; all date are expressed as the means ± SEM. A P value <0.05 was defined as statistically significant. All statistical analyses were performed using the SYSTAT 8.0 program (SYSTAT Inc., Evanston, IL, USA).

3. Results

3.1. Quantitation of Ingredients in AI. A chromatogram of AI extract was obtained using an HPLC-PDA. Under optimized chromatography conditions, six compounds were eluted within 35 min in the sample analysis using mobile phases comprising solvent A (1.0%, v/v, acetic acid in water) and solvent B (1.0%, v/v, acetic acid in acetonitrile).

The linearity of the peak area (y) versus concentration (x, μg/mL) curve for each component was used to calculate the contents of the main components in the AI extract. The correlation coefficients (r^2) of the calibration curves for the six main constituents were ≥0.9999. The line equations and r^2 values for the calibration curves are summarized in Table 1. The retention times of chlorogenic acid, caffeic acid, scopoletin, isoquercitrin, isochlorogenic acid A, and isorhamnetin were 11.63, 14.80, 15.55, 19.78, 21.63, and 30.53, respectively. Figure 1 shows the HPLC chromatogram of standard solution and water extracts of AI. Isochlorogenic acid A was a major ingredient (20.63 ± 0.26 mg/g) in our analytical system, and the contents of the six constituents ranged from 0.64 to 20.63 mg/g. The analytical results for each component identified are summarized in Table 2.

3.2. Inhibitory Effects of AI on NO, PGE_2, and Histamine Production. AI was shown to inhibit the inflammatory and allergic responses of *in vitro* systems. LPS-induced NO production was significantly reduced by AI extract in a dose-dependent manner compared to the group treated with LPS alone ($P < 0.05$, Figure 2(a)); however, there was no difference in the PGE_2 production (data not shown). Histamine production was inhibited by AI in the PMA- and A23187-stimulated MC/9 cells ($P < 0.05$, Figure 2(b)).

3.3. Dermatitis Scores in Nc/Nga Mice. In representative photographs for each group, the mice developed macroscopic lesions on the dorsal skin and ears starting at the second week after the initiation of *D. farinae* extract treatment (Figure 3(a)). The dorsal skin and ear lesion severity of the AI group were significantly reduced compared to those of the control group at the third and fourth weeks ($P < 0.05$). However, the dermatitis scores of the Protopic-treated positive control group were no different than those of the control group. The maximum dermatitis scores were recorded following the fourth week of *D. farinae* extract application in all groups. The scores for each group were as follows: 0.0 ± 0.00 (normal), 7.1 ± 0.43 (control), 8.1 ± 0.54 (Protopic), and 4.9 ± 0.60 (AI) (Figure 3(b)).

3.4. Histological Observations. The control group showed significant dorsal skin and ear lesions and hemorrhage, hypertrophy, and hyperkeratosis of the epidermis in the dorsal region (Figure 3(c)). These changes were significantly improved in the AI group; however, there were no changes in the Protopic group. The infiltration of mast cells was reduced by the application of AI in the dorsal skin (Figure 3(c)).

3.5. Plasma Levels of Histamine and IGE. The plasma histamine levels were elevated by *D. farinae* extract-sensitization (control group, 39.85 ± 5.44 ng/mL) compared to the normal group (28.56 ± 2.56 ng/mL). The histamine levels were reduced in the AI treatment groups (27.83 ± 4.60 ng/mL); however, there was no significant difference compared to

Table 1: Calibration curves for the six ingredients of *A. iwayomogi* ($n = 3$).

Component	Linear range (μg/mL)	Regression equation[a]	r^2	LOD (ng/mL)	LOQ (ng/mL)
Chlorogenic acid	0.78–50.00	$Y = 32627.70x - 4523.06$	1.0000	126.49	421.62
Caffeic acid	0.16–10.00	$Y = 60172.54x - 1297.07$	0.9999	43.64	145.45
Scopoletin	0.78–50.00	$Y = 34832.43x + 3393.40$	0.9999	52.00	173.33
Isoquercitrin	0.16–10.00	$Y = 26489.61x + 23.88$	1.0000	38.40	128.00
Isochlorogenic acid A	2.34–150.00	$Y = 38075.16x - 21283.50$	0.9999	51.62	172.06
Isorhamnetin	0.16–10.00	$Y = 40367.16x - 376.39$	1.0000	35.56	118.52

[a]Y represents peak area (mAU); x represents concentration (μg/mL).

Table 2: Contents of the six ingredients in the 70% ethanol extract of *A. iwayomogi* ($n = 3$).

Compound	Content (mg/g)		
	Mean	SD	RSD (%)
Chlorogenic acid	9.04	0.08	0.89
Caffeic acid	0.96	0.02	1.64
Scopoletin	8.23	0.01	0.12
Isoquercitrin	1.43	0.02	1.21
Isochlorogenic acid A	20.63	0.26	1.27
Isorhamnetin	0.64	0.01	1.46

the control group ($P > 0.05$). In the Protopic treatment group, the histamine levels (25.54 ± 1.93 ng/mL) were decreased, compared to the control group ($P < 0.05$, Figure 4(a)).

Additionally, the total plasma IgE levels were significantly increased in the control group (211.3 ± 13.4 ng/mL) compared to the normal group (41.56 ± 7.02 ng/mL, $P < 0.01$). AI treatment inhibited increased plasma IgE levels (139.0 ± 27.6 ng/mL) in *D. farinae*-sensitized mice ($P < 0.01$). However, there was no significant difference in the Protopic group (175.4 ± 20.4 ng/mL, Figure 4(b)).

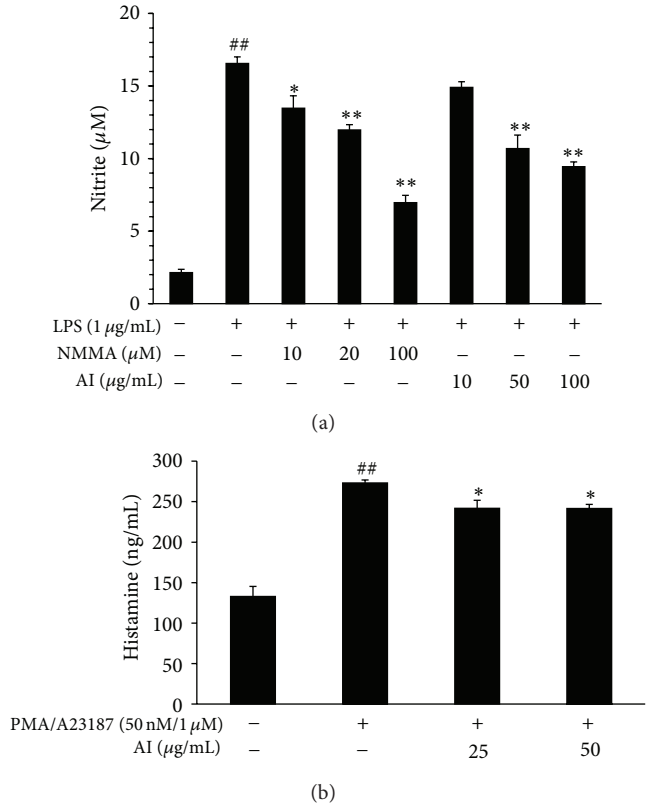

Figure 2: *A. iwayomogi* (AI) extract inhibited NO and histamine production. (a) AI inhibited NO production in LPS-stimulated (1 μg/mL, 24 hr) RAW264.7 cells in a concentration-dependent manner. Each data value represents the mean ± SEM of triplicate experiments ($^{\#\#}P < 0.01$ compared with the control group, $^{*}P < 0.05$ and $^{**}P < 0.01$ compared with the LPS-treated group). (b) Histamine production was reduced by AI in PMA- and A23187-treated (50 nM and 1 μM, 24 hr) MC/9 cells. Each data value represents the mean ± SEM of triplicate experiments ($^{\#\#}P < 0.01$ compared with the control group, $^{*}P < 0.05$ compared with the PA-treated group).

4. Discussion

Allergic reactions, including atopic dermatitis (AD), are developed due to an imbalance of Th1 and Th2 cells that is mediated by IgE and histamine levels. AD is characterized by the overexpression of inflammatory cytokines such as IL-10 and by high IgE levels. The involvement of Th2 cells both helps to explain the joint involvement of IgE-producing B cells (via IL-4 and IL-13), mast cells (via IL-4 and IL-10), and eosinophils (via IL-5) in the allergic inflammatory process and accounts for the other pathophysiologic features of allergies [13].

Artemisia herbs, including AI, have been used for liver disorders and inflammatory diseases. We investigated the anti-inflammatory and anti-AD effects of AI treatment using *in vitro* and *in vivo* systems because AD is strongly associated with the inflammatory response. AI suppressed the production of NO in LPS-stimulated RAW264.7 macrophage cells. Histamine production was also inhibited by AI in PMA- and A23187-stimulated MC/9 mast cells. Nc/Nga mice are characterized by AD-like skin lesions and elevated levels of blood IgE. The skin changes that developed in the Nc/Nga mice closely mimic human AD, which conventionally develops following infection with mites [14]. The most important allergens associated with human AD are house dust mite allergens, and *D. farinae* is the most common house dust mite present in the environment. The infiltration of mast cells is another important factor in AD development [15]. AI treatment reduced the dermatitis scores after the third

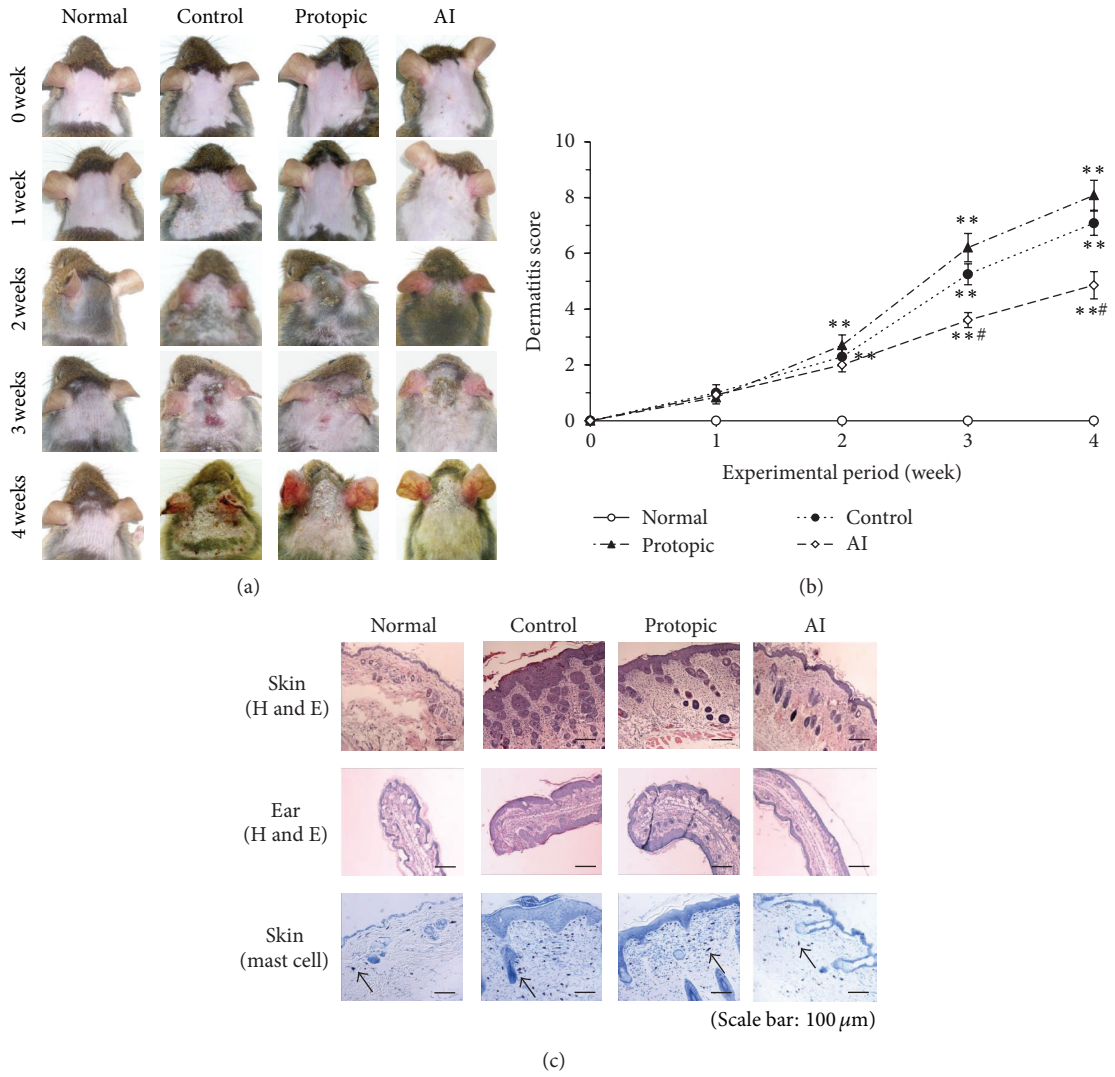

Figure 3: *A. iwayomogi* (AI) extract reduced the dermatitis scores and histological changes in *D. farinae* extract-sensitized Nc/Nga mice. (a) Macroscopic changes following the consecutive administration of AI or Protopic ointment onto *D. farinae*-induced, AD-like lesions on the back and ears in Nc/Nga mice. The images show the backs and ears for four weeks after sensitization. (b) The dermatitis scores of *D. farinae*-induced, AD-like skin lesions on the backs and ears (mean ± SEM ($n = 5$), $^{*}P < 0.05$ and $^{**}P < 0.01$, compared with the normal group, $^{\#\#}P < 0.01$, compared with the *D. farinae*-induced control group). AI (10 mg/mouse/day) and Protopic ointment (50 mg/mouse/day) were topically applied on the back and ears once daily for four weeks. (c) Histological features of the back and ears. The tissues were stained with hematoxylin and eosin (H and E) or toluidine blue to estimate epidermal inflammation or mast cell infiltration. The mast cells are indicated by arrows.

week in *D. farinae*-sensitized Nc/Nga mice. In addition, AI suppressed the histological features of the disease, including edema, cornification of the epidermis, and mast cell infiltration in the dorsal skin and ear. Furthermore, treatment with AI reduced the plasma levels of histamine and IgE in *D. farinae*-sensitized Nc/Nga mice.

In the Protopic group, a positive control group, dermatitis scores were not reduced compared with those of control group. As one of the adverse effects of Protopic ointment, the patients experienced skin irritation and burning at the site of application [6]. Therefore, we expected that the high dermatitis scores in the Protopic group would be caused by increased itching behaviors at the application area of the ointment. However, the plasma levels of histamine and IgE were reduced in the mice.

In the present study, the chemical contents of the AI extract were analyzed using a high performance liquid chromatography (HPLC) system. Isochlorogenic acid A, chlorogenic acid, and scopoletin were detected as the major compounds in the AI extract. Isochlorogenic acid A has been reported to have hepatoprotective effects and antioxidative properties through the induction of HO-1 [16] and immunopotentiation properties mediated through the NF-κB-induced release of NO from macrophages [17]. Chlorogenic acid has been reported to inhibit the production of inflammatory mediators and cytokines [18, 19]. Moreover,

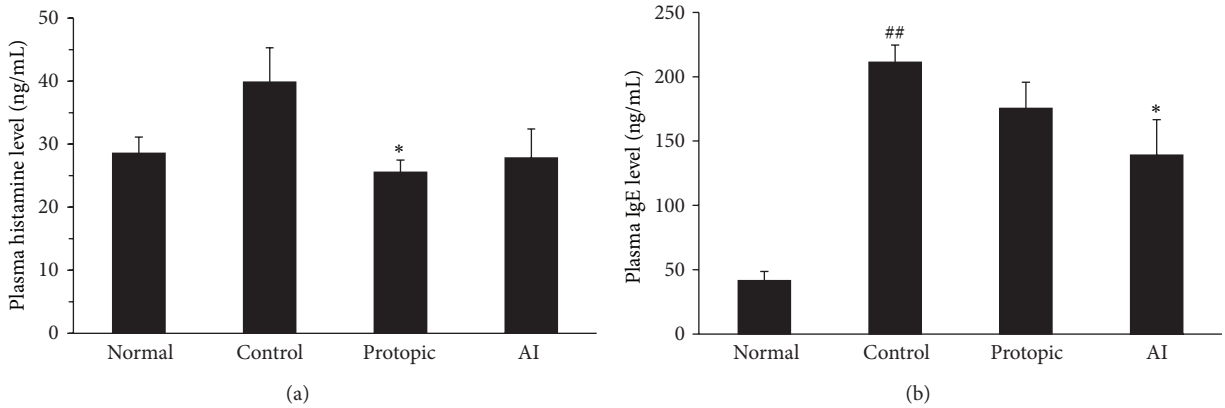

Figure 4: *A. iwayomogi* (AI) extract reduced the plasma levels of histamine (a) and IgE (b) in *D. farinae* extract-sensitized Nc/Nga mice. AI (10 mg/mouse/day) and Protopic ointment (50 mg/mouse/day) were topically applied on the backs and ears once daily for 4 weeks. The concentrations of histamine and IgE were measured by ELISA methods (mean ± SEM, $n = 5$), $^{\#\#}P < 0.01$ compared with the normal group, $^{*}P < 0.05$ compared with the *D. farinae*-induced control group.

chlorogenic acid exhibits antibacterial, antioxidant, antihepatic injuries, and antiallergic activities [20, 21]. Lee et al. reported that scopoletin has been shown to suppress the osteoclastogenesis from RAW264.7 cells [22] by scavenging reactive oxygen species (ROS). Scopoletin significantly inhibited interleukin-4 (IL-4), IL-5, and IL-10 production [23]. The antiallergic properties of scopoletin might be mediated by the downregulation of cytokine expression in Th2 cells. Therefore, the analytical method of using HPLC to distinguish the major ingredients of AI, isochlorogenic acid A, chlorogenic acid, and scopoletin, might be a useful quality control method for these AI remedies.

5. Conclusions

These results suggest that AI inhibits AD-like skin lesions to reduce the generation of IgE, the inflammatory response on the skin, and the release of preformed mediators, such as histamine, on *D. farinae*-sensitized Nc/Nga mouse model. We conclude that AI should be explored as a potential therapeutic agent to treat allergic diseases, including AD.

Conflict of Interests

No conflict of interests exists in the present paper.

Acknowledgment

This research was supported by a Grant for "Construction of Scientific Evidence for Herbal Medicine Formulas (K13030)," from the Korea Institute of Oriental Medicine (KIOM).

References

[1] J. M. Han, H. G. Kim, M. K. Choi et al., "Aqueous extract of Artemisia iwayomogi Kitamura attenuates cholestatic liver fibrosis in a rat model of bile duct ligation," *Food and Chemical Toxicology*, vol. 50, no. 10, pp. 3505–3513, 2012.

[2] Y. Choi, Y. Yanagawa, S. Kim, W. K. Whang, and T. Park, "Artemisia iwayomogi extract attenuates high-fat diet-induced obesity by decreasing the expression of genes associated with adipogenesis in mice," *Evidence-Based Complement and Alternative Medicine*, vol. 2013, Article ID 915953, 11 pages, 2013.

[3] T. Terui, "Analysis of the mechanism for the development of allergic skin inflammation and the application for its treatment: overview of the pathophysiology of atopic dermatitis," *Journal of Pharmacological Sciences*, vol. 110, no. 3, pp. 232–236, 2009.

[4] H. Nagai, H. Teramachi, and T. Tuchiya, "Recent advances in the development of anti-allergic drugs," *Allergology International*, vol. 55, no. 1, pp. 35–42, 2006.

[5] H. Aoyama, N. Tabata, M. Tanaka, Y. Uesugi, and H. Tagami, "Successvul treatment of resistant facial lesions of atopic dermatitis with 0.1% FK506 ointment," *British Journal of Dermatology*, vol. 133, no. 3, pp. 494–496, 1995.

[6] D. M. Ashcroft, P. Dimmock, R. Garside, K. Stein, and H. C. Williams, "Efficacy and tolerability of topical pimecrolimus and tacrolimus in the treatment of atopic dermatitis: meta-analysis of randomised controlled trials," *British Medical Journal*, vol. 330, no. 7490, pp. 516–522, 2005.

[7] M. Boguniewicz, V. C. Fiedler, S. Raimer, I. D. Lawrence, D. Y. M. Leung, and J. M. Hanifin, "A randomized, vehicle-controlled trial of tacrolimus ointment for treatment of atopic dermatitis in children. Pediatric Tacrolimus Study Group," *Journal of Allergy and Clinical Immunology*, vol. 102, no. 4, part 1, pp. 637–644, 1998.

[8] N. S. Tomi and T. A. Luger, "The treatment of atopic dermatitis with topical immunomodulators," *Clinics in Dermatology*, vol. 21, no. 3, pp. 215–224, 2003.

[9] S. Moncada, R. M. J. Palmer, and E. A. Higgs, "Nitric oxide: physiology, pathophysiology, and pharmacology," *Pharmacological Reviews*, vol. 43, no. 2, pp. 109–142, 1991.

[10] T. P. Ramesh, Y. D. Kim, M. S. Kwon, C. D. Jun, and S. W. Kim, "Swiprosin-1 regulates cytokine expression of human mast cell line HMC-1 through actin remodeling," *Immune Network*, vol. 9, no. 6, pp. 274–284, 2009.

[11] H. Lee, J. K. Lee, H. Ha, M.-Y. Lee, C.-S. Seo, and H. K. Shin, "*Angelicae Dahuricae* radix inhibits dust mite extract-induced atopic dermatitis-like skin lesions in NC/Nga mice,"

Evidence-based Complementary and Alternative Medicine, vol. 2012, Article ID 743075, 7 pages, 2012.

[12] J. M. Hanifin, K. D. Cooper, V. C. Ho et al., "Guidelines of care for atopic dermatitis, developed in accordance with the American Academy of Dermatology (AAD)/American Academy of Dermatology Association 'Administrative Regulations for Evidence-Based Clinical Practice Guidelines'," *Journal of the American Academy of Dermatology*, vol. 50, no. 3, pp. 391–404, 2004.

[13] S. Romagnani, "Cytokines and chemoattractants in allergic inflammation," *Molecular Immunology*, vol. 38, no. 12-13, pp. 881–885, 2002.

[14] H. Jin, R. He, M. Oyoshi, and R. S. Geha, "Animal models of atopic dermatitis," *The Journal of Investigative Dermatology*, vol. 129, no. 1, pp. 31–40, 2009.

[15] T. Fukuyama, Y. Tajima, K. Hayashi, H. Ueda, and T. Kosaka, "Prior or coinstantaneous oral exposure to environmental immunosuppressive agents aggravates mite allergen-induced atopic dermatitis-like immunoreaction in NC/Nga mice," *Toxicology*, vol. 289, no. 2-3, pp. 132–140, 2011.

[16] B. J. Hao, Y. H. Wu, J. G. Wang et al., "Hepatoprotective and antiviral properties of isochlorogenic acid A from Laggera alata against hepatitis B virus infection," *Journal of Ethnopharmacology*, vol. 144, no. 1, pp. 190–194, 2012.

[17] K. Tomimori, S. Nakama, R. Kimura, K. Tamaki, C. Ishikawa, and N. Mori, "Antitumor activity and macrophage nitric oxide producing action of medicinal herb, *Crassocephalum crepidioides*," *BMC Complement and Alternative Medicine*, vol. 12, no. 78, 2012.

[18] D. A. Chagas-Paula, R. B. D. Oliveira, V. C. Da Silva et al., "Chlorogenic acids from *Tithonia diversifolia* demonstrate better anti-inflammatory effect than indomethacin and its sesquiterpene lactones," *Journal of Ethnopharmacology*, vol. 136, no. 2, pp. 355–362, 2011.

[19] N. Huang, L. Rizshsky, C. C. Hauck, B. J. Nikolau, P. A. Murphy, and D. F. Birt, "The inhibition of lipopolysaccharide-induced macrophage inflammation by 4 compounds in *Hypericum perforatum* extract is partially dependent on the activation of SOCS3," *Phytochemistry*, vol. 76, pp. 106–116, 2012.

[20] N. Yun, J.-W. Kang, and S.-M. Lee, "Protective effects of chlorogenic acid against ischemia/reperfusion injury in rat liver: molecular evidence of its antioxidant and anti-inflammatory properties," *Journal of Nutritional Biochemistry*, vol. 23, no. 10, pp. 1249–1255, 2012.

[21] H.-T. Trinh, E.-A. Bae, Y.-J. Hyun et al., "Anti-allergic effects of fermented Ixeris sonchifolia and its constituents in mice," *Journal of Microbiology and Biotechnology*, vol. 20, no. 1, pp. 217–223, 2010.

[22] S. H. Lee, Y. Ding, X. T. Yan, Y. H. Kim, and H. D. Jang, "Scopoletin and scopolin isolated from artemisia iwayomogi suppress differentiation of osteoclastic macrophage RAW 264.7 cells by scavenging reactive oxygen species," *Journal of Natural Products*, vol. 74, no. 4, pp. 615–620, 2013.

[23] A. S. Cheng, Y. H. Cheng, and T. L. Chang, "Scopoletin attenuates allergy by inhibiting Th2 cytokines production in EL-4 T cells," *Food and Function*, vol. 3, no. 8, pp. 886–890, 2012.

Hindawi Publishing Corporation
Evidence-Based Complementary and Alternative Medicine
Volume 2014, Article ID 981046, 14 pages
http://dx.doi.org/10.1155/2014/981046

Research Article

Antidiabetic and Antihyperlipidemic Effects of *Clitocybe nuda* on Glucose Transporter 4 and AMP-Activated Protein Kinase Phosphorylation in High-Fat-Fed Mice

Mei-Hsing Chen,[1] Cheng-Hsiu Lin,[2] and Chun-Ching Shih[3]

[1] *Plant Pathology Division, Taiwan Agricultural Research Institute, Council of Agriculture, Executive Yuan, Wufeng District, Taichung City 41362, Taiwan*
[2] *Department of Internal Medicine, Fongyuan Hospital, Ministry of Health and Welfare, Fengyuan District, Taichung City 42055, Taiwan*
[3] *Graduate Institute of Pharmaceutical Science and Technology, College of Health Science, Central Taiwan University of Science and Technology, No. 666 Buzih Road, Beitun District, Taichung City 40601, Taiwan*

Correspondence should be addressed to Chun-Ching Shih; ccshih@ctust.edu.tw

Received 22 July 2013; Revised 8 December 2013; Accepted 9 December 2013; Published 16 January 2014

Academic Editor: Mohamed Eddouks

The objective of this study was to evaluate the antihyperlipidemic and antihyperglycemic effects and mechanism of the extract of *Clitocybe nuda* (CNE), in high-fat- (HF-) fed mice. C57BL/6J was randomly divided into two groups: the control (CON) group was fed with a low-fat diet, whereas the experimental group was fed with a HF diet for 8 weeks. Then, the HF group was subdivided into five groups and was given orally CNE (including C1: 0.2, C2: 0.5, and C3: 1.0 g/kg/day extracts) or rosiglitazone (Rosi) or vehicle for 4 weeks. CNE effectively prevented HF-diet-induced increases in the levels of blood glucose, triglyceride, insulin ($P < 0.001$, $P < 0.01$, $P < 0.05$, resp.) and attenuated insulin resistance. By treatment with CNE, body weight gain, weights of white adipose tissue (WAT) and hepatic triacylglycerol content were reduced; moreover, adipocytes in the visceral depots showed a reduction in size. By treatment with CNE, the protein contents of glucose transporter 4 (GLUT4) were significantly increased in C3-treated group in the skeletal muscle. Furthermore, CNE reduces the hepatic expression of glucose-6-phosphatase (G6Pase) and glucose production. CNE significantly increases protein contents of phospho-AMP-activated protein kinase (AMPK) in the skeletal muscle and adipose and liver tissues. Therefore, it is possible that the activation of AMPK by CNE leads to diminished gluconeogenesis in the liver and enhanced glucose uptake in skeletal muscle. It is shown that CNE exhibits hypolipidemic effect in HF-fed mice by increasing ATGL expression, which is known to help triglyceride to hydrolyze. Moreover, antidiabetic properties of CNE occurred as a result of decreased hepatic glucose production via G6Pase downregulation and improved insulin sensitization. Thus, amelioration of diabetic and dyslipidemic states by CNE in HF-fed mice occurred by regulation of GLUT4, G6Pase, ATGL, and AMPK phosphorylation.

1. Introduction

The prevalence of diabetes mellitus (DM) represents a significant and growing global health problem. Type 2 diabetes mellitus (T2D) accounts for 90% to 95% of all patients [1]. Diabetes mellitus is characterized by hyperglycemia that involves abnormalities in either insulin secretion or action at peripheral tissues, resulting in reducing insulin sensitivity at skeletal muscle and adipose and liver tissues, which represents insulin resistance. Both genetic (heredity) and environmental factors (obesity and leisure life style) play an important role in T2D.

Clitocybe nuda (Fr.) Bigelow and Smith (*Lepista nuda,* commonly known as wood blewit or blue stalk mushroom) is an edible woodland mushroom found in Europe, North America, Asia, and Australia [2]. Due to its special fragrance and delicate texture, it has been cultivated in France, Holland, Britain, and Taiwan. Several bioactive extracts from *C. nuda*

have been found to exhibit antioxidant and antimicrobial properties [3–6]. The ethanol extracts of *C. nuda* exerted antioxidant activity by flavonoid amount being 8.21 μg mg^{-1} quercetin equivalent, while the phenolic compound amount was 48.01 μg mg^{-1} pyrocatechol equivalent [5]. Flavonoids have been proven to display a wide range of pharmacological actions such as antimicrobial and antithrombotic activities [7]. In food systems flavonoids can act as free radical scavengers and terminate the radical chain reactions that occur during the oxidation of triglyceride [5]. It was reported that the antioxidant activity of plant materials was well correlated with the content of their phenolic compounds [8].

A new drimane sesquiterpenoid including 3-keto-drimenol, 3beta-hydroxydrimenol, and 3beta, 11, 12-trihydroxydrimene had been shown to exert inhibitory activities against two isozymes of 11 beta-hydroxysteroid dehydrogenases (11β-HSD1), which catalyze the interconversion of active cortisol and inactive cortisone [9]. Inhibitors of 11β-HSD1 are known to have a potential treatment for the metabolic syndrome [10].

Insulin resistance is known to be associated with reduced glucose uptake and utilization by skeletal muscle and adipose tissues and is related to reduced glucose transporter 4 (GLUT4) gene expressions [11, 12]. Impairment of GLUT4 expression, GLUT4 translocation, and/or insulin signaling may affect insulin-stimulated glucose uptake, and that would result in insulin resistance and hyperglycemia [13, 14]. Therefore, the improvements of GLUT4 contents and/or translocation to the plasma membrane have long been regarded as a potential target in the treatment of diabetes mellitus.

The identification of AMP-activated protein kinase (AMPK) phosphorylation as a likely mechanism is particularly interesting in relation to diabetes and obesity because activation of AMPK inhibits lipid synthesis and can improve insulin action [15, 16]. Because AMPK regulates a variety of different metabolic disorders, it is widely recognized as a useful and safe target for the treatment of metabolic disorders such as T2D and dyslipidemia [15, 16].

Many oral agents for the treatment of DM cause adverse effects. As a result, attempts have been made to discover new antidiabetic regiments derived from plants. Many traditional plant treatments for diabetes are used throughout the world, which are frequently considered to be less toxic and result in fewer side effects than synthetic compounds. Anthocyanins (cyanidin or cyanidin 3-glucoside) were reported to have the potency of a unique therapeutic advantage for prevention obesity and diabetes [17]. *C. nuda* is reported to inhibit 11β-HSD1 [9]. Inhibition of 11β-HSD1 could improve insulin resistance [10]. Based on the fact that the gills of *C. nuda* are of intense bluish-purple color, the total phenolic content on the antioxidant activity of this mushroom extract [8] and the sesquiterpenoid from *C. nuda* could inhibit 11β-HSD1; we hypothesized that extract of *Clitocybe nuda* (CNE) could ameliorate insulin resistance. The present study was to investigate the effects of the CNE-mediated glucose and lipid lowering in a diabetic and dyslipidemic mice model. High-fat (HF) diet could induce C57BL6J mice to hyperglycemia, hyperlipidemia, and hypercholesterolemia [18]. AMPK is considered as a therapeutic target for treatment of diabetes and dyslipidemia [15, 16]. Since activation of the AMPK results in increased lipid and glucose catabolism [19] and GLUT4 is involved in glucose transport, the effect of CNE on AMPK activity and GLUT4 is investigated in mice fed with a HF diet. Phosphorylation of Thr 172 of α subunits is essential for AMPK activity [20]. As one of the possible mechanisms of action, this study also examined its effect on the expression of genes involved in gluconeogenesis, lipogenesis, and triglyceride lipase in the liver tissue.

2. Materials and Methods

2.1. Materials and Preparation of Extract of Clitocybe nuda (CNE). The mushroom (or fungal) strain of *Clitocybe nuda* (Tainung stain no. 1) was cultured under compost extract agar medium. The preparation of grain spawn was as follows: wheat grains were washed with distilled water, then boiled for 20 min, and removed from water by filtration. Then, they were added with 1% $CaCO_3$, mixed well, then transferred to the flask, and sterilized at 121°C and 1.2 kg/cm^3 for 1 h. After one day, the hyphal chunk of the described above *C. nuda* was implanted to the flask at 24°C for 15 days for mycelia to cover grains, called grain spawn. The fruiting of *C. nuda* was as follows: the grain spawn of *C. nuda* was mixed with the fermented rice straw compost, incubated at 24°C for 21–28 days for spawn running, and covered with 1-2 cm peat and the condition was 13°C, 90–95% relative humidity, 1000 ppm CO_2 concentration, and at daylight for 8 h. During this period, they were periodically supplied with water until fruiting, and then the mushrooms were harvested. After being lyophilized, 30 g of the dried mushroom samples was homogenized and extracted with 40 time volumes of hot water under reflux at 100°C for 40 min. The aqueous extract was filtered over Whatman no. 1 paper and the filtrate was evaporated to a small volume. The filtrate was lyophilized, designated the hot-water soluble fraction (CNE), and was stored frozen at −20°C until required. Nutrients contents were as follows: the fruiting of *C. nuda* (per 100 g) contained crude fat, crude ash, and carbohydrate contents are 3.4~5.0 g, 8.0~12.0 g, and 56.0~67.5 g, respectively; mineral contents are 3.8~6.2 g. The total phenolic contents were determined by the Folin-Ciocalteau method [21]. The total phenolic contents of CNE were 1.29%. The polysaccharides of CNE were 12.62% by phenol-sulfuric acid method [22]. The total anthocyanin contents of CNE were 0.045%. The CNE was diluted and adjusted and then was administrated orally to mice in a volume of 0.2, 0.5, and 1.0 g/kg body weight (C1: 0.2, C2: 0.5, and C3: 1.0 g/kg body weight), respectively. Distilled water was administered in a similar volume to control mice.

2.2. Animals and Experimental Design. All animal procedures were performed as per guidelines provided by the Institutional Animal Care and Use Committee of Central Taiwan University of Science and Technology. The study contained two parts, part 1: oral glucose tolerance test (OGTT). The ICR mice normal mice ($n = 5$) were fasted for 12 h but were allowed to access to 0.2 g/kg, 0.5 g/kg, and 1.0 g/kg extracts of CNE or an equivalent amount of normal

vehicle (water) was given orally 30 min before an oral glucose load (1 g/kg body weight). Blood samples were collected from the retroorbital sinus of fasting mice at the time of the glucose administration (0) and every 30 minutes until 3 hours after glucose administration to determine the levels of glucose. Part 2: animal study was as follows: C57BL/6J mice (4-5 weeks old) were purchased from the National Laboratory Animal Breeding and Research Center, National Science Council. Animals were maintained on a 12 h light/dark cycle (light cycle: 7 a.m. to 7 p.m.). Seven days after acclimation, the C57BL/6J mice were divided randomly into two groups. The control (CON) group ($n = 9$) was fed low-fat diet (Diet 12450B, Research Diets, Inc., New Brunswick, NJ, USA), whereas the experimental group ($n = 45$) was fed a 45% high-fat diet (Diet 12451, Research Diets, Inc., New Brunswick, NJ, USA) for 12 weeks. The low-fat diet was composed of protein 20%, carbohydrate 70%, and fat 10%, whereas high-fat diet was composed of protein 20%, carbohydrate 35%, and fat 45% (of total energy, % kcal). After 8-week diet-induction period, the high-fat-treated mice were randomly subdivided into 5 groups ($n = 9$ per group). Extracts of CNE (including 0.2, 0.5, and 1.0 g/kg/day) or rosiglitazone (Rosi; 1% methylcellulose of 10 mg/kg body weight, obtained from GlaxoSmithKline Product number BRL49653 C) were administrated through oral gavage 1 time per day from 9 to 12 weeks of the experiment, and the mice were still on the high-fat diet, while the CON and high-fat control (HF) mice were treated with vehicle only. The body weight was measured weekly throughout the study. The compositions of the experimental diets are shown as described in [23]. At the end of the study, we deprive animal from food (from p.m. 10:00–a.m. 10:00). The next day (the 85th day), the mice were sacrificed for blood and tissue collection and analysis. The mice were untreated with CNE or Rosi at the 85th day. Livers and white adipose tissues (WATs) (including epididymal, mesenteric, and retroperitoneal WATs) were excised according to the defined anatomical landmarks, and the weights of the tissues were measured. Tissues were immediately frozen using liquid nitrogen and then kept at −80°C for the analysis of target gene expression. Heparin (30 units/mL) (Sigma) was added into blood sample. Plasma samples were collected by centrifugation at 1600 ×g for 15 min at 4°C. The separation of the plasma was finished within 30 min. Plasma was obtained for insulin and leptin assay.

2.3. Body Weight and Food Intake Assay. Body weight and food intake were monitored. Body weight was measured weekly throughout the study. The pellet food was weighed and followed by placing in the cage food container. After 24 h, the remaining food was weighed, and the difference represented the daily food intake. Unconsumed pellet HF food was discarded each day and fresh pellet high-fat diet was provided to ensure consistent food quality throughout the study. The HF food was stored at 4°C.

2.4. Blood Parameters Assay. Blood samples (0.8 mL) were collected from the retro-orbital sinus of fasting mice and the level of glucose was measured by the glucose oxidase method (Model 1500; Sidekick Glucose Analyzer; YSI Incorporated, Yellow Springs, OH, USA). Plasma triglycerides (TG), total cholesterol (TC), and free fatty acids (FFA) were analyzed using commercial assay kits according to the manufacturer's directions (triglycerides-*E* test, cholesterol-*E* test, and FFA-*C* test, Wako Pure Chemical, Osaka, Japan).

2.5. Adipocytokine Levels Assay. The levels of insulin and leptin were analyzed by ELISA using a commercial assay kit according to manufacturer's directions (mouse insulin ELISA kit, Shibayagi, Gunma, Japan, and mouse leptin ELISA kit, Morinaga, Yokohama, Japan).

2.6. Histopathology of Adipose and Liver Tissue. Small pieces of epididymal WAT and liver tissue were fixed with formalin (200 g/kg) neutral buffered solution and embedded in paraffin. Sections (8 μm) were cut and stained with hematoxylin and eosin. For microscopic examination, a microscope (Leica, DM2500) was used, and the images were taken using a Leica Digital camera (DFC-425-C).

2.7. Measurement of Hepatic Lipids. Hepatic lipids were extracted using a previously described protocol [24]. For the hepatic lipid extraction, the 0.375 g liver samples were homogenized with 1 mL distilled water for 5 min. Finally, the dried pellet was resuspended in 0.5 mL ethanol and analyzed using a triglycerides kit as used for serum lipids.

2.8. Isolation of RNA and Relative Quantization of mRNA Indicating Gene Expression. Total RNA from the epididymal WAT, skeletal muscle, and liver tissue was isolated with a Trizol Reagent (Molecular Research Center, Inc., Cincinnati, OH, USA) according to the manufacturer's directions. The integrity of the extracted total RNA was examined by 2% agarose gel electrophoresis, and the RNA concentration was determined by the ultraviolet (UV) light absorbency at 260 nm and 280 nm (Spectrophotometer U-2800A, Hitachi). The quality of the RNA was confirmed by ethidium bromide staining of 18S and 28S ribosomal RNA after electrophoresis on 2% agarose gel containing 6% formaldehyde. Total RNA (1 μg) was reverse transcribed to cDNA in a reaction mixture containing buffer, 2.5 mM dNTP (Gibco-BRL, Grand Island, NY, USA), 1 mM of the oligo(dT) primer, 50 mM dithiothreitol, 40 U Rnase inhibitor (Gibco-BRL, Grand Island, NY, USA), and 5 μL Moloney murine leukemia virus reverse transcriptase (Epicentre, Madison, WI, USA) at 37°C for 1 h and then heated at 90°C for 5 min to terminate the reaction. The polymerase chain reaction (PCR) was performed in a final 25 μL containing 1U Blend Taq-Plus (TOYOBO, Japan), 1 μL of the RT first-strand cDNA product, 10 μM of each forward (F) and reverse (R) primer, 75 mM Tris-HCl (pH = 8.3) containing 1 mg/L Tween 20, 2.5 mM dNTP, and 2 mM $MgCl_2$. Preliminary experiments were carried out with various cycles to determine the nonsaturating conditions of the PCR amplification for all the genes studied. The primers are shown in Table 1. The products were run on 2% agarose gels and stained with ethidium bromide. The relative density of the band was evaluated using AlphaDigiDoc 1201

Table 1: Primers used in this study.

Gene	Accession numbers	Forward primer and reverse primer	PCR product (bp)	Annealing temperature (°C)
		Liver		
ApoC-III	NM_023114.3	F: CAGTTTTATCCCTAGAAGCA R: TCTCACGACTCAATAGCTG	349	47
G6Pase	NM_008061.3	F: GAACAACTAAAGCCTCTGAAAC R: TTGCTCGATACATAAAACACTC	350	50
PPARα	NM_011144	F: ACCTCTGTTCATGTCAGACC R: ATAACCACAGACCAACCAAG	352	55
SREBP1c	NM_011480	F: GGCTGTTGTCTACCATAAGC R: AGGAAGAAACGTGTCAAGAA	219	50
ATGL	AY894805	F: AGG ACA GCT CCA CCA ACA TC R: TGG TTC AGT AGG CCA TTC CT	165	50
GAPDH	NM_031144	F: TGTGTCCGTCGTGGATCTGA R: CCTGCTTCACCACCTTCTTGA	99	55

software (Alpha Innotech Co., San Leandro, CA, USA). All the measured PCR products were normalized to the amount of cDNA of GAPDH in each sample.

2.9. Western Immunoblotting Analysis. Protein extractions and immunoblots for the determination of phospho-AMPK (Thr172) and GLUT4 proteins were carried out on frozen skeletal muscle, liver, and adipose tissue from mice according to a previous report [25]. Briefly, samples (0.1 g) were powdered under liquid nitrogen and homogenized for 20 s in 500 μL buffer containing 20 mM Tris-HCl (pH = 7.4 at 4°C), 2% SDS, 5 mM EDTA, 5 mM EGTA, 1 mM DTT, 100 mM NaF, 2 mM sodium vanadate, 0.5 mM phenylmethylsulfonyl fluoride, 10 μg/mL leupeptin, and 10 μL/mL pepstatin. 40 μg of each homogenate was mixed with an equal amount of 2 × standard SDS sample loading buffer containing 125 mM Tris-HCl (pH = 6.8), 4% SDS, 20% glycerol, 10% β-mercaptoethanol, and 0.25% bromophenol blue and boiled for 10 min before electrophoresis.

The protein contents of both phospho-AMPK (Abcam Inc, Cambridge, MA, USA) and GLUT4 (Santa Cruz Biotechnology, CA, USA) were detected by immunoblotting using a rabbit polyclonal antibody. About 0.1 g of liver, muscle, and adipose tissue of mice ($n = 9$) were used for the homogenate samples containing lysis buffer (pH = 6.4) and protease inhibitors. The protein concentration in supernatant was determined with a BCA protein assay kit (Thermo Scientific, Rockford, IL, USA). Twenty micrograms of proteins were separated by electrophoresis on a polyacrylamide gel 10% (SDS-PAGE) and transferred to a nitrocellulose membrane. The membranes were blocked with 5% slim milk in Tris-buffered saline (TBS) (Amersham BioSciences, Uppsala, Sweden) containing 0.05% Tween-20 (Bio Rad, CA, USA) and incubated overnight at 4°C with antiphospho-AMPK and anti-GLUT4 at 1 : 200 dilution. Subsequently, the membranes were washed three times with TBS containing 0.05% Tween-20 and incubated with secondary antibody anti-rabbit (1 : 1000) (JacksonImmuno Research, Laboratories, Inc., PA, USA) for 1 h. Immunoreactive bands were detected with ECL reagent kit (GE Healthcare BioSciences, Buckinghamshire, UK). The density blotting was analyzed using Alpha Easy FC software (Alpha innotech corporation, Randburg, South Africa). Structural proteins GADPH (Santa Cruz Biotechnology, CA, USA) and β-actin (Santa Cruz Biotechnology, CA, USA) were obtained by stripping the nitrocellulose membrane proteins of liver, muscle, and adipose tissue, respectively.

2.10. Statistical Analysis. Data were expressed as mean ± S.E. values. Whenever possible, data were subjected to analysis of variance, followed by Dunnett's multiple range tests, using SPSS software (SPSS Inc., Chicago, IL, USA). $P < 0.05$ was considered to be statistically significant.

3. Results

3.1. Oral Glucose Tolerance Test. The effect of CNE on OGTT is shown in Figure 1. By the treatment of the ICR mice with 0.2 g/kg, 0.5, and 1.0 g/kg of CNE, the levels of blood glucose were significantly decreased at 30, 60, 90, 120, and 180 min glucose loading when compared with those of the control.

3.2. Body Weight, Body Weight Gain, Food Intake and Tissue Weight. All mice groups started with similar mean body weights (17.5 ± 0.1 g). At weeks 8 and 12, the body weight of all the high-fat diet treated mice is significantly greater than that of the CON group ($P < 0.001$, $P < 0.001$, resp.). At week 12, treatment with C2 and C3 showed a significant reduction in body weight compared with that in the HF group ($P < 0.05$, $P < 0.05$, resp.) (Table 2). At week 12, the body weight gain of the HF group is greater than that of the CON group ($P < 0.001$). All the CNE-treated groups showed a significant reduction in body weight gain compared with the HF group (Figure 2(a)). At week 12, the HF group is significantly greater than the CON group in the 4-week

Table 2: Absolute tissue weight, weight gain over 4-week treatment (g), liver lipids, and blood profiles.

Parameter	CON	HF	HF + C1 0.2[a]	HF + C2 0.5[a]	HF + C3 1.0[a]	HF + Rosi 0.01[a]
Absolute tissue weight (g)						
MWAT	0.310 ± 0.016	0.594 ± 0.044$^{\#\#\#}$	0.450 ± 0.051**	0.405 ± 0.031***	0.402 ± 0.025***	0.359 ± 0.038***
RWAT	0.093 ± 0.063	0.516 ± 0.068$^{\#\#\#}$	0.288 ± 0.040**	0.294 ± 0.044**	0.272 ± 0.034***	0.163 ± 0.031***
BAT	0.078 ± 0.005	0.062 ± 0.006	0.065 ± 0.005	0.054 ± 0.006	0.053 ± 0.004	0.071 ± 0.004
Liver (g)	0.873 ± 0.030	0.873 ± 0.029	0.869 ± 0.026	0.841 ± 0.025	0.825 ± 0.030	0.929 ± 0.021
Spleen	0.061 ± 0.004	0.068 ± 0.003	0.078 ± 0.004	0.074 ± 0.002	0.068 ± 0.002	0.074 ± 0.004
Food intake (g/mouse)	76.41 ± 1.57	67.12 ± 1.01$^{\#\#\#}$	58.97 ± 0.91***	58.71 ± 1.16***	58.71 ± 1.19***	68.11 ± 1.64
Liver lipids						
Total lipid (mg/g)	57.6 ± 2.8	93.8 ± 5.7$^{\#\#\#}$	75.2 ± 3.9*	65.1 ± 4.5**	63.9 ± 3.9**	64.4 ± 4.9**
Triacylglycerol (μmol/g)	35.6 ± 3.7	78.4 ± 6.9$^{\#\#\#}$	58.9 ± 6.1*	43.2 ± 4.6***	44.0 ± 5.9***	46.5 ± 5.4***
Blood profiles						
FFA (meq/L)	1.529 ± 0.068	2.472 ± 0.063$^{\#}$	1.404 ± 0.192*	1.329 ± 0.161*	1.231 ± 0.156**	1.359 ± 0.173*
TC (mg/dL)	100.3 ± 4.6	154.0 ± 5.5$^{\#\#\#}$	148.8 ± 3.4	142.6 ± 6.0	130.8 ± 8.8*	134.9 ± 3.5
Leptin (μg/mL)	1.767 ± 0.172	1.958 ± 0.272	1.292 ± 0.092*	1.269 ± 0.121*	1.112 ± 0.173*	1.429 ± 0.161
Insulin (μg/L)	1.567 ± 0.040	1.813 ± 0.101$^{\#}$	1.517 ± 0.081*	1.387 ± 0.073**	1.384 ± 0.056**	1.363 ± 0.082***
Adiponectin (ng/mL)	10.05 ± 0.23	8.94 ± 0.49	9.85 ± 0.61	10.57 ± 0.46*	11.21 ± 0.33**	12.19 ± 0.75*
Semiquantitative RT-PCR analysis for mRNA expression in liver tissue						
ApoC-III	1.148 ± 0.039	1.023 ± 0.087	0.990 ± 0.037	0.996 ± 0.063	0.846 ± 0.016*	0.797 ± 0.046**

All values are mean ± S.E. ($n = 9$). $^{\#}P < 0.05$, $^{\#\#}P < 0.01$, and $^{\#\#\#}P < 0.001$ were compared with those of the control (CON) group; $^{*}P < 0.05$, $^{**}P < 0.01$, and $^{***}P < 0.001$ were compared with those of the high-fat + vehicle (distilled water) (HF) group. C1, C2, and C3: extracts of *Clitocybe nuda*. (C1: 0.2, C2: 0.5, and C3: 1.0 g/kg bodyweight); Rosi: rosiglitazone (0.01 g/kg body weight); BAT: brown adipose tissue; RWAT: retroperitoneal white adipose tissue; MWAT: mesenteric white adipose tissue; FFA: plasma-free fatty acid; TC: total cholesterol. Total RNA (1 μg) isolated from tissue was reverse transcripted by MMLV-RT, 10 μL of RT products was used as template for PCR. Signals were quantitated by image analysis; each value was normalized by GAPDH. [a]Dose (g/kg/day).

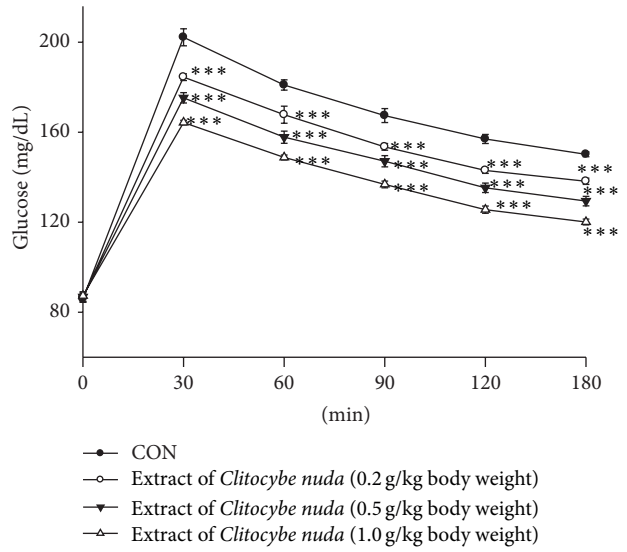

Figure 1: Effects of the extract of *Clitocybe nuda* on oral glucose tolerance in ICR normal mice. Animals in all groups received oral glucose 30 minutes after the extract administration. Blood samples were collected and centrifuged at 3000 rpm for 10 minutes. Each point is the mean ± S.E. of 5 separate mice. $^{***}P < 0.001$ was significantly different compared with that of the control group at the same time by ANOVA.

cumulative food intake (kcal) ($P < 0.05$). All the CNE-treated groups showed a significant reduction in the 4-week cumulative food intake (kcal) ($P < 0.001$) (Figure 2(b)). At week 12, the weights of absolute adipose tissue (epididymal WAT, visceral fat, mesenteric WAT, and retroperitoneal WAT) were markedly greater in the HF group than those in the CON group (epididymal WAT 265.7%, visceral fat 303.9%, mesenteric WAT 91.6%, and retroperitoneal WAT 454.8.0%) ($P < 0.001$, $P < 0.001$, $P < 0.001$, and $P < 0.001$, resp.) (Table 2 and Figures 2(c) and 2(d)). All the CNE- and Rosi-treated groups showed a significant decrease in the weights of absolute epididymal WAT, visceral fat, mesenteric WAT, and retroperitoneal WAT compared with the HF group. No significant difference in the weights of liver and spleen was observed in all the CNE- and Rosi-treated groups compared with the HF group (Table 2).

3.3. Plasma Glucose Levels. At the beginning of the study, all of mice started with similar levels. At weeks 8 and 12, the glucose levels of the HF group were significantly greater than those of the CON group ($P < 0.001$, $P < 0.001$, resp.). Treatment with C1, C2, C3, and Rosi showed a significant reduction in plasma glucose compared with the HF group ($P < 0.001$, $P < 0.001$, $P < 0.001$, and $P < 0.001$, resp.) (Figure 2(e)).

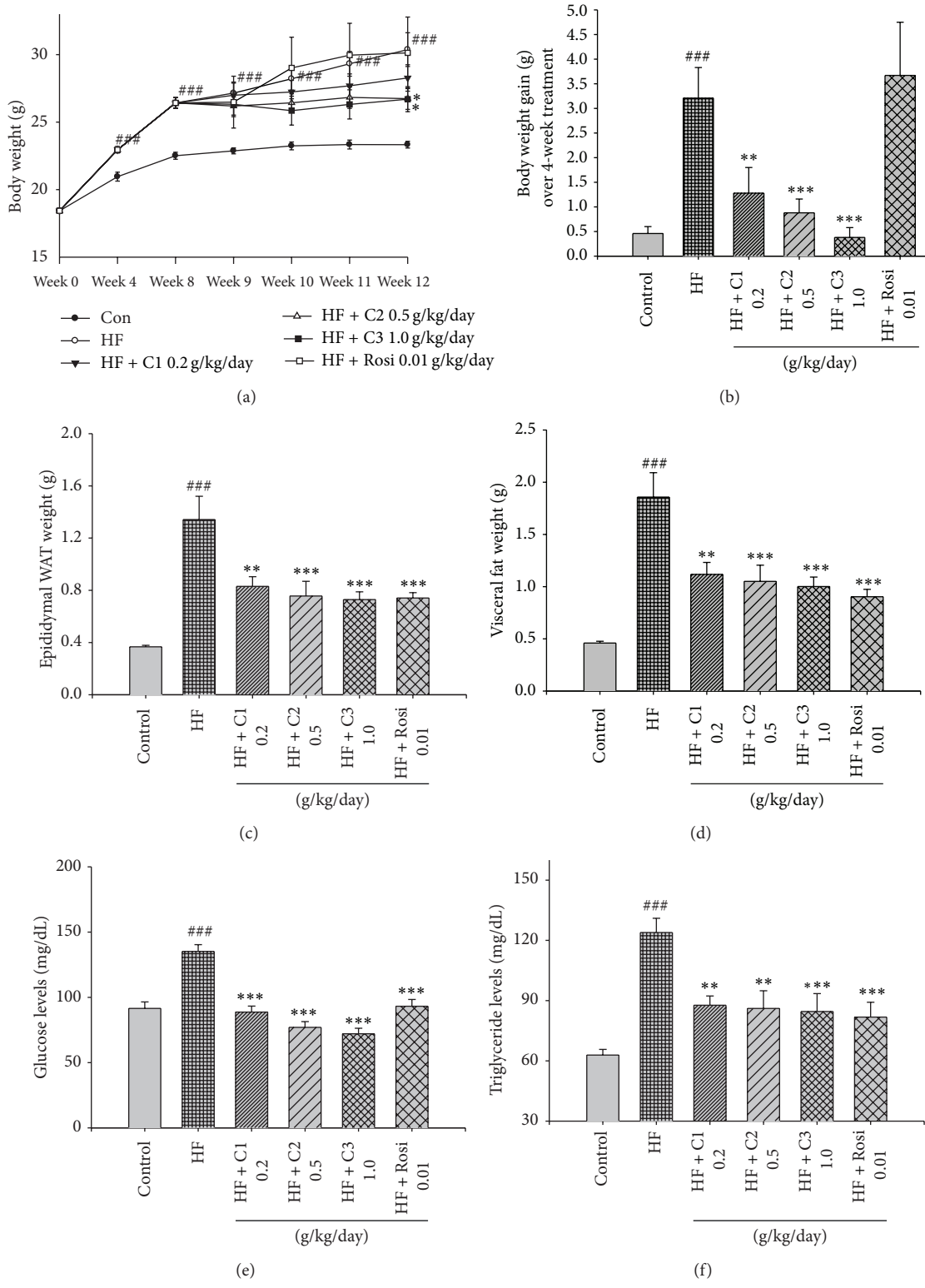

Figure 2: Effects of the extract of *Clitocybe nuda* on (a) body weight at week 12, (b) body weight gain over 4-week treatment, (c) epididymal WAT weights, (d) visceral fat weight, (e) blood glucose levels, and (f) circulating triglyceride levels at week 12. Mice were fed with 45% high-fat diet (HF) or low-fat diet (CON) for 12 weeks. After 8 weeks, the HF mice were treated with vehicle (water; p.o.), extract of *Clitocybe nuda*, or rosiglitazone (p.o.) accompanied with HF diet for 4 weeks. All values are mean ± S.E. ($n = 9$). $^{\#}P < 0.05$, $^{\#\#}P < 0.01$, and $^{\#\#\#}P < 0.001$ were compared with those of the control (CON) group; $^{*}P < 0.05$, $^{**}P < 0.01$, and $^{***}P < 0.001$ were compared with those of the high-fat + vehicle (distilled water) (HF) group by ANOVA. C1, C2, and C3: extracts of *Clitocybe nuda* (C1: 0.2, C2: 0.5, and C3: 1.0 g/kg body weight); Rosi: rosiglitazone (0.01 g/kg body weight). WAT: white adipose tissue; epididymal WAT + retroperitoneal WAT: visceral fat.

3.4. Plasma and Liver Lipid. As time passed, the hypercholesterolaemic phenomenon was evident for the HF diet. As shown in Table 2 and Figure 2(f), at week 12, the levels of TC, TG, and FFA were 62.4%, 97.0%, and 60.8% greater in the HF group than in the CON group ($P < 0.001$, $P < 0.001$, and $P < 0.05$, resp.). All the CNE- and Rosi-treated groups suppressed the HF diet-induced increases in the concentrations of TG. Treatment with C3 suppressed the HF diet-induced increases in the concentrations of TC. Treatment with C2, C3, and Rosi suppressed the high-fat diet-induced increases in the concentrations of FFA. The liver total lipids and triacylglycerol concentrations were 62.8% and 120.2% greater, respectively, in the HF group than those in the CON group (Table 2). Treatment with C1, C2, C3, and Rosi significantly suppressed the HF diet-induced increase in the liver total lipids and triacylglycerol concentrations (Table 2).

3.5. Leptin and Insulin Concentrations. As shown in Table 2, at week 12, the concentrations of insulin were greater in the HF group than in the CON group ($P < 0.05$). ALL the CNE-treated groups significantly decreased leptin levels, whereas C2-, C3-, and Rosi-treated groups increased adiponectin levels compared with the HF group. C1-, C2-, C3-, and Rosi-treated groups significantly decreased the levels of insulin compared with the HF group ($P < 0.05$, $P < 0.01$, $P < 0.01$, and $P < 0.001$, resp.).

3.6. Histopathology of Adipose and Liver Tissue. As shown in Figure 3(a), feeding the HF diet induced hypertrophy of the adipocytes compared with the CON group in epididymal WAT. Treatment with C1, C2, and C3 decreased the hypertrophy compared with the HF group. As shown in Figure 3(b), feeding the HF diet induced the ballooning of hepatocyte compared with the CON group in liver tissue. Afterwards, treatment with C2 and C3 decreased the ballooning compared with the HF group. These morphological results strongly suggest that treatment with CNE inhibits the hepatic TG accumulation. The results obtained from the other mice are similar to those shown in Figure 3.

3.7. Expressions of ATGL, G6Pase, PPARα, ApoC-III, and SREBP1c in Liver Tissue. As shown Figure 4 and Table 2, at week 12, there were no significant differences in the mRNA levels of ATGL and PPARα between the HF group and the CON group. At week 12, the mRNA levels of G6Pase and SREBP1c were higher in the HF group than in the CON group ($P < 0.001$, $P < 0.05$, resp.). Following treatment, the C1-, C2-, C3-, and Rosi-treated groups significantly decreased the mRNA level of G6Pase ($P < 0.001$, $P < 0.001$, $P < 0.001$, and $P < 0.001$, resp.) (Figure 4(a)). Following treatment, the C1-, C2-, and C3-treated groups increased the mRNA level of ATGL ($P < 0.05$, $P < 0.01$, and $P < 0.05$, resp.) (Figure 4(b)). The C2-treated group increased the mRNA levels of PPARα (Figure 4(c)), whereas the C3- and Rosi-treated groups decreased the apoC-III expression ($P < 0.05$, $P < 0.01$, resp.) (Table 2). The C3- and Rosi-treated groups decreased the SREBP1c expression as compared with the HF group ($P < 0.05$) (Figure 4(d)).

3.8. The Phospho-AMPK (Thr172) Protein Contents in Liver Tissue, Skeletal Muscle, and Adipose Tissue. At week 12, the protein contents of phospho-AMPK protein were lower in the HF group than those in the CON group in liver, skeletal muscle, and adipose tissue ($P < 0.05$, $P < 0.05$, and $P < 0.01$, resp.). After treatment, the protein contents of hepatic phospho-AMPK were increased in the C2-, C3-, and Rosi-treated groups compared with those in the HF group ($P < 0.01$, $P < 0.001$, and $P < 0.01$, resp.) (Figure 5(a)). Following treatment, the muscular protein contents of phospho-AMPK were increased in the C1-, C2-, C3-, and Rosi-treated groups compared with the HF group ($P < 0.05$, $P < 0.01$, $P < 0.01$, and $P < 0.01$, resp.) (Figure 5(b)). After treatment, the protein contents of adipose phospho-AMPK were increased in the C1-, C2-, C3-, and Rosi-treated groups compared with those in the HF group in liver tissue ($P < 0.01$, $P < 0.01$, $P < 0.05$, and $P < 0.05$, resp.) (Figure 5(c)).

3.9. The GLUT4 Protein Contents in Skeletal Muscle and Adipose Tissue. At week 12, there were no significant differences in GLUT4 protein between the HF group and the CON group in skeletal muscle and adipose tissue. After treatment, the skeletal muscular protein contents of GLUT4 were greater in C3- and Rosi-treated groups than those in the HF group ($P < 0.01$, $P < 0.05$, resp.) (Figure 5(d)). Following treatment, the adipose protein contents of GLUT4 were greater in C2-treated groups than those in the HF group ($P < 0.01$) (Figure 5(e)).

4. Discussion

Clitocybe nuda is an edible woodland mushroom found in Europe; because of its special fragrance and delicacy, it has been cultivated in France and even in Taiwan. The season variation had no effect on the amount of antioxidants property in this mushroom, because the culture is under environmental controls. However, the antidiabetic and antihyperlipidemia activities of *Clitocybe nuda* are not well defined. This study showed that feeding mice with high-fat diet induced hyperglycemia, hyperinsulinemia, hypertriglycemia and hypercholesterolemia. Following treatment of HF-fed mice with CNE, blood glucose, visceral fat mass, and the levels of triglycerides were decreased and improved insulin resistance. This could be because the lowered insulin and glucose levels reflect the glucose output and insulin secretion.

In this study, we found that CNE increased the protein contents of GLUT4 and had favorable effects on glucose uptake into the peripheral tissues and reduced circulating blood glucose. Furthermore, CNE not only increased the phosphorylation of AMPK in tissues, but also improved lipid metabolism. The AMPK activator AICAR has been shown to lower plasma glucose and ameliorate insulin resistance in animal studies [26, 27]. Based on our described findings, we found that CNE is effective in improving insulin resistance and dyslipidemia in a mouse model of type 2 diabetes and dyslipidemia and CNE may have favorable effects on glucose

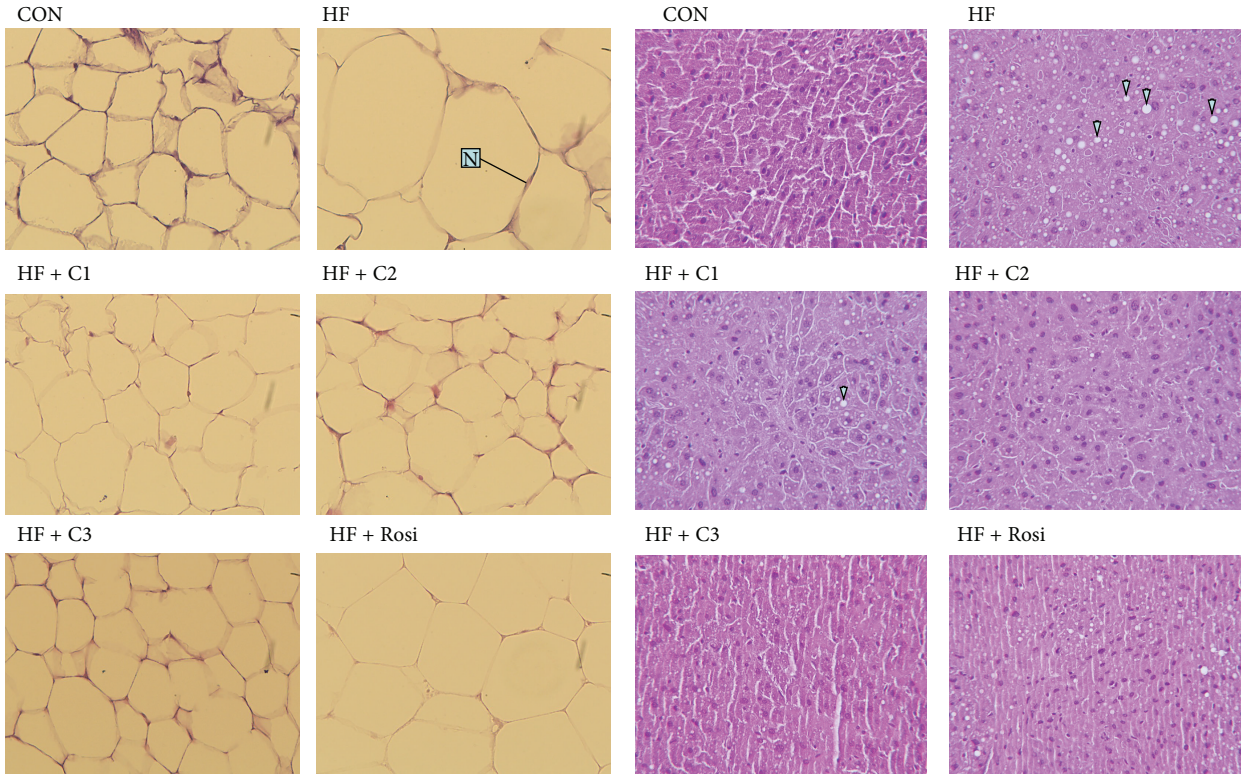

Figure 3: Effects of the extract of *Clitocybe nuda* on liver tissue morphology in the low-fat (Con), high-fat (HF), HF + C1, HF + C2, HF + C3, or HF + Rosi groups. Pictures of hematoxylin and eosin-stained sections of (a) epididymal adipocytes (magnification: 10 (ocular) × 20 (object lens)) from mice fed with extract of *Clitocybe nuda*. White adipose tissue (named adipocytes) is polyhedral by H&E stain, and the appearance showed string-like cytosol surrounding a vacuole. This is because they were embedded in paraffin as immersed in lipid solvents, and finally all the fats were removed. Unobvious nucleus (N) in the other side of cells was carefully observed, and (b) liver tissue (magnification: 10 (ocular) × 40 (object lens)) was obtained from mice fed with extract of *Clitocybe nuda*. The high-fat diet induced the hepatic ballooning degeneration in the HF group as compared with the CON group. The ballooning degeneration is a form of liver parenchymal cell death and the nucleolus was squeezed into the other side named balloon (as the arrow indicated). This may be due to the heap of glycogen in the nucleus. High-fat diet induced obesity and insulin resistance. Insulin levels affected the storage of hepatic glycogen. Treatment with C2 and C3 significantly decreased the degree of ballooning degeneration. Each presented is typical and representative of nine mice. C1, C2, and C3: extracts of *Clitocybe nuda* (C1: 0.2, C2: 0.5, and C3: 1.0 g/kg body weight); Rosi: rosiglitazone (0.01 g/kg body weight).

level and lipid metabolism. These findings are involved in the results of GLUT4 contents and AMPK activation.

To investigate the antidiabetic properties of CNE, we chose GLUT4 proteins in skeletal muscle as the major tissues. GLUT4 is a protein that is encoded by the GLUT4 gene found in skeletal muscle. Skeletal muscle is the major tissue responsible for insulin-mediated glucose utilization. Insulin stimulates glucose uptake in skeletal muscle by promoting the translocation of of the GLUT4 to the plasma membrane [28]. Diabetic animals with defective glucose uptake in skeletal muscle appear to be the result of low level of GLUT4 expression [29]. Therefore, the improvements of GLUT4 contents and/or translocation to the plasma membrane have long been regarded as a potential target in the treatment of diabetes mellitus. In the present study there was an increase in the muscular GLUT4 protein contents in the C3-treated HF mice. Increased protein contents of GLUT4 indicated that CNE improved glucose utilization in skeletal muscle by restoring translocation of GLUT4 to the plasma membrane.

The first aim of this study was to investigate the antidiabetic effect and mechanism of CNE. Since the lowering of glucose by CNE and rosiglitazone occurs possibly by different mechanisms, the levels of insulin were measured. Rosiglitazone lowered glucose by insulin sensitizing; therefore, the levels of insulin in the groups of mice treated with Rosi and CNE showed reduction of insulin as a result of insulin utilization. To clarify the mechanism of glucose lowering as well as insulin lowering, mRNA of key transcription factor that included G6Pase gene in the liver was quantitated.

Liver gluconeogenesis is driven by the availability of gluconeogenic substrates and the activity of the important gluconeogenic enzymes like glucose-6-phosphatase (G6Pase) [30]. In the re-feeding state, insulin suppresses gluconeogenesis by transcriptional downregulation of G6pase [31]. Following treatment with CNE, the G6Pase expression was restored to a level lower than the CON group. The hypoglycemic effect is known to be principally attributed to hepatic gluconeogenesis

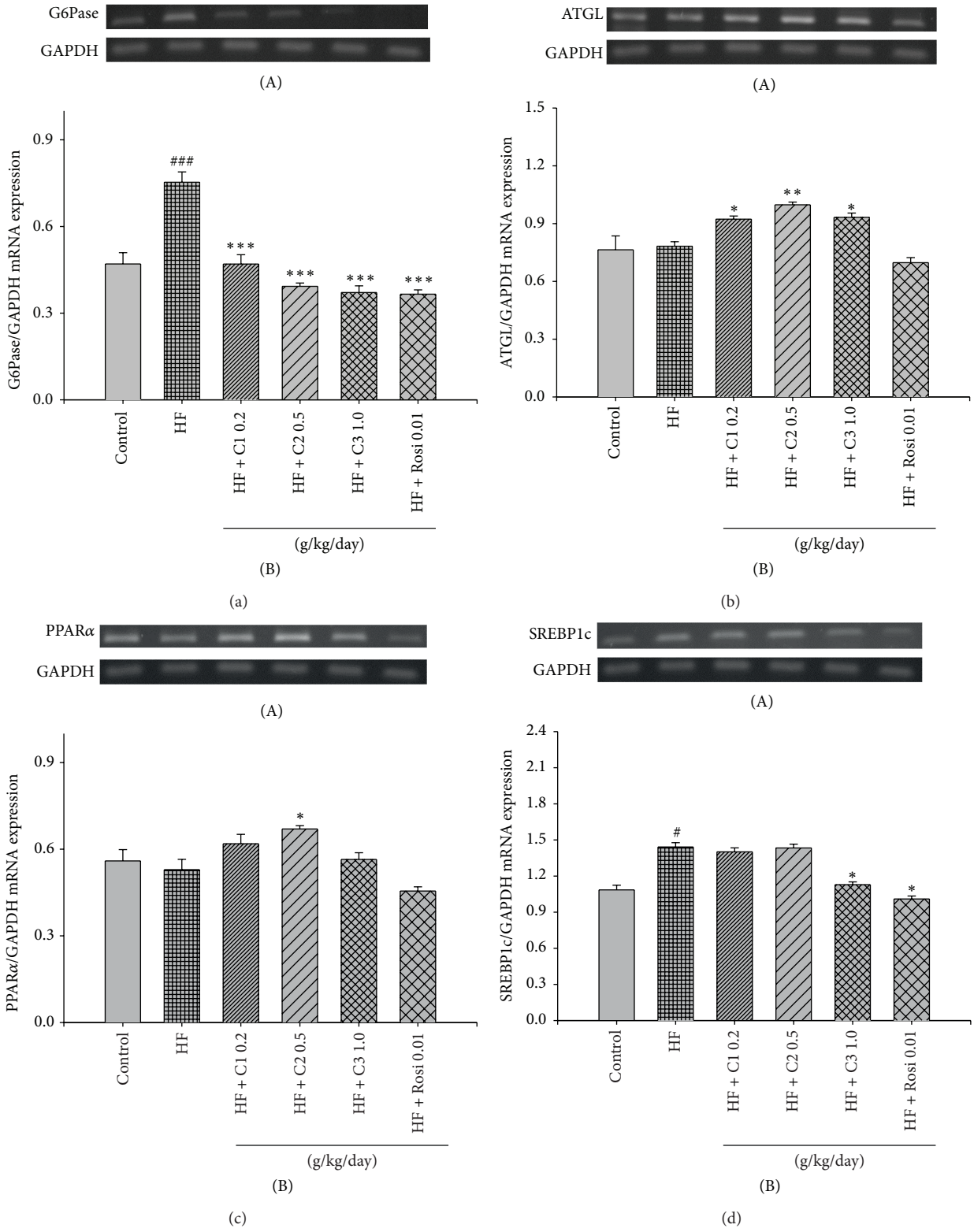

Figure 4: Semiquantative RT-PCR analysis on (a) ATGL, (b) G6Pase, (c) PPARα, and (d) SREBP1c mRNA expressions in liver tissue of the mice by oral gavage extracts of *Clitocybe nuda* (C1: 0.2, C2: 0.5, and C3: 1.0 g/kg body weight); Rosi: rosiglitazone (0.01 g/kg body weight). Total RNA (1 μg) isolated from tissue was reverse transcripted by MMLV-RT, and 10 μL of RT products was used as template for PCR. The expression levels of ATGL, G6Pase, PPARα, and SREBP1c mRNA were measured and quantified by image analysis. Values were normalized to GAPDH mRNA expression. All values are mean ± S.E. ($n = 9$). $^{\#}P < 0.05$ and $^{\#\#\#}P < 0.001$ were compared with those of the control (CON) group; $^{*}P < 0.05$ and $^{***}P < 0.001$ were compared with those of the high-fat + vehicle (distilled water) (HF) group.

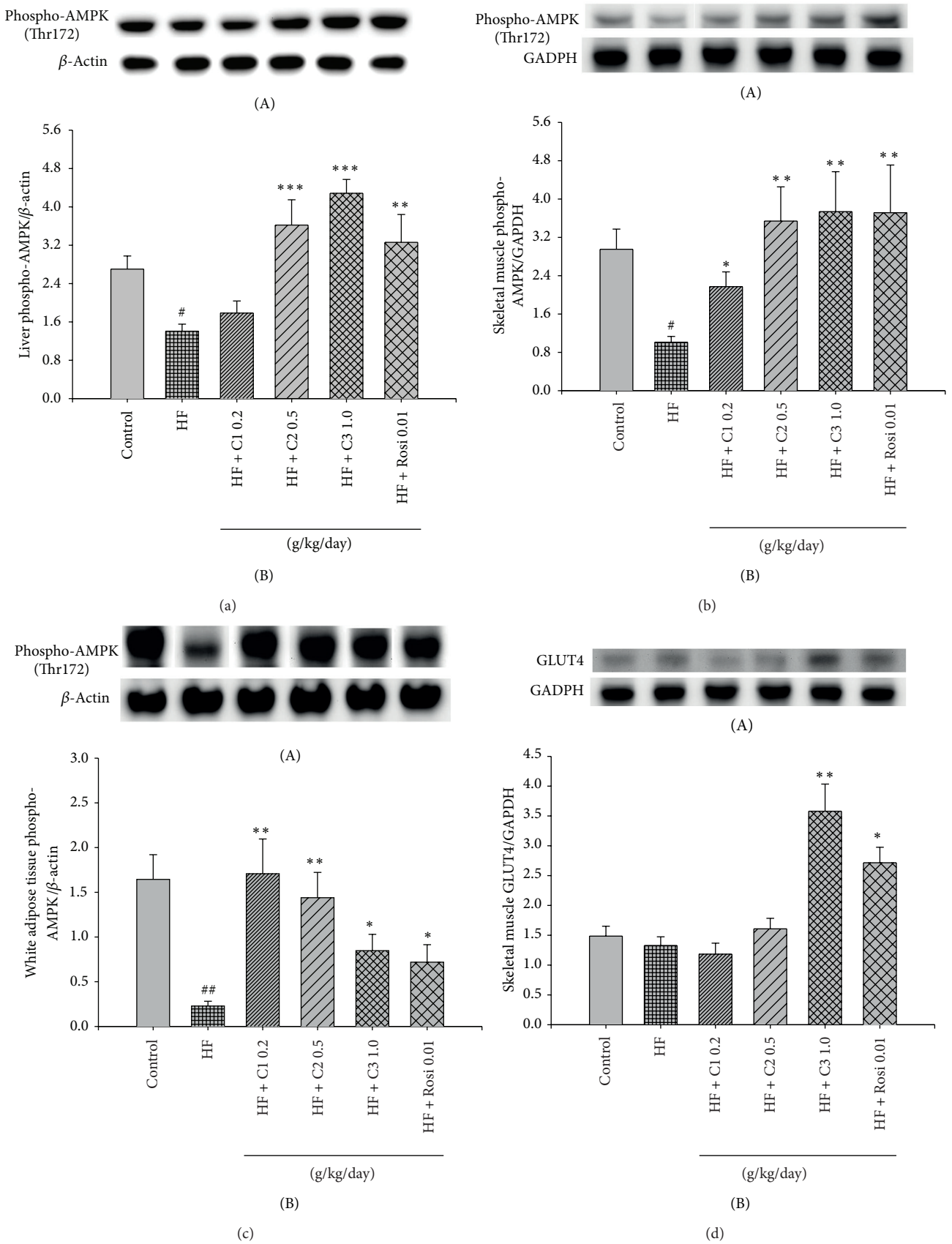

Figure 5: Continued.

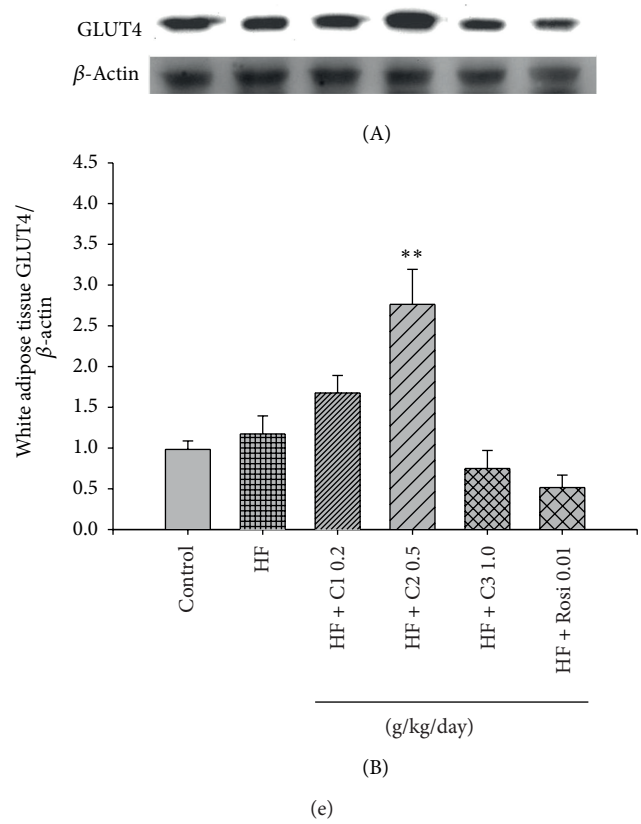

Figure 5: The phospho-AMPK (Thr172) protein contents in (a) liver, (b) skeletal muscle, and (c) white adipose tissue and GLUT4 protein contents in (d) skeletal muscle and (e) adipose tissue of the mice by oral gavage extract of *Clitocybe nuda* for 4 weeks. Protein was separated by 12% SDS-PAGE detected by western blot. All values are mean ± S.E. ($n = 9$). $^{\#}P < 0.05$ and $^{\#\#}P < 0.01$ were compared with the control (CON) group; $^{*}P < 0.05$, $^{**}P < 0.01$, and $^{***}P < 0.001$ were compared with the high-fat + vehicle (distilled water) (HF) group. C1, C2, and C3: extract of *Clitocybe nuda* (C1: 0.2, C2: 0.5, and C3: 1.0 g/kg bodyweight); Rosi: rosiglitazone (0.01 g/kg body weight).

suppression [31], suggesting the lowering of glucose effects of CNE involved in the suppression of hepatic gluconeogenesis.

AMPK activation results in increased glucose uptake in skeletal muscle [32, 33] but decreased hepatic glucose production. AMPK regulates glucose metabolism both via the direct phosphorylation of metabolic enzymes and effects on gene expression [34]. The previous findings suggested that increased AMPK activation is associated with increases in GLUT4 [35]. Once activated, AMPK promotes muscle glucose uptake and inhibits hepatic gluconeogenesis by repressing PEPCK and G6Pase expressions [36]. The present study implicated that CNE exerted hypoglycemic activity and significantly increased the protein contents of phospho-AMPK, whereas expressions of G6Pase were decreased in the liver of all CNE- and rosi-treated mice. Therefore, this might also indicate that CNE by AMPK activation leads to increased GLUT4 contents and decreased G6Pase expression, with stimulation of peripheral glucose uptake and inhibition of hepatic glucose production, thus resulting in the lowering of glucose levels.

GLUT4 translocation is mainly regulated by two independent pathways: the insulin signaling pathway and the AMPK pathway [37]. The kinase, AMPK, has also been shown to regulate GLUT4 translocation [37]. The AMPK pathway is involved in regulation of GLUT4 translocation during exercise or in response to some antidiabetic agents such as AICAR and metformin [37]. In the study, treatment with C2 and C3 was able to increase the phosphorylation of AMPK to a level, suggesting that the AMPK activation is likely responsible for the stimulation of GLUT4 translocation by this CNE. Further studies are needed to shed light on the molecular mechanism involved in the phosphorylation of AS160 pathway.

AMPK activation also has numerous effects on lipid metabolism [38], which leads to the inhibition of fatty acid, triglyceride and sterol biosynthesis in hepatocytes [39, 40], and activation of fatty acid oxidation in skeletal muscle and hepatocytes [41]. In these cases, the effects are known to be due to the direct phosphorylation of metabolic enzyme. Based on a number of studies showing that AMPK regulates a variety of metabolic syndromes, it is widely recognized as a useful target for the treatment of metabolic disorders such as T2D and dyslipidemia [27, 42]. Hence, our findings of activation of AMPK by CNE may implicate this extract as a novel phytonutrient with therapeutic potential for insulin resistant states by targeting AMPK.

The lipid-lowering efficacy of CNE was also caused by upregulation of another enzyme, adipose triglyceride lipase

(ATGL), which is responsible for triacylglycerol hydrolase activity in cells that control the rate-limiting step of lipolysis in many insulin sensitive tissues. ATGL exhibits high specificity for triglyceride to hydrolyze into diglyceride and free fatty acid [43]. It is known that activation of AMPK may in turn increase ATGL expression and decrease intracellular lipid droplet accumulation [44]. Recently, ATGL has been considered as a possible therapeutic target for dyslipidemia and fatty liver [45]. In this study, we showed that CNE caused AMPK phosphorylation and increased ATGL expression, which could help triglyceride to hydrolyze, suggesting that CNE could be a possible therapeutic supplementary for dyslipidemia.

In this study, treatment with CNE, the levels of triglycerides were lowered. SREBP-1c plays an important role in response to activation of lipogenic enzyme expression, fatty acid synthesis, and triglyceride accumulation [46]. In PPARα-deficient mice, dysregulation of SREBP-mediated lipogenic genes was noticed [47], suggesting the role of PPARα in SREBP-mediated regulation of lipogenic genes. This study confirmed CNE's lipid-lowering effects partly via downregulation of genes involved in lipid synthesis. Metformin acts by increasing the phosphorylation and activation of AMP kinase, a key enzyme involved in the regulation of gene expression, fuel metabolism, and energy balance [19]. Activation of AMP kinase in liver leads to reduced transcriptional activity of the nuclear factor SREBP1c on the expression of lipogenic enzymes. Therefore, there is a possibility that CNE inactivated these enzymes and/or downregulated gene expression through AMPK activation.

Following treatment with CNE, hepatic PPARα expressions were increased in C2-treated group but leptin levels were decreased in CNE-treated groups. However, we could not exclude the possibility that CNE stimulates PPARα function through leptin-dependent actions. It is known that PPARα is involved in regulation of lipid metabolism and fatty acid oxidation. According to a previous study [48], leptin stimulates fatty acid oxidation through the activation of AMPK and the induction of gene expression, such as PPARα. Thus, further study should shed the light on whether CNE-activated PPARα functions are mediated by leptin-AMPK pathway.

We knew that the gills of *C. nuda* are of intense bluish-purple color. Anthocyanins (cyanidin or cyanidin 3-glucoside) were reported to have the potency of a unique therapeutic advantage for prevention of obesity and diabetes in isolated rat adipocytes [17]. Treatment of adipocytes with anthocyanins enhanced adiponectin secretion and AMPK activation which plays a key role in the metabolic regulation of lipids and glucose uptake in adipocyte [17]. Moreover, dietary cyanidin 3-O-β-D-glucoside-rich "purple corn color" (PCC) prevents obesity and ameliorates hyperglycemia in HF-diet-induced mice, and the findings provide a nutritional basis for the use of PCC and anthocyanins as a functional food factor that may have benefits for the prevention of obesity and diabetes [49]. This mushroom extract contained antioxidant properties of the total phenolic content [5]. Our study demonstrated that CNE contained the total phenolic contents. Dietary polyphenols such as resveratrol, catechins, epicatechin, and gallic acid, possess wide therapeutic benefits [50]. Several studies demonstrated the antidiabetic action of polyphenolic class of compounds [51–53]. In the present study, it is possible that the phenolic-rich and anthocyanin contained in CNE may be one of bioactive principles responsible for CNE improved carbohydrate and lipid metabolism in type II diabetic mice. The researcher's interest in polyphenol-rich foods as a dietary source of antioxidants has increased in response to the recognition of the importance of oxidative damage in the pathogenesis of many diseases. Our present investigation provides information that explains, at least in part, the potential benefits of CNE in mice with type II diabetes. However further research is required to establish whether CNE polyphenol in being beneficial for insulin sensitizing and attenuating hyperlipidemic process due to its activity of AMPK activation and glucose uptake by increasing adiponectin levels.

In conclusion, this study demonstrated that CNE increased insulin sensitivity appears to be related to not only increased phosphorylation of AMPK but also increased protein contents of GLUT4 in C3-treated group in skeletal muscle and in C2-treated group in adipose tissue, whereas it is related to a reduction in G6Pase expression, which is one of rate-limiting enzymes of hepatic gluconeogenesis, resulting in reduced glucose level in HF-fed mice. In the other hand, by increasing the phosphorylation of AMPK in liver tissue, CNE should partly decrease hepatic fatty acid synthesis but increase ATGL, which is responsible for hydrolyzing triacyl glycerol, which in turn contributed to the lowering of circulating triglycerides. Therefore, CNE might be a good metabolic regulator and insulin sensitizer. This biological function of CNE might be associated with the increased activity of AMPK. Our findings demonstrated that CNE had the therapeutic potential for the protection against diabetes and hyperlipidemia.

Abbreviations

AMPK:	AMP-activated protein kinase
ATGL:	Adipose triglyceride lipase
BAT:	Brown adipose tissue
CON:	Control
EWAT:	Epididymal white adipose tissue
FFA:	Free fatty acid
GAPDH:	Glyceraldehyde-3-phosphate dehydrogenase
GLUT4:	Glucose transporter 4
G6Pase:	Glucose-6-phosphatase
HF:	High-fat control
HOMA-IR:	Homeostasis model assessment for insulin resistance
MWAT:	Mesenteric white adipose tissue
PPARα:	Peroxisome proliferator-activated receptor α
PPARs:	Peroxisomal proliferator-activated receptors
Rosi:	Rosiglitazone
RT-PCR:	Reverse transcription polymerase chain reaction
RWAT:	Retroperitoneal white adipose tissue
SREBP-1:	Sterol regulatory element binding protein 1

TC: Total cholesterol
TG: triglyceride
WAT: White adipose tissue.

Conflict of Interests

The authors declare that there is no conflict of interests regarding publishing of this paper.

Acknowledgments

This work was supported in part by Grants CTU102-TARI-001 from the Agricultural Research Institute, Council of Agriculture, Executive Yuan, Taiwan, and Central Taiwan University of Science and Technology.

References

[1] S. O'Rahilly, R. C. Turner, and D. R. Matthews, "Impaired pulsatile secretion of insulin in relatives of patients with non-insulin-dependent diabetes," *The New England Journal of Medicine*, vol. 318, no. 19, pp. 1225–1230, 1988.

[2] L. Barros, B. A. Venturini, P. Baptista, L. M. Estevinho, and I. C. F. R. Ferreira, "Chemical composition and biological properties of Portuguese wild mushrooms: a comprehensive study," *Journal of Agricultural and Food Chemistry*, vol. 56, no. 10, pp. 3856–3862, 2008.

[3] B. Dulger, C. C. Ergul, and F. Gucin, "Antimicrobial activity of the macrofungus *Lepista nuda*," *Fitoterapia*, vol. 73, no. 7-8, pp. 695–697, 2002.

[4] M. A. Murcia, M. Martínez-Tomé, A. M. Jiménez, A. M. Vera, M. Honrubia, and P. Parras, "Antioxidant activity of edible fungi (truffles and mushrooms): losses during industrial processing," *Journal of Food Protection*, vol. 65, no. 10, pp. 1614–1622, 2002.

[5] N. Mercan, M. E. Duru, A. Turkoglu, K. Gezer, I. Kivrak, and H. Turkoglu, "Antioxidant and antimicrobial properties of ethanolic extract from *Lepista nuda* (Bull.) Cooke," *Annals of Microbiology*, vol. 56, no. 4, pp. 339–344, 2006.

[6] J. T. Chen, H. J. Su, and J. W. Huang, "Isolation and identification of secondary metabolites of *Clitocybe nuda* inhibition of zoospore germination of *Phytophthora capsici*," *Journal of Agricultural and Food Chemistry*, vol. 60, no. 30, pp. 7341–7344, 2012.

[7] C. Kandaswami and E. Middleton, "Flavonoids as antioxidants," in *Natural Antioxidants: Chemistry, Health Effects and Practical Applications*, F. Shahidi, Ed., pp. 174–194, The American Oil Chemists Society, Champaign, lll, USA, 1997.

[8] Y. S. Velioglu, G. Mazza, L. Gao, and B. D. Oomah, "Antioxidant activity and total phenolics in selected fruits, vegetables, and grain products," *Journal of Agricultural and Food Chemistry*, vol. 46, no. 10, pp. 4113–4117, 1998.

[9] D. Xu, Y. Sheng, Z.-Y. Zhou, R. Liu, Y. Leng, and J.-K. Liu, "Sesquiterpenes from cultures of the basidiomycete *Clitocybe conglobata* and their 11β-hydroxysteroid dehydrogenase inhibitory activity," *Chemical and Pharmaceutical Bulletin*, vol. 57, no. 4, pp. 433–435, 2009.

[10] D. J. St. Jean Jr., M. Wang, and C. Fotsch, "Inhibitors of 11β-HSD1: a potential treatment for the metabolic syndrome," *Current Topics in Medicinal Chemistry*, vol. 8, no. 17, pp. 1508–1523, 2008.

[11] J. Berger, C. Biswas, P. P. Vicario, H. V. Strout, R. Saperstein, and P. F. Pilch, "Decreased expression of the insulin-responsive glucose transporter in diabetes and fasting," *Nature*, vol. 340, no. 6228, pp. 70–72, 1989.

[12] B. B. Kahn, S. W. Cushman, and J. S. Flier, "Regulation of glucose transporter-specific mRNA levels in rat adipose cells with fasting and refeeding. Implications for in vivo control of glucose transporter number," *The Journal of Clinical Investigation*, vol. 83, no. 1, pp. 199–204, 1989.

[13] R. T. Watson and J. E. Pessin, "Intracellular organization of insulin signaling and GLUT4 translocation," *Recent Progress in Hormone Research*, vol. 56, pp. 175–194, 2001.

[14] S. Sujatha, S. Anand, K. N. Sangeetha et al., "Biological evaluation of (3β)-STIGMAST-5-EN-3-OL as potent anti-diabetic agent in regulating glucose transport using *in vitro* model," *International Journal of Diabetes Mellitus*, vol. 2, no. 2, pp. 101–109, 2010.

[15] M. Foretz, N. Toleux, B. Guigas et al., "Regulation of energy metabolism by AMPK: a novel therapeutic approach for the treatment of metabolic and cardiovascular diseases," *Médecine/Sciences*, vol. 22, no. 4, pp. 381–388, 2006.

[16] B. Viollet, L. Lantier, J. Devin-Leclerc et al., "Targeting the AMPK pathway for the treatment of type 2 diabetes," *Frontiers in Bioscience*, vol. 14, no. 9, pp. 3380–3400, 2009.

[17] T. Tsuda, Y. Ueno, H. Aoki et al., "Anthocyanin enhances adipocytokine secretion and adipocyte-specific gene expression in isolated rat adipocytes," *Biochemical and Biophysical Research Communications*, vol. 316, no. 1, pp. 149–157, 2004.

[18] A. E. Petro, J. Cotter, D. A. Cooper, J. C. Peters, S. J. Surwit, and R. S. Surwit, "Fat, carbohydrate, and calories in the development of diabetes and obesity in the C57BL/6J mouse," *Metabolism*, vol. 53, no. 4, pp. 454–457, 2004.

[19] G. Zhou, R. Myers, Y. Li et al., "Role of AMP-activated protein kinase in mechanism of metformin action," *The Journal of Clinical Investigation*, vol. 108, no. 8, pp. 1167–1174, 2001.

[20] S. C. Stein, A. Woods, N. A. Jones, M. D. Davison, and D. Cabling, "The regulation of AMP-activated protein kinase by phosphorylation," *Biochemical Journal*, vol. 345, no. 3, pp. 437–443, 2000.

[21] T. Swain and W. E. Hills, "The phenolic constituents of *Punnus domestica*. I.—the quantitative analysis of phenolic constituents," *Journal of the Science of Food and Agriculture*, vol. 10, no. 1, pp. 63–68, 1959.

[22] M. Dubois, K. A. Gilles, J. K. Hamilton, P. A. Rebers, and F. Smith, "Colorimetric method for determination of sugars and related substances," *Analytical Chemistry*, vol. 28, no. 3, pp. 350–356, 1956.

[23] C.-C. Shih, C.-H. Lin, and W.-L. Lin, "Effects of *Momordica charantia* on insulin resistance and visceral obesity in mice on high-fat diet," *Diabetes Research and Clinical Practice*, vol. 81, no. 2, pp. 134–143, 2008.

[24] C.-C. Shih, C.-H. Lin, and J.-B. Wu, "*Eriobotrya japonica* improves hyperlipidemia and reverses insulin resistance in high-fat-fed mice," *Phytotherapy Research*, vol. 24, no. 12, pp. 1769–1780, 2010.

[25] Q. W. Shen, C. S. Jones, N. Kalchayanand, M. J. Zhu, and M. Du, "Effect of dietary α-lipoic acid on growth, body composition, muscle pH, and AMP-activated protein kinase phosphorylation in mice," *Journal of Animal Science*, vol. 83, no. 11, pp. 2611–2617, 2005.

[26] M. A. Iglesias, J.-M. Ye, G. Frangioudakis et al., "AICAR administration causes an apparent enhancement of muscle

and liver insulin action in insulin-resistant high-fat-fed rats," *Diabetes*, vol. 51, no. 10, pp. 2886–2894, 2002.

[27] J.-M. Ye, N. B. Ruderman, and E. W. Kraegen, "AMP-activated protein kinase and malonyl-CoA: targets for treating insulin resistance?" *Drug Discovery Today*, vol. 2, no. 2, pp. 157–163, 2005.

[28] H.-G. Joost, G. I. Bell, J. D. Best et al., "Nomenclature of the GLUT/SLC2A family of sugar/polyol transport facilitators," *American Journal of Physiology: Endocrinology and Metabolism*, vol. 282, no. 4, pp. E974–E976, 2002.

[29] P. Daisy, K. Balasubramanian, M. Rajalakshmi, J. Eliza, and J. Selvaraj, "Insulin mimetic impact of Catechin isolated from *Cassia fistula* on the glucose oxidation and molecular mechanisms of glucose uptake on Streptozotocin-induced diabetic Wistar rats," *Phytomedicine*, vol. 17, no. 1, pp. 28–36, 2010.

[30] A. Barthel and D. Schmoll, "Novel concepts in insulin regulation of hepatic gluconeogenesis," *American Journal of Physiology: Endocrinology and Metabolism*, vol. 285, no. 4, pp. E685–E692, 2003.

[31] Y. Pan, J.-M. Zheng, H.-Y. Zhao, Y.-J. Li, H. Xu, and G. Wei, "Relationship between drug effects and particle size of insulin-loaded bioadhesive microspheres," *Acta Pharmacologica Sinica*, vol. 23, no. 11, pp. 1051–1056, 2002.

[32] T. Hayashi, M. F. Hirshman, E. J. Kurth, W. W. Winder, and L. J. Goodyear, "Evidence for 5′AMP-activated protein kinase mediation of the effect of muscle contraction on glucose transport," *Diabetes*, vol. 47, no. 8, pp. 1369–1373, 1998.

[33] E. J. Kurth-Kraczek, M. F. Hirshman, L. J. Goodyear, and W. W. Winder, "5′AMP-activated protein kinase activation causes GLUT4 translocation in skeletal muscle," *Diabetes*, vol. 48, no. 8, pp. 1667–1671, 1999.

[34] P. A. Lochhead, I. P. Salt, K. S. Walker, D. G. Hardie, and C. Sutherland, "5-Aminoimidazole-4-carboxamide riboside mimics the effects of insulin on the expression of the 2 key gluconeogenic genes PEPCK and glucose-6-phosphatase," *Diabetes*, vol. 49, no. 6, pp. 896–903, 2000.

[35] W. W. Winder, "AMP-activated protein kinase: possible target for treatment of type 2 diabetes," *Diabetes Technology & Therapeutics*, vol. 2, no. 3, pp. 441–448, 2000.

[36] Y. D. Kim, K.-G. Park, Y.-S. Lee et al., "Metformin inhibits hepatic gluconeogenesis through AMP-activated protein kinase-dependent regulation of the orphan nuclear receptor SHP," *Diabetes*, vol. 57, no. 2, pp. 306–314, 2008.

[37] S. Huang and M. P. Czech, "The GLUT4 glucose transporter," *Cell Metabolism*, vol. 5, no. 4, pp. 237–252, 2007.

[38] Y. Li, S. Xu, M. M. Mihaylova et al., "AMPK phosphorylates and inhibits SREBP activity to attenuate hepatic steatosis and atherosclerosis in diet-induced insulin-resistant mice," *Cell Metabolism*, vol. 13, no. 4, pp. 376–388, 2011.

[39] N. Henin, M.-F. Vincent, H. E. Gruber, and G. Van den Berghe, "Inhibition of fatty acid and cholesterol synthesis by stimulation of AMP- activated protein kinase," *The FASEB Journal*, vol. 9, no. 7, pp. 541–546, 1995.

[40] D. M. Muoio, K. Seefeld, L. A. Witters, and R. A. Coleman, "AMP-activated kinase reciprocally regulates triacylglycerol synthesis and fatty acid oxidation in liver and muscle: evidence that sn-glycerol-3-phosphate acyltransferase is a novel target," *Biochemical Journal*, vol. 338, no. 3, pp. 783–791, 1999.

[41] G. F. Merrill, E. J. Kurth, D. G. Hardie, and W. W. Winder, "AICA riboside increases AMP-activated protein kinase, fatty acid oxidation, and glucose uptake in rat muscle," *American Journal of Physiology: Endocrinology and Metabolism*, vol. 273, no. 6, pp. E1107–E1112, 1997.

[42] N. Musi, "AMP-activated protein kinase and type 2 diabetes," *Current Medicinal Chemistry*, vol. 13, no. 5, pp. 583–589, 2006.

[43] R. Zimmermann, J. G. Strauss, G. Haemmerle et al., "Fat mobilization in adipose tissue is promoted by adipose triglyceride lipase," *Science*, vol. 306, no. 5700, pp. 1383–1386, 2004.

[44] M. P. Gaidhu, S. Fediuc, N. M. Anthony et al., "Prolonged AICAR-induced AMP-kinase activation promotes energy dissipation in white adipocytes: novel mechanisms integrating HSL and ATGL," *The Journal of Lipid Research*, vol. 50, no. 4, pp. 704–715, 2009.

[45] M. Kato, N. Higuchi, and M. Enjoji, "Reduced hepatic expression of adipose tissue triglyceride lipase and CGI-58 may contribute to the development of non-alcoholic fatty liver disease in patients with insulin resistance," *Scandinavian Journal of Gastroenterology*, vol. 43, no. 8, pp. 1018–1019, 2008.

[46] H. Shimano, N. Yahagi, M. Amemiya-Kudo et al., "Sterol regulatory element-binding protein-1 as a key transcription factor for nutritional induction of lipogenic enzyme genes," *The Journal of Biological Chemistry*, vol. 274, no. 50, pp. 35832–35839, 1999.

[47] D. D. Patel, B. L. Knight, D. Wiggins, S. M. Humphreys, and G. F. Gibbons, "Disturbances in the normal regulation of SREBP-sensitive genes in PPARa-deficient mice," *Journal of Lipid Research*, vol. 42, no. 3, pp. 328–337, 2001.

[48] A. Suzuki, S. Okamoto, S. Lee, K. Saito, T. Shiuchi, and Y. Minokoshi, "Leptin stimulates fatty acid oxidation and peroxisome proliferator-activated receptor α gene expression in mouse C2C12 myoblasts by changing the subcellular localization of the α2 form of AMP-activated protein kinase," *Molecular and Cellular Biology*, vol. 27, no. 12, pp. 4317–4327, 2007.

[49] T. Tsuda, F. Horio, K. Uchida, H. Aoki, and T. Osawa, "Dietary cyanidin 3-O-β-D-glucoside-rich purple corn color prevents obesity and ameliorates hyperglycemia in mice," *The Journal of Nutrition*, vol. 133, no. 7, pp. 2125–2130, 2003.

[50] I. D. Postescu, C. Tatomir, G. Chereches et al., "Spectroscopic characterization of some grape extracts with potential role in tumor growth inhibition," *Journal of Optoelectronics and Advanced Materials*, vol. 9, no. 3, pp. 564–567, 2007.

[51] H.-C. Su, L.-M. Hung, and J.-K. Chen, "Resveratrol, a red wine antioxidant, possesses an insulin-like effect in streptozotocin-induced diabetic rats," *American Journal of Physiology: Endocrinology and Metabolism*, vol. 290, no. 6, pp. E1339–E1346, 2006.

[52] V. R. Drel and N. Sybirna, "Protective effects of polyphenolics in red wine on diabetes associated oxidative/nitrative stress in streptozotocin-diabetic rats," *Cell Biology International*, vol. 34, no. 12, pp. 1147–1153, 2010.

[53] R. T. R. Tan, S. Mohamed, G. F. Samaneh, M. M. Noordin, Y. M. Goh, and M. Y. A. Manap, "Polyphenol rich oil palm leaves extract reduce hyperglycaemia and lipid oxidation in STZ-rats," *International Food Research Journal*, vol. 18, no. 1, pp. 179–188, 2011.

Hindawi Publishing Corporation
Evidence-Based Complementary and Alternative Medicine
Volume 2013, Article ID 297154, 8 pages
http://dx.doi.org/10.1155/2013/297154

Research Article

Effect of Xiaoyaosan Decoction on Learning and Memory Deficit in Rats Induced by Chronic Immobilization Stress

Zhen-Zhi Meng,[1,2] Jia-Xu Chen,[1,3] You-Ming Jiang,[1] and Han-Ting Zhang[4]

[1] *School of Preclinical Medicine, Beijing University of Chinese Medicine, No. 11, Beisanhuan Donglu, Chaoyang, Beijing 100029, China*
[2] *School of Preclinical Medicine, Youjiang Medical University for Nationalities, Baise, Guangxi 533000, China*
[3] *Department of Basic Theory in Chinese Medicine, Henan University of Traditional Chinese Medicine, Zhengzhou 450008, China*
[4] *Department of Behavioral Medicine & Psychiatry, West Virginia University Health Sciences Center, Morgantown, WV 26506-9137, USA*

Correspondence should be addressed to Jia-Xu Chen; chenjiaxu@hotmail.com

Received 6 June 2013; Revised 16 October 2013; Accepted 16 October 2013

Academic Editor: Mohamed Eddouks

Xiaoyaosan (XYS) decoction is a famous prescription which can protect nervous system from stress and treat liver stagnation and spleen deficiency syndrome (LSSDS). In this experiment, we observed the effect of XYS decoction on chronic immobilization stress (CIS) induced learning and memory deficit in rats from behaviors and changes of proteins in hippocampus. We used XYS decoction to treat CIS induced learning and memory deficit in rats with rolipram as positive control, used change of body weight and behavioral tests to determine whether the rats have LSSDS and have learning and memory deficit or not. We used Western blotting to determine the content of postsynaptic density protein 95 (PSD-95) and synaptophysin (SYP) in hippocampus. Results showed that XYS could improve the situation of slow weight gain induced by CIS, improve the ability of learning and memory, reverse the symptom of liver stagnation and spleen deficiency syndrome (LSSDS) in rats, and increase the levels of PSD-95 and SYP on the hippocampal nerve synapses. These findings suggested that XYS decoction may be helpful in reversing CIS induced learning and memory deficit by increasing the levels of PSD-95 and SYP on the hippocampal nerve synapses and improving synaptic plasticity.

1. Introduction

Learning and memory deficit is a very important symptom in central nervous system injury [1, 2]. Hippocampal synaptic plasticity plays a key role in learning and memory [3]. Hippocampus is a target of stress [4]. CIS significantly decreases the hippocampal volume by 3%–6.3% [5, 6], attenuates long-term potentiation (LTP) in hippocampal slices [7], and causes hippocampal CA3 apical dendritic retraction which parallels spatial memory impairments in male rats [8]. CIS causes dendritic atrophy of the hippocampal pyramidal neurons and alterations in the levels of neurotransmitters in the hippocampus [9]. Research found 602 genes in the hippocampus were differentially expressed in CIS (3 h per day for a 7-day period) induced rats, as well as 566 genes in hippocampus were differentially expressed in CIS (3 h per day for a 21-day period) induced rats [10]. CIS can not only induce spatial learning and memory deficit [11], but also result in rats with liver stagnation and spleen deficiency syndrome (LSSDS) in traditional Chinese medicine [12].

Traditional Chinese medicine (TCM) has an active effect on chronic disease and psychiatry. XYS decoction which was created in Song Dynasty (960-1127 AD) contains *Radix Angelicae Sinensis, Poria, Radix Paeoniae Alba, Radix Glycyrrhizae, Radix Bupleuri, Rhizoma Atractylodis Macrocephalae, Herba Menthae, and Rhizoma Zingiberis Recens*. The chemical constituent of XYS includes peoniflorin, saikoside, ferulic acid, atractylol, glycyrrhetate, curcumin, and menthone [13]. XYS decoction has been mainly used to treat LSSDS and mental disorders in TCM clinic [14, 15]. The function of XYS decoction is to soothe the liver, improve the circulation of qi, relieve depression, strengthen the spleen, and nourish blood.

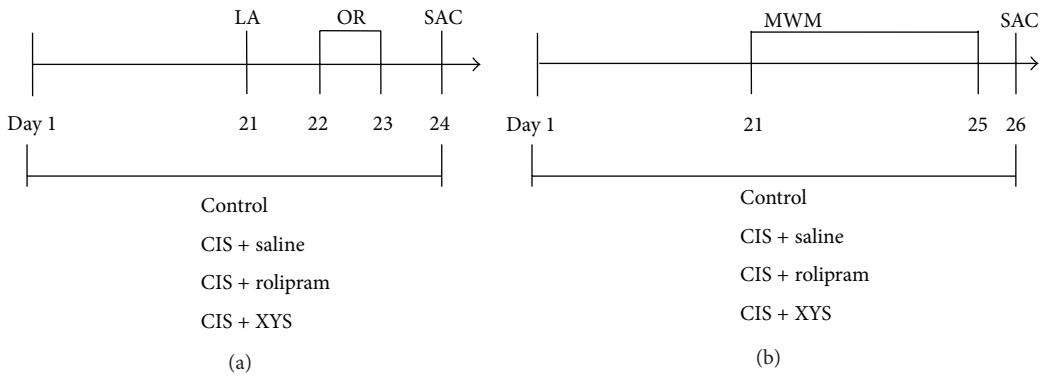

Figure 1: Schedule of drug treatments and behavioral tests. Saline and XYS were taken (i.g.) and rolipram (0.3 mg/kg) was injected (i.p.) once daily through the whole experiment. CIS was given 30 min after saline, XYS, or rolipram. Behavioral tests were carried out on day 21 (after the CIS). After all behavioral tests, animals were killed. (a) Schedule of drug treatments and behavioral tests except MWM test for rats. (b) Schedule of drug treatments and MWM test for rats. LA: locomotor activity. OR: object recognition. MWM: Morris water maze. SAC: sacrifice.

It is a safe and useful prescription in clinic. XYS decoction can protect nervous system from stress [16] and play a good role in the treatment of LSSDS [15, 17].

Our recently studies showed the XYS decoction reverse CIS-induced decreases in brain-derived neurotropic factor (BDNF) and increases tyrosine hydroxylase (TrkB) and neurotropic 3 (NT-3) in the frontal cortex and the hippocampal CA1 subregion [18]. The XYS decoction can significantly downregulate the contents of leptin and leptin receptor (*ob-R*) at the arcuate nucleus (ARC) in the basal of hypothalamus of chronic stressed rats [19]. Meanwhile, the XYS decoction containing serum significantly improves mitochondrial membrane potential and apoptotic rate of hippocampus neuron induced by oxidative stress [20].

The purpose of this study was to observe the effect of XYS decoction on chronic immobilization stress-induced learning and memory deficit in rats from behaviors and changes of proteins in hippocampus.

2. Materials and Method

2.1. Animal. Adult male Sprague-Dawley rats (Harlan, Indianapolis, IN.) weighing 227.2 ± 3.6 g (mean ± SD) were used for the experiments. Animals were housed in a temperature controlled room (22 ± 2°C) with a 12-h on/12-h off light cycle (lights on from 06:00 to 18:00). Water and food were freely available. All experiments were carried out according to the NIH Guide for the Care and Use of Laboratory Animals (NIH Publications No. 80-23, revised 1996). The procedures were approved by the Animal Care and Use Committees of West Virginia University Health Sciences Center.

2.2. Preparation of Extracts of the XYS Decoction. The XYS decoction consists of the following dried raw materials: 150 g of *Poria cocos* (Schw.) Wolf (Poria), 300 g of *Paeonia lactiflora* Pall. (Radix Paeoniae Alba), 150 g of *Glycyrrhiza uralensis* Fisch. (Radix Glycyrrhizae), 300 g of *Bupleurum chinense* DC. (Radix Bupleuri), 300 g of *Angelica sinensis* (Oliv.) Diels (Radix Angelicae Sinensis), 300 g of *Atractylodes macrocephala* Koidz. (Rhizoma Atractylodis macrocephalae), 100 g of *Mentha haplocalyx* Briq. (Herba Menthae), and 100 g of *Zingiber officinale* Rosc. (Rhizoma Zingiberis Recens). These eight herbs were purchased from Medicinal Materials Company of Beijing Tongrentang, processed in Sino-Japan Friendship Hospital (Beijing). We process herbs abiding by Regulation on Processing of Traditional Chinese Medical Herbal Pieces of Beijing.

2.3. Drugs and Treatments. XYS decoction (3.854 g/kg/d) was mixed by XYS powder and saline. Saline was mixed by NaCl (purchased from Fisher Scientific) and deionized water. The volume for XYS decoction or saline (i.g.) is 1 mL/100 g body weight. Rolipram was purchased from A. G. Scientific and was dissolved in saline containing 5% dimethyl sulfoxide (DMSO). The injection (i.p.) volume was 1 mL/kg body weight. Rolipram (0.3 mg/mL) was given once daily through the whole experiment.

Rats were divided into 4 groups, that is, control group, CIS + saline group, CIS + rolipram group, and CIS + XYS group. Every group had 10 rats. All groups, except control group, were immobilized for 3 hours per day through the whole experiment [11, 21, 22]. Saline or rolipram or XYS was given 30 min prior to CIS in the whole experiment. On 21st day, behavior tests such as locomotor activity, object recognition, or Morris water maze were taken after stress.

2.4. CIS Procedure. All groups, except the control group, were exposed to CIS. CIS was performed by putting rats in a breathable plastic decapicones for 3 h per day in the whole experiment until rats were sacrificed. It took first 21 days in the experiment to impair the ability of learning and memory and induce symptom of LSSDS in rats. The control group had access to food and water freely; however, food and water were not provided during stress.

2.5. Body Weight Monitoring and Behavioral Test Procedures. Body weight and general state were recorded before treatments. On day 21, behavior tests such as locomotor activity,

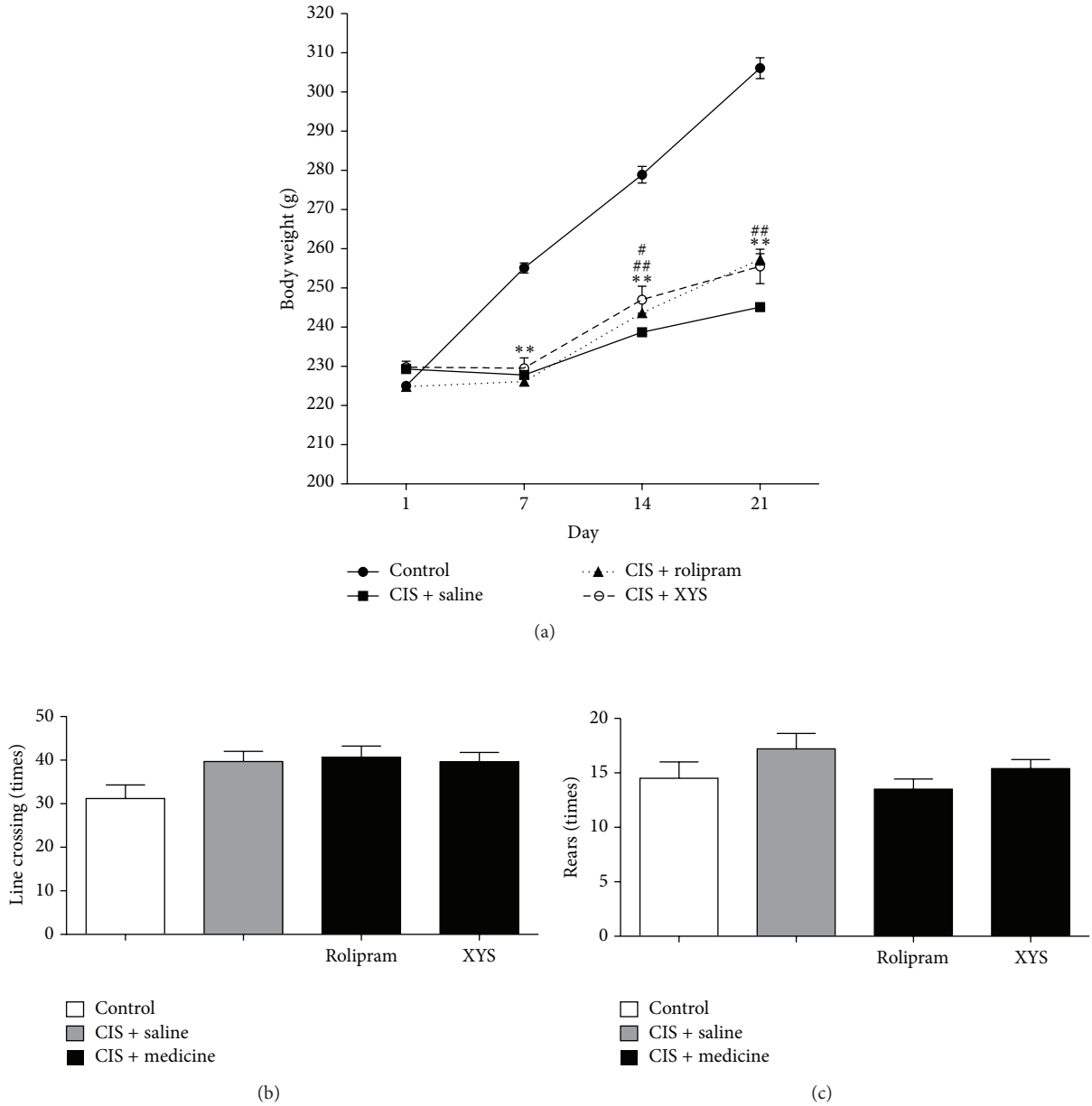

Figure 2: Effects of XYS on body weights and locomotor activity test. (a) After 1-week treatment, body weight gain of the CIS + saline group, and the CIS + rolipram group, the CIS + XYS group decreased markedly compared with that of the control group ($P < 0.01$). After 2-week treatment, body weight gain of the CIS + saline group, the CIS + rolipram group, and the CIS + XYS group increased compared with themselves after 1-week treatment. These differences were not significant. After 2-week treatment, body weight gain of the CIS + saline group, the CIS + rolipram group, and the CIS + XYS group decreased markedly compared with that of the control group ($P < 0.01$). Body weight gain of the CIS + XYS group increased compared with that of the CIS + saline group significantly ($P < 0.05$). After 3-week treatment, body weight gain of the CIS + saline group, the CIS + rolipram group, and the CIS + XYS group decreased markedly compared with that of the control group ($P < 0.01$). Body weight gain of the CIS + rolipram group and the CIS + XYS group increased compared with the CIS + saline group significantly ($P < 0.05$). (b) There is no significant difference between any two groups in four groups in locomotor activity, as assessed by line crossings and rears after stress on day 21. Values shown are means ± SD of ten rats per group. $^{**}P < 0.01$ versus the control group. $^{\#}P < 0.05$, $^{\#\#}P < 0.01$ versus the CIS + saline group.

object recognition, or Morris water maze were performed after stress. Rats were placed in the testing room 30 min before the behavioral tests for habituation. All the behavioral data were recorded manually by an unbiased observer.

2.5.1. Locomotor Activity Test. This was performed as described previously [23] with minor modifications. On day 21 (Figure 1(a)), after the stress rats were placed individually in a black wooden box (80 × 80 × 40 cm) which was with the

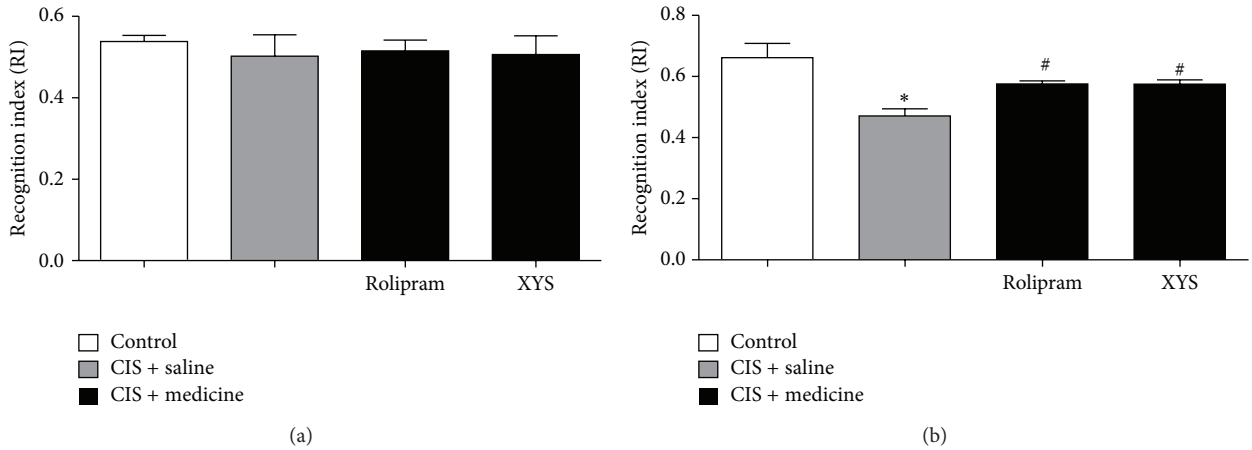

Figure 3: Effects of XYS on object recognition test. (a) There was no significant difference in RI between any two groups in the control group, the CIS + saline group, the CIS + rolipram group, and the CIS + XYS group when object A and object B were identical. (b) When object A was different from object C, RI of the CIS + saline group was lower than that of the control group significantly ($P < 0.05$). RIs of the CIS + rolipram group and the CIS + XYS group were higher than these of the CIS + saline group significantly ($P < 0.05$). Values shown are means ± SD of ten rats per group. $^{*}P < 0.05$ versus the control group. $^{\#}P < 0.05$ versus the CIS + saline group.

floor divided into four identical squares. Line crossings (with all four paws placed into a new square) and rears (with both front paws raised from the floor) were recorded in a 5-min period.

2.5.2. Object Recognition Test. The test was carried out as described previously [23]. On day 21 (Figure 1(a)), each rat was allowed to move freely in a black wooden box for 5 min as habituation; locomotor activity was simultaneously recorded (see locomotor activity test part). Twenty-four hours later, rats were individually placed in the center of the box containing two identical objects (Lego blocks) located in the two diagonal corners. The cumulative time spent in exploring each object (object A and object B) was recorded separately during 5-min period.

Exploration was defined as touching or smelling or being close to (within 2 cm) the object. On day 23, each rat was tested for memory using the same procedure except that one of the familiar objects was replaced with a totally novel object (object C replacing object B). The cumulative time spent in exploring each object was recorded, respectively, during 5-min period. Formula RI = $T2/(T1+T2)$ was used to calculate the recognition index (RI). $T2$ is the cumulative time in exploring object B or object C. $T1$ is the cumulative time in exploring object A.

2.5.3. Morris Water Maze Test. The role of XYS in memory was further confirmed using the Morris water maze test. This test was carried out as described previously [23]. The apparatus consisted of a circular, plastic pool (174 cm diameter, 72.5 cm high) located in a well-illuminated room with external cues visible from the inside of the pool, which was filled with opaque water (22–24°C). On day 21 (Figure 1(b)), a visible circular platform (10 cm diameter) was 2 cm higher than the water in one of the four quadrants. Rats were trained to escape by swimming to the platform. On day 22, a hidden circular platform (10 cm diameter) was submerged 2 cm under the water in one of four quadrants. The acquisition trials (training to escape to the hidden platform) were carried out for three consecutive days (6 trials for 2 days and 4 trials for 1 day) (Figure 1(b)). The latency (the time taken to climb onto the platform) for each rat was recorded and the cut-off time is 90 sec. On day 25, the probe trial was performed with the platform removed to assess spatial memory. Rat was allowed to swim for 90 sec. The numbers of entries into the target quadrant and time spent in the target quadrant where the platform was previously located were recorded.

2.6. Western Blotting. Hippocampal tissues were processed and Western blot analysis was performed as described previously [24]. Samples were separated using SDS-PAGE and then transferred to PVDF membranes. Sample loading quantity for PSD-95 is 10 μg and that for SYP is 3 μg. Membranes were incubated with Mouse Anti-PSD-95 (1 : 500) or Mouse Anti-Synaptophysin (1 : 50000). Both of antibodies were purchased from BD Transduction Laboratories. Beta-actin (1 : 1000) was purchased from Sigma. Membranes were incubated overnight with primary antibodies. After washing, the membranes were incubated with goat anti-mouse secondary antibody (1 : 10000, Li-COR) for 1 h. The detection and quantification of specific bands were carried out using a fluorescence scanner (Odyssey Infrared Imaging System, LI-COR Biotechnology) at 800 nm wavelength.

2.7. Statistical Analysis. Data shown were expressed as mean value ± standard deviation (SD) and analyzed using one-way ANOVA except for the data of the body weight and acquisition training of the Morris water maze, which were analyzed by two-way ANOVA. Newman-Keuls tests were used for post hoc multiple treatment comparisons. Statistical significance was considered when $P < 0.05$.

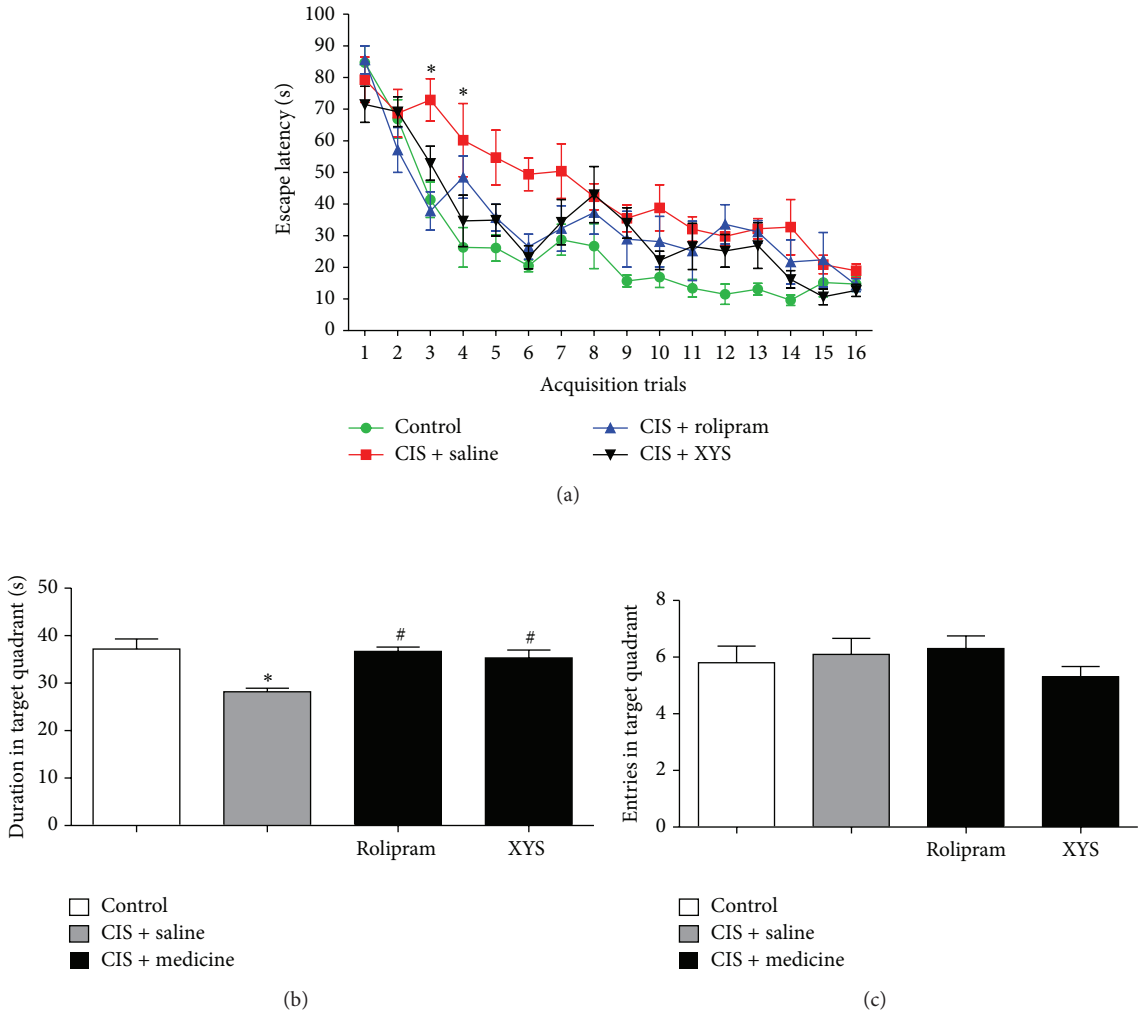

FIGURE 4: Effects of XYS on Morris water maze. (a) During the 3-day acquisition training, all the rats displayed progressive decreases in the escape latency to reach the hidden platform. Overall statistic compared by two-way ANOVA did not reveal significant changes, except in the 3rd and 4th acquisition trials ($P < 0.05$). (b) In the probe trial test performed 24 h after the last acquisition trial, CIS + saline group displayed significant decrease compared with the control group ($P < 0.05$) in duration in target quadrant. CIS + rolipram group and CIS + XYS group displayed significant increase compared with CIS + saline group ($P < 0.05$) in duration in target quadrant. (c) As entries in target quadrant, there are no significant changes in groups. Values shown are means ± SD of ten rats per group. $^{*}P < 0.05$ versus the control group. $^{\#}P < 0.05$ versus the CIS + saline group.

3. Results

3.1. Effects of XYS on Body Weights and Locomotor Activity Test. In this experiment, body weights of rats were monitored throughout 21 days to evaluate the potential effect of XYS. Body weight gain in all groups except the control group tended to be decreased statistically from the control group through whole 21 days. After 2-week and 3-week treatments, XYS and rolipram led to a slower gain of body weights. (Figure 2(a)) The treatment did not display significant changes in locomotor activity (Figures 2(b) and 2(c)).

3.2. Effects of XYS on Object Recognition Test. In this experiment, rats in the CIS + saline group displayed worse recognition index in object recognition test compared with the control group. Rolipram or XYS treatments increased the recognition index compared with the CIS + saline group (Figure 3).

3.3. Effects of XYS on Morris Water Maze. In the experiment, rats displayed progressive decreases in the escape latency to reach the hidden platform during the 3-day acquisition training, especially in the 3rd and 4th acquisition trials for the CIS + saline group (Figure 4(a)). CIS + saline group displayed significant decrease compared with the control group in duration in target quadrant. CIS + rolipram group and CIS + XYS group displayed significant increase compared with the CIS + saline group in duration in target quadrant (Figure 4(b)). As entries in target quadrant, there are no significant changes in groups (Figure 4(c)).

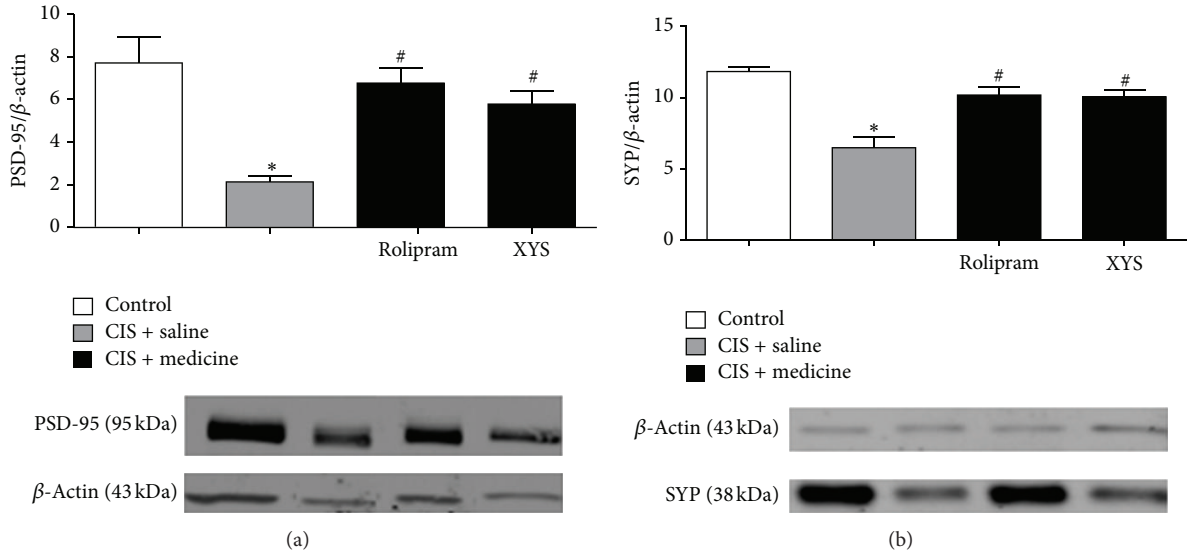

Figure 5: Effect of XYS on PSD-95, SYP in the hippocampus. Changes in expression of PSD-95 (a) or SYP (b) in the hippocampus. Bottom panels were representative immunoblots of PSD-95 or SYP detected by Western blotting. Top panels were the corresponding quantification. (a) PSD-95 in the CIS + saline group displayed decrease significantly in the hippocampus compared with that in the control group ($P < 0.05$). PSD-95 in the CIS + rolipram group and CIS + XYS group displayed increase significantly compared with that in the CIS + saline group ($P < 0.05$). (b) SYP in the CIS + saline group displayed decrease significantly in the hippocampus compared with that in the control group ($P < 0.05$). SYP in the CIS + rolipram group and CIS + XYS group displayed increase significantly compared with that in the CIS + saline group ($P < 0.05$). Values shown are means ± SD of ten rats per group. Values shown are means ± SD of ten rats per group. $^{*}P < 0.05$ versus the control group. $^{\#}P < 0.05$ versus the CIS + saline group.

3.4. Effect of XYS on PSD-95, SYP in the Hippocampus. In this experiment, Western blotting results indicated that the CIS + saline group displayed decrease significantly in PSD-95 (Figure 5(a)) and SYP (Figure 5(b)) in the hippocampus compared with the control group. The CIS + rolipram group and CIS + XYS group displayed significant increase in PSD-95 (Figure 5(a)) and SYP (Figure 5(b)) in the hippocampus compared with the CIS + saline group (Figure 5).

4. Discussion

The purpose of this experiment was to dig out the mechanism of XYS on CIS induced learning and memory deficit in rats.

In TCM, the syndrome of stagnation of liver qi can lead to poor digestion and weight loss [25]. CIS can slow weight gain of rats; especially CIS was given in the morning [26, 27]. Symptoms of LSSDS include poor digestion, weight loss, diarrhea, bad appetite, and so on. Stress exposure 3 hours per day for 21 days leads to LSSDS, XYS decoction can soothe the liver and strengthen the spleen, and our previous study suggests that leptin receptor (ob-R) in the arcuate nucleus may act as the target of XYS in regulating the symptoms such as appetite and bodyweight loss under chronic stress with LSSDS [19]. Normal function of the liver and the spleen plays a beneficial role in turning the foods and drinks into nutrition. Nutrition can not only keep physical normality such as regular weight gain but also keep mental health such as memory and learning.

CIS leads to learning and memory deficit in object recognition test [28]. Chronic stress prolongs the latent period and decreases the times crossing the target quadrant in Morris water maze [29]. Chronic multiple stress can prolong the escape latency and duration of exploring in the target quadrant [30]. The memory enhancing effect of XYS is verified in Morris water maze task [31, 32].

Synaptic plasticity is the important part of neurobiology for learning and memory ability [33]. Synapse is the key to neuron networking and information transmission [34]. Reduction of neuronal synaptic plasticity and function deficit do harm to the ability of learning and memory [35]. PSD-95 is the postsynaptic membrane marker and SYP is the presynaptic membrane marker [36].

PSD-95 knocked out mice or PSD-95-mutant mice have LTP and learning and memory deficit [37, 38]. Chronic restraint stress leads to PSD-95 decreases in hippocampal CA3 areas of rats and the stress leads to the impairment of learning and memory ability [39]. Analog 165 can obviously improve the learning and memory ability and also increase the expression of PSD-95 [40]. Environmental enrichment significantly improves the memory damage induced by cerebral ischemia and upregulated the expression of PSD-95 mRNA in the ipsilateral cortex and hippocampus of occluding the right middle cerebral artery rats [41].

Immobilization stress exposure decreases expression of SYP in the hippocampus [42]. Patients with Alzheimer's disease were found that their PSD-95 and SYP decrease in the hippocampus [43, 44]. Cognitive decline of patients

with Alzheimer's disease correlates with changes in the hippocampus and the content of cortical presynaptic vesicle protein SYP content [45, 46].

The above data suggested that XYS could improve the situation of slow weight gain induced by CIS, improve the ability of learning and memory, reverse the symptom of liver stagnation and spleen deficiency syndrome (LSSDS) in rats, and increase the levels of PSD-95 and SYP on the hippocampal nerve synapses to improve synaptic plasticity. Several groups of bioactive nature products have been identified from the herbs in the XYS decoction as cited by our previous published paper [18], combined with our previously reported data that XYS decoction ameliorates impairment of cellular plasticity and resilience underlying pathophysiology of mood disorders [18], and there were some inclusions appearing that low-dose XYS (1.927 g/kg/d) decoction containing serum decreases apoptotic rate of neuron significantly *in vitro* and XYS decoction (3.854 g/kg/d) improved chronic immobilization stress induced learning and memory deficit *in vivo* [20].

Further studies will be focused on the relationship between different doses of XYS decoction serum concentration and improvement of learning and memory deficit induced by CIS in rats.

Ethical Approval

The study was approved by the Ethics Committee of Beijing University of Chinese Medicine in China.

Conflict of Interests

There is no conflict of interests.

Acknowledgments

This work was supported by the National Natural Science Foundation of China (No. 30672578 and No. 81072756), the China National Funds for Distinguished Young Scientists (No. 30825046), and the Program for Innovative Research Team in Beijing University of Chinese Medicine (2011CXTD-07) to Jia-Xu Chen.

References

[1] P. Ballerini, P. Di Iorio, F. Caciagli et al., "P2Y2 receptor up-regulation induced by guanosine or UTP in rat brain cultured astrocytes," *International Journal of Immunopathology and Pharmacology*, vol. 19, no. 2, pp. 293–308, 2006.

[2] W. Zhu, K. J. Mantione, F. M. Casares, M. H. Sheehan, R. M. Kream, and G. B. Stefano, "Cholinergic regulation of endogenous morphine release from lobster nerve cord," *Medical Science Monitor*, vol. 12, no. 9, pp. BR295–BR301, 2006.

[3] S. J. Martin, P. D. Grimwood, and R. G. M. Morris, "Synaptic plasticity and memory: an evaluation of the hypothesis," *Annual Review of Neuroscience*, vol. 23, pp. 649–711, 2000.

[4] J. J. Kim and D. M. Diamond, "The stressed hippocampus, synaptic plasticity and lost memories," *Nature Reviews Neuroscience*, vol. 3, no. 6, pp. 453–462, 2002.

[5] T. Lee, T. Jarome, S. J. Li, J. J. Kim, and F. J. Helmstetter, "Chronic stress selectively reduces hippocampal volume in rats: a longitudinal magnetic resonance imaging study," *NeuroReport*, vol. 20, no. 17, pp. 1554–1558, 2009.

[6] B. N. Srikumar, T. R. Raju, and B. S. S. Rao, "Contrasting effects of bromocriptine on learning of a partially baited radial arm maze task in the presence and absence of restraint stress," *Psychopharmacology*, vol. 193, no. 3, pp. 363–374, 2007.

[7] D. T. Radecki, L. M. Brown, J. Martinez, and T. J. Teyler, "BDNF protects against stress-induced impairments in spatial learning and memory and LTP," *Hippocampus*, vol. 15, no. 2, pp. 246–253, 2005.

[8] K. J. McLaughlin, J. L. Gomez, S. E. Baran, and C. D. Conrad, "The effects of chronic stress on hippocampal morphology and function: an evaluation of chronic restraint paradigms," *Brain Research*, vol. 1161, no. 1, pp. 56–64, 2007.

[9] K. Ramkumar, B. N. Srikumar, B. S. S. Rao, and T. R. Raju, "Self-stimulation rewarding experience restores stress-induced CA3 dendritic atrophy, spatial memory deficits and alterations in the levels of neurotransmitters in the hippocampus," *Neurochemical Research*, vol. 33, no. 9, pp. 1651–1662, 2008.

[10] X. H. Li, J. X. Chen, G. X. Yue et al., "Gene expression profile of the hippocampus of rats subjected to chronic immobilization stress," *PLoS ONE*, vol. 8, no. 3, Article ID e57621, 2013.

[11] H. N. Wang, X. Jin, H. Zheng et al., "The effect of different intensity and duration of chronic immobilization stress on the ability of special learning and memory in rats," *Chinese Journal of Behavioral Medical Science*, vol. 17, no. 8, pp. 691–693, 2008.

[12] W. Li, J. X. Chen, J. X. Yang et al., "The effect of compounds of soothing liver, invigorating spleen, tonifying kidney on the praxiology and immunological function of chronic immobilization stressed rats," *Acta Laboratorium Animalis Scientia Sinica*, vol. 11, no. 1, pp. 251–252, 2003.

[13] M. T. Li and H. Xiang, "Advances in effective ingredients and pharmacological action of Xiaoyao Pill or Xiaoyao San research," *Journal of Chinese Medicinal Materials*, vol. 33, no. 12, pp. 1968–1972, 2010.

[14] J. X. Chen, B. Ji, Z. Lu, and L. S. Hu, "Effects of Chai Hu (Radix Burpleuri) containing formulation on plasma β-endorphin, epinephrine and dopamine in patients," *The American Journal of Chinese Medicine*, vol. 33, no. 5, pp. 737–745, 2005.

[15] H. Zhao, X. Wan, and J. Chen, "A mini review of traditional Chinese medicine for the treatment of depression in China," *The American Journal of Chinese Medicine*, vol. 37, no. 2, pp. 207–213, 2009.

[16] W. Li and J. X. Chen, "Changes of BDNF TrkB NT3 in hippocampus of rats of chronic immobilization stress model and effect of Xiaoyaosan," *Chinese Archives of Traditional Chinese Medicine*, vol. 23, no. 7, pp. 1205–1208, 2005.

[17] W. F. Zhu and Q. H. He, *The Modern TCM Clinical Diagnostics*, People's Health Publishing House, Beijing, China, 2003.

[18] J. X. Chen, W. Li, X. Zhao, and J. X. Yang, "Effects of the Chinese traditional prescription Xiaoyaosan decoction on chronic immobilization stress-induced changes in behavior and brain BDNF, TrkB, and NT-3 in rats," *Cellular and Molecular Neurobiology*, vol. 28, no. 5, pp. 745–755, 2008.

[19] S. X. Wang, J. X. Chen, G. X. Yue, M. H. Bai, M. J. Kou, and Z. Y. Jin, "Xiaoyaosan decoction regulates changes in neuropeptide Y and leptin receptor in the rat arcuate nucleus after chronic immobilization stress," *Evidence-Based Complementary and Alternative Medicine*, vol. 2012, Article ID 381278, 16 pages, 2012.

[20] Z. Z. Meng, J. H. Hu, J. X. Chen, and G. X. Yue, "Xiaoyaosan decoction, a traditional Chinese medicine, inhibits oxidative-stress-induced hippocampus neuron apoptosis in vitro," *Evidence-Based Complementary and Alternative Medicine*, vol. 2012, Article ID 489254, 8 pages, 2012.

[21] B. M. Andrus, K. Blizinsky, P. T. Vedell et al., "Gene expression patterns in the hippocampus and amygdala of endogenous depression and chronic stress models," *Molecular Psychiatry*, vol. 17, no. 1, pp. 49–61, 2012.

[22] J. Thome, B. Pesold, M. Baader et al., "Stress differentially regulates synaptophysin and synaptotagmin expression in hippocampus," *Biological Psychiatry*, vol. 50, no. 10, pp. 809–812, 2001.

[23] Y. F. Li, Y. F. Cheng, Y. Huang et al., "Phosphodiesterase-4D knock-out and RNA interference-mediated knock-down enhance memory and increase hippocampal neurogenesis via increased cAMP signaling," *Journal of Neuroscience*, vol. 31, no. 1, pp. 172–183, 2011.

[24] R. K. Carlin, D. J. Grab, R. S. Cohen, and P. Siekevitz, "Isolation and characterization of postsynaptic densities from various brain regions: enrichment of different types of postsynaptic densities," *Journal of Cell Biology*, vol. 86, no. 3, pp. 831–845, 1980.

[25] C. Yan, Z. C. Zhang, and Z. Y. Deng, "Clinical and experimental study of immunological mechanism of 'liver bears the dispersive effect'," *Chinese Journal of Basic Medicine in Traditional Chinese Medicine*, vol. 1, no. 3, p. 36, 1995.

[26] B. M. Andrus, K. Blizinsky, P. T. Vedell et al., "Gene expression patterns in the hippocampus and amygdala of endogenous depression and chronic stress models," *Molecular Psychiatry*, vol. 17, no. 1, pp. 49–61, 2012.

[27] I. I. Rybkin, Y. Zhou, J. Volaufova, G. N. Smagin, D. H. Ryan, and R. B. S. Harris, "Effect of restraint stress on food intake and body weight is determined by time of day," *The American Journal of Physiology—Regulatory Integrative and Comparative Physiology*, vol. 273, no. 5, pp. R1612–R1622, 1997.

[28] K. D. Beck and V. N. Luine, "Food deprivation modulates chronic stress effects on object recognition in male rats: role of monoamines and amino acids," *Brain Research*, vol. 830, no. 1, pp. 56–71, 1999.

[29] Y. Y. Cai, W. G. Zhang, and S. X. Shi, "Effects of chronic stress on learning ability and expression of neuronal cell adhesion molecule in hippocampus in rats," *Shanghai Archives of Psychiatry*, vol. 20, no. 5, pp. 285–287, 2008.

[30] G. Zheng, W. J. Luo, Y. M. Chen, M. C. Liu, J. L. Ma, and J. Y. Chen, "Effects of chronic multiple stress on learning and memory and the expression and phosphorylation of cerebral ERK of rats," *Chinese Journal of Applied Physiology*, vol. 27, no. 1, pp. 33–36, 2011.

[31] R. G. M. Morris, P. Garrud, J. N. P. Rawlins, and J. O'Keefe, "Place navigation impaired in rats with hippocampal lesions," *Nature*, vol. 297, no. 5868, pp. 681–683, 1982.

[32] M. Remodes and E. M. Schuman, "Role for a cortical input to hippocampal area CA1 in the consolidation of a long-tem memory," *Nature*, vol. 431, no. 7009, pp. 699–703, 2004.

[33] C. G. Zhu, *Neuroanatomy*, People's Health Publishing House, Beijing, China, 2002.

[34] J. H. Kim, Y. K. Park, J. H. Kim, T. H. Kwon, and H. S. Chung, "Transient recovery of synaptic transmission is related to rapid energy depletion during hypoxia," *Neuroscience Letters*, vol. 400, no. 1-2, pp. 1–6, 2006.

[35] P. Coleman, H. Federoff, and R. Kurlan, "A focus on the synapse for neuroprotection in Alzheimer disease and other dementias," *Neurology*, vol. 63, no. 7, pp. 1155–1162, 2004.

[36] T. G. Oliveira, R. B. Chan, H. Tian et al., "Phospholipase D2 ablation ameliorates Alzheimer's disease-linked synaptic dysfunction and cognitive deficits," *Journal of Neuroscience*, vol. 30, no. 49, pp. 16419–16428, 2010.

[37] M. B. Kennedy, "Signal-processing machines at the postsynaptic density," *Science*, vol. 290, no. 5492, pp. 750–754, 2000.

[38] M. Migaud, P. Charlesworth, M. Dempster et al., "Enhanced long-term potentiation and impaired learning in mice with mutant postsynaptic density-95 protein," *Nature*, vol. 396, no. 6710, pp. 433–439, 1998.

[39] M. Liao, N. B. Liu, M. H. Zhang et al., "The change of synapsin and PSD 95 expression in the hippocampal neurons of rats with learning and memory impairment by chronic restraint stress," *Journal of Huazhong University of Science and Technology (Health Science Edition)*, vol. 32, no. 4, pp. 367–370, 2003.

[40] S. Lu, Y. P. Lei, P. W. Wang, R. Wang, S. L. Sheng, and J. Z. Tian, "The effects of analog 165 of APP 5-mer peptide on praxiology, expression of PSD95 and Shank 1 in Alzheimer disease rats," *Chinese Journal Neuroimmunology and Neurology*, vol. 14, no. 4, pp. 183–187, 2007.

[41] L. J. Ye, X. H. Xu, Y. M. Wang et al., "The effects of enriched environment on structural modification of synaptic interface and PSD-95 mRNA of rats after transient focal cerebral ischemia," *Acta Psychologica Sinica*, vol. 40, no. 6, pp. 709–716, 2008.

[42] J. Thome, B. Pesold, M. Baader et al., "Stress differentially regulates synaptophysin and synaptotagmin expression in hippocampus," *Biological Psychiatry*, vol. 50, no. 10, pp. 809–812, 2001.

[43] R. D. Terry, E. Masliah, D. P. Salmon et al., "Physical basis of cognitive alterations in Alzheimer's disease: synapse loss is the major correlate of cognitive impairment," *Annals of Neurology*, vol. 30, no. 4, pp. 572–580, 1991.

[44] C. Sze, J. C. Troncoso, C. Kawas, P. Mouton, D. L. Price, and L. J. Martin, "Loss of the presynaptic vesicle protein synaptophysin in hippocampus correlates with cognitive decline in Alzheimer disease," *Journal of Neuropathology and Experimental Neurology*, vol. 56, no. 8, pp. 933–944, 1997.

[45] I. Antonova, O. Arancio, A. Trillat et al., "Rapid increase in clusters of presynaptic proteins at onset of long-lasting potentiation," *Science*, vol. 294, no. 5546, pp. 1547–1550, 2001.

[46] L. K. Siew, S. Love, D. Dawbarn, G. K. Wilcock, and S. J. Allen, "Measurement of pre- and post-synaptic proteins in cerebral cortex: effects of post-mortem delay," *Journal of Neuroscience Methods*, vol. 139, no. 2, pp. 153–159, 2004.

Hindawi Publishing Corporation
Evidence-Based Complementary and Alternative Medicine
Volume 2013, Article ID 948627, 10 pages
http://dx.doi.org/10.1155/2013/948627

Research Article

Metabolic Effects of Mulberry Leaves: Exploring Potential Benefits in Type 2 Diabetes and Hyperuricemia

A. Hunyadi,[1] E. Liktor-Busa,[1] Á. Márki,[2] A. Martins,[3,4] N. Jedlinszki,[1] T. J. Hsieh,[5] M. Báthori,[1] J. Hohmann,[1] and I. Zupkó[2]

[1] *Institute of Pharmacognosy, Faculty of Pharmacy, University of Szeged, Eötvös u. 6, Szeged 6720, Hungary*
[2] *Department of Pharmacodynamics and Biopharmacy, Faculty of Pharmacy, University of Szeged, Eötvös u. 6, Szeged 6720, Hungary*
[3] *Department of Medical Microbiology and Immunobiology, Faculty of Medicine, University of Szeged, Dóm tér 13, Szeged 6720, Hungary*
[4] *Unidade de Parasitologia e Microbiologia Médica, Instituto de Higiene e Medicina Tropical, Universidade Nova de Lisboa, Rua da Junqueira 100, 1349-008 Lisboa, Portugal*
[5] *Department of Genome Medicine, College of Medicine, Kaohsiung Medical University, Shih Chuan 1st Rd. 100, Kaohsiung 807, Taiwan*

Correspondence should be addressed to A. Hunyadi; hunyadi.a@pharm.u-szeged.hu and I. Zupkó; zupko@pharm.u-szeged.hu

Received 24 July 2013; Accepted 18 October 2013

Academic Editor: C. S. Cho

The leaves of *Morus alba* L. have a long history in Traditional Chinese Medicine and also became valued by the ethnopharmacology of many other cultures. The worldwide known antidiabetic use of the drug has been suggested to arise from a complex combination effect of various constituents. Moreover, the drug is also a potential antihyperuricemic agent. Considering that type 2 diabetes and hyperuricemia are vice-versa in each other's important risk factors, the use of mulberry originated phytotherapeutics might provide an excellent option for the prevention and/or treatment of both conditions. Here we report a series of relevant *in vitro* and *in vivo* studies on the bioactivity of an extract of mulberry leaves and its fractions obtained by a stepwise gradient on silica gel. *In vivo* antihyperglycemic and antihyperuricemic activity, plasma antioxidant status, as well as *in vitro* glucose consumption by adipocytes in the presence or absence of insulin, xanthine oxidase inhibition, free radical scavenging activity, and inhibition of lipid peroxidation were tested. Known bioactive constituents of *M. alba* (chlorogenic acid, rutin, isoquercitrin, and loliolide) were identified and quantified from the HPLC-DAD fingerprint chromatograms. Iminosugar contents were investigated by MS/MS, 1-deoxynojirimycin was quantified, and amounts of 2-*O*-alpha-D-galactopyranosyl-1-deoxynojirimicin and fagomine were additionally estimated.

1. Introduction

Chronically elevated uric acid concentration in the serum has impact on human health at various levels; it frequently leads to the development of gout [1], and it is a relevant risk factor of several further chronic diseases. For example, it represents a significant risk for various cardiovascular and cerebrovascular diseases [2–4], and a tight connection between hyperuricemia and diabetes has recently been revealed; apparently, these two diseases mutually increase each other's incidence [5]. Hyperinsulinemia in type 2 diabetes can significantly increase reabsorption of uric acid in the proximal tubules, while its overproduction due to an increased activity of xanthine-oxidase usually also takes place [5, 6]. On the other hand, high uric acid levels might predict the development of metabolic syndrome consequentially leading to diabetes [7, 8] and can also increase severity of the already developed disease by leading to a higher incidence of certain diabetic complications [9]. The mechanism by which these metabolic states are interconnected seems yet to be clarified, although there is evidence that hyperuricemia, metabolic syndrome, and type II diabetes share the same causal origin in which insulin resistance would play a key role [5]. Anyhow, development of novel therapeutic agents targeting both diabetes

and hyperuricemia appears to be a highly relevant strategy for overcoming difficulties attributed to the current therapeutic approaches. Appropriately chosen phytotherapeutics [10, 11], representing complex bioactivity profiles, might serve as excellent tools to fulfill this objective, either as monotherapy or in combination with already existing approaches.

Mulberry leaves are probably best known by their role in the silk production, but medicinal use of this drug also dates back at least two thousand years; it is already mentioned in the "Divine Farmer's Materia Medica" (pinyin: Shénnóng Běncǎo Jīng) written during the reign of the Han dynasty. In Traditional Chinese Medicine, leaves of *M. alba* possess sweet, slightly bitter, and slightly cold properties, and their primary uses are described as "to expel wind and heat from the lungs, as well as to clear the liver and the eyes" [12]. Anti-diabetic use of mulberry leaves had also been popular; moreover, this indication became part of the local traditional medicine wherever the tree has been naturalized [13–16]. Based on this, a large number of herbal preparations (including many food supplements) are worldwide available for diabetes treatment and easily accessible to everyone even via online shopping. This activity of mulberry leaves has been verified by a number of studies including several animal experiments [14–16] and a few human trials as well [17, 18], but, to our knowledge, the active constituents and their role in the activity still remain to be fully described. Nevertheless, a complex cocktail of various bioactive constituents is thought to be responsible for this activity [19], among which the role of iminosugars [18] and certain phenolics mainly chlorogenic acid and rutin [16] might be the most significant.

Furthermore, several traditional Chinese preparations utilize the branch of *Morus alba* for the treatment of gout, arthritis, and rheumatism [20]. Various constituents of the drug were found to have significant antihyperuricemic potential, including mulberroside A, a stilbene glycoside [21], and a number of flavonoids, primarily morin [22, 23].

Based on the above, our objectives were to explore the potential of *Morus alba* leaves as dual-target phytotherapeutics to prevent and treat both diabetes and hyperuricemia and to investigate whether a simple chromatographic fractionation can lead to the enrichment of the main bioactive constituents valuable for both therapeutic targets of interest.

2. Materials and Methods

2.1. Plant Material, Chemicals, and Reagents. The leaves of *Morus alba* were collected near Ásotthalom (nearby Szeged, Hungary) in May, 2007, and botanically identified by A. Hunyadi. A voucher specimen (MA052007) was deposited in the Institute of Pharmacognosy, University of Szeged, Szeged, Hungary. All chemicals, if otherwise not specified, were purchased from Sigma-Aldrich (Budapest, Hungary). Rutin (**2**) and isoquercitrin (**3**) were purchased from ChromaDex (Irvine, CA, USA) and Extrasynthése (Genay, France), respectively. Loliolide (**4**) was previously isolated from the dry leaves of *Morus alba* [19], and 1-Deoxynojirimicin (1-DN) was purchased from Wako Pure Chemical Industries (Osaka, Japan). HPLC grade methanol was obtained from Fischer Scientific; ultrapure water was obtained by using a Millipore Direct-Q UV3 equipment.

2.2. Extraction and Chromatographic Fractionation. 2.5 kg of the dried and ground plant material was extracted by percolation with 30 L of 70% aqueous methanol and the solvent was evaporated under vacuum at 50°C to obtain 675.36 g dry extract (EX). 170 g of the dry material was further processed; it was dissolved in 1000 mL of water and extracted with 10 × 500 mL of n-butanol. After solvent evaporation, dry residue of the aqueous (FR-W) and organic phase (FR-B) was 78.4 and 88.09 g, respectively. The butanol phase was adsorbed onto triple amount (276 g) of silica (Kieselgel 60, Merck, Darmstadt, Germany) and administered on the top of a previously prepared silica column of 1840 g. A stepwise gradient of CH_2Cl_2, CH_2Cl_2 : EtOH (95 : 5, 9 : 1, 8 : 2, 7 : 3, 6 : 4, and 1 : 1), and EtOH was used, and one single fraction per solvent was collected. After the first fraction of 18 L, each following was of 10 L volume. After solvent evaporation, dry residues of the fractions were 13.72, 9.76, 4.48, 8.19, 10.52, 9.93, 5.50, and 10.87 g, respectively. Based on high similarities in their TLC fingerprints, the last three fractions were joined; hence, finally six fractions, referred to as FR1-6, were used for the experiments discussed here.

2.3. HPLC-DAD Analysis of Fractions FR1-6. Diode-array detected high performance liquid chromatography (HPLC-DAD) was performed on a gradient system of two Jasco PU2080 pumps connected to a Jasco MD-2010 Plus diode-array detector (DAD) and equipped with a Jasco AS-2055Plus autosampler (Jasco Co., Tokyo, Japan), by using a Zorbax Eclipse XDB-C8 (5 μm, 4.6 × 150 mm) analytical column. Samples were dissolved in 30% of aqueous MeOH at 2 mg/mL, and 30 μL of each was injected. Gradient elution was performed from 30 to 100% of aqueous MeOH in 13 minutes, kept at 100% for four more minutes, and returned to 30% at 17.1 min. Chromatograms were recorded for 24 min, and DAD data was collected from 200 to 650 nm. Baselines were corrected by subtracting the chromatogram of a single 30 μL injection of 30% MeOH.

*2.4. Quantitative Analysis of Compounds **1–4**.* Single-point quantitative analysis was performed for the previously identified major constituents in their respective fractions such as chlorogenic acid (**1**), rutin (**2**), and isoquercitrin (**3**) in EX, FR-B and FR5-6 and loliolide (**4**) in FR2. Calibration curves were taken by analysing dilutions of a 1 mg/mL stock solution of the corresponding standard, at concentrations of 1, 0.5, 0.4, 0.3, 0.2, 0.1, and 0.05 mg/mL. R^2 values were 0.9970, 0.9990, 0.9904, and 0.9978 for the calibration lines of **1–4**, respectively. In case of FR5 and FR6, peaks of **2** and **3** were partially overlapping; deconvolution was performed by using Gaussian approximations with the Fityk 0.9.7 software (Free Software Foundation, Poland) and quantities were calculated based on the peak areas revealed this way.

2.5. Determination of Iminosugars. Iminosugar content was qualitatively investigated by thin-layer chromatography

(TLC) in each fraction, by using DC-Alufolien Kieselgel $60F_{254}$ plates (Merck, Darmstadt, Germany) and CH_2Cl_2 : MeOH : NH_3 (3 : 6 : 2, v/v/v) as solvent system. For quantitative analysis, an API 2000 MS/MS spectrometer was used with a Shimadzu autosampler and an electrospray ionization (ESI) interface set in positive mode. 1-DN, 2-*O*-alpha-D-galactopyranosyl-1-deoxynojirimicin (Gal-DN), and fagomine contents were investigated in FR-W, FR-B, and FR4-6. Injected samples were washed into the spectrometer with 50% aqueous MeOH at a flow rate of 200 μL/min; temperature of the ion source was 300°C. Multiple reaction monitoring (MRM) was used with transitions of m/z 164 → 69 for 1-DN, m/z 326 → 164 for GAL-DN, and m/z 148 → 86 for fagomine, according to literature data [24]. Parameter optimization and data acquisition and evaluation were performed by using the Analyst 1.5.1 software. Calibration line of 1-DN (R^2 = 1.0000) was obtained by means of six measurement points in triplicates.

2.6. In Vitro Assay on Xanthine Oxidase (EC 1.17.3.2) Inhibition. The activity of the enzyme was calculated from the increase of uric acid concentration determined by microplate-based kinetic photometry [25]. Briefly, the absorption of uric acid generated from xanthine (50 μM at start-up) was followed at λ = 290 nm for 125 s (Spectrostar Nano, BMG Labtech, Ortenberg, Germany). The activity of xanthine oxidase was described as the slope of the absorbance versus time curve and allopurinol was used as positive control. Stock solutions prepared with dimethylsulfoxide were used for the *in vitro* assays and any substantial effect of the solvent was excluded. All *in vitro* assays were carried out in duplicates.

2.7. Determination of Free Radical Scavenging Activity by DPPH Assay In Vitro. The activity for scavenging 1,1-diphenyl-2-picrylhydrazyl (DPPH) radicals was tested for each fraction as described earlier [26]. Briefly, different amounts of the samples were added to 0.1 mM DPPH dissolved in ethanol. The mixture was shaken and allowed to stand for 30 min, and then the absorbance of the solution was measured at λ = 517 nm. trolox (6-hydroxy-2,5,7,8-tetramethylchroman-2-carboxylic acid), a water-soluble analog of vitamin E, was used as positive control.

2.8. Determination of Lipid Peroxidation Inhibitory Activity. The antioxidant properties of the fractions were additionally measured by means of inhibition of the autooxidation of unsaturated fatty acids present in animal brain tissue [27]. A lipid-rich fraction was prepared from the brains of male Sprague-Dawley rats (Charles River Laboratories, Budapest, Hungary; body mass: 250–300 g) by homogenization and centrifugation. The fatty acids in such a fraction get spontaneously oxidized during an incubation of 1 h at 37°C, and this oxidation can be inhibited by antioxidants. The oxidized products were determined by colorimetry at 532 nm after reaction with thiobarbituric acid. All *in vitro* experiments were carried out in duplicates and statistically evaluated. Sigmoid curves were fitted to the results of both antioxidant assays, and IC_{50} values were calculated by using GraphPad Prism 4 (GraphPad Software, San Diego, CA, USA).

2.9. Testing the Effect on the Glucose Consumption of Adipocytes. Effect of each fraction was tested on the *in vitro* glucose consumption of adipocytes as published before, at concentrations of 200 μg/mL [19]. Briefly, 3T3-L1 preadipocytes (5×10^5 cells, BCRC no. 60159; Bioresource Collection and Research Center, Taiwan) were seeded and cultured in 10% CS DMEM containing 5.5 mM D-glucose. The cells were induced to differentiate, and, at day 3, samples dissolved in DMSO were added to the cells at 200 μg/mL either in presence or absence of 0.32 μM insulin. 24 h changes in the glucose contents of the testing media were recorded and compared to those before the addition of the samples.

2.10. Animal Studies. Animals were treated in accordance with the European Communities Council Directives (86/609/ECC) and the Hungarian Act for the Protection of Animals in Research (XXVIII.tv.32.§). Experiments involving animal subjects were carried out with the approval of the Hungarian Ethical Committee for Animal Research (registration no. IV./01758-2/2008). Male Sprague-Dawley rats (Charles River Laboratories, Budapest, Hungary; body mass: 180–200 g; 8 animals in each group) were housed in temperature (20–23°C), humidity (40–60%), and light (12 h of light, 12 h of dark) regulated rooms, with tap water and rodent food (Bioplan, Isaszeg, Hungary) intake available *ad libitum*. The tested extracts were orally administered in 0.25% methylcellulose containing 2% Cremophor EL using a dosing volume of 5 mL/kg. Three doses of all extracts (30, 60, and 120 mg/kg) were selected for daily treatment for 3 consecutive days and each treatment was performed after 16 hours of fasting. One-way analysis of variance (ANOVA) with Dunnett's multiple comparison test by GraphPad Prism 4 was used for statistical evaluation of all *in vivo* experiments.

2.11. Determination of Antihyperuricemic, Antihyperglycemic, and Antioxidant Properties of the Fractions In Vivo. In order to minimize the number of animals, antihyperuricemic, antihyperglycemic, and antioxidant properties effects were determined from the same groups of rats. Experimental hyperuricemia model induced by uricase inhibitor potassium oxonate was utilized to assess the antihyperuricemic properties of the tested fractions [28]. 250 mg/kg potassium oxonate was suspended in 0.25% methylcellulose and administered intraperitoneally at the time of the third oral treatment. 50 mg/kg of allopurinol, a clinically used antigout drug, was orally administered as a positive control. One hour later rats were orally treated with 2.5 g/kg starch suspension in a dosing volume of 5 mL/kg in order to characterize the antihyperglycemic effects of the fractions [25]. After another one hour, venous blood samples were obtained from the tail, and the plasma glucose concentrations were determined by a commercially available kit (Reanal, Budapest, Hungary) based on the glucose oxidase-peroxidase method [29]. Immediately after blood sampling, rats were anesthetized in 4% isoflurane and additional blood samples were collected by

cardiac puncture for determination of uric acid concentration and total antioxidant capacity. Since inhalational anesthetics are reported to substantially elevate the blood glucose level, separate blood samplings were needed for determination of all the planned parameters [30]. Serum samples were prepared by centrifugation and stored at –70°C until the analyses. All determinations by colorimetric uric acid (BioAassay Systems, Hayward, CA, USA) and antioxidant (Sigma-Aldrich, Budapest, Hungary) assay kits were performed in duplicates according to the manufacturers' suggestions. Separate groups orally treated with glibenclamide and trolox (10 mg/kg for both) were included as reference for the antihyperglycemic and antioxidant assays, respectively.

3. Results and Discussion

3.1. Chemical Composition of the Fractions Obtained. The fractions, obtained by solvent-solvent extraction and a rough chromatographic separation of the organic phase on silica, represented fundamentally different chemical compositions (Figure 1). As expected, highly water soluble, hydrophilic compounds (including iminosugars of the plant, see below) remained in the water phase (Figure 1(b)), while most of the still polar chlorogenic acid (**1**) could already be detected in the organic phase (Figure 1(c)) along with vast majority of the supposedly "drug-like" secondary metabolites of mulberry leaves. These would be the compounds with the highest probability for therapeutic value; mainly the too low log *P* value typically results in poor penetration through membranes (iminosugars, a constituent group of possible exception to this, are discussed below). As seen from the DAD fingerprints, FR1 (Figure 1(d)) and FR2 (Figure 1(e)) mostly contained compounds with lower wavelengths of UV absorbance maxima probably including several terpenoids and/or phenylpropanes [19]. The dominant peak of FR2 was detected and quantified as loliolide (**4**) (0.33%), a monoterpene lactone we have recently reported from *M. alba* leaves [19]. Of all fractions, FR3 (Figure 1(f)) contained the smallest amount of UV absorbing material; its main constituents remained unidentified. Based on its UV spectrum and retention time, chief constituent of FR4 (Figure 1(g)) is suggested to be a flavone aglycone (3.42–3.50%, expressed in equivalents of isoquercitrin (**3**) or rutin (**2**)), while **3** (2.42%) was also present in this fraction. FR5 (Figure 1(h)) contained the majority of **3** (9.79%) along with a smaller amount of **2** (3.77%), while the previously mentioned unidentified flavonoid could still be detected. FR6 (Figure 1(i)), the most polar fraction obtained from the column chromatography, contained **1** (8.99%), **2** (10.41%), and **3** (5.64%) as major UV active constituents.

Both the extract and the fractions contained very small amounts of iminosugars. By means of MS/MS, 1-DN contents were found as low as 0.2694‰ (EX), 0.3007‰ (FR-W), 0.0742‰ (FR-B), ~0.016‰ (FR4; around detection limit), 0.0558‰ (FR5), and 0.2770‰ (FR6). On the other hand, slope of the calibration lines of GAL-DN and fagomine is around 13 and 6 times higher, respectively, as compared to that of 1-DN, based on a recent publication using the same MRM transitions with ESI-MS/MS [24]. This allowed only a rough estimation on the quantity of these compounds by using our calibration obtained for 1-DN. Amounts of GAL-DN were about 0.02‰ (EX), 0.03‰ (FR-W), 0.003‰ (FR-B) and 0.009‰ (FR6), and trace amounts of this compound were detected in FR4 and FR5. Fagomine contents could be estimated as around 0.03‰ (EX), 0.04‰ (FR-W), 0.01‰ (FR-B), 0.01‰ (FR5) and 0.03‰ (FR6), with a trace amount of this compound also present in FR4. Structures of the compounds identified from the fractions are shown in Figure 2.

3.2. Inhibition of Xanthin Oxidase In Vitro. All fractions were tested at the final concentration of 5 μg/mL. The enzyme activity determined in the solvent-treated condition was considered 100% and all other conditions were compared to that control. None of the prepared fractions exerted any substantial action on the enzyme xanthine oxidase, while, as expected, the reference compound allopurinol resulted in a nearly complete (>90%) inhibition of the enzyme activity at 5 μg/mL, and its IC_{50} value was determined as 1.03 μg/mL. Based on these results, XO inhibition does not seem to be an important mechanism for neither the antihyperuricemic nor the antioxidant activity of mulberry preparations.

3.3. In Vitro Antioxidant Properties. Two different bioassays were utilized to investigate the *in vitro* antioxidant properties of the fractions: DPPH assay and lipid peroxidation (LOX) assay. Even though the results obtained by these two methods are frequently parallel, certain agents can exhibit substantial differences in these assays [31]. Generally, a compound effective in the DPPH assay can be considered as a free radical scavenger functioning in an organic solvent against a chemically pure molecule (i.e., the DPPH radical). LOX assay, on the other hand, is performed in a more complex *ex vivo* biological system containing lipids with unsaturated fatty acids; a substance active in this assay may protect these lipids from the spontaneous oxidation in aqueous conditions.

DPPH assay was performed with the concentration range of 0.001–0.15 mg/mL to characterize the free radical scavenging capacity of the prepared fractions. Fractions FR1 and FR2 exhibited no substantial activities in the utilized concentrations. Fractions FR3 and FR4 were moderately active, while FR5 and FR-W showed the highest potencies. FR6, containing significant amounts of phenolic compounds (compounds **1–3**), was equipotent with the reference agent trolox. In agreement with these, lipid peroxidation assay showed that the antioxidant capacities of fractions FR3 and FR6 were close to that of trolox, while FR5 and FR-W were slightly less active. Fractions FR2 and FR4 exhibited moderate activities, and, similarly to the case of the DPPH assay, FR1 was inactive. Results of both assays are summarized in Table 1.

3.4. Effect on the In Vitro Glucose Consumption of Adipocytes. Although some minor changes could be observed in this bioassay, no statistically significant activities were found. This was somewhat surprising, since a lipophilic fraction, obtained by a simple solvent-solvent distribution from the hot water extract of the same plant collection, was previously

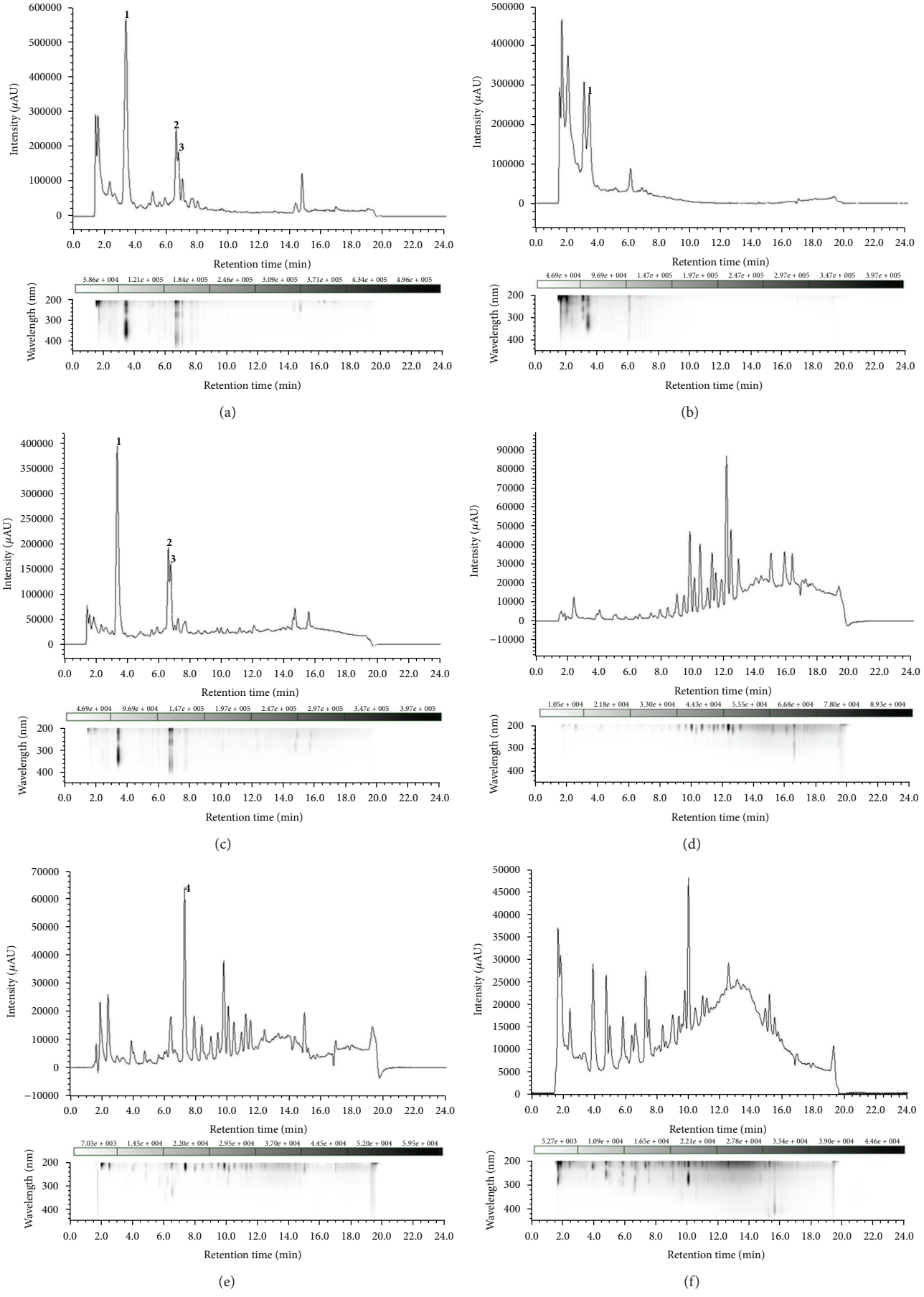

Figure 1: Continued.

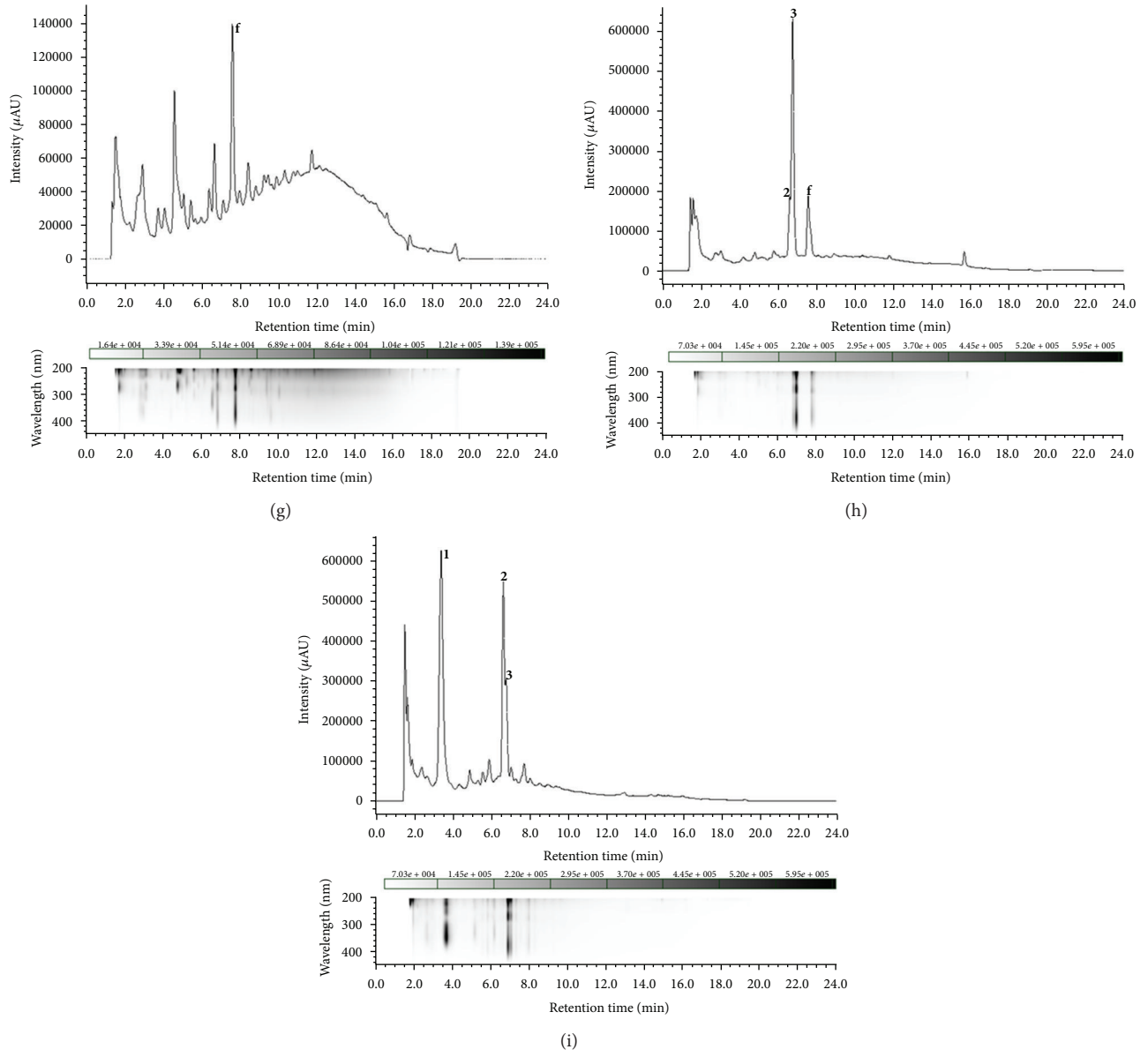

Figure 1: HPLC-DAD fingerprints of the samples and the corresponding maximum absorbance chromatograms from $\lambda = 200$ to 450 nm. (a) Crude extract (EX), (b) FR-W, (c) FR-B, and (d)–(i) FR1-FR6, respectively. Marked peaks represent chlorogenic acid (**1**), rutin (**2**), isoquercitrin (**3**), loliolide (**4**), and an unidentified flavone derivative (**f**).

found to exert strong effect in this test [19]. The most likely explanation is the low relative amount of the constituents responsible for this effect, based on which we can also conclude that increasing the glucose consumption of adipose tissue has little importance in the complex anti-diabetic activity of less processed phytotherapeutics originated from mulberry leaves.

3.5. Determination of the Antihyperuricemic Effects of the Fractions In Vivo. The serum uric acid concentration in rats is considerably low because it is metabolized into allantoin by the enzyme uricase. Therefore, uric acid accumulation was induced by a single administration of K-oxonate for the *in vivo* investigation of the antihyperuricemic properties of the fractions. Results are shown in Figure 3. Allopurinol (50 mg/kg intraperitoneally), used as positive control, substantially and significantly decreased the accumulation of uric acid. The lowest dose (30 mg/kg) of FR1, the highest dose (120 mg/kg) of FR2, and 60 mg/kg of FR5 exerted antihyperuricemic actions comparable to that of allopurinol. Unexpectedly, treatment with FR-W (60 and 120 mg/kg) resulted in an elevation of serum uric acid levels. No clear dose-response relationships were detected for some of the fractions.

The renal excretion of uric acid is a complex and species-dependent procedure involving its glomerular filtration, tubular secretion, and tubular reabsorption. Since these processes can independently be modulated with exogenous

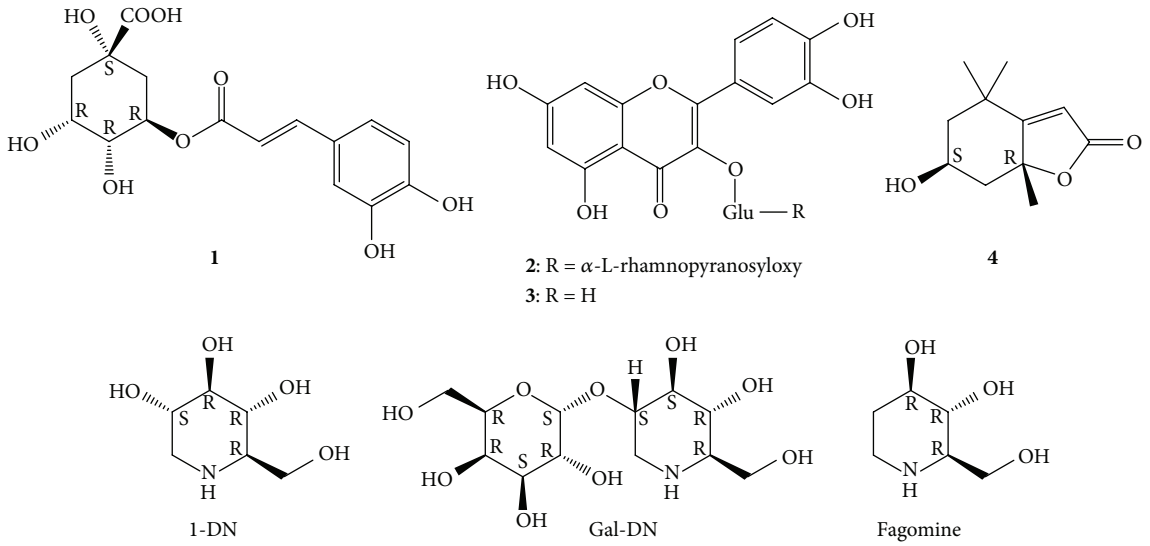

Figure 2: Chemical structures of the compounds identified in the fractions: chlorogenic acid (**1**), rutin (**2**), isoquercitrin (**3**), loliolide (**4**), 1-deoxynojirimycin (1-DN), 2-*O*-alpha-D-galactopyranosyl-1-deoxynojirimycin (Gal-DN), and fagomine. Glu: β-D-glucopyranosyloxy.

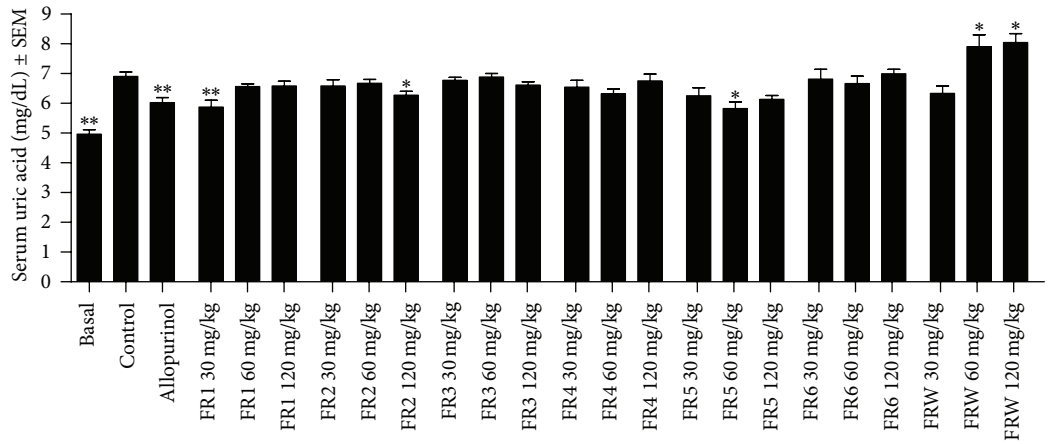

Figure 3: *In vivo* antihyperuricemic activity of the fractions obtained. Hyperuricemia was induced by a single administration of K-oxonate, 50 mg/kg of allopurinol was used as positive control, and samples were tested at 30, 60, and 120 mg/kg. $*$ and $**$: $P < 0.05$ and 0.01, respectively, as compared to the negative control by means of one-way ANOVA followed by Dunnett's multiple comparison test; $n = 8$.

substances, the overall action of a drug is frequently biphasic. Aspirin at dosages of >3 g/day promotes uricosuria by inhibition of the reabsorption while lower dosages (1-2 g/day) may cause uric acid retention, presumably by interfering with the tubular secretion [32]. This, together with the chemical complexity of the fractions, could provide a simple explanation for the unclear dose-response relationships observed in certain cases; several interactions between various constituents of the fractions might take place, in which the active components would influence these renal functions differently.

3.6. Determination of the Serum Antioxidant Capacity. The antioxidant capacities of the serum samples of the treated animals were determined by means of a photometric assay in which 2,2′-azino-bis(3-ethylbenzthiazoline-6-sulfonic acid) (ABTS) is converted into a chromogen radical cation ($ABTS^{\bullet+}$). The generation of radical cation is suppressed by antioxidants and can be detected as a decrease of color intensity; results of this assay are shown in Figure 4. Treatment with trolox (10 mg/kg) resulted in a substantial increase in the antioxidant capacity (expressed as trolox equivalents) but most of the tested fractions failed to induce significant change in this serum parameter. The higher doses of FR6 (60 and 120 mg/kg) exhibited similar antioxidant effects to that of trolox, which effect can most likely be attributed to the high chlorogenic acid (**1**), rutin (**2**), and isoquercitrin (**3**) content of this fraction. On the other hand, 30 mg/kg of FR3 decreased the oxidative status of the serum, indicating a prooxidant potential for certain constituents.

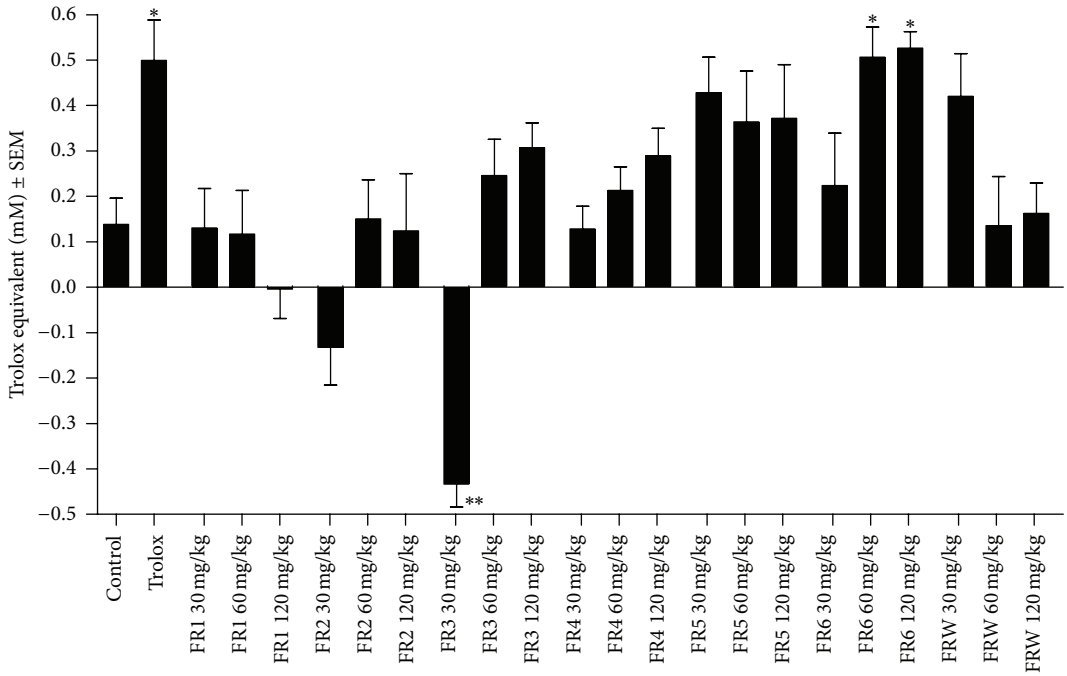

Figure 4: Effects on the serum antioxidant capacity *in vivo*. $^{*}P < 0.05$ as compared to the negative control by one-way ANOVA followed by Dunnett's multiple comparison test; $n = 8$.

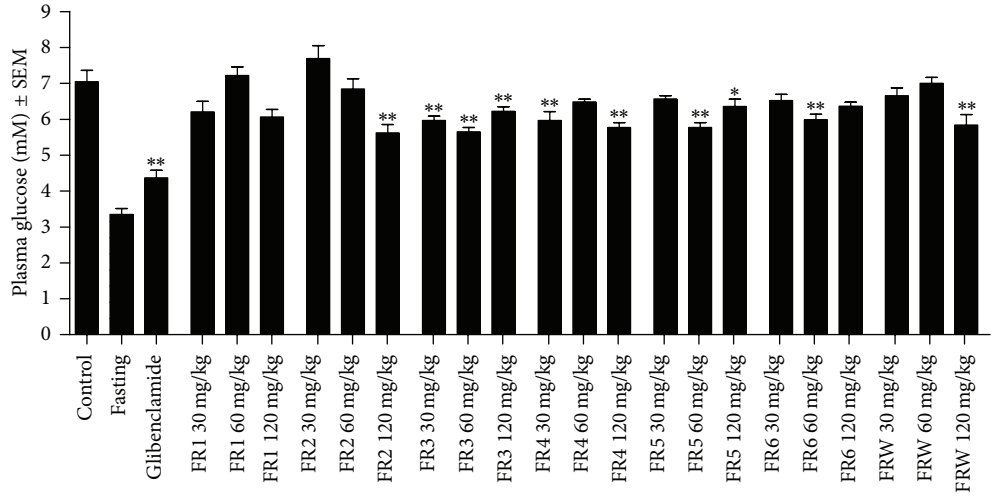

Figure 5: Effects on the postprandial hyperglycemia of normal rats after starch loading. $*$ and $**$: $P < 0.05$ and 0.01, respectively, as compared to the negative control by one-way ANOVA followed by Dunnett's multiple comparison test; $n = 8$. The fasting blood glucose level was determined in preliminary experiments, and its dataset was not included in the statistical evaluation.

3.7. Determination of the Postprandial Plasma Glucose Levels. Treatment with the positive control glibenclamide (10 mg/kg) resulted in a substantial and significant decrease of the postprandial plasma glucose levels obtained in the starch load model. FR1 was inactive up to 120 mg/kg, while FR3 exhibited antihyperglycemic action at all applied doses. Fractions FR2, FR-W, and FR5 were effective at 120, 60, and 120 mg/kg, respectively. Fractions FR4 and FR6 exhibited some antihyperglycemic properties but no clear dose-response relationships were observed; results are shown in Figure 5. It is worthy to note, however, that the present *in vivo* model investigated the effect of a single-dose administration on the postprandial hyperglycemia of normal rats after starch loading; therefore, these results can hardly be compared with those we obtained previously for a longer treatment in type 2 diabetic rats with *ad libitum* access to standard food [16].

4. Conclusions

The investigated extract of *M. alba* showed multiple beneficial bioactivities in view of both targeted chronic metabolic diseases. It can also be concluded, based on the different

Table 1: *In vitro* antioxidant activities as calculated from the DPPH assay and from the inhibition of the spontaneous lipid peroxidation.

Sample	DPPH EC_{50} (μg/mL)	Lipid peroxidation IC_{50} (μg/mL)
FR-W	72.2	71.0
FR1	—[a]	—[a]
FR2	—[a]	138.0
FR3	186.0	47.3
FR4	245.0	114.0
FR5	55.0	77.7
FR6	21.7	55.8
Trolox	21.8	42.5

Trolox: positive control in both cases.
[a]Exhibited no substantial activity in the applied concentration range.

effects exerted by the fractions, that separate compound groups are responsible for the individual actions, which have a significant potential for a positive combined effect.

FR1, FR2, and FR5 are of interest in view of the antihyperuricemic activity as potential uricosuric agents. FR2–6 were all found valuable for their antihyperglycemic activities, but FR3 was the strongest exerting significant effects at all administered doses. Somewhat unsurprisingly, FR6, containing most of the phenolic constituents, was found to be the strongest antioxidant both *in vitro* and *in vivo*, which makes this fraction particularly useful against the high oxidative stress present in both diabetes and chronic hyperuricemia.

Furthermore, considering our original objectives, fractions of relatively low value could also be revealed. Although the water phase of the first solvent-solvent extraction (FR-W) could effectively scavenge DPPH radicals *in vitro* and showed at least a weak antihyperglycemic activity *in vivo* (possibly due to the low iminosugar content of our sample), this fraction was also found to significantly increase the plasma uric acid levels; hence, it is potentially unwanted in a well-designed mulberry preparation. FR1, the less polar fraction that was eluted with dichloromethane from the silica column, was found inactive in most bioactivity tests except for its non-dose-dependent antihyperuricemic activity at 30 mg/kg *in vivo*. This might be of interest for further research, but, due to the nearly 20% amount of this fraction by weight in the dry butanolic phase, removing this polarity range of constituents could as well be considered for increasing the overall therapeutic benefits of a phytotherapeutic product.

Acknowledgments

This work was supported by the Hungarian National Research Fund (OTKA PD75383), and it was performed within the framework of a bilateral mobility Grant from the National Science Council, Taiwan, and the Hungarian Academy of Sciences (102-2911-I-037-501 and SNK-79/2013). The authors acknowledge financial support from the Pick Szeged Zrt., Szeged, Hungary, Grants from the European Union cofunded by the European Social Fund (TAMOP-4.2.2/B-10/1-2010-0012, and TAMOP-4.2.2A-11/1/KONV-2012-0035), the Grant from the National Science Council of Taiwan (NSC 101-2314-B-037-033), and support of the Fundação para a Ciência e a Tecnologia, Portugal (PEsT-OE/SAU/UI0074/2011). A. Martins acknowledges the Grant SFRH/BPD/81118/2011, FCT, Portugal and Professor Leonard Amaral for scientific discussion. The authors wish to express their special thanks to Ibolya Hevérné Herke for her contribution to the lab work.

References

[1] E. W. Campion, R. J. Glynn, and L. O. DeLabry, "Asymptomatic hyperuricemia: risks and consequences in the normative aging study," *The American Journal of Medicine*, vol. 82, no. 3, pp. 421–426, 1987.

[2] E. Krishnan, B. J. Pandya, L. Chung, and O. Dabbous, "Hyperuricemia and the risk for subclinical coronary atherosclerosis: data from a prospective observational cohort study," *Arthritis Research & Therapy*, vol. 13, p. R66, 2011.

[3] P. Higgins, J. Dawson, and M. Walters, "The potential for xanthine oxidase inhibition in the prevention and treatment of cardiovascular and cerebrovascular disease," *Cardiovascular Psychiatry and Neurology*, vol. 2009, Article ID 282059, 9 pages, 2009.

[4] P. Pacher, A. Nivorozhkin, and C. Szabó, "Therapeutic effects of xanthine oxidase inhibitors: renaissance half a century after the discovery of allopurinol," *Pharmacological Reviews*, vol. 58, no. 1, pp. 87–114, 2006.

[5] L. Changgui, H. Ming-Chia, and C. Shun-Jen, "Metabolic syndrome, diabetes, and hyperuricemia," *Current Opinion in Rheumatology*, vol. 25, no. 2, pp. 210–216, 2013.

[6] M. A. Suriyajothi, R. Sangeetha, and R. Venkateswari, "Activity of Xanthine oxidase in diabetics: its correlation with aging," *Pharmacologyonline*, vol. 2, pp. 128–133, 2011.

[7] S. Ryu, J. Song, B.-Y. Choi et al., "Incidence and risk factors for metabolic syndrome in Korean male workers, ages 30 to 39," *Annals of Epidemiology*, vol. 17, no. 4, pp. 245–252, 2007.

[8] X. Sui, T. S. Church, R. A. Meriwether, F. Lobelo, and S. N. Blair, "Uric acid and the development of metabolic syndrome in women and men," *Metabolism*, vol. 57, no. 6, pp. 845–852, 2008.

[9] H. Ito, M. Abe, M. Mifune et al., "Hyperuricemia is independently associated with coronary heart disease and renal dysfunction in patients with type 2 diabetes mellitus," *PloS ONE*, vol. 6, no. 11, Article ID e27817, 2011.

[10] C. L. T. Chang, Y. Lin, A. P. Bartolome, Y. C. Chen, S. C. Chiu, and W. C. Yang, "Herbal therapies for type 2 diabetes mellitus: chemistry, biology, and potential application of selected plants and compounds," *Evidence-Based Complementary and Alternative Medicine*, vol. 2013, Article ID 378657, 33 pages, 2013.

[11] Z. Wang, J. Wang, and P. Chan, "Treating type 2 diabetes mellitus with traditional Chinese and Indian medicinal herbs," *Evidence-Based Complementary and Alternative Medicine*, vol. 2013, Article ID 343594, 17 pages, 2013.

[12] D. Bensky and A. Gamble, *Chinese Herbal Medicine, Materia Medica*, Eastland Press, Seattle, Wash, USA, 1986.

[13] J. Anjaria, M. Parabia, G. Bhatt, and R. Khamar, *Nature Heals, A Glossary of Selected Indigenous Medicinal Plants of India*, Sristi Innovations, Ahmedabad, India, 2002.

[14] A. N. B. Singab, H. A. El-Beshbishy, M. Yonekawa, T. Nomura, and T. Fukai, "Hypoglycemic effect of Egyptian *Morus alba* root bark extract: effect on diabetes and lipid peroxidation of

streptozotocin-induced diabetic rats," *Journal of Ethnopharmacology*, vol. 100, no. 3, pp. 333–338, 2005.

[15] I. Lemus, R. García, E. Delvillar, and G. Knop, "Hypoglycaemic activity of four plants used in Chilean popular medicine," *Phytotherapy Research*, vol. 13, no. 2, pp. 91–94, 1999.

[16] A. Hunyadi, A. Martins, T. J. Hsieh, A. Seres, and I. Zupkó, "Chlorogenic acid and rutin play a major role in the in vivo antidiabetic Activity of *Morus alba* leaf extract on type II diabetic rats," *PloS ONE*, vol. 7, no. 11, Article ID e50619, 2012.

[17] M. Mudra, N. Ercan-Fang, L. Zhong, J. Furne, and M. Levitt, "Influence of mulberry leaf extract on the blood glucose and breath hydrogen response to ingestion of 75 g sucrose by type 2 diabetic and control subjects," *Diabetes Care*, vol. 30, no. 5, pp. 1272–1274, 2007.

[18] T. Kimura, K. Nakagawa, H. Kubota et al., "Food-grade mulberry powder enriched with 1-deoxynojirimycin suppresses the elevation of postprandial blood glucose in humans," *Journal of Agricultural and Food Chemistry*, vol. 55, no. 14, pp. 5869–5874, 2007.

[19] A. Hunyadi, K. Veres, B. Danko et al., "In vitro anti-diabetic activity and chemical characterization of an apolar fraction of *Morus alba* leaf water extract," *Phytotherapy Research*, vol. 27, pp. 847–851, 2013.

[20] Y. W. Shia, C. P. Wang, X. Wang et al., "Uricosuric and nephroprotective properties of *Ramulus Mori* ethanol extract in hyperuricemic mice," *Journal of Ethnopharmacology*, vol. 143, no. 3, pp. 896–904, 2012.

[21] C.-P. Wang, Y. Wang, X. Wang et al., "Mulberroside A possesses potent uricosuric and nephroprotective effects in hyperuricemic mice," *Planta Medica*, vol. 77, no. 8, pp. 786–794, 2011.

[22] Z. Yu, P. F. Wing, and C. H. K. Cheng, "The dual actions of morin (3,5,7,2′,4′-pentahydroxyflavone) as a hypouricemic agent: uricosuric effect and xanthine oxidase inhibitory activity," *Journal of Pharmacology and Experimental Therapeutics*, vol. 316, no. 1, pp. 169–175, 2006.

[23] Z. Yu, P. F. Wing, and C. H. K. Cheng, "Morin (3,5,7,2′,4′-pentahydroxyflavone) exhibits potent inhibitory actions on urate transport by the human urate anion transporter (hURAT1) expressed in human embryonic kidney cells," *Drug Metabolism and Disposition*, vol. 35, no. 6, pp. 981–986, 2007.

[24] K. Nakagawa, K. Ogawa, O. Higuchi, T. Kimura, T. Miyazawa, and M. Hori, "Determination of iminosugars in mulberry leaves and silkworms using hydrophilic interaction chromatography-tandem mass spectrometry," *Analytical Biochemistry*, vol. 404, no. 2, pp. 217–222, 2010.

[25] H. G. Vogel, Ed., *Drug Discovery and Evaluation: Pharmacological Assays*, Springer, Berlin, Germany, 2002.

[26] Z. Hajdú, J. Hohmann, P. Forgo et al., "Diterpenoids and flavonoids from the fruits of Vitex agnus-castus and antioxidant activity of the fruit extracts and their constituents," *Phytotherapy Research*, vol. 21, no. 4, pp. 391–394, 2007.

[27] I. Zupkó, J. Hohmann, D. Rédei, G. Falkay, G. Janicsák, and I. Máthé, "Antioxidant activity of leaves of Salvia species in enzyme-dependent and enzyme-independent systems of lipid peroxidation and their phenolic constituents," *Planta Medica*, vol. 67, no. 4, pp. 366–368, 2001.

[28] I. Fridovich, "The competitive inhibition of uricase by oxonate and by related derivatives of s-triazines," *The Journal of biological chemistry*, vol. 240, pp. 2491–2494, 1965.

[29] P. Trinder, "Determination of glucose in blood using oxidase with an alternative oxygen acceptor," *Annals of Clinical Biochemistry*, vol. 6, pp. 24–27, 1969.

[30] C. J. Zuurbier, F. J. Hoek, J. Van Dijk et al., "Perioperative hyperinsulinaemic normoglycaemic clamp causes hypolipidaemia after coronary artery surgery," *British Journal of Anaesthesia*, vol. 100, no. 4, pp. 442–450, 2008.

[31] R. Minorics, T. Szekeres, G. Krupitza et al., "Antiproliferative effects of some novel synthetic solanidine analogs on HL-60 human leukemia cells in vitro," *Steroids*, vol. 76, no. 1-2, pp. 156–162, 2011.

[32] D. Caspi, E. Lubart, E. Graff, B. Habot, M. Yaron, and R. Segal, "The effect of mini-dose aspirin on renal function and uric acid handling in elderly patients," *Arthritis and Rheumatism*, vol. 43, pp. 103–108, 2000.

Hindawi Publishing Corporation
Evidence-Based Complementary and Alternative Medicine
Volume 2013, Article ID 984797, 8 pages
http://dx.doi.org/10.1155/2013/984797

Research Article

Effects of the Chinese Traditional Prescription Xiaoyaosan Decoction on Chronic Immobilization Stress-Induced Changes in Behavior and Ultrastructure in Rat Hippocampus

Yuan Liang,[1,2] Xiao-Ling Guo,[1,3] Jia-Xu Chen,[1,4] and Guang-Xin Yue[2]

[1] *School of Pre-Clinical Medicine, Beijing University of Chinese Medicine, Beijing 100029, China*
[2] *Institute of Basic Theory in Chinese Medicine, China Academy of Chinese Medical Sciences, Beijing 100700, China*
[3] *Fangzhuang Community Health Center, Beijing 100078, China*
[4] *Department of Basic Theory in Chinese Medicine, Henan University of Traditional Chinese Medicine, Zhengzhou 450008, China*

Correspondence should be addressed to Jia-Xu Chen; chenjiaxu@hotmail.com

Received 17 June 2013; Accepted 1 November 2013

Academic Editor: Mohamed Eddouks

Xiaoyaosan (XYS) decoction has been widely used as a traditional medicine for treating stress and depression-related disorders in China for thousands of years. *Aim of the Study*. To observe the potential mechanism of XYS decoction's antidepressant-like effect in α-amino-3-hydroxy-5-methyl-4-isoxazolepropionic acid (AMPA) receptors related to synaptic plasticity in the hippocampus rats induced by chronic immobilization stress (CIS). *Materials and Methods*. Animals were randomly divided into five groups: (1) control group; (2) sham-operated group; (3) CIS group, in which rats were conducted CIS for 21 days; (4) XYS decoction treatment group; (5) 6-cyano-7-nitroquinoxaline-2,3-dione (CNQX) positive group, in which the amygdala of CIS rats was unilaterally microinjected with a competitive glutamate receptor antagonist, CNQX. After CIS for 21 days, the open field test (OPT) and elevated plus-maze test (EPM) were measured, the ultrastructure of hippocampus CA_1 subregion was observed by the electron microscopy; both the GluR1 and GluR2 mRNA level of AMPA receptor subunits in hippocampus CA_1 subregion were detected by real-time qPCR. *Results*. Rats subjected to CIS exhibited increases in time in central zone and decreases in total distance traveled in the OPT. In the EPM, they also showed decreases in center zone time and entries, open arm time and entries, and an increase in close arm time. Ultrastructural damage in the hippocampus CA_1 was also observed. XYS decoction and CNQX showed significant improvement behavioral changes and the ultrastructural damage of the hippocampus CA_1; XYS decoction also reversed CIS-induced decreases in GluR2 mRNA and increases in GluR1 mRNA in the hippocampus CA_1 as well as CNQX. *Conclusions*. XYS decoction may effectively produce an antidepressant-like effect, which appears to be involved AMPA receptors related synaptic plasticity of hippocampus.

1. Introduction

There is abundant evidence demonstrating that chronic stress can cause hippocampal damage, such as dendritic remodeling, synaptic plasticity, dendrites retracting, decreased neurogenesis, and apoptosis [1]. Synaptic plasticity is one of the key factors indicating how stress response is transforming to damage; the changes of α-amino-3-hydroxy-5-methyl-4-isoxazolepropionic acid (AMPA) receptors in the synapses have a relation with synaptic plasticity [2]. However, stress induced anxiety and depression involve multiple areas of the brain, such as amygdale and the prefrontal cortex.

Both the hippocampus and the amygdala are important aspects of the limbic system which plays a dominant role in stress response. Anatomically, the amygdala projects to several hippocampal regions (including the CA_1 area) [3, 4]. And functionally, both of them control the systems involved in stress. But it seems that they have different actions during stress response. There were findings about enlarged amygdala volume and reduced hippocampus volume in young women

with major depression [5]. Considerable evidence indicates that the amygdala is critically involved in mediating stress-related effects on behavior and modulating hippocampal function. Furthermore, the hippocampus and anterior cingulate cortex inhibit stress-induced HPA activation, whereas the amygdala may enhance glucocorticoid secretion [6].

AMPA receptors mediate the majority of rapid excitatory synaptic transmission in the central nervous system [2, 7]. It is known that glutamate is a potent neuronal excitotoxin [8], and when it is combined with the AMPA receptor α-amino-3-hydroxy-5-methyl-4-isoxazolepropionic acid (AMPA) receptors, it produces depolarization and neuronal excitation. The excitation triggers either rapid or delayed neurotoxicity which may be an important cause of stress-induced neural damage. AMPA receptors are composed of a homo or heteromeric complex of four subunits, GluR1, GluR2, GluR3, and GluR4 [2]. In the mature hippocampus, most of the AMPARs are composed of GluR1-GluR2 or GluR2-GluR3 combinations [9]. AMPA receptors are mainly distributed in the postsynaptic membrane of the excitatory synapses. They are not static components of the synapses, but they are continuously being delivered and removed in and out of the synapses in response to neuronal activity [10]. The changes of the amount or certain subunits of the AMPA receptors may influence the activity and transmission effect of excitatory synapses. This dynamic process probably plays a key role in the synaptic plasticity that is thought to trigger aspects of learning and memory and also being one of the causative factors of neural damage under stress.

Our previous research [11] found that the expression of AMPA receptors decreased in hippocampus CA_1 subregion while increased in basolateral nucleus of amygdala (BLA) after exposure to CIS, and XYS decoction had a regulation effect on the above changes.

Therefore, in the present study, 6-cyano-7-nitroquinoxaline-2,3-dione (CNQX), a competitive glutamate receptor antagonist, was microinjected in the amygdala to block the AMPA receptors as positive control. The purpose of this study was to further investigate the potential regulation mechanism of XYS decoction in synaptic plasticity relevant to the AMPA receptor in the central nervous system especially in hippocampus CA_1 of rats with CIS.

2. Materials and Methods

2.1. Animals. A total of 100 male Sprague-Dawley rats (Beijing Weitong Lihua Research Center for Experimental Animals), weighing (230 ± 10) g, were used in the experiments. They were randomly divided into five groups: (1) control group; (2) sham-operated group; (3) CIS group; (4) XYS decoction treatment group (XYS group); (5) CNQX positive group.

The animals were housed in a room with routine care (20–24°C, relative humidity of 30–40%) and free access to food and water. This study was performed in strict accordance with the recommendations in the Guide for the Care and Use of Laboratory Animals of the P. R. China. The protocol was approved by the Committee on the Ethics of Animal Experiments of the Beijing University of Chinese Medicine (BUCM). All the surgery was performed under sodium pentobarbital anesthesia, and every effort was made to minimize animal suffering.

2.2. Preparation of Extracts of the XYS Decoction. The XYS decoction was composed of the following dried raw materials: Poria cocos (Schw.) Wolf (Poria), Paeonia lactiflora Pall. (Radix Paeoniae Alba), Glycyrrhiza uralensis Fisch. (Radix Glycyrrhizae), Bupleurum chinense DC. (Radix Bupleuri), Angelica sinensis (Oliv.) Diels (Radix Angelicae Sinensis), Atractylodes macrocephala Koidz. (Rhizoma Atractylodis Macrocephalae), Mentha haplocalyx Briq. (Herba Menthae), and Zingiber officinale Rosc. (Rhizoma Zingiberis Recens). These eight herbs were purchased from Medicinal Materials Company of Beijing Tongrentang and authenticated by Qi Junjie, BUCM, before processing the following procedures provided by the Department of Preparation for Herbs, Sino-Japan Friendship Hospital in Beijing, as previously described [12].

2.3. Surgery. All the rats except those in control group were anesthetized with pentobarbital sodium (40–50 mg/kg, i.p.) after adaption for three days. The animal was secured in a stereotaxic instrument by using nonpuncture ear bars and a bite bar. A stainless steel guide cannula (0.8 mm o.d.) was aimed to the right amygdala (coordinates: AP: −4.0 mm, L: 4.4 mm, DV: 8.0 mm) [13]. The cannula tip was 1.5 mm above the injection site, the cannula was attached to the skull bone with stainless steel screws and acrylic cement, and a stiletto inside the cannula prevented obstruction [14]. After the rats with CIS established for 1 week were performed surgeries, penicillin was given by the intramuscular injection to against infection. The histological site of cannula was verified by dye infusion at the end of the experiment, and demonstrated the accurateness.

2.4. Stress Procedure and XYS Treatment. The rats in CIS, XYS, and CNQX groups were carried out the immobilization stress 3 h per day for 21 days as described previously. The XYS decoction-treated rats were given via gavage the extracted mixture (5.32 g/kg) [15], 1 hour before CIS each day for 21 days. The rats in the other groups were given distilled water.

2.5. Intracerebral Injection. CNQX (Sigma-Aldrich Company), a selective AMPA receptor antagonist, was dissolved in 99.5% dimethyl sulfoxide (DMSO) (Sigma-Aldrich Company) and then diluted with sterile 0.9% saline to a final concentration of 0.5 μg/0.5 μL CNQX. Infusion was performed according to the method of Padovan et al. with minor modifications [14]. Briefly, a thin needle (0.4 o.d.) was introduced through the guide cannula until its tip was 1.5 mm below the cannula end. A polyethylene catheter (PE 10) was interposed between the upper end of the dental needle and the microsyringe. A volume of 0.5 mL was injected in 1 min using a Hamilton (USA) microsyringe. The movement of an air bubble inside the polyethylene catheter confirmed drug flow and the injector was left in place for an additional 1 min. Unilateral intra-amygdala infusion of CNQX (0.5 μL) was administered to rats of CNQX group on the 1st, 4th, 7th, 10th,

13th, 16st, 19th, and 21st day; vehicle (sterile saline) was used as a control.

2.6. Behavioral Procedures: Open-Field Test (OFT). The OFT was performed according to previously described procedure [12]. Briefly, at 8:00 of the 22nd day, all rats were put in a quiet, closed room around with black curtains for 10 min before the test, avoiding the unfavorable disturbances from the surroundings. Each rat was placed in the center zone (50 cm × 50 cm) of open-field box (100 cm × 100 cm × 40 cm) lightly; total distance traveled (cm) and time in central zone (sec) were recorded and calculated by EthoVision tracking software (Noldus Information Technology Inc., Holland). The apparatus was cleaned thoroughly with 95% ethanol after each animal was tested in case that the smell influenced the next rat.

Elevated Plus-Maze Test (EPM). The EPM test was performed the following procedures. After the OFT for two hours, each rat was put in the center zone of elevated plus maze with head faced to an open arm. Entry times in central zone, open arms and closed arms and time in central zone, open arms, and closed arms in 5 minutes were recorded and calculated by EthoVision tracking software. When one rat finished its test, the maze was cleaned by 95% ethanol.

2.7. Electron Microscopy. After the behavioral test, three animals of each group were analyzed by electron microscopy, and the animals were anaesthetized with 2% pentobarbital sodium (40 mg/kg) and perfused with cold 0.9% NaCl solution followed by perfusate solution (4% paraformaldehyde, 2.5% glutaraldehyde, and 0.1 mol PBS). Then, the brain was isolated and postfixed in 2.5% paraformaldehyde for 24 hours; the right CA_1 region of hippocampus (2 mm × 2 mm × 2 mm) was cut out macroscopically from brain tissues.

For embedding electron microscopy, the sections were rinsed 8 times for 48 hours in 0.1 M phosphate buffer, postfixed with 2% osmium tetroxide for 1.5 hours, washed 5 times for 5 min in PBS, dehydrated through a series of alcohols acetone I (50%, 70%, 80%, 90%, 95%, and 100%, for 10 minutes each), further dehydrated in 100% acetone II, III twice for 40 minutes each, soaked in a ratio of 1 : 1 of solution of acetone and araldite resin for 1.5 hours, and then immersed in pure resin at room temperature for 3 hours, 37°C for 12 hours, 45°C for 12 hours, and 60°C for 48 h. Blocks were serially sectioned with a Leica UCT ultramicrotome into 70 nm. The sections were positioned onto 1 mm slotted, piloform-covered, copper coated grids, stained with 8% uranyl acetate and 0.4% lead citrate. Ultrathin sections were scanned at 80 kV with a JEOL-1230 transmission electron microscope (TEM).

2.8. Real-Time qPCR. Five samples of each group were detected by real-time qPCR. The animals were anaesthetized with 2% pentobarbital sodium (40 mg/kg) and decapitated and the brains were immediately removed on ice. Contralateral hippocampus CA_1 region in individual animals was quickly isolated as Lein ES reported [16], put into 1.5 mL sterile centrifuge tube, and then frozen and stored at −70°C. Total RNA was extracted with Trizol reagent (Invitrogen) according to a standard protocol. The RNA was diluted in 40 μL ultra pure water, and the RNA concentration was determined by NanoDrop ND-100 Spectrophotometer (Thermo Fisher Scientific, Wilmington, DE).

Total RNA from each sample was used to synthesize cDNA using High Capacity cDNA Reverse Transcription Kit with Gene Amp PCR System 9700 (Applied Biosystems, USA). A final concentration of 1 μg/100 μL was obtained. Real-time PCR primers were designed on the basis of the reported cDNA sequences. The sequences for primers are as follows: β-actin, forward 5′-CCTCTATGCCAACACAGT-GC-3′ and reverse 5′-GTACTCCTGCTTGCTGATCC-3′; GluR1, forward 5′-GAGGGGAGGGAAGACCAA-3′ and reverse 5′-GCCGCATGTTCCTGTGAT-3′; GluR1, forward 5′-AGAGGACCCTTGTCTGTC-3′ and reverse 5′-GTG-TTTGATGGCTTGAGT-3′; GluR2, forward 5′-CTACCA-ATGGGATAAGTTCGC-3′ and reverse 5′-TTCGCAGTC-AAGGATTACACG-3′. Real-time PCR was performed using an ABI 7700 Real-Time PCR System (Applied Biosystems, USA) and an SYBR Green PCR Master Mix (Applied Biosystems) in a final volume of 25 μL with the following thermal cycling conditions: 95°C for 30 min, followed by 40 cycles of 95°C for 15 s, 59°C for 20 s, 72°C for 20 s, and 83°C for 15 s. β-actin was used as an internal control.

Samples were assayed in triplicate. Relative amount of each expression of mRNA in each sample was calculated as the ratio of mRNA/β-actin. The relative amount of amplified product was performed using the comparative threshold cycle method as described in the manufacturer's manual.

2.9. Statistical Analysis. Data are expressed as means ± standard error of the mean (SEM). Differences among means were measured by one-way analysis of variance (ANOVA) and Student's t tests, the correlations corrected for multiple comparisons. Statistical significance was defined as $P < 0.05$.

3. Results

3.1. Behavioral Test

3.1.1. OPT. The OPT is a behavioral test to measure the excited or depressed state of rats, commonly used to evaluate the exploratory behavior and reflect the emotional response of rats in new environment. In the present study, this test was used to verify whether the CIS model was successful. As shown in Figures 1(a) and 1(b), compared to the sham-operated rats, rats in CIS group showed decreased total distance traveled in 5 min ($P < 0.01$) and increased time in central zone ($P > 0.05$) after being put into the open field area. The decreased total distance traveled was effectively reversed by the treatment with CNQX or XYS decoction ($P < 0.01$); the time in central zone decreased after treatment, but no statistical difference was shown ($P > 0.05$). Both XYS and CNQX significantly ameliorated the behavioral abnormality of CIS rats.

3.1.2. EPM. The elevated plus-maze test is also commonly used as an anxiety test. CIS decreased the entry times and the time spent in central zone, compared to the control

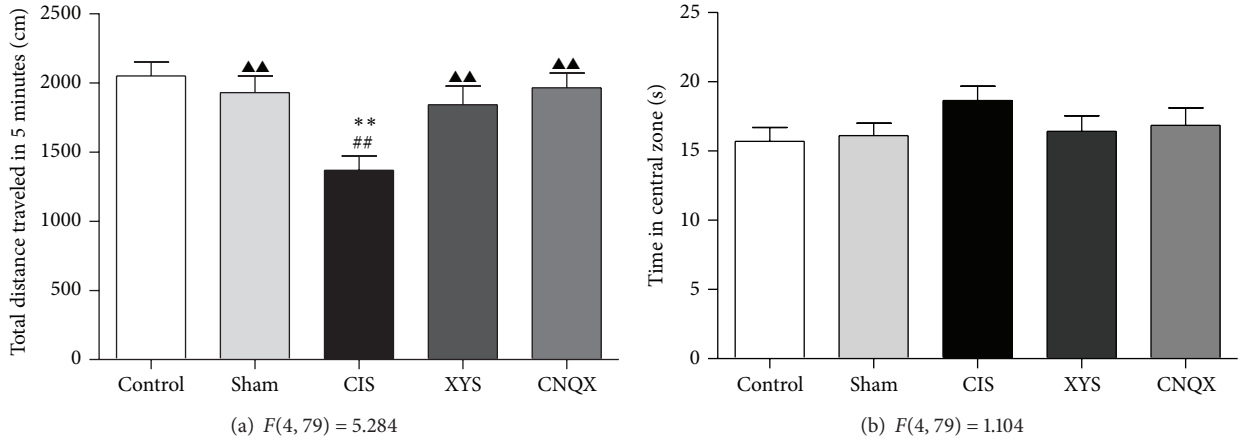

(a) $F(4, 79) = 5.284$ (b) $F(4, 79) = 1.104$

FIGURE 1: Performance of rats in the OPT: (a) total distance traveled in 5 minutes; (b) time in central zone of the test. Results are expressed as means ± SEM. $^{**}P < 0.01$ versus control group, $^{\#\#}P < 0.01$ versus sham-operated group, and $^{\blacktriangle\blacktriangle}P < 0.01$ versus CIS group.

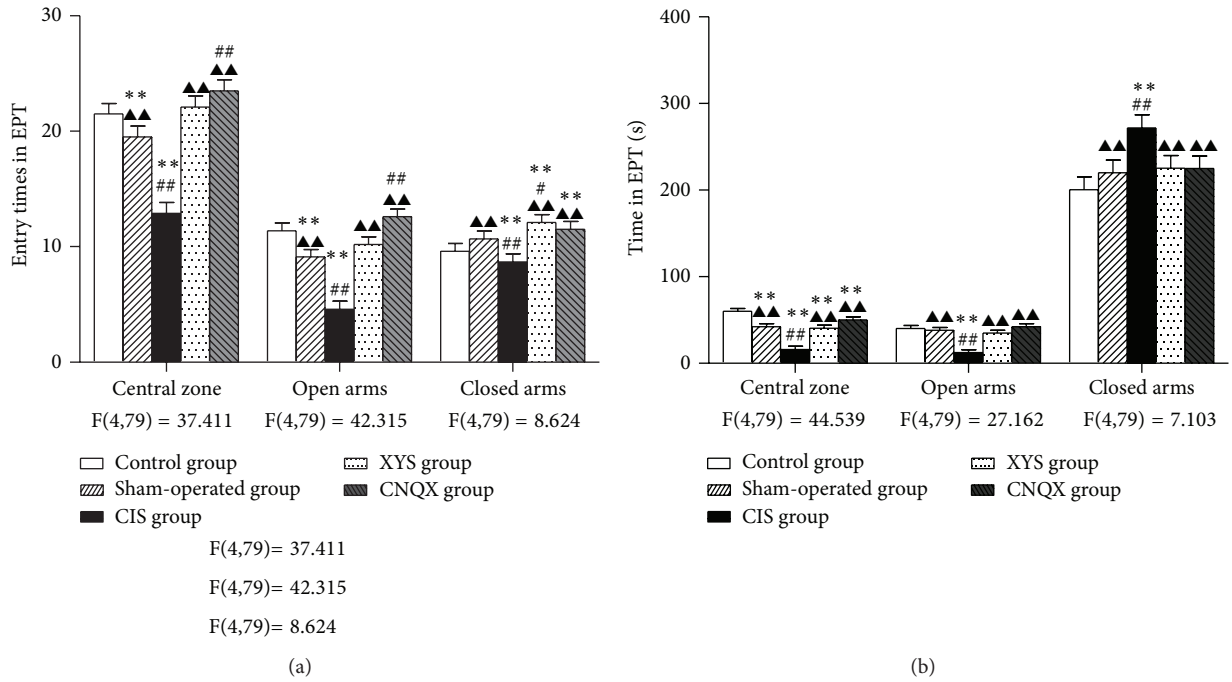

(a) (b)

FIGURE 2: Performance of rats in the EPM: (a) entry times in central zone, open arms, and closed arms; (b) time spent in central zone, open arms, and closed arms in 5 minutes. Results are expressed as means ± SEM. $^{**}P < 0.01$ versus control group, $^{\#}P < 0.05$ $^{\#\#}P < 0.01$ versus sham-operated group, and $^{\blacktriangle\blacktriangle}P < 0.01$ versus CIS group.

and sham-operated rats ($P < 0.01$, Figure 2(a); $P < 0.01$, Figure 2(b)). The decreases were reversed by the administration of CNQX ($P < 0.01$, Figures 2(a) and 2(b)) or XYS decoction ($P < 0.01$, Figures 2(a) and 2(b)).

Compared to the control and sham-operated group rats' activities, the entry times in open arms were decreased after CIS ($P < 0.01$, Figure 2(a)). Similar effects were found in the time spent in the open arms ($P < 0.01$, Figure 2(b)). XYS decoction increased the entry times and time spent in open arms ($P < 0.01$, Figures 2(a) and 2(b)). The CNQX showed better upregulation effects compared to the XYS and almost reached the normal level compared to the control group (Figures 2(a) and 2(b)).

No significant difference was found in the number of closed arm entries and time in the closed arms between control and sham-operated group (Figures 2(a) and 2(b)). The time spent in the closed arms was significantly increased after CIS compared to the control and sham-operated rats ($P < 0.01$, Figure 2(b)). XYS decoction decreased the time spent in closed arms; CNQX showed similar effects ($P < 0.01$, Figure 2(b)).

3.1.3. TEM. In subregion hippocampus CA_1 of control and sham-operated control group, the membrane of hippocampal pyramidal cell nucleus was very smooth, and the caryotin was evenly distributed (Figure 3(a)). All kinds of organelles,

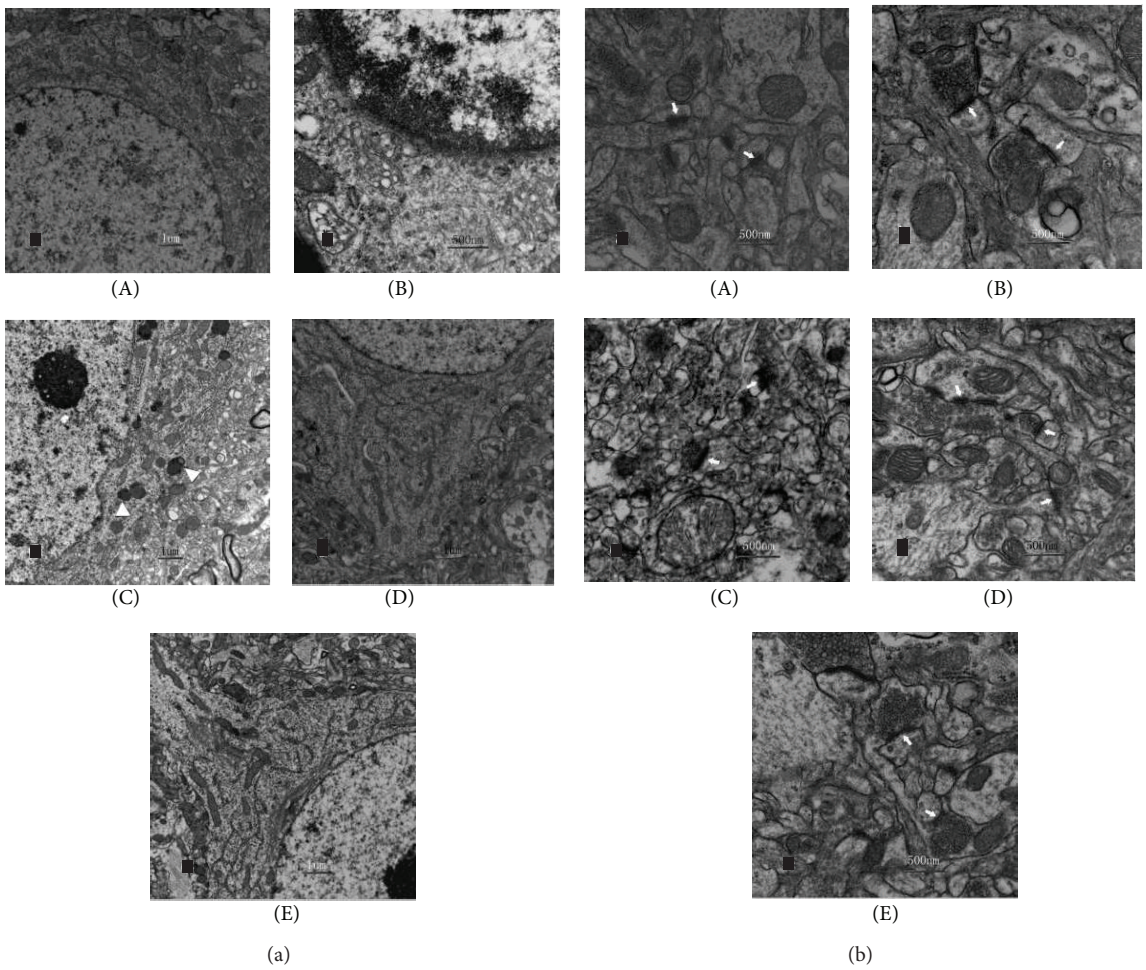

Figure 3: Ultrastructural changes of the hippocampus CA_1 subregion in control (A), sham-operated (B), CIS (C), XYS (D), and CNQX (E) groups, respectively. (a) The morphology and structure of hippocampal pyramidal cells, including the nucleus and most of the organelles. Mitochondria, rough endoplasmic reticulum, Golgi's body, and free ribosome can be identified near the nucleus. A curly nucleus (C) and several cytolysosomes (triangle, (a)(C)) in the cytolymph are shown in CIS-induced hippocampus. (b) Synapses in hippocampus CA_1. The synaptic structure is not clear and the fusion of pre- and postsynaptic membranes is visible in CIS-induced hippocampus (arrowheads, (b)(C)).

morphologically normal mitochondria rough endoplasmic reticulum, Golgi's body, and free ribosome were identified easily near the nucleus (Figure 3(a)). The synaptic structure was normal; both pre- and postsynaptic membranes were clearly visualized; the synaptic cleft,spherical and vesicles were also clearly present (Figure 3(b)). The synaptic vesicles within these synapses were typically clear and round (Figure 3(b)). And of those in CIS group, nucleus of hippocampal pyramidal cell was shrunken and metamorphotic, exhibiting pyknotic nuclei, irregular, dispersed chromatin clumps, with deformation of mitochondria and several cytolysosomes in cytolymph (Figure 3(a)). Both the synaptic structure synaptic cleft and synaptic cleft were unclear, in contrast, the fusion of pre- and postsynaptic membranes could be visualized clearly (Figure 3(b)).

After XYS decoction treatment, no obvious changes were observed between hippocampus neurons and synapses compared with control group (Figures 3(a) and 3(b)).

3.1.4. Real-Time qPCR. Real-time qPCR analysis revealed that, in hippocampus CA_1, 21-day stress increased the contents of GluR1 mRNA ($P < 0.05$, Figure 4(a)) in contrast to the sham-operated group; the level of GluR1 mRNA was decreased after XYS decoction treatment, but no significance was found comparing with CNQX positive control group ($P > 0.05$, Figure 4(a)). In contrast to the sham-operated group, the level of GluR2 mRNA was lower in the CIS group ($P < 0.05$, Figure 4(b)). However, XYS decoction treatment effectively reversed the GluR2 mRNA expression as well as CNQX positive group ($P < 0.05$, Figure 4(b)).

4. Discussion

OFT is one of the most popular assessment methods in behavioral research and often used to evaluate the environmental manipulations applying on the emotions of rodents [17, 18]. In our experiment, we additionally observed the animals' behavior by utilizing the EPM. This instrument has

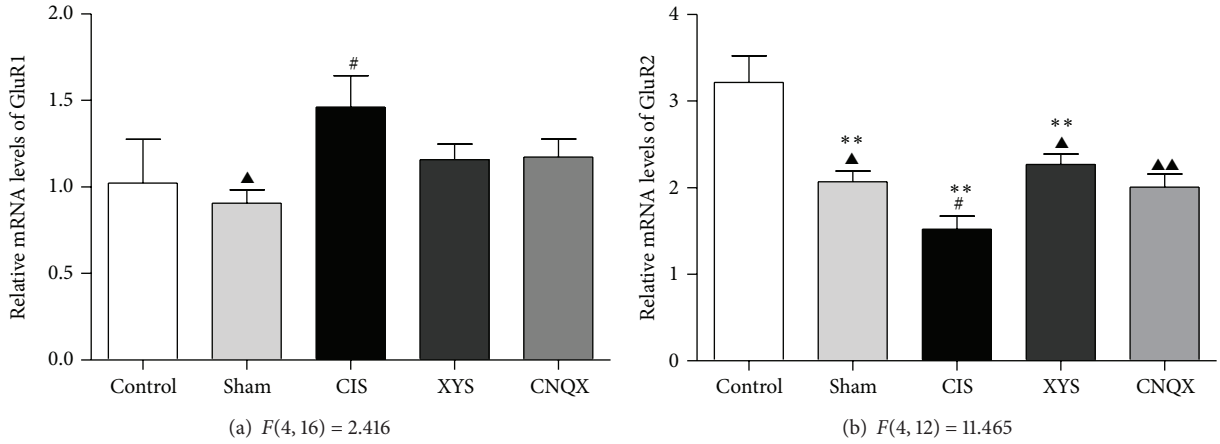

(a) $F(4, 16) = 2.416$ (b) $F(4, 12) = 11.465$

FIGURE 4: The expression of GluR1 and GluR2 mRNA in the hippocampus CA_1. Results are expressed as means ± SEM. $^{**}P < 0.01$ versus control group, $^{\#}P < 0.05$ versus sham-operated group, and $^{\blacktriangle}P < 0.05$ $^{\blacktriangle\blacktriangle}P < 0.01$ versus CIS group.

also been thoroughly validated as an extremely useful tool used to assess the emotional status of rodents [19]. Several variables can be measured in the open field; for instance, time spent in the center is considered to indicate emotional reactivity, and total distance traveled is thought to indicate locomotor and exploratory activity [17, 18]. The increased time spent in the center zone and decreased total distance of CIS rats showed a statement of limited spontaneous activity, anxiety, and depression, which caused decreased responsiveness, cognitive ability, and movement when the rats were placed in a novel environment. XYS decoction reversed CIS-induced changes, corroborating our previous findings [12], and CNQX showed the similar effect. This may reflect that both XYS and CNQX have some inhibitory influence on rat with chronic stress.

In our EPM test, 21 days' CIS rats showed increased occupancy of the closed arms and decreased occupancy of the open arms and center zone that are considered to indicate anxiety or depression. It is reported that animals with early restraint exhibited a significant decrease in the percent time spent and in the number of entries on the open arms; in addition, restraint induced a reduction in the total number of entries [20], which means exposure to hostile environment may produce behavioral and neuroendocrine changes that involve plasticity of central nervous system. In our investigation, it was found that XYS decoction effectively reversed CIS-induced behavior changes in EPM as well as CNQX positive control. These behavioral results of the present study clearly corroborated and extended previous findings that continuous administration of the XYS decoction exerts an antidepressant-like effect.

CNQX, a competitive AMPA (non-NMDA glutamate) receptor antagonist, was found to inhibit the locomotor activity of naive rats, and no symptoms of behavioral excitation were observed [21]. In our research, an increase in the exploratory behavior and motor activity in CIS rats after an intra-amygdala injection of CNQX was observed. These findings appear to provide that blocking AMPA receptors in particular brain regions might play an important role in relieving or aggravating depression-like behavior induced by chronic stress.

The results of electron microscopy showed that, in hippocampus CA_1, a series of ultrastructural damages of cellular organs such as nucleus and mitochondria in pyramidal neurons and synaptic contacts were observed in CIS rats. Mitochondria are the main energy providers for the neurons. Mitochondrial damage or other dysfunction will cause serious obstruction in the production of ATP and reduction in the primary neural capacity and give rise to different changes in cells structure and function disorder. Information from one neuron flows to another neuron across a synapse. Decreased number or structure damage of synapses can induce obstruction of neuronal information transfer caused by changes of neurotransmitter delivery. Consistent with previous findings of repeated stress can cause loss of the pyramidal neurons [22], profound changes in the morphology of the mossy fiber terminals, and significant loss of synapses in both CA_3 and CA_1 of the hippocampus [23], we have proved that synaptic plasticity in the central nervous system was changed by chronic stress.

Chronic stress may serve as an experimental model to evaluate the underlying cellular and molecular alterations associated with some of the consequences of recurrent depressive illness. Our previous study found that, generally, CIS decreased the level of AMPA receptors in the hippocampus while increased them in the amygdala BLA [11]. The present data demonstrated that the level of GluR1 increased, whereas GluR2 decreased in the hippocampus CA_1 after exposure to CIS. The opposite expression trends between GluR1 and GluR2 may be attributed to the differences in their process of synthesis, trafficking, and internalization. The high expression of GluR1 is probably attributed to the glutamate enhancement caused by chronic stress-induced HPA axis excitability, and the accumulated glutamate activates GluR1-containing AMPAR receptors [24, 25].

GluR2 expression may serve as a "molecular switch" leading to the formation of Ca^{2+}-permeable AMPA receptors [26]. In fact, receptors containing the GluR2 subunit are

calcium impermeable; only receptors lacking the GluR2 subunit (e.g., heteromers of GluR1/3) are calcium permeable [27, 28]. The position of GluR2 subunit in AMPA receptors can be replaced by GluR1 and GluR3 subunits when downregulation of GluR2 expression and stimulation of these calcium permeable receptors enhance excitotoxicity of endogenous glutamate following a neurological insult.

Some evidence has reported that mRNA and protein expression of the glutamate receptor subunit GluR2 in the hippocampus CA_1 were suppressed by transient global ischemia, sustained or kainate seizures; CNQX altered the downregulation of GluR2 subunit and prevented the hippocampal neurons from the neurotoxicity [29–31]. During the chronic stress processed, the combined action of polygenic, multilevel, and multisignal pathways leads to the disorder of the immunologic functions of the hippocampus, hippocampal apoptosis, and proliferation disequilibrium [32]. This is consistent with the protective effect of microstructure of CNQX, and XYS decoction downregulation of GluR1 and upregulation of GluR2 in hippocampus CA_1 respond to the 21-day stress in the present study.

It is well known that XYS decoction plays important roles in the clinical therapy of depression-related disorders in China [33], and several bioactive natural products have been identified from the herbs in the XYS decoction [33]. In Chinese medicinal theory, XYS decoction releases constraint and encourages the free-flow of Liver qi, allowing for open mindedness and rambling spirit [34]. Our previous clinic and experimental study demonstrated that the main ingredient of the XYS decoction is Radix Angelicas Sinensis (i.e., Chai Hu in Chinese), which acts as a nervous system sedative and a pituitary adrenocortical stimulant and is used for treatment of menstrual disorders [35–38].

In conclusion, this study demonstrated that XYS decoction can reverse the depression-like behavioral changes caused by CIS and produce an effect similar to the AMPA receptors in CNQX positive control, which indicates that one of the mechanisms of XYS decoction may attenuate the stimulation of the hippocampus CA_1 to relieve its damage. Further research may be needed to prove that XYS decoction may effectively regulate the balance of the AMPA receptors excitability between hippocampus and amygdala.

Ethical Approval

This study received permission from the Animal Ethics Committee of Beijing University of Chinese Medicine, China.

Conflict of Interests

The authors declare that there is no conflict of interests.

Authors' Contribution

Yuan Liang and Xiao-Ling Guo performed animal experiments and drafted the paper; the two authors contributed equally to this work. Guang-Xin Yue performed some of the experiments. Jia-Xu Chen was responsible for designing, supervising experiment, and correcting the manuscript. All authors read and corrected the paper, and approved the final version.

Acknowledgments

This study was supported by the National Natural Science Foundation of China (30672578, 81072756), China National Funds for Distinguished Young Scientists (30825046), and Program for Innovative Research Team in Beijing University of Chinese Medicine (2011CXTD-07). We are grateful to Dr. Xiu-Fang Ding who works at Beijing University of Chinese Medicine for her revised English grammar and words.

References

[1] M. Joëls, H. Karst, D. Alfarez et al., "Effects of chronic stress on structure and cell function in rat hippocampus and hypothalamus," *Stress*, vol. 7, no. 4, pp. 221–231, 2004.

[2] C. Lohmann and H. Kessels, "The developmental stages of synaptic plasticity," *Journal of Physiology*, 2013.

[3] J. E. Krettek and J. L. Price, "Projections from the amygdaloid complex and adjacent olfactory structures to the entorhinal cortex and to the subiculum in the rat and cat," *Journal of Comparative Neurology*, vol. 172, no. 4, pp. 723–752, 1977.

[4] J. P. Aggleton, "A description of amygdalo-hippocampal interconnections in the macaque monkey," *Experimental Brain Research*, vol. 64, no. 3, pp. 515–526, 1986.

[5] C. Lange and E. Irle, "Enlarged amygdala volume and reduced hippocampal volume in young women with major depression," *Psychological Medicine*, vol. 34, no. 6, pp. 1059–1064, 2004.

[6] J. P. Herman, M. M. Ostrander, N. K. Mueller, and H. Figueiredo, "Limbic system mechanisms of stress regulation: hypothalamo-pituitary- adrenocortical axis," *Progress in Neuro-Psychopharmacology and Biological Psychiatry*, vol. 29, no. 8, pp. 1201–1213, 2005.

[7] M. Hollmann and S. Heinemann, "Cloned glutamate receptors," *Annual Review of Neuroscience*, vol. 17, pp. 31–108, 1994.

[8] J. W. Olney, "Excitatory transmitter neurotoxicity," *Neurobiology of Aging*, vol. 15, no. 2, pp. 259–260, 1994.

[9] R. J. Wenthold, R. S. Petralia, J. Blahos II, and A. S. Niedzielski, "Evidence for multiple AMPA receptor complexes in hippocampal CA_1/CA_2 neurons," *Journal of Neuroscience*, vol. 16, no. 6, pp. 1982–1989, 1996.

[10] D. S. Bredt and R. A. Nicoll, "AMPA receptor trafficking at excitatory synapses," *Neuron*, vol. 40, no. 2, pp. 361–379, 2003.

[11] G.-X. Yue, Z.-F. Wang, and Q.-L. Zhang, "Changes of central AMPA receptor subunits and related protein mRNA expression in immobilization stressed rats and effect of Xiaoyaosan on them," *Chinese Journal of Integrated Traditional and Western Medicine*, vol. 27, no. 12, pp. 1110–1115, 2007.

[12] J.-X. Chen, W. Li, X. Zhao, and J.-X. Yang, "Effects of the chinese traditional prescription Xiaoyaosan decoction on chronic immobilization stress-induced changes in behavior and brain BDNF, TrkB, and $NT\text{-}_3$ in rats," *Cellular and Molecular Neurobiology*, vol. 28, no. 5, pp. 745–755, 2008.

[13] X. M. Bao and S. Y. Shu, *Stereotaxic Atlas of the Rat Brain*, People's Medical Publishing House, Beijing, China, 2004.

[14] C. M. Padovan, E. A. Del Bel, and F. S. Guimarães, "Behavioral effects in the elevated plus maze of an NMDA antagonist

injected into the dorsal hippocampus: influence of restraint stress," *Pharmacology Biochemistry and Behavior*, vol. 67, no. 2, pp. 325–330, 2000.

[15] Z.-Z. Meng, J.-H. Hu, J.-X. Chen, and G.-X. Yue, "Xiaoyaosan decoction, a traditional chinese medicine, inhibits oxidative-stress-induced hippocampus neuron apoptosis in vitro," *Evidence-Based Complementary and Alternative Medicine*, vol. 2012, Article ID 489254, 8 pages, 2012.

[16] E. S. Lein, X. Y. Zhao, and F. H. Gage, "Defining a molecular atlas of the hippocampus using DNA microarrays and high-throughput In situ hybridization," *Journal of Neuroscience*, vol. 24, no. 15, pp. 3879–3889, 2004.

[17] X.-C. Ma, D. Jiang, W.-H. Jiang et al., "Social isolation-induced aggression potentiates anxiety and depressive-like behavior in male mice subjected to unpredictable chronic mild stress," *Plos One*, vol. 6, no. 6, Article ID e20955, 2011.

[18] G. Liebsch, A. Montkowski, F. Holsboer, and R. Landgraf, "Behavioral profiles of two Wistar rat lines selectively bred for high or low anxiety-related behaviour," *Behavioural Brain Research*, vol. 94, no. 2, pp. 301–310, 1998.

[19] R. J. Rodgers and A. Dalvi, "Anxiety, defence and the elevated plus-maze," *Neuroscience and Biobehavioral Reviews*, vol. 21, no. 6, pp. 801–810, 1997.

[20] I. D. Martijena, N. Calvo, M. Volosin, and V. A. Molina, "Prior exposure to a brief restraint session facilitates the occurrence of fear in response to a conflict situation: behavioral and neurochemical correlates," *Brain Research*, vol. 752, no. 1–2, pp. 136–142, 1997.

[21] J. Maj, Z. Rogoz, G. Skuza, and T. Jaros, "Some behavioral effects of CNQX and NBQX, AMPA receptor antagonists," *Polish Journal of Pharmacology*, vol. 47, no. 4, pp. 269–277, 1995.

[22] B. S. McEwen and R. M. Sapolsky, "Stress and cognitive function," *Current Opinion in Neurobiology*, vol. 5, no. 2, pp. 205–216, 1995.

[23] N. Sousa, N. V. Lukoyanov, M. D. Madeira, O. F. X. Almeida, and M. M. Paula-Barbosa, "Reorganization of the morphology of hippocampal neurites and synapses after stress-induced damage correlates with behavioral improvement," *Neuroscience*, vol. 97, no. 2, pp. 253–266, 2000.

[24] M. T. Lowy, L. Gault, and B. K. Yamamoto, "Adrenalectomy attenuates stress-induced elevations in extracellular glutamate concentrations in the hippocampus," *Journal of Neurochemistry*, vol. 61, no. 5, pp. 1957–1960, 1993.

[25] J. N. Flak, M. M. Ostrander, J. G. Tasker, and J. P. Herman, "Chronic stress-induced neurotransmitter plasticity in the PVN," *Journal of Comparative Neurology*, vol. 517, no. 2, pp. 156–165, 2009.

[26] D. E. Pellegrini-Giampietro, J. A. Gorter, M. V. L. Bennett, and R. S. Zukin, "The GluR2 (GluR-B) hypothesis: Ca^{2+}-permeable AMPA receptors in neurological disorders," *Trends in Neurosciences*, vol. 20, no. 10, pp. 464–470, 1997.

[27] N. Burnashev, H. Monyer, P. H. Seeburg, and B. Sakmann, "Divalention permeability of AMPA receptor channels is dominated by the edited form of a single subunit," *Neuron*, vol. 8, no. 1, pp. 189–198, 1992.

[28] I. H. Greger, L. Khatri, and E. B. Ziff, "RNA editing at Arg607 controls AMPA receptor exit from the endoplasmic reticulum," *Neuron*, vol. 34, no. 5, pp. 759–772, 2002.

[29] L. K. Friedman, "Selective reduction of GluR2 protein in adult hippocampal CA_3 neurons following status epilepticus but prior to cell loss," *Hippocampus*, vol. 8, no. 5, pp. 511–525, 1998.

[30] K. Oguro, N. Oguro, T. Kojima et al., "Knockdown of AMPA receptor GluR2 expression causes delayed neurodegeneration and increases damage by sublethal ischemia in hippocampal CA_1 and CA_3 neurons," *Journal of Neuroscience*, vol. 19, no. 21, pp. 9218–9227, 1999.

[31] S.-Y. Li, J.-H. Ni, D.-S. Xu, and H.-T. Jia, "Down-regulation of GluR2 is associated with Ca^{2+}-dependent protease activities in kainate-induced apoptotic cell death in culturd rat hippocampal neurons," *Neuroscience Letters*, vol. 352, no. 2, pp. 105–108, 2003.

[32] X. H. Li, J. X. Chen, G. X. Yue et al., "Gene expression profile of the hippocampus of rats subjected to chronic immobilization stress," *Plos One*, vol. 8, no. 3, Article ID e57621, 14 pages, 2013.

[33] Y. Xu, B.-S. Ku, H.-Y. Yao et al., "The effects of curcumin on depressive-like behaviors in mice," *European Journal of Pharmacology*, vol. 518, no. 1, pp. 40–46, 2005.

[34] D. Bensky and R. Barolet, *Chinese Herbal Medicine: Formulas and Strategies*, Eastland Press, Seattle, Wash, USA, 3rd edition, 1990.

[35] J.-X. Chen, B. Ji, Z.-L. Lu, and L.-S. Hu, "Effects of *Chai Hu* (radix burpleuri) containing formulation on plasma β-endorphin, epinephrine and dopamine in patients," *American Journal of Chinese Medicine*, vol. 33, no. 5, pp. 737–745, 2005.

[36] S.-X. Wang, J.-X. Chen, G.-X. Yue, M.-H. Bai, M.-J. Kou, and Z.-Y. Jin, "Xiaoyaosan decoction regulates changes in neuropeptide Y and leptin receptor in the rat arcuate nucleus after chronic immobilization stress," *Evidence-Based Complementary and Alternative Medicine*, vol. 2012, Article ID 381278, 16 pages, 2012.

[37] Z. Z. Meng, J. X. Chen, Y. M. Jiang, and H. T. Zhang, "Effect of Xiaoyaosan decoction on learning and memory deficit in rats induced by chronic immobilization stress," *Evidence-Based Complementary and Alternative Medicine*. In press.

[38] H.-Z. Cui, L.-M. Wang, X. Zhao et al., "Metabonomics-based study of clinical urine samples in suboptimal health with different syndromes," *Evidence-Based Complementary and Alternative Medicine*, vol. 2013, Article ID 509134, 7 pages, 2013.

Hindawi Publishing Corporation
Evidence-Based Complementary and Alternative Medicine
Volume 2013, Article ID 759615, 7 pages
http://dx.doi.org/10.1155/2013/759615

Research Article

Citrus bergamia Risso Elevates Intracellular Ca^{2+} in Human Vascular Endothelial Cells due to Release of Ca^{2+} from Primary Intracellular Stores

Purum Kang,[1] Seung Ho Han,[2] Hea Kyung Moon,[1] Jeong-Min Lee,[3] Hyo-Keun Kim,[3] Sun Seek Min,[2] and Geun Hee Seol[1]

[1] *Department of Basic Nursing Science, School of Nursing, Korea University, 145 Anam-ro, Seongbuk-gu, Seoul 136-701, Republic of Korea*
[2] *Department of Physiology and Biophysics, School of Medicine, Eulji University, Youngdu-dong, Jung-gu, Daejeon 301-746, Republic of Korea*
[3] *KT&G Research Institute, Daejeon 305-805, Republic of Korea*

Correspondence should be addressed to Sun Seek Min; ssmin@eulji.ac.kr and Geun Hee Seol; ghseol@korea.ac.kr

Received 26 June 2013; Revised 28 October 2013; Accepted 28 October 2013

Academic Editor: Mohamed Eddouks

The purpose of the present study is to examine the effects of essential oil of *Citrus bergamia* Risso (bergamot, BEO) on intracellular Ca^{2+} in human umbilical vein endothelial cells. Fura-2 fluorescence was used to examine changes in intracellular Ca^{2+} concentration $[Ca^{2+}]_i$. In the presence of extracellular Ca^{2+}, BEO increased $[Ca^{2+}]_i$, which was partially inhibited by a nonselective Ca^{2+} channel blocker La^{3+}. In Ca^{2+}-free extracellular solutions, BEO increased $[Ca^{2+}]_i$ in a concentration-dependent manner, suggesting that BEO mobilizes intracellular Ca^{2+}. BEO-induced $[Ca^{2+}]_i$ increase was partially inhibited by a Ca^{2+}-induced Ca^{2+} release inhibitor dantrolene, a phospholipase C inhibitor U73122, and an inositol 1,4,5-triphosphate (IP_3)-gated Ca^{2+} channel blocker, 2-aminoethoxydiphenyl borane (2-APB). BEO also increased $[Ca^{2+}]_i$ in the presence of carbonyl cyanide m-chlorophenylhydrazone, an inhibitor of mitochondrial Ca^{2+} uptake. In addition, store-operated Ca^{2+} entry (SOC) was potentiated by BEO. These results suggest that BEO mobilizes Ca^{2+} from primary intracellular stores via Ca^{2+}-induced and IP3-mediated Ca^{2+} release and affect promotion of Ca^{2+} influx, likely via an SOC mechanism.

1. Introduction

Bergamot essential oil (BEO) is obtained from bergamot (*Citrus bergamia* Risso), a roughly pear-shaped citrus fruit. BEO is widely used in aromatherapy to alleviate symptoms of stress-induced anxiety, mild mood disorders, and cancer pain [1] and it has anxiolytic [2] and analgesic [1, 3, 4] effects in rodents.

Besides these effects of BEO, bergamottin, isolated from nonvolatile fraction of BEO, significantly decreased the typical electrocardiographic signs of coronary arterial spasm, the force of the contraction and the incidence of cardiac arrhythmias induced by vasopressin in the guinea pig [5]. Given the potential roles of bergamottine in cardiovascular function, it is of interest to know the roles of BEO in Ca^{2+} mobilization in endothelial cells. Vasorelaxant effect of BEO may involve Ca^{2+} mobilization from intracellular stores and/or from the extracellular pool in endothelial cells. Several studies demonstrating the relationship between endothelial cells and smooth muscle relaxation have been reported. Our previous study implicated that a change in cytosolic Ca^{2+} levels during stimulation of endothelial cells was a basic mechanism by which endothelial cells modulate vasomotor activity [6]. Another report indirectly supports this view, demonstrating that the vasorelaxant effect of the essential oil of *Ocimum gratissimum* is partly dependent on the integrity of the vascular endothelium [7].

Up till now, the effects of BEO on $[Ca^{2+}]_i$ in endothelial cells and the mechanisms by which BEO modulates the intracellular Ca^{2+} concentration ($[Ca^{2+}]_i$) are not revealed. In the present study, we investigate the intracellular Ca^{2+}-regulating properties of BEO in endothelial cells and present evidence that BEO increases $[Ca^{2+}]_i$ via release from intracellular Ca^{2+} stores and through store-operated Ca^{2+} entry (SOC).

2. Materials and Methods

2.1. Human Vascular Endothelial Cell Culture. A human endothelium-derived cell line EA.hy926 was purchased from the American Type Culture Collection (Manassas, VA, USA) [8]. EA cells were grown in Dulbecco's Modified Eagle Medium (DMEM) containing 20% fetal bovine serum (FBS) and 10% hypoxanthine-aminopterin-thymidine 50 supplement (Life Technologies). Cell cultures were maintained at 37°C in a fully humidified 95% air 5% CO_2 atmosphere. The media were removed and replaced with fresh medium three times in a week. The cells were detached by exposure to trypsin, reseeded on gelatin-coated coverslips, and maintained in culture for 2 to 4 days before use. Measurements were performed on subconfluent cells.

2.2. Cell Viability Assays. The thiazolyl blue tetrazolium bromide (MTT) assay was used to determine the effects of BEO on cell viability. EA cells were cultured using DMEM with 100% (v/v) FBS (Gibco Invitrogen), 100 units/mL penicillin, 100 μg/mL streptomycin (Gibco Invitrogen), and MEM nonessential amino acids (Invitrogen) in 96-well plates (Nunclon, Denmark) for 48 h until 80–90% confluence has been reached. To evaluate the effect of BEO, cells were for 15 min with varying concentrations (0.001, 0.005, 0.01, 0.05, or 0.1% [v/v in DMSO]) of the BEO and 0.25% DMSO. Then cells were washed with fresh PBS and replaced with serum-free media. In addition, cells were loaded with 10 μL MTT (5 mg/mL) and incubated at 37°C for 3 h. MTT solution was removed and replaced with 100 μL DMSO in a dark place for 2 h. The change in color was read at 540 nm using a plate reader.

2.3. Ca^{2+} Measurements. Cells were loaded with fura-2 AM, and $[Ca^{2+}]_i$ was measured using a microfluorometer system consisting of an inverted microscope (IX71, Olympus, Japan) and a PTI Filter Scan power illuminator system (Photon Technology International). Fura-2 AM (2 μM) was added to the bath and the cells were incubated for 25 min at 37°C. The cells were illuminated alternatively at wavelengths of 340 and 380 nm through a chopper wheel (frequency = 50 Hz). Fluorescence was measured at 510 nm, and autofluorescence was subtracted from the signals obtained. The Ca^{2+}-free concentration was calculated from the ratio of the fluorescence signals emitted at each excitation wavelength. The calibration procedure was identical to that described previously [9].

2.4. Solutions and Chemicals. The external solution contained the following (in mM): 150 NaCl, 6 KCl, 1.5 $CaCl_2$, 1 $MgCl_2$, 10 HEPES, and 10 glucose; pH was adjusted to 7.4 with NaOH. Ca^{2+}-free solution contained 5 mM EGTA in place of Ca^{2+}. The osmolarity of this solution, as measured with a vapor pressure osmometer (FISKE, USA), was 320 ± 5 mOsm. ATP, 2-aminoethoxydiphenyl borane (2-APB), 2,5-di-t-butyl-1,4-benzohydroquinone (BHQ), carbonyl cyanide m-chlorophenylhydrazone (CCCP), dantrolene, U73122, and MTT were purchased from Sigma; Fura-2 AM was obtained from molecular probes. BHQ, U73122, and essential oil (0.001%, 0.005%, 0.01%, 0.05%, 0.1%, or 0.2% v/v) were applied from a stock solution in dimethyl sulfoxide (DMSO). Final concentration of DMSO was less than 1%. 2-APB was applied from a stock solution in ethanol. The final concentrations of DMSO and ethanol were less than 0.05%. BEO (batch no. 110824) was purchased from Aromarant Co. Ltd., Röttingen, Germany, and came from locally cultivated plants in Italy.

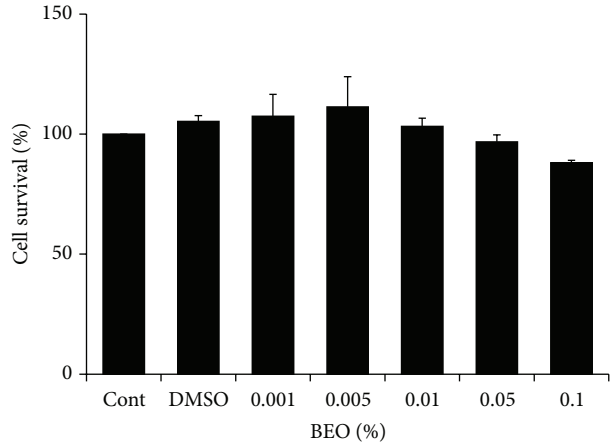

Figure 1: The cell survival percentage measured using MTT assay after 15 min posttreatment of bergamot essential oil, one-way ANOVA followed by Scheffe's post hoc test ($n = 4$).

2.5. Statistical Analysis. Pooled data are presented as means ± SEMs and significant differences were determined using paired t-test or ANOVA followed by Scheffe's post-hoc analysis. A value of $P < .05$ was considered significant.

3. Results

3.1. Cell Viability. The MTT assay was used to determine explored effect of varying concentrations of BEO in EA cells. Each cell was treated with media (control), DMSO (vehicle, 0.25% [v/v]), or BEO (0.001%, 0.005%, 0.01%, 0.05%, or 0.1% [v/v in DMSO]) for 15 min (Figure 1). Differences between groups were analyzed using the ANOVA followed by Scheffe's post-hoc analysis. There was no significant effect to the percentage of viable cells at all concentrations of BEO in EA cells ($F_{(6.27)} = 1.541$, $P = .214$).

3.2. Elevation of $[Ca^{2+}]_i$ by BEO in Human Vascular Endothelial Cells. BEO increased $[Ca^{2+}]_i$ in a concentration-dependent manner in EA cells (Figure 2(a)). The

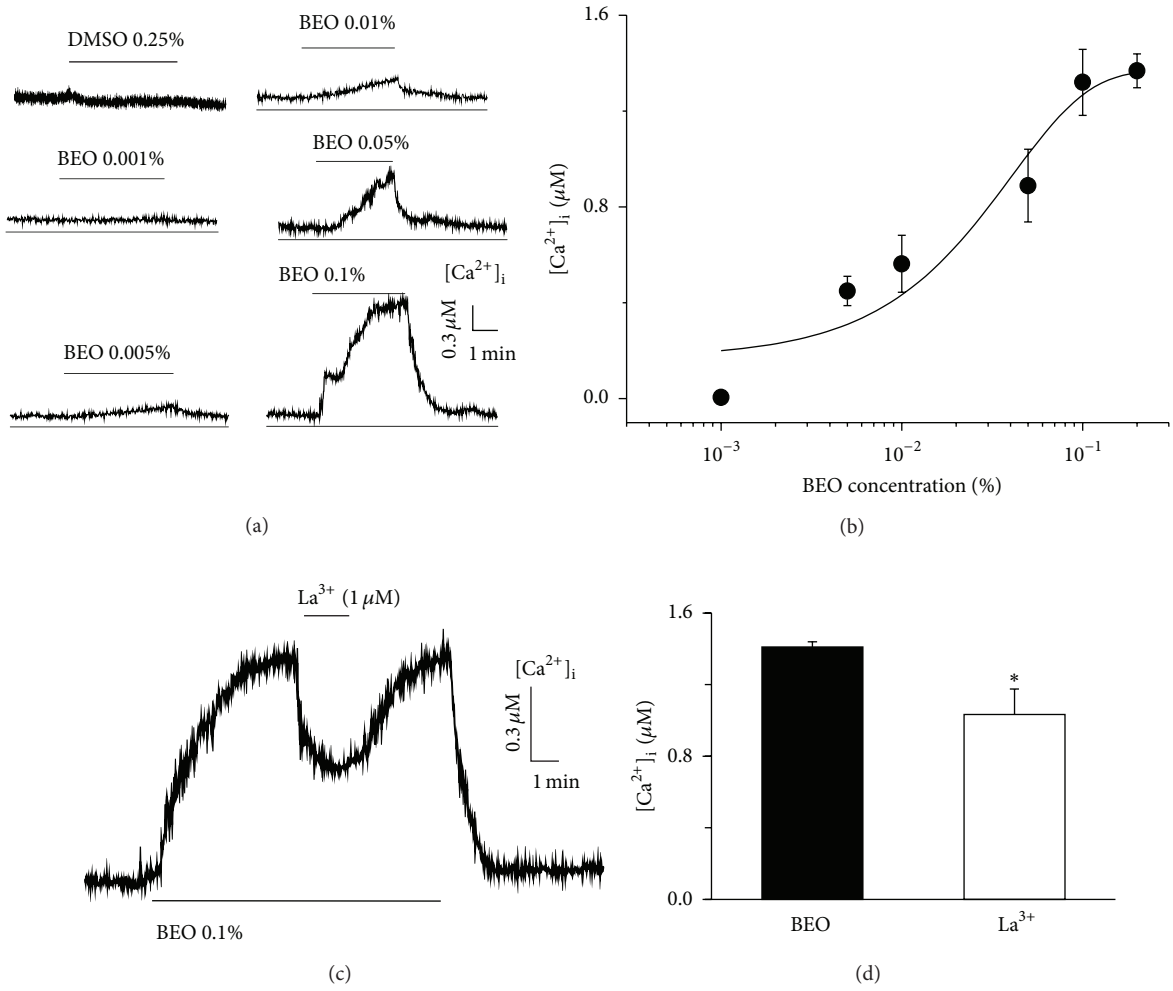

Figure 2: Application of BEO increased $[Ca^{2+}]_i$ in a concentration-dependent manner (a). Summary data describing the concentration-response relationship for BEO effects on $[Ca^{2+}]_i$ (b). Data are means ± SEMs. Applications of BEO or drugs are indicated by upper or bottom lines. Effects of BEO on $[Ca^{2+}]_i$ in human vascular endothelial cells. In the presence of extracellular Ca^{2+}, application of BEO (0.1% v/v) induced an increase in $[Ca^{2+}]_i$ that was significantly inhibited by La^{3+} (1 μM) ((c), (d)). $^*P < .05$ compared to the BEO group; n = 10~13 cells/group.

concentration-response relationship for mobilization of Ca^{2+} from intracellular stores by BEO is summarized in Figure 2(b). The concentration of BEO was nonlinearly related to the increase in $[Ca^{2+}]_i$ as revealed by fitting the Hill equation type dose-response curve. The half maximal increase in $[Ca^{2+}]_i$ (EC_{50}) was obtained at 0.04 ± 0.01%. DMSO (0.25% v/v) itself did not change intracellular Ca^{2+} levels. The cells showed no morphological change after treatment with BEO. Then we investigated whether BEO changed $[Ca^{2+}]_i$ in the presence of extracellular Ca^{2+} in EA cells. Application of BEO increased $[Ca^{2+}]_i$ to 1.41 ± 0.14 μM, which was partially and reversibly inhibited by the non-selective Ca^{2+} channel blocker La^{3+} (1 μM). $[Ca^{2+}]_i$ was reduced to 1.03 ± 0.09 μM by La^{3+} ($P = .019$, $n = 13$, Figures 2(c) and 2(d)), indicating that BEO induces Ca^{2+} influx from extracellular pool and Ca^{2+} release from intracellular stores.

3.3. Ca^{2+} Release from Endoplasmic Reticulum and Mitochondrial Ca^{2+} Stores by BEO. We next performed experiments to determine which of the two main dynamic intracellular Ca^{2+} stores, namely, the endoplasmic reticulum (ER) and mitochondria, is affected by BEO in EA cells. Ca^{2+} release from the ER depends on two mechanisms: Ca^{2+}-induced Ca^{2+} release (CICR), involving ryanodine receptors, and IP_3-induced Ca^{2+} release (IICR), involving inositol 1,4,5-triphosphate (IP_3) receptors [10]. BEO-induced intracellular Ca^{2+} increase was significantly and reversibly inhibited by the CICR inhibitor, dantrolene ($P < .001$, $n = 10$, Figure 3(a)). These data indicate that BEO elevates $[Ca^{2+}]_i$ in part by the release of Ca^{2+} from intracellular stores via a CICR mechanism. To determine whether BEO releases Ca^{2+} from intracellular Ca^{2+} stores via IICR, we tested the effects of BEO in the presence of U73122, the specific inhibitor of

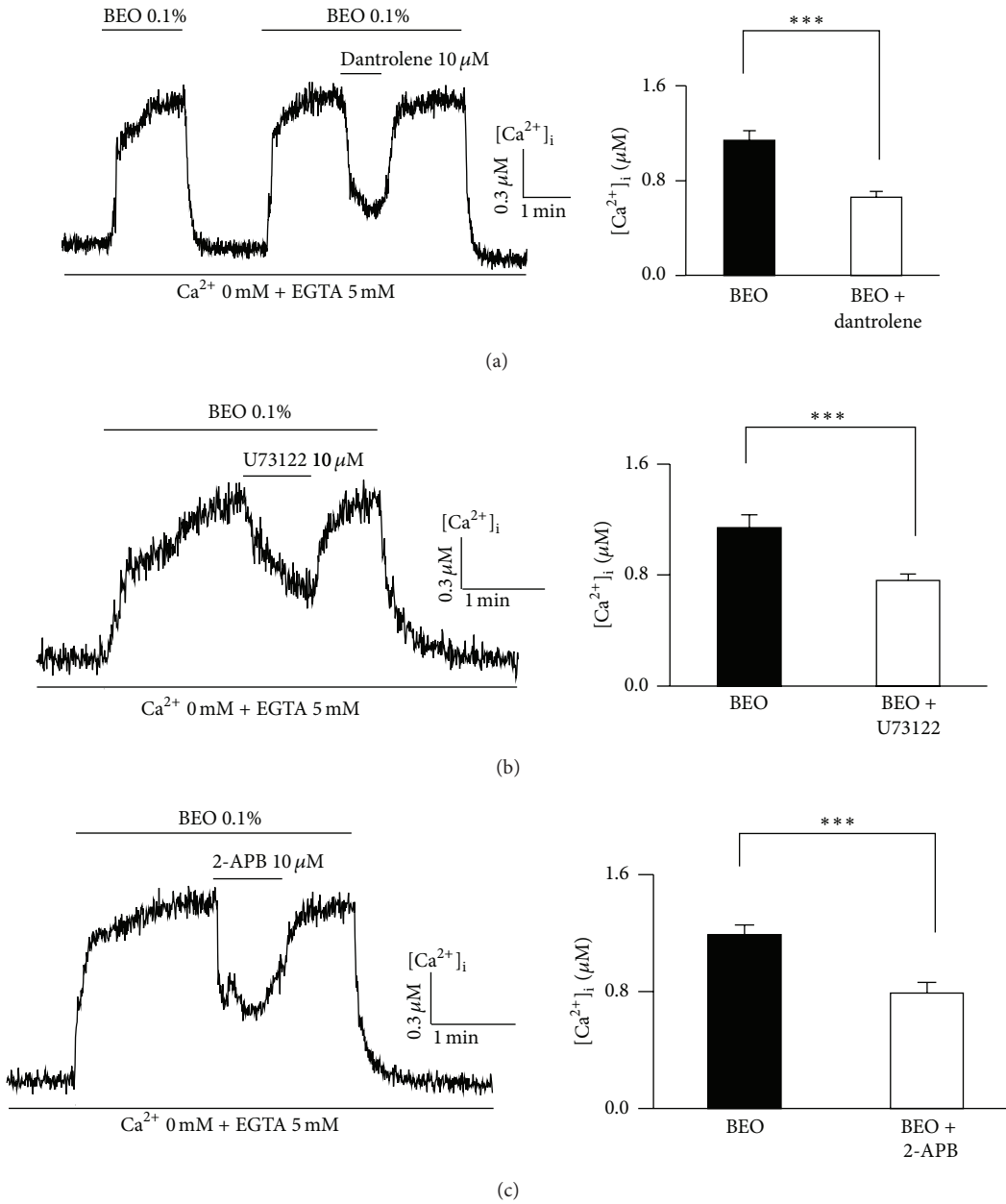

Figure 3: Involvement of CICR and IICR on BEO-induced intracellular Ca^{2+} release. Effects of CICR inhibitor, dantrolene (10 μM) on BEO-induced intracellular Ca^{2+} release. Application of dantrolene partially attenuated increase in $[Ca^{2+}]_i$ by BEO (the first upper line) (a). Involvement of IICR pathways in BEO-induced intracellular Ca^{2+} release ((b), (c)). Increased $[Ca^{2+}]_i$ by BEO was significantly inhibited by inhibitors of PLC (U73122, 10 μM) or IP_3 receptors (2-APB, 10 μM).

phospholipase C (PLC) [11], to inhibit IP_3 synthesis, or 2-APB, a membrane-permeable inhibitor of IP_3-gated ER Ca^{2+} channels [12]. BEO-induced intracellular Ca^{2+} increase was significantly inhibited by both U73122 ($P < .001$, $n = 10$, Figure 3(b)) and 2-APB ($P < .001$, $n = 15$, Figure 3(c)). These data indicate that PLC-mediated synthesis of IP_3 and IP_3 binding to IP_3-gated Ca^{2+} channels in the ER contribute to BEO-induced Ca^{2+} release from intracellular stores.

A portion of Ca^{2+} released from the ER is taken up by proximate mitochondria, which can also release Ca^{2+} and thereby regulate $[Ca^{2+}]_i$. To determine whether mitochondria participate in the reuptake of BEO-induced Ca^{2+} release, we examined the effects of BEO on $[Ca^{2+}]_i$ in a Ca^{2+}-free solution in the presence of BHQ (an SR/ER Ca^{2+}-ATPase inhibitor) and CCCP (a mitochondrial Ca^{2+} uptake inhibitor). In cells treated with BHQ and/or CCCP, $[Ca^{2+}]_i$ transiently increased and then decreased slowly to a steady state, suggesting that an SR/ER Ca^{2+}-ATPase and mitochondrial Ca^{2+} uptake participate in the regulation of $[Ca^{2+}]_i$ under basal conditions (Figure 4(a)). Increase in $[Ca^{2+}]_i$ in

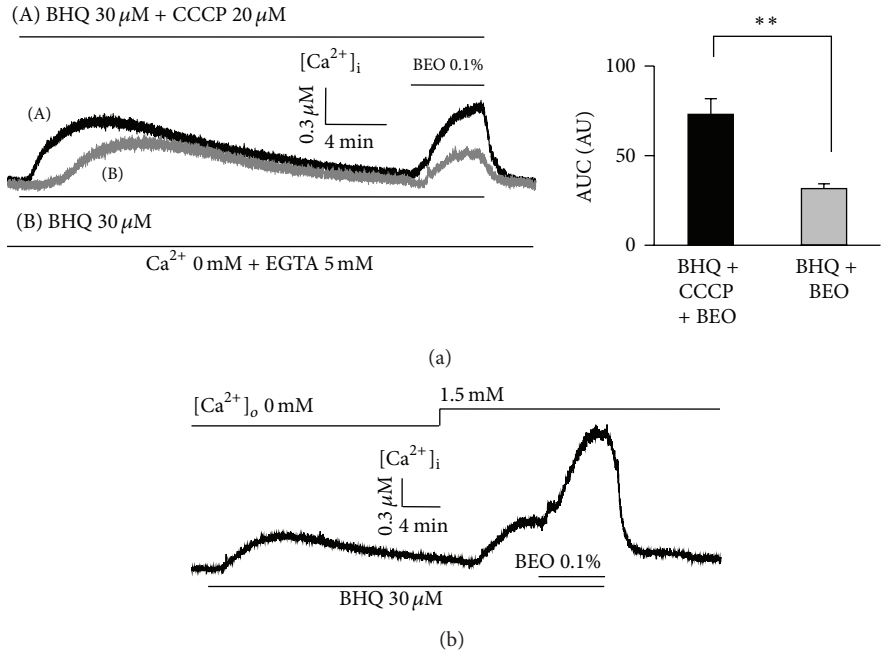

Figure 4: Involvement of mitochondrial Ca^{2+} uptake and SOC pathway on BEO-induced Ca^{2+} release. Inhibition of mitochondrial Ca^{2+} uptake and SR/ER Ca^{2+}-ATPase on BEO-induced Ca^{2+} release with CCCP (20 μM) and BHQ (30 μM), respectively (a). Increase in $[Ca^{2+}]_i$ by subsequent application of BEO in the presence of BHQ and CCCP (black trace a) was higher than that in the presence of BHQ only (gray trace b). Effects of SOC pathway in BEO-induced intracellular Ca^{2+} release. SOC was induced by reintroduction of extracellular Ca^{2+} following SR/ER Ca^{2+}-ATPase inhibition with BHQ (b). Intracellular Ca^{2+} levels were further enhanced by subsequent addition of BEO. Data are means ± SEMs. $^{**}P < .01$; $n = 15$ cells/group. Applications of BEO or drugs are indicated by upper or bottom lines.

EA cells by subsequent application of BEO in the presence of BHQ and CCCP was higher than that in the presence of BHQ only. An area under the curve in each condition was 72.97 ± 8.81 and 31.62 ± 2.75 arbitrary unit, respectively. The difference between two conditions was 41.35 ± 8.12 arbitrary unit, suggesting that mitochondrial Ca^{2+} stores may contribute to the regulation of the BEO-induced increase in $[Ca^{2+}]_i$.

Considering the inhibitory effect of La^{3+}, noted above, it is suggested that Ca^{2+}-entry pathway(s) is (are) activated by BEO. Thus, we next examined whether BEO modulated Ca^{2+} entry via an SOC mechanism. Exposure of EA cells to the BHQ in a Ca^{2+}-free solution induced a transient increase in $[Ca^{2+}]_i$, which then decreased slowly to a steady state (Figure 4(a)). Reapplication of extracellular Ca^{2+} following emptying of intracellular Ca^{2+} stores with BHQ caused an increase in $[Ca^{2+}]_i$, indicating activation of an SOC mechanism. When BEO was applied after SOC was evoked, SOC was further enhanced, suggesting that BEO also activates Ca^{2+} influx through an SOC pathway (Figure 4(b)). However, using this protocol alone in this experiment does not rule out that other calcium entry pathways may be activated by BEO.

4. Discussion

In the present study, we firstly demonstrate that BEO mobilized Ca^{2+} from extracellular and intracellular sources in endothelial cells. Our present results also suggest that BEO increased intracellular Ca^{2+} level through both mobilization of intracellular Ca^{2+} stores, ER and mitochondria, and promotion of Ca^{2+} influx, via an SOC mechanism. These findings will provide insight into the physiological mechanisms involved in Ca^{2+} regulation in endothelial cells following exposure to BEO.

Some essential oils contain photoactive molecules like furocoumarins. For instance, essential oil of *Citrus bergamia* contains psoralens which bind to DNA under ultraviolet A light exposure producing mono- and biadducts that are cytotoxic and highly mutagenic [13]. Therefore, the results observed in the present study may be results from the effects of photoirritation of BEO. Since, however, intracellular Ca^{2+} level rapidly returned to a baseline level after washing out of BEO and cell viability was normal in doses tested, we think that phototoxic or cytotoxic effect is little on intracellular Ca^{2+} level by BEO. In addition, *in vitro* studies have shown that BEO reduces glutamate receptor-mediated cell death induced by N-methyl-D-aspartate [14]. Nevertheless, further researches are necessary to evaluate phototoxic potential of BEO in endothelial cells.

BEO has been reported to decrease the blood pressure in healthy human and have dilating effect on mouse artery [15, 16]. In the recent study, limonene, one of the major components of BEO (37.26%), increased cytosolic Ca^{2+} concentration by the direct activation of adenosine A_{2A} receptors [17]. In endothelium, an adenosine A_{2A} receptor

has an important role in NO release. Adenosine A_{2A} receptor induced NO-dependent vasodilation by intracellular Ca^{2+} increase [18]. Thus, we suggest that the effect of BEO may be attributable to limonene by activation of adenosine A_{2A} receptors.

Contraction and relaxation of smooth muscle are regulated not only by changes in cytoplasmic calcium concentration but also by other important signaling mechanisms, that is, independent of the changes in $[Ca^{2+}]_i$, known as Ca^{2+} sensitization [19]. Although the increase in $[Ca^{2+}]_i$ initiates smooth muscle contraction via activating myosin light chain kinase, Ca^{2+} sensitization mediates smooth muscle contraction by modulating myosin light chain phosphatase [20]. The increase in $[Ca^{2+}]_i$ in endothelial cell plays a role in synthesis and the release of vasoactive compounds such as nitric oxide or prostaglandins [21], thereby altering Ca^{2+} sensitization in smooth muscle cells. It has been reported that linalyl acetate, one of the main components of BEO, induces relaxation of the smooth muscle via partially endothelium-dependent pathway [22]. Further research will be needed to reveal the mechanism by which the calcium releasing actions by BEO in endothelial cells regulate to the vasodilator action.

In conclusion, before BEO can be considered for use in treating vascular-related diseases, further studies are necessary to define the Ca^{2+}-elevating pathways enlisted by BEO under pathological conditions.

Conflict of Interests

The authors declare they have no conflict of interests.

Authors' Contribution

Purum Kang, Seung Ho Han, and Hea Kyung Moon contributed equally to this work.

Acknowledgment

This work was supported by the National Research Foundation of Korea (NRF) grant funded by the Korean government (MEST) (2012-0004065, 2012-007145).

References

[1] G. Bagetta, L. A. Morrone, L. Rombolà et al., "Neuropharmacology of the essential oil of bergamot," *Fitoterapia*, vol. 81, no. 6, pp. 453–461, 2010.

[2] S. Saiyudthong and C. A. Marsden, "Acute effects of bergamot oil on anxiety-related behaviour and corticosterone level in rats," *Phytotherapy Research*, vol. 25, no. 6, pp. 858–862, 2011.

[3] T. Sakurada, H. Kuwahata, S. Katsuyama et al., "Intraplantar injection of bergamot essential oil into the mouse hindpaw: effects on capsaicin-induced nociceptive behaviors," *International Review of Neurobiology*, vol. 85, pp. 237–248, 2009.

[4] T. Sakurada, H. Mizoguchi, H. Kuwahata et al., "Intraplantar injection of bergamot essential oil induces peripheral antinociception mediated by opioid mechanism," *Pharmacology Biochemistry and Behavior*, vol. 97, no. 3, pp. 436–443, 2011.

[5] F. Occhiuto and C. Circosta, "Cardiovascular properties of the non-volatile total residue from the essential oil or *Citrus bergamia*," *International Journal of Pharmacognosy*, vol. 34, no. 2, pp. 128–133, 1996.

[6] G. H. Seol, S. C. Ahn, J. A. Kim, B. Nilius, and S. H. Suh, "Inhibition of endothelium-dependent vasorelaxation by extracellular K^+: a novel controlling signal for vascular contractility," *American Journal of Physiology—Heart and Circulatory Physiology*, vol. 286, no. 1, pp. H329–H339, 2004.

[7] L. F. L. Interaminense, D. M. Jucá, P. J. C. Magalhães, J. H. Leal-Cardoso, G. P. Duarte, and S. Lahlou, "Pharmacological evidence of calcium-channel blockade by essential oil of Ocimum gratissimum and its main constituent, eugenol, in isolated aortic rings from DOCA-salt hypertensive rats," *Fundamental and Clinical Pharmacology*, vol. 21, no. 5, pp. 497–506, 2007.

[8] C. J. S. Edgell, C. C. McDonald, and J. B. Graham, "Permanent cell line expressing human factor VIII-related antigen established by hybridization," *Proceedings of the National Academy of Sciences of the United States of America*, vol. 80, no. 12, pp. 3734–3737, 1983.

[9] B. Nilius, G. Schwartz, M. Oike, and G. Droogmans, "Histamine-activated, non-selective cation currents and Ca^{2+} transients in endothelial cells from human umbilical vein," *Pflugers Archiv—European Journal of Physiology*, vol. 424, no. 3-4, pp. 285–293, 1993.

[10] M. Iino, "Calcium-induced calcium release mechanism in guinea pig taenia caeci," *Journal of General Physiology*, vol. 94, no. 2, pp. 363–383, 1989.

[11] E. Gabev, J. Kasianowicz, T. Abbott, and S. McLaughlin, "Binding of neomycin to phosphatidylinositol 4,5-bisphosphate (PIP2)," *Biochimica et Biophysica Acta*, vol. 979, no. 1, pp. 105–112, 1989.

[12] T. Maruyama, T. Kanaji, S. Nakade, T. Kanno, and K. Mikoshiba, "2APB, 2-aminoethoxydiphenyl borate, a membrane-penetrable modulator of Ins(l,4,5)P3-induced Ca^{2+} release," *Journal of Biochemistry*, vol. 122, no. 3, pp. 498–505, 1997.

[13] F. Bakkali, S. Averbeck, D. Averbeck, and M. Idaomar, "Biological effects of essential oils—a review," *Food and Chemical Toxicology*, vol. 46, no. 2, pp. 446–475, 2008.

[14] M. T. Corasaniti, J. Maiuolo, S. Maida et al., "Cell signaling pathways in the mechanisms of neuroprotection afforded by bergamot essential oil against NMDA-induced cell death in vitro," *British Journal of Pharmacology*, vol. 151, no. 4, pp. 518–529, 2007.

[15] K.-M. Chang and C.-W. Shen, "Aromatherapy benefits autonomic nervous system regulation for elementary school faculty in Taiwan," *Evidence-Based Complementary and Alternative Medicine*, vol. 2011, Article ID 946537, 7 pages, 2011.

[16] P. Kang, S. H. Suh, S. S. Min, and G. H. Seol, "The essential oil of *Citrus bergamia* Risso induces vasorelaxation of the mouse aorta by activating K^+ channels and inhibiting Ca^{2+} influx," *Journal of Pharmacy and Pharmacology*, vol. 65, no. 5, pp. 745–749, 2013.

[17] H. M. Park, J. H. Lee, J. Yaoyao, H. J. Jun, and S. J. Lee, "Limonene, a natural cyclic terpene, is an agonistic ligand for adenosine A_{2A} receptors," *Biochemical and Biophysical Research Communications*, vol. 404, no. 1, pp. 345–348, 2011.

[18] C. J. Ray and J. M. Marshall, "The cellular mechanisms by which adenosine evokes release of nitric oxide from rat aortic endothelium," *Journal of Physiology*, vol. 570, part 1, pp. 85–96, 2006.

[19] M. Hori and H. Karaki, "Regulatory mechanisms of calcium sensitization of contractile elements in smooth muscle," *Life Sciences*, vol. 62, no. 17-18, pp. 1629–1633, 1998.

[20] A. P. Somlyo and A. V. Somlyo, "Ca^{2+} sensitivity of smooth muscle and nonmuscle myosin II: modulated by G proteins, kinases, and myosin phosphatase," *Physiological Reviews*, vol. 83, no. 4, pp. 1325–1358, 2003.

[21] F. Lantoine, L. Iouzalen, M.-A. Devynck, E. Millanvoye-Van Brussel, and M. David-Dufilho, "Nitric oxide production in human endothelial cells stimulated by histamine requires Ca^{2+} influx," *Biochemical Journal*, vol. 330, no. 2, pp. 695–699, 1998.

[22] R. Koto, M. Imamura, C. Watanabe et al., "Linalyl acetate as a major ingredient of lavender essential oil relaxes the rabbit vascular smooth muscle through dephosphorylation of myosin light chain," *Journal of Cardiovascular Pharmacology*, vol. 48, no. 1, pp. 850–856, 2006.

Hindawi Publishing Corporation
Evidence-Based Complementary and Alternative Medicine
Volume 2013, Article ID 145925, 7 pages
http://dx.doi.org/10.1155/2013/145925

Research Article

Effect of *Nelumbo nucifera* Petal Extracts on Lipase, Adipogenesis, Adipolysis, and Central Receptors of Obesity

Chandrasekaran Chinampudur Velusami,[1,2] Amit Agarwal,[1] and Vijayalakshmi Mookambeswaran[2]

[1] *R&D Centre, Natural Remedies Pvt. Ltd., Plot No. 5B, Veerasandra Industrial Area, 19th K.M. Stone, Hosur Road, Bangalore, Karnataka 560100, India*
[2] *Center for Bioseparation Technology, VIT University, Vellore, Tamil Nadu 632014, India*

Correspondence should be addressed to Chandrasekaran Chinampudur Velusami; cvc@naturalremedy.com

Received 22 July 2013; Revised 30 September 2013; Accepted 2 October 2013

Academic Editor: C. S. Cho

N. nucifera is one among the important medicinal plants assessed for its antiobesity action in various preclinical models. The present study was aimed at investigating the antiobesity effect of methanol and successive water extracts of petals of *N. nucifera* by studying its effect on adipogenesis, adipolysis, lipase, serotonin (5-HT_{2C}), cannabinoid (CNR_2), melanocyte concentrating hormone ($MCHR_1$), and melanocortin (MC_4R) receptors. Both methanol and successive water extracts of *N. nucifera* petals had an effect on inhibition of lipid storage in adipocytes and on increasing lipolysis. *N. nucifera* petal methanol extract exhibited the concentration-dependent inhibitory effect on lipase activity with an IC_{50} value of 47 μg/mL. *N. nucifera* petal extracts showed evident agonist and antagonist activity towards 5-HT_{2C} and CNR_2 receptors, respectively, while it showed no effect towards $MCHR_1$ and MC_4R receptors. Overall, methanol extract of *N. nucifera* petals showed better activity than successive water extract.

1. Introduction

Several herbs have been indicated for weight management [1]. One such plant used for weight management is *Nelumbo nucifera* Gaertn. *N. nucifera*, known by a number of names including Indian lotus, sacred lotus, bean of India, or simply lotus, is one of two species of aquatic plant in the family Nelumbonaceae. Almost all parts of *N. nucifera* are edible, and in many Asian countries it was found in the recipe of food [2]. Extracts of *N. nucifera* flowers, seeds, rhizomes, and leaves have been reported to have varied therapeutic potential including antistress [3], antiobesity [4], antioxidant [5], hepatoprotective [6], antidiabetic activity [7], anti-inflammatory [8, 9], antipyretic [10], antibacterial [11], and immunomodulatory [12, 13] activities.

Several bioactive phytocompounds derived from these plant parts were belonging to different chemical groups, including alkaloids, flavonoids, glycosides, triterpenoid, and vitamins [14]. Leaves, root, and the embryonic stage of *N. nucifera* have been reported to contain alkaloids such as roemerine, nuciferine, nornuciferine, nelumboside, anonaine, 5-methoxy-6-hydroxyaporphine, liensinine, and asimilobine [15]. Bisbenzylisoquinoline alkaloids from *N. nucifera* were shown to be bioavailable after oral administration to rats at a dose of 20 mg/kg [16]. *N. nucifera* alkaloid was shown to inhibit 3T3-L1 preadipocyte differentiation and improve high-fat diet-induced obesity and body fat accumulation in rats [17].

Several flavonoids and nonflavonoids from flowers of *N. nucifera* reported by several authors were consolidated in a review by Mukherjee et al. [14]. Flavonoids include myricetin-3-O-b-D-glucopyranoside, quercetin-3-O-b-D-glucuronide, astragalin, quercetin, 3,4-dihydroxybenzoic, kaempferol, p-hydroxybenzoic acid, and b-sitosterol which were isolated from ethanol extract of the petals of *N. nucifera* [18]. Nonflavonoid compounds, including adenine, myo-inositol, arbutin, and sitosterol glucopyranoside, were identified in flower extract [14]. Wu et al. [19] demonstrated the antiobesity effect of a flavonoid-enriched extract from *N. nucifera* leaf (NLFE) in high-fat diet (HFD) fed C57BL/6 mice and

concluded its action via lipid-regulated enzymes, thereby attenuating body lipid accumulation and preventing obesity. Antiobesity action of leaves and seeds of *N. nucifera* was extensively studied in *in vitro* and *in vivo* models by many researchers [4, 20–22]. The present study was designed to investigate the effect of *N. nucifera* petal extracts on lipase, adipogenesis, adipolysis, and central receptors *in vitro*.

2. Materials and Methods

2.1. Chemicals. Dexamethasone, isobutylmethylxanthine (IBMX), oil red O, porcine lipase enzyme, thiazolyl blue tetrazolium bromide (MTT), 4-methyl umbelliferyl oleate, GW 803430, melanocyte concentrating hormone (MCH), melanotan II, DL-isoproterenol hydrochloride, and orlistat were procured from Sigma-Aldrich. AM630, CP 55,940, AL34662, cell plating reagent-3, cell assay buffer, substrate reagent 1, and substrate reagent 2 were obtained from DiscoveRx (USA). Insulin was procured from Biocon. Fetal bovine serum (FBS) and bovine calf serum (BCS) were purchased from Hyclone. Enzychrom glycerol detection kit was procured from BioAssay systems. DMEM was obtained from Gibco Life Technologies.

2.2. Plant Material. The petals of *N. nucifera* (100 g each) were procured from a local commercial supplier and were authenticated at National Institute of Science Communication and Information Resources (NISCAIR), New Delhi. A voucher specimen (no. 811) was deposited in our herbarium. Dried petals were extracted with methanol (~400 mL) by refluxing at 70°C for 1 hour. Extract solution was filtered, and the remaining raw material was subjected to methanol extraction by repeating the above steps twice. The liquid filtrates were combined and concentrated by distillation under vacuum to a thick paste, followed by drying under vacuum at temperature 70°C. The dried extract was named as methanol extract and utilized to perform *in vitro* experiments. Phytochemical investigation of methanol extract of *N. nucifera* was carried out by subjecting methanol extract to HPLC analysis to identify the flavonoids as per the method described by Xingfeng et al. [23].

Methanol extraction of the raw material was carried out as mentioned above. The leftover raw material after methanol extraction was further boiled with water at 85–90°C (3 times each with 500–600 mL water for 1 h) and filtered each time. The liquid filtrates were combined and concentrated by distillation under vacuum to a thick paste, followed by drying under vacuum at temperature 80°C. The dried extract was named as successive water extract and used to perform *in vitro* experiments.

2.3. Cell Lines and Culture Conditions. 3T3-L1 cell line was procured from American Type Culture Collection (ATCC). 3T3-L1 fibroblasts were cultured in DMEM supplemented with 10% BCS and incubated at 37°C; 5% CO_2. The U2OS cell line coupled with 5-HT_{2C} or MC_4 receptor and CHO-K1 cell line coupled with CNR_2 or $MCHR_1$ receptor were obtained from DiscoveRx. U2OS and CHO-K1 cells were maintained in cell plate reagent in 96-well tissue culture plates for 48 h and 24 h, respectively.

2.4. Cell Viability Determination. Initial experiments using 3T3-L1, CHO-K1, and U2OS cells were conducted to assess the cytotoxic concentrations of both methanol and successive water extracts of *N. nucifera*. Cell viability was determined by a colorimetric MTT assay as described by Mosmann [24]. In brief, cells were cultured in 96-well plates at a seeding density of 5×10^3 cells/well. After 24 h of seeding, the cells were treated with and without *N. nucifera* extracts up to a concentration of 100 μg/mL. Thereafter, the cells were rinsed and further incubated with MTT for 1 h. After 1 h, MTT crystals were dissolved in 200 μL DMSO. Optical density was read at 570 nm, and, consequently, the noncytotoxic concentrations were chosen for conducting *in vitro* studies.

2.5. Adipogenesis Assay. Effect of *N. nucifera* petal extracts on adipogenesis was evaluated by examining their ability to inhibit the differentiation of preadipocytes to adipocytes using 3T3-L1 cells as a test system. On day 0, mouse 3T3-L1 fibroblasts were seeded at a density of 3×10^4 cells/well in a 48-well plate containing DMEM supplemented with 10% BCS. On day 1, cells were changed to DMEM medium supplemented with FBS (5%), IBMX (0.5 mM), insulin (10 μg/mL), and dexamethasone (1 μM) with and without *N. nucifera* extracts. Guggulsterone was used as a reference control. On day 3, cells were changed to DMEM supplemented with FBS (5%) and insulin (5 μg/mL) with and without *N. nucifera* petal extracts. On days 5 and 7, the cells were changed to DMEM supplemented with 5% FBS. On day 8, 3T3-L1 adipocytes were rinsed with PBS and fixed using 10% formalin for 30 min followed by another rinse with 60% isopropanol solution and allowed to dry. The cells were stained with oil red O solution (0.5% oil red O in isopropanol, diluted in proportion of 3 parts of oil red O stock and two parts of distilled water) for 15 min at room temperature. Dye retained in adipocytes was extracted with isopropanol and quantified by measuring the absorbance at 500 nm.

2.6. Adipolysis Assay. Adipolysis assay was performed to evaluate the possible lipolytic activity of *N. nucifera* petal extracts by examining their ability to release glycerol from differentiated 3T3-L1 cells. On day 0, 3T3-L1 cells were seeded at a density of 3×10^4 cells/well in a 48-well plate containing DMEM medium supplemented with 10% BCS. On day 1, cells were changed to DMEM supplemented with 5% FBS, IBMX (0.5 mM), insulin (10 μg/mL), and dexamethasone (1 μM). On day 2, cells were changed to DMEM, supplemented with FBS (5%) and insulin (5 μg/mL), and left undisturbed for 2 days. On day 4, the cells were allowed to grow in FBS (5%) for consecutive three days. On day 7, the cells were starved overnight with DMEM containing 2% BSA. On day 8, cells were treated with noncytotoxic concentrations of *N. nucifera* extracts and DL-isoproterenol hydrochloride (reference control) separately for 4 hr in KRB (Krebs-Ringer Bicarbonate) buffer (pH 7.2). The supernatant was collected and estimated for glycerol content by adding 100 μL of

glycerol working reagent and 10 μL of sample/standard per well in a 96-well assay plate. Plate was tapped to mix and incubated at room temperature for 20 min. Read the color intensity at 570 nm in VersaMax plate reader.

2.7. Lipase Assay. The inhibitory effect of *N. nucifera* on porcine pancreatic lipase was evaluated. The assay was based on the principle of conversion of the substrate 4-methyl umbelliferyl oleate to 4-methyl umbelliferone by an active porcine lipase enzyme [25]. In brief, the total reaction volume of 50 μL contained 15 μL of Tris buffer/reference control (orlistat)/*N. nucifera* extract, 5 μL of lipase enzyme, 5 μL of demineralized water, and 25 μL of substrate (4-methyl umbelliferyl oleate). Mix these reagents and determine the change in fluorescence at 25°C for 20 min at an excitation and emission wavelength of 360 nm and 460 nm, respectively, using FLUOstar Optima.

2.8. Receptor Assays. Both methanol and successive water extracts of petals of *N. nucifera* were screened for possible agonistic and antagonistic activity towards selected receptors at a concentration of 10 μg/mL.

2.8.1. Agonist Assays

$5HT_{2C}$ and MC_4R Receptor Assays. The U2OS cell line coupled with either 5-HT_{2C} or MC_4R receptor was plated at a density of 10^4 cells/well in 96-well tissue culture plates, containing cell plating reagent. After 48 h incubation, *N. nucifera* petal extracts or reference agonist, (AL34662 for 5-HT_{2C}; melanotan II for MC_4R) were added in separate wells at noncytotoxic concentrations and incubated for 90 min at 37°C; 5% CO_2. 55 μL of prepared detection reagent solution was added to each well. After 60 min incubation at room temperature, the plate was read using luminescence plate reader (FLUOstar).

2.8.2. Antagonist Assays

Cannabinoid Receptor 2 (CNR_2). Effect of both methanol and successive water extracts of *N. nucifera* on inhibition of CP 55,940 (CNR_2 agonist) elicited CNR_2 activity in Gi/Go coupled CHO-K1 cell line was studied. 10^4 cells/well were plated in 96-well tissue culture plates containing cell plating reagent. After 48 h incubation, *N. nucifera* or reference antagonist (AM630) was added to the respective wells and incubated for 30 min at 37°C; 5% CO_2. 5 μL of agonist compound (CP 55,940) was added to the respective wells in a final volume of 110 μL and incubated for 90 min. 55 μL of prepared detection reagent solution was added to each well and incubated for 60 min at room temperature, and plate was read using luminescence plate reader (FLUOstar).

Melanin Concentrating Hormone Receptor ($MCHR_1$) Assay. Antagonistic potential of *N. nucifera* extracts on $MCHR_1$ receptor was studied using $MCHR_1$ Gi coupled CHO-K1 cells. Cell density of 3×10^4 cells/well was plated in 96-well tissue culture plates containing cell plating reagent and incubated for 24 h. After incubation, the entire medium was aspirated and 45 μL of cell assay buffer and antibody mixture was added to each well. *N. nucifera* or reference antagonist (GW 803430) was added to the respective wells and incubated for 15 min at 37°C and 5% CO_2. Agonist compound (MCH—62.5 nM + Forskolin 20 μM) was added to the respective wells and incubated for 30 min. 60 μL of prepared detection reagent solution and cAMP solution D was added to each well and incubated for 60 min at room temperature in the dark. 60 μL of cAMP Solution A was added and incubated for 3 hr at room temperature in the dark. Plate was read using luminescence plate reader (FLUOstar).

2.9. Data Analysis. For adipogenesis and adipolysis assays, statistical analysis was performed by one-way analysis of variance using the Graphpad Prism statistical software. Results are represented as Mean ± SD from three replicates per treatment group. Differences with $P < 0.05$ in comparison to control were considered to be statistically significant. For lipase assay, mean of the relative fluorescence unit (RFU) of *N. nucifera*/reference control tested in triplicate was calculated. From the mean values, percentage inhibition (%I) was calculated using the following equation:

$$\%I = \frac{(\text{RFU of Control} - \text{RFU of Sample})}{(\text{RFU of Control})} \times 100. \quad (1)$$

IC_{50} was calculated by the Finney software. For receptor assays, Student's t-test was performed using GraphPad Prism 5 statistical software to test for differences among all treatments. Differences with $P < 0.05$ were considered to be significant.

3. Results

3.1. Effect of N. nucifera on Differentiation of 3T3-L1 Cells. Noncytotoxic concentrations up to 50 μg/mL and 100 μg/mL were selected for methanol and successive water extract of *N. nucifera,* respectively, for *in vitro* cell-based assays. To test whether *N. nucifera* extracts inhibit adipocyte differentiation, the differentiated adipocytes were stained by oil red O. The staining results showed that incubation of *N. nucifera* during the differentiation period significantly inhibited 3T3-L1 adipogenesis. It was found that treatment of 3T3-L1 cells with *N. nucifera* successive water extract significantly decreased the cell differentiation and lipid accumulation in a dose-dependent manner, compared with control cells. Methanol extract of *N. nucifera* exhibited significant inhibition of adipocyte differentiation by 19% at a concentration of 2 μg/mL. The reference control, guggulsterone, demonstrated a potent inhibitory activity towards lipid accumulation at 20 μM with a percentage inhibition of 48 (Figure 1).

3.2. Lipolytic Effect of N. nucifera on Differentiated 3T3-L1 Cells. *N. nucifera* petal extracts displayed lipolytic activity as evident by significant increase of glycerol release from the differentiated 3T3-L1 cells. Methanol extract of *N. nucifera* showed significant dose-dependent release of glycerol at

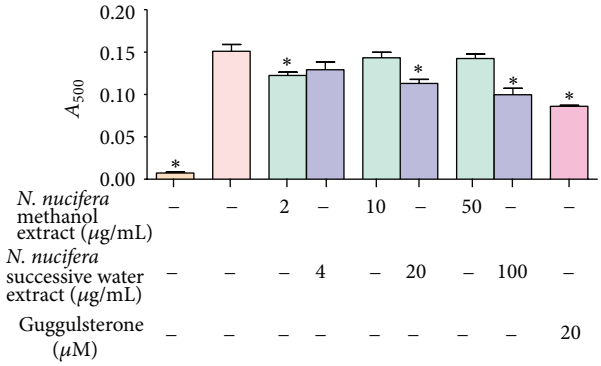

Figure 1: Effect of *N. nucifera* on adipogenesis using 3T3-L1 cells.

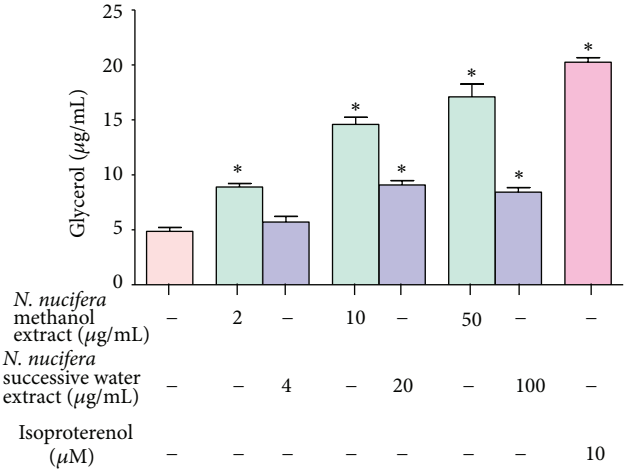

Figure 2: Effect of *N. nucifera* on glycerol release from differentiated 3T3-L1 cells.

concentrations ranging from 2 μg/mL to 50 μg/mL. Maximum lipolytic activity of 3.5-fold increase was observed with methanol extract of *N. nucifera* at a concentration of 50 μg/mL. Successive water extract showed significant increase of glycerol levels at highest concentrations (20 and 100 μg/mL), where a fold increase of 1.9 was observed. Isoproterenol, a known lipolytic agent, elicited a marked glycerol release by fat cells at the tested concentration of 10 μM with a 4-fold increase over control (Figure 2).

3.3. Lipase Inhibitory Effect of N. nucifera. Pancreatic lipase inhibition of both methanol and successive water extracts of *N. nucifera* was determined at a screening concentration of 50 μg/mL. Percent lipase inhibitory effect of methanol and successive water extract at 50 μg/mL of *N. nucifera* was found to be 52 and 10, respectively. Further, lipase inhibitory potential of methanol extract was tested to determine the IC_{50} (the concentration required to inhibit a lipase activity by 50%). Methanol extract of *N. nucifera* exhibited a dose-dependent lipase inhibitory effect with an IC_{50} value of 47 μg/mL. However, it was not more effective than orlistat which showed an IC_{50} value of 26 ng/mL (Table 1).

3.4. Central Target Action of N. nucifera

3.4.1. 5-HT_{2c} and MC_4 Receptor Assays. Both methanol and successive water extracts of *N. nucifera* at 10 μg/mL showed significant equipotent stimulatory activity of about 4-fold increase towards 5-HT_{2C} receptor (Table 2). The reference control AL34662 demonstrated a potent dose-dependent agonist activity towards 5-HT_{2C} receptor with an EC_{50} value of ~10.8 nM. Both methanol and successive water extracts did not show significant agonist activity towards MC_4 receptor at a concentration of 10 μg/mL (Table 2). Melanotan II, a known MC_4R agonist, demonstrated a concentration-dependent potent agonist activity towards MC_4R receptor with an EC_{50} value of ~3.3 nM.

3.4.2. CNR_2 and $MCHR_1$ Receptor Assays. At a concentration of 10 μg/mL, methanol extract of *N. nucifera* petals displayed 26.2% antagonism against CP 55,940 activity towards CNR_2 receptor, whereas the successive water extract was found to be inactive at a concentration of 10 μg/mL (Table 2). AM630, a known CNR_2 antagonist, demonstrated a potent antagonist activity towards CP 55,940 activated CNR_2 receptor with an IC_{50} value of ~62.3 nM. Both of these two extracts did not show antagonist activity towards $MCHR_1$ (Table 2). GW 803430, a known $MCHR_1$ antagonist, demonstrated a potent antagonist activity towards MCH induced $MCHR_1$ receptor with an IC_{50} value of ~13 nM.

3.5. Phytochemical Analysis of Methanol Extract of N. nucifera. HPLC analysis of crude methanol extract of *N. nucifera* confirmed the presence of flavonoids as major phytochemicals. HPLC followed by UV spectral analysis confirmed the identity of flavonoid glycosides (quercetin and kaempferol glycosides) which is in compliance with the earlier report by Xingfeng et al. [23].

4. Discussion

Dietary fat is not directly absorbed by the intestine unless the fat has been subjected to the action of pancreatic lipase. Therefore, pancreatic lipase is one of the most widely studied mechanisms for determining natural products and potential efficacy as antiobesity agents [26]. In this study, we report the inhibitory effects of *Nelumbo nucifera* petal extracts on pancreatic lipase. Methanol extract elicited an inhibitory effect on lipase enzyme with an IC_{50} value of 47 μg/mL. Similar to our study but on lotus leaf, authors have showed antiobesity activity through a concentration-dependent inhibition of lipase enzyme and also upregulated the lipid metabolism [4]. *Nelumbo nucifera* is known as sacred lotus and found to have various pharmacologically active substances including alkaloids, flavonoids, triterpenoids, polyphenols, steroids, and glycosides [23]. A phytochemical investigation of *N. nucifera* leaves led to the isolation of eight alkaloids and some of these significantly inhibited pancreatic lipases [20]. Total flavonoids from *N. nucifera* leaves showed high inhibitory

Table 1: Effect of *N. nucifera* extracts on pancreatic lipase activity.

Test sample	Concentration	% Lipase inhibition	IC_{50}
Nelumbo nucifera methanol extract	12.5 μg/mL	14.78	47 μg/mL
	25 μg/mL	29.28	
	50 μg/mL	51.81	
	100 μg/mL	71.94	
	200 μg/mL	89.87	
Nelumbo nucifera successive water extract	50 μg/mL	10	—
Orlistat (reference standard)	5 ng/mL	28.31	26 ng/mL
	10 ng/mL	36.89	
	25 ng/mL	44.88	
	50 ng/mL	66.15	
	100 ng/mL	68.22	
	200 ng/mL	71.91	

Table 2: Effect of petal extracts of *N. nucifera* on central receptors.

Name of the test item	Solvent	Concentration	RLU (Mean ± SD)			
			$5HT_{2C}$	MC_4R	$MCHR_1$	CNR_2
Negative	—	NA	35947.0 ± 410.12	2322.3 ± 111.11	NA	NA
DMSO	—	0.1%	36188.5 ± 3324.11	2405.3 ± 246.41	NA	NA
N. nucifera methanol extract	DMSO	10 μg/mL	146121.5 ± 3987.37*	2276.5 ± 289.21 (NS)	321.5 ± 38.89 (NS)	106480.0 ± 2791.66*
N. nucifera successive water extract	DMEM	10 μg/mL	150760.5 ± 15262.89*	2071.5 ± 282.14 (NS)	320.0 ± 46.67 (NS)	122709.0 ± 6588.82 (NS)
Agonist AL-34662 (reference standard)	DMSO	50 nm*	136099.9 ± 2258.78*	NA	NA	NA
Agonist melanotan II acetate salt (reference standard)	DMSO	950 nm*	NA	11798.5 ± 27.58*	NA	NA
Agonist CP 55,940	DMSO	4.5 nm[1]	NA	NA	NA	144375.5 ± 7012.38
Agonist MCH	DMSO	62.5 nm[1]	NA	NA	545.0 ± 1.41	NA
Antagonist AM630 (reference standard)	DMSO	173.2 nm*	NA	NA	NA	4025.4 ± 994.31*
Antagonist GW-803430 (reference standard)	DMSO	18.1 nm*	NA	NA	1294.5 ± 142.13*	NA

RLU: relative luminescence units; NA: not applicable; *indicates a concentration at which maximum response of reference controls was observed; [1]indicates EC_{80} concentration of agonist against which *N. nucifera* petal extracts/reference controls were evaluated for their antagonistic potential.
$P < 0.05$.
NS: not significant.

activity against porcine pancreatic lipase, α-amylase, and α-glucosidase. Also, it lowered total cholesterol, triglycerides, low-density lipoprotein cholesterol, and malondialdehyde and raised the high-density lipoprotein cholesterol *in vivo* system. Moreover, it alleviated high-fat diet-induced lipid accumulation in the liver [27].

Adipocytes primarily store triglycerides and release them in the form of free fatty acid with the change of energy demand in the body. *N. nucifera* petal extracts demonstrated significant dose-dependent inhibitory effects on lipid accumulation in 3T3-L1 adipocytes. Alkaloids isolated from *N. nucifera* showed stronger inhibitory effect on adipocyte differentiation [20] and could probably contribute to the activity of petals of *N. nucifera*. Similar to this study but on lotus seed, epicarp extracts of *N. nucifera* were studied using an *in vitro* 3T3-L1 preadipocyte cell model. Results showed that the lotus seed epicarp extracts inhibited preadipocyte differentiation to adipocyte in a concentration-dependent manner [21]. Antiobesity effect of *N. nucifera* leaves extract (NNE) using high-fat diet-induced obesity in mice was studied. NNE significantly decreased the high-fat diet-induced weight gain, parametrial adipose tissue weight, and liver triacylglycerol levels in mice. Authors concluded that NNE impaired digestion, inhibited absorption of lipids and carbohydrates, accelerated lipid metabolism, and upregulated energy expenditure [4].

In this study, we have demonstrated that the petal extracts of *N. nucifera* clearly exhibit lipolytic activity in a dose-dependent manner in murine 3T3-L1 fibroblasts. Previous studies have reported that a liquid leaf extract of *Nelumbo nucifera* stimulated lipolysis activity in differentiated adipocytes. Also, authors have showed that treatment of adipocyte cultures with 0.5% lotus leaf extract solution significantly increased the content of free glycerol. Likewise, cultivation of cells with 1% lotus leaf extract solution induced a significant release of free glycerol compared to control cells [28]. In another study, 50% ethanol (EtOH) extract prepared from the leaves of *N. nucifera* stimulated lipolysis in the white adipose tissue (WAT) of mice and possible involvement of beta-adrenergic receptor (beta-AR) pathway was attributed to this effect. *N. nucifera* in preventing diet-induced obesity emerged to be due to various flavonoids and that the activation of beta-AR pathway was involved, at least in part [29].

Based on the 5-HT_{2C} receptor study, *N. nucifera* petal extracts showed significant agonist activity towards 5-HT_{2C} receptor and antagonistic activity towards CNR_2 indicating its role in central targets of obesity as appetite suppressant. Alkyl 4-hydroxybenzoates were isolated from seeds of *N. nucifera* and shown to enhance and inhibit 5-HT-stimulated inward current (I(5-HT)) mediated by the human 5-HT(3)A receptors expressed in Xenopus oocytes [30]. Similar to this study, Oh et al. [31] demonstrated that chronic treatment with ethanol extract from *Morus alba* leaves exerts an antiobesity effect in diet-induced obese mice via its direct MCH_1 receptor antagonism. Various phytocompounds, namely, alkaloids, anthocyanin, and nonanthocyanin flavonoids, have been isolated from petals of *N. nucifera* [32, 33] and shown to have other biological activities; however, their role in antiobesity activity needs to be determined.

Flavonoid-enriched *N. nucifera* leaf extract significantly inhibited the high-fat diet-induced abnormal blood lipids and liver damage [27]. Galleano et al. [34] consolidated the proof linking flavonoid intake with metabolic disorders, namely, obesity, hypertriglyceridemia, hypercholesterolemia, hypertension, and insulin resistance. However, a number of molecular mechanisms have been identified; the effects of flavonoids on endpoints of metabolic syndrome are still inconclusive. These convolutions were explained by the complex associations among the risk factors of metabolic syndrome, the multiple biological targets controlling these risk factors, and the high number of flavonoids (including their metabolites) present in the diet and potentially responsible for the *in vivo* effects. As a result, extensive basic and clinical research is warranted to assess the relevance of flavonoids for the treatment of metabolic syndrome [34].

Acute and subchronic oral toxicity studies of *N. nucifera* stamens extract in rats were performed and found to have safety threshold for acute toxicity which is above 5000 mg/kg bodyweight, and no-observed-adverse-effect level (NOAEL) of the extract for both male and female rats is considered to be 200 mg/kg/day [35].

In conclusion, *N. nucifera* petal extract showed antilipase activity, lipolytic and antiadipogenesis effect in adipocytes *in vitro*. *N. nucifera* extract showed agonist and antagonistic effect towards central receptors involved in food intake. Thus, it is worthwhile to further investigate *N. nucifera* petal extract and phytoconstituents for its potential pharmacological effect in metabolic disorders, in particular obesity.

Conflict of Interests

All authors declare that they have no conflict of interests.

Acknowledgment

This research received support from DBT, India, under Indo-Spanish joint call for collaboration in the field of biotechnology.

References

[1] C. V. Chandrasekaran, M. A. Vijayalakshmi, K. Prakash, V. S. Bansal, J. Meenakshi, and A. Amit, "Review: herbal approach for obesity management," *American Journal of Plant Sciences*, vol. 3, pp. 1003–1014, 2012.

[2] W. La-Ongsri, C. Trisonthi, and H. Balslev, "Management and use of *Nelumbo nucifera* Gaertn. in Thai wetlands," *Wetlands Ecology and Management*, vol. 17, no. 4, pp. 279–289, 2009.

[3] M. Kulkarni and A. Juvekar, "Attenuation of acute and chronic restraint stress-induced perturbations in experimental animals by *Nelumbo nucifera* Gaertn," *Indian Journal of Pharmaceutical Sciences*, vol. 70, no. 3, pp. 327–332, 2008.

[4] Y. Ono, E. Hattori, Y. Fukaya, S. Imai, and Y. Ohizumi, "Anti-obesity effect of *Nelumbo nucifera* leaves extract in mice and rats," *Journal of Ethnopharmacology*, vol. 106, no. 2, pp. 238–244, 2006.

[5] S. Rai, A. Wahile, K. Mukherjee, B. P. Saha, and P. K. Mukherjee, "Antioxidant activity of *Nelumbo nucifera* (sacred lotus) seeds," *Journal of Ethnopharmacology*, vol. 104, no. 3, pp. 322–327, 2006.

[6] D.-H. Sohn, Y.-C. Kim, S.-H. Oh, E.-J. Park, X. Li, and B. Lee, "Hepatoprotective and free radical scavenging effects of *Nelumbo nucifera*," *Phytomedicine*, vol. 10, no. 2-3, pp. 165–169, 2003.

[7] P. K. Mukherjee, K. Saha, J. Das, M. Pal, and B. P. Saha, "Effect of *Nelumbo nucifera* rhizome extract on blood sugar level in rats," *Journal of Ethnopharmacology*, vol. 58, no. 3, pp. 207–213, 1997.

[8] P. K. Mukherjee, K. Saha, J. Das, M. Pal, and B. P. Saha, "Studies on the anti-inflammatory activity of rhizomes of *Nelumbo nucifera*," *Planta Medica*, vol. 63, no. 4, pp. 367–369, 1997.

[9] P. V. Chakravarthi and N. Gopakumar, "Anti-inflammatory activity of red and white lotus seeds (*Nelumbo nucifera*) in albino rats," *Veterinary World*, vol. 3, no. 4, pp. 157–159, 2010.

[10] P. K. Mukherjee, J. Das, K. Saha, S. N. Giri, M. Pal, and B. P. Saha, "Antipyretic activity of *Nelumbo nucifera* rhizome extract," *Indian Journal of Experimental Biology*, vol. 34, no. 3, pp. 275–276, 1996.

[11] M. Li and Z. Xu, "Quercetin in a lotus leaves extract may be responsible for antibacterial activity," *Archives of Pharmacal Research*, vol. 31, no. 5, pp. 640–644, 2008.

[12] D. Mukherjee, A. Biswas, S. Bhadra et al., "Exploring the potential of *Nelumbo nucifera* rhizome on membrane stabilization, mast cell protection, nitric oxide synthesis, and expression of costimulatory molecules," *Immunopharmacology and Immunotoxicology*, vol. 32, no. 3, pp. 466–472, 2010.

[13] D. Mukherjee, T. N. Khatua, P. Venkatesh, B. P. Saha, and P. K. Mukherjee, "Immunomodulatory potential of rhizome and seed extracts of *Nelumbo nucifera* Gaertn," *Journal of Ethnopharmacology*, vol. 128, no. 2, pp. 490–494, 2010.

[14] P. K. Mukherjee, D. Mukherjee, A. K. Maji, S. Rai, and M. Heinrich, "The sacred lotus (*Nelumbo nucifera*): phytochemical and therapeutic profile," *Journal of Pharmacy and Pharmacology*, vol. 61, no. 4, pp. 407–422, 2009.

[15] R. P. Rastogi and B. N. Mehrotra, *Compendium of Indian Medicinal Plants*, vol. 1 of *(1960–1969), pp. 288-289*, Central Drug Research Institute, Lucknow and Publications & Information Directorate, New Delhi, India, 1991.

[16] Y. Huang, L. Zhao, Y. Bai, P. Liu, J. Wang, and J. Xiang, "Simultaneous determination of liensinine, isoliensinine and neferine from seed embryo of *Nelumbo nucifera* Gaertn. in rat plasma by a rapid HPLC method and its application to a pharmacokinetic study," *Arzneimittel-Forschung*, vol. 61, no. 6, pp. 347–352, 2011.

[17] B. Xie, J. Wan, W. Wang, C. Shi, X. Hou, and J. Fang, "*Nelumbo nucifera* alkaloid inhibits 3T3-L1 preadipocyte differentiation and improves high-fat diet-induced obesity and body fat accumulation in rats," *Journal of Medicinal Plant Research*, vol. 5, no. 10, pp. 2021–2028, 2011.

[18] X. Shuangshuang, D. Wenjuan, F. Lei, S. Yu, D. Hongjing, and W. Xiao, "Isolation and characterization of chemical constituents from the petals of *Nelumbo nucifera*," *Asian Journal of Chemistry*, vol. 24, pp. 4619–4622, 2012.

[19] C. Wu, M. Yang, K. Chan, P. Chung, T. Ou, and C. Wang, "Improvement in high-fat diet-induced obesity and body fat accumulation by a *Nelumbo nucifera* leaf flavonoid-rich extract in mice," *Journal of Agricultural and Food Chemistry*, vol. 58, no. 11, pp. 7075–7081, 2010.

[20] J. H. Ahn, E. S. Kim, C. Lee et al., "Chemical constituents from *Nelumbo nucifera* leaves and their anti-obesity effects," *Bioorganic and Medicinal Chemistry Letters*, vol. 23, no. 12, pp. 3604–3608, 2013.

[21] S. Qi and D. Zhou, "Lotus seed epicarp extract as potential antioxidant and anti-obesity additive in Chinese Cantonese Sausage," *Meat Science*, vol. 93, no. 2, pp. 257–262, 2013.

[22] J. S. You, Y. J. Lee, K. S. Kim, S. H. Kim, and K. J. Chang, "Antiobesity and hypolipidemic effects of *Nelumbo nucifera* seed ethanol extract in human preadipocytes and rats fed a high-fat diet," *Journal of the Science of Food and Agriculture*.

[23] G. Xingfeng, W. Daijie, D. Wenjuan, D. Jinhua, and W. Xiao, "Preparative isolation and purification of four flavonoids from the petals of *Nelumbo nucifera* by high-speed counter-current chromatography," *Phytochemical Analysis*, vol. 21, no. 3, pp. 268–272, 2010.

[24] T. Mosmann, "Rapid colorimetric assay for cellular growth and survival: application to proliferation and cytotoxicity assays," *Journal of Immunological Methods*, vol. 65, no. 1-2, pp. 55–63, 1983.

[25] US patent publication number: US, 2008/0317821 A1, dated December 2008.

[26] R. B. Birari and K. K. Bhutani, "Pancreatic lipase inhibitors from natural sources: unexplored potential," *Drug Discovery Today*, vol. 12, no. 19-20, pp. 879–889, 2007.

[27] S. Liu, D. Li, B. Huang, Y. Chen, X. Lu, and Y. Wang, "Inhibition of pancreatic lipase, α-glucosidase, α-amylase, and hypolipidemic effects of the total flavonoids from *Nelumbo nucifera* leaves," *Journal of Ethnopharmacology*, vol. 149, pp. 263–269, 2013.

[28] R. Siegner, S. Heuser, U. Holtzmann et al., "Lotus leaf extract and L-carnitine influence different processes during the adipocyte life cycle," *Nutrition and Metabolism*, vol. 7, article 66, 2010.

[29] E. Ohkoshi, H. Miyazaki, K. Shindo, H. Watanabe, A. Yoshida, and H. Yajima, "Constituents from the leaves of *Nelumbo nucifera* stimulate lipolysis in the white adipose tissue of mice," *Planta Medica*, vol. 73, no. 12, pp. 1255–1259, 2007.

[30] U. J. Youn, J. Lee, Y. J. Lee, J. W. Nam, H. Bae, and E. Seo, "Regulation of the 5-HT3A receptor-mediated current by alkyl 4-hydroxybenzoates isolated from the seeds of *Nelumbo nucifera*," *Chemistry and Biodiversity*, vol. 7, no. 9, pp. 2296–2302, 2010.

[31] K. Oh, S. Y. Ryu, S. Lee et al., "Melanin-concentrating hormone-1 receptor antagonism and anti-obesity effects of ethanolic extract from *Morus alba* leaves in diet-induced obese mice," *Journal of Ethnopharmacology*, vol. 122, no. 2, pp. 216–220, 2009.

[32] S. Chen, Y. Xiang, J. Deng, Y. Liu, and S. Li, "Simultaneous analysis of anthocyanin and non-anthocyanin flavonoid in various tissues of different lotus (Nelumbo) cultivars by HPLC-DAD-ESI-MS(n)," *Public Library of Science One*, vol. 8, no. 4, Article ID e62291, 2013.

[33] S. Nakamura, S. Nakashima, G. Tanabe et al., "Alkaloid constituents from flower buds and leaves of sacred lotus (*Nelumbo nucifera*, Nymphaeaceae) with melanogenesis inhibitory activity in B16 melanoma cells," *Bioorganic Medicinal Chemistry*, vol. 21, no. 3, pp. 779–787, 2013.

[34] M. Galleano, V. Calabro, P. D. Prince et al., "Flavonoids and metabolic syndrome," *Annals of the New York Academy of Sciences*, vol. 1259, pp. 87–94, 2012.

[35] P. Kunanusorn, A. Panthong, P. Pittayanurak, S. Wanauppathamkul, N. Nathasaen, and V. Reutrakul, "Acute and subchronic oral toxicity studies of *Nelumbo nucifera* stamens extract in rats," *Journal of Ethnopharmacology*, vol. 134, no. 3, pp. 789–795, 2011.

Hindawi Publishing Corporation
Evidence-Based Complementary and Alternative Medicine
Volume 2013, Article ID 869061, 7 pages
http://dx.doi.org/10.1155/2013/869061

Research Article

Greenselect Phytosome for Borderline Metabolic Syndrome

Gianni Belcaro, Andrea Ledda, Shu Hu, Maria Rosa Cesarone, Beatrice Feragalli, and Mark Dugall

Department of Biomedical Sciences, Irvine3 Circulation/Vascular Labs & San Valentino Vascular Screening Project, Gabriele D'Annunzio University, Chieti, Italy

Correspondence should be addressed to Gianni Belcaro; cardres@abol.it

Received 22 July 2013; Revised 26 September 2013; Accepted 27 September 2013

Academic Editor: Mohamed Eddouks

The beneficial effects of Greenselect Phytosome, a proprietary lecithin formulation of a caffeine-free green tea catechin extract, were evaluated in a controlled registry study on 50 asymptomatic subjects borderline for metabolic syndrome factors and with increased plasma oxidative stress. After 24 weeks of intervention, improvement in weight, blood lipid profile, and blood pressure positioned 68% of subjects in the treatment arm out of the metabolic syndrome profile, while 80% of the subjects in the control group still remained in their initial borderline disease signature. Compared to the control (lifestyle and dietary changes alone), Greenselect Phytosome was especially effective for weight/waist changes. These results highlight the relevance of addressing multiple factors involved in the development of metabolic syndrome with a pleiotropic agent capable of improving the beneficial effects of lifestyle and dietary changes and foster the attainment of a globally improved health profile.

1. Introduction

Tea is probably the most consumed beverage in the world after water, and its pharmacological potential has been extensively investigated [1]. The phytochemical profile of tea depends on the extent of oxidation (*fermentation* in the tea lingo) of its catechin constituents, and most studies have focused on green tea that maintains the original polyphenolic profile of the leaves and is the source of sinecatechins, a registered drug for the topical management of genital warts [1]. Cancer prevention [2, 3], weight loss [4, 5], and diabetes [6–9] are some of the other hot areas of clinical investigation where green tea catechins have proved potentially useful both as a stand-alone agent and in combination with lifestyle and pharmacological intervention strategies.

According to an estimation from 2010 [10], more than 35% of adults and 17% of children and adolescents are medically obese (BMI > 30) in North America, and obesity rates are rapidly increasing not only in affluent Western countries but also in poorer nations, presumably because of the growing popularity of the obesogenic Western lifestyle [11, 12]. Green tea extracts enriched in catechins have shown promising results in reducing body mass index in over-weight subjects, especially when associated with lifestyle changes and diet [13–18]. A synergistic effect of catechins and caffeine on reducing obesity has been observed, presumably due to a complementary increase in adrenergic tone and its associated signal translation in adipose tissue [19], but the detrimental effects of caffeine on glucose control and blood pressure make this association questionable in the context of overall prevention of the metabolic syndrome (MetS) [20]. Thus, obesity is often associated, especially in adults, with detrimental changes in glucose control and variously related cardiovascular risk factors (dyslipidemia, hypertension). Epigallocatechin gallate (EGCG), the major catechin of green tea, is a well-known thermogenic agent [21] that, unlike caffeine, also shows beneficial effects toward several markers of the metabolic syndrome, especially glucose control and dyslipidemia [22].

Greenselect Phytosome (GSP) is a green tea extract devoid of caffeine and formulated in lecithin to improve the absorption of catechins [23]. Because of its domesticated profile compared to other green tea extracts in terms of phytochemical profile and bioavailability, it was selected, in the form of coated tablets (Monoselect Camellia, MonCam), for a single blind, controlled study on 50 asymptomatic subjects borderline for all five MetS factors, who were also showing an

increased plasma oxidative stress. According to the new International Diabetes Federation (IDF) definition [24], metabolic syndrome patients are featuring central obesity as well as two (or more) of the following four factors:

(i) raised triglycerides level: ≥150 mg/dL (1.7 mmol/L) or need for treatment for this lipid abnormality;

(ii) reduced HDL cholesterol: <40 mg/dL (1.03 mmol/L) in males and <50 mg/dL (1.29 mmol/L) in females or need for treatment for this lipid abnormality;

(iii) raised blood pressure: systolic BP ≥ 130 or diastolic BP ≥ 85 mm Hg or treatment of previously diagnosed hypertension;

(iv) raised fasting plasma glucose: FPG ≥ 100 mg/dL (5.6 mmol/L) or previously diagnosed Type II diabetes.

MetS is associated with an increased risk of cardiovascular events (i.e. coronary disease, myocardial infarction, and stroke) and to the development of type-2 diabetes [25–28]; its management should be aggressive, constant, and effective, involving primary intervention (lifestyle modification with calorie restriction, increase of physical activity, and change in dietary composition) to achieve a 10% loss of body weight in the first year. Even a modest weight loss is associated with a significant risk reduction for Type II diabetes and cardiovascular disease [29–31]. When lifestyle change is not possible or not adequate and in subjects considered at higher risk for cardiovascular disease, a secondary intervention [32–34] resorting to drug therapy may be required to treat MetS, and there is a dire need of agents to control its risk factors. However, since the actual molecular mechanism(s) underlying the development of MetS are still largely elusive, no specific pharmacological agents are currently available to globally control the cardiovascular and diabetic risk associated to MetS [35–37]. The relevance of each single factor in the development of metabolic syndrome is indeed difficult to evaluate and might even be different in distinct populations [32, 38]. In the present study, we wanted to evaluate whether GSP is able to support the beneficial effects of lifestyle and dietary changes and foster the attainment of a globally improved health profile, thanks to its pleiotropic effect able to address multiple factors involved in the development of metabolic syndrome.

2. Materials and Methods

2.1. Subjects. Inclusion criteria were an asymptomatic status, a borderline profile for all the 5 MetS factors, and an increased oxidative stress. Exclusion criteria for subjects were fasting blood glucose values exceeding 162 mg/dL and any other metabolic or clinical conditions requiring medical treatment. Pregnant or breastfeeding females, individuals with any clinical condition, psychiatric disorders including depression, and subjects who participated in another study less than 30 days before the start of this study were excluded as well.

2.2. Study Design. The present study was randomized, single-blinded, parallel design comparing GSP tablets versus a corresponding blank formulation, in association with lifestyle and dietary interventions.

2.3. Study Protocol. At inclusion, subjects were unaware of the presence of MetS and of the value of the MetS factors. The study was performed according to the Declaration of Helsinki, and all patients gave an informed consent prior to their participation to the study. After briefing and evaluation of their interest to participate in the study, the volunteers were divided into two groups using the same management plans.

(i) Group 1: management plan + MonCam (1 tablet at 10 AM and one at 6 PM) equivalent to overall 300 mg/day of GSP.

(ii) Group 2: management plan + corresponding blank formulation.

Volunteers had a defined management plan: changes in diet, thus avoiding junk food and limiting high calorie elements, and a precise individual exercise plan. Diet produced a caloric deficit (750 kcal/day in females and 1000 kcal/day in males) compared to the individual estimated energy requirements and contained 17–22% proteins, 23–25% fats, and 55–58% carbohydrates. Individual exercise plan foresaw 210 minutes/week of physical activity (70% moderate aerobic, 30% muscular strengthening). None of the included subjects had important (at ultrasound scans) atherosclerotic lesions (plaques or intima-media thickening) in the studied arteries (carotids, femoral, aorta). No other nutritional elements, vitamins, or drugs were used in the observation period. No other clinical condition was present.

Based upon published data about the efficacy of lifestyle changes on MetS [39, 40], an estimate of not less than 25 subjects completing the study in each group was considered necessary to obtain clinically meaningful data on the treatment outcome. The safety population, as planned in the protocol, was effectively composed of all the subjects recruited into the study, who received at least one dose (product or blank formulation) and having at least one post baseline safety evaluation (one week). The intention-to-treat (ITT) efficacy analysis included all the subjects who had received at least one dose of medication and had had at least one post baseline measurement of the primary efficacy items. Subjects having treatment compliance <70% were excluded. The ITT analysis was performed comparing "all treated subjects" versus control subjects. The per-protocol (PP) analysis had to include all subjects available for the ITT analysis, who completed the planned duration of treatment, were complying with the regimen, had a valid efficacy evaluation, and did not violate the protocol in any way liable to influence the efficacy outcome. A range of compliance of at least 85% was adopted as a criterion to select subjects for the PP analysis. Therefore, subjects with compliance <85% were excluded, as well as all the subjects who did not meet the criteria for the "Population for efficacy analysis." Additional ("post-hoc") analysis was made to assess the minimum effective time "dose" to reach significant results. These tests were performed using closed testing procedures. The fixed-sequence Dunnett test was applied to determine the time

needed to have results on each MetS item. All hypothesis tests were two sided. All statistical tests (nonparametric) were performed at a 5% significance level ($P < 0.05$).

2.4. Products. Both the ingredient Greenselect Phytosome (GSP) and its oral formulation in tablets Monoselect Camellia (MonCam) are commercially available products from Indena (Milan, Italy) and from PharmExtracta (Pontenure, Italy), respectively. GSP is a decaffeinated, standardized extract from green tea having the following specifications:

(i) epigallocatechin-3-O-gallate (EGCG) ≥ 13%;

(ii) polyphenols 19%–25%;

(iii) caffeine ≤ 0.1%.

Each MonCam tablet has been manufactured to contain 150 mg of GSP. No side effects were reported during the execution of the study, formulation tolerability (both for GSP and the corresponding blank formulation) being excellent, with overall more than 93% of GSP tablets and more than 91% of blank formulation having been correctly used.

2.5. Blood Tests. At inclusion and at 24 weeks (end of observation), a panel of additional blood tests was carried out (ALT, AST, gamma-GT, Alkaline Phosphatase, CRP, Serum creatinine, Leptin as well as blood cell count and fibrinogen, aPTT, and PT-Quick's value and hematocrit).

2.6. Anthropometric Measures. At inclusion and at 24 weeks (end of observation) the following anthropometric parameters were taken in all subjects: body weight, body mass index (BMI), and waist circumference.

2.7. Data Analysis. The clinical efficacy assessed by weight and blood test score was examined using a B-W-Subject Anova model, a mixed analysis of variance design for differences mean, which is the only model that can be correctly applied to the experimental data [41]. Analysis of difference between active and blank formulation groups was performed by Tukey-Kramer test for pairwise comparisons between means.

3. Results and Discussion

We have been interested in the possibility to improve the outcome of MetS primary prevention by complementing lifestyle changes with dietary ingredients capable to address the various dysfunctions in which the syndrome is declined, and, as discussed above, green tea catechins show indeed the potential to do so. To explore this enticing possibility, we hence carried out a single blind controlled study on 50 asymptomatic subjects borderline for all the five mentioned MetS factors and also showing increased plasma oxidative stress. The study lasted 24 weeks, and 48 (25 men and 23 women) out of 50 subjects in the treatment group completed the study, with no dropouts being due to medical reasons; 50 comparable control volunteers were also followed for all the duration of the study, with no dropouts. The groups characteristics are summarized in Table 1.

The results, which are detailed in Table 2, confirmed the efficacy of the management plan to achieve an overall amelioration, both at the anthropometric and blood parameters level. Compared to the control group, though, who took the blank formulation, the group who took MonCam performed remarkably better, achieving for all the parameters observed a better outcome, statistically significant both versus the baseline and versus the control group, even for items where the control group did not obtain a significant result (waist circumference in women, HDL cholesterol, blood pressure, and fasting glucose).

The panel of additional blood tests did not show any significant variations (within the normal range at inclusion and after the evaluation period, as may be expected in borderline volunteers).

GSP clearly promoted weight loss and reduced waist circumference (see Table 2) when compared to management plan alone. The improvement in GSP subjects in borderline MetS was also associated with lipids and blood pressure beneficial variations. Finally, the value of plasma free radicals (PFR) decreased at 24 weeks in the GSP group (−33.04%; $P < 0.05$ versus inclusion) in a much more marked way compared to the control (decreasing only −4.14%; n.s. versus inclusion, $P < 0.022$ between groups).

Overall, GSP appears to have a moderate, yet significant, action on each single parameter of MetS, with particular emphasis on weight/waist changes. It was also interesting to evaluate the global impact of the treatment protocol (lifestyle + GSP versus lifestyle + blank formulation) on the various parameters defining metabolic syndrome (Table 3). In accordance with the inclusion criteria, 100% of subjects had borderline values for all the five parameters of MetS. At the end of the study, 68.75% of GSP subjects (33 out of 48) were outside the metabolic syndrome profile, 7 had reached a limit profile for MetS, while only 8 were still lingering in MetS area. Conversely, in the control group, 80% of subjects were still in MetS area at 24 weeks and 10 out of 50 (20%) had still a borderline profile for MetS. Therefore, a significant improvement in all risk conditions and a more significant progressive exit from the MetS area were observed in the GSP branch. In the ITT analysis, 40 out of a total 48 GSP subjects (83.33%) improved in comparison with 20% of controls (10/50), a statistically significant ($P < 0.02$) difference.

4. Discussion

This study confirms GSP's efficacy in weight loss when associated with proper lifestyle modifications and a low-calorie diet [18]. This result was achieved despite the absence of caffeine in the product, thus going beyond results found with caffeine-containing green tea extracts [19, 22] and confirming that catechins alone can have an important role in controlling weight, most likely through the increase of fat oxidation [21]. Spurred by epidemiological data, some investigations have been undertaken to evaluate the usefulness of green tea and green tea extracts in MetS [42, 43]; for the time being, the heterogeneity of the studies available in literatures

Table 1: Group characteristics at inclusion.

Group	Number of subjects	Men/women ratio	Age (average; ±s.d.; range)	Percentage of subjects with borderline MetS values (for all 5 items)
Treated group (Management plan + MonCam)	50	25/25	47.6 yr.; ±5.5; 45–55	100%
Control group (Management plan + blank formulation)	50	24/26	45.3 yr.; ±3.55; 45–55	100%

Table 2: Anthropometric and blood parameters in treated and control groups at the inclusion and at the end of the observation period (24 weeks).

ITEM (inclusion criteria)	Reference for MetS according to NCEP ATP III		Inclusion	24 weeks	*P*
Weight (kg)		GSP	88.4; 2.4	76.6; 2.5	* #
		range	83.2–92.5	72.3–82.8	
		control	88.9; 2.1	83.0; 1.8	*
		range	84.4–91.3	87.0–77.6	
BMI	Normal 18.5 to 25 Overweight 25 to 30	GSP	31.0; 2.0	26.7; 1.7	* #
		control	30.9; 2.6	28.9; 2.5	*
Central obesity (waist circumference)	>102 cm (men) >88 cm (women)	GSP	M 107.0; 1.3 F 91.0; 1.6	95.6; 1.3 82.7; 2.3	* # * #
		control	M 105.6; 2.5 F 90.0; 2.4	101; 2.0 88.5; 2.5	* ns
Fasting glucose	>110 mg/dL	GSP	116.1; 5.3	107.9; 3.0	* #
		control	115.7; 3.7	113.7; 3.0	ns
Triglycerides	>150 mg/dL	GSP	168.0; 8.7	154.7; 7.0	* #
		control	163.8; 8.4	160.0; 7.3	*
HDL cholesterol	M < 40 mg/dL F < 50 mg/dL	GSP	M 34.4; 2.2 F 46.4; 2.5	41.8; 3.3 54.2; 2.2	* #
		control	M 36.0; 3.4 F 44.5; 3.4	36.7; 3.2 45.8; 2.0	ns
Plasma free radicals		GSP	466.4; 38	312; 42	* #
		control	458.3; 34	439.3; 33	*
Blood pressure	Systolic BP > 130 mm Hg Diastolic BP > 85 mm Hg	GSP	Sys 136.8; 4.1	129.6; 2.1	* #
			Dia 88.8; 2.9	83.6; 2.2	* #
		control	Sys 137.4; 3.5	137.5; 2.4	ns
			Dia 89.4; 2.4	86.2; 2.8	ns

$P < 0.05$; *better than inclusion; #better than controls.

Table 3: MetS factors presence in 98 subjects (48 treated and 50 controls) at inclusion and at the end of the study.

MetS factors affecting subjects	Inclusion		24 weeks			
			GSP treated (48)		Controls (50)	
	subjects	%	subjects	%	subjects	%
Metabolic syndrome area						
5 over 5	98	100%	1	2%	18	36%
4 over 5	—	—	2	4%	12	24%
3 over 5	—	—	5	10%	10	20%
Borderline						
2 over 5	—	—	7	15%	10	20%
Out of metabolic syndrome area						
1 over 5	—	—	11	23%	0	0%
none	—	—	22	46%	0	0%

and their still limited numbers makes it difficult to compare our results with those obtained in other studies, although featuring coherent outcomes.

In terms of body weight specifically, it is worth mentioning that the results described above were obtained treating volunteers with a dose of GSP corresponding to 40 mg/day catechins, while other studies on green tea and green tea extracts in weight loss area (although in a different type of population) were done treating volunteers with much higher doses of green tea catechins (375–1200 mg/day) typically associated with caffeine (150–600 mg/day) [15, 44–48]. While the exact composition of green tea infusions and green tea extracts used in the studies available from the literature cannot always be clearly identified, we assume that the achievement of a significant weight loss resorting to a catechins intake which is significantly lower than in other studies can be explained by an improved bioavailability provided by the lecithin component of GSP [49]. Also, the use of a standardized, reproducible extract, as in the case of GSP, allows making future comparisons in case of additional clinical experiences in weight loss and MetS.

Another important aspect to be evaluated when comparing studies obtained with different green tea derivatives is the presence of caffeine, in addition to the content, composition, and bioavailability of catechins. The role of caffeine is, in fact, double-edged: if, from one side, it can increase the metabolic rate and calorie expenditure [50], on the other side, it is able to disrupt insulin sensitivity at low doses even in healthy volunteers [51], possibly leading to an undesirable weight loss outcome as a result of these two opposite effects. Hence, we cannot exclude that the absence of caffeine in the tested product may have had an additional positive role in the study.

5. Conclusions

Body weight reduction is considered the hallmark target to reduce the detrimental effects of MetS on health, and the attainment of this aim requires changes in lifestyle and nutrition [52], promoting exercise, and caloric restriction. The increase of calories expenditures obtained by exercise can be complemented by the use of thermogenic food ingredients, that is, compounds that promote brown adipose tissue activity and, in general, the degradation of fats in a non-ATP producing way. Thermogenic compounds could also provide help in counteracting the metabolic homeostatic adjustments associated to diet, increasing its overall efficacy [53]. The effect of green tea, the best-known dietary thermogenic agent, is therefore expected to be most evident when associated to a lifestyle intervention that involves both dietary restriction and exercise. We have evaluated this possibility in a controlled registry study in borderline MetS individuals, associating a lecithin-formulated decaffeinated catechin extract (GSP) to a controlled hypocaloric diet and exercise schedule. Compared to a control characterized by the same lifestyle intervention scheme, significant beneficial effects were observed not only on weight but also on other markers of cardiovascular and diabetic risk associated with the conditions, making it tempting to speculate that green tea might promote these improvements not only indirectly via weight loss but also directly, owing to its antioxidant and anti-inflammatory activity. We believe that the study we have outlined is worth expanding in terms of both recruitment and duration, also focusing on the chronic subclinical inflammation commonly associated with MetS and obesity. Inflammation strongly contributes to the persistence of the MetS and to the clinical consequences of the syndrome [54–58], and inflammatory markers, often in association with an increased oxidative stress, are usually found in MetS, contributing to its progression to higher risk levels [59].

References

[1] S. Bansal, N. Syan, P. Mathur, and S. Choudhary, "Pharmacological profile of green tea and its polyphenols: a review," *Medicinal Chemistry Research*, vol. 21, no. 11, pp. 3347–3360, 2012.

[2] C. S. Yang and X. Wang, "Green tea and cancer prevention," *Nutrition and Cancer*, vol. 62, no. 7, pp. 931–937, 2010.

[3] K. Boehm, F. Borrelli, E. Ernst et al., "Green tea (Camellia sinensis) for the prevention of cancer," *Cochrane Database of Systematic Reviews*, no. 3, Article ID CD005004, 2009.

[4] T. M. Jurgens, A. M. Whelan, L. Killian, S. Doucette, S. Kirk, and E. Foy, "Green tea for weight loss and weight maintenance in overweight or obese adults," *Cochrane Database of Systematic Reviews*, vol. 12, Article ID CD008650, 2012.

[5] R. Hursel, W. Viechtbauer, and M. S. Westerterp-Plantenga, "The effects of green tea on weight loss and weight maintenance: a meta-analysis," *International Journal of Obesity*, vol. 33, no. 9, pp. 956–961, 2009.

[6] J. H. Park, J. Y. Jin, W. K. Baek et al., "Ambivalent role of gallated catechins in glucose tolerance in humans: a novel insight into non-absorbable gallated catechin-derived inhibitors of glucose absorption," *Journal of Physiology and Pharmacology*, vol. 60, no. 4, pp. 101–109, 2009.

[7] K. Maruyama, H. Iso, S. Sasaki, and Y. Fukino, "The association between concentrations of green tea and blood glucose levels," *Journal of Clinical Biochemistry and Nutrition*, vol. 44, no. 1, pp. 41–45, 2009.

[8] T. Miura, T. Koike, and T. Ishida, "Antidiabetic activity of green tea (*Thea sinensis* L.) in genetically type 2 diabetic mice," *Journal of Health Science*, vol. 51, no. 6, pp. 708–710, 2005.

[9] M. E. Waltner-Law, X. L. Wang, B. K. Law, R. K. Hall, M. Nawano, and D. K. Granner, "Epigallocatechin gallate, a constituent of green tea, represses hepatic glucose production," *Journal of Biological Chemistry*, vol. 277, no. 38, pp. 34933–34940, 2002.

[10] C. L. Ogden, M. D. Carroll, B. K. Kit, and K. M. Flegal, "Prevalence of obesity in the United States, 2009-2010," *NCHS Data Brief*, no. 82, pp. 1–8, 2012.

[11] S. Kumanyika, R. W. Jeffery, A. Morabia, C. Ritenbaugh, and V. J. Antipatis, "Obesity prevention: the case for action," *International Journal of Obesity*, vol. 26, no. 3, pp. 425–436, 2002.

[12] P. Hossain, B. Kawar, and M. El Nahas, "Obesity and diabetes in the developing world—a growing challenge," *The New England Journal of Medicine*, vol. 356, no. 3, pp. 213–215, 2007.

[13] M. Bose, J. D. Lambert, J. Ju, K. R. Reuhl, S. A. Shapses, and C. S. Yang, "The major green tea polyphenol, (-)-epigallocatechin-3-gallate, inhibits obesity, metabolic syndrome, and fatty liver disease in high-fat-fed mice," *Journal of Nutrition*, vol. 138, no. 9, pp. 1677–1683, 2008.

[14] T. Nagao, T. Hase, and I. Tokimitsu, "A green tea extract high in catechins reduces body fat and cardiovascular risks in humans," *Obesity*, vol. 15, no. 6, pp. 1473–1483, 2007.

[15] A. G. Dulloo, C. Duret, D. Rohrer et al., "Efficacy of a green tea extract rich in catechin polyphenols and caffeine in increasing 24-h energy expenditure and fat oxidation in humans," *American Journal of Clinical Nutrition*, vol. 70, no. 6, pp. 1040–1045, 1999.

[16] S. Wolfram, Y. Wang, and F. Thielecke, "Anti-obesity effects of green tea: from bedside to bench," *Molecular Nutrition and Food Research*, vol. 50, no. 2, pp. 176–187, 2006.

[17] Q. Shixian, B. VanCrey, J. Shi, Y. Kakuda, and Y. Jiang, "Green tea extract thermogenesis-induced weight loss by epigallocatechin gallate inhibition of catechol-O-methyltransferase," *Journal of Medicinal Food*, vol. 9, no. 4, pp. 451–458, 2006.

[18] F. Di Pierro, A. B. Menghi, A. Barreca, M. Lucarelli, and A. Calandrelli, "GreenSelect Phytosome as an adjunct to a low-calorie diet for treatment of obesity: a clinical trial," *Alternative Medicine Review*, vol. 14, no. 2, pp. 154–160, 2009.

[19] G. Zheng, K. Sayama, T. Okubo, L. R. Juneja, and I. Oguni, "Anti-obesity effects of three major components of green tea, catechins, caffeine and theanine, in mice," *In Vivo*, vol. 18, no. 1, pp. 55–62, 2004.

[20] J. A. Greenberg, C. N. Boozer, and A. Geliebter, "Coffee, diabetes, and weight control," *American Journal of Clinical Nutrition*, vol. 84, no. 4, pp. 682–693, 2006.

[21] M. Boschmann and F. Thielecke, "The effects of epigallocatechin-3-gallate on thermogenesis and fat oxidation in obese men: a pilot study," *The Journal of the American College of Nutrition*, vol. 26, no. 4, pp. 389S–395S, 2007.

[22] C. Gosselin and F. Haman, "Effects of green tea extracts on non-shivering thermogenesis during mild cold exposure in young men," *British Journal of Nutrition*, vol. 110, no. 2, pp. 282–288, 2013.

[23] P. Pietta, P. Simonetti, C. Gardana, A. Brusamolino, P. Morazzoni, and E. Bombardelli, "Relationship between rate and extent of catechin absorption and plasma antioxidant status," *Biochemistry and Molecular Biology International*, vol. 46, no. 5, pp. 895–903, 1998.

[24] G. Alberti, P. Zimmet, J. Shaw, and S. M. Grundy, *The IDF Consensus Worldwide Definition of the Metabolic Syndrome, IDF Communications*, Brussels, Belgium, 2006.

[25] E. Bonora, S. Kiechl, J. Willeit et al., "Prevalence of insulin resistance in metabolic disorders: the Bruneck Study," *Diabetes*, vol. 47, no. 10, pp. 1643–1649, 1998.

[26] J. D. Brunzell and A. F. Ayyobi, "Dyslipidemia in the metabolic syndrome and type 2 diabetes mellitus," *American Journal of Medicine A*, vol. 115, supplement 8, pp. 24S–28S, 2003.

[27] R. W. Nesto, "The relation of insulin resistance syndromes to risk of cardiovascular disease," *Reviews in Cardiovascular Medicine*, vol. 4, no. 6, pp. S11–S18, 2003.

[28] M.-C. Pouliot, J.-P. Despres, S. Lemieux et al., "Waist circumference and abdominal sagittal diameter: best simple anthropometric indexes of abdominal visceral adipose tissue accumulation and related cardiovascular risk in men and women," *American Journal of Cardiology*, vol. 73, no. 7, pp. 460–468, 1994.

[29] J. Lindström, A. Louheranta, M. Mannelin et al., "The Finnish Diabetes Prevention Study (DPS): lifestyle intervention and 3-year results on diet and physical activity," *Diabetes Care*, vol. 26, no. 12, pp. 3230–3236, 2003.

[30] S. J. Robins, D. Collins, J. T. Wittes et al., "Relation of gemfibrozil treatment and lipid levels with major coronary events. VA-HIT: a randomized controlled trial," *Journal of the American Medical Association*, vol. 285, no. 12, pp. 1585–1591, 2001.

[31] J. Tuomilehto, J. Lindström, J. G. Eriksson et al., "Prevention of type 2 diabetes mellitus by changes in lifestyle among subjects with impaired glucose tolerance," *The New England Journal of Medicine*, vol. 344, no. 18, pp. 1343–1350, 2001.

[32] A. V. Chobanian, G. L. Bakris, H. R. Black et al., "Seventh report of the joint national committee on prevention, detection, evaluation, and treatment of high blood pressure," *Hypertension*, vol. 42, no. 6, pp. 1206–1252, 2003.

[33] R. Collins, J. Armitage, S. Parish, P. Sleigh, and R. Peto, "MRC/BHF Heart Protection Study of cholesterol-lowering with simvastatin in 5963 people with diabetes: a randomised placebo-controlled trial," *The Lancet*, vol. 361, no. 9374, pp. 2005–2016, 2003.

[34] S. M. Haffner, C. M. Alexander, T. J. Cook et al., "Reduced coronary events in simvastatin-treated patients with coronary heart disease and diabetes or impaired fasting glucose levels: subgroup analyses in the scandinavian simvastatin survival study," *Archives of Internal Medicine*, vol. 159, no. 22, pp. 2661–2667, 1999.

[35] J.-L. Chiasson, R. G. Josse, R. Gomis, M. Hanefeld, A. Karasik, and M. Laakso, "Acarbose treatment and the risk of cardiovascular disease and hypertension in patients with impaired glucose tolerance: the STOP-NIDDM trial," *Journal of the American Medical Association*, vol. 290, no. 4, pp. 486–494, 2003.

[36] W. C. Knowler, E. Barrett-Connor, S. E. Fowler et al., "Reduction in the incidence of type 2 diabetes with lifestyle intervention or metformin," *The New England Journal of Medicine*, vol. 346, no. 6, pp. 393–403, 2002.

[37] J. S. Torgerson, J. Hauptman, M. N. Boldrin, and L. Sjöström, "XENical in the Prevention of Diabetes in Obese Subjects (XENDOS) Study: a randomized study of orlistat as an adjunct to lifestyle changes for the prevention of type 2 diabetes in obese patients," *Diabetes Care*, vol. 27, no. 1, pp. 155–161, 2004.

[38] C. X. Romero, T. E. Romero, J. C. Shlay, L. G. Ogden, and D. Dabelea, "Changing trends in the prevalence and disparities of obesity and other cardiovascular disease risk factors in three racial/ethnic groups of USA adults," *Advances in Preventive Medicine*, vol. 2012, Article ID 172423, 8 pages, 2012.

[39] M. R. Goldstein, L. Mascitelli, and F. Pezzetta, "On treating metabolic syndrome: emphasise lifestyle change," *The Lancet Oncology*, vol. 11, no. 5, article 415, 2010.

[40] T. Wilsgaard and B. K. Jacobsen, "Lifestyle factors and incident metabolic syndrome. The Tromsø Study 1979–2001," *Diabetes Research and Clinical Practice*, vol. 78, no. 2, pp. 217–224, 2007.

[41] R. E. Kirk, *Experimental Design: Procedures for the Behavioral Sciences*, Brooks/Cole, Belmont, Mass, USA, 1982.

[42] A. Basu, N. M. Betts, A. Mulugeta, C. Tong, E. Newman, and T. J. Lyons, "Green tea supplementation increases glutathione and plasma antioxidant capacity in adults with the metabolic syndrome," *Nutrition Research*, vol. 33, no. 3, pp. 180–187, 2013.

[43] A. E. Vieira Senger, C. H. Schwanke, I. Gomes, and M. G. Valle Gottlieb, "Effect of green tea (Camellia sinensis) consumption on the components of metabolic syndrome in elderly," *The Journal of Nutrition, Health & Aging*, vol. 16, no. 9, pp. 738–742, 2012.

[44] S. Bérubé-Parent, C. Pelletier, J. Doré, and A. Tremblay, "Effects of encapsulated green tea and Guarana extracts containing

a mixture of epigallocatechin-3-gallate and caffeine on 24 h energy expenditure and fat oxidation in men," *British Journal of Nutrition*, vol. 94, no. 3, pp. 432–436, 2005.

[45] A. M. Hill, A. M. Coates, J. D. Buckley, R. Ross, F. Thielecke, and P. R. C. Howe, "Can EGCG reduce abdominal fat in obese subjects?" *Journal of the American College of Nutrition*, vol. 26, no. 4, pp. 396S–402S, 2007.

[46] K. C. Maki, M. S. Reeves, M. Farmer et al., "Green tea catechin consumption enhances exercise-induced abdominal fat loss in overweight and obese adults," *Journal of Nutrition*, vol. 139, no. 2, pp. 264–270, 2009.

[47] T. Komatsu, M. Nakamori, K. Komatsu et al., "Oolong tea increases energy metabolism in Japanese females," *Journal of Medical Investigation*, vol. 50, no. 3-4, pp. 170–175, 2003.

[48] W. Rumpler, J. Seale, B. Clevidence et al., "Oolong tea increases metabolic rate and fat oxidation in men," *Journal of Nutrition*, vol. 131, no. 11, pp. 2848–2852, 2001.

[49] P. Pietta, P. Simonetti, C. Gardana, A. Brusamolino, P. Morazzoni, and E. Bombardelli, "Relationship between rate and extent of catechin absorption and plasma antioxidant status," *Biochemistry and Molecular Biology International*, vol. 46, no. 5, pp. 895–903, 1998.

[50] R. Hursel, W. Viechtbauer, A. G. Dulloo et al., "The effects of catechin rich teas and caffeine on energy expenditure and fat oxidation: a meta-analysis," *Obesity Reviews*, vol. 12, no. 7, pp. e573–e581, 2011.

[51] M. S. Beaudoin, B. Allen, G. Mazzetti, P. J. Sullivan, and T. E. Graham, "Caffeine ingestion impairs insulin sensitivity in a dose-dependent manner in both men and women," *Applied Physiology, Nutrition, and Metabolism*, vol. 38, no. 2, pp. 140–147, 2013.

[52] G. Belcaro, M. Cesarone, E. Silvia et al., "Daily consumption of reliv glucaffectÛ for 8 weeks significantly lowered blood glucose and body weight in 50 subjects," *Phytotherapy Research*, vol. 23, no. 12, pp. 1673–1677, 2009.

[53] N. Boon, "Health potential for functional green teas?" *International Journal for Vitamin and Nutrition Research*, vol. 78, no. 6, pp. 275–281, 2008.

[54] T. Adar, A. Ben Ya'acov, G. Lalazar et al., "Oral administration of immunoglobulin G-enhanced colostrum alleviates insulin resistance and liver injury and is associated with alterations in natural killer T cells," *Clinical and Experimental Immunology*, vol. 167, no. 2, pp. 252–260, 2012.

[55] N. Gupta, K. Goel, P. Shah, and A. Misra, "Childhood obesity in developing countries: epidemiology, determinants, and prevention," *Endocrine Reviews*, vol. 33, no. 1, pp. 48–70, 2012.

[56] A. Nguyen Dinh Cat and F. Jaisser, "Extrarenal effects of aldosterone," *Current Opinion in Nephrology and Hypertension*, vol. 21, no. 2, pp. 147–156, 2012.

[57] L. Soares-Miranda, G. Sandercock, S. Vale et al., "Metabolic syndrome, physical activity and cardiac autonomic function," *Diabetes/Metabolism Research and Reviews*, vol. 28, no. 4, pp. 363–369, 2012.

[58] I. Stelzer, S. Zelzer, R. B. Raggam et al., "Link between leptin and interleukin-6 levels in the initial phase of obesity related inflammation," *Translational Research*, vol. 159, no. 2, pp. 118–124, 2012.

[59] A. Barac, H. Wang, N. M. Shara et al., "Markers of inflammation, metabolic risk factors, and incident heart failure in American Indians: the strong heart study," *Journal of Clinical Hypertension*, vol. 14, no. 1, pp. 13–19, 2012.

Hindawi Publishing Corporation
Evidence-Based Complementary and Alternative Medicine
Volume 2013, Article ID 989670, 12 pages
http://dx.doi.org/10.1155/2013/989670

Research Article

Traditional Chinese Medicine Tang-Luo-Ning Ameliorates Sciatic Nerve Injuries in Streptozotocin-Induced Diabetic Rats

Da-Wei Zou,[1] Yan-Bin Gao,[1] Zhi-Yao Zhu,[1] Hui Zhou,[2] Tao-Jing Zhang,[2] Bu-Man Li,[3] Jin-Yang Wang,[1] Min-Zhou Li,[2] Ming-Fei Ma,[2] and Na Zhang[1]

[1] *School of Traditional Chinese Medicine, Capital Medical University, Number 10 Youanmenwai Xitoutiao, Fengtai District, Beijing 100069, China*
[2] *Endocrinology Department, Oriental Hospital of Beijing University of Chinese Medicine, Beijing, China*
[3] *Traditional Chinese Medicine Department, Shougang Hospital of Peking University, Beijing, China*

Correspondence should be addressed to Yan-Bin Gao; gaoyb111@hotmail.com

Received 16 July 2013; Accepted 1 September 2013

Academic Editor: Vincenzo De Feo

Diabetic peripheral neuropathy (DPN) is a common microvascular complication of diabetes associated with high disability rate and low quality of life. Tang-Luo-Ning (TLN) is an effective traditional Chinese medicine for the treatment of DPN. To illustrate the underlying neural protection mechanisms of TLN, the effect of TLN on electrophysiology and sciatic nerve morphology was investigated in a model of streptozotocin-induced DPN, as well as the underlying mechanism. Sciatic motor nerve conduction velocity and digital sensory nerve conduction velocity were reduced in DPN and were significantly improved by TLN or α-lipoic acid at 10 and 20 weeks after streptozotocin injection. It was demonstrated that TLN intervention for 20 weeks significantly alleviated pathological injury as well as increased the phosphorylation of ErbB2, Erk, Bad (Ser112), and the mRNA expression of neuregulin 1 (Nrg1), GRB2-associated binding protein 1 (Gab1), and mammalian target of rapamycin (Mtor) in injured sciatic nerve. These novel therapeutic properties of TLN to promote Schwann cell survival may offer a promising alternative medicine for the patients to delay the progression of DPN. The underlying mechanism may be that TLN exerts neural protection effect after sciatic nerve injury through Nrg1/ErbB2 → Erk/Bad Schwann cell survival signaling pathway.

1. Introduction

Diabetic peripheral neuropathy (DPN) is a common microvascular complication of diabetes and affects more than 50% of diabetic patients [1]. DPN is a progressive disease characterized by pain and paresthesia and can even develop diabetic foot or gangrene [2]. Recent studies showed that the incidence of DPN is a complex mechanism mainly including (1) hyperglycemia and metabolism disorders such as activation of polyol pathway [3], nonenzymatic glycosylation [4], and activation of protein kinase C [5]; (2) activation of mitogen-activated protein kinases (MAPK) pathways [6]; (3) oxidative stress [7]; (4) lack of neurotrophic support and vascular pathologies [8]; (5) apoptosis of Schwann cells (SCs) [9].

As an important neuron in peripheral nerve system, SCs have become a center for many research studies in recent years as they play a key role in myelination, neurotrophic support, homeostasis, and repair after peripheral nerve injury [10–13]. Moreover, physiological interactions and reciprocal signaling between axons and SCs play critical roles in nerve development and survival, and Nrg1 is an essential modulator of SCs during development, nerve repair, and remyelination [14]. However, conventional therapy techniques for DPN, including controlling hyperglycemia, improving microcirculation, alleviating metabolic disorder, and suppressing oxidative stress, have failed to halt functional and structural changes of peripheral nerve in both humans and experimental animals [15]. Significantly, this suggests that the injuries of SCs have been activated by hyperglycemia induced

metabolic disturbance, and then SCs can act independently to further exacerbate the structural and functional injuries of sciatic nerve. The therapies above could not reverse the occurred peripheral nerve injuries such as axonal degeneration, demyelination, and cell apoptosis. Consequently, improvement of SCs survival and recovery of peripheral nerve regeneration ability are of vital importance to delay the progress of DPN.

As is well known, the incidence of DPN could be attributed to a multiple mechanisms. Traditional Chinese medicine (TCM), which has the advantage of hitting multiple targets at the same time, may be a good choice for such therapeutic agents [16]. Tang-Luo-Ning (TLN) is an effective Chinese recipe in TCM for the treatment of DPN [17, 18]. According to the theory of TCM, TLN recipe mainly contains three different traditional Chinese herbs: *Astragalus membranaceus* (Fisch.) Bge (Huangqi), *Salvia miltiorrhiza* Bge. (Danshen), and *Paeonia lactiflora* Pall. (Chishao) (detailedly shown in Section 2). This recipe functions to tonify qi promote the blood circulation and remove the blood stasis. It has been reported that *Astragalus membranaceus* could reduce the serum glucose and triglyceride level and inhibit advanced glycation end products-induced inflammation as well in the diabetic individuals [19, 20]. Moreover, Astragaloside IV, the major active component of TLN recipe, could exert protective effects against DPN in streptozotocin- (STZ-) induced diabetes in rats through several interrelated mechanisms [21]. Previously, we demonstrated that TLN exerted protective effects against the progression of DPN through several interrelated mechanisms, such as improvement of oxidative damage, inhibition of dorsal root ganglion and sciatic nerve apoptosis [22, 23] in streptozotocin-induced diabetic rats (STZ-R). However, whether TLN intervention attenuates sciatic nerve injury and promotes recovery of it through enhancing SCs survival is unknown.

In our study, due to multiple-target characteristic of Chinese herbal compound, microarray expression analysis was used to screen cell-survival related genes and pathways regulated by TLN, followed further validation by quantitative real time polymerase chain reaction (qPCR) and western blot.

2. Materials and Methods

2.1. The TLN Extract Preparation and Quality Control. TLN recipe mainly contains the ingredients from three different traditional Chinese herbs: the dried root of *Astragalus membranaceus* (Fisch.) Bge. (Huangqi, amount used 30 g per day), the dried root and rhizome of *Salvia miltiorrhiza* Bge. (Danshen, amount used 30 g per day), and the dried root of *Paeonia lactiflora* Pall. (Chishao, amount used 20 g per day) as well. All herbs were purchased from Oriental Hospital of Beijing University of Chinese Medicine (BUCM, Beijing, China). The crude drugs were carefully authenticated and then decocted and made into particle in the Manufacturing Laboratory of Oriental Hospital of BUCM. In brief, the weight proportion of *Astragalus membranaceus* (Fisch.) Bge., *Salvia miltiorrhiza* Bge., and *Paeonia lactiflora* Pall. is 3 : 3 : 2. The herbs were extracted three times with 60% ethanol (600 mL per 100 g herbs) for 1.5 h each time. The ethanol extract was pooled and concentrated to stronger liquor with a relative density of 1.25–1.30 at 70°C. The above liquor was evaporated under reduced pressure and ground into fine powder to obtain the TLN extract. The TLN extract and excipients were mixed at a ratio of 1 : 1 with 80% ethanol to pelletize. A content of 0.7875 mg/g Astragaloside IV, which is the main active component in TLN, was detected in TLN particles by HPLC-ELSD (shown in Supplementary Figure 1, available on line at http://dx.doi.org/10.1155/2013/989670). TLN particles were suspended in the distilled water at appropriate concentration for the animal treatment.

2.2. Animal Model and Drug Intervention. Male Sprague Dawley rats weighting 180 g–220 g were purchased from Vital River Laboratories (Beijing, China, certificate No. SCXK 2006–0009). The animals were housed in separate cages at constant temperature (20–22°C) and humidity (50%–67%) under a 12-hour light/dark cycle in specific pathogen free animal laboratory of BUCM. The animals had free access to standard chow diet (Vital River, Beijing, China) and sterilized drinking water during the period of this experiment. The experimental protocol was approved by the ethics committee of BUCM. All animal experiments were conducted in accordance with the NIH guide for the care and use of laboratory animals (NIH Publication No. 80-23; revised 1978).

After one week of acclimatization, rats were given STZ (Sigma, 60 mg/kg body weight), and 72 hours later rats with fasting blood glucose more than 16.7 mmol/L were considered successfully induced for diabetes. The diabetic rats were randomly divided into three groups including STZ induced diabetic group (STZ group), Tang-Luo-Ning group (TLN group), and alpha-lipoic acid group (α-LA group); there was also a non-STZ induced group as control group (CTL group). Rats in intervention groups were administrated separate drug by gavage (5 mL/kg) from the next day at a dose of either 10 g/kg body weight (TLN group) or 20 mg/kg body weight (α-LA group), and the rats in CTL group or STZ group were treated at the same volume of distill water (5 mL/kg) by gavage for 20 weeks. The α-LA was purchased from Puritan's Pride Inc. (Oakdale, NY, USA). The batch number of the α-LA used in this experiment was 250597-09. Determination of the dose of TLN used in the present study was based on our previous works. After the last administration, all rats were fasted for 12 hours before experiment but allowed free access to water. The animals were anesthetized using 10% chloral hydrate (300–350 mg/kg) to get sciatic nerve. The sciatic nerve tissue from each mouse was also divided into two parts, one part was immediately frozen in liquid nitrogen for western blot, RNA extraction, and microarray, and another part was fixed with 4% glutaraldehyde for electron microscope, respectively.

2.3. Electrophysiological Measurements. Sciatic motor nerve conduction velocity (MNCV) and distal digital sensory nerve conduction velocity (SNCV) were measured after induction of anesthesia with 10% chloral hydrate (300–350 mg/kg) at two points (10 weeks and 20 weeks after intervention). Body

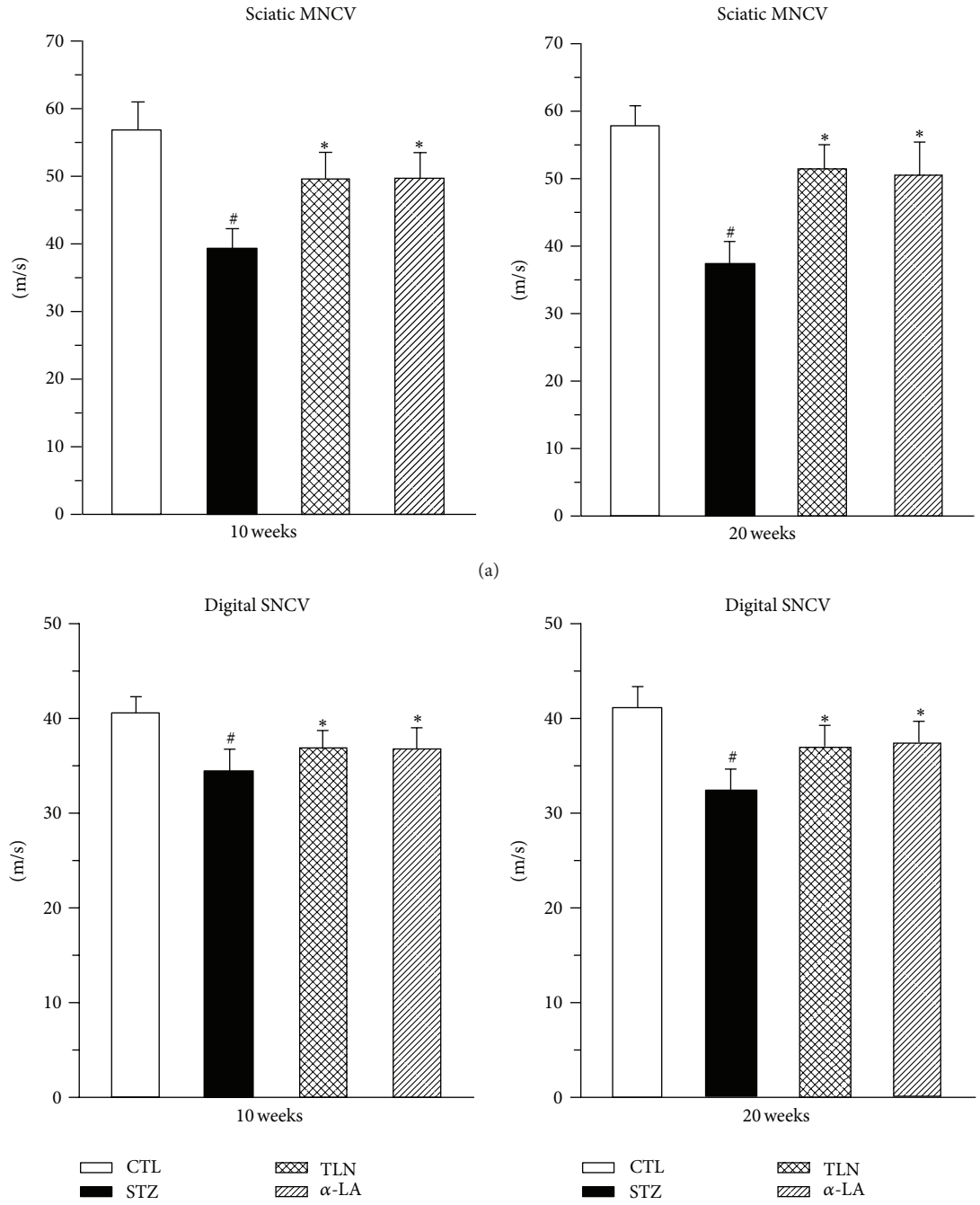

Figure 1: Effects of TLN and α-LA on (a) sciatic MNCV and (b) distal digital SNCV at 10 and 20 weeks after streptozotocin injection. $n = 8$ per group. Data are expressed as mean ± SD. $^{\#}P < 0.05$ versus CTL group, $^{*}P < 0.05$ versus STZ group; sciatic MNCV and distal digital SNCV of STZ group rats with streptozotocin injection decreased compared with CTL group ($P < 0.05$). Tang-Luo-Ning and alpha-lipoic acid intervention both increased sciatic MNCV and distal digital SNCV of injured sciatic nerve compared with STZ group ($P < 0.05$). MNCV: Motor nerve conduction velocity. SNCV: sensory nerve conduction velocity. Four groups: CTL group: nonstreptozotocin-induced group, STZ group: streptozotocin-induced diabetic group, TLN group: Tang-Luo-Ning group, and α-LA group: alpha-lipoic acid group.

temperature was maintained at 37°C with a warming pad. For sciatic measurement, the left sciatic motor conduction system was stimulated at the sciatic notch where sciatic nerve exits and at ipsilateral ankle via bipolar electrodes with a width of 0.1 ms. The threshold was determined when the compound muscle action appeared or disappeared, and we set at 1.5-fold above the threshold as stimulus intensity. The recorded bipolar electrodes were placed at the first interosseous muscle

of the hind-paw, as well as reference electrode was placed 1 cm away from the recording electrode but between the stimulating and the recording electrode. Hind-limb SNCV was recorded in the digital nerve to the second toe by stimulating with a square-wave pulse duration of 0.05 ms using the smallest intensity current that resulted in a maximal amplitude response. The sensory nerve action potential was recorded behind the medial malleolus. The maximal SNCV was calculated from the latency to the onset of the initial negative deflection and the distance between stimulating and recording electrodes. The latencies of action potentials were measured as described below by physiological data recording system (MacLab/400, ADI, Australia) and dual-beam memory oscilloscope (VC-10, Nihon Kohden Corporation, Japan). Average conduction time was calculated after 7–10 measurements. Sciatic MNCV and distal digital SNCV were measured and calculated based on the method [24].

2.4. Morphological Observation of the Sciatic Nerve. Approximately 0.1 cm of sciatic nerve was removed from the lower edge of the left piriformis and cut into pieces about 1 mm^3 by volume. After prefixing with cold, 4% glutaraldehyde nerve tissues were fixed with 1% osmic acid and dehydrated and embedded in 1 : 100 mixture of Epon 812 and 100% aceton. Semithin sections were cut and stained with toluidine blue before they were further cut into 50 nm ultrathin sections using an ultramicrotome (8800, LKB, Bromma, Sweden). After double staining with uranyl acetate and lead nitrate, morphological changes of the sciatic nerves were observed by transmission electron microscopy (H-600, Hitachi, Japan). Images were taken by imaging systems (Moticam 2306, Motic Instruments Inc., Canada).

2.5. RNA Extraction and Microarray. RNA extraction and microarray were performed according to manufacturer's protocols by Shanghai Biotechnology Co., Ltd. TRIZOL Reagent (Catalogue number 15596-018, Life technologies, Carlsbad, CA, USA) was added into sciatic nerve, and total RNA was isolated using RNeasy Kit (Qiagen). RNA integrity number (RIN) and 28 s/18 s ratio were determined by Agilent BioAnalyzer 2100. RNAs with RIN $\geq$ 7.0 and 28S/18S $>$ 0.7 were deemed to be of sufficient quality. RNA concentration and A260/A280 ratio were determined by Nanodrop ND-1000. RNAs were purified by QIAGEN RNeasy Kit, followed by cDNA synthesis and cRNA fluorescent labeling, purifying, and shearing. Probes were hybridized with Rat Gene Expression Microarray slides (4 $\times$ 44 K microarray, Agilent, Catalogue number G2519F-014879) in a hybridization oven (Agilent G2545A). After thorough washing, array slides were scanned by Agilent scanner with both 100% and 10% PMT setting. Results were analyzed by Agilent software.

2.6. Microarray Data Analysis. With threshold of fold change between experimental samples (TLN group) and control samples (STZ group, CTL group) set at 2, genes that were differentially regulated by TLN were identified. Genes that were first downregulated >2-fold (compared with CTL) by STZ and then upregulated >2-fold (compared with STZ) by TLN were considered as upregulated genes, and the downregulated genes were opposite. Differentially regulated genes by TLN were analyzed using an online SAS system for hierarchical clustering, Gene ontology (GO) enrichment analysis and Kyoto Encyclopedia of Genes and Genomes pathway analysis (enrichment $P < 0.05$).

2.7. qPCR. To confirm microarray data and further screen cell survival related pathway, Nrg1, GRB2-associated binding protein 1 (Gab1), mammalian target of rapamycin (Mtor), and phosphoinositide-3-kinase, catalytic, beta polypeptide (Pik3cb) were selected for validation by qPCR. Primers were designed by Sheng Gong Biotech (Shanghai, China) using Primer Premier 5.0 software (PREMIER Biosoft International, CA, USA). The sequences of Nrg1, Pik3cb, Mtor, Gab1, and GAPDH were the following: Nrg1: forward primer 5′-TGGCACATCCATCCAAATAC-3′, reverse primer 5′-GTAGCATGCTGCTGGGTCTA-3′; Pik3cb: forward primer 5′-AGATGTTGCTCAGCTTCAGG-3′, reverse primer 5′-TT CATCACTCATCTGTCGCA-3′; Mtor: forward primer 5′-AGAACCACATGCCACACAGT-3′, reverse primer 5′-CTTTGGCATTTGTGTCCATC-3′; Gab1: forward primer 5′-CTCCTGAGACCACAAAGCAA-3′, Reverse primer 5′-AACGCTAGCTGCTTCTCACA-3′; GAPDH: Forward primer 5′-CAACTCCCTCAAGAT-TGTCAGCAA-3′, Reverse primer: 5′-GGCATGGACTGT-GGTCATGA-3′. RNA was reverse transcribed by M-MLV Reverse Transcriptase (CK2801A, Takara) according to manufacturer's protocols, and qPCR was performed on qPCR machine (ABI 7500, Life Technologies, USA) with the following program settings: 94°C for 15 min, 94°C for 15 s, 60°C for 34 s, and 72°C for 15 s for 40 cycles followed by 72°C for 10 min. All qPCRs were performed in duplicate, and relative expression was calculated using the $2^{-\Delta\Delta CT}$ method [25].

2.8. Western Blot. To determine the expression level of (P-) ErbB2, extracellular signal-regulated kinase (Erk), P-Erk, protein kinase B (PKB/Akt), P-Akt, bad, and P-bad Ser112/Ser136, the sciatic nerve tissues were quickly pulverized in prechilled mortar and then fractionated by SDS-PAGE. 40 μg of protein was separated by electrophoresis and transferred to Nitrocellulose membrane (Millipore, USA). Membrane was blocked in 5% nonfat dry milk in Tris-buffered saline (containing 0.1% Tween-20, PH = 7.6) for 1 h and incubated with primary antibodies at 4°C overnight. The primary antibodies were as follows: mouse monoclonal anti-Erk1/2 antibody (dilution: 1 : 3000), mouse monoclonal anti-Phospho-Erk1/2 antibody (dilution: 1 : 2000), rabbit monoclonal anti-Bad (D24A9) antibody (dilution: 1 : 2000), rabbit monoclonal anti-Phospho-Bad (Ser112) (40A9) antibody (dilution: 1 : 500), rabbit monoclonal anti-Phospho-Bad (Ser136) (D25H8) antibody (dilution: 1 : 500), rabbit monoclonal anti-Akt antibody (dilution: 1 : 3000), and rabbit monoclonal anti-Phospho-Akt (Ser473) antibody (dilution: 1 : 2000); the antibodies above were all purchased from Cell Signaling Technology (USA). Rabbit polyclonal anti-ErbB2 antibody (dilution: 1 : 4000, Novus, Biologicals, Inc.; Littleton, CO, USA), Rabbit polyclonal anti-Phospho-ErbB2

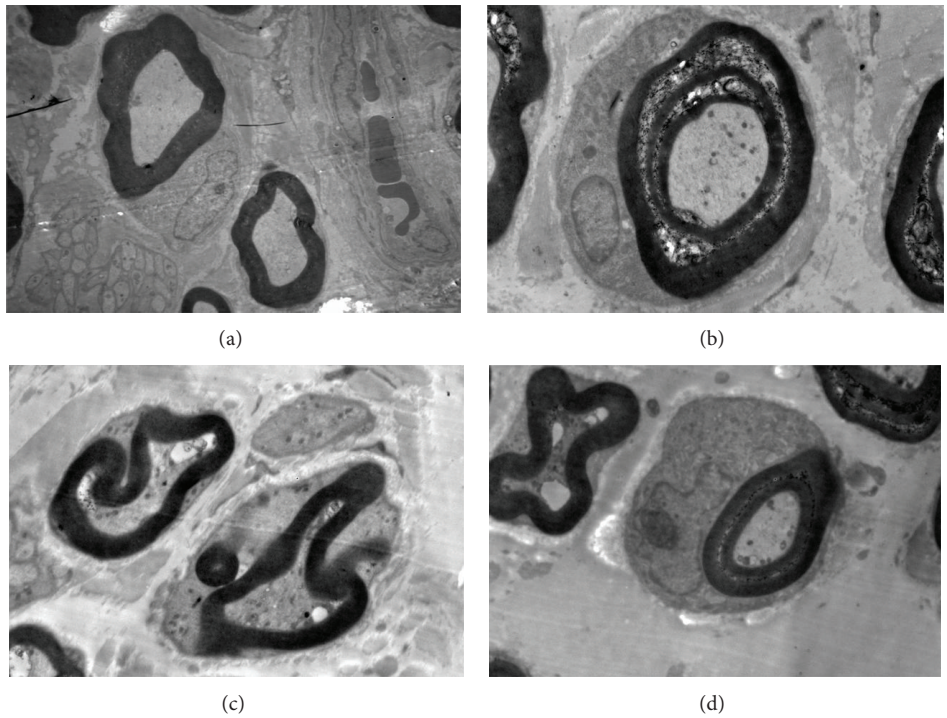

Figure 2: Transmission electron micrographs showing the ultrastructure of sciatic nerve fiber (×10000) (a) CTL rats: intact myelinated axon. (b) STZ rats: serious demyelination, axial degeneration, and Schwann cell proliferation. (c) TLN rats: moderate segmental demyelination and axial degeneration. (d) α-LA rats: moderate segmental demyelination, axial degeneration, and Schwann cell proliferation. Four groups: CTL group: nonstreptozotocin-induced group, STZ group: streptozotocin-induced diabetic group, TLN group: Tang-Luo-Ning group, and α-LA group: alpha-lipoic acid group.

(Tyr1248) antibody (dilution: 1 : 3000, Novus, Biologicals, Inc.; Littleton, CO, USA), after washing 3 × 10 min with Tris-buffered saline, horseradish peroxidase conjugated secondary antibody (dilution 1 : 1000: P-Bad ser112/ser136, 1 : 2000: other antibodies) was added and incubated for 1 hr with shaking. Target proteins were visualized using enhanced chemiluminescence reagents and exposed to X-Ray film in dark room. Densitometry analysis was performed on protein bands using software IPP 6.0 (Media Cybernetics Inc., USA).

2.9. Statistical Analysis. Differential gene expression and bioinformatics analysis were performed using online SAS analysis system provided by Shanghai Biotechnology Corporation. All other data were statistically analyzed by SPSS13.0 software. Average value ± standard deviation (Mean ± SD) were calculated, one-way ANOVA (analysis of variance) and LSD-t test (least significant difference t test) for multiple samples multiple comparison were performed, and $P < 0.05$ were considered as statistically significant.

3. Results

3.1. Function and Morphology of Sciatic Nerve

3.1.1. TLN Increases Nerve Conduction Velocity in STZ-Induced Diabetic Rats. Compared with the STZ group, an obvious improvement of sciatic MNCV and distal digital SNCV were observed after 10 weeks of TLN treatment (Figure 1), and this trend was even more profound after 20 weeks of TLN treatment. Moreover, the trend of MNCV after α-LA treatment was consistent with published data [26]. In brief, results demonstrated that TLN intervention increased MNCV and distal digital SNCV of injured sciatic nerve and improved the lower nerve function.

3.1.2. TLN Alleviates Pathological Injury of Sciatic Nerve. In control rats, there were fair-arranged nerve fibers, mainly with myelinated nerve of thick myelin and large axon diameter simultaneously. In diabetic rats, serious demyelination, axial degeneration and reduced number of myelinated nerve fibers were observed on transmission electron microscope, and the pathological injury in this study corresponded to typical morphological changes of DPN. Likewise, the pathologic and morphological changes in the sciatic nerves of diabetic rats treated with TLN and α-LA were both greatly alleviated (Figure 2). No significant changes were observed in the number and proportion of myelinated and unmyelinated nerve fibers in TLN and α-LA group. The results demonstrated that TLN could be counteracting against the pathological morphology changes of sciatic nerve in STZ-induced diabetic rats.

3.2. Schwann Cells Survival of Sciatic Nerve

3.2.1. Microarray Bioinformatics Analysis of Differentially Regulated Genes by TLN. Using an online SAS system, cluster

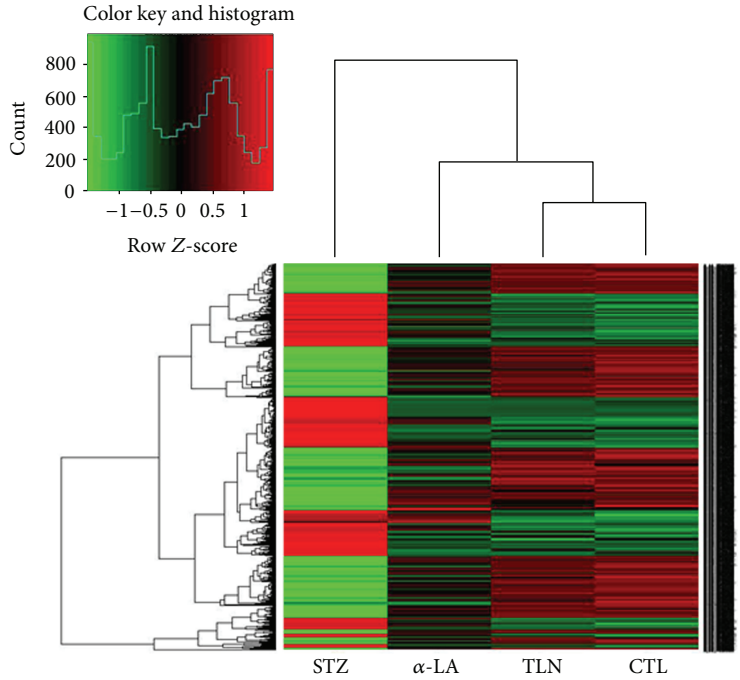

Figure 3: Heat map showed the differentially expressed genes regulated by TLN between four groups. Red color indicates over expressed genes, whereas green color indicates the opposite. The color scale bar is shown. Four groups: CTL group: nonstreptozotocin-induced group, STZ group: streptozotocin-induced diabetic group, TLN group: Tang-Luo-Ning group, and α-LA group: alpha-lipoic acid group.

analysis was performed and the resultant heat map allowed us to visualize the differential gene expression patterns between the experimental groups (Figure 3). GO analysis encompasses three domains: molecular function, biological process, and cellular component. GO analysis showed that the functions of genes that were differentially regulated by TLN mainly focused on cellular homeostasis, cell development, and anatomical structure formation (Figure 4). Pathway analysis showed that cell survival related pathways regulated by TLN contained ErbB signaling pathway, neurotrophin signaling pathway, and phosphatidylinositol signaling system (Table 1). These results indicated that TLN may exert protective effects against morphological changes of sciatic nerve through regulating these genes of above pathways, such as Nrg1, Pik3cb, Mtor, and Gab1 (Tables 1 and 2).

Table 1: Cell survival-related pathways regulated by TLN.

Pathway name	Positive and negative genes	Enrichment test P value
ErbB signaling pathway	Nrg1 Pik3cb Gab1 Mtor	0.0121
Neurotrophin signaling pathway	Pik3cb Gab1	$5.0E-4$
Phosphatidylinositol signaling system	Pik3cb	0.0057

Enrichment test P value ($P < 0.05$) means significant. Some genes listed are involved in more than one pathway. Nrg1: Neuregulin 1; Mtor: Mammalian target of rapamycin; Gab1: GRB2-associated binding protein 1.

3.2.2. TLN Upregulates Gene Expression of Nrg1, Mtor, and Gab1 in Sciatic Nerve of Diabetic Rats. Cell-survival genes (Nrg1, Mtor, Gab1, and Pi3kcb) identified from the microarray analysis were selected and performed qPCR for validation. Results showed that the TLN intervention upregulated the Nrg1, Mtor, and Gab1 expression levels, while the expression pattern of Pi3kcb were not consistent with the microarray data (Table 2 and Figure 5). Since Pi3kcb is the crucial gene of the Neurotrophin signaling pathway and phosphatidylinositol signaling system, there was no sense to do deeper study the two pathways.

3.2.3. TLN Upregulates Expression of P-ErbB2, P-Erk, and P-Bad (Ser112) in Sciatic Nerve of Diabetic Rat. In brief, we focused on Nrg1/ErbB2 pathway and do further validation by western blot. It is demonstrated that there was little variation of total ErbB2, Erk, Bad, Akt, and P-Akt after STZ injection ($P > 0.05$), and the phosphor-Bad (Ser136) cannot be detected by western blot. Likewise, phosphorylated levels of ErbB2, Erk, and Bad (Ser112) declined 3.6-fold, 1.9-fold, 4.4-fold in the STZ group (no intervention after STZ injection) when compared with the control group, respectively. In contrast, the expression levels of phosphorylated protein were similar to normal rat with TLN and α-LA intervention after STZ injection (Figure 6).

Taken together, these results from western blot and qPCR demonstrated that TLN could enhance NRG/ErbB2 → Erk/Bad dependent SCs-survival signal pathway (Figures 5 and 6).

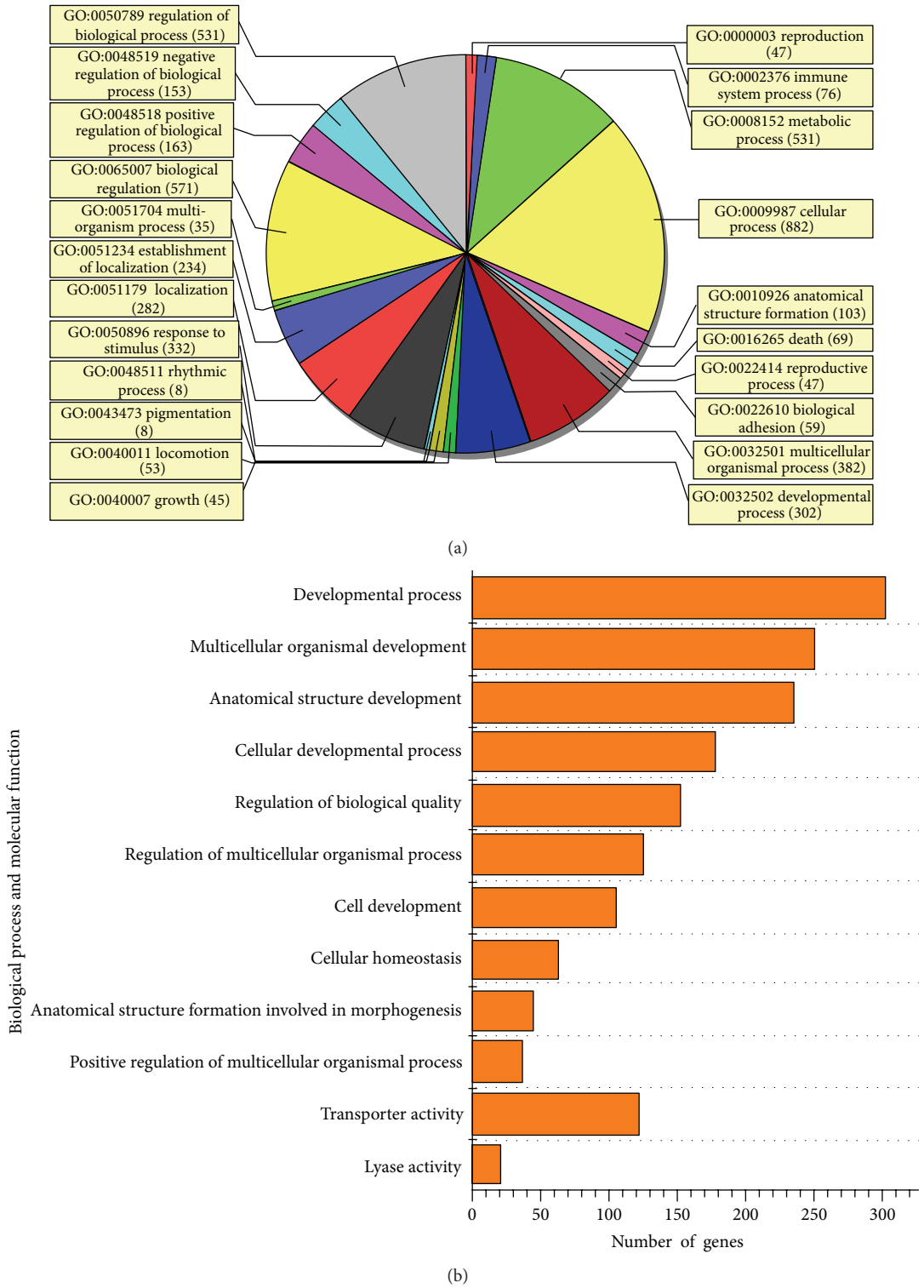

Figure 4: GO analysis and significantly altered categories regulated by TLN. (a) Gene ontology category of biological process for differentially expressed genes regulated by TLN. (b) The significant GO categories for differently expressed genes. The vertical axis represents the GO category, and the horizontal axis represents the number of genes changed in each category. There are 12 categories that were significantly altered (enrichment P value < 0.05 and number of changed genes >20). The first 10 categories are involved in biological process; the last two are involved in molecular function. GO: gene ontology.

Table 2: Major genes in cell survival-related pathways upregulated by TLN.

Probe Id	Gene Id	Gene symbol	Gene name	FC: STZ versus CTL	FC: TLN versus STZ	FC: α-LA versus STZ
A_44_P438143	112400	Nrg1	Neuregulin 1	0.3638	2.2264	2.1083
A_43_P12820	85243	Pik3cb	Phosphoinositide-3-kinase, catalytic, and beta polypeptide	0.3298	3.3562	2.8317
A_44_P191924	56718	Mtor	Mechanistic target of rapamycin (serine/threonine kinase)	0.3786	2.2988	1.9853
A_44_P176342	361388	Gab1	GRB2-associated binding protein 1	0.2205	4.8388	3.8136

FC: fold change.

4. Discussion

The present study provides direct evidence for a crucial role of TLN in function and morphology of sciatic nerve after diabetes. The protective effects of the compound recipe TLN may be attributed to promote SCs-survival through the activation of Nrg1/ErbB2 → Erk/Bad (Ser112) signal pathway by increasing the phosphorylation of ErbB2, Erk, and Bad (Ser112) at a protein level and mRNA expression of Nrg1, Mtor, and Gab1. This finding supports the hypothesis that TLN was a critical regulator in SCs survival and recovery of peripheral nerve regeneration ability. Recently there has been a great deal of interest in SCs due to the key role of it in myelination regeneration and repair after peripheral nerve injury.

DPN is a long-term common complication of diabetes. In this study, STZ was used to induce diabetic neuropathy model, which was widely performed in Sprague—Dawley rats [21], Wistar rats [27], and transgenic mice [28]. The STZ-induced diabetic rats beard the typical characteristics of DPN including demyelination and axial degeneration of sciatic nerve and reduction of peripheral nerve conduction velocity, which were consistent with published observations [29]. In addition, α-LA was selected as a positive control in the present study because of its antioxidative activity [30, 31].

In fact, ErbB2 signal pathway was most closely linked to SCs survival among the three screened signal pathways by microarray (Table 1), and Nrg1, Mtor, and Gab1 are key genes of ErbB2 signal pathway. Mtor is a conserved serine/threonine protein kinase and a member of the phosphatidylinositol 3-kinase-related kinase family. Mtor plays key roles in sensing nutrition signal, regulation of cell growth and proliferation [32], and regulation of insulin response by the insulin response element [33]. Meanwhile, due to the proapoptosis effect of c-Jun-NH2-terminal kinase pathway activation, Gab1 has an indirect antiapoptosis effect. Biochemical analysis suggested Gab1 played a positive role in coupling the signal relay between cytokine receptors and the Erk pathway [34]. More important, Nrg1, also known as glial growth factor, is mainly produced by SCs and transported by axons and plays a crucial role in SCs survival. Nrg1 belongs to Neuregulin gene family which contains four members termed as Nrg1, Nrg2, Nrg3, and Nrg4. Among them, Nrg1 is the most characteristic gene, and it is believed to be able to rescue SCs from apoptosis and act as a predominant survival factor during SCs maturation [35]. Recently studies also demonstrated that NRG signal provided trophic support to myelin-producing cells and contributed to myelination in peripheral nerve system and velocity of conduction [36, 37]. In our study, these three genes discussed above appeared to be key factors through which TLN might promote SCs survival.

The binding and activation of Nrg1 and ErbB2/ErbB3 coreceptor to activate the downstream signal pathways is very important to transmit SCs survival signal. Being a family member of polypeptide growth/differentiation factors containing an epidermal growth factor-like motif, Nrg1 could activate membrane-associated ErbB tyrosine kinase receptors and mediate SCs differentiation, proliferation, and migration through binding and activation of a heterodimeric ErbB2/ErbB3 coreceptor [38]. ErbB2 itself does not bind to NRG, while ErbB3 alone could bind to NRG but could not transmit signals. Since it is necessary for ErbB2 and ErbB3 to form a high affinity coreceptor complex to transmit SCs survival signal, the expression level of P-ErbB2 could reflect NRG receptor downstream signal intensity. In this study, the expression level of P-ErbB2 decreased after STZ induction, suggesting that there was a close relationship between Nrg1-ErbB2 signal transduction and sciatic nerve morphology change/conduction velocity. These data contradict with some reports [39] but agree with some others [40–42]. The underlying causes for this discrepancy are unknown. The present study also showed that TLN enhanced NRG receptor signal intensity through increasing Nrg1 mRNA expression and phosphorylation of ErbB2 at a protein level after peripheral nerve injury in STZ-R.

In addition, after binding to the high-affinity ErbB2/ErbB3 coreceptor complex, Nrg could potentially activate several distinct signaling pathways, mainly including p21Ras/Raf-1/MEK/Erk cascade [43] and PI3K/Akt signaling pathway [44]. The phosphorylation of bad either on serine 112 by Erk or serine 136 by Akt promotes its dissociation from the cytosolic protein 14-3-3, leading to the release of Bcl-2 and Bcl-xl to inhibit SCs apoptosis. Obviously, the phosphorylation of bad is the key link for TLN to promote SCs survival. One study showed that NRG-ErbB2 receptor signaling promoted SCs survival through a downstream PI3K/Akt/Bad pathway [41]. In this study, we detected that the significant change of phospho-Erk and phospho-Bad (Ser112), accompanying insignificant variation of phospho-Akt and no detection of phospho-Bad at the ser 136 residue,

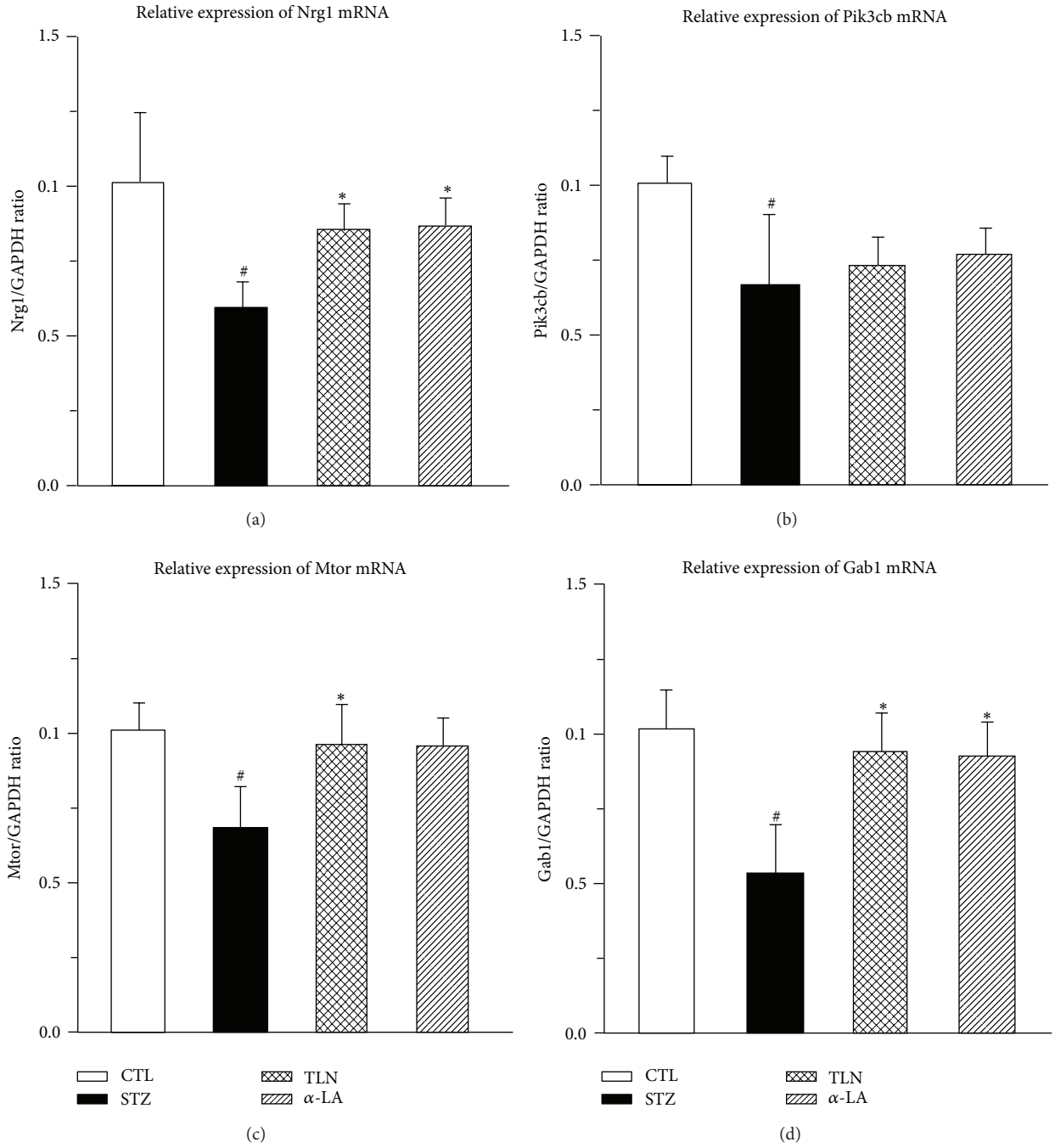

FIGURE 5: Effect of TLN and α-LA on cell survival related genes in sciatic nerve of streptozotocin-induced rats. Relative expression level change ($2^{-\Delta\Delta CT}$) of 4 genes in qPCR, (a) Nrg1, (b) Pik3cb, (c) Mtor, and (d) Gab1. Statistical analysis was performed using the ANOVA procedure t test (LSD). Data are expressed as mean ± SD. $^{\#}P < 0.05$, when compared with CTL group; $^{*}P < 0.05$, when compared with STZ group. The mRNA expression of Nrg1, Pik3cb, Mtor, and Gab1 decreased compared with CTL group ($P < 0.05$); TLN intervention could increase the expression level of Nrg1, Mtor, and Gab1 compared with STZ group ($P < 0.05$). The alpha-lipoic acid intervention trend was consistent with Tang-Luo-Ning except Gab1. There were no significant differences of Pik3cb mRNA between the three groups (STZ, α-LA, and TLN). Four groups: CTL group: nonstreptozotocin-induced group, STZ group: streptozotocin-induced diabetic group, TLN group: Tang-Luo-Ning group, and α-LA group: alpha-lipoic acid group. ANOVA: analysis of variance; LSD-t test: least significant difference t test; qPCR: quantitative real time polymerase chain reaction.

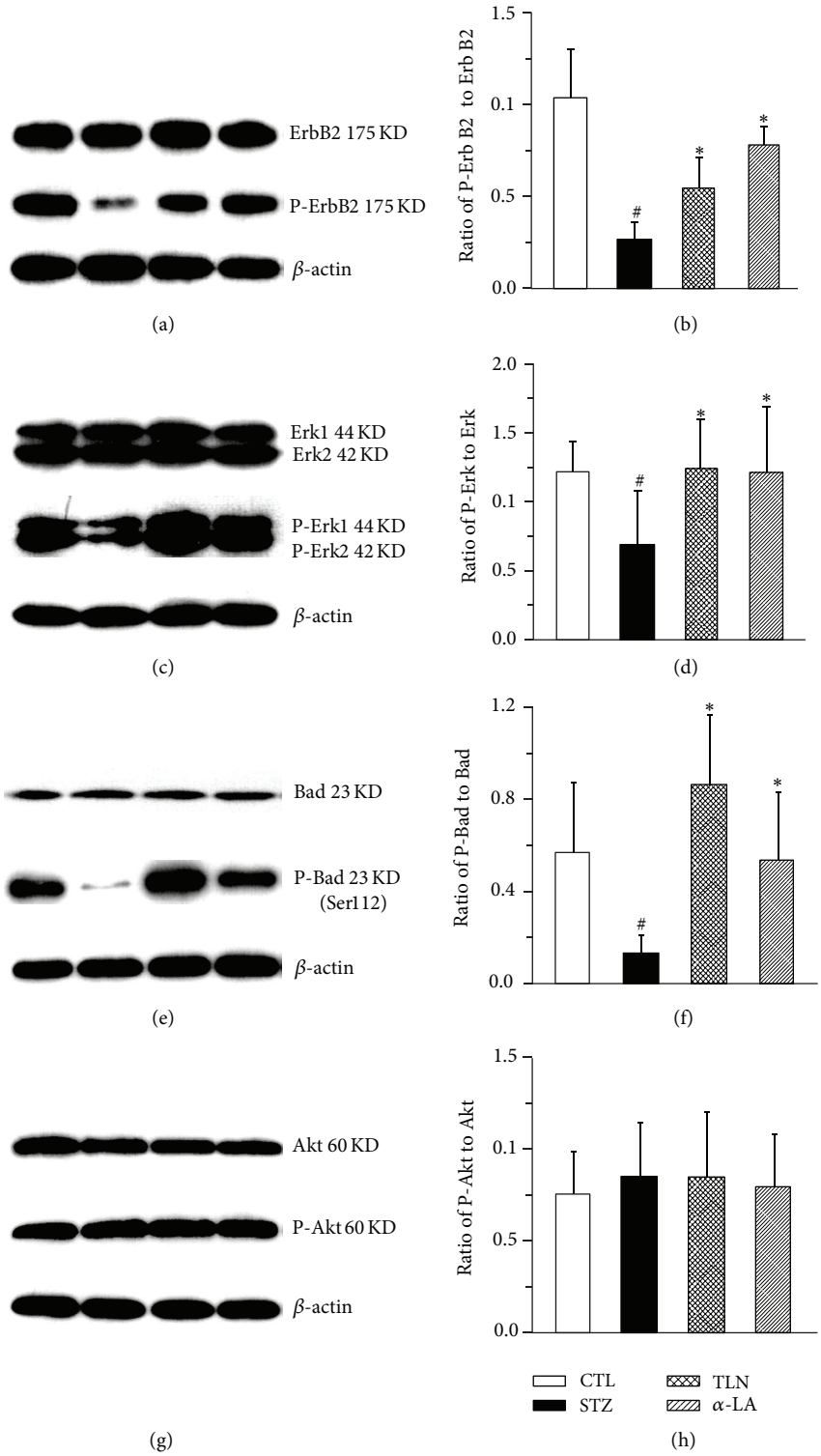

Figure 6: Effect of TLN and α-LA on Nrg1/ErbB2 downstream signal pathway in sciatic nerve of streptozotocin-induced rats. A representative western blot ((a), (c), (e), and (g)) and the grey value analyses of protein expression ((b), (d), (f), and (h)) in sciatic nerves from different experimental groups. ((a), (b)) Ratio of P-ErbB2 to T-ErbB2 (P/T); ((c), (d)) ratio of P-Erk to T-Erk (P/T); ((e), (f)) ratio of P-Bad (Ser112) to T-Bad (P/T); ((g), (h)) ratio of P-Akt to T-Akt (P/T). Statistical analysis was performed using the ANOVA procedure t test (LSD). Data are expressed as mean ± SD. $^{\#}P < 0.05$ versus CTL group, $^{*}P < 0.05$ versus STZ group. $n = 4$ per group. The protein expression of ratio of ErbB2 Erk, Bad (P/T) decreased compared with CTL group ($P < 0.05$), while Tang-Luo-Ning and alpha-lipoic acid intervention could increase the ratio above compared with STZ group ($P < 0.05$). There were no significant differences of ratio of Akt (P/T) between the four groups. Four groups: CTL group: nonstreptozotocin-induced group, STZ group: streptozotocin-induced diabetic group, TLN group: Tang-Luo-Ning group, and α-LA group: alpha-lipoic acid group. ANOVA: analysis of variance; LSD-t test: least significant difference t test.

suggesting that SCs-survival effect by TLN could be due to the Erk/Bad (Ser112) signal but not the PI3K/Akt/Bad (Ser136) signal.

Despite a marked improvement in the function and morphology of sciatic nerve with TLN intervention after STZ injection, administration of TLN did not completely halt the progression of sciatic nerve injury. This suggests that there may be other signaling pathways involved in pathogenesis of nerve damage. Furthermore, although the Nrg1/ErbB2 receptor dependent SCs-survival effect of TLN is explicit in this *in vivo* animal model, its biologic relevance *in vitro* remains unclear. It will be important to evaluate the therapeutic role of TLN in future *in vitro* studies.

5. Conclusion

In conclusion, the findings of the current study provide support to the hypothesis that compound recipe TLN could inhibit SC apoptosis, which lead to an improvement in sciatic MNCV, distal digital SNCV and sciatic nerve pathological injury, suggesting TLN offering a promising alternative medicine for the DPN patients to delay the progression. The mechanism of the protective effect of TLN on promoting SCs survival may be partly due to activate Nrg1/ErbB2 → Erk/bad signal pathway.

Conflict of Interests

The authors declare that they have no conflict of interests, financial or otherwise.

Acknowledgments

This work was supported by National Natural Science Foundation of China (NSFC) (no. 30873253). Thus, the authors thank NSFC for financial support. The authors also thank Shanghai Biotechnology Co., Ltd for providing technical assistance related to the study.

References

[1] S. Tesfaye and D. Selvarajah, "Advances in the epidemiology, pathogenesis and management of diabetic peripheral neuropathy," *Diabetes/Metabolism Research and Reviews*, vol. 28, supplement 1, pp. 8–14, 2012.

[2] A. J. Boulton, A. I. Vinik, J. C. Arezzo et al., "Diabetic neuropathies: a statement by the American Diabetes Association," *Diabetes Care*, vol. 28, no. 4, pp. 956–962, 2005.

[3] P. J. Oates, "Polyol pathway and diabetic peripheral neuropathy," *International Review of Neurobiology*, vol. 50, pp. 325–328, 2002.

[4] J. L. Wautier and P. J. Guillausseau, "Diabetes, advanced glycation endproducts and vascular disease," *Vascular Medicine*, vol. 3, no. 2, pp. 131–137, 1998.

[5] K. J. Way, N. Katai, and G. L. King, "Protein kinase C and the development of diabetic vascular complications," *Diabetic Medicine*, vol. 18, no. 12, pp. 945–959, 2001.

[6] T. Purves, A. Middlemas, S. Agthong et al., "A role for mitogen-activated protein kinases in the etiology of diabetic neuropathy," *The FASEB Journal*, vol. 15, no. 13, pp. 2508–2514, 2001.

[7] M. Brownlee, "The pathobiology of diabetic complications: a unifying mechanism," *Diabetes*, vol. 54, no. 6, pp. 1615–1625, 2005.

[8] A. M. Schmidt, S. D. Yan, J. L. Wautier, and D. Stern, "Activation of receptor for advanced glycation end products: a mechanism for chronic vascular dysfunction in diabetic vasculopathy and atherosclerosis," *Circulation Research*, vol. 84, no. 5, pp. 489–497, 1999.

[9] J. Yu, Y. Zhang, S. Sun et al., "Inhibitory effects of astragaloside IV on diabetic peripheral neuropathy in rat," *Canadian Journal of Physiology and Pharmacology*, vol. 84, no. 6, pp. 579–587, 2006.

[10] L. Q. Sun, B. Xue, X. J. Li et al., "Inhibitory effects of salvianolic acid B on apoptosis of Schwann cells and its mechanism induced by intermittent high glucose," *Life Sciences*, vol. 90, no. 3-4, pp. 99–108, 2012.

[11] L. Q. Sun, Y. Y. Chen, X. Wang et al., "The protective effect of alpha lipoic acid on Schwann cells exposed to constant or intermittent high glucose," *Biochemical Pharmacology*, vol. 84, no. 7, pp. 961–973, 2012.

[12] L. Eckersley, "Role of the Schwann cell in diabetic neuropathy," *International Review of Neurobiology*, vol. 50, pp. 293–321, 2002.

[13] L. Stenberg, M. Kanje, K. Dolezal, and L. B. Dahlin, "Expression of activating transcription factor 3 (ATF 3) and caspase 3 in Schwann cells and axonal outgrowth after sciatic nerve repair in diabetic BB rats," *Neuroscience Letters*, vol. 515, no. 1, pp. 34–38, 2012.

[14] A. Krishnan, "Neuregulin-1 type I: a hidden power within Schwann cells for triggering peripheral nerve remyelination," *Science Signaling*, vol. 6, no. 270, article jc1, 2013.

[15] D. S. Skundric and R. P. Lisak, "Role of neuropoietic cytokines in development and progression of diabetic polyneuropathy: from glucose metabolism to neurodegeneration," *Experimental Diabesity Research*, vol. 4, no. 4, pp. 303–312, 2003.

[16] Q. L. Wu and X. C. Liang, "Survey of current experimental studies of effects of traditional Chinese compound recipe on diabetic peripheral neuropathy," *Zhongguo Zhong Yao Za Zhi*, vol. 32, no. 9, pp. 775–778, 2007.

[17] Y. B. Gao, R. H. Liu, X. C. Yu et al., "Clinical observation on patients of diabetic peripheral nervous lesion," *Journal of Beijing University of TCM*, vol. 20, no. 4, pp. 50–53, 1997.

[18] H. Zhou, Y. B. Gao, T. H. Liu et al., "Clinical trial of tangluoning for treating diabetic peripheral neuropathy," *Journal of Beijing University of TCM*, vol. 25, no. 4, pp. 59–62, 2002.

[19] W. L. Li, H. C. Zheng, J. Bukuru, and N. de Kimpe, "Natural medicines used in the traditional Chinese medical system for therapy of diabetes mellitus," *Journal of Ethnopharmacology*, vol. 92, no. 1, pp. 1–21, 2004.

[20] Q. Qin, J. Niu, Z. Wang, W. Xu, Z. Qiao, and Y. Gu, "Astragalus membranaceus inhibits inflammation via phospho-P38 mitogen-activated protein kinase (MAPK) and nuclear factor (NF)-κB pathways in advanced glycation end product-stimulated macrophages," *International Journal of Molecular Sciences*, vol. 13, no. 7, pp. 8379–8387, 2012.

[21] J. Yu, Y. Zhang, S. Sun et al., "Inhibitory effects of astragaloside IV on diabetic peripheral neuropathy in rats," *Canadian Journal of Physiology and Pharmacology*, vol. 84, no. 6, pp. 579–587, 2006.

[22] Y. B. Gao, Z. Y. Zhu, D. W. Zou, B. M. Li, and J. S. Peng, "Effect of TangluoNing on cell apoptosis of dorsal root ganglion in diabetic rats," *Chinese Journal of Basic Medicine in Traditional Chinese Medicine*, vol. 18, no. 6, pp. 616–618, 2012.

[23] D. W. Zou, Z. Y. Zhu, and Y. B. Gao, "Effects of traditional Chinese medicine on oxidative stress and ultrastructure of diabetic rats' sciatic nerve," *China Journal of Traditional Chinese Medicine and Pharmacy*, vol. 27, no. 5, pp. 1253–1256, 2012.

[24] M. J. Stevens, I. Obrosova, X. Cao, C. van Huysen, and D. A. Greene, "Effects of DL-alpha-lipoic acid on peripheral nerve conduction, blood flow, energy metabolism, and oxidative stress in experimental diabetic neuropathy," *Diabetes*, vol. 49, no. 6, pp. 1006–1015, 2000.

[25] M. W. Pfaffl, "A new mathematical model for relative quantification in real-time RT-PCR," *Nucleic Acids Research*, vol. 29, no. 9, article e45, 2001.

[26] N. E. Cameron, M. A. Cotter, D. H. Horrobin, and H. J. Tritschler, "Effects of alpha-lipoic acid on neurovascular function in diabetic rats: interaction with essential fatty acids," *Diabetologia*, vol. 41, no. 4, pp. 390–399, 1998.

[27] S. S. Kamboj, R. K. Vasishta, and R. Sandhir, "N-acetylcysteine inhibits hyperglycemia-induced oxidative stress and apoptosis markers in diabetic neuropathy," *Journal of Neurochemistry*, vol. 112, no. 1, pp. 77–91, 2010.

[28] R. Stavniichuk, H. Shevalye, H. Hirooka, J. L. Nadler, and I. G. Obrosova, "Interplay of sorbitol pathway of glucose metabolism, 12/15-lipoxygenase, and mitogen-activated protein kinases in the pathogenesis of diabetic peripheral neuropathy," *Biochemical Pharmacology*, vol. 83, no. 7, pp. 932–940, 2012.

[29] S. Yagihashi, M. Kamijo, and K. Watanabe, "Reduced myelinated fiber size correlates with loss of axonal neurofilaments in peripheral nerve of chronically streptozotocin diabetic rats," *The American Journal of Pathology*, vol. 136, no. 6, pp. 1365–1373, 1990.

[30] M. Nagamatsu, K. K. Nickander, J. D. Schmelzer et al., "Lipoic acid improves nerve blood flow, reduces oxidative stress, and improves distal nerve conduction in experimental diabetic neuropathy," *Diabetes Care*, vol. 18, no. 8, pp. 1160–1167, 1995.

[31] Z. G. Xu, C. G. Wu, L. Wang, Y. N. Chen, and Y. Chen, "Effects of alpha lipoic acid on oxidative stress and apoptosis of sciatic nerve in diabetic rat," *Journal of Jiangsu University*, vol. 21, no. 1, pp. 15–17, 2011.

[32] E. Buck, A. Eyzaguirre, J. D. Haley, N. W. Gibson, P. Cagnoni, and K. K. Iwata, "Inactivation of Akt by the epidermal growth factor receptor inhibitor erlotinib is mediated by HER-3 in pancreatic and colorectal tumor cell lines and contributes to erlotinib sensitivity," *Molecular Cancer Therapeutics*, vol. 5, no. 8, pp. 2051–2059, 2006.

[33] C. Taha, Z. Liu, J. Jin, H. Al-Hasani, N. Sonenberg, and A. Klip, "Opposite translational control of GLUT1 and GLUT4 glucose transporter mRNAs in response insulin. Role of mammalian target of rapamycin, protein kinase B, and phosphatidylinositol 3-kinase in GLUT1 mRNA translation," *The Journal of Biological Chemistry*, vol. 274, no. 46, pp. 33085–33091, 1999.

[34] Y. Sun, J. Yuan, H. Liu et al., "Role of Gab1 in UV-induced c-Jun NH2-terminal kinase activation and cell apoptosis," *Molecular and Cellular Biology*, vol. 24, no. 4, pp. 1531–1539, 2004.

[35] Z. Ma, J. Wang, F. Song, and J. A. Loeb, "Critical period of axoglial signaling between neuregulin-1 and brain-derived neurotrophic factor required for early Schwann cell survival and differentiation," *Journal of Neuroscience*, vol. 31, no. 26, pp. 9630–9640, 2011.

[36] G. V. Michailov, M. W. Sereda, B. G. Brinkmann et al., "Axonal neuregulin-1 regulates myelin sheath thickness," *Science*, vol. 304, no. 5671, pp. 700–703, 2004.

[37] C. Taveggia, G. Zanazzi, A. Petrylak et al., "Neuregulin-1 type III determines the ensheathment fate of axons," *Neuron*, vol. 47, no. 5, pp. 681–694, 2005.

[38] S. Heermann, J. Schmücker, U. Hinz et al., "Neuregulin 1 type III/ErbB signaling is crucial for schwann cell colonization of sympathetic axons," *PLoS ONE*, vol. 6, no. 12, Article ID e28692, 2011.

[39] J. F. McGuire, S. Rouen, E. Siegfreid, D. E. Wright, and R. T. Dobrowsky, "Caveolin-1 and altered neuregulin signaling contribute to the pathophysiological progression of diabetic peripheral neuropathy," *Diabetes*, vol. 58, no. 11, pp. 2677–2686, 2009.

[40] S. Chen, M. O. Velardez, X. Warot et al., "Neuregulin 1-erbB signaling is necessary for normal myelination and sensory function," *Journal of Neuroscience*, vol. 26, no. 12, pp. 3079–3086, 2006.

[41] Y. Li, G. I. Tennekoon, M. Birnbaum, M. A. Marchionni, and J. L. Rutkowski, "Neuregulin signaling through a PI3K/Akt/Bad pathway in Schwann cell survival," *Molecular and Cellular Neuroscience*, vol. 17, no. 4, pp. 761–767, 2001.

[42] J. M. Newbern, X. Li, S. E. Shoemaker et al., "Specific functions for ERK/MAPK signaling during PNS development," *Neuron*, vol. 69, no. 1, pp. 91–105, 2011.

[43] J. Newbern and C. Birchmeier, "Nrg1/ErbB signaling networks in Schwann cell development and myelination," *Seminars in Cell and Developmental Biology*, vol. 21, no. 9, pp. 922–928, 2010.

[44] Z. Liu, H. Jiang, H. Li, H. Liu, X. Xu, and Z. Li, "The effects of neuregulin-1beta on neuronal phenotypes of primary cultured dorsal root ganglion neurons by activation of PI3K/Akt," *Neuroscience Letters*, vol. 511, no. 1, pp. 52–57, 2012.

Hindawi Publishing Corporation
Evidence-Based Complementary and Alternative Medicine
Volume 2013, Article ID 432097, 8 pages
http://dx.doi.org/10.1155/2013/432097

Research Article

Si Shen Wan Inhibits mRNA Expression of Apoptosis-Related Molecules in p38 MAPK Signal Pathway in Mice with Colitis

Hai-Mei Zhao,[1,2] Xiao-Ying Huang,[1] Feng Zhou,[2] Wen-Ting Tong,[1] Pan-Ting Wan,[1] Min-Fang Huang,[1] Qing Ye,[3] and Duan-Yong Liu[1,2]

[1] *Jiangxi University of Traditional Chinese Medicine, Nanchang, Jiangxi 330004, China*
[2] *Jiangxi University of Traditional Chinese Medicine, Science and Technology College, 666 Fusheng Road, Nanchang, Jiangxi 330025, China*
[3] *Jiangxi University of Traditional Chinese Medicine, School of Computer, 18 Yunwan Road, Nanchang, Jiangxi 330004, China*

Correspondence should be addressed to Qing Ye; 78466490@qq.com and Duan-Yong Liu; liuduanyong@163.com

Received 26 July 2013; Revised 28 August 2013; Accepted 28 August 2013

Academic Editor: William C. S. Cho

Si Shen Wan (SSW) is used to effectively treat ulcerative colitis (UC) as a formula of traditional Chinese medicine. To explore the mechanism of SSW-inhibited apoptosis of colonic epithelial cell, the study observed mRNA expression of apoptosis-related molecules in p38 MAPK signal pathway in colonic mucosa in colitis mice treated with SSW. Experimental colitis was induced by 2,4,6-trinitrobenzene sulfonic acid (TNBS) in mice; meanwhile, the mice were administrated daily either SSW (5 g/kg) or p38 MAPK inhibitor (2 mg/kg) or vehicle (physiological saline) for 10 days. While microscopical evaluation was observed, apoptosis rate of colonic epithelial cell and mRNA expression of apoptosis-related molecules were tested. Compared with colitis mice without treatment, SSW alleviated colonic mucosal injuries and decreased apoptosis rate of colonic epithelial cell, while the mRNA expressions of p38 MAPK, p53, caspase-3, c-jun, c-fos, Bax, and TNF-α were decreased in the colonic mucosa in colitis mice treated with SSW, and Bcl-2 mRNA and the ratio of Bcl-2/Bax were increased. The present study demonstrated that SSW inhibited mRNA expression of apoptosis-related molecules in p38 MAPK signal pathway to downregulate colonic epithelial cells apoptosis in colonic mucosa in mice with colitis.

1. Introduction

Ulcerative colitis (UC) is a chronic, inflammatory disease of colonic mucosa characterized by a relapsing-remitting course. Although the exact pathogenesis of UC is unclear, it is well known that excessive apoptosis with insufficient proliferation in crypt proliferative zones has been proposed as a mechanism for mucosal ulceration in UC [1]. Increased apoptosis of colonic epithelial cells in the acute inflammatory sites was a hallmark of ulcerative colitis [2]. Apoptosis of colonic epithelial cells was induced by using murine models with DSS- or TNBS-induced colitis in previous studies [3, 4]. Apoptosis of colonic epithelial cells can disrupt intestinal mucosal integrity and barrier function and lead to other changes associated with colitis. Therefore, inhibiting apoptosis of colonic epithelial cells will be one of the main attempts to treat UC [5].

Mitogen-activated protein kinases (MAPKs), a family of serine/threonine kinases, encompass the extracellular signal-regulated kinases, p38 MAPKs, and so on [6]. Many studies had provided evidence that p38 MAPK activation was responsible for apoptosis of colonic epithelial cells in ulcerative colitis [7]. The primary pathways to control apoptosis were correlative with the function of p38 MAPK (i.e., reinforcing expression of c-myc [8], phosphorylating p53 [9], participating Fas/Fas L signal [10], activating c-jun and c-fos [11], inducing transposition of Bax [12], augmenting production of TNF-α [13], and ect.)

Si Shen Wan (SSW) is a famous traditional Chinese herbal medicine formula, which was used to treat UC, allergic colitis, chronic colitis, and so on [14, 15]. The reported effective rate of SSW was above 90% when it was used to treat chronic colitis by oral administration or enema [16]. But the

Table 1: Characterization of the herbs included in Si Shen Wan.

Herbs	Percentage content (%)	Identified compounds	Effects	References
Evodia rutaecarpa (Juss.) Benth (Wu Zhu Yu)	6.67	Evodiamine rutaecarpine	Bacteriostasis, analgesia, antiemetic	[28]
Psoralea corylifolia L. (Bu Gu Zhi)	26.67	Psoralen isopsoralen	Anti-aging, antineoplastic	[29]
Fructus *Schisandra chinensis* (Turcz.) Baill. (Wu Wei Zi)	13.33	Schisandrin	Anti-free radical, boost immunity.	[30]
Myristica fragrans Houtt. (Rou Dou Kou)	13.33	Ursolic acid	Bacteriostasis, antineoplastic	[31]
Zingiber officinale Rosc. (Sheng Jiang)	26.67	Gingerol	Gastroprotective effects	[32]
Ziziphus Jujuba Mill. (Da Zao)	13.33	Polysaccharides	Antioxidative, antiglycative, antiapoptotic efects	[33]

mechanism of SSW is unclear. In our previous studies, we had demonstrated that SSW effectively alleviated colonic injury of rats with experimental colitis, regulated colonic epithelial cell cycle, and inhibited expression of Fas in colonic mucosa [17, 18]. However, the pathway is illdefined that SSW inhibited apoptosis to protect colonic epithelial cells in treatment of UC.

2. Materials and Methods

2.1. Animals. C57/BL mice (half males and half females) weighting 22–26 g (the animal certificate number was SCXK 2009-0004) were purchased from Sino-British Sippr/BK Laboratory Animal Co. Ltd. (Changsha, China). The animals were caged at 20 ± 1°C with a humidity of 50% ± 5% in a 12 h light/dark cycle. Standard diet and water were provided ad libitum throughout the experiments. The animals were acclimatized for 3 days before experiments and handled according to the Guidelines of the Jiang Xi University of Traditional Chinese Medicine Animal Research Committee. These mice were randomly assigned to 4 groups: the Normal group (mice were induced and administrated by physiological saline), the TNBS 10 d group (mice were induced by TNBS and administrated by physiological saline), the TNBS 10 d + SSW group (mice were induced by TNBS and treated with SSW), and the TNBS 10 d + SB203580 group (mice were induced by TNBS and treated with p38 MAPK inhibitor (SB203580)). Ten animals were in each group.

2.2. Drugs. SSW is a traditional Chinese herbal medicine formula, which is composed of *Evodia rutaecarpa* (Juss.) Benth (Wu Zhu Yu), *Psoraleacorylifolia* L. (Bu Gu Zhi), Fructus *Schisandra chinensis* (Turcz.) Baill. (Wu Wei Zi), *Myristica fragrans* Houtt. (Rou Dou Kou), *Zingiber officinale* Rosc. (Sheng Jiang), and *Ziziphus Jujuba* Mill. (Da Zao). All medicinal herbs were purchased from Huang Qing Ren Drugstore (Nanchang, China) and identified by professor Xiao-lan Chu of Jiangxi University of Traditional Chinese Medicine. The major identified effective phytochemical compound of each herb included in SSW is illustrated in Table 1. 2,4,6-trinitrobenzene sulfonic acid (TNBS) (batch number 2508-19-2) and p38 MAPK inhibitor (SB203580, batch number 152121-47-6) were from Sigma-Aldrich, St. Louis, MO, USA.

2.3. Trinitrobenzene Sulfonic Acid-Induced Colitis. According to the previous study [19], the experimental colitis was induced by TNBS in mice. Briefly, after 12 h absolute diet, the mice were lightly anesthetized with pentobarbital and administrated TNBS solution (100 mg·kg^{-1} body TNBS was dissolved in 0.15 mL of 30% ethanol) by enema. The freshly prepared solution was injected into the colon 4 cm proximal to the anus by a plastic hose tube (the diameter is 1.5 mm). The mice were maintained in a head-down position for 1 min.

2.4. Preparation of SSW Powder and Therapeutic Protocol. All medicinal herbs were extracted twice by refluxing with water (1 : 10, v/v) for 1 h per time. The water extract was filtered and evaporated by rotary evaporation below 60°C under reduced pressure. And then the residue was freeze-dried; the powder was taken (25.2% w/w of the crude drugs), stored at 4°C, and dissolved at the desired concentration with distilled water before use [20]. The quality control of SSW extract was reported in our previous article [20]. And SSW powder in the present study was the same batch as in our previous study.

The animals in the TNBS 10 d + SSW group received SSW extracts daily by gavage at a dose of 5 g/kg for 10 days, while the mice in the TNBS 10 d + SB203580 group were injected intraperitoneally with 2 mg/kg p38 MAPK inhibitor. And the animals in the Normal and TNBS 10 d group received the equivalent volume of physiological saline.

2.5. Microscopical Evaluation. On day 11, all animals were killed after anesthesia with intraperitoneally administrated urethane (2.0 g/kg). The colon of mouse was separated rapidly into two parts. One part was used to test apoptosis rate of colonic epithelial cell and to isolate total RNA. The other specimens were processed for paraffin sectioning and hematoxylin-eosin (HE) staining ($n = 8$). Histological injuries were evaluated according to the previously described scales [20, 21], taking into consideration both inflammatory

Table 2: Primer sequences for RT-PCR (mouse).

Gene	Primer sequences	Annealing temperature (°C)	Products (bp)
GAPDH	F: 5′GGAAAGCTGTGGCGTGAT3′ R: 5′AAGGTGGAAGAATGGGAGTT3′	59	308
caspase-3	F: 5′GCTGGACTGCGGTATTGAGA3′ R: 5′CCATGACCCGTCCCTTGA3′	59	142
p38MAPK	F: 5′GACGAATGGAAGAGCCTGAC3′ R: 5′AGATACATGGACAAACGGACA3′	59	260
TNF-α	F: 5′CTCAGCCTCTTCTCATTCCT3′ R: 5′ATTTGGGAACTTCTCCTCCT3′	59	101
Bcl-2	F: 5′TGGGATGCCTTTGTGGAAC3′ R: 5′CATATTTGTTTGGGGCAGGTC3′	59	167
Bax	F: 5′TGCTACAGGGTTTCATCCAG3′ R: 5′ATCCACATCAGCAATCATCC3′	59	175
c-fos	F: 5′TGCGTTGCAGACCGAGA3′ R: 5′GAAACAAGAAGTCATCAAAGGG3′	59	293
p53	F: 5′TGCTGAGTATCTGGACGACA3′ R: 5′CAGCGTGATGATGGTAAGG3′	59	166
c-jun	F: 5′GGCTGTTCATCTGTTTGTCTTCA3′ R: 5′TTCTTTACGGTCTCGGTGGC3′	59	300
c-myc	F: 5′GCTCAAAGCCTAACCTCACAA3′ R: 5′AAAGAAAGAAGATGGGAAGCA3′	59	117

cell infiltration and tissue damage. Scores for infiltration: 0, no infiltration; 1, increased number of inflammatory cells in the lamina propria; 2, inflammatory cells extending into the submucosa; 3, transmural inflammatory infiltrates; and for tissue damage: 0, no mucosal damage; 1, discrete epithelial lesions; 2, erosions or focal ulcerations; 3, severe mucosal damage with extensive ulceration extending into the bowel wall.

2.6. Apoptosis Rate of Colonic Epithelial Cell Was Analyzed by Flow Cytometry (FCM). The colonic tissue ($n = 8$) was clipped into fragments in icebath and filtrated to collect colonic epithelial cells. These cells were washed in cold phosphate-buffered saline (PBS), recentrifuged, and resuspended in annexin-binding buffer. The cell density was determined and diluted into 1×10^6 cells/mL. 5 μL Alexa Fluor 488 annexin V and 1 μL 100 μg/mL PI (propidium iodide) working solution was added to each 100 μL of cell suspension. After the incubation for 15 minutes at room temperature, the stained cells were analyzed by flow cytometry at 530 nm.

2.7. Real-Time-Polymerase Chain Reaction (PCR). Assessment of mRNA was performed by real-time-polymerase chain reaction according to the previous study [22]. Total RNA ($n = 5$) was isolated from fresh full-thickness colonic tissue by using Trizol reagent (Invitrogen Life Technologies Co. Ltd., USA) method as described earlier. Total RNA aliquots were reverse transcribed to assay for p38 MAPK, p53, c-myc, c-jun, c-fos, caspase-3, Bax, Bcl-2, and TNF-α. The thermal cycle involved a 3-minute hot start at 95°C, followed by 40 cycles at 95°C (15 seconds), 60°C (20 seconds), 72°C (20 seconds), and 82°C (20 seconds). Primers, annealing temperatures, and products length used for each gene are shown in Table 2. All resulting products were analyzed by agarose gel electrophoresis (visual absence of significant 28S and 18S band 3degradation) and quantified by spectrophotometry on a Bio-Rad Gel Doc 1000 (BioRad, Hercules, CA, USA). Results were standardized to GAPDH.

2.8. Statistical Analysis. All parameters were expressed as mean ± standard deviation (SD). For comparison of >2 conditions, a one-way analysis of variance (ANOVA) with Tukey post hoc test was used by SPSS 13.0 software (SPSS Inc., Chicago, IL, USA). Differences with $P < 0.05$ were considered significant.

3. Results

3.1. SSW Alleviates the Colonic Mucosal Injuries Induced by TNBS. These colonic mucosal injuries persisted till day 10, including epithelial necrosis, epithalaxy, impaired mucosa involving submucosa with hyperemia and edema, and ulcer accompanied with numerous inflammatory cell infiltrations (Figure 1(a), (a2)), but alleviated by treatment with SSW (Figure 1(a), (a3)). The colonic histological injury scores were higher (Figure 1(b)) in TNBS 10 d groups compared to Normal groups, all of which were ameliorated significantly by SSW treatment. These results revealed a significant improvement of histology in TNBS 10 d + SSW group compared with TNBS alone group.

3.2. SSW Decreases Apoptosis Rate of Colonic Epithelial Cell in Mice with Colitis. Excessive apoptosis of colonic epithelial cell is an important event in the pathogenesis of ulcerative

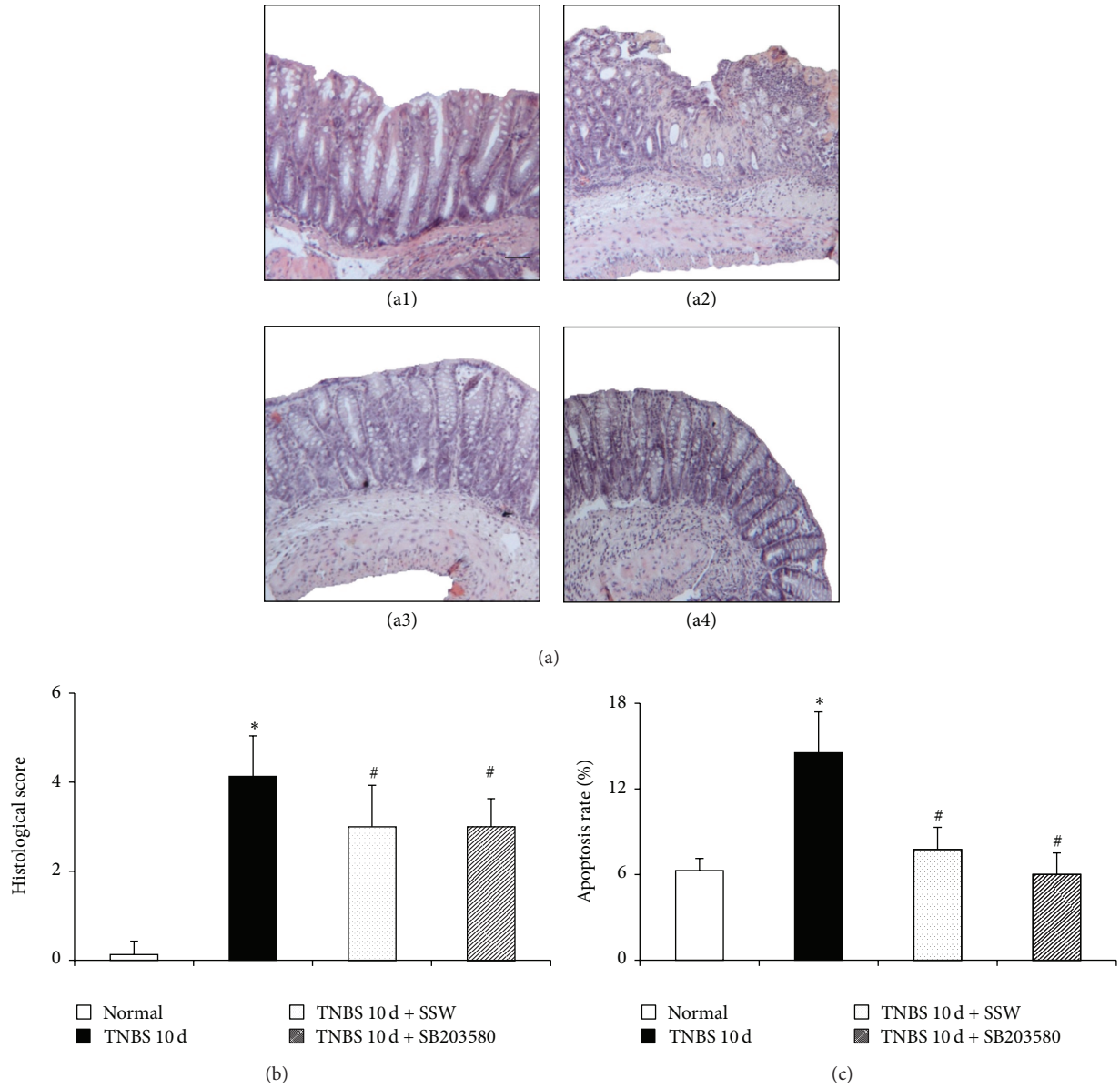

Figure 1: Representative histological images and scores and apoptosis rate of colonic epithelial cell. (a) Representative histological images stained by HE: (a1) Normal (mice were induced and administrated by physiological saline), (a2) TNBS 10 d (mice were induced by TNBS and administrated by physiological saline), (a3) TNBS 10 d + SSW (mice were induced by TNBS and treated by SSW), and (a4) TNBS 10 d + SB203580 (mice were induced by TNBS and treated with p38 MAPK inhibitor (SB203580)); Bar = 100 μm. (b) Histological scores. (c) Apoptosis rates. Data were mean ± SD ($n = 8$). $^{*}P < 0.05$ versus Normal group; $^{\#}P < 0.05$ versus TNBS 10 d group.

colitis. In the present study, compared with the Normal group, apoptosis rate of colonic epithelial cell in mice in the TNBS 10 d group was elevated significantly (Figure 1(c)) ($P < 0.05$). This enhancement was blunted significantly by SSW and SB203580 treatment (Figure 1(c)) ($P < 0.05$).

3.3. SSW Inhibits mRNA Expression of Apoptosis-Related Molecules in p38 MAPK Signal Pathway in Mice with Colitis. To investigate the mechanism of SSW in regulating apoptosis of colonic epithelium to protect colonic mucosa, the study principally observed mRNA expression of apoptosis-related molecules in p38 MAPK signal in colonic mucosa. As seen in Figures 2 and 3, compared with the Normal group, the expression of p38 MAPK (Figures 2(a) and 2(b)), p53 (Figures 2(a) and 2(b)), TNF-α (Figures 2(a) and 2(e)), caspase-3 (Figures 2(a) and 2(b)), c-jun (Figures 3(a) and 3(b)), c-fos (Figures 3(a) and 3(b)), and Bax mRNA (Figures 2(a) and 2(c)) was remarkably increased in the colonic mucosa in mice in the TNBS 10 d group ($P < 0.05$), while Bcl-2 mRNA expression (Figures 2(a) and 2(c)) and the ratio of Bcl-2/Bax (Figures 2(a) and 2(d)) were transparently decreased ($P < 0.05$). However, the expression of p38 MAPK (Figures 2(a) and 2(b)), p53 (Figures 2(a) and 2(b)), caspase-3 (Figures 2(a) and 2(b)), c-jun (Figures 3(a) and 3(b)), c-fos (Figures 3(a)

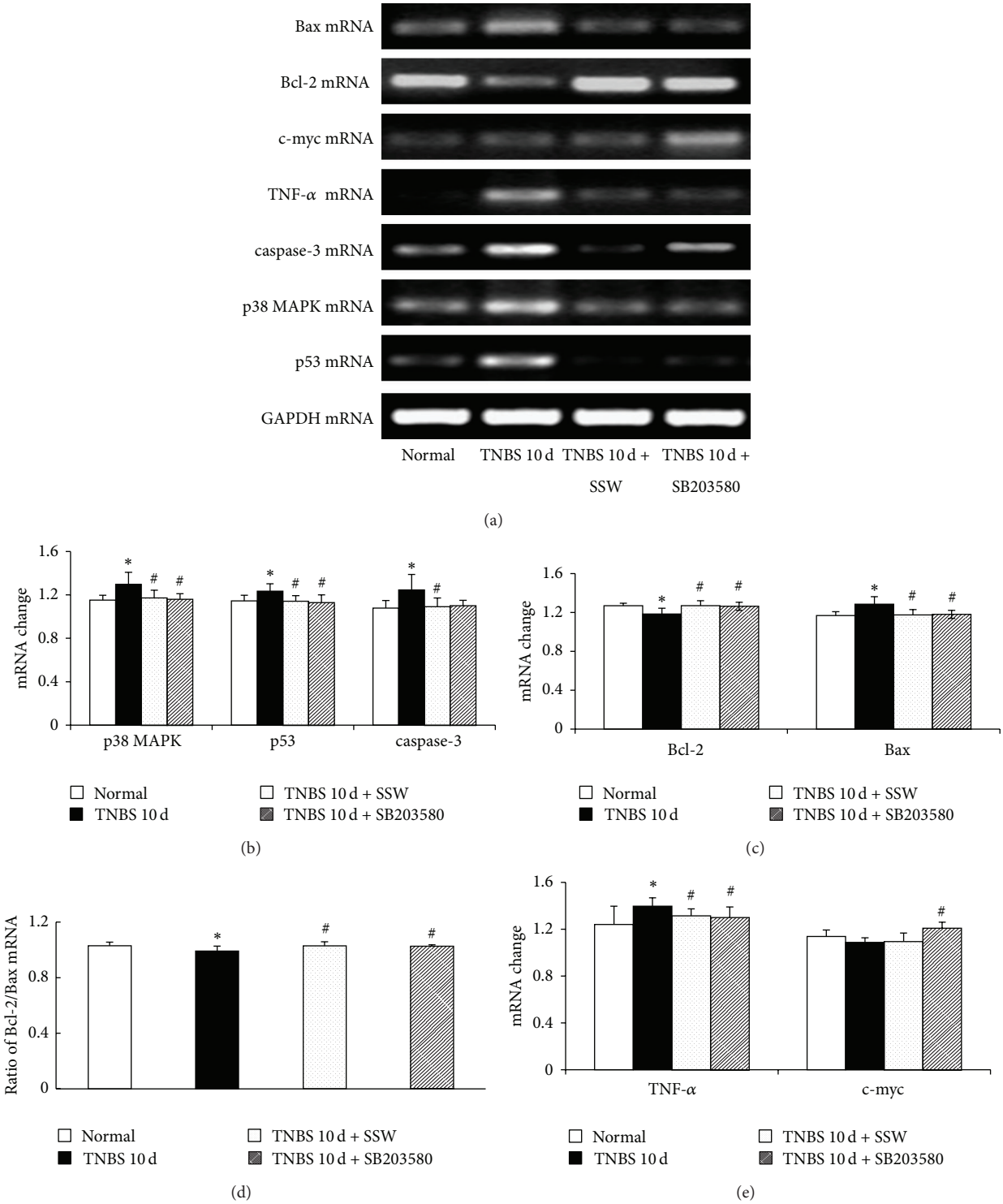

Figure 2: mRNA expression of p38 MAPK, p53, caspase-3, TNF-α, c-myc, Bcl-2, and Bax. (a) Representative electrophoretograms of p38 MAPK, p53, caspase-3, TNF-α, c-myc, Bcl-2, Bax, and GAPDH; (b) p38 MAPK, p53, and caspase-3 mRNA change; (c) Bcl-2 and Bax mRNA change; (d) ratio of Bcl-2/Bax mRNA change; (e) TNF-α and c-myc mRNA change. Data were mean ± SD ($n = 5$). $^{*}P < 0.05$ versus Normal group; $^{\#}P < 0.05$ versus TNBS 10 d group.

and 3(b)), Bax (Figures 2(a) and 2(c)), and TNF-α mRNA (Figures 2(a) and 2(c)) in the TNBS 10 d + SSW group was lower than in the TNBS 10 d group ($P < 0.05$), but Bcl-2 mRNA expression (Figures 2(a) and 2(c)) and the ratio of Bcl-2/Bax (Figures 2(a) and 2(d)) were upregulated ($P < 0.05$). All results had shown that overexpression of mainly apoptosis genes in p38 MAPK signal pathway existed in the pathogenesis of UC and was inhibited after treatment by SSW.

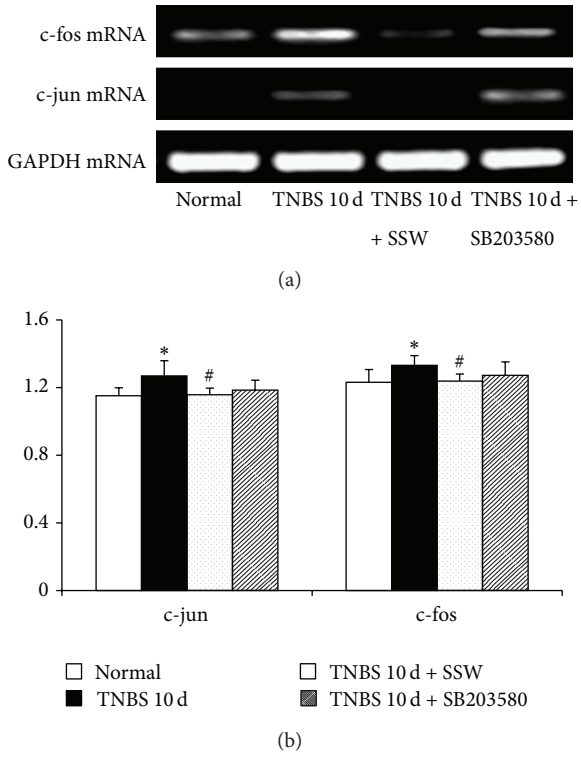

Figure 3: mRNA expression of c-jun and c-fos. (a) Representative electrophoretograms of c-jun, c-fos, and GAPDH. (b) c-jun and c-fos mRNA change. Data were mean ± SD ($n = 5$). $^{*}P < 0.05$ versus Normal group; $^{\#}P < 0.05$ versus TNBS 10 d group.

4. Discussion

The evidences of SSW therapeutic effects were reported in our previous study including decreased colon wet weight, colon organ coefficient, and colonic damage score; shorted colon length; improved pathological injury [20]. In the present study, TNBS administration successfully induced colonic mucosal injuries in mice, as evidenced by microscopic manifestations. Significantly, apoptosis rate of colonic epithelial cells was increased in the TNBS 10 d group and was inhibited by SSW treatment. It demonstrated that its therapeutic effects on TNBS-induced colonic mucosal injury were intimately related to inhibited apoptosis of colonic epithelial cells.

Increased apoptosis of colonic epithelial cells in crypt enterocytes plays an important role in the pathogenesis of UC [19]. The p38 MAPK signal pathway was closely related to apoptosis of colonic epithelial cells in UC colonic mucosa [7]. In the present study, p38 MAPK mRNA was overexpressed in colitis mice induced by TNBS, while the expression of p53, caspase-3, c-jun, c-fos, Bax, and TNF-α mRNA was increased in the colonic mucosa of mice from the model group. These molecules are wellknown and are important signals to induce/inhibit apoptosis in p38 MAPK signal pathway. On one hand, these facts have shown that the p38 MAPK signal pathway was activated and played a crucial role in the pathogenesis of colitis induced by TNBS, and on the other hand, the results were coincident with many documents [7, 23].

Others researchers had indicated their correlations with p38 MAPK and abovementioned factors. (1) p38-MAPK is necessary for Bax activation and apoptosis in vitro [12]. Bax seems to be necessary for induction of apoptosis, and Bcl-2 is a suppressor gene of apoptosis. Increased expression of Bcl-2 can combine with Bax to form more stable heterodimers to inhibit apoptosis, so the ratio of Bcl-2/Bax can regulate apoptosis [24]. (2) Expression of TNF-α and TNF-α receptor-mediated signaling is required for p38 activation [16]. (3) The p38 MAPK signaling cascades in the regulation of AKT-dependent cyclin D1 and c-myc internal ribosome entry site (IRES) activity, while as a downstream of p38 MAPK signaling, IRES mediated the synthesis of c-myc during apoptosis [8]. (4) As an important marker of apoptosis, caspases, Bcl-2, and p53 proteinase family related genes were activated after Fas and Fas L were integrated in the initial phase, while overexpression of caspases subsequently activated MAPKs signal pathway to phosphorylate p38 and c-jun and expressed transcription factor (p53 and Fas L) to induce apoptosis [25, 26].

In the present study, SSW had inhibited the expression of p38 MAPK mRNA in colonic mucosa in colitis mice. The results had hinted that activation of p38 MAPK signal was restrained by SSW. Furthermore, SSW had refrained expression of p53, caspase-3, c-jun, c-fos, Bax, and TNF-α mRNA and improved the level of Bcl-2 mRNA and the ratio of Bcl-2/Bax in colitis mice treated with SSW. Our previous studies had proved that SSW inhibited the expression of Fas to decrease apoptosis of colonic epithelial cells in colitis mice treated with SSW [17, 18]. And in our previous study, SSW increased the expression of IL-4 and IL-10 mRNA which inhibit the production of proinflammatory factor (TNF-α, IL-1) as anti-inflammatory cytokine [20]. In addition, the c-myc can keep dynamic equilibrium between cell proliferation and apoptosis [27]. The activated c-myc improves growth vigor of cell to restore injury and induce cell apoptosis [27]. The phenomenon is coincident with the pathogenesis of UC which is excessive in inflammatory cell proliferation and epithelial cell apoptosis [1, 2]. While p38 MAPK inhibitor (SB203580) increased expression of c-myc mRNA in some situation as activated PTEN [8]. However, it is not an emphasis in the present study, but is worth studying that the recovery effect of p38 MAPK inhibitor is or not related with over-expression of c-myc mRNA. In conclusion, SSW effectively inhibited mRNA expression of apoptosis-related molecules in p38 MAPK signal pathway to downregulate colonic epithelial cells apoptosis in colonic mucosa in mice with colitis.

Conflict of Interests

The authors have declared that there is no conflict of interests.

Acknowledgments

This work was supported by the Science and Technology project from the Department of Education of Jiangxi Province

(no. GJJ09285, GJJ13611) and by the Science and Technology Project of TCM from the Department of Health of Jiangxi Province (no. 2012A020).

References

[1] K. Croitoru and P. Zhou, "T-cell-induced mucosal damage in the intestine," *Current Opinion in Gastroenterology*, vol. 20, no. 6, pp. 581–586, 2004.

[2] R. Dirisina, R. B. Katzman, T. Goretsky et al., "P53 and PUMA independently regulate apoptosis of intestinal epithelial cells in patients and mice with colitis," *Gastroenterology*, vol. 141, no. 3, pp. 1036–1045, 2011.

[3] L. Eckmann, T. Nebelsiek, A. A. Fingerle et al., "Opposing functions of IKKβ during acute and chronic intestinal inflammation," *Proceedings of the National Academy of Sciences of the United States of America*, vol. 105, no. 39, pp. 15058–15063, 2008.

[4] M. R. Frey, K. L. Edelblum, M. T. Mullane, D. Liang, and D. B. Polk, "The ErbB4 growth factor receptor is required for colon epithelial cell survival in the presence of TNF," *Gastroenterology*, vol. 136, no. 1, pp. 217–226, 2009.

[5] X. Han, X. Ren, I. Jurickova et al., "Regulation of intestinal barrier function by signal transducer and activator of transcription 5b," *Gut*, vol. 58, no. 1, pp. 49–58, 2009.

[6] L. Chang and M. Karin, "Mammalian MAP kinase signalling cascades," *Nature*, vol. 410, no. 6824, pp. 37–40, 2001.

[7] X. Zhao, B. Kang, C. Lu et al., "Evaluation of P38 MAPK pathway as a molecular signature in ulcerative colitis," *Journal of Proteome Research*, vol. 10, no. 5, pp. 2216–2225, 2011.

[8] Y. Shi, A. Sharma, H. Wu, A. Lichtenstein, and J. Gera, "Cyclin D1 and c-myc internal ribosome entry site (IRES)-dependent translation is regulated by AKT activity and enhanced by rapamycin through a p38 MAPK- and ERK-dependent pathway," *Journal of Biological Chemistry*, vol. 280, no. 12, pp. 10964–10973, 2005.

[9] F. Lin, J. Hsu, C. Chou, W. Wu, C. Chang, and H. Liu, "Activation of p38 MAPK by damnacanthal mediates apoptosis in SKHep 1 cells through the DR5/TRAIL and TNFR1/TNF-α and p53 pathways," *European Journal of Pharmacology*, vol. 650, no. 1, pp. 120–129, 2011.

[10] J. K. Pru, I. R. Hendry, J. S. Davis, and B. R. Rueda, "Soluble Fas ligand activates the sphingomyelin pathway and induces apoptosis in luteal steroidogenic cells independently of stress-activated p38MAPK," *Endocrinology*, vol. 143, no. 11, pp. 4350–4357, 2002.

[11] T. Peng, T. Zhang, X. Lu, and Q. Feng, "JNK1/c-fos inhibits cardiomyocyte TNF-α expression via a negative crosstalk with ERK and p38 MAPK in endotoxaemia," *Cardiovascular Research*, vol. 81, no. 4, pp. 733–741, 2009.

[12] D. Wakeman, J. Guo, J. A. Santos et al., "P38 MAPK regulates Bax activity and apoptosis in enterocytes at baseline and after intestinal resection," *American Journal of Physiology*, vol. 302, no. 9, pp. G997–G1005, 2012.

[13] S. Chen, B. Jin, and Y. Li, "TNF-α regulates myogenesis and muscle regeneration by activating p38 MAPK," *American Journal of Physiology*, vol. 292, no. 5, pp. C1660–C1671, 2007.

[14] F. Wang, L. Yu, and Y. R. Li, "Effect of Si Shen Wan treated 45 UC patients," *Journal of Practical Traditional Chinese Internal Medicine*, vol. 22, no. 7, p. 35, 2008.

[15] S. Xie and J. J. Li, "Effect of four miraculous herbs decoction ultrafine particle in retention enema on 58 cases of ulcerative colitis with Yang deficiency of spleen and kidney," *Chinese Medicine Modern Distance Education of China*, vol. 8, no. 15, pp. 17–19, 2010.

[16] C. Hua, "Sishen Wan treated 87 patients with spleen-kidney yang vacuity of chronic colitis," *Fujian Journal of TCM*, vol. 9, no. 3, pp. 38–39, 2011.

[17] D. Y. Liu, Y. M. Guan, H. M. Zhao et al., "Therapeutic effect of Sishen Wan on lipid peroxidization injury in rats with experimental colitis treated by different ways of administration," *CJTCMP*, vol. 26, no. 5, pp. 1168–1171, 2011.

[18] H. M. Zhao, D. Y. Liu, F. Tang, and Z. Q. Zuo, "Protective effect of Sishen Wan to injury colonic mucosa from mouse with experimental colitis," *Chinese Traditional Patent Medicine*, vol. 31, no. 12, pp. 1935–1937, 2009.

[19] J. P. Segain, D. R. De la Blétière, V. Sauzeau et al., "Rho kinase blockade prevents inflammation via nuclear factor κB inhibition: evidence in Crohn's disease and experimental colitis," *Gastroenterology*, vol. 124, no. 5, pp. 1180–1187, 2003.

[20] D. Y. Liu, Y. M. Guan, H. M. Zhao et al., "The protective and healing effects of Si Shen Wan in trinitrobenzene sulphonic acid-induced colitis," *Journal of Ethnopharmacology*, vol. 143, no. 2, pp. 435–440, 2012.

[21] N. Schmidt, E. Gonzalez, A. Visekruna et al., "Targeting the proteasome: partial inhibition of the proteasome by bortezomib or deletion of the immunosubunit LMP7 attenuates experimental colitis," *Gut*, vol. 59, no. 7, pp. 896–906, 2010.

[22] S. A. Bustin, "Absolute quantification of mrna using real-time reverse transcription polymerase chain reaction assays," *Journal of Molecular Endocrinology*, vol. 25, no. 2, pp. 169–193, 2000.

[23] T. Yoshida, T. Sekine, K. Aisaki, T. Mikami, J. Kanno, and I. Okayasu, "CITED2 is activated in ulcerative colitis and induces p53-dependent apoptosis in response to butyric acid," *Journal of Gastroenterology*, vol. 46, no. 3, pp. 339–349, 2011.

[24] I. K. Bukholm and J. M. Nesland, "Protein expression of p53, p21 (WAF1/CIP1), bcl-2, Bax, cyclin D1 and pRb in human colon carcinomas," *Virchows Archiv*, vol. 436, no. 3, pp. 224–228, 2000.

[25] M. A. Moosavi, R. Yazdanparast, and A. Lotfi, "ERK1/2 inactivation and p38 MAPK-dependent caspase activation during guanosine 5′-triphosphate-mediated terminal erythroid differentiation of K562 cells," *International Journal of Biochemistry and Cell Biology*, vol. 39, no. 9, pp. 1685–1697, 2007.

[26] N. Matsumoto, R. Imamura, and T. Suda, "Caspase-8- and JNK-dependent AP-1 activation is required for Fas ligand-induced IL-8 production," *FEBS Journal*, vol. 274, no. 9, pp. 2376–2384, 2007.

[27] A. Gregorieff and H. Clevers, "Wnt signaling in the intestinal epithelium: from endoderm to cancer," *Genes and Development*, vol. 19, no. 8, pp. 877–890, 2005.

[28] J. Du, X. F. Wang, Q. M. Zhou et al., "Evodiamine induces apoptosis and inhibits metastasis in MDA MB-231 human breast cancer cells *in vitro* and *in vivo*," *Oncology Reports*, vol. 30, no. 2, pp. 685–694, 2013.

[29] G. Marzaro, A. Guiotto, M. Borgatti et al., "Psoralen derivatives as inhibitors of NF-κB/DNA interaction: synthesis, molecular modeling, 3D-QSAR, and biological evaluation," *Journal of Medicinal Chemistry*, vol. 56, no. 5, pp. 1830–1842, 2013.

[30] R. Checker, R. S. Patwardhan, D. Sharma et al., "Schisandrin B exhibits anti-inflammatory activity through modulation of the redox-sensitive transcription factors Nrf2 and NF-κB," *Free Radical Biology & Medicine*, vol. 53, no. 7, pp. 1421–1430, 2012.

[31] J. Wang, L. Liu, H. Qiu et al., "Ursolic Acid simultaneously targets multiple signaling pathways to suppress proliferation and induce apoptosis in colon cancer cells," *PLoS One*, vol. 8, no. 5, Article ID e63872, 2013.

[32] X. H. Li, K. C. McGrath, V. H. Tran et al., "Attenuation of proinflammatory responses by S-[6]-gingerol via inhibition of ROS/NF-Kappa B/COX2 activation in HuH7 cells," *Evidence-Based Complementary and Alternative Medicine*, vol. 2013, Article ID 146142, 8 pages, 2013.

[33] W. Zhong, N. Liu, Y. Xie, Y. Zhao, X. Song, and W. Zhong, "Antioxidant and anti-aging activities of mycelial polysaccharides from Lepista sordida," *International Journal of Biological Macromolecules C*, vol. 25, no. 60, pp. 355–359, 2013.

Hindawi Publishing Corporation
Evidence-Based Complementary and Alternative Medicine
Volume 2013, Article ID 346438, 9 pages
http://dx.doi.org/10.1155/2013/346438

Research Article

Ampelopsis Radix Protects Dopaminergic Neurons against 1-Methyl-4-phenylpyridinium/1-methyl-4-phenyl-1,2,3,6-tetrahydropyridine-Induced Toxicity in Parkinson's Disease Models *In Vitro* and *In Vivo*

Hanbyeol Park,[1] Jin Sup Shim,[2] Hyo Geun Kim,[2] Hyejung Lee,[3] and Myung Sook Oh[1,2]

[1] *Department of Life and Nanopharmaceutical Science, Kyung Hee University, No. 1 Hoegi-dong, Dongdaemun-gu, Seoul 130-701, Republic of Korea*
[2] *Department of Oriental Pharmaceutical Science, College of Pharmacy and Kyung Hee East-West Pharmaceutical Research Institute, Kyung Hee University, No. 1 Hoegi-dong, Dongdaemun-gu, Seoul 130-701, Republic of Korea*
[3] *Studies of Translational Acupuncture Research (STAR), Acupuncture & Meridian Science Research Center (AMSRC), Kyung Hee University, No. 1 Hoegi-dong, Dongdaemun-gu, Seoul 130-701, Republic of Korea*

Correspondence should be addressed to Myung Sook Oh; msohok@khu.ac.kr

Received 29 May 2013; Revised 2 August 2013; Accepted 20 August 2013

Academic Editor: William C. S. Cho

Ampelopsis Radix, the root of *Ampelopsis japonica* (Thunb.) Makino (Vitaceae), is a herbal medicine which has been widely used in East Asia. The present study was done to explore whether the standardized extract of Ampelopsis Radix (AJW) protects dopaminergic neurons via antioxidant mechanisms in Parkinson's disease (PD) models. The effects of AJW on primary mesencephalic cultures stressed with 1-methyl-4-phenylpyridinium were investigated using tyrosine hydroxylase (TH) immunohistochemistry and reactive oxygen species measurement. The eliminative effects of AJW on the 2,2-diphenyl-1-picrylhydrazyl and 2,2′-azino-bis-(3-ethylbenzthiazoline-6-sulphonic acid) radicals were explored using colorimetric methods. The effects of AJW on the mice treated with 1-methyl-4-phenyl-1,2,3,6-tetrahydropyridine (MPTP) were determined by pole test as well as TH and 8-hydroxydeoxyguanosine immunohistochemistry. AJW protected dopaminergic neurons by inhibiting reactive oxygen species generation *in vitro*. Moreover, AJW showed potent radical scavenging activities *in vitro*. In the mouse PD model, AJW protected the dopaminergic neurons in the brain, leading to motor improvements. AJW inhibited the MPTP-evoked accumulation of 8-hydroxydeoxyguanosine in the brain. These data suggest that AJW has neuroprotective effects with antioxidant mechanisms in PD models.

1. Introduction

Oxidative stress occurs as a result of imbalance of the free radical generation and antioxidant defense system [1]. Even under natural physiological states, however, the oxygen consumption by aerobes, which is necessary for their immediate survival, leads to the potentially detrimental reactive oxygen metabolites generation [2]. The brain is deemed to be vulnerable to oxidative damage because of its high metabolic rate and relatively low cellular regeneration ability compared with other organs [3]. In addition, dopaminergic neurons in the substantia nigra pars compacta (SNc) are thought to be more prone to oxidative stress because the self-metabolism of dopamine generates reactive oxygen species (ROS), including various peroxides and radicals [4]. Therefore, oxidative stress might contribute to the pathogenesis of Parkinson's disease (PD), a common degenerative brain disease, which is featured by selective dopaminergic neurodegeneration from the SNc to the striatum and by clinical symptoms of bradykinesia, resting tremor, and rigidity [5]. Supporting this oxidative stress hypothesis, considerable levels of oxidative damaged macromolecules such as proteins, lipids, and DNA have been reported in PD brains [6].

As a very common neurotoxin for PD models, 1-methyl-4-phenyl-1,2,3,6-tetrahydropyridine (MPTP) causes clinical and chemical alterations in humans and rodents similar to those that occur in PD [7, 8]. After administration, MPTP rapidly passes through the brain and is converted into its active form, 1-methyl-4-phenylpyridinium (MPP^+), by an oxidizing enzyme in astrocytes [9]. MPP^+ is transferred to dopaminergic neurons through the dopamine transporter, where it inhibits the respiratory chain by disrupting mitochondrial complex I, and leads to oxidative stress via mitochondria-dependent or -independent pathways [10]. The oxidative stress generated by MPP^+ subsequently results in the peroxidation of macromolecules, ultimately resulting in cell death [10].

Ampelopsis Radix, the root of *Ampelopsis japonica* (Thunb.) Makino, belongs to the grape family (Vitaceae) and has been widely used as a traditional medicine to treat pain and fever in East Asia [11]. It contains well-known bioactive components, including resveratrol, schizandriside, catechins, and other polyphenol compounds [11, 12]. Researches on (+)-catechin and (−)-epicatechin demonstrated that they have the strong free radical eliminating activities and protective effects against 6-hydroxydopamine (6-OHDA) neurotoxicities [13, 14]. (+)-Catechin further exerted neuroprotective effects via antioxidant mechanisms against 6-OHDA- or MPP^+-induced toxicities in various cellular systems [15]. In addition, resveratrol protects neurons in an injured-spinal-cord rat model with its antioxidant properties, which increase superoxide dismutase activity and decrease malondialdehyde levels [16]. Nevertheless, few studies have examined the pharmacological properties of Ampelopsis Radix, and particularly the possible protective effects in PD models have not been demonstrated. Therefore, we explored the effects of an aqueous extract of Ampelopsis Radix on mesencephalic dopaminergic cells stressed with MPP^+ and C57BL/6 mice stressed with MPTP. We also examined the possible antioxidant mechanisms of this protection.

2. Materials and Methods

2.1. Materials. Minimal essential medium was purchased from Gibco (Carlsbad, CA, USA). Fetal bovine serum (FBS) was purchased from Hyclone Lab Inc. (Logan, UT, USA). (+)-Catechin, (−)-epicatechin, 2,2-diphenyl-1-picrylhydrazyl (DPPH), 2,2′-azino-bis-(3-ethylbenzthiazoline-6-sulphonic acid) (ABTS), potassium persulfate, poly-L-lysine (PLL), glucose, glutamine, MPTP, MPP^+, 2,7-dichlorodihydrofluorescein diacetate (H_2DCF-DA), phosphate-buffered saline (PBS), paraformaldehyde (PFA), 3,3-diaminobenzidine (DAB), sucrose, and bovine serum albumin (BSA) were purchased from Sigma-Aldrich (St. Louis, MO, USA). Rabbit anti-tyrosine hydroxylase (TH) antibody was purchased from Chemicon International Inc. (Temecula, CA, USA). Mouse anti-8-hydroxydeoxyguanosine (8-OHdG) antibody was purchased from JaICA (Shizuoka, Japan). Biotinylated anti-rabbit and anti-mouse antibodies, normal goat serum, and avidin-biotin-peroxidase complex (ABC) standard kit were purchased from Vector Lab (Burlingame, CA, USA). Zoletil was purchased from Virbac (Carros, France).

2.2. Preparation of Extract and Standardization. A dried root of *A. japonica* was obtained from Jung Do Hrbal Drug Co. (Seoul, Republic of Korea). The voucher specimen (KHUOPS-MH023) was deposited in the herbarium of the College of Pharmacy, Kyung Hee University (Seoul, Republic of Korea). It was extracted with distilled water at 100°C for 2 h. The powder (AJW) was made from the extracts by filtering and lyophilization. The yield of AJW was 16.10% and it was kept at 4°C. AJW was standardized with (+)-catechin and (−)-epicatechin known as constituents in *A. japonica* [11], using reverse-phase high-performance liquid chromatography system consisting of a Waters (Miliford, MA, USA) model 515 pump, a 717 autosampler, and a 996 photodiode array detector. Separation was conducted using Atlantis C18 column (150 × 4.6 mm, 3 μm; Waters, Miliford, MA, USA) at 25°C. Mobile phases included aqueous solution of 0.2% acetonitrile (eluent M1) and methanol (eluent M2). The gradient elution was carried in the way that the eluent M2 was linearly increased from 0 to 50% for 0 to 24 min and from 50 to 100% for 24 to 40 min at a flow rate of 1.2 mL/min. The injection volume was 10 μL, and the detector wavelength was set at 280 nm. AJW and reference to the calibration curve obtained with (+)-catechin and (−)-epicatechin were analyzed in triplicates. (+)-Catechin and (−)-epicatechin were found in AJW at a mean level of 1.81 ± 0.16 mg/g and 1.40 ± 0.04 mg/g, respectively.

2.3. Primary Cultures of Rat Mesencephalic Cells. Mesencephalic cell cultures were derived from 14-day embryos of Sprague-Dawley rat (Daehan Biolink Co., Eumseong, Republic of Korea). Mesencephalons were dissected, collected, dissociated, and seeded in PLL precoated 24-well plates at a density of 1.0×10^5 cells/well. Cultures were maintained in a humidified incubator of 5% CO_2 at 37°C in minimal essential medium with 6 g/L glucose, 2 mM glutamine, and 10% FBS. On the 6th day *in vitro*, cells were treated with AJW for 1 h and stressed with 12 μM MPP^+ for a further 23 h. An equal volume of vehicles was given to the control and toxin groups. Then, cells were fixed with 4% PFA at room temperature for 30 min. The cells were stored in PBS at 4°C for immunohistochemistry.

2.4. Determination of Intracellular ROS Level. Intracellular ROS was measured using a fluorescent probe, H_2DCF-DA. Intracellular H_2O_2 or low-molecular weight peroxides oxidize H_2DCF-DA to the highly fluorescent compound dichlorofluorescein (DCF). Cells were seeded in PLL precoated 24-well plates at a density of 1.0×10^5 cells/well, and on the 6th day *in vitro*, cells were treated with AJW for 1 h and stressed with 12 μM MPP^+ for a further 23 h. An equal volume of vehicles was given to the control and toxin groups. Cells were incubated with 20 μM H_2DCF-DA at 37°C for 30 min, the cells on cover slips were mounted on gelatin-coated glass slides; they were photographed with a fluorescence microscope (BX51T-32F01; Olympus Co., Tokyo, Japan). The fluorescence intensity of DCF was measured by a fluorescence microscope, and was expressed as a percentage of the value in the vehicle-treated control group.

2.5. Measurement of DPPH Radical Scavenging Activity. AJW at various concentrations of 1–1000 μg/mL was mixed with 0.2 mM DPPH ethanol solution (1 : 1). After incubation at room temperature in the dark for 30 min; the absorbance of the mixture was determined at 517 nm using spectrophotometer (VersaMax microplate reader; Molecular Device, Sunnyvale, CA, USA). Also, the activity of AJW was expressed as half maximal inhibiting concentration (IC_{50}) which is defined as the concentration of AJW required to scavenge 50% of DPPH radicals. IC_{50} values were estimated by a nonlinear regression using the GraphPad Prism software (GraphPad Software Inc., San Diego, CA, USA).

2.6. Measurement of ABTS Radical Cation Scavenging Activity. ABTS solution of 7.4 mM was added to 2.6 mM potassium persulfate for 1 day before starting the experiment in the dark. AJW at various concentrations of 1–1000 μg/mL was mixed with 7.4 mM ABTS solution with 2.6 mM potassium persulfate. After incubation at room temperature for 5 min, the absorbance of the mixture was determined at 732 nm using spectrophotometer. Also, the activity of AJW was expressed as IC_{50} which is defined as the concentration of AJW required to scavenge 50% of ABTS radical cations. IC_{50} values were estimated by a nonlinear regression using the GraphPad Prism software.

2.7. Animals and Treatment. Animal maintenance and treatment were carried out in accordance with the Principles of Laboratory Animal Care (NIH publication number 85-23, revised 1985) and the Animal Care and Use guidelines of Kyung Hee University, Seoul, Republic of Korea. Male C57BL/6 mice (8 weeks old) were purchased from Daehan Biolink. Animals were assigned to four groups: (1) Group 1 (vehicle-treated group), (2) Group 2 (MPTP-only treated group), (3) Group 3 (MPTP + AJW 10 mg/kg/day treated group), and (4) Group 4 (MPTP + AJW 100 mg/kg/day treated group). The mice were housed at an ambient temperature of 23 ± 1°C and a relative humidity of 60 ± 10% under a 12-h light/dark cycle and were allowed free access to water and food. AJW dissolved in saline was administered orally at 10 or 100 mg/kg/day for 7 days. MPTP (MPTP base form; 20 mg/kg) in saline was injected intraperitoneally four times at 2 h intervals on the last day of AJW treatment.

2.8. Behavioral Test and Brain Tissue Preparation. We performed the pole test, on the seventh day after the last MPTP injection. The mice were placed head upward near the top of a vertical rough-surfaced pole (diameter 8 mm, height 55 cm). The time taken for the mice to turn completely downward (time to turn, T-turn) and the time taken to reach the floor (locomotion activity time, T-LA) were recorded, with a cut-off limit of 30 sec. After the pole test, the mice were anesthetized with 50 mg/kg Zoletil (intramuscularly) and were rapidly perfused transcardially with PBS, followed by 4% PFA in 0.1 M phosphate buffer (PB). Then, brains were rapidly taken out, postfixed in 4% PFA, and processed for cryoprotection in 30% sucrose at 4°C. Frozen brains were cut into 30 μm coronal sections using a cryostat microtome (CM3000; Leica, Wetzlar, Germany). Then, the tissues were stored in storing solution containing glycerin, ethylene glycol, and PB at 4°C for immunohistochemistry.

2.9. Immunohistochemistry. Fixed mesencephalic cells on cover slips and free-floating brain sections were rinsed in PBS at room temperature before immunostaining. They were pretreated with 1% H_2O_2 in PBS for 15 min. For dopaminergic neuron detection, they were incubated with a rabbit anti-TH antibody (1 : 2000 dilution) overnight at 4°C. For detection of oxidative DNA damage, the treated brain sections were heated in citric acid (0.1 M, 90°C) for 5 min for antigen retrieval, incubated in blocking solution (10% goat serum + 1% BSA in PBS) for 1 h, and incubated with mouse anti-8-OHdG antibody (1 : 50 dilution in blocking solution) overnight at 4°C. They were then incubated with a biotinylated anti-mouse and anti-rabbit IgG, respectively, for 1 h followed by incubation in ABC solution for 1 h at room temperature. The activity was visualized with DAB for 3 min. After every incubation step, the cells and tissues were washed three times with PBS. Finally, the mesencephalic cells on cover slips were mounted on gelatin-coated glass slides and air-dried. The free-floating brain tissues were mounted on gelatin-coated slides, dehydrated, cleared with xylene, and cover-slipped using histomount medium. All of them were photographed with an optical light microscope (BX51T-32F01; Olympus Co.). For quantification of the effect of AJW in the mesencephalic dopaminergic cells, TH-positive cells were counted on at least four cover slips from independent experiments for each condition. Quantification of the effect of AJW in brain tissues was performed by counting the TH-positive cell numbers and the 8-OHdG-positive cell numbers in the SNc at ×100 magnification under a microscope and by measuring the optical density of TH-positive fibers in the striatum at ×40 magnification using an ImageJ software (Bethesda, MD, USA). Data were expressed as a percentage of the value in the vehicle-treated control group.

2.10. Statistical Analysis. The data were expressed as mean ± standard error of the mean (SEM). Statistical significance was determined by one-way analysis of variance, followed by Tukey's multiple comparison test, using GraphPad Prism software. In all analyses, $P < 0.05$ was deemed to indicate statistical significance.

3. Results

3.1. Protective Effects of AJW against MPP^+-Induced Toxicity in Primary Dopaminergic Neurons. To evaluate the protective effects of AJW against MPP^+ toxicity in primary dopaminergic neurons, we counted TH-positive cell numbers. Exposure to 12 μM MPP^+ exhibited remarkably reduced numbers of TH-positive cells as 42.50±2.45% relative to the control group and the treated cells had shrunken bodies and shortened neurites. Treatment of AJW at 1 μg/mL protected dopaminergic cells, showing increased survival rate by 61.96±3.70% relative to the control group and better neuronal morphology of TH-positive cells (Figure 1).

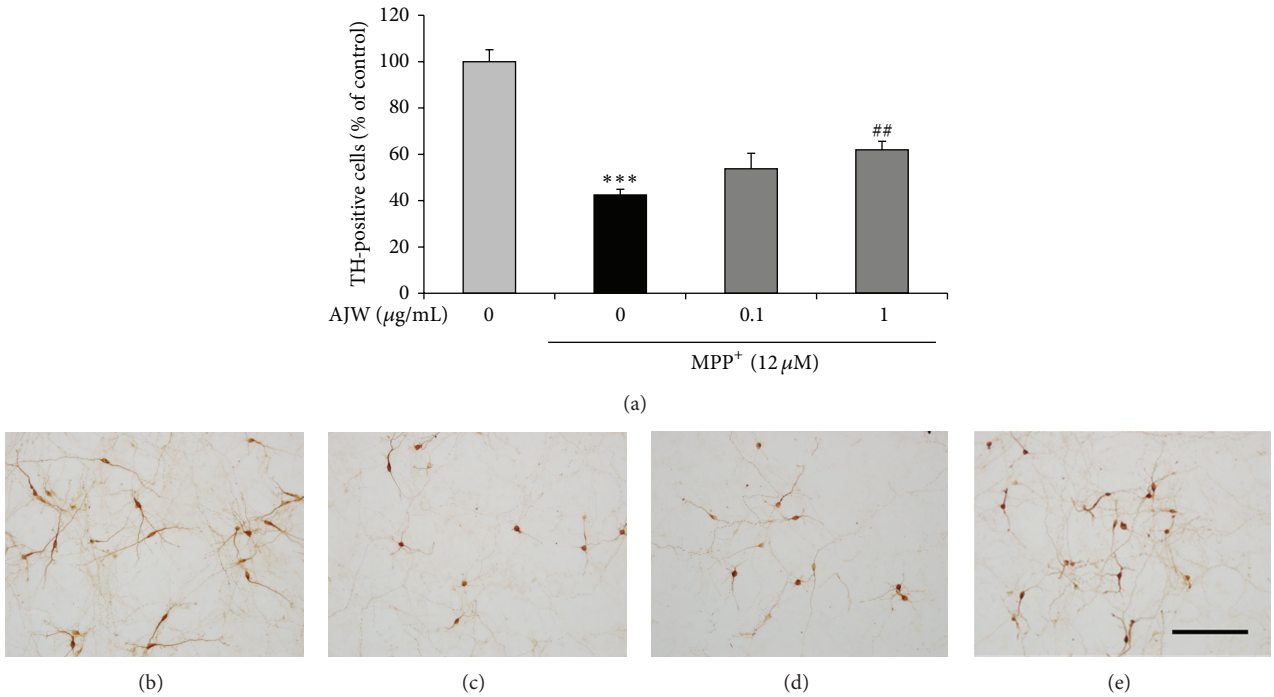

Figure 1: Protective effects of AJW against MPP^+-induced toxicity in primary dopaminergic neurons. Cells were treated with AJW at 0.1, 1 μg/mL, or vehicle for 1 h before exposure to 12 μM MPP^+ for 23 h. The numbers of TH-positive neurons were counted (a), and the representative images are shown ((b)–(e)). Control group (b), MPP^+-only treated group (c), MPP^+ + AJW 0.1 μg/mL treated group (d), and MPP^+ + AJW 1 μg/mL treated group (e). Scale bar = 100 μm. Values are indicated as the mean ± SEM. $^{***}P < 0.001$ compared with the control group, $^{\#\#}P < 0.01$ compared with the MPP^+-only treated group.

3.2. Inhibitory Effects of AJW on ROS Production by MPP^+ in Primary Mesencephalic Cells. To evaluate the inhibitory effects of AJW on ROS generation by MPP^+ in primary mesencephalic cells, we used H_2DCF-DA. Exposure to 12 μM MPP^+ exhibited significantly increased intensity of DCF by 171.15 ± 5.37% relative to the control group, while the treatment with AJW at 0.1 and 1 μg/mL showed markedly decreased intensity by 144.87 ± 5.51 and 129.51 ± 5.79% relative to the control group, respectively (Figure 2).

3.3. Radical Scavenging Activities of AJW. To examine the antioxidant capacities of AJW, we performed DPPH free radical and ABTS radical cation scavenging activity assays. In both assays, AJW exhibited dose-dependently increased activities similar to the water extract of Scutellariae Radix (SBE), used as a positive control. AJW at 1000 μg/mL exhibited 96.12 ± 0.52% and 93.64 ± 0.04% of scavenging activities in DPPH (Figure 3(a)) and ABTS (Figure 3(b)) assays, respectively. DPPH IC_{50}s for AJW and SBE were 36.12 ± 2.79 and 39.28 ± 1.02 μg/mL, whereas ABTS IC_{50}s for AJW and SBE were 64.26 ± 0.06 and 54.30 ± 0.33 μg/mL, respectively.

3.4. Inhibitory Effects of AJW on Behavioral Impairment by MPTP in Mice. To confirm the effect of AJW on dopaminergic neurons in an *in vivo* PD model, we treated mice with AJW and/or MPTP and carried out the pole test. As a result, T-turn and T-LA of MPTP-only treated mice were markedly prolonged as 25.15 ± 4.17 sec and 26.74 ± 3.26 sec, compared with the control group (T-turn: 3.64 ± 1.49 sec; T-LA: 8.91 ± 1.88 sec) (Figure 4). However, the times of AJW 10 mg/kg/day treated group were shortened as 19.20 ± 6.14 sec and 21.49 ± 5.28 sec, respectively, and the AJW 100 mg/kg/day treated group showed more shortened T-turn as 4.06 ± 0.87 sec and T-LA as 9.39 ± 0.94 sec (Figure 4).

3.5. Inhibitory Effects of AJW on Dopaminergic Neuronal Loss by MPTP in Mice. In the mouse brain, MPTP induced severe dopaminergic cell death in the SNc and the striatum. In the MPTP-only treated mice, the number of TH-positive cells in the SNc and the optical density in the striatum were decreased by 37.46 ± 3.46 and 39.53 ± 1.38% relative to the control group, respectively (Figure 5). However, these values are significantly increased by AJW 10 mg/kg/day treatment as 53.83 ± 9.54 and 45.34 ± 4.41% relative to the control group (Figure 5). Also, the values of AJW 100 mg/kg/day treated group more largely increased as 60.48 ± 4.68 and 58.48 ± 3.09% relative to the control group.

3.6. Inhibitory Effects of AJW on 8-OHdG Accumulation by MPTP in Mice. To evaluate the inhibitory effects of AJW on 8-OHdG accumulation by MPTP in mice, we used anti-8-OHdG antibody. In the SNc of MPTP-only treated mice, large accumulation of 8-OHdG occurred, whereas in the control group, there is nothing shown (Figure 6). This accumulation

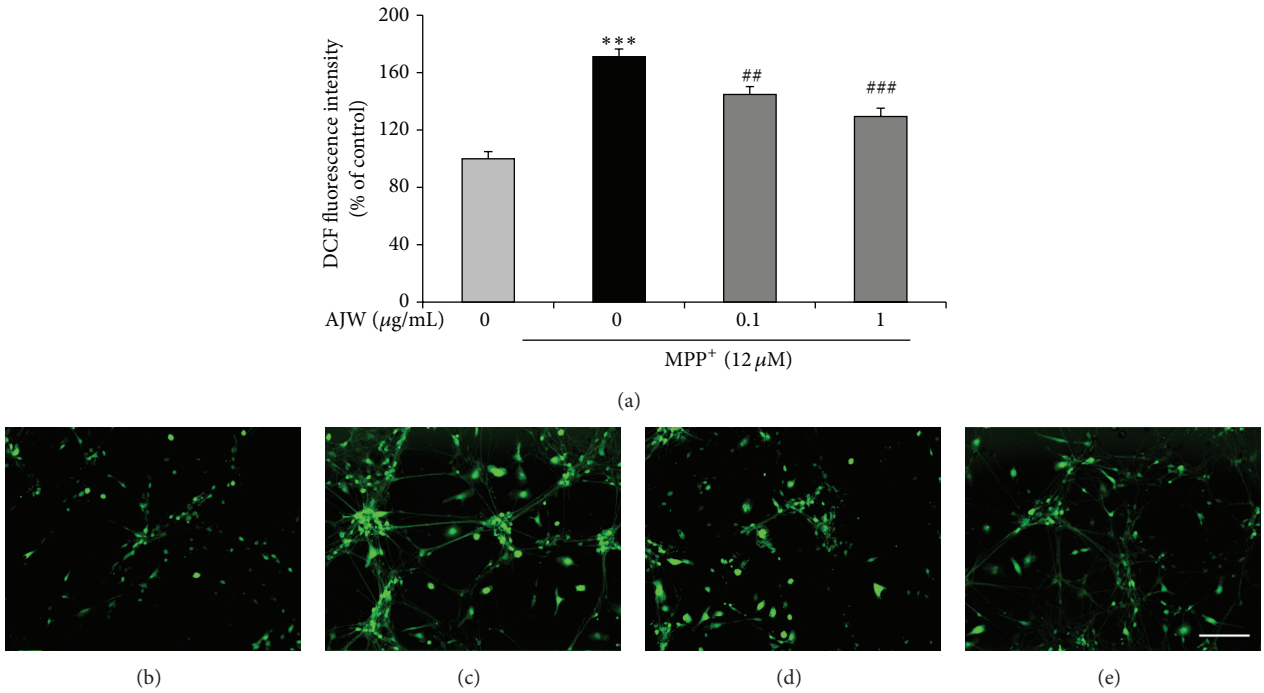

Figure 2: Inhibitory effects of AJW on ROS generation by MPP^+ in primary mesencephalic cells. Cells were treated with AJW at 0.1, 1 μg/mL, or vehicle for 1 h before exposure to 12 μM MPP^+ for 23 h. The fluorescence intensity of DCF was measured (a), and the representative images are shown ((b)–(e)). Control group (b), MPP^+-only treated group (c), MPP^+ + AJW 0.1 μg/mL treated group (d), and MPP^+ + AJW 1 μg/mL treated group (e). Scale bar = 100 μm. Values are indicated as the mean ± SEM. $^{***}P < 0.001$ compared with the control group, $^{\#\#}P < 0.01$, and $^{\#\#\#}P < 0.001$ compared with the MPP^+-only treated group.

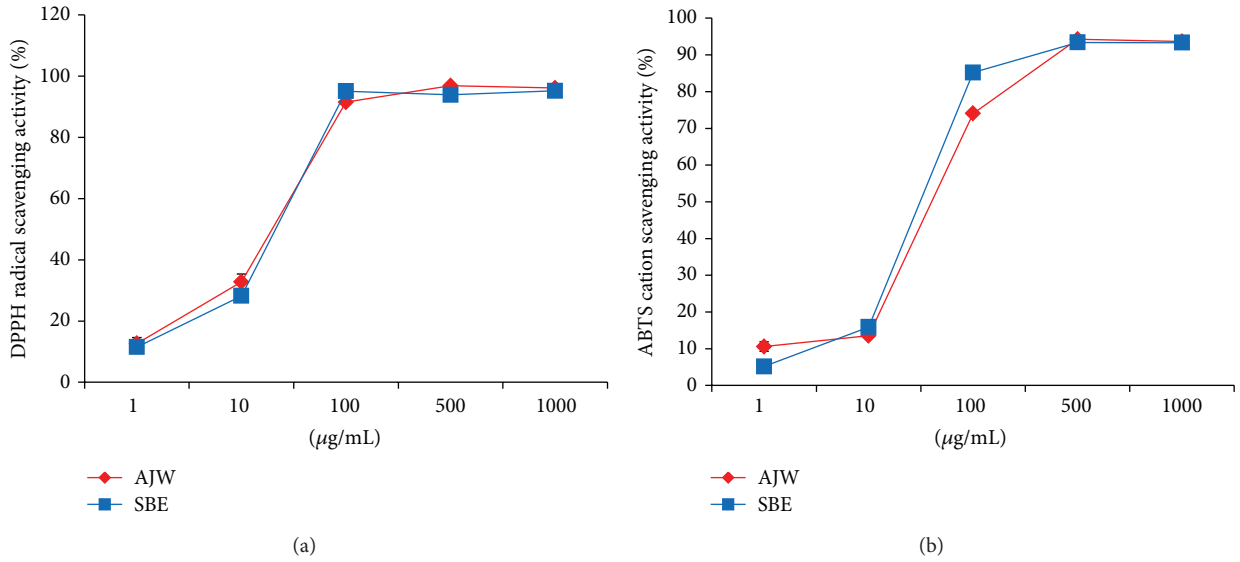

Figure 3: Radical scavenging activities of AJW. AJW and SBE, a positive control, showed DPPH free radical scavenging activity (a) and ABTS radical cation scavenging activity (b) in a dose-dependent manner at concentrations of 1–1000 μg/mL. SBE = water extract of Scutellariae Radix. Values are indicated as the mean ± SEM.

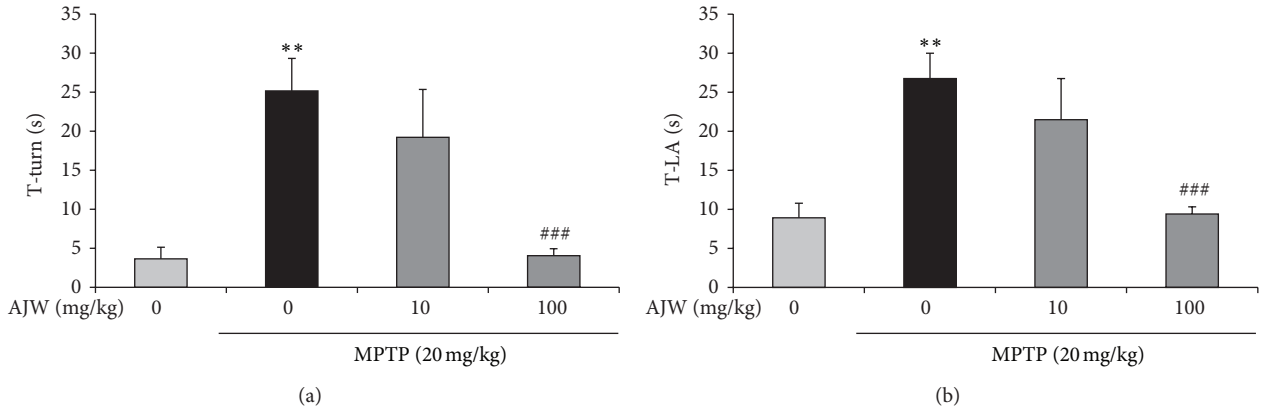

Figure 4: Inhibitory effects of AJW on behavioral impairment by MPTP in mice. Saline or AJW at 10 or 100 mg/kg/day was administered orally for 7 days, and MPTP 20 mg/kg was injected intraperitoneally four times at 2 h intervals on the last day of AJW treatment. Seven days after the last MPTP injection, we conducted the pole test. The time taken for the mice to turn completely downward ((a); T-turn) and the time taken to reach the floor ((b); T-LA) were recorded. Values are indicated as the mean ± SEM. $^{**}P < 0.01$ compared with the control group, $^{###}P < 0.001$ compared with the MPTP-only treated group.

is effectively prevented by treatment with AJW at 10 and 100 mg/kg/day as 85.48 ± 6.31 and 35.26 ± 13.92% of the value in the MPTP-only treated group (Figure 6).

4. Discussion

In this study, we demonstrated that AJW protects dopaminergic neurons against MPP^+ toxicities in a primary culture system and against MPTP toxicities in mice through antioxidant mechanisms.

First, to investigate whether AJW protects dopaminergic neurons from MPP^+ toxicity, we performed an immunohistochemistry of TH, the crucial enzyme in dopamine biosynthesis [17], in primary cultured mesencephalic cells. MPP^+, the active metabolite of MPTP, is known to result in selective dopaminergic neuronal degeneration via inhibiting mitochondrial complex I and increasing calcium permeability of the mitochondrial membrane generating ROS in cellular PD models [18]. In this study, AJW remarkably protected dopaminergic neurons against MPP^+ toxicity, leading to an increase in the TH-positive cell numbers and preservation of TH-positive cell morphologies.

Next, to explore the protective mechanisms of AJW from MPP^+-induced neurotoxicity, we measured intracellular ROS level in primary cultured mesencephalic cells treated with MPP^+ and/or AJW. ROS, generated mostly during the incomplete metabolic reduction of oxygen to water in aerobes, include superoxide, nitric oxide, hydroxyl radical, H_2O_2, and peroxynitrite [3]. All of these species are redox-active and can interact with nearby cellular components, resulting in wide-ranging damage [3]. Moreover, as one of the toxic events induced by MPP^+, the overproduction of ROS readily damages dopaminergic neurons, which are especially vulnerable to oxidative stress [1, 19, 20]. In this study, AJW remarkably inhibited the intracellular ROS production triggered by MPP^+ in primary mesencephalic cells. In addition, AJW showed potent radical scavenging activity comparable to SBE, a positive control that has strong antioxidant and neuroprotective effects [21], in DPPH and ABTS assays, suggesting that AJW scavenges the free radicals overproduced by MPP^+.

Next, to evaluate the effects of AJW *in vivo*, we performed behavioral tests and brain tissue stereology after treating C57BL/6 mice with MPTP and/or AJW. The MPTP-treated mouse has been widely used as an *in vivo* PD model because MPTP induces PD-like motor deficits such as bradykinesia and rigidity and selective dopaminergic neuronal loss in the SNc [22]. In the pole test, which measures bradykinesia [23], AJW-treated mice showed significant improvement in the T-turn and T-LA to the level of the control group, compared with the MPTP-only treated group. We confirmed these effects of AJW in TH immunohistochemistry, showing that the AJW treatment protects both dopaminergic neurons in the SNc and its fibers in the striatum compared with the MPTP-only treated group. During MPTP-induced neurotoxicities, oxidative stress increases markedly and leads to the peroxidation of macromolecules [10]. Therefore, we examined the inhibitory effects of AJW on 8-OHdG accumulation in the SNc. 8-OHdG is the major DNA oxidative adduct, and it increases in the SNc and in the urine of PD patients [5]. Moreover, 8-OHdG levels in urine have been suggested to be a potential biomarker for investigating the progress of PD [5]. In our study, the MPTP-only treated mice showed significantly increased 8-OHdG accumulation in the SNc, whereas the control group showed nothing in the same region. However, AJW treatment prevented this accumulation, suggesting that AJW has inhibitory effects on the oxidative stress induced by MPTP. From these results, we confirmed that AJW protects dopaminergic neurons against MPTP-induced neurotoxicities through antioxidant mechanisms in PD models both *in vitro* and *in vivo*.

Most neurodegenerative diseases are heterogeneous and genetically complex. In PD, more than 90% of the cases are not linked to a single mutation [24]. Due to this multiplicity in the pathological processes of neurodegenerative diseases, materials that target more than one pathophysiological event

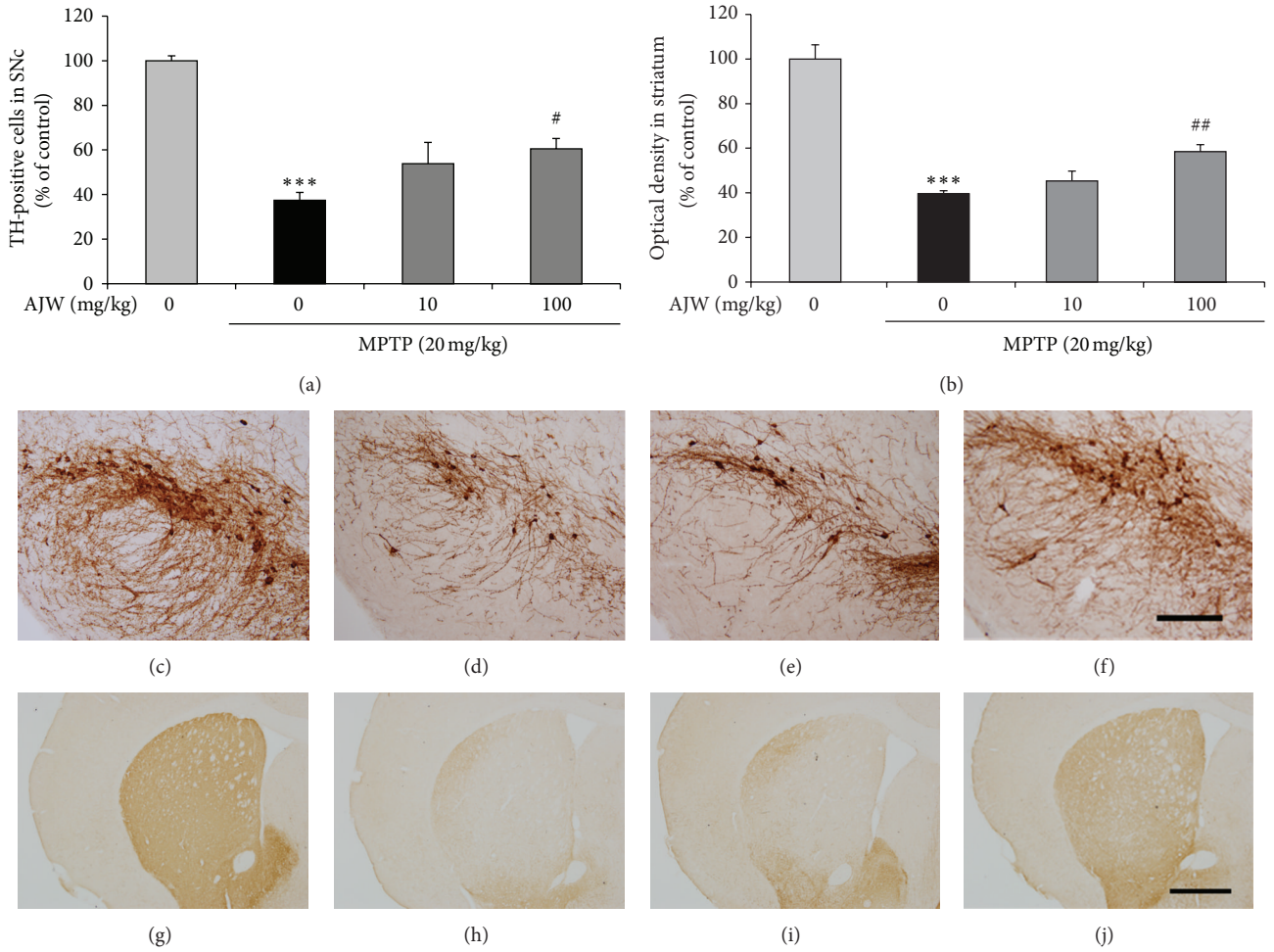

Figure 5: Protective effects of AJW on dopaminergic neuronal loss by MPTP in mice. Saline or AJW at 10 or 100 mg/kg/day was administered orally for 7 days, and MPTP 20 mg/kg was injected intraperitoneally four times at 2 h intervals on the last day of AJW treatment. After the behavioral test, dopaminergic neurons were determined using TH-immunohistochemistry. The numbers of TH-positive neurons in the SNc were counted (a) and the optical density of TH positive fibers in the striatum was measured (b). Representative images are shown of the SNc ((c)–(f)) and the striatum ((g)–(j)) of each group. Control group ((c) and (g)), MPTP-only treated group ((d) and (h)), MPTP + AJW 10 mg/kg/day treated group ((e) and (i)), and MPTP + AJW 100 mg/kg/day treated group ((f) and (j)). Scale bar = 100 μm ((c)–(f)) and 400 μm ((g)–(j)). Values are indicated as the mean ± SEM. $^{***}P < 0.001$ compared with the control group, $^{\#\#\#}P < 0.001$ compared with the MPTP-only treated group.

in cell death cascades have been investigated [25]. And many drugs with single target often fail to show the expected effect in further studies [24]. However, because herbal medicines contain multiple compounds, they potentially could have multiple functions and produce stronger effects than a single compound via the synergism of their constituents [26]. Therefore, candidate herbal medicines have been evaluated recently [27]. For example, *Cassia obtusifolia* L. seed extract showed protective effects in experimental models of memory impairment, hippocampal cell death, ischemia, and PD [22]. Similarly, the root extract of *Polygala tenuifolia* Willd was reported to confer neuroprotection in various experimental models, such as memory impairment, cerebral ischemia, chronic stress, anxiety, and PD [17]. In addition, *Scutellaria baicalensis* Georgi root extract, another herbal medicine, protected neurons against ischemia, PD, Alzheimer's disease, and spinal cord injury in various experimental models [22]. Chemical profile of Ampelopsis Radix is rarely known, but Kim discovered that it contains resveratrol, (+)-catechin, (−)-epicatechin, schizandriside, (+)-gallocatechin, and (−)-epicatechin gallate, showing that (+)-catechin is the highest constituent in Ampelopsis Radix [11] and the content is similar to our result. Although the content of (+)-catechin in AJW, 0.18%, is not high, it could be enough to show activities in that (+)-catechin has been demonstrated to have strong neuroprotective activities in MPTP-treated mice even at 0.3 mg/kg [28] and to have good bioavailability [29]. In addition to (+)-catechin, (−)-epicatechin and resveratrol, which are known to be neuroprotective in various PD models [13, 15, 30], have been demonstrated to cross blood-brain barrier [31, 32]. Furthermore, the mixture of (+)-catechin and (−)-epicatechin was reported to have synergistic neuroprotective

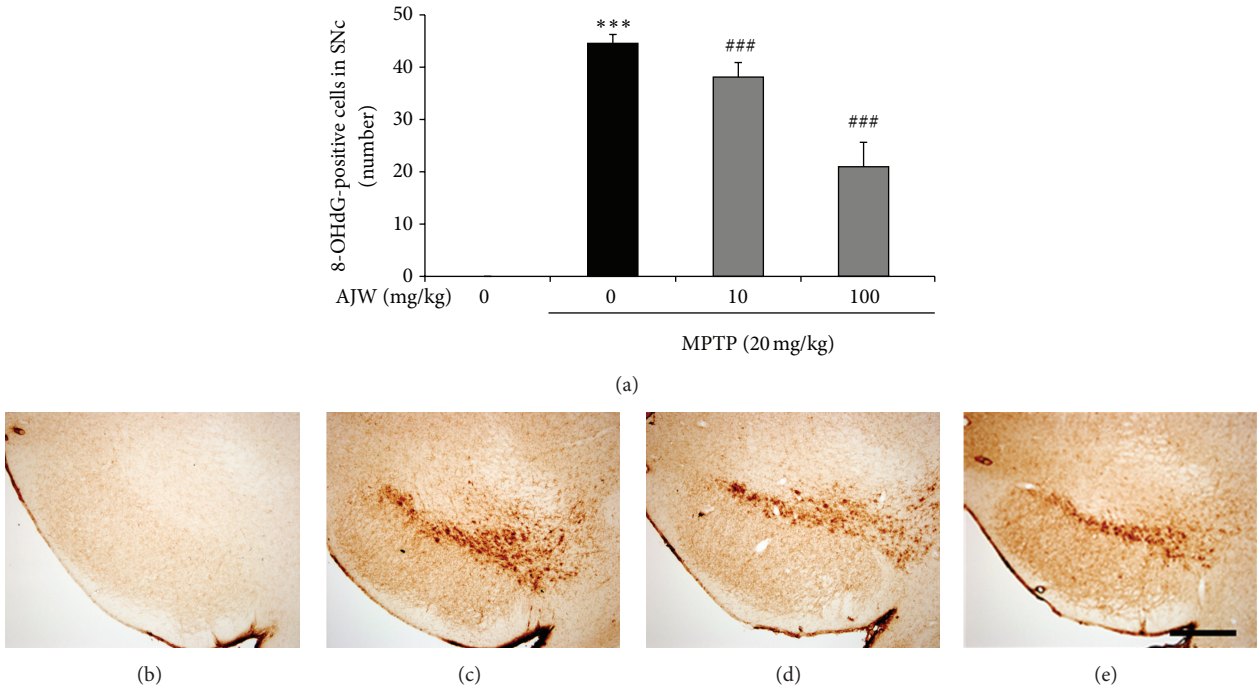

Figure 6: Inhibitory effects of AJW on 8-OHdG accumulation by MPTP in mice. Saline or AJW at 10 or 100 mg/kg/day were administered orally for 7 days, and MPTP 20 mg/kg was injected intraperitoneally four times at 2-h intervals on the last day of AJW treatment. After the behavioral tests, oxidative DNA damage in the cells of the SNc was detected using 8-OHdG-immunohistochemistry. The numbers of 8-OHdG-positive cells in the SNc were counted (a), and the representative images are shown ((b)–(e)). Control group (b), MPTP-only treated group (c), MPTP + AJW 10 mg/kg/day treated group (d), and MPTP + AJW 100 mg/kg/day treated group (e). Scale bar = 200 μm. Values are indicated as the mean ± SEM. $^{***}P < 0.001$ compared with the control group, $^{###}P < 0.001$ compared with the MPTP-only treated group.

effects against amyloid β toxicities *in vitro* [33]. Taken together, the beneficial effects of AJW might be due to (+)-catechin mainly, and also other unknown compounds in AJW might synergistically contribute to the effects. Furthermore, those compounds could make AJW have potential to be applied to various neurodegenerative disease models, as the other herbal medicines mentioned above do. Nevertheless, the possible multimodal neuroprotective effects of AJW and the active compounds in AJW need to be further studied.

5. Conclusions

AJW protected dopaminergic cells from MPP^+ toxicities in primary mesencephalic cultures and against MPTP toxicities in C57BL/6 mice. The neuroprotective effects of AJW are due to the antioxidant activities including inhibition of ROS, free radicals, and 8-OHdGs. These results indicated that AJW is a potential candidate as a neuroprotective agent in PD, although the major active ingredients in AJW and the possible protective effects of AJW in other PD models need to be further studied.

Acknowledgment

This research was supported by Basic Science Research Program through the National Research Foundation of Korea (NRF) funded by the Ministry of Education, Science and Technology (no. 2005-0049404).

References

[1] N. A. Simonian and J. T. Coyle, "Oxidative stress in neurodegenerative diseases," *Annual Review of Pharmacology and Toxicology*, vol. 36, no. 1, pp. 83–106, 1996.

[2] R. S. Sohal and R. Weindruch, "Oxidative stress, caloric restriction, and aging," *Science*, vol. 273, no. 5271, pp. 59–63, 1996.

[3] J. K. Andersen, "Oxidative stress in neurodegeneration: cause or consequence?" *Nature Medicine*, vol. 10, supplement, pp. S18–S25, 2004.

[4] Y. Saito, K. Nishio, Y. Ogawa et al., "Molecular mechanisms of 6-hydroxydopamine-induced cytotoxicity in PC12 cells: involvement of hydrogen peroxide-dependent and -independent action," *Free Radical Biology & Medicine*, vol. 42, no. 5, pp. 675–685, 2007.

[5] A. Oyagi, Y. Oida, H. Hara et al., "Protective effects of SUN N8075, a novel agent with antioxidant properties, in *in vitro* and *in vivo* models of Parkinson's disease," *Brain Research*, vol. 1214, pp. 169–176, 2008.

[6] Q. Xu, A. G. Kanthasamy, and M. B. Reddy, "Phytic acid protects against 6-hydroxydopamine-induced dopaminergic neuron apoptosis in normal and iron excess conditions in a cell culture model," *Parkinson's Disease*, vol. 2011, Article ID 431068, 6 pages, 2011.

[7] R. E. Heikkila, L. Manzino, F. S. Cabbat, and R. C. Duvoisin, "Protection against the dopaminergic neurotoxicity of 1-methyl-4-phenyl-1,2,5,6-tetrahydropyridine by monoamine oxidase inhibitors," *Nature*, vol. 311, no. 5985, pp. 467–469, 1984.

[8] L. Turski, K. Bressler, K.-J. Rettig, P.-A. Loschmann, and H. Wachtel, "Protection of substantia nigra from MPP+ neurotoxicity by N-methyl-D-aspartate antagonists," *Nature*, vol. 349, no. 6308, pp. 414–418, 1991.

[9] V. Jackson-Lewis and R. J. Smeyne, "MPTP and SNpc DA neuronal vulnerability: role of dopamine, superoxide and nitric oxide in neurotoxicity. Minireview," *Neurotoxicity Research*, vol. 7, no. 3, pp. 193–201, 2005.

[10] D. Blum, S. Torch, N. Lambeng et al., "Molecular pathways involved in the neurotoxicity of 6-OHDA, dopamine and MPTP: contribution to the apoptotic theory in Parkinson's disease," *Progress in Neurobiology*, vol. 65, no. 2, pp. 135–172, 2001.

[11] I. H. Kim, M. Umezawa, N. Kawahara, and Y. Goda, "The constituents of the roots of Ampelopsis japonica," *Journal of Natural Medicines*, vol. 61, no. 2, pp. 224–225, 2007.

[12] Y. Wensheng, C. Xinmin, and Y. Lei, "Studies on the polyphenol constituents of ampelopsis japonica (part II)," *Journal of Chinese Medicinal Materials*, vol. 6, 1995.

[13] G. Nie, C. Jin, Y. Cao, S. Shen, and B. Zhao, "Distinct effects of tea catechins on 6-hydroxydopamine-induced apoptosis in PC12 cells," *Archives of Biochemistry and Biophysics*, vol. 397, no. 1, pp. 84–90, 2002.

[14] C. Ao, T. Higa, H. Ming, Y.-T. Ding, and S. Tawata, "Isolation and identification of antioxidant and hyaluronidase inhibitory compounds from Ficus microcarpa L. fil. bark," *Journal of Enzyme Inhibition and Medicinal Chemistry*, vol. 25, no. 3, pp. 406–413, 2010.

[15] Y.-P. Lin, T.-Y. Chen, H.-W. Tseng, M.-H. Lee, and S.-T. Chen, "Neural cell protective compounds isolated from Phoenix hanceana var. formosana," *Phytochemistry*, vol. 70, no. 9, pp. 1173–1181, 2009.

[16] C. Liu, Z. Shi, L. Fan, C. Zhang, K. Wang, and B. Wang, "Resveratrol improves neuron protection and functional recovery in rat model of spinal cord injury," *Brain Research*, vol. 1374, pp. 100–109, 2011.

[17] J. G. Choi, H. G. Kim, M. C. Kim et al., "Polygalae radix inhibits toxin-induced neuronal death in the Parkinson's disease models," *Journal of Ethnopharmacology*, vol. 134, no. 2, pp. 414–421, 2011.

[18] T. Hashimoto, K. Nishi, J. Nagasao, S. Tsuji, and K. Oyanagi, "Magnesium exerts both preventive and ameliorating effects in an *in vitro* rat Parkinson disease model involving 1-methyl-4-phenylpyridinium (MPP^+) toxicity in dopaminergic neurons," *Brain Research*, vol. 1197, pp. 143–151, 2008.

[19] D. Di Monte, M. S. Sandy, G. Ekstrom, and M. T. Smith, "Comparative studies on the mechanisms of paraquat and 1-methyl-4-phenylpyridine (MPP+) cytotoxicity," *Biochemical and Biophysical Research Communications*, vol. 137, no. 1, pp. 303–309, 1986.

[20] G. U. Höglinger, G. Carrard, P. P. Michel et al., "Dysfunction of mitochondrial complex I and the proteasome: Interactions between two biochemical deficits in a cellular model of Parkinson's disease," *Journal of Neurochemistry*, vol. 86, no. 5, pp. 1297–1307, 2003.

[21] Z. Gao, K. Huang, X. Yang, and H. Xu, "Free radical scavenging and antioxidant activities of flavonoids extracted from the radix of Scutellaria baicalensis Georgi," *Biochimica et Biophysica Acta*, vol. 1472, no. 3, pp. 643–650, 1999.

[22] M. S. Ju, H. G. Kim, J. G. Choi et al., "Cassiae semen, a seed of Cassia obtusifolia, has neuroprotective effects in Parkinson's disease models," *Food and Chemical Toxicology*, vol. 48, no. 8-9, pp. 2037–2044, 2010.

[23] T. Karl, R. Pabst, and S. von Hörsten, "Behavioral phenotyping of mice in pharmacological and toxicological research," *Experimental and Toxicologic Pathology*, vol. 55, no. 1, pp. 69–83, 2003.

[24] P. T. Lansbury Jr., "Back to the future: the "old-fashioned" way to new medications for neurodegeneration," *Nature Medicine*, vol. 10, supplement, pp. S51–S57, 2004.

[25] M. B. H. Youdim, W. J. Geldenhuys, and C. J. Van der Schyf, "Why should we use multifunctional neuroprotective and neurorestorative drugs for Parkinson's disease?" *Parkinsonism & Related Disorders*, vol. 13, supplement 3, pp. S281–S291, 2007.

[26] H. G. Kim and M. S. Oh, "Herbal medicines for the prevention and treatment of Alzheimer's disease," *Current Pharmaceutical Design*, vol. 18, no. 1, pp. 57–75, 2012.

[27] D.-S. Hwang, H. G. Kim, H.-J. Kwon et al., "Dangguijakyak-san, a medicinal herbal formula, protects dopaminergic neurons from 6-hydroxydopamine-induced neurotoxicity," *Journal of Ethnopharmacology*, vol. 133, no. 2, pp. 934–939, 2011.

[28] H. Ruan, Y. Yang, X. Zhu, X. Wang, and R. Chen, "Neuroprotective effects of (±)-catechin against 1-methyl-4-phenyl-1,2,3,6-tetrahydropyridine (MPTP)-induced dopaminergic neurotoxicity in mice," *Neuroscience Letters*, vol. 450, no. 2, pp. 152–157, 2009.

[29] K. S. Kang, N. Yamabe, Y. Wen, M. Fukui, and B. T. Zhu, "Beneficial effects of natural phenolics on levodopa methylation and oxidative neurodegeneration," *Brain Research*, vol. 1497, pp. 1–14, 2013.

[30] F. Jin, Q. Wu, Y.-F. Lu, Q.-H. Gong, and J.-S. Shi, "Neuroprotective effect of resveratrol on 6-OHDA-induced Parkinson's disease in rats," *European Journal of Pharmacology*, vol. 600, no. 1–3, pp. 78–82, 2008.

[31] M. M. Abd El Mohsen, G. Kuhnle, A. R. Rechner et al., "Uptake and metabolism of epicatechin and its access to the brain after oral ingestion," *Free Radical Biology and Medicine*, vol. 33, no. 12, pp. 1693–1702, 2002.

[32] J. Blanchet, F. Longpré, G. Bureau et al., "Resveratrol, a red wine polyphenol, protects dopaminergic neurons in MPTP-treated mice," *Progress in Neuro-Psychopharmacology and Biological Psychiatry*, vol. 32, no. 5, pp. 1243–1250, 2008.

[33] H. Jin Heo and C. Y. Lee, "Epicatechin and catechin in cocoa inhibit amyloid β protein induced apoptosis," *Journal of Agricultural and Food Chemistry*, vol. 53, no. 5, pp. 1445–1448, 2005.

Hindawi Publishing Corporation
Evidence-Based Complementary and Alternative Medicine
Volume 2013, Article ID 313142, 5 pages
http://dx.doi.org/10.1155/2013/313142

Research Article

Grape Seed Procyanidins in Pre- and Mild Hypertension: A Registry Study

Gianni Belcaro, Andrea Ledda, Shu Hu, Maria Rosa Cesarone, Beatrice Feragalli, and Mark Dugall

Department of Biomedical Sciences, Irvine3 Circulation-Vascular Labs and San Valentino Vascular Screening Project, Gabriele D'Annunzio University, SS 16 Bis 94, Spoltore, Pescara, Italy

Correspondence should be addressed to Gianni Belcaro; cardres@abol.it

Received 22 July 2013; Accepted 20 August 2013

Academic Editor: Vincenzo De Feo

The efficacy of a standardized grape seed procyanidins extract (GSPE, Enovita) to decrease blood pressure when associated with nondrug intervention (diet and lifestyle modifications) was investigated in a controlled registry study involving 119 healthy, pre- and mildly hypertensive subjects. Two dosages of Enovita were evaluated (150 and 300 mg/die), using blood pressure and heart rate as the primary endpoints and complementing these observations with a laser Doppler flowmetry (LDF) investigation of the microcirculation state and an evaluation of the plasma oxidative status. After four months of treatment, a statistically significant higher, and dose-dependent, improvement in all endpoints was observed in the treatment groups compared to that of the control, with blood pressure normalizing in 93% of the higher dosage (300 mg) treatment group. Taken together, these observations suggest that GSPEs have beneficial cardiovascular effects that complement current intervention strategies in the hypertension area. The effect on blood pressure adds to the beneficial effects of GSPEs on the cardiovascular disease (CVD) phenotype associated with the oxidation of membrane lipids (endothelial dysfunction, formation of oxidized LDL, and activation of phagocytic cells).

1. Introduction

The concept that the nutritional properties of food cannot be recapitulated by, and go substantially beyond, its profile of essential macronutrients (proteins, sugars, and lipids) and micronutrients (vitamins and minerals) is now firmly entrenched in both human and animal nutrition [1]. It explains various once puzzling observations, from the difference between the pharmacological profile of alcohol and wine [2] to the higher susceptibility to parasite infection associated with the nutrition of bees with sugar solutions rather than with honey [3]. Within the differences between alcohol and red wine, one of the most remarkable ones regards the effect on blood pressure [2, 4]. While the regular consumption of alcohol elevates blood pressure of approximately 1 mm Hg for each 10 g of alcohol consumed [2, 4], red wine, at least when associated with moderate drinking (1–4 standard drinks a day), can substantially reverse alcohol-related hypertension and have a beneficial effect on hypertension and overall cardiac morbidity [2]. This effect has been associated with the phenolic constituents of wine, mostly procyanidins (GSPs) [5], and two preliminary intervention studies on prehypertensive patients have supported the view that GSPs lower blood pressure [6, 7]. The mechanist details of this activity have been worked out. Thus, procyanidins directly inhibit angiotensin-converting enzyme (ACE) [8] and indirectly increase the lifetime of endothelially generated nitrogen oxide by inhibiting the production of superoxide, its major physiological scavenger, from endothelial NADP oxidase [9]. The overall result of a decreased peripheral resistance is a reduction of both systolic and diastolic blood pressures, with potential beneficial effects for all risk factors associated with hypertension (stroke, heart disease, congestive heart failure, and kidney disease).

Conventionally, high blood pressure is associated with values of systolic and diastolic pressure higher than 139 mm Hg and 89 mm Hg, respectively, while the corresponding normal values are considered those <120 mm Hg

and <80 mm Hg [10]. The grey area between normality and hypertension has been named prehypertension and is generally treated only with diet and lifestyle modifications (self-monitoring, exercise, and relaxation), as often happens for the stage 1 of hypertension, the one associated with 140–159/90–95 mm Hg values [10]. Severe hypertension is an important risk factor for coronary artery disease, more important than high non-HDL cholesterol or obesity [11], but there is mounting evidence that also chronic prehypertension is detrimental for cardiovascular health. Nevertheless, the side-effect profile of hypotensive drugs (diuretics, beta-blockers, and ACE-inhibitors) makes their generalized use in prehypertensive patients questionable [10], providing a rationale to investigate the potential of supplementation with diet-derived agents to promote the attainment of healthy values of blood pressure in this population. In this context, GSPs are the best validated dietary constituents, due to their occurrence in red wine, where contents in the range of 1 g/L are not uncommon, and their identification as the molecular link between wine and its protective cardiovascular properties [5].

GSP is an umbrella name that covers a wide range of products, differing for their contents of monomeric catechins and their degree of oligomerization and decoration with galloyl moieties [12]. GSPs are type B procyanidins, characterized by a single interflavane bond, and represent the best investigated class of condensed tannins [13]. Only the lower homologues (2–5 units) have been shown to be absorbed, either directly or after microbial metabolization. Although the extent of absorption is controversial [14], mass balance experiments with radiolabeled procyanidin B2, a dimeric condensed tannin, have shown an overall significant (>60%) systemic label absorption [15]. For these reasons, we have selected a standardized GSPE (Enovita) enriched in lower oligomers for this study.

2. Material and Methods

Enovita, a standardized grape seed extract, and the corresponding blank formulation were provided by Indena (Milan, Italy). Enovita contains ca. 8.6% (HPLC) monomeric procyanidins (catechin, epicatechin, and epicatechin gallate) and ca. 91% OPC (GPC), of which 9% (HPLC) are of the dimeric type. The water content is ca. 5%.

Inclusion criteria for this study were a general good health and borderline hypertension, defined as prehypertension (120–139 mm Hg/80–89 mm Hg) and stage 1 hypertension (140–159 mm Hg/90–99 mm Hg) [10]. The evaluation of general good health involved clinical evaluation and history, full blood test panel to rule out alterations in the lipid profile, fasting glucose or hepatitis markers, an overall normal hematocrit, and proteins profile and coagulation, as well as exclusion of hormonal alterations (thyroid and adrenal).

The nondrug intervention included diet (reduction of salt, alcohol, and caffeinated drinks) and lifestyle (regular exercise, improvement of sleep time, relaxation, and reduction of smoke). No other nutritional elements, vitamins, or drugs were used in the observation period. The same management plan was assigned to all subjects, who were then divided into three groups:

(i) group 1—300 mg Enovita/day + management plan;

(ii) group 2—150 mg Enovita/day + management plan;

(iii) group 3: controls—management plan only.

Group 1 was made of 37 subjects (14 females), group 2 of 35 subjects (18 females), and group 3 of 47 subjects (19 females) (Table 1). The age range for volunteers was 45–55 years, and the mean age was 51.33 ± 5.31 years in group 1, 49.90 ± 5.31 in group 2, and 49.40 ± 3.00 in group 3. Also, the average BMI was fairly similar within the three groups, namely, 25.41 ± 0.80 Kg/m^2 in the high dosage group (group 1), 25.20 ± 0.73 Kg/m^2 in the low dosage group (group 2), and 25.11 ± 0.70 Kg/m^2 in the control group (group 3) (Table 1). No side effects were reported during the execution of the study, and formulation tolerability (both for Enovita and the corresponding blank formulation) was very good. Based on the number of used capsules, compliance was >94% in group 1 and >95% in group 2. Blood pressure and heart rate were measured digitally. LDF measurements were taken after 30 minutes of supine rest and acclimatization at 21°C for additional 30 minutes. A linear probe (Vasamedics Laserflo, St. Paul, USA) was used for all measurements, taken on the dorsum of foot, and expressed in flux unit [16]. In hypertensive subjects, flux is generally decreased due to vasoconstriction and is increased by treatment, exercise, and control of the risk factors associated with lifestyle.

All measured target parameters (Table 1) have a non-normal, skewed, or unknown distribution. Therefore, the ANOVA (with the Bonferroni correction) was used to evaluate the before-after results and the Mann-Whitney *U* test for the evaluation of statistically significant differences. A numerosity of at least 20 comparable subjects per group (treatment versus control) was considered necessary to overcome the possible, unavoidable even under the best experimental conditions, differences due to the variability of the microcirculatory target measurements, particularly the laser Doppler test.

3. Results and Discussion

GSPs are endowed with high antioxidant activity, orders of magnitude higher than vitamin C, and have been extensively investigated for their capacity to interfere with the development of the cardiovascular disease (CVD) phenotype associated with the oxidation of membrane lipids (endothelial dysfunction, formation of oxidized LDL, and activation of phagocytic cells) [13]. Epidemiological evidence related to the so-called French paradox suggests that GSPs can substantially buffer a high income of animal fats in the diet, although evidence for this activity is controversial because of the difficulty of recapitulating a complex dietary lifestyle in a controlled clinical experiment [5]. On the other hand, there is growing evidence that GSPs can also address another important element of the CVD phenotype, namely, hypertension, and two controlled studies have suggested that the preclinical observations on procyanidins and blood

Table 1: Key parameters at inclusion, 4, 8, 12, and 16 weeks.

Time	Systolic pressure			Diastolic pressure			Laser Doppler flux			Heart rate			Plasma-free radicals		
	Enovita 300 mg	Enovita 150 mg	Control	Enovita 300 mg	Enovita 150 mg	Control	Enovita 300 mg	Enovita 150 mg	Control	Enovita 300 mg	Enovita 150 mg	Control	Enovita 300 mg	Enovita 150 mg	Control
Inclusion	149; 4.5	150; 3	153.3; 4.4	91; 3.2	91.3; 2	90.4; 2.5	1.1; 0.01	1.1; 0.2	1.1; 0.01	78; 3.5	77.3; 4	77.2; 3.3	378; 22	382; 21	383; 23
4 weeks	121.3; 5.4$^{*\#}$	129; 2.2$^{*\#}$	142.3; 5*	86.3; 3.9*	88; 2*	88.4; 3*	1.28; 0.01$^{*\#}$	1.2; 0.1	1.16; 0.01	73; 2.2*	73; 3.2*	74; 3.2*	—	—	—
8 weeks	119; 4.9$^{*\#}$	125; 3$^{*\#}$	142; 3.9	84.4; 2.8$^{*\#}$	86.1; 2.1*	87; 3.6	2.13; 0.1$^{*\#}$	1.6; 0.2$^{*\#}$	1.22; 0.1	71; 3.1*	73; 2.1	74; 3.1	324; 19$^{*\#}$	339; 32$^{*\#}$	376; 29*
12 weeks	113; 3.3$^{*\#}$	122; 3.2$^{*\#}$	139; 3.5	83; 3.3$^{\#}$	86.3; 2$^{\#}$	88; 2.2	2.22; 0.2$^{*\#}$	1.9; 0.2$^{*\#}$	1.3; 0.1	69; 2.3*	72.2; 2$^{\#}$	74; 2.3	—	—	—
16 weeks	112; 3.5$^{*\#}$	123; 2.1$^{*\#}$	141; 4.3	82.3; 3$^{\#}$	85.3; 2$^{\#}$	88.9; 3.2	2.23; 0.1$^{\#}$	1.9; 0.2$^{\#}$	1.2; 0.1	70; 1.5	72; 2.3	73.2; 2.2	317; 22$^{*\#}$	342; 28$^{\#}$	374; 22

*($P < 0.05$) indicates statistical variations in comparison with previous value.
#: better than controls.

Table 2: Subjects details.

Treatment	Number of subjects completing the study	Age	Compliance	Tolerability	Dropouts
150 mg + best management	37 (14 females)	51.33; 5.31	94%	Very good	0
300 mg + best management	35 (18 females)	49.9; 5.2	95%	Very good	0
Best management	47 (19 females)	49.4; 3	95%	Very good	3

pressure have indeed a clinical translation [6, 7]. These studies were carried out in subjects with avert metabolic syndrome and were of short duration (four weeks). We have now investigated the activity of GSPs in a controlled and longer registry study (four months) on mildly hypertensive but otherwise healthy and only slightly overweight subjects, complementing the observation on blood pressure with a series of other parameters of relevance for the predisease status of the population in study that included heart rate, ECG analysis, and measurements of the microcirculatory status by LDF.

The borderline hypertensive subjects (119) were sorted out in three groups, similar in terms of age and all the objective parameters evaluated, namely, systolic and diastolic blood pressures, microcirculatory status (LDF), heart rate, and plasma oxidative status (Table 2). Group 1 (37 subjects) and group 2 (35 subjects) complemented the management plan with Enovita at two different daily dosages (300 mg/day for group 1 and 150 mg/day for group 2), while in subjects from group 3 (47), only the management plan was implemented and served as the control. The endpoints of the study were evaluated monthly, that is, at weeks 4, 8, and 12, in order to assess the kinetics of development of any beneficial effect.

A decrease of systolic blood pressure was observed in all four groups of the study at month 1, but the decrease was significantly higher in the treatment group ($P < 0.05$). Thus, the average drop of systolic pressure was 28 mm Hg in the high dosage branch and 21 mm Hg in the lower dosage group, while in their respective control groups the decrease was more modest (11 mm Hg). During the next checks, the systolic pressure underwent a further, but much lower, decrease to eventually reach, at the end of the study, an average value of 112 mm Hg in the high dosage group, 123 mm Hg in the lower dosage group, and 141 mm Hg in the control group. In this latter group, no significant further decrease in systolic pressure was observed after the first check. The decrease was, as expected, lower for the diastolic pressure, but a difference between the treatment and the control could still be observed. Thus, in the two treatment groups, a decrease of the diastolic pressure was also observed and developed more gradually in time, eventually reaching 82.3 ± 3.0 mm Hg (from 91.3 ± 2.0 mm Hg) for group 1 and 85.3 ± 2.0 mm Hg (from 91.3 mm Hg) for group 2 (Table 2). Conversely, the decrease was marginal in the control group (from 90.4 ± 2.5 mm Hg to 88.9 ± 3.2 mm Hg). As expected from the data on blood pressure, heart rate was also significantly better reduced in the interventional arms compared to their controls (Table 1), decreasing from 78 ± 3.5 mm Hg to 70 ± 1.5 mm Hg in group 1, from 77 ± 3.4 mm Hg to 72 ± 2.0 mm Hg in group 2, and from 77.2 ± 3.3 mm Hg to 73.2 ± 2.2 mm Hg in the control (group 3).

GSPs have been reported to improve endothelial function and promote microcirculation [16], decreasing the plasma oxidative status [17], and both activities were confirmed in our study (Table 1).

Taken together, our data suggest that GSPs, at least in the profile associated with Enovita, are worth considering to complement dietary and lifestyle changes associated with the attainment of a healthy blood pressure status. The data on blood pressure complement the beneficial activity of GSPs on the CVD phenotype associated with the oxidation of membrane lipids (endothelial dysfunction, formation of oxidized LDL, and activation of phagocytic cells) [17], suggesting that this class of condensed tannins, at least as fractions enriched in lower oligomers, is worth systematic studies for cardiovascular prevention in subjects at risk, providing, for borderline patients, a nondrug option that is better accepted than mainstream medication.

References

[1] G. Hardy, "Nutraceuticals and functional foods: introduction and meaning," *Nutrition*, vol. 16, no. 7-8, pp. 688–689, 2000.

[2] C. Carollo, R. L. Presti, and G. Caimi, "Wine, diet, and arterial hypertension," *Angiology*, vol. 58, no. 1, pp. 92–96, 2007.

[3] R. J. Barker and Y. Lehner, "Acceptance and sustentative values of honey, the sugars of honey, and sucrose fed to caged honey bee workers," *American Bee Journal*, vol. 113, pp. 370–371, 1973.

[4] I. B. Puddey and L. J. Beilin, "Alcohol is bad for blood pressure," *Clinical and Experimental Pharmacology and Physiology*, vol. 33, no. 9, pp. 847–852, 2006.

[5] R. Corder, W. Mullen, N. Q. Khan et al., "Oenology: red wine procyanidins and vascular health," *Nature*, vol. 444, no. 7119, p. 566, 2006.

[6] B. Siva, I. Edirisinghe, J. Randolph, F. Steinberg, and T. Kappagoda, "Effect of a polyphenoics extracts of Grape Seeds (GSE) on Blood Pressure (BP) in patients with the Metabolic Syndrome (MetS)," *The FASEB Journal*, vol. 20, p. A305, 2006.

[7] B. Sivaprakasapillai, I. Edirisinghe, J. Randolph, F. Steinberg, and T. Kappagoda, "Effect of grape seed extract on blood pressure in subjects with the metabolic syndrome," *Metabolism*, vol. 58, no. 12, pp. 1743–1746, 2009.

[8] J. I. Ottaviani, L. Actis-Goretta, J. J. Villordo, and C. G. Fraga, "Procyanidin structure defines the extent and specificity of angiotensin I converting enzyme inhibition," *Biochimie*, vol. 88, no. 3-4, pp. 359–365, 2006.

[9] E. Álvarez, B. K. Rodiño-Janeiro, M. Jerez, R. Ucieda-Somoza, M. J. Núñez, and J. R. González-Juanatey, "Procyanidins from grape pomace are suitable inhibitors of human endothelial NADPH oxidase," *Journal of Cellular Biochemistry*, vol. 113, no. 4, pp. 1386–1396, 2012.

[10] E. Pimenta and S. Oparil, "Management of hypertension in the elderly," *Nature Reviews Cardiology*, vol. 9, no. 5, pp. 286–296, 2012.

[11] R. Kones, "Rosuvastatin, inflammation, C-reactive protein, JUPITER, and primary prevention of cardiovascular disease—a perspective," *Drug Design, Development and Therapy*, vol. 4, pp. 383–413, 2010.

[12] S. Quideau, D. Deffieux, C. Douat-Casassus, and L. Pouységu, "Plant polyphenols: chemical properties, biological activities, and synthesis," *Angewandte Chemie—International Edition*, vol. 50, no. 3, pp. 586–621, 2011.

[13] J. Shi, J. Yu, J. E. Pohorly, and Y. Kakuda, "Polyphenolics in grape seeds—biochemistry and functionality," *Journal of Medicinal Food*, vol. 6, no. 4, pp. 291–299, 2003.

[14] J. I. Ottaviani, C. Kwik-Uribe, C. L. Keen, and H. Schroeter, "Intake of dietary procyanidins does not contribute to the pool of circulating flavanols in humans," *American Journal of Clinical Nutrition*, vol. 95, no. 4, pp. 851–858, 2012.

[15] S. Stoupi, G. Williamson, F. Viton et al., "In vivo bioavailability, absorption, excretion, and pharmacokinetics of [14C]procyanidin B2 in male rats," *Drug Metabolism and Disposition*, vol. 38, no. 2, pp. 287–291, 2010.

[16] A.-M. Salmasi, G. Belcaro, and A. N. Nicolaides, "Impaired venoarteriolar reflex as a possible cause for nifedipine-induced ankle oedema," *International Journal of Cardiology*, vol. 30, no. 3, pp. 303–307, 1991.

[17] R. Maffei Facino, M. Carini, G. Aldini, E. Bombardelli, P. Morazzoni, and R. Morelli, "Free radicals scavenging action and anti-enzyme activities of procyanidines from Vitis vinifera. A mechanism for their capillary protective action," *Arzneimittel-Forschung*, vol. 44, no. 5, pp. 592–601, 1994.

Hindawi Publishing Corporation
Evidence-Based Complementary and Alternative Medicine
Volume 2013, Article ID 819296, 10 pages
http://dx.doi.org/10.1155/2013/819296

Research Article

Skimmin, a Coumarin from *Hydrangea paniculata*, Slows down the Progression of Membranous Glomerulonephritis by Anti-Inflammatory Effects and Inhibiting Immune Complex Deposition

Sen Zhang, Hongqi Xin, Yan Li, Dongming Zhang, Jing Shi, Jingzhi Yang, and Xiaoguang Chen

State Key Laboratory of Bioactive Substances and Functions of Natural Medicines, Institute of Materia Medica, Chinese Academy of Medical Sciences and Peking Union Medical College, Beijing 100050, China

Correspondence should be addressed to Xiaoguang Chen; chxg@imm.ac.cn

Received 28 April 2013; Revised 8 July 2013; Accepted 8 July 2013

Academic Editor: Mohamed Eddouks

Skimmin is one of the major pharmacologically active molecules present in *Hydrangea paniculata*, a medical herb used in the traditional Chinese medicine as an anti-inflammatory agent. In the current study, we attempted to investigate its renoprotective activity and underlying mechanisms in a rat model of membranous glomerulonephritis induced by cationic bovine serum albumin (c-BSA). Sprague-Dawley (SD) rats were divided into five groups, including normal control, model control, Mycophenolate Mofetil-treated group, and two skimming-treated groups (15 mg/kg and 30 mg/kg). Our research showed that treatment with skimmin significantly reduced the levels of blood urea nitrogen (BUN), urinary albumin excretion (UAE), and serum creatinine (Scr) as compared with model control after experimental induction of membranous glomerulonephritis ($P < 0.01$). Moreover, glomerular hypercellularity, tubulointerstitial injury, and glomerular deposition of IgG were less intense after skimmin treatment. By immunochemistry analysis, we demonstrated that skimmin could significantly inhibit interleukin-1β (IL1β) and IL-6 expression ($P < 0.05$), reduce the loss of nephrin and podocin, and suppress the infiltration of renal interstitium by CD3-positive T cell and CD20-positive B cell. These results suggest that treatment with skimmin can significantly improve renal function and suppress the IgG deposition as well as the development of glomerular lesions in a rat model of membranous glomerulonephritis.

1. Introduction

Hydrangea paniculata (family Hydrangeaceae) possesses anti-inflammatory and antipyretic properties. Water extract of branches and stems of *Hydrangea paniculata* has been used to treat numerous kidney diseases for decades. Skimmin that belongs to coumarin family is a common chemical compound present in many medical plants, such as *Aegle marmelos* (L.) *Correa* and *Adina cordifolia* [1–3]. Skimmin is also present in *Hydrangea paniculata*, accounting for approximately 55% of the total constituents in the water extract of its branches and stems.

In our previous study, we demonstrated a renal protective activity for skimmin in a rat model of streptozotocin-induced diabetic nephropathy [4]. Skimmin treatment significantly decreased plasma creatinine, improved creatinine clearance, and reduced the incidence of glomerulosclerosis and tubulointerstitial injuries in animals following diabetic nephropathy induction. Downregulation of expression of TGFβ1 and TGFβ receptor I [4], which play an important role in renal fibrosis of end-stage renal disease, is one of the possible mechanisms underlying the renoprotective activity of skimmin.

Given the demonstrated activity of skimmin in protecting against renal injury in diabetic nephropathy, we hypothesize that skimmin may also have renoprotective effect in membranous nephropathy which is caused by immune complex localization in the subepithelial area of the glomerulus [5]. Inhibition of inflammatory mediators is one of the important target pathways for intervention of membranous nephropathy. In this study, we treated SD rats with cationic

bovine serum albumin (C-BSA) to create an animal model of membranous glomerulonephritis and investigated the therapeutic effect of skimmin in protecting against renal injury in this model. Specifically, we assessed how skimmin modulated changes in the renal function and albuminuria, kidney cell morphology, IgG deposition, and expression of cytokines such as IL-1β and IL-6 induced by C-BSA. We also analyzed the expression of nephrin and podocin to assess the podocyte injuries and the renal interstitial infiltration by B cells and T cells to understand involvement of immune system in skimmin's renoprotective action in membranous nephropathy.

2. Materials and Methods

2.1. Skimmin Preparation. Skimmin was provided by the Laboratory of Plant Natural Products, Institute of *Materia Medica*, Chinese Academy of Medical Sciences, which was prepared as follows. Air-dried stems of *H. paniculata* (5 kg) were powdered and extracted with H_2O (2 × 20 L, each for 2 h). The H_2O extract was passed through macroporous resin (D101, 5 kg) column and eluted with H_2O (6 L), 30% EtOH (9 L), 70% EtOH (9 L), and 95% EtOH (8 L). The 30% EtOH fraction (A) was dried in vacuum, and the residue (120 g) was subjected to silica gel column chromatography (200–300 mesh, 1.5 kg) and eluted with $CHCl_3$-MeOH-H_2O (80 : 20 : 2, 6 L) to obtain eight fractions (Fr A-1~A-8). The precipitate was formed from the Fr A-4 after concentration and then filtered. The solid was repeatedly recrystallized in MeOH to yield skimmin (10.2 g). The purity of the compound was >95%, as determined by HPLC.

2.2. Preparation of C-BSA. To prepare C-BSA, crystallized unmodified BSA was chemically cationized according to Border's method [6]. An anhydrous ethylenediamine (EDA, Sigma-Aldrich, Germany) solution was prepared by mixing 67 mL of EDA and 500 mL of distilled water. The pH was adjusted to 4.75 with 350 mL of 6 M HCl at 25°C. After addition of 1.8 g 1-ethyl-[(3-dimethylaminopropyl)-carbodiimide hydrochloride] (EDC, Sigma-Aldrich, Germany), 5 g native BSA (Amresco, Solon, USA) dissolved in 25 mL of distilled water was added to the EDA solution. With continuous stirring the reaction was continued for 120 min, before being stopped by adding 30 mL 4 M acetate buffer. The product was dialyzed 48 h against distilled water at 4°C, lyophilized, and stored at −80°C.

2.3. Animals. Female SD rats, 10 weeks old and weighing 160–180 g, were obtained from the Institute of Laboratory Animal Science, Chinese Academy of Medical Sciences, Beijing, China. Rats were maintained under a 12 h light/dark cycle at 25°C and a humidity of 60 ± 10%. Experiments were performed in accordance with the institutional regulations on the use of experimental animals. Experimental design followed the methods of Border et al. [6] and Mirshafiey et al. [7]. A total of 50 rats were randomly divided into five groups: normal vehicle treatment (N group), model (M group), low skimmin treatment at 15 mg/kg body weight (L group), and high skimmin treatment at 30 mg/kg body weight (H group). Mycophenolate Mofetil (MMF group) at 20 mg/kg was used as a positive control. Rats in the M, MMF, L, and H groups were injected subcutaneously with 0.5 mg incomplete Freund's adjuvant at day 1 to prevent autoimmunity, followed by injection of C-BSA (50 mg/kg, administered at 10 mg/mL in 0.01 MPBS, pH 7.4) through the tail vein every other day from days 8 to 36 to induce membranous glomerulonephritis. Rats in the N group were injected with saline every other day during the same time. From days 37 to 66, rats in the MMF, L, and H groups received daily intragastric MMF and skimmin (MMF group: 20 mg/kg; L group: 15 mg/kg; H group: 30 mg/kg), while rats in the N and M groups received daily intragastric saline. All animals were sacrificed on day 66.

All the animal experiments were approved by the Ethics Committee of Laboratory Animals of Peking Union Medical College (Beijing, China); the protocol was approved on, June, 15, 2011 (approval number 002463).

2.4. Blood and Urine Chemistry. Before sacrifice, blood was sampled from all animals through the eyes under anesthesia with diethyl ether. 24-hour urine collections were performed in each animal after placement in metabolic cage the day before blood sample collection. BUN, Ucr, and Scr were measured with the commercial kits (BHKT clinical reagent Co. LTD, Beijing, China). Creatinine clearance ratio (Ccr) was calculated according to the following formula:

$$\text{Ccr} = \text{Urinary creatinine } (\text{mg/mL}) \times \frac{\text{urine volume } (\text{mL/kg})}{\text{creatinine in plasma } (\text{mg/mL})}. \quad (1)$$

See [8].

2.5. Competitive ELISA of Rat Urinary Albumin Excretion. Urinary albumin excretion was calculated from albumin concentration of urine samples collected in metabolic cage for 24 h. Indirect ELISA was used to quantitatively measure urinary albumin concentrations. Briefly, the 96-well plate was coated with rat serum albumin (RSA, 1 μg/mL, 50 μL, Sigma, MO, USA) and then blocked. Following a thorough washing, 50 μL PBS-diluted rat urine or RSA standards (0–10 μg/mL) were added to the wells and incubated. Then 50 μL HRP conjugated sheep anti-rat albumin antibody (0.1 μg/mL, Bethyl, TX, USA) was added and the color was developed by TMB (3,3′,5,5″-tetramethylbenzidine). Urinary albumin excretion was expressed as mg/day.

2.6. Histological Examination. Kidney specimens were processed by light and immunofluorescence microscopic examination. For the light microscopy, the right kidneys from each animal were fixed in 10% phosphate-buffered formalin solution and embedded in paraffin. Sections of 2 μm thickness were cut and stained with hematoxylin and eosin (HE) and periodic acid-Schiff (PAS). To evaluate the glomerular hypercellularity, at least 10 glomeruli were examined for

each animal, the number of cells in each glomeruli (including endothelial cells, mesangial cells, and podocytes) was counted and average number was calculated; meanwhile, the incidence of glomerular basement membrane thickening or mesangial proliferation among 100 glomeruli was calculated too.

To assess the tubulointerstitial damage, a semiquantitative method of renal histology using a grading scale of 0–4 was applied: 0: normal; 1: lesions in <25% of the area; 2: lesions in 25% to 50% of the area; 3: lesions in >50% of the area; and 4: lesions involving the entire area [9, 10]. Tubular atrophy, dilation, casts, interstitial inflammation, and fibrosis were assessed in 10 kidney fields at a magnification of ×100.

For immunofluorescence microscopy, tissue blocks from the left kidney were instantaneously frozen in n-hexane precooled to −70°C, and 4 μm cryostat sections were stained with fluorescein isothiocyanate- (FITC-) conjugated anti-rat IgG. The degree of deposition of immune complex was calculated quantitatively on the basis of the staining intensity and distribution.

2.7. ELISA Analysis of IL-1β and IL-6 in Plasma. Plasma levels of IL-1β and IL-6 were measured by with ELISA kit following the manufacturer's instructions (R&D systems, USA). Briefly, a monoclonal antibody specific for IL-1β or IL-6 was precoated onto a microplate. The standards and test samples were then pipetted into the wells to allow binding of IL-1β or IL-6 to the immobilized antibodies. After washing away any unbound substances, an enzyme-linked polyclonal antibody specific for IL-1β or IL-6 was added to the wells. Following removal of unbound antibody-enzyme reagent through washing, a substrate solution was added to the wells and color was developed. The optical density of each well was measured at the wave length of 450 nm or 510 nm on a microreader (S190, Molecular Devices, USA). The concentration of IL-1β or IL-6 was accordingly calculated.

2.8. Immunohistochemistry. The expression of IgG, IL-1β, and IL-6 in kidney was assessed by the streptavidin-peroxidase-biotin (SP) immunohistochemical method [11–13]. The kidney tissue sections (4 μm) were made and were mounted onto immunohistochemical slides. After dehydration with xylene and alcohol, the antigen retrieval was accomplished. Sections were then incubated in a blocking solution of 10% normal goat serum diluted in PBS and incubated with polyclonal rabbit anti-rat IgG (Abcam, USA), IL-1β (Abcam, USA) and IL-6 (Abcam, USA), antibodies (1 : 200) for 2 h and then incubated for 10 min at room temperature with biotinylated goat anti-rabbit secondary antibody (1 : 500). After that, sections were exposed to streptavidin-biotin complex conjugated to HRP. Signals were then visualized with diaminobenzene (DAB) and observed at 200x magnification under a light microscope (Leica, Germany). Signals in three random fields on each slide were quantitated using Image-Pro Plus software (Bethesda, MD, USA). Results were expressed as percentage of positive area per glomerulus.

To understand whether skimmin had protective effect on podocytes, we evaluated the expression of nephrin and podocin in glomeruli by immunohistochemistry following the similar procedure described before. Monoclonal anti-nephrin (Santa Cruz, USA) and monoclonal antipodocin (Abcam, USA) were used, respectively.

To assess the distribution of B cell and T cell infiltration into the renal interstitium, immunohistochemistry with an anti-CD3 (Abcam, USA) antibody and an anti-CD20 antibody (Santa Cruze, USA) was used. The same immunohistochemistry procedures as mentioned before were followed.

2.9. Statistical Analysis. Data were expressed as the means ± standard deviation (S.D.) and analyzed by One-Way Analysis of Variance (One-Way-ANOVA) followed by and post hoc Bonferroni test. Pearson's correlation analysis was used to determine the relationship between IL-1β or IL-6 with the values of IgG deposition and the degree of tubulointerstitial damage. Difference was considered significant when $P < 0.05$ and $P < 0.01$.

3. Results

3.1. Effect of Skimmin on Renal Function. As shown in Table 1, C-BSA markedly caused severe deterioration of renal functions compared to the normal control. The average level of albuminuria increased from 0.22 (mg/day) to 5.64 (mg/day) dramatically (normal versus model, $P < 0.01$). Skimmin treatment at 15 mg/kg and 30 mg/kg decreased average albuminuria level by 13.5% ($P < 0.05$), and 36.0% ($P < 0.05$), respectively. MMF treatment at 20 mg/kg also decreased albuminuria level by 30.4% ($P < 0.05$). In the model group, levels of Scr and BUN were significantly higher than those in the normal control group (Table 1). Skimmin (30 mg/kg) treatment reduced BUN by 42.7% ($P < 0.05$) and Scr by 55.7% ($P < 0.05$), respectively, compared to model group. Compared to the model group, skimmin treatment (30 mg/kg) increased the Ucr by 51.6% ($P < 0.05$) and increased Ccr by 67.8% ($P < 0.05$). These biochemical analysis results indicated that skimmin at a dose of 30 mg/kg was effective in the protection against renal injury.

3.2. Morphological Changes. Shown in Figure 1 are light microscopic graphs (100x) of renal glomeruli and tubules in different groups of animals. As compared to vehicle controls (Normal group), C-BSA treatment produced numerous slightly enlarged renal glomeruli, capillary stenosis, and thickened capillary walls with scattered short subepithelial basement membrane projections (Model group). Treatment with 15 or 30 mg/kg skimmin reduced these C-BSA-induced morphological changes. The incidences of glomerular hypercellarity, glomerular basement membrane thickening or mesangial proliferation, and tubulointerstitial injuries were all significantly reduced in the skimmin treatment groups than in the model control ($P < 0.01$, Table 2).

Immunofluorescent microscopic investigation of glomeruli revealed deposits of immune complexes in the mesangial areas and along the capillary walls of all animals. But

Table 1: Renal function in the membranous glomerulonephritis model rats after treatment with the skimmin for 30 days.

Index	Sham control	Model control	Groups		
			MMF (20 mg/kg)	Skimmin (15 mg/kg)	Skimmin (30 mg/kg)
N	10	10	10	10	10
Body weight (g)	311.25 ± 18.15	293.65 ± 28.46	287.00 ± 28.79	284.50 ± 28.79	281.70 ± 20.00
Urine creatinine (mM)	4.34 ± 1.58	2.87 ± 1.17*	3.02 ± 1.74	3.00 ± 1.51	4.35 ± 1.10$^{\#}$
Blood urea nitrogen (mM)	7.53 ± 1.40	21.08 ± 17.30*	16.21 ± 10.13	22.25 ± 11.80	12.08 ± 10.09$^{\#}$
Serum creatinine (mM)	0.16 ± 0.10	1.22 ± 1.31*	0.98 ± 1.17	1.24 ± 0.91	0.54 ± 0.87$^{\#}$
Creatinine clearance (mL/min)	2.57 ± 0.01	1.43 ± 0.03*	1.26 ± 0.02	0.75 ± 0.05	2.40 ± 0.07$^{\#}$
Urinary albumin excretion (mg/day)	0.22 ± 0.15	5.64 ± 3.01**	3.93 ± 2.23$^{\#}$	4.88 ± 2.96$^{\#\#}$	3.61 ± 2.14$^{\#\#}$

$^{*}P < 0.05$, $^{**}P < 0.01$, versus normal control; $^{\#}P < 0.05$, $^{\#\#}P < 0.01$, versus model control, by One-Way-ANOVA followed by post hoc test.

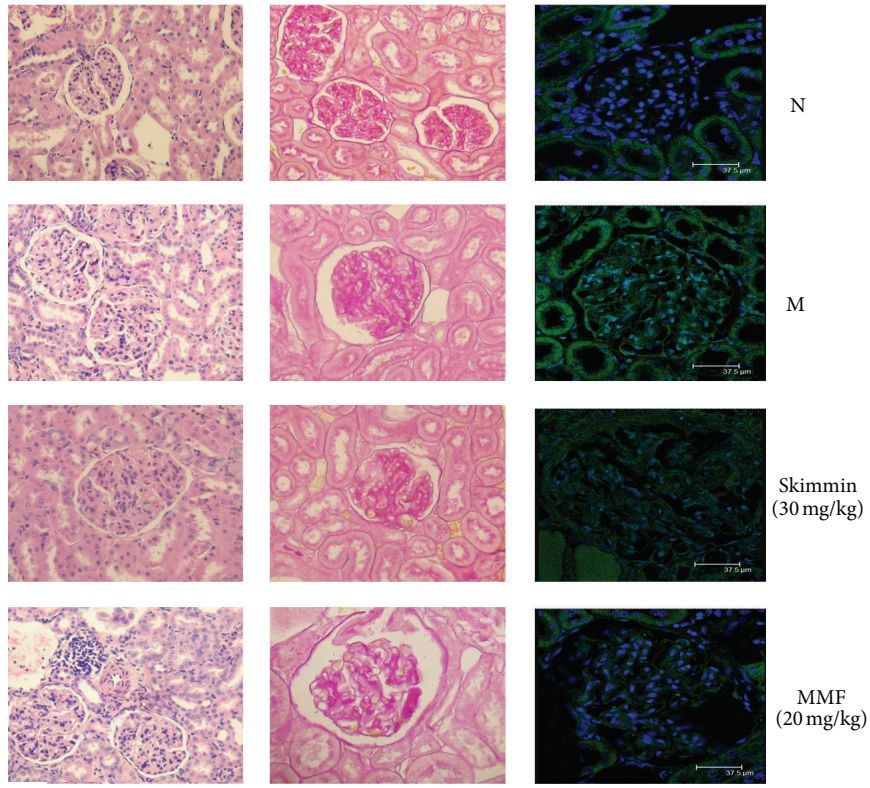

Figure 1: Representative images of HE-stained and PAS-stained kidneys and immunofluorescent microscopy of IgG deposition (100x).

Table 2: Light microscopic and immunofluorescent findings of kidney histological lesions.

Groups	*N*	Cell number per glomerulus	Case of mesangial proliferation (per 10 glomeruli)	Tubulointerstitial injury scores	IgG deposition (% positive area in glomerulus)
N	10	72.92 ± 12.52	0.30 ± 0.48	0	8.17 ± 3.52
M	10	99.28 ± 18.83**	4.73 ± 1.43**	1.20 ± 1.25**	45.86 ± 7.97**
MMF (20 mg/kg)	10	103.04 ± 21.69	3.40 ± 2.46	1.20 ± 0.76	21.99 ± 6.64$^{\#\#}$
Skimmin (15 mg/kg)	10	110.92 ± 29.38	1.10 ± 0.88$^{\#\#}$	1.27 ± 1.56	36.17 ± 4.76$^{\#\#}$
Skimmin (30 mg/kg)	10	81.80 ± 17.92$^{\#\#}$	1.20 ± 1.34$^{\#\#}$	0.33 ± 0.47$^{\#}$	26.00 ± 5.376$^{\#\#}$

Note: $^{**}P < 0.01$, versus normal control; $^{\#}P < 0.05$, $^{\#\#}P < 0.01$, versus model control, by One Way-ANOVA followed by post hoc test.

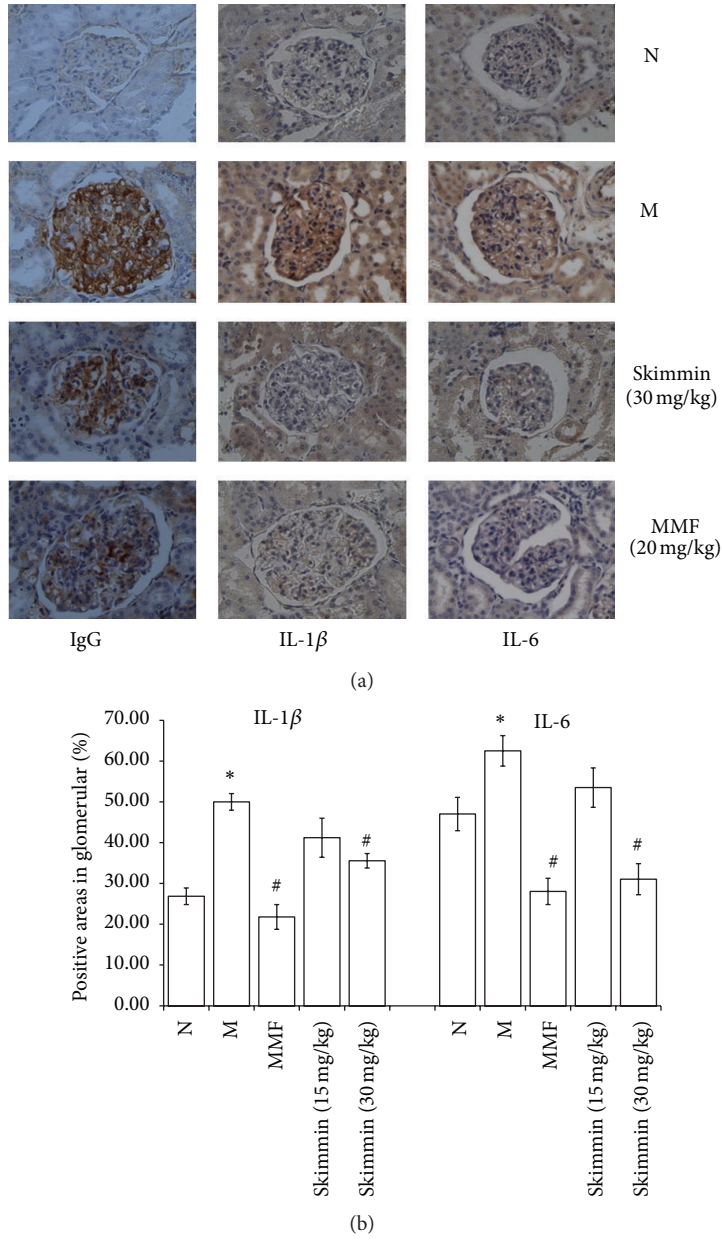

FIGURE 2: Immunohistochemical staining, showing the expression of IgG, IL-1β, and IL-6 (200x, designated by percentage of positive areas in glomerulus). $^{*}P < 0.05$; $^{**}P < 0.01$, versus normal control; $^{\#}P < 0.05$, $^{\#\#}P < 0.01$, versus model control, by One-Way-ANOVA followed by post-Hoc test.

the deposition was significantly less intense in skimmin and MMF treated animals than that in the vehicle controls; at the dose of 30 mg/kg, skimmin reduced the IgG positive staining area by 41% compared to model group ($P < 0.01$, Figure 1, Table 2).

3.3. Expression of IgG, IL-1β, and IL-6 by IHC and ELISA. As shown in Figure 2, immunohistochemistry demonstrated that C-BSA induction markedly increased the IgG accumulation and the expression of IL-1β and IL-6 (M group) in glomeruli compared with vehicle controls (N group) ($P < 0.05$). The IHC results on IgG accumulation in glomeruli were consistent with fluorescent microscopic results. Skimmin dose dependently decreased the expression of IL-1β and IL-6 in glomeruli ($P < 0.05$). However, skimmin at 30 mg/kg was less potent than MMF at 20 mg/kg.

ELISA analysis showed that plasma concentrations of IL-1β and IL-6 were significantly decreased in the high (30 mg/kg) skimmin and MMF treatment groups, as compared with the model control groups ($P < 0.05$, Figure 3).

3.4. Changes in Nephrin and Podocin Expression in the Glomeruli. Changes in expression of nephrin and podocin related to podocyte injuries were examined by immunohistochemical staining. As shown in Figure 4, immunoreactivity for nephrin and podocin in the glomerular regions of rats in

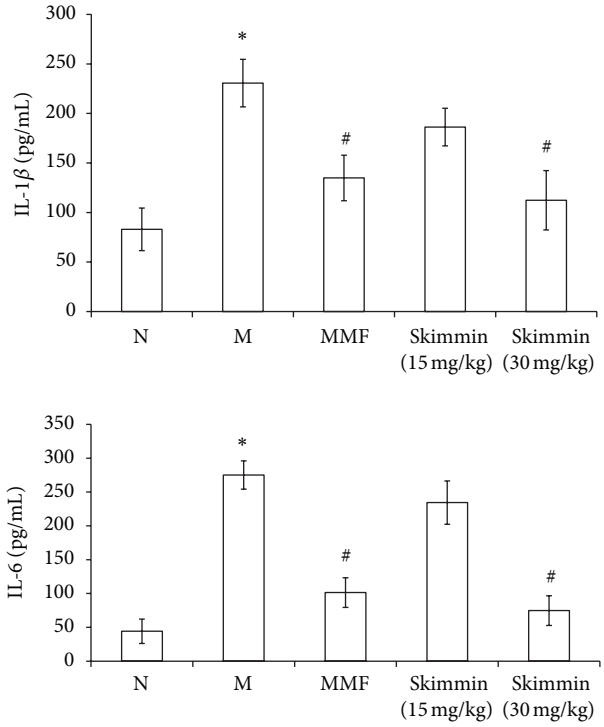

Figure 3: ELISA presented IL-1β and IL-6 levels in plasma of skimmin-treated rats were reduced significantly than the model control rats. $^{*}P < 0.01$ as compared with the normal rats; $^{\#}P < 0.05$ as compared with model control rats.

the model group was significantly decreased, and skimmin (30 mg/kg) and MMF treatment effectively ameliorated the C-BSA-induced aberration in the expression of nephrin and podocin ($P < 0.05$).

3.5. CD20 Positive B Cell and CD3 Positive T Cell Infiltration of Interstitium. To further characterize lymphocyte infiltration of the renal interstitium, we performed immunohistochemistry to detect the distribution of CD3 mature T lymphocyte and CD20 mature B lymphocyte in the interstitium. Obvious focal or diffuse interstitial CD20 positive B cell infiltration was seen in the model group but not in the normal control group; in the MMF and skimmin (30 mg/kg) treatment groups, weak and moderate CD20 positive staining was detected, suggesting both MMF and skimmin were able to reduce the CD20 mature B cell infiltration significantly ($P < 0.05$, Figure 5).

Under microscopic view, small aggregates of CD3 positive T-cells were detectable in the renal interstitium in the model group (Figure 5). In the MMF and skimmin (30 mg/kg) treatment groups, positive CD3 cells was less aggregated were found, and most of them were singly present in the interstitium, suggesting that both MMF and skimmin could ameliorate the CD3 T cell infiltration ($P < 0.05$, Figure 5).

3.6. Correlation between IL-1β and IL-6 with IgG Deposition and the Degree of Tubulointerstitial Damage. Finally, we examined the correlation of IL-6 and IL-1β as inflammatory markers with the values of IgG deposition and the degree of tubulointerstitial damage. A positive correlation between IgG deposition and levels of IL-6 or IL-1β was demonstrated in all animals ($P < 0.01$); similar correlation was also observed between the degree of tubulointerstitial damage and levels of IL-6 or IL-1β (Figure 6). Together, these results suggested that changes in IL-6 or IL-1β concentrations are closely related to the pathogenesis of membranous glomerulonephritis.

4. Discussion

Membranous glomerulonephropathy is the most frequent cause of nephrotic syndrome in adults [14, 15], but currently there is no effective medicines. The major pathological characteristic about membranous glomerulonephropathy is the presence of subepithelial immunoglobulin-containing deposits along the glomerular basement membrane, which was found in the model group in the current study. In the clinical practice, angiotensin converting enzyme (ACE) inhibition or angiotensin receptor blockade is still most common strategy against membranous nephropathy or, rather, more aggressive treatment using glucocorticoids and alkylating agents [5]. Recent progress in the molecular pathways of inflammation and immunologic regulation holds the promise of offering futuristic alternatives and/or supplements to the standard regimen, such as inhibition of proinflammatory mediators and T and B cell proliferation and activation; besides, proteinuria control and suppressing activation of TGFβ-smad pathway are also potential alternative strategies.

The present study evaluated the therapeutic effect of skimmin on glomerulonephritis in a rat model of C-BSA induced membranous glomerulonephritis. C-BSA administration dramatically increased BUN, Scr, and albuminuria, caused morphologically structural changes and increased IgG deposition and expression of some cytokines, such as IL-1β and IL-6. Skimmin treatment suppressed all these abnormalities significantly.

In the current study, skimmin treatment, especially at a high dose, significantly alleviated the tubulointerstitial injuries ($P < 0.01$). It was able to reduce the albumin content in the urine significantly. Previous studies have demonstrated that, under proteinuric conditions, albumin is the major protein in the ultrafiltrate and nephrotic urine, which plays an active role in the pathogenesis of chronic tubulointerstitial damage [16–18]. We assume that albuminuria reduction is one of mechanisms by which skimmin alleviates tubulointerstitial injuries.

Podocytes function to maintain the permeability of the glomerular filtration barrier; their dysfunction and depletion contribute greatly to albuminuria [19, 20]. Studies have established an association between the development of progressive kidney disease and podocyte failure [21, 22], as seen in gene mutations of podocyte-specific proteins leading to nephrotic syndrome, renal injury, and failure [23–27]. Several molecules synthesized by podocytes, such as podocin, nephrin, CD2-associated protein (CD2AP), NcK, ZO-1, and actinin [27, 28], play key roles in the maintaining of integrity of the glomerular filtration barrier. In the current study, low

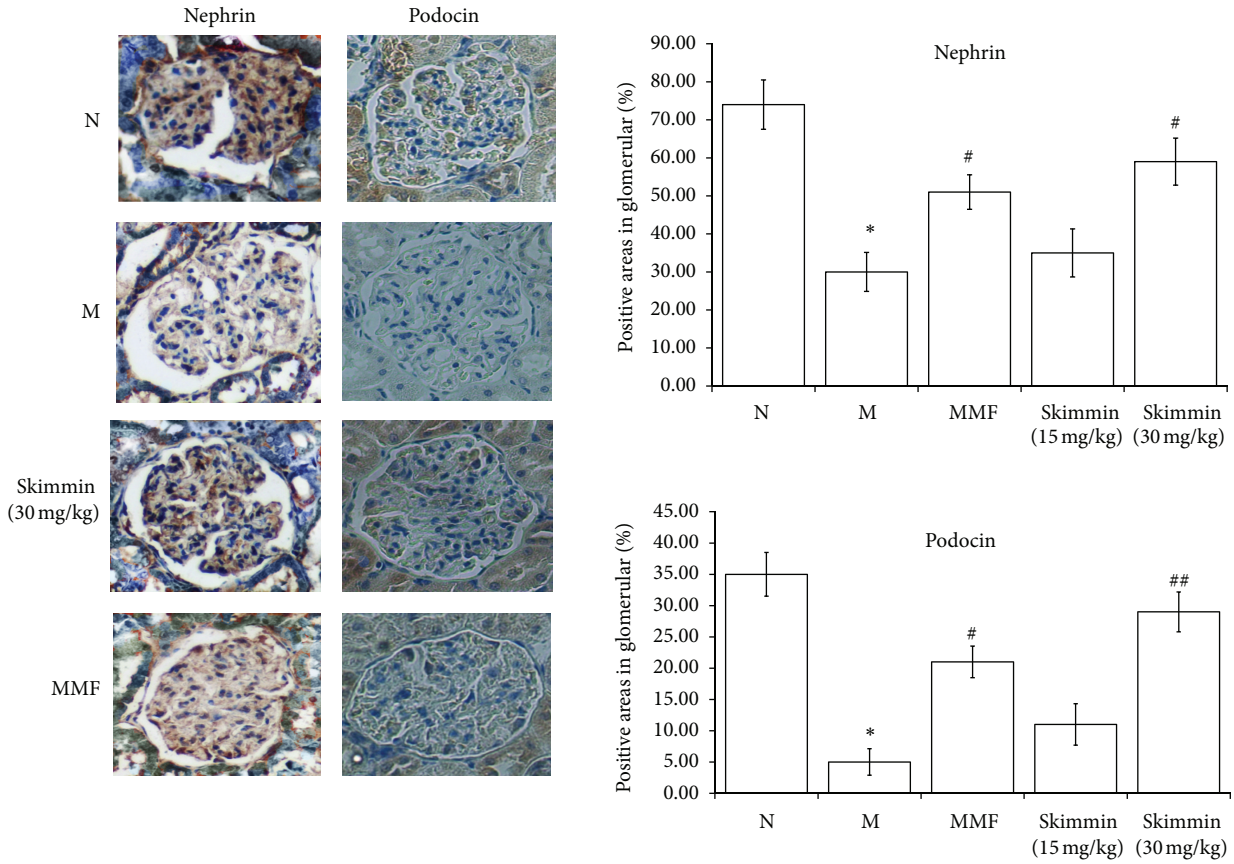

Figure 4: Expression and quantitation analysis of podocin and nephrin in the glomeruli, (200x, designated by percentage of positive areas in glomerulus). $^{*}P < 0.01$ as compared with the normal rats; $^{\#}P < 0.05$, $^{\#\#}P < 0.01$ as compared with model control rats.

expression of podocyte biomarkers (nephrin and podocin) was observed in the glomeruli of animals in the model group, in consistency with significantly higher albuminuria in the model group. Skimmin treatment significantly inhibited the loss of nephrin and podocin expression in a dose dependent manner. This suggests that skimmin protection of podocytes may partially contribute to its albuminuria-lowering activity.

The effect that skimmin suppresses glomerulonephritis might be also attributable to its ability to inhibit the expression of some pro-inflammatory cytokines. Both IL-1β and IL-6 are important cytokines which are essential mediators of immune response and inflammatory reactions in patients with chronic renal failure [29]. In the current study, by correlation analysis, we prove that IL-1β and IL-6 expressions are positively correlated with tubulointerstitial injuries and IgG deposition. Possibly, skimmin may exhibit its anti-inflammatory effect and subsequent renoprotection through inhibiting IL-1β and IL-6.

Focal or diffuse interstitial B cell infiltration was detected by immunostaining with anti-CD20 antibody in the model group. By contrast, this infiltration was less significant in the skimmin treatment groups. CD3 positive T cell infiltration was much weaker than CD20 B cell infiltration in the renal interstitium in the current study. B cell and T cell infiltration is important pathological characteristics in membranous nephritis [30, 31]. By suppressing T cell and B cell infiltration, skimmin may ameliorate the severity of inflammation and slow down the development of renal dysfunction.

Membranous glomerulonephritis is an antibody-mediated disease induced by deposits of immunoglobulins and complement components on the subepithelial layer of the glomerular capillary wall [32]. This immune deposition promotes injury to the glomerular filtering barrier, proteinuria, and eventual renal failure [33]. Results in experimental membranous glomerulonephritis have shown that the inhibition of B cell function is associated with beneficial effects on proteinuria [34] and human studies clearly demonstrated that the inhibition of B cells with alkylating agents induces remission of the nephrotic syndrome [35]. In B cell development, IL-6 has been shown to induce terminal maturation of B lymphocytes into antibody producing plasma cells [36, 37]. Immunohistochemistry results in the present study suggest that skimmin may inhibit B cell maturation and function by decreasing IL-6 levels in kidneys, leading to beneficial effect on membranous glomerulonephritis.

MMF has been used successfully as an immunosuppressive medication in lupus nephritis and other primary glomerular diseases [38]. Lots of experimental animal models of nephritis and clinical trials have proved that MMF could

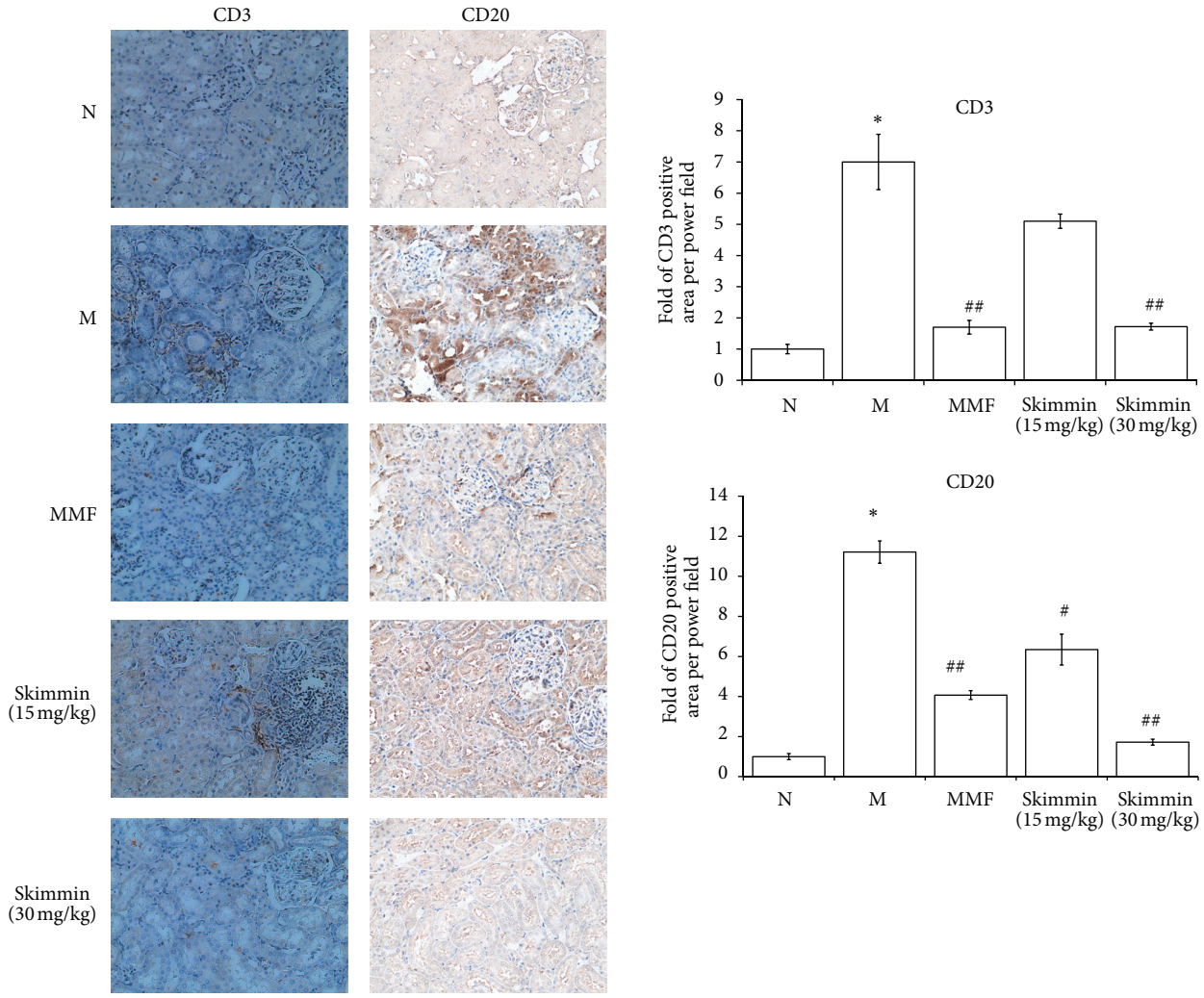

FIGURE 5: Representation and quantification of the infiltrates by digital morphometry, determined as the percentage of area staining positive. Arrows refer to CD3 positive T cells, 200x. $^{*}P < 0.01$ as compared with the normal rats; $^{\#}P < 0.05$, $^{\#\#}P < 0.01$ as compared with model control rats.

slow down the progress of several glomerular diseases, partially from inhibiting both mesangial cell proliferation and lymphocyte migration into renal tissue [39, 40]. Such inhibition results from impaired glycosylation, which, in turn, leads to alterations in adhesion molecule functioning [41]. In the current study, as a positive control, at 20 mg/kg dosage, MMF shows similar beneficial effect on membranous nephropathy as skimmin, which gives us more confidence to further explore the skimmin's potential usage in the clinical treatment.

5. Conclusions

In summary, despite the use of *H. paniculata* as an anti-inflammatory agent in Chinese traditional medicine for long, its renoprotective activity and the underlying mechanism in the membrane glomerulonephritis have not been established. This study is the first to report the effects of skimmin, a major constituent present in *H. paniculata*, on IL-1β and IL-6 protein expression in membranous glomerulonephritis. Our observations suggest that skimmin is a promising therapeutic agent for glomerulonephritis.

Conflict of Interests

The authors have no declaration of interests to report.

Authors' Contribution

Sen Zhang and Hongqi Xin contributed equally to this paper.

Acknowledgment

This study was supported by the Major Special Program of National Science and Technology in Twelfth Five-year Plan, China; the number is 2012ZX09301002-006.

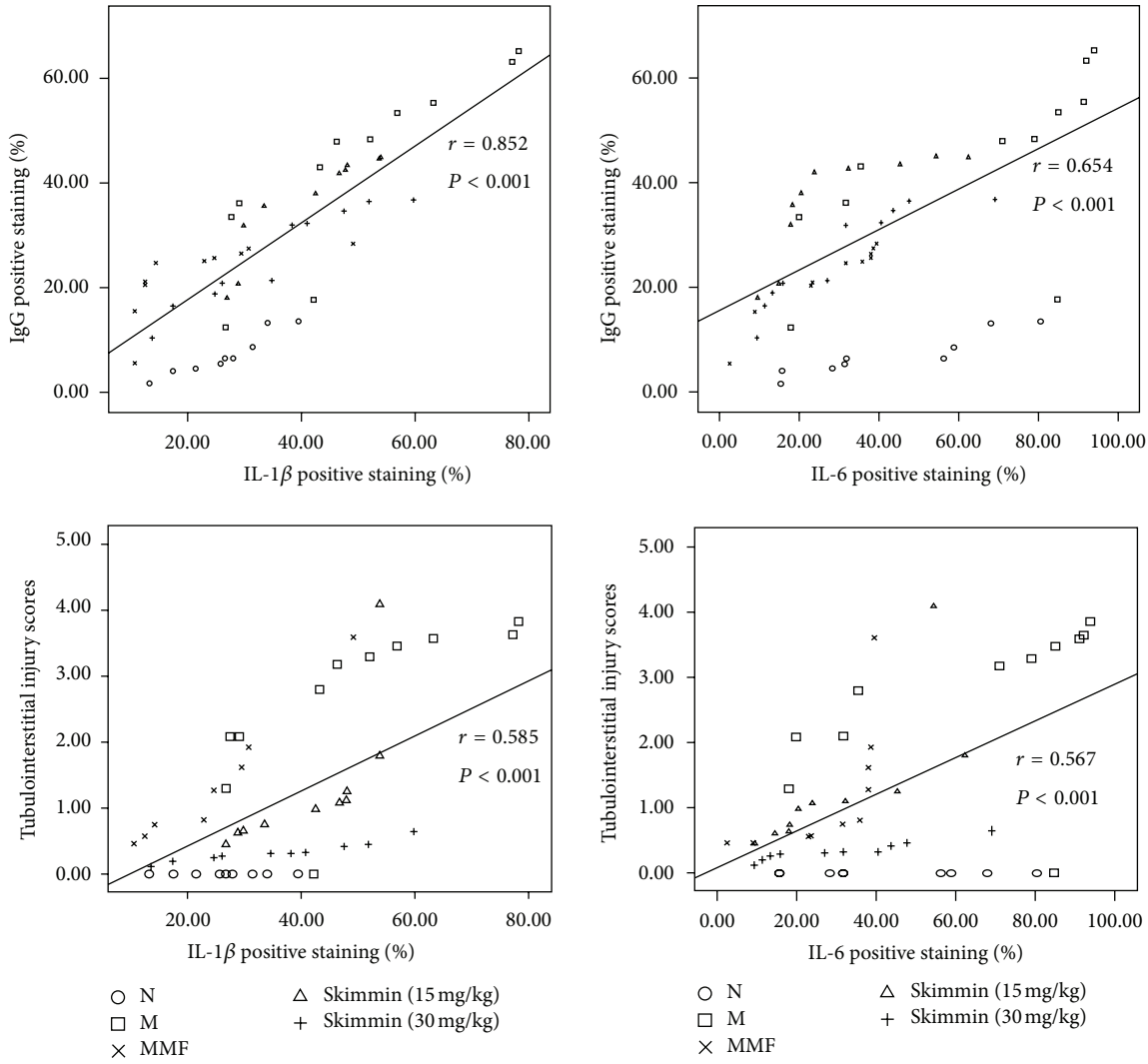

Figure 6: Correlation between IL-1β and IL-6 with the values of IgG deposition and the degree of tubulointerstitial damage.

References

[1] K. Doi, T. Kojima, M. Makino, Y. Kimura, and Y. Fujimoto, "Studies on the constituents of the leaves of Morus alba L," *Chemical and Pharmaceutical Bulletin*, vol. 49, no. 2, pp. 151–153, 2001.

[2] K. Kai, B.-I. Shimizu, M. Mizutani, K. Watanabe, and K. Sakata, "Accumulation of coumarins in *Arabidopsis thaliana*," *Phytochemistry*, vol. 67, no. 4, pp. 379–386, 2006.

[3] P. F. Iqbal, A. R. Bhat, and A. Azam, "Antiamoebic coumarins from the root bark of *Adina cordifolia* and their new thiosemicarbazone derivatives," *European Journal of Medicinal Chemistry*, vol. 44, no. 5, pp. 2252–2259, 2009.

[4] S. Zhang, J. Yang, H. Li et al., "Skimmin, a coumarin, suppresses the streptozotocin-induced diabetic nephropathy in wistar rats," *European Journal of Pharmacology*, vol. 692, no. 1–3, pp. 78–83, 2012.

[5] A. V. Kshirsagar, P. H. Nachman, and R. J. Falk, "Alternative therapies and future intervention for treatment of membranous nephropathy," *Seminars in Nephrology*, vol. 23, no. 4, pp. 362–372, 2003.

[6] W. A. Border, H. J. Ward, E. S. Kamil, and A. H. Cohen, "Induction of membranous nephropathy in rabbits by administration of an exogenous cationic antigen," *Journal of Clinical Investigation*, vol. 69, no. 2, pp. 451–461, 1982.

[7] A. Mirshafiey, B. Rehm, M. Sotoude, A. Razavi, R. S. Abhari, and Z. Borzooy, "Therapeutic approach by a novel designed anti-inflammatory drug, M2000, in experimental immune complex glomerulonephritis," *Immunopharmacology and Immunotoxicology*, vol. 29, no. 1, pp. 49–61, 2007.

[8] E. J. Sohn, C.-S. Kim, Y. S. Kim et al., "Effects of magnolol (5,5′-diallyl-2,2′-dihydroxybiphenyl) on diabetic nephropathy in type 2 diabetic Goto-Kakizaki rats," *Life Sciences*, vol. 80, no. 5, pp. 468–475, 2007.

[9] I. Pörsti, M. Fan, P. Kööbi et al., "High calcium diet down-regulates kidney angiotensin-converting enzyme in experimental renal failure," *Kidney International*, vol. 66, no. 6, pp. 2155–2166, 2004.

[10] P. Li, L. L. Ma, R. J. Xie et al., "Treatment of 5/6 nephrectomy rats with sulodexide: a novel therapy for chronic renal failure," *Acta Pharmacologica Sinica*, vol. 33, no. 5, pp. 644–651, 2012.

[11] M. Sugiyama, K. Kinoshita, K. Kishimoto et al., "Deletion of IL-18 receptor ameliorates renal injury in bovine serum albumin-induced glomerulonephritis," *Clinical Immunology*, vol. 128, no. 1, pp. 103–108, 2008.

[12] Y. Fu, C. Xie, J. Chen et al., "Innate stimuli accentuate end-organ damage by nephrotoxic antibodies via Fc receptor and TLR stimulation and IL-1/TNF-α production," *Journal of Immunology*, vol. 176, no. 1, pp. 632–639, 2006.

[13] S. Yung, R. C. W. Tsang, Y. Sun, J. K. H. Leung, and T. M. Chan, "Effect of human anti-DNA antibodies on proximal renal tubular epithelial cell cytokine expression: implications on tubulointerstitial inflammation in lupus nephritis," *Journal of the American Society of Nephrology*, vol. 16, no. 11, pp. 3281–3294, 2005.

[14] A. Segarra, M. Praga, N. Ramos et al., "Successful treatment of membranous glomerulonephritis with rituximab in calcineurin inhibitor-dependent patients," *Clinical Journal of the American Society of Nephrology*, vol. 4, no. 6, pp. 1083–1088, 2009.

[15] S. Aaltonen and E. Honkanen, "Outcome of idiopathic membranous nephropathy using targeted stepwise immunosuppressive treatment strategy," *Nephrology Dialysis Transplantation*, vol. 26, no. 9, pp. 2871–2877, 2011.

[16] M. M. Van Timmeren, M.-L. Gross, W. Hanke et al., "Oleic acid loading does not add to the nephrotoxic effect of albumin in an amphibian and chronic rat model of kidney injury," *Nephrology Dialysis Transplantation*, vol. 23, no. 12, pp. 3814–3823, 2008.

[17] H. Birn and E. I. Christensen, "Renal albumin absorption in physiology and pathology," *Kidney International*, vol. 69, no. 3, pp. 440–449, 2006.

[18] M. Abbate, C. Zoja, and G. Remuzzi, "How does proteinuria cause progressive renal damage?" *Journal of the American Society of Nephrology*, vol. 17, no. 11, pp. 2974–2984, 2006.

[19] B. Zhang, S. Xie, W. Shi, and Y. Yang, "Amiloride off-target effect inhibits podocyte urokinase receptor expression and reduces proteinuria," *Nephrology, Dialysis, Transplantation*, vol. 27, no. 5, pp. 1746–1755, 2012.

[20] A. Fukuda, L. T. Wickman, M. P. Venkatareddy et al., "Angiotensin II-dependent persistent podocyte loss from destabilized glomeruli causes progression of end stage kidney disease," *Kidney International*, vol. 81, no. 1, pp. 40–55, 2012.

[21] D. J. Davies, A. Messina, C. M. Thumwood, and G. B. Ryan, "Glomerular podocytic injury in protein overload proteinuria," *Pathology*, vol. 17, no. 3, pp. 412–419, 1985.

[22] H. Pavenstädt, W. Kriz, and M. Kretzler, "Cell biology of the glomerular podocyte," *Physiological Reviews*, vol. 83, no. 1, pp. 253–307, 2003.

[23] J.-L. R. Michaud and C. R. J. Kennedy, "The podocyte in health and disease: insights from the mouse," *Clinical Science*, vol. 112, no. 5-6, pp. 325–335, 2007.

[24] S. Dittrich, K. Kurschat, I. Dähnert, M. Vogel, C. Müller, and P. E. Lange, "Cyanotic nephropathy and use of non-ionic contrast agents during cardiac catherization in patients with cyanotic congenital heart disease," *Cardiology in the Young*, vol. 10, no. 1, pp. 8–14, 2000.

[25] H. Lu, G. Kapur, T. K. Mattoo, and W. D. Lyman, "Hypoxia decreases podocyte expression of slit diaphragm proteins," *International Journal of Nephrology and Renovascular Disease*, vol. 5, pp. 101–107, 2012.

[26] T. Nakatsue, H. Koike, G. D. Han et al., "Nephrin and podocin dissociate at the onset of proteinuria in experimental membranous nephropathy," *Kidney International*, vol. 67, no. 6, pp. 2239–2253, 2005.

[27] K. Tryggvason, T. Pikkarainen, and J. Patrakka, "Nck links nephrin to actin in kidney podocytes," *Cell*, vol. 125, no. 2, pp. 221–224, 2006.

[28] P. Fauchald, D. Albrechtsen, T. Leivestad, P. Pfeffer, T. Talseth, and A. Flatmark, "Renal replacement therapy in patients over 60 years of age," *Transplantation Proceedings*, vol. 20, no. 3, pp. 432–433, 1988.

[29] J. Rysz, M. Banach, A. Cialkowska-Rysz et al., "Blood serum levels of IL-2, IL-6, IL-8, TNF-alpha and IL-1beta in patients on maintenance hemodialysis," *Cellular & Molecular Immunology*, vol. 3, no. 2, pp. 151–154, 2006.

[30] F. Heller, M. T. Lindenmeyer, C. D. Cohen et al., "The contribution of B cells to renal interstitial inflammation," *American Journal of Pathology*, vol. 170, no. 2, pp. 457–468, 2007.

[31] H. Hopfer, J. Holzer, S. Hünemörder et al., "Characterization of the renal CD^{4+} T-cell response in experimental autoimmune glomerulonephritis," *Kidney International*, vol. 82, no. 1, pp. 60–71, 2012.

[32] D. Kerjaschki and M. G. Farquhar, "Immunocytochemical localization of the Heymann nephritis antigen (GP330) in glomerular epithelial cells of normal Lewis rats," *Journal of Experimental Medicine*, vol. 157, no. 2, pp. 667–686, 1983.

[33] P. Ronco and H. Debiec, "New insights into the pathogenesis of membranous glomerulonephritis," *Current Opinion in Nephrology and Hypertension*, vol. 15, no. 3, pp. 258–263, 2006.

[34] L. Biancone, G. Andres, H. Ahn, C. DeMartino, and I. Stamenkovic, "Inhibition of the CD40-CD40ligand pathway prevents murine membranous glomerulonephritis," *Kidney International*, vol. 48, no. 2, pp. 458–468, 1995.

[35] C. Ponticelli, P. Zucchelli, P. Passerini et al., "A 10-year follow-up of a randomized study with methylprednisolone and chlorambucil in membranous nephropathy," *Kidney International*, vol. 48, no. 5, pp. 1600–1604, 1995.

[36] K. Takatsu, "Cytokines involved in B-cell differentiation and their sites of action," *Proceedings of the Society for Experimental Biology and Medicine*, vol. 215, no. 2, pp. 121–133, 1997.

[37] S. Chen-Kiang, "Regulation of terminal differentiation of human B-cells by IL-6," *Current Topics in Microbiology and Immunology*, vol. 194, pp. 189–198, 1994.

[38] A. S. Appel and G. B. Appel, "An update on the use of mycophenolate mofetil in lupus nephritis and other primary glomerular diseases," *Nature Clinical Practice Nephrology*, vol. 5, no. 3, pp. 132–142, 2009.

[39] L. Senthil Nayagam, A. Ganguli, M. Rathi et al., "Mycophenolate mofetil or standard therapy for membranous nephropathy and focal segmental glomerulosclerosis: a pilot study," *Nephrology Dialysis Transplantation*, vol. 23, no. 6, pp. 1926–1930, 2008.

[40] C. K. Fujihara, D. M. A. C. Malheiros, I. D. L. Noronha, G. De Nucci, and R. Zatz, "Mycophenolate mofetil reduces renal injury in the chronic nitric oxide synthase inhibition model," *Hypertension*, vol. 37, no. 1, pp. 170–175, 2001.

[41] I. A. Hauser, L. Renders, H.-H. Radeke, R. B. Sterzel, and M. Goppelt-Struebe, "Mycophenolate mofetil inhibits rat and human mesangial cell proliferation by guanosine depletion," *Nephrology Dialysis Transplantation*, vol. 14, no. 1, pp. 58–63, 1999.

Hindawi Publishing Corporation
Evidence-Based Complementary and Alternative Medicine
Volume 2013, Article ID 751658, 17 pages
http://dx.doi.org/10.1155/2013/751658

Review Article

Updates on Antiobesity Effect of *Garcinia* Origin (−)-HCA

Li Oon Chuah,[1] Wan Yong Ho,[2] Boon Kee Beh,[3] and Swee Keong Yeap[4]

[1] *School of Industrial Technology, University Science Malaysia, 11800 Penang, Malaysia*
[2] *School of Biomedical Sciences, The University of Nottingham Malaysia Campus, Jalan Broga, 43300 Semenyih, Selangor, Malaysia*
[3] *Department of Bioprocess Technology, Faculty of Biotechnology and Biomolecular Sciences, University Putra Malaysia, 43400 Serdang, Selangor, Malaysia*
[4] *Institute of Bioscience, University Putra Malaysia, 43300 Serdang, Selangor, Malaysia*

Correspondence should be addressed to Swee Keong Yeap; skyeap2005@gmail.com

Received 15 June 2013; Accepted 7 July 2013

Academic Editor: Vincenzo De Feo

Garcinia is a plant under the family of Clusiaceae that is commonly used as a flavouring agent. Various phytochemicals including flavonoids and organic acid have been identified in this plant. Among all types of organic acids, hydroxycitric acid or more specifically (−)-hydroxycitric acid has been identified as a potential supplement for weight management and as antiobesity agent. Various *in vivo* studies have contributed to the understanding of the anti-obesity effects of *Garcinia*/hydroxycitric acid via regulation of serotonin level and glucose uptake. Besides, it also helps to enhance fat oxidation while reducing *de novo* lipogenesis. However, results from clinical studies showed both negative and positive antiobesity effects of *Garcinia*/hydroxycitric acid. This review was prepared to summarise the update of chemical constituents, significance of *in vivo*/clinical anti-obesity effects, and the importance of the current market potential of *Garcinia*/hydroxycitric acid.

1. Introduction

The world is in health transition. Infection as a major cause of suffering and death is giving way to new epidemics of noncommunicable disorders such as cancer, cardiovascular diseases, and diabetes, which continue to plague the world at an alarming rate [1]. A trend of increasing prevalence of obesity and obesity-related comorbidity and mortality was observed over the last few decades [2]. The International Association of the Study of Obesity (IASO) reported on the country rankings in terms of percentage global prevalence of adult obesity (BMI $\geq 30\,kg/m^2$) in the year of 2012, where Tonga ranks first with 56.0% obese adults (46.6% of obese male and 70.3% of obese female). In the United States, IASO reported that 35.5% of men and 35.8% women were obese (BMI ≥ 30) [1, 3]. Overweight and obesity are diagnosed zbased on the body mass index (BMI), which is defined as quotient of body weight (kg) over the square of stature (m^2). According to the World Health Organization (WHO) standard, overweight subjects are diagnosed with BMI values in the range of 25–29.99. Obesity itself, defined as BMI ≥ 30, is associated with several chronic and debilitating health problems including hyperlipidemia, hypertension, coronary heart disease, diabetes, cancer, disease of the gall bladder, osteoarthritis, shortage of breath, abnormal dilation of the veins, backache, and even psychological problems [2, 4].

There are a few drugs in the market to ameliorate or prevent obesity, but there are costs, efficacy, and side effects to be considered. For example, the currently available pharmacological agents, Sibutramine, Rimonabant, Orlistat, and Phentermine which are licensed for weight reduction therapy, appear to possess some adverse effects [5–7]. Phentermine, for instance, has been reported to cause dry mouth, insomnia, headache, dizziness, fatigue, and palpitation [6, 7]. In year 2010, FDA had announced the market withdrawal of Meridia (Sibutramine) due to its risk of serious cardiovascular events [6, 7]. Natural products and plant-based dietary supplements have been used by people for centuries. Evidence is starting to emerge to shed light on the consumption of herbs as an effective strategy for disease treatment and health maintenance. Several ethnobotanical studies have reported the bioprospecting surveys on the positive application of herbs

Table 1: Comparison of *G. cambogia*, *G. atroviridis*, and *G. indica* [9, 11, 13, 44].

Species	Common name	Origin	Feature
G. cambogia	Asam Gelugor	India: found commonly in the evergreen forests of Western Ghats, from Konkan southward to Travancore, and in the Shola forests of Nilgiri.	Small- or medium-sized tree with a rounded crown and horizontal or drooping branches, under the family of Guttiferae. Its fruits are ovoid, about 5 cm in diameter, yellow or red when ripe with six to eight grooves, enclosing six to eight seeds, and are edible.
G. atroviridis	Asam Gelugor	Southeast Asia	Small- or medium-sized fruit tree, with drooping branches and ovoid fruits. The fruits are bright orange-yellow when ripe, globose with 12–16 grooves, about 7–10 cm in diameter, and fluted with a firmly textured outer rind and a rather thin and translucent pulp surrounding the seeds.
G. indica	Kokum	India: the tropical rain forests of Western Ghats, from Konkan southward to Mysore, Coorg, and Wayanad	Slender evergreen tree with drooping branches. Its fruits are globose or spherical, 2–4 cm in diameter, dark purple when ripe with five to eight large seeds surrounded.

in the treatments for obesity [8]. *Garcinia* has been used for centuries in Asian countries for culinary purposes as a condiment and flavoring agent in place of tamarind or lemon and to make meals more filling [9, 10]. Besides its use as a flavouring agent, the dried rind of *G. cambogia* combined with salt and other organic acids can help to lower the pH and thus provides a bacteriostatic effect in curing fish. *G. cambogia* contains large amounts of hydroxycitric acid (HCA). Similar to *G. cambogia*, *G. atroviridis* and *G. indica* also contain significant HCA content and are sometimes used interchangeably with *G. cambogia* in food preparation. The different features among these three different types of *Garcinia* are summarised in Table 1 [9, 11–14].

A myriad of health effects have been attributed to *Garcinia* (including *G. cambogia, G. atroviridis*, and *G. indica*), such as antiobesity effects [15–17], antiulcerogenic [18–20], antioxidative [21–24], antidiabetes [25], antimicrobial [22, 26–28], antifungal [29], anti-inflammatory [30, 31], and anticancer effects [22, 32–34]. In particular, the antiobesity effects of *Garcinia* or more specifically of its HCA content have been elucidated with unprecedented clarity over the last few decades. Besides its efficacy in the reduction of body weight and food intake, *Garcinia*/HCA has been proven to be beneficial in ameliorating obesity-related complications such as inflammation, oxidative stress, and insulin resistance [21]. The results obtained from several studies supported the positive effects of HCA administration alone or in combination with other ingredients on body weight loss, reduced food intake, increased fat oxidation, or energy expenditure (EE) [16, 17, 35–39] whereas some studies did not [40–42].

In spite of the vastly reported prominent role of HCA in inducing satiety, reduced energy intake and weight gain, and improved blood parameters and substrate oxidation, controversial results regarding its efficacy and safety as an antiobesity dietary supplement had also been reported. Evidence from the *in vitro*, *in vivo*, and clinical trials on the safety of *Garcinia*/HCA as a dietary supplement for treating obesity had been extensively reviewed [43]. However, the efficacy of *Garcinia*/HCA remains the subject of debate. Despite the previously stated issues, on conclusive evidence for HCA's efficacy in promoting weight loss and suppressing food intake, the marketing of a plethora of over-the-counter slimming aids containing HCA has taken place. The aim of this review is to critically assess the evidence from a very broad range of reports, rigorous clinical trials, systematic reviews, and meta-analyses on the efficacy and potential of *Garcinia*/HCA as an antiobesity dietary supplement.

2. Uses in Traditional Medical Systems

Botanical dietary supplements usually contain a complex mixture of phytochemicals which have additive or synergistic interactions. Aside from its use as a preservative and as a condiment in cuisine, *Garcinia* extract has been used in the traditional Ayurvedic medical system [9, 13]. A decoction of *G. cambogia* is given as purgative in the treatment of intestinal worms and other parasites, for bilious digestive conditions, for dysentery, rheumatism, and in the treatment of tumours. Less commonly, extracts are employed as cardiotonics to treat angina. In veterinary medicine, it is used as a rinse for diseases of the mouth in cattle [12, 77]. The fruit rind is used in rickets and enlargement of spleen and to heal bone fractures [13]. In Southeast Asian folkloric medicine, a decoction of *G. atroviridis* (leaves and roots) is sometimes used for the treatment of cough, dandruff, earache, stomach pains associated with pregnancy, and throat irritation [49]. The dried fruit of *G. atroviridis* is used for improving blood circulation, for the treatment of coughs, as a laxative, and as a expectorant. The fruit is used in a lotion with vinegar to rub over the abdomen of women after confinement [9]. Fruit of *G. indica* is antiscorbutic, cholagogue, cooling, antibilious, emollient, and demulcent. The anthelmintic properties of the fruit of *G. indica* contributed to its use in haemorrhoids, dysentery, tumor, pains, and heart complaints. Bilious affected sites are treated with syrup from the fruit juice. Kokum butter is astringent and demulcent and is used in diarrhea and dysentery. It is also applied externally for ulcerations, sinuses, fissures of hand, lip, chapped skin, and skin diseases [12, 13, 44, 77].

3. Phytoconstituents

The several compounds which have been isolated from various species of *Garcinia* are summarised in Table 2. Several

Table 2: Phytochemicals of *Garcinia*.

Phytochemicals	*G. cambogia*	*G. indica*	*G. atroviridis*
Organic acids			
(−)-HCA	Fruit rind [45, 46]	Fruit rind [45]	Fruit rind [45]
Citric acid	Fruit rind [46]	Leave and fruit rind [47]	Herbal products [48]
Tartaric acid	[46]nd	[47]nd	Herbal products [48]
Malic acid	Fruit rind [46]	[47]nd	Herbal products [48]
Succinic acid	—	[47]nd	—
Prenylated benzoquinone			
Atrovirinone	—	—	Root [27]
Prenylated depsidone			
Atrovirisidone	—	—	Root [27]
Atrovirisidone B	—	—	Root [49]
Prenylated hydroquinone			
4-Methylhydroatrovirinone	—	—	Root [50]
1,4-cis-Docosenoic acid	—	—	Root [50]
14-cis-Docosenoic acid	—	—	Root [50]
Flavonoid			
Morelloflavone	—	—	Root [50]
Fukugiside	—	—	Root [50]
Naringenin			Root [49]
3,8″-Binaringenin			Root [49]
Xanthone			
Garbogiol	Root [51]	—	—
Rheediaxanthone A	Bark [51]	—	—
Dioxygenated xanthone			
1,7-Dihydroxyxanthone	—	Heartwood [52]	—
Tetraoxygenated xanthone			
Atroviridin	—	—	Stem bark [53]
Tetracyclic xanthone			
Oxyguttiferone K	Fruit [54]	—	—
Polyisoprenylated benzophenone			
Garcinol/camboginol (enantiomer of xanthochymol)	Fruit rinds [55, 56] Latex [57] Bark [51]	[55]nd Fruit rinds [58]	—
Isogarcinol/cambogin (enantiomer of isoxanthohumol)	Latex [57] Bark [51]	Fruit rinds [58]	—
Isoxanthohumol	Fruit rinds [55]	[55]nd	—
Guttiferone I	Fruit [54]		—
Guttiferone J	Fruit [54]		—
Guttiferone K	Fruit [54]		—
Guttiferone M	Fruit [54]		—
Guttiferone N	Fruit [54]		—

nd: none detected; —: not reported.

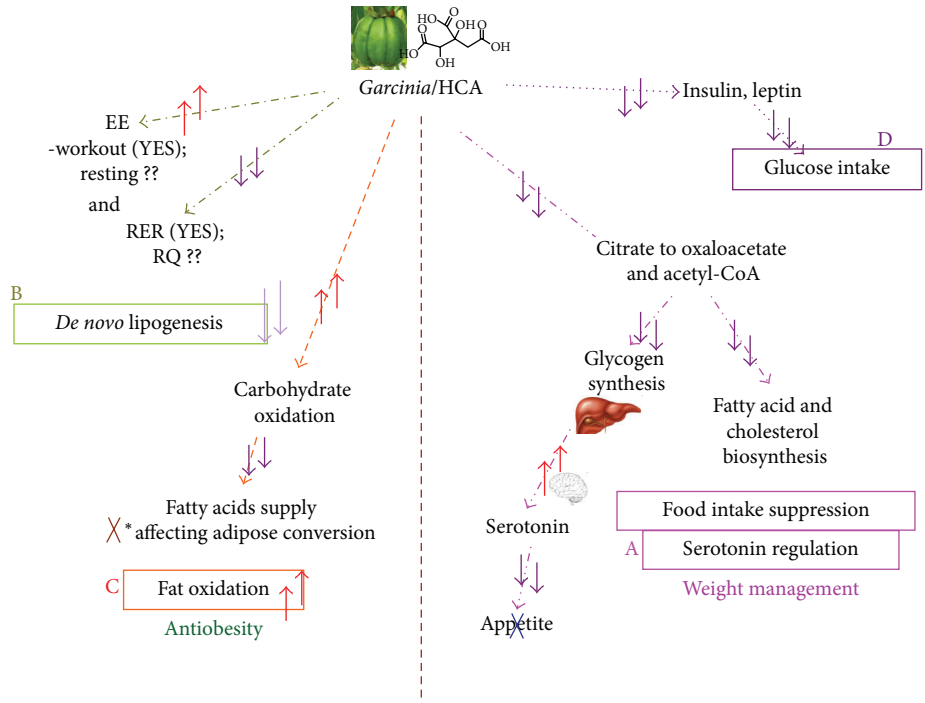

Figure 1: Possible multiple mechanisms that contribute to antiobesity effect of *Garcinia*/HCA. ↑ indicated increase or stimulation; ↓ indicated reduce or inhibition while ?? indicated that the effect is yet to be confirmed. (A) summary of Serotonin regulation and food intake suppression; (B) summary of reduction of *de novo* lipogenesis; (C) summary of stimulation on fat oxidation; (D) summary of reduce on glucose intake; (A) and (B) contribute to the weight management effect of *Garcinia*/HCA while (B) and (C) contribute to antiobesity of *Garcinia*/HCA.

types of organic acids such as HCA, citric, tartaric, malic, and succinic acids are isolated from *Garcinia*. However, HCA is the principal acid of the fruit rinds of *G. cambogia*, *G. indica*, and *G. atroviridis* [12, 27, 45], with its content ascending as listed [46–48]. A substantial amount of (−)-HCA, up to 30% by weight is present in the pericarp of the fruit of *G. cambogia*. In similar studies conducted by Sullivan et al. [78, 79] and Stallings et al. [80], they observed that of the four isomers of HCA [(−)-HCA, (+)-HCA, (−)-allo-HCA, and (+)-allo-HCA], (−)-HCA, which is also known as (2S, 3S)-HCA, was the only potent inhibitor of ATP citrate lyase. (−)-HCA can be chemically synthesized using citric acid as starting material. Synthetic (−)-HCA offers several advantages including higher purity and lactone stable as compared to natural (−)-HCA [81]. On the other hand, (−)-HCA is a good starting material to synthesize other important chiral synthons and compounds [82].

(−)-HCA is one of the important supplements for antiobesity and weight management. Its effect on weight management is mainly contributed by giving the feeling of full and satisfaction while the antiobesity effect is by reduction of *de novo* lipogenesis and acceleration of fat oxidation (Figure 1). In this paper, we aimed to review the mechanism for antiobesity and weight management effects by (−)-HCA (hereafter referred to as HCA)/*G. cambogia*/*G. atroviridis*/*G. indica* extracts and the assessment of these effects in the clinical settings.

4. Salts of HCA

On account to the discovery of (−)-HCA as an effective compound in weight management, market demand for the acid has increased tremendously. The commercially available *G. cambogia* extracts which contain approximately 50% (−)-HCA are prepared from the fruit rind [12, 69]. HCA can exist as a free acid or in the lactone form. The former form is considered to be biologically active. However, the free acid is unstable and is usually converted to its less active lactone form to attain higher stability. To prevent the cyclization of HCA into its less potent lactone, the acid has been combined with various counter ions to form stable salts [83].

Commercial HCA is available in free acid form and as single, double, or triple salts. Preparations with different counter ions contribute to different degree of solubility as well as bioavailability [84]. For example, Na^+ salt of HCA had been shown to be more effective than its lactone in inhibiting lipogenesis. However, Na^+ salt is highly hygroscopic when bound to (−)-HCA, which would deemed unfavorable for the production of pharmaceuticals for dry delivery [85].

To address the need to achieve higher solubility and stability, recent approaches have been focused more on the preparation of (−)-HCA in the form of a double or triple salt. Similar to its single salts, these double or triple salts also serve as good supply for essential ions [84]. A remarkable example of these would be the Ca^{2+}/K^+ salt of (−)-HCA (HCA-SX) or Super CitriMax. In contrast to the single salts,

HCA-SX is completely soluble in water and thus confers higher bioavailability [84]. A number of studies on the safety of HCA-SX had been reported [43]. Daily intake of HCA-SX at this dosage was shown to be effective in reducing body weight and BMI of healthy and obese adults after clinical trials of 8 weeks [16, 64]. Gene expression studies also provided additional evidence for the safety of HCA-SX, where genes essential for mitochondrial/nuclear proteins and for fundamental support of adipose tissue were shown to be independent of the regulation by HCA-SX [17, 86].

A typical reduction of food appetite and an increased serotonin availability were observed in all the weight control studies of HCA-SX on both animal and human subjects. These were associated with reduced levels of total cholesterol, LDL, triglycerides, and serum leptin as well as increased HDL level and urinary excretion of fat metabolites [15, 16, 64, 84, 87]. In rats, the salt also caused downregulation of genes encoding abdominal fat leptin while expressions of the plasma leptin genes remained unaltered [17]. Nevertheless, it was postulated that a set of obesity regulatory genes [84] and inhibition to the uptake of [^{3}H]-5-HT release in the brain [15] are involved in the appetite suppressing activity of HCA-SX.

In relation to this, gene expression profiling carried out by a research group demonstrated the modulation of a specific set of genes (about 1% of 9960 genes and ESTs) in the adipocytes by dietary HCA-SX supplementation [17]. Further study on cultured mature human adipocytes revealed significant upregulation of 366 and downregulation of 348 the fat- and obesity-related genes [88]. Notably also in the microarray analyses, HCA-SX demonstrated a distinct effect on appetite suppression whereby genes encoding serotonin receptors were shown to be selectively upregulated by the salt [17]. Besides, HCA-SX was also found to be capable of activating hypoxia inducible factor (HIF), a transcription factor involved in energy metabolism [88] and restored the increase in oxidative stress, inflammation, and insulin resistance in obese Zucker rats [21].

5. Antiobesity Effects of *Garcinia*/HCA

Obesity, particularly caused by accumulation of visceral fat, is a serious risk factor of various life-style diseases such as coronary heart disease, diabetes, hyperlipidemia, hypertension, and cancer [2, 4]. Human obesity is influenced by genetic and environmental factors and particularly by changes in diet and physical activity, which contributes greatly to the development of insulin resistance, a most common underlying abnormality in human obesity [89]. Studies on food sources exerting antiobesity effects have focused on the development of herbal extracts or functional food which can suppress the accumulation of body fat. Several studies were conducted to provide scientific basis on the extensive usage of *G. cambogia* and *G. atroviridis* associated with high-fat diet- (HFD-) induced obesity where dyslipidemia, fatty liver, insulin resistance, and hyperleptinemia were acquired along with the overexpression of leptin, TNF-α, resistin, PPARγ2, C/EBPα, and SREBP1c genes in epididymal adipose tissue. The effect of *G. cambogia* was largely attributed to its HCA content [90, 91]. Subsequent researches proved that the antiobesity effects of *G. cambogia*/HCA resulted from the combined actions of several mechanisms including suppressing *de novo* fatty acid biosynthesis and appetite [16, 60] and increasing energy expenditure [39], subsequently reducing body fat accumulation and weight gain in experimental animals [37, 38, 92]. In this review, we arranged the antiobesity effects of *Garcinia*/HCA based on their distinct mechanisms: (1) serotonin regulation and food intake suppression, (2) decreased *de novo* lipogenesis, (3) increased fat oxidation, and (4) downregulation of a spectrum of obesity-associated genes.

5.1. Serotonin (5-Hydroxytryptamine, 5-HT) Regulation and Food Intake Suppression. HCA, the primary acid in the fruit rinds of *G. cambogia*, *G. atroviridis*, and *G. indica* [45], has been reported as the active ingredient in inhibiting ATP citrate lyase (EC 4.1.3.8) [78, 93]. ATP citrate lyase, which is an extramitochondrial enzyme catalyzing the cleavage of citrate to oxaloacetate and acetyl-CoA, was inhibited by HCA. Thus, the availability of two-carbon units required for the initial steps of fatty acid and cholesterol biosynthesis during carbohydrate feeding was limited [78, 79, 94–97]. As a result, the consumed carbon source was diverted to glycogen synthesis in liver. A signal was then sent to the brain due to this metabolic alteration, resulting in rising of serotonin level concomitant with a reduced appetite. HCA might exhibite its anorectic effect by a second possible mechanism, namely, reducing acetyl CoA, subsequently decreasing malonyl CoA levels and thereby reducing negative feedback on carnitine acyltransferase (CPT-1). The substrate of CPT-1, long-chain acyl CoA(s), may act as a mediator(s) of appetite [98, 99]. More recently, neuropeptide Y (NPY) had also been implicated in the appetite suppression of HCA. Basal concentration of the neurotransmitter was claimed to be significantly reduced in the hypothalamic tissues as a result of supplementation with HCA-SX [84]. However, the role of NPY in this is still vague to date. Several reports supported the serotonin regulation of HCA. Ohia et al. [100] demonstrated that HCA-SX enhanced serotonin availability in isolated rat brain cortex by acting as a mild serotonin receptor reuptake inhibitor (SRRI), without stimulating the central nervous system. Kaur and Kulkarni [36] conducted a study to elucidate the effect of OB-200G, a polyherbal preparation containing aqueous extracts of *G. cambogia*, *Gymnema sylvestre*, *Zingiber officinale*, *Piper longum,* and resin from *Commiphora mukul* on the modulation of food intake by serotonin modulators in female mice. The results obtained were compared with fluoxetine, a drug that was reported to enhance 5-HT neurotransmission [101]. Both OB-200G and fluoxetine significantly ($P < 0.05$) antagonized the hyperphagic effect of p-chlorophenylalanine (PCPA), 8-hydroxy-2-(di-N-propylamino)-Tetralin (8-OH-DPAT), cyproheptadine, and 2-deoxy-D-glucose (2-DG) which further instigate possible serotonergic involvement in the effects of OB-200G on food intake in female mice. Preuss et al. [16] reported that HCA caused a significant reduction in appetite, weight loss, and plasma leptin level, concomitant with an increase in the serum serotonin level and a favorable lipid profile in human clinical trials. Similar results were also obtained in a study conducted by Asghar et al. [87] They reported on increased brain serotonin level in obese Zucker

rats receiving *G. cambogia* extract, suggesting that the ability of HCA in body weight gain reduction was most probably due to its combined effects on the metabolic and serotonin pathways. In addition, Roy et al. [17] reported that HCA-SX supplementation upregulated prostaglandin D synthase (PDS), aldolase B (AldB), and lipocalin (LCN2) genes in abdominal fat tissue. Further mapping of the candidate genes of known pathways associated with fat metabolism by using functional categorization and pathway construction software showed that supplementation of HCA-SX targeted on the serotonin receptor.

Leonhardt et al. [102] reported that HCA reduced body weight regain in rats after a period of substantial body weight loss. Besides, HCA temporarily reduced food intake of rats with diets of varying nutrient contents (grounded standard rat chow, high glucose, and high glucose + fat). HCA supplementation caused pronounce suppression of food intake during the entire 10 days of ad libitum feeding period in rats fed with high glucose + fat diet, a diet that had a nutritionally relevant level of dietary fat (24% of energy). These data therefore extended those of the previous studies which reported on the anorectic effects of HCA [96, 97, 103–105]. Moreover, the results obtained were consistent with studies which reported on particularly strong food intake suppression by HCA with high glucose + fat diet and a smaller but still significant suppression with the high glucose diet in other rat models and in different orders [37, 39, 102]. Hence, the feed conversion efficiency [cumulative body weight regain (g)/cumulative food intake (MJ)] in the high glucose and high glucose + fat groups during the 10 ad libitum days was reduced, which indirectly supported that HCA increased energy expenditure in these groups.

Leonhardt and Langhans [39] then extended their study on the long-term effects of HCA on body weight regain and food intake, as well as the effects of HCA on the circadian distribution of food intake and on meal patterns during the dark and light phases. HCA administration significantly reduced the food intake of rats fed with 12% fat diet, but not 1% fat diet, concomitant with significant reduction in weight regain (overall $P < 0.01$) in both groups. In the study, the rats underwent restrictive feeding for 10 days prior to ad libitum feeding (Experiment 1: normal 1% fat diet and 1% fat diet + 3% HCA; Experiment 2: normal 12% fat diet and 12% fat diet + 3% HCA). The control groups of both experiments had compensated the body weight loss, whereas the HCA-fed rats groups regained only 68 ± 4% (1% fat diet) and 61 ± 8% (12% fat diet) of the body weight regained by their respective control groups after 22 days of such ad libitum feeding. Despite significant reduction in weight regain in rats fed with 1% and 12% fat diet, long-term suppression of HCA on food intake was only detected in combination with 12% fat diet (Experiment 2). This was in line with the results obtained by Leonhardt et al. [106] who suggested that HCA increased energy expenditure. Studies on the effects of HCA on the circadian distribution of food intake and on meal patterns showed that the suppression of food intake occurred predominantly during the dark phase of the first ad libitum days. However later on, HCA suppression of food intake was more effective during the light phase. Further experiments elucidating the effects of HCA in combination with the 12% fat diet on meal size and meal number during the light phase revealed that HCA markedly reduced the meal number, but not the meal size. HCA did not affect any metabolic variables tested (plasma glucose, lactate, triacylglycerol, HDL, free fatty acids, β-hydroxybutyrate, and insulin, hepatic fact, and glycogen concentrations) in both experiments, except decreasing plasma triacylglycerol levels and increasing the liver fat concentration in Experiment 2 (rats fed with 12% fat diet). The fact that HCA did not affect plasma β-hydroxybutyrate (BHB) levels did not support the hypothesis that HCA suppressed food intake via increased hepatic fatty acid oxidation.

However, contradicting results were obtained by Kovacs et al. [41, 71] who reported that two-week supplementation with HCA and HCA combined with medium-chain triglycerides did not result in increased satiety. The findings were in line with previous reports where no significant treatment effects were observed on appetite indices (inclusive of mean, peak or nadir hunger ratings, mean ratings of desire to eat, prospective consumption, fullness or sensations of thirst, stomach growling, headache, distraction, irritability, or, as a check on malingering, itchiness) [69]. The lack of efficacy and transient food intake suppression by HCA raised questions about its clinical significance. While negative findings are always open to methodological questions, several questions need to be answered before drawing a definite conclusion. First, the diet administered to the subjects should not promote extreme sensations in the evaluation of the food intake suppression effects of HCA under conditions of energy restriction. However, Mattes and Bormann imposed mild restrictions and thus ruled out this possibility as evidenced by ratings falling in the middle range of the response scales. Second, an energy-restricted diet would prevent the required enzyme alterations (reduction of acetyl-CoA and suppression of formation of carnitine palmitoyltransferase I inhibitor malonyl CoA) which altered substrate metabolism and satiety. However, it was unlikely that the moderate energy restricted diet prescribed in the study conducted by Mattes and Bormann [69] hindered the satiety effect of HCA as it still contained at least 30% of energy from fat.

Several factors might contribute to the controversial results of the efficacy of HCA in human studies. One of contributing factors is the highly variable doses used in the human trials which ranged from 5 to 250 mg/kg of HCA per day [42, 70]. Besides, the discrepancy might also be due to the differences in the preparation or extraction of HCA. For instance, the extraction method might increase the formation of HCA in a lactone form, which is less potent in the inhibition of ATP citrate lyase [85, 107]. In order to prevent the cyclization of HCA into the less potent lactone form, preparation using different counte rions (such as potassium, sodium, or calcium) had been applied [84], which contributed to the different degrees of stability, bioavailability, or solubility of HCA [86]. In this respect, Louter-Van De Haar et al. [83] conducted a study on the efficacy of three commercially available HCA products on suppression of food intake in male Wistar rats. Many human studies which reported lack of efficacy used Super CitriMax at considerably lower

doses [41, 70, 71]. On the contrary, Preuss et al. [16] reported that high doses of Super CitriMax exerted significant effects in human. Thus, Louter-Van De Haar et al. [83] suggested that the reported lack of efficacy of HCA in suppressing food intake in human subjects might be due to the low doses of a relatively low-effective HCA preparation. Nevertheless, significant suppression of food intake was observed in the studies conducted by Leonhardt and Langhans [39] where Sprague-Dawley rats were supplemented with HCA for 10 days after substantial, fasting-induced weight loss. It seemed that HCA might be more effective in regulating weight gain than promoting weight loss; thus it was more useful for weight maintenance after an initial loss [39, 102]. Hence, differences in the experimental setups such as the difference in rat strains could contribute to such discrepancy.

5.2. Decreased De Novo Lipogenesis. The reduction of the acetyl-CoA by HCA and thus limiting the availability of building blocks required for fatty acid and cholesterol biosynthesis has led to suggestions that HCA inhibited lipogenesis. Several studies conducted by Sullivan and colleagues had confirmed the inhibition of *in vivo* and *in vitro* rates of lipogenesis in several tissues reported to convert carbohydrate into fatty acids (such as liver, adipose tissue, and small intestine), in which HCA was predominantly given to rodent models [78, 79, 85, 96, 97, 108]. Lowenstein [108] demonstrated that HCA greatly inhibited *in vivo* fatty acid synthesis in rat liver. The rats were placed on chow diet for 7–10 days, followed by 45 h of fasting prior to a scheduled diet high in fructose or glucose for 10 to 15 days. The sodium salt of HCA at dose levels of 2 to 20 mM was administered by intraperitoneal injections 45 min before injection of ^3H_2O. Fatty acid biosynthesis in rat liver (μ moles ^3H_2O incorporated/g liver/h) was measured 3.5–5 h after starting of the final feeding. Profound decrease in fatty acid synthesis by 25 to 30 days was obtained with an intraperitoneal dose of 0.1 mmole per kg of body weight (equivalent to approximately 2.9 mg of HCA per 150 g rat). In addition, 50% of inhibition was detected at a dose level of 0.28 mmole per kg body weight.

It was reported that *G. cambogia*/HCA affected respiratory quotient (RQ) and EE in rats and human. Lim et al. [109, 110] showed that short-term administration of HCA decreased the RQ in athletes and in untrained women. Leonhardt et al. [106] further extended their study to determine the effect of HCA on RQ and EE in rats fed ad libitum after a period of substantial weight loss. They reported that HCA markedly decreased RQ and EE during the first two days of ad libitum, reflecting suppression of *de novo* lipogenesis in rats, which is consistent with the findings of Westerterp-Plantenga and Kovacs [61] in humans.

In this respect, Kovacs and Westerterp-Plantenga [60] further extended their study where the effects of HCA on net fat synthesis as *de novo* lipogenesis were investigated. A double-blind, placebo-controlled, randomized, and crossover design experiment was conducted on 10 sedentary male subjects. The subjects performed glycogen depletion exercise, followed by a 3-day high-fat low-carbohydrate (F/CHO/P, 60/25/15% energy; 100% of EE; depletion period) intake in order to create a similar glycogen storage capacity. Subsequently, a 7-day high-carbohydrate diet (F/CHO/P, <5/>85/10% energy; 130–175% of EE; overfeeding period) supplemented with either 500 mg of regulator HCA (HOB Ireland Ltd.) or placebo was administered. Each intervention ended with a 60 h stay in the respiratory chamber (days 9 and 10). *De novo* lipogenesis occurred as indicated by RQ > 1.00 in all subjects. Significantly, lower 24 h EE ($P < 0.05$; on day 9), resting metabolic rate ($P < 0.01$; on day 10), and RQ at night ($P < 0.05$; on day 10) were detected with HCA as compared to placebo. Fat balance and thus net fat synthesis as *de novo* lipogenesis tended to be lower ($P < 0.1$) with HCA as compared to placebo. Taken all together, Kovacs and Westerterp-Plantenga concluded that the administration of HCA during overfeeding of carbohydrates may reduce *de novo* lipogenesis.

However, opinions differ widely with respect to this issue. The mechanism underlying the anorectic effect of HCA is still unclear. Furthermore, whether the suppression of body weight regained was solely due to reduced food intake or whether there was involvement of increased EE remained unknown. Contradictory results were reported on the effects of HCA on EE. Previous reports by Leonhardt and colleagues [39, 102] and the results obtained in pair-feeding studies [103] showed reduction of body weight regain and energy conversion ratio by HCA supporting the finding that HCA increased EE. However, reduced energy conversion ratio could be due to decreased nutrient absorption. Vasselli et al. [111] demonstrated an increment in 24 h EE in rats fed with mixed high-carbohydrate diet ad libitum by directly measuring the EE in a whole-body respirometer, albeit no effect on the RQ was detected. Another study conducted by Leray et al. [112] reported that 6 months of HCA administration did not affected EE in adult neutered cats. Besides, most human studies [41, 42, 70] reported that HCA had no effect on EE. Kriketos et al. [42] reported that HCA administration exhibited no effect on lipid oxidation in men during either rest or moderately intense exercise on a cycle ergometer. However, in these studies, the subjects received a much smaller dose, namely, a daily dose of 3.0 g per subject [nearly equal to 1.5 mg/day/mouse]. Furthermore, their experimental period of 3 days was quite short when compared with other studies.

Blunden [113] reported that when *Garcinia* extract and insulin were added simultaneously, the number of larger droplets markedly decreased while the smaller droplets (10–20 μm^2 or <10 μm^2) increased in 3T3-L1 cell. The activity of cytosolic glycerophosphate dehydrogenase (GPDH) which converts dihydroxyacetne phosphate to glycerol 3-phosphate (predominant substrate for triglyceride synthesis) increased from undetectable levels to between 100 and 187 U/mg of cytosolic protein after adipose conversion. However, no significant decrease in enzymatic activity was detected after administration of the *Garcinia* extract. Taken together, the authors therefore suggested that *Garcinia* extract interferes with lipid synthesis in fat cells via fatty acid supply inhibition without affecting adipose conversion.

5.3. Increased Fat Oxidation. Ishihara et al. [35] conducted a study on acute and chronic effects of HCA on energy metabolism. Acute administration of 10 mg/100 μL of a 0.48 mol/L HCA solution per mice significantly increased

($P < 0.05$) serum free fatty acid levels and concentration of glycogen in the gastrocnemius muscle, even though the respiratory exchange ratio was not different from that in the control group. On the other hand, chronic administration of 10 mg HCA twice a day significantly lowered ($P < 0.01$) the RQ during resting and exercising conditions in mice. Lipid oxidation, calculated from RQ, and oxygen consumption were significantly enhanced, and carbohydrate oxidation was significantly less in these mice during the early stages of running ($P < 0.01$). Taken all together, the authors therefore suggested that chronic administration of HCA augmented the endurance exercise performance in mice via the attenuation of glycogen consumption caused by the promotion of lipid oxidation during running exercise. Furthermore, Ishihara et al. [35] suggested that chronic HCA administration might have increased EE during the 3-week experimental period.

In addition, Lim et al. [109, 110] also showed that short-term administration of HCA increased fat oxidation during exercise in athletes and in untrained women. Lim et al. [110] conducted a randomized, placebo-controlled study where subjects (athletes) consumed HCA (250 mg) or placebo for 5 days, after each time performing cycle ergometer exercise at 60% VO_2 max for 60 min followed by 80% VO_2 max until exhaustion. The results obtained showed that the respiratory exchange ratio (RER) was significantly lower in the HCA trial than in the control trial ($P < 0.05$). Fat oxidation was significantly increased by short-term administration of HCA, and carbohydrate oxidation was significantly decreased ($P < 0.05$) during exercise in athletes. In a continuation of their study, Lim et al. [109] conducted a similar study to evaluate the effects of HCA administration on fat oxidation during exercise in untrained women. The results showed that HCA decreased the RER and carbohydrate oxidation during 1 hour of exercise. In addition, exercise time to exhaustion was significantly enhanced ($P < 0.05$).

A more recent approach for determining fat metabolism by HCA was conducted by measuring urinary concentration of malondialdehyde (MDA), acetaldehyde (ACT), formaldehyde (FA), and acetone (ACON) of the tested subjects. The urinary excretion of these four metabolites was proposed to be a consequence of enhanced β-oxidation of fats in body tissues [16]. The effect of HCA-SX had been studied extensively by Preuss et al. on obese human subjects [16, 64] as well as on male and female Sprague-Dawley rats. In the randomized, double-blind, and placebo-controlled clinical studies on obese human, a group of subjects were given 4,667 mg of HCA-SX daily (provided 2,800 mg HCA/day) while the other given a combination of HCA-SX 4,667 mg, 4 mg of niacin-bound chromium (NBC), and 400 mg of gymnema sylvestre extract (GSE) daily. The control group received placebo in 3 equal doses daily at 30 to 60 min before meals. In the trial involving 30 subjects, urinary excretion of fat metabolites was increased by approximately 125–258% whereas in trial involving 60 and 90 obese subjects, the metabolite excretion increased by about 35.6–106.4% [16] and 32–109% [64], respectively. As excretion of fat metabolites was enhanced in groups receiving the combination formula, it was also suggested that HCS-SX, either alone or in combination with NBC and GSE, could effectively promote breakdown of fats [16, 64].

5.4. Downregulation of a Spectrum of Obesity-Associated Genes. Lipogenic transcription factors, including SREBP1c, liver X receptors, PPARγ, and C/EBPα, are highly expressed in the adipose tissue and actively participate in the lipid metabolism of adipocytes by coordinating lipogenic and adipocyte-specific gene expression [114]. PPARγ interacts with several other transcription factors. C/EBPα and PPARγ interact via a positive feedback loop in the differentiated adipocytes, to induce each other's expression [115]. Besides, coexpression of PPARγ with SREBP1c increases the transcriptional activity of PPARγ [116]. aP2 (a marker of terminal adipocyte differentiation), together with several adipocyte-specific genes, including adiponectin, insulin receptor, leptin, glucose transporter 4 (GLUT4), and glycerol phosphate dehydrogenase, are induced during the adipogenic differentiation process [114]. Leptin, a 167-amino acid hormone and a biomarker of the obesity regulatory gene, is produced by fat tissue and is known to regulate energy intake and metabolism. Leptin binds to the medial nucleus of the hypothalamus and induces a sensation of satiety and thus controlling the appetite [98, 117, 118].

Fatty acid synthase, acetyl-CoA carboxylase 1, and SREBP1c mRNA concentrations were decreased in the adipose tissue of the obese animal models [119]. On the contrary, the mRNA and protein expression of TNFα (which is involved in proinflammation, apoptosis, lipid metabolism, and insulin resistance) were increased in the adipose tissues of the obese rodents and humans [120]. A high level of TNFα suppressed transcription factors such as PPARγ and C/EBPα which, in turn, activated the GLUT4 gene [121, 122].

Hayamizu et al. [123] evaluated the effects of *G. cambogia* fruit rind extract containing 60% (–)-HCA on serum leptin and insulin in mice. *G. cambogia* extract reduced serum total cholesterol, triacylglycerol, and nonesterified fatty acids in mice. Nevertheless, the body weight gain and fat pad weight were not affected in the treatment. No significant difference in blood glucose level was detected between groups, but a significant reduction of serum insulin ($P < 0.05$) was detected, suggesting that the *G. cambogia* extract efficiently improved glucose metabolism in the treated animals. In addition, the treatment decreased serum leptin levels and the leptin/WAT ratio. Besides, the changed ratio of body weight correlated positively with leptin levels in their study. Furthermore, it had been reported that leptin suppressed the signal transduction of insulin via cytokine interactions [124, 125]. Hayamizu et al. [123] suggested that the observed effect of *G. cambogia* extract on serum insulin in their study occurred through leptin-like activity.

The antiobesity effects of *Garcinia* on visceral fat mass, lipid profiles in the serum and liver, serum adipocytokine levels, and regulation of the expression of multiple adipose tissue genes were reviewed. Kim et al. [37] reported the antiobesity effects of a mixture composed of aqueous extract of *G. cambogia*, soy peptide, and L-carnitine (1.2 : 0.3 : 0.02, w/w/w) on rats rendered obese by high-fat diet (HFD). An HFD (40% fat calories) with identical composition of

Table 3: Summary of clinical studies of *Garcinia*/HCA that have shown significant antiobesity effect.

Duration	Subject	Treatment	Outcome	References
10 days	44 healthy volunteers	4 g for the 1st day followed by 3 g until day 10.	Not recorded	[59]
11 days	Normal, groups: placebo, HCA of total 10 sedentary male under high-fat diet	1500 mg HCA daily	No significant effects on body weight gain, appetite-related, and plasma parameters but decreased fat deposition **Comments: suggest that (−)-HCA may reduce net fat deposition from *de novo* lipogenesis during weight gain	[60]
2 weeks	BMI 27.5, groups: placebo, HCA of 24 subjects each (12 males, 12 females)	300 mg HCA	Reduced of energy intake and slight decreased of body weight	[61]
4 weeks	Obese, hypocaloric diet, groups: placebo, 1 capsule, 2 capsule, (50 subjects each group)	55 mg *G cambogia* + 19 mg chromium + 240 mg chitosan/day	Weight loss associated with lower TC/LDL and higher HDL	[62]
8 weeks	BMI 25–35, groups: placebo, treatment of 20 each	1000 mg HCA/day	Reduced of visceral and subcutaneous fat area	[63]
8 weeks	Moderate obese, groups: placebo, HCA-SX, HCA-SX + NBC + GSE of total 60	HCA-SX 4667 mg (60% HCA), 4667 mg HCA-SX + 400 μg niacin-bound chromium + 400 mg Gymnema sylvestre extract	Significant ($P < 0.05$) decrease in BMI, food intake, total cholesterol, low-density lipoproteins, triglycerides, and serum leptin levels, increase in high-density lipoprotein levels, and enhanced excretion of urinary fat metabolites (biomarker of fat oxidation, including malondialdehyde, acetaldehyde, formaldehyde, and acetone) in HCA and HCA-NBC-GSE groups	[16]
8 weeks	BMI 30–50, groups: placebo, 2800 mg HCA; 2800 mg HCA + 400 μg chromium of 30 subjects each	2800 mg HCA; 2800 mg of HCA-SX + 400 μg chromium + 100 mg gymnemic acid/day	Decreased of body weight, BMI, LDL, and TG and increased fat oxidation	[64]
8 weeks	Normal, group: 35 healthy subjects on diets 1000, 1200, or 1500 kcal	1500 mg *G. cambogia* extract daily	Significant reduction of total cholesterol, triacylglycerol, and body weight associated with reduced appetite	[65]
8 weeks	Obese, groups: placebo and treatment of total 50 F	3.45 g *G. atroviridis*	Significant reduction of body weight, BMI, body fat, lean body mass, and anthropometric parameters (biceps, subscapular, suprailiac crest skinfold thicknesses, and upper arm circumference) but no change of serum lipid profile	[66]
60 days	Over weight to obese, groups: placebo and treatment of total 58	285 mg (−)-HCA in Slim339 *G. cambogia* extract daily	Significant reduced of body weight (4.7%)	[67]
12 weeks	BMI 27.5–39, groups: placebo and treatment (18 females/2 males each) of total 40	300 mg *G. cambogia* + 1200 mg *Phaseolus vulgaris* + 1200 mg inulin/day	Significant body weight lost (3.5 kg versus 1.2 kg)	[68]
12 weeks	BMI ~28, groups: placebo: 47; treatment: 42	2400 mg *G. cambogia*/day	Significant body weight lost	[69]

the high-fat control diet (CD) applied in the study was fed to five-week-old male Sprague-Dawley rats for 9 weeks to create an obese conditions in rats that mimic to human obesity. Body weight gain, visceral fat-pad weight, and serum and hepatic biochemistry of rats were measured. The 0.38% mixture-supplemented HFD (D + M) reduced the total body weight and the accumulation of visceral fat mass and lowered the blood and hepatic lipid levels, which led to the improvement of insulin resistance in the HFD-induced obese rats. Moreover, the mixture of *G. cambogia*, soy peptide, and L-carnitine improved dyslipidemia in rat models with HFD-induced obesity. Downregulation of the expression of leptin, tumor necrosis factor-alpha, and sterol regulatory element binding protein 1c genes in the epididymal fat tissue of rats fed with CD + M diet was obtained. In contrary, upregulation of the uncoupling protein 2 (UCP2) gene in epididymal adipose tissues was induced with CD + M diet. No effect on the food intake of the animals was observed in the study, suggesting

Table 4: Summary of clinical studies of *Garcinia*/HCA that have shown none significant antiobesity effect.

Duration	Subject	Treatment	Outcome	References
1 day	Normal, groups: placebo, HCA of total 10 cyclists	4300 g HCA	No significant changes in total fat and carbohydrate oxidation rates	[70]
2 weeks	Normal-moderately obese, group: placebo, HCA, and HCA + MCT of total 7 males and 14 females	500 mg HCA; 500 mg HCA + 3 g medium chain triacylglycerols (MCT)	No significant differences in satiety, daily energy intake and body weight loss within all groups **Comment: subjects were under negative energy balance conditions (eliminating the possibility of *de novo* lipogenesis and reservation of glycogen reserves had occurred; thus, the only possible remaining mechanism increased hepatic fatty acid oxidation)	[71]
2 weeks	Normal-moderately obese, groups: placebo, HCA, and HCA + MCT of total 11 male	500 mg HCA; 500 mg HCA + 3 g medium chain triacylglycerols (MCT)	No significant differences in body weight reduction, EE, appetite ratings, and substrates oxidation (protein, fat, and carbohydrate oxidation) within all groups **Comment: 2-week intervention is too short	[41]
2 weeks	Normal-moderately obese, groups: placebo, HCA of total 10 sedentary males, with or without moderately intense exercise	3 g (−)-HCA daily	No significant difference in RQ, EE, and blood parameters during rest nor during exercise	[42]
8 weeks	39 subjects	1500 mg *G. cambogia* + 300 μg chromium picolinate/day	No significant difference in control and placebo	[72]
10 weeks	Overweight, groups: treatment: 29; placebo: 29	2 g *G. cambogia* extract daily	No clinically significant differences in body composition, plasma lipid profiles, antioxidant enzyme activity, and plasma adipocytokines	[73]
12 week	Obese, treatment: 5 M, 61 F; placebo: 14 M, 55 F	*G. cambogia* extract: 3000 mg of (50% of HCA); Diet: 5020 kJ/day (1200 kcal/day)	No significant difference in body weight and fat mass loss	[40]
12 weeks	Obese, groups: treatment: 36 F, 11 M; placebo: 41 F, 10 M	Botanical extract (1000 mg HCA daily)	No difference between placebo and treatment group but significant change of the body composition improvement index, body free fat mass, weight, BMI, and some other anthropometric measurements in both treatment and placebo groups	[74]
12 weeks	Obese, groups: treatment: 25 F, 7 M; placebo: 21 F, 5 M.	2.4 g *G. cambogia* (52.4% HCA) + 1.5 g *A. konjac* (94.9% glucomannan)	No significantvariation in body weight/other anthropometric and calorimetric parameters but significant hypercholesterolemic	[75]
12 weeks	BMI 28, groups: placebo: 23; treatment: 21	1,667.3 mg of *G. cambogia* extract/day (1,000 mg HCA/day)	No significant effect	[76]

that the mixture exerted antiobesity effect via modulation of the metabolic derangement induced by HFD during which interactions between the multiple genes implicated in the process of adipogenesis might be involved, rather than simply suppressing appetite. A similar observation was obtained by Kim et al. [38], where in addition to the reduction of food intake, the food efficiency ratio (FER) was also significantly lower in the *G. cambogia* diet administrated group than in the HFD mice, implying less efficient transformation of the feed mass into body mass.

6. Human Clinical Trials

The antiobesity effects of *G. cambogia* in terms of promoting weight loss and lowering cholesterol level were extensively studied. However, evidence for the effectiveness of *G. cambogia* or its derivative products was largely derived from animal studies [126]. Despite the intriguing evidence of antiobesity effects of *G. cambogia* from *in vitro* and animal studies, more equivocal results were obtained from randomized double-blind placebo-controlled experiments dealing with

Table 5: Commercialized dietary supplements that contain *G. cambogia* extract/HCA.

Product name	Company	Concentration of HCA	Doses recommended (daily)	Formulation of supplement
Super CitriMax HCA-600-SXS	Inter health N.I.	60% (−)-HCA in its free form, 1.0% (−)-HCA in its lactone form	3 capsules, 3 times daily, 30–60 min before meal	3 capsules per serving: *G. cambogia* extract 1500 mg (providing 900 mg of HCA), calcium 150 mg, potassium 225 mg, 0.5% sodium, 0.1% magnesium, 0.03% iron, 0.05% total phytosterols, 0.3% total protein, 4.5% moisture, and 8.5% soluble dietary fiber
GarCitrin	Sabinsa Corporation	50% (−)-HCA	500 mg, 3 times daily	500 mg of GarCitrin (providing 250 mg of HCA) and 5% Garcinol
Sci-Fit Pro Cut		50% (−)-HCA	4 capsules, 2-3 times daily, 30–60 min before meal	4 capsules per serving: *G. cambogia* 1000 mg (providing 500 mg of HCA), green tea extract 500 mg (98% polyphenols) (45% epigallocatechin/EGCG), guarana extract 910 mg (22% caffeine), caffeine 100 mg, L-carnitine 100 mg, white willow bark extract 100 mg (standardized for 15% salicin), dandelion 100 mg, juniper berry extract 100 mg, buchu extract 100 mg, and chromium 200 mg
G. cambogia and Kola Nut 450 mg	TerraVita	—	1 capsule, 3 times daily, with meals	225 mg *G. cambogia* fruit, 225 mg kola nut
G. cambogia	ProThera, Inc.	50% (−)-HCA	1–6 capsules daily, before meals.	500 mg *G. cambogia* (providing min. 250 mg of HCA), vegetarian capsule (hydroxypropyl methylcellulose, water), cellulose, magnesium stearate, and silicon dioxide
G. cambogia Plus	Atrium Inc	50% (−)-HCA	2 capsules, 3 times daily	Chromium 166 μg (as Cr picolinate 500 mg and Cr arginate 160 mg), *G. cambogia* 340 mg (providing 170 mg of HCA), atractylodes 80 mg, citrus aurantii 80 mg, gelatin, rice powder, and magnesium staerate
G. cambogia Plus	BioCare Ltd.	50% (−)-HCA	3 capsules daily, 20 min before food	*G. cambogia* 500 mg, vitamin B5 (calcium pantothenate) 6 mg, vitamin C (ascorbic acid) 5 mg, manganese gluconate(providing 270 μg elemental manganese) 2.5 mg, and chromium polynicotinate 0.9 mg (providing 100 μg elemental chromium)
Garcinia 1000	Source Naturals	50% (−)-HCA	1 tablet, twice daily, 1 hour before meal	Chromium (as chromiumpolynicotinate [ChromeMate] and chromium picolinate) 150 μg, sodium 25 mg, *G. cambogia* fruit extract (providing 500 mg of HCA) 1 g
Garcinia 1000 hydroxycitric acid	Nature's life	50% (−)-HCA	—	*G. cambogia* rind concentrate (providing 500 mg of HCA) 1 g, cellulose, silicon dioxide, magnesium stearate and "*Micro-Cellulose*" coating
Citrin	Natural Nirvana	—	1 capsule, 2 times daily	*G. cambogia* 495 mg, BioPerine 5 mg
HCA 450 mg tablet	Higher nature	450 mg HCA per tablet	1-2 tablets, 3 times daily, 30 min before meal	Tamarind fruit extract, microcrystalline cellulose, magnesium stearate (vegetarian source), hydroxypropyl methylcellulose coating, silicon dioxide, and acacia powder
HCA Hydroxy citric acid	Viridian Nutrition Ltd.	50% (−)-HCA	1 capsule, 3 times daily, before meal	*G. cambogia* (providing 250 mg HCA) 500 mg, viridian bilberry extract, alfalfa, spirulina blend 150 mg, and vegetarian cellulose capsule 120 mg
HCA hydroxycitric acid	Life Extension Foundation	50% (−)-HCA	1 capsule, 3 times daily, 45 min before meals with 1 capsule of CitriChrome	*G. cambogia* (fruit) (providing 250 mg of HCA) 500 mg
Hydroxycitrate	Solgar	50% (−)-HCA	1 capsule, 30–60 min before meal	*G. cambogia* fruit powdered extract (providing 250 mg [50%] HCA) 500 mg, hydroxypropylmethyl cellulose, vegetable magnesium stearate, and silicon dioxide
Hydroxycitrate Plus	Metagenics	—	1 tablet, 3 times daily, 30–60 min before meal	*Garcinia* fruit extract (*G. cambogia*) 500 mg, L-carnitine 100 mg, niacin (as niacinamide) 50 mg, pantothenic acid (as D-calcium pantothenate) 25 mg, riboflavin 10 mg, manganese (as manganese arginine) 750 μg, and chromium (as chromium nicotinate glycinate) 75 μg

human subjects [127–130]. Hayamizu et al. [59] conducted a crossover design randomized controlled trials (RCTs) to determine the "no observed adverse effect level (NOAEL)" of *G. cambogia* extract in 44 healthy volunteers (22 males and 22 females) and concluded that *G. cambogia* is generally safe to be consumed. Several equivocal findings of RCTs were reported on the effectiveness of supplements containing HCA (Table 3). Some studies reported that HCA exerted no significant effects as compared to the placebo group [40, 42, 70] (Table 4). All the above findings were in agreement with the most recent meta-analysis of RCTs which revealed that *G. cambogia* extract possessed limited or no effects on weight-loss in human subjects [131]. Moreover, this study showed no effect on satiety or calorie intake in overweight individuals consuming their habitual diet, which is in agreement with past studies [41, 60, 75]. However, such comparisons must be made with caution as the variations in the formulations, doses administered, RCTs designs, and study populations might contribute to the discrepancy of the results.

Preclinical studies using rodent models have confirmed the body weight reduction, appetite suppression, and subsequently food intake reduction effects of HCA in rats. Clinically, however, HCA failed to perform well. Several factors that might contribute to this scenario are the ATP citrate lyase which might be important only at very high carbohydrate diets, a type of diet that most studies did not prescribe. Besides, a high-fiber diet can bind to HCA and block it, thus reducing its efficacy. HCA and *G. cambogia* exerted potential effects in weight management, but clinical studies have yet to prove optimum conditions for HCA to be effective. For instance, Sullivan et al. [85] reported that hepatic lipid synthesis was reduced only if HCA was administered before the beginning of feeding, reaching optimum 30–60 minutes prior to feeding. The reason for this remains unknown.

7. Patents and Commercialization

The claims on enhanced human health associated with *Garcinia*/HCA had been reviewed in Section 4. In particular, the antiobesity effects of *Garcinia*/HCA were extensively reported. This has resulted in the availability of numerous commercialized weight-management products derived from *Garcinia*/HCA (Table 5). Several products of *G. cambogia* or its derivatives had been patented and commercialized. As of August 2012, a total of 66 patents that apply to *G. cambogia* or HCA derived from *Garcinia* were filed with the US Patent and Trademark Office (USPTO) since 1976 (search of US Patents and Trademark Office in year 2012 using Google patent search). These patents are on various aspects, including HCA enrichment from *Garcinia* rind, HCA and food products/dietary supplements prepared therefrom, methods of production, and their use. The majority of the patents are related to *G. cambogia/atroviridis* and/or HCA derived from *Garcinia* on obesity and weight loss. The patent numbers are as follows: 8,197,867, 8,097,286, 8,017,147, 8,003,138, 7,943,186, 7,943,183, 7,927,636, 7,858,128, 7,846,970, 7,772,428, 7,741,370, 7,687,082, 7,550,161, 7,507,421, 7,431,951, 7,335,651, 7,311,929, 7,230,131, 7,214,823, 7,208,615, 7,189,416, 7,179,488, 7,063,861, 6,982,098, 6,899,891, 6,875,891, 6,855,358, 6,770,782, 6,706,899, 6,676,977, 6,610,277, 6,565,847, 6,541,026, 6,489,492, 6,485,710, 6,476,071, 6,447,807, 6,428,806, 6,426,077, 6,413,545, 6,399,089, 6,395,296, 6,277,396, 6,221,901, 6,217,898, 6,160,172, 6,147,228, 6,113,949, 6,054,128, 5,972,357, 5,911,992, 5,783,603, 5,656,314, 5,612,039, 5,536,516, 4,007,208, 4,006,166, 4,005,086, 7,119,110, 3,994,927, 3,993,668, 7,153,877, 3,993,667, 4,028,397, 7,153,528, 7,015,250, 6,638,542, 6,579,866, 6,482,858, 6,441,041, 6,383,482, 6,207,714, 5,817,329, 5,626,849, and 3,965,121.

8. Conclusions

The nutraceutical industry is flourishing, and interest in establishing scientific credibility has attained importance for many companies and scientists. In the recent years, more clinical trials had been conducted to elucidate the functional effects of *Garcinia*/HCA supplementation on promoting human health. A multitude of metabolic functions had been reported for HCA or HCA-containing *Garcinia* extract, such as reducing blood lipids, inducing weight loss, suppressing appetite, and reducing food intake based on results obtained in both animal trials and human clinical trials (Figure 1). These discoveries make the development of evidence-based adjuvant modalities to curb the trend of the increasing prevalence of obesity and obesity-related comorbidity and mortality possible. We have previously reviewed and concluded that *Garcinia* extract and HCA were generally safe to be consumed. Collective results from 17 clinical studies which involved 873 subjects demonstrated the safety of HCA and HCA-SX for human consumption [43]. These studies provided scientific evidence that intake of HCA and HCA-SX alone did not produce adverse effects and a dietary dosage of up to 2800 mg/day was regarded as the "no observed adverse effect level (NOAEL)" of HCA-SX in human [84]. Based on these animal and human safety data, HCA-SX also received self-affirmed GRAS status in the USA by the Burdock Group in year 2003 [132]. However, definitive conclusions that *Garcinia*/HCA supplements are efficient tools against various health problems especially obesity remain to be proven in larger-scale and longer-term clinical trials, despite substantial public interest in such supplements. Many diet supplements containing *Garcinia*/HCA marketed as weight management products are the combination of active ingredients rather than containing a single agent. Thus it is difficult to evaluate the effectiveness of single agents when the combination products are tested. In addition, awareness of the safety and efficacy of the weight management supplements available in the market should be raised among health care providers in order to assist their patients in analyzing the risks and benefits of the dietary supplements. Thus, scientific investigations on the potential health promoting effects of herbal preparations as diet supplement are prerequisites for new discoveries of alternative therapies.

Acknowledgment

The authors would like to thanks Professor S. G. Tan for the proofreading of this paper.

References

[1] WHO, "Global database on body mass index," http://apps.who.int/bmi/index.jsp, 2012.

[2] W. H. O. expert consultation, "Appropriate body-mass index for Asian populations and its implications for policy and intervention strategies," *The Lancet*, vol. 363, pp. 157–163, 2004.

[3] International Association for the Study of Obesity (IASO), "% Global prevalence of adult obesity (BMI ≥ 30 kg/m2): country rankings 2012," http://www.iaso.org/site_media/uploads/Global_prevalence_of_adult_obesity_Ranking_by_country_2012.pdf, 2012.

[4] WHO, "Obesity: preventing and managing the global epidemic, report of a WHO consultation," WHO Technical Report Series 894, World Health Organization, Geneva, Switzerland, 2000.

[5] G. A. Bray and F. L. Greenway, "Pharmacological treatment of the overweight patient," *Pharmacological Reviews*, vol. 59, no. 2, pp. 151–184, 2007.

[6] United States Food and Drug Administration, Center for Drug Evaluation and Research, "Endocrinologic and metabolic drugs advisory committee," http://www.fda.gov/downloads/AdvisoryCommittees/CommitteesMeetingMaterials/Drugs/EndocrinologicandMetabolicDrugsAdvisoryCommittee/UCM224180.pdf, 2012.

[7] United States Food and Drug Administration, "Meridia (sibutramine): market withdrawal due to risk of serious cardiovascular events," http://www.fda.gov/safety/medwatch/safetyinformation/safetyalertsforhumanmedicalproducts/ucm228830.htm , 2010.

[8] D. Heber, "Herbal preparations for obesity: are they useful?" *Primary Care*, vol. 30, no. 2, pp. 441–463, 2003.

[9] T. K. Lim, *Edible Medicinal and Non-Medicinal Plants*, vol. 2 of *Fruits*, Springer, Heidelberg, Germany, 2012.

[10] W. Sergio, "A natural food, the Malabar Tamnarind, may be effective in the treatment of obesity," *Medical Hypotheses*, vol. 27, no. 1, pp. 39–40, 1988.

[11] H. Drury, *The Useful Plants of India: With Notices of Their Chief Value in Commerce, Medicine, and the Arts*, William H. Allen & Co., London, UK, 2nd edition, 1873.

[12] B. S. Jena, G. K. Jayaprakasha, R. P. Singh, and K. K. Sakariah, "Chemistry and biochemistry of (−)-hydroxycitric acid from Garcinia," *Journal of Agricultural and Food Chemistry*, vol. 50, no. 1, pp. 10–22, 2002.

[13] C. P. Khare, *Indian Medicinal Plants: An Illustrated Dictionary*, Springer, Berlin, Germany, 2007.

[14] A. Sreenivasan and R. Venkataraman, "Chromatographic detection of the organic constituents of Gorikapuli (*Garcinia cambogia* Desr.) used in pickling fish," *Current Science*, vol. 28, pp. 151–152, 1959.

[15] S. E. Ohia, C. A. Opere, A. M. LeDay, M. Bagchi, D. Bagchi, and S. J. Stohs, "Safety and mechanism of appetite suppression by a novel hydroxycitric acid extract (HCA-SX)," *Molecular and Cellular Biochemistry*, vol. 238, no. 1-2, pp. 89–103, 2002.

[16] H. G. Preuss, D. Bagchi, M. Bagchi, C. V. S. Rao, D. K. Dey, and S. Satyanarayana, "Effects of a natural extract of (−)-hydroxycitric acid (HCA-SX) and a combination of HCA-SX plus niacin-bound chromium and *Gymnema sylvestre* extract on weight loss," *Diabetes, Obesity and Metabolism*, vol. 6, no. 3, pp. 171–180, 2004.

[17] S. Roy, C. Rink, S. Khanna et al., "Body weight and abdominal fat gene expression profile in response to a novel hydroxycitric acid-based dietary supplement," *Gene Expression*, vol. 11, no. 5-6, pp. 251–262, 2003.

[18] A. B. Deore, V. D. Sapakal, N. L. Dashputre, and N. S. Naikwade, "Antiulcer activity of *Garcinia indica* linn fruit rinds," *Journal of Applied Pharmaceutical Science*, vol. 1, pp. 151–154, 2011.

[19] P. Mahendran, A. J. Vanisree, and C. S. Shyamala Devi, "The antiulcer activity of *Garcinia cambogia* extract against indomethacin induced gastric ulcer in rats," *Phytotherapy Research*, vol. 16, no. 1, pp. 80–83, 2002.

[20] F. Yamaguchi, M. Saito, T. Ariga, Y. Yoshimura, and H. Nakazawa, "Free radical scavenging activity and antiulcer activity of garcinol from *Garcinia indica* fruit rind," *Journal of Agricultural and Food Chemistry*, vol. 48, no. 6, pp. 2320–2325, 2000.

[21] M. Asghar, E. Monjok, G. Kouamou, S. E. Ohia, D. Bagchi, and M. F. Lokhandwala, "Super CitriMax (HCA-SX) attenuates increases in oxidative stress, inflammation, insulin resistance, and body weight in developing obese Zucker rats," *Molecular and Cellular Biochemistry*, vol. 304, no. 1-2, pp. 93–99, 2007.

[22] M. M. Mackeen, A. M. Ali, N. H. Lajis et al., "Antimicrobial, antioxidant, antitumour-promoting and cytotoxic activities of different plant part extracts of *Garcinia atroviridis* Griff. ex T. Anders," *Journal of Ethnopharmacology*, vol. 72, no. 3, pp. 395–402, 2000.

[23] F. Yamaguchi, T. Ariga, Y. Yoshimura, and H. Nakazawa, "Antioxidative and anti-glycation activity of garcinol from *Garcinia indica* fruit rind," *Journal of Agricultural and Food Chemistry*, vol. 48, no. 2, pp. 180–185, 2000.

[24] Y. Yonei, Y. Takahashi, S. Hibino, M. Watanabe, and T. Yoshioka, "Effects on the human body of a dietary supplement containing L-carnitine and *Garcinia cambogia* extract: a study using double-blind tests," *Journal of Clinical Biochemistry and Nutrition*, vol. 42, no. 2, pp. 89–103, 2008.

[25] P. Y. Wielinga, R. E. Wachters-Hagedoorn, B. Bouter et al., "Hydroxycitric acid delays intestinal glucose absorption in rats," *American Journal of Physiology*, vol. 288, no. 6, pp. G1144–G1149, 2005.

[26] P. S. Negi and G. K. Jayaprakasha, "Control of foodborne pathogenic and spoilage bacteria by garcinol and *Garcinia indica* extracts, and their antioxidant activity," *Journal of Food Science*, vol. 69, no. 3, pp. FMS61–FMS65, 2004.

[27] D. Permana, N. H. Lajis, M. M. Mackeen et al., "Isolation and bioactivities of constitutents of the roots of *Garcinia atroviridis*," *Journal of Natural Products*, vol. 64, no. 7, pp. 976–979, 2001.

[28] K. N. Varalakshmi, C. G. Sangeetha, A. N. Shabeena, S. R. Sunitha, and J. Vapika, "Antimicrobial and cytotoxic effects of *Garcinia indica* fruit rind extract," *American-Eurasian Journal of Agricultural & Environmental Sciences*, vol. 7, pp. 652–656, 2010.

[29] M. M. Mackeen, A. M. Ali, N. H. Lajis, K. Kawazu, H. Kikuzaki, and N. Nakatani, "Antifungal garcinia acid esters from the fruits of *Garcinia atroviridis*," *Zeitschrift fur Naturforschung C*, vol. 57, no. 3-4, pp. 291–295, 2002.

[30] S. B. D. Reis, C. C. De Oliveira, S. C. Acedo et al., "Attenuation of colitis injury in rats using *Garcinia cambogia* extract," *Phytotherapy Research*, vol. 23, no. 3, pp. 324–329, 2009.

[31] A. Syahida, D. A. Israf, D. Permana et al., "Atrovirinone inhibits pro-inflammatory mediator release from murine macrophages and human whole blood," *Immunology and Cell Biology*, vol. 84, no. 3, pp. 250–258, 2006.

[32] E. A. Mazzio and K. F. A. Soliman, "In vitro screening for the tumoricidal properties of international medicinal herbs," *Phytotherapy Research*, vol. 23, no. 3, pp. 385–398, 2009.

[33] M. A. Parasramka and S. V. Gupta, "Garcinol inhibits cell proliferation and promotes apoptosis in pancreatic adenocarcinoma cells," *Nutrition and Cancer*, vol. 63, no. 3, pp. 456–465, 2011.

[34] S. Prasad, J. Ravindran, B. Sung, M. K. Pandey, and B. B. Aggarwal, "Garcinol potentiates TRAIL-induced apoptosis through modulation of death receptors and antiapoptotic proteins," *Molecular Cancer Therapeutics*, vol. 9, no. 4, pp. 856–868, 2010.

[35] K. Ishihara, S. Oyaizu, K. Onuki, K. Lim, and T. Fushiki, "Chronic (−)-hydroxycitrate administration spares carbohydrate utilization and promotes lipid oxidation during exercise in mice," *Journal of Nutrition*, vol. 130, no. 12, pp. 2990–2995, 2000.

[36] G. Kaur and S. K. Kulkarni, "Investigations on possible serotonergic involvement in effects of OB-200G (polyherbal preparation) on food intake in female mice," *European Journal of Nutrition*, vol. 40, no. 3, pp. 127–133, 2001.

[37] Y. J. Kim, K. Kim, M. S. Kim, J. H. Lee, K. P. Lee, and T. Park, "A mixture of the aqueous extract of *Garcinia cambogia*, soy peptide and L-carnitine reduces the accumulation of visceral fat mass in rats rendered obese by a high fat diet," *Genes and Nutrition*, vol. 2, no. 4, pp. 353–358, 2008.

[38] K. Kim, H. N. Lee, Y. J. Kim, and T. Park, "*Garcinia cambogia* extract ameliorates visceral adiposity in C57BL/6J mice fed on a high-fat diet," *Bioscience, Biotechnology and Biochemistry*, vol. 72, no. 7, pp. 1772–1780, 2008.

[39] M. Leonhardt and W. Langhans, "Hydroxycitrate has long-term effects on feeding behavior, body weight regain and metabolism after body weight loss in male rats," *Journal of Nutrition*, vol. 132, no. 7, pp. 1977–1982, 2002.

[40] S. B. Heymsfield, D. B. Allison, J. R. Vasselli, A. Pietrobelli, D. Greenfield, and C. Nunez, "*Garcinia cambogia* (hydroxycitric acid) as a potential antiobesity agent: a randomized controlled trial," *Journal of the American Medical Association*, vol. 280, no. 18, pp. 1596–1600, 1998.

[41] E. M. R. Kovacs, M. S. Westerterp-Plantenga, and W. H. M. Saris, "The effects of 2-week ingestion of (−)-hydroxycitrate and (−)-hydroxycitrate combined with medium-chain triglycerides on satiety, fat oxidation, energy expenditure and body weight," *International Journal of Obesity*, vol. 25, no. 7, pp. 1087–1094, 2001.

[42] A. D. Kriketos, H. R. Thompson, H. Greene, and J. O. Hill, "(−)-Hydroxycitric acid does not affect energy expenditure and substrate oxidation in adult males in a post-absorptive state," *International Journal of Obesity*, vol. 23, no. 8, pp. 867–873, 1999.

[43] L. O. Chuah, S. K. Yeap, W. Y. Ho, B. K. Beh, and N. Banu Alitheen, "*In vitro* and *in vivo* toxicity of *Garcinia* or hydroxycitric acid: a review," *Evidence-Based Complementary and Alternative Medicine*, vol. 2012, Article ID e197920, 12 pages, 2012.

[44] P. C. Sharma, M. B. Yelne, and T. J. Dennis, *Database on Medicinal Plants Used in Ayurveda*, vol. 2, Central Council for Research in Ayurveda & Siddha, New Delhi, India, 2005.

[45] Y. S. Lewis and S. Neelakantan, "(−)-Hydroxycitric acid-the principal acid in the fruits of *Garcinia cambogia* desr," *Phytochemistry*, vol. 4, no. 4, pp. 619–625, 1965.

[46] G. K. Jayaprakasha and K. K. Sakariah, "Determination of organic acids in *Garcinia cambogia* (Desr.) by high- performance liquid chromatography," *Journal of Chromatography A*, vol. 806, no. 2, pp. 337–339, 1998.

[47] G. K. Jayaprakasha and K. K. Sakariah, "Determination of organic acids in leaves and rinds of *Garcinia indica* (Desr.) by LC," *Journal of Pharmaceutical and Biomedical Analysis*, vol. 28, no. 2, pp. 379–384, 2002.

[48] L. Muensritharam, V. Tolieng, C. Chaichantipyuth, A. Petsom, and T. Nhujak, "Capillary zone electrophoresis for separation and analysis of hydroxycitric acid and hydroxycitric acid lactone: application to herbal products of *Garcinia atroviridis* Griff," *Journal of Pharmaceutical and Biomedical Analysis*, vol. 46, no. 3, pp. 577–582, 2008.

[49] D. Permana, F. Abas, M. Maulidiani et al., "Atrovirisidone B, a new prenylated depsidone with cytotoxic property from the roots of *Garcinia atroviridis*," *Zeitschrift fur Naturforschung C*, vol. 60, no. 7-8, pp. 523–526, 2005.

[50] D. Permana, N. H. Lajis, K. Shaari et al., "A new prenylated hydroquinone from the roots of *Garcinia atroviridis* Griff ex T. Anders (Guttiferae)," *Zeitschrift fur Naturforschung B*, vol. 58, no. 4, pp. 332–335, 2003.

[51] M. Iinuma, T. Ito, R. Miyake, H. Tosa, T. Tanaka, and V. Chelladurai, "A xanthone from *Garcinia cambogia*," *Phytochemistry*, vol. 47, no. 6, pp. 1169–1170, 1998.

[52] P. J. Cotterill, F. Scheinmann, and G. S. Puranik, "Phenolic compounds from the heartwood of *Garcinia indica*," *Phytochemistry*, vol. 16, no. 1, pp. 148–149, 1977.

[53] J. Kosin, N. Ruangrungsi, C. Ito, and H. Furukawa, "A xanthone from *Garcinia atroviridis*," *Phytochemistry*, vol. 47, no. 6, pp. 1167–1168, 1998.

[54] M. Masullo, C. Bassarello, H. Suzuki, C. Pizza, and S. Piacente, "Polyisoprenylated benzophenones and an unusual polyisoprenylated tetracyclic xanthone from the fruits of *Garcinia cambogia*," *Journal of Agricultural and Food Chemistry*, vol. 56, no. 13, pp. 5205–5210, 2008.

[55] S. Kumar, S. Sharma, and S. K. Chattopadhyay, "High-performance liquid chromatography and LC-ESI-MS method for identification and quantification of two isomeric polyisoprenylated benzophenones isoxanthochymol and camboginol in different extracts of Garcinia species," *Biomedical Chromatography*, vol. 23, no. 8, pp. 888–907, 2009.

[56] S. K. Chattopadhyay and S. Kumar, "A rapid liquid chromatography-tandem mass spectrometry method for quantification of a biologically active molecule camboginol in the extract of *Garcinia cambogia*," *Biomedical Chromatography*, vol. 21, no. 1, pp. 55–66, 2007.

[57] A. V. Rama Rao, G. Venkatswamy, and A. D. Pendse, "Camboginol and cambogin," *Tetrahedron Letters*, vol. 21, no. 20, pp. 1975–1978, 1980.

[58] N. Krishnamurthy, Y. S. Lewis, and B. Ravindranath, "On the structures of garcinol, isogarcinol and camboginol," *Tetrahedron Letters*, vol. 22, no. 8, pp. 793–796, 1981.

[59] K. Hayamizu, Y. Ishii, I. Kaneko, M. Shen, Y. Okuhara, H. Sakaguchi et al., "No-Observed-Adverse-Effect Level (NOAEL) and sequential-high- dose administration study on *Garcinia cambogia* extract in humans," *Journal of Oleo Science*, vol. 51, pp. 365–369, 2002.

[60] E. M. R. Kovacs and M. S. Westerterp-Plantenga, "Effects of (−)-hydroxycitrate on net fat synthesis as de novo lipogenesis," *Physiology and Behavior*, vol. 88, no. 4-5, pp. 371–381, 2006.

[61] M. S. Westerterp-Plantenga and E. M. R. Kovacs, "The effect of (−)-hydroxycitrate on energy intake and satiety in overweight humans," *International Journal of Obesity*, vol. 26, no. 6, pp. 870–872, 2002.

[62] M. Girola, M. De. Bernardi, and S. Contos, "Dose effect in lipid lowering activity of a new dietary integrator (Chitosan,

Garcinia cambogia extract, and Chrome)," *Acta Toxicologica Et Therapeutica*, vol. 17, pp. 25–40, 1996.

[63] K. Hayamizu, Y. Ishii, I. Kaneko et al., "Effects of *Garcinia cambogia* (Hydroxycitric Acid) on visceral fat accumulation: a double-blind, randomized, placebo-controlled trial," *Current Therapeutic Research*, vol. 64, no. 8, pp. 551–567, 2003.

[64] H. G. Preuss, R. I. Garis, J. D. Bramble et al., "Efficacy of a novel calcium/potassium salt of (−)-hydroxycitric acid in weight control," *International Journal of Clinical Pharmacology Research*, vol. 25, no. 3, pp. 133–144, 2005.

[65] R. Roman Ramos, J. Flores Saenz, and M. C. F. Alarcon Aguilar en, "Control of obesity with *Garcinia cambogia* extract," *Investigacion Medica Internacional*, vol. 22, no. 3, pp. 97–100, 1996.

[66] C. Roongpisuthipong, R. Kantawan, and W. Roongpisuthipong, "Reduction of adipose tissue and body weight: Effect of water soluble calcium hydroxycitrate in *Garcinia atroviridis* on the short term treatment of obese women in Thailand," *Asia Pacific Journal of Clinical Nutrition*, vol. 16, no. 1, pp. 25–29, 2007.

[67] E. Toromanyan, G. Aslanyan, E. Amroyan, E. Gabrielyan, and A. Panossian, "Efficacy of Slim339 in reducing body weight of overweight and obese human subjects," *Phytotherapy Research*, vol. 21, no. 12, pp. 1177–1181, 2007.

[68] E. Thom, "A randomized, double-blind, placebo-controlled trial of a new weight-reducing agent of natural origin," *Journal of International Medical Research*, vol. 28, no. 5, pp. 229–233, 2000.

[69] R. D. Mattes and L. Bormann, "Effects of (−)-hydroxycitric acid on appetitive variables," *Physiology and Behavior*, vol. 71, no. 1-2, pp. 87–94, 2000.

[70] L. J. C. Van Loon, J. J. M. Van Rooijen, B. Niesen, H. Verhagen, W. H. M. Saris, and A. J. M. Wagenmakers, "Effects of acute (−)-hydroxycitrate supplementation on substrate metabolism at rest and during exercise in humans," *American Journal of Clinical Nutrition*, vol. 72, no. 6, pp. 1445–1450, 2000.

[71] E. M. R. Kovacs, M. S. Westerterp-Plantenga, M. De Vries, F. Brouns, and W. H. M. Saris, "Effects of 2-week ingestion of (−)-hydroxycitrate and (−)-hydroxycitrate combined with medium-chain triglycerides on satiety and food intake," *Physiology and Behavior*, vol. 74, no. 4-5, pp. 543–549, 2001.

[72] A. A. Conte, "A non-prescription alternative in weight reduction therapy," *American Journal of Bariatric Medicine*, pp. 17–19, summer1993.

[73] J. Kim, S. Jeon, K. Park et al., "Does Glycine max leaves or *Garcinia cambogia* promote weight-loss or lower plasma cholesterol in overweight individuals: a randomized control trial," *Nutrition Journal*, vol. 10, no. 1, article 94, 2011.

[74] T. Opala, P. Rzymski, I. Pischel, M. Wilczak, and J. Woźniak, "Efficacy of 12 weeks supplementation of a botanical extract-based weight loss formula on body weight, body composition and blood chemistry in healthy, overweight subjects—a randomised double-blind placebo-controlled clinical trial," *European Journal of Medical Research*, vol. 11, no. 8, pp. 343–350, 2006.

[75] C. A. R. Vasques, S. Rossetto, G. Halmenschlager et al., "Evaluation of the pharmacotherapeutic efficacy of *Garcinia cambogia* plus amorphophallus konjac for the treatment of obesity," *Phytotherapy Research*, vol. 22, no. 9, pp. 1135–1140, 2008.

[76] K. Hayamizu, H. Tomi, I. Kaneko, M. Shen, M. G. Soni, and G. Yoshino, "Effects of *Garcinia cambogia* extract on serum sex hormones in overweight subjects," *Fitoterapia*, vol. 79, no. 4, pp. 255–261, 2008.

[77] *The Wealth of India: Raw Materials IV*, CSIR, New Delhi, India, 1956.

[78] A. C. Sullivan, J. Triscari, and H. E. Spiegel, "Metabolic regulation as a control for lipid disorders. I. Influence of, (−)-hydroxycitrate on experimentally induced obesity in the rodent," *American Journal of Clinical Nutrition*, vol. 30, pp. 767–776, 1977.

[79] A. C. Sullivan, J. Triscari, and H. E. Spiegel, "Metabolic regulation as a control for lipid disorders. II. Influence of (−)-hydroxycitrate on genetically and experimentally induced hypertriglyceridemia in the rat," *American Journal of Clinical Nutrition*, vol. 30, no. 5, pp. 777–784, 1977.

[80] W. C. Stallings, J. F. Blount, P. A. Srere, and J. P. Glusker, "Structural studies of hydroxycitrates and their relevance to certain enzymatic mechanisms," *Archives of Biochemistry and Biophysics*, vol. 193, no. 2, pp. 431–448, 1979.

[81] J. Kjeldstadli and E. Thom, "Synthetically prepared composition for treatment and/or prophylaxis of overweight, and use thereof," US patent, EP, 1007027 A2, 2000.

[82] S. Haleema, P. V. Sasi, I. Ibnusaud, P. L. Polavarapu, and H. B. Kagan, "Enantiomerically pure compounds related to chiral hydroxy acids derived from renewable resources," *RSC Advances*, vol. 2, pp. 9257–9285, 2012.

[83] J. Louter-Van De Haar, P. Y. Wielinga, A. J. W. Scheurink, and A. G. Nieuwenhuizen, "Comparison of the effects of three different (−)-hydroxycitric acid preparations on food intake in rats," *Nutrition and Metabolism*, vol. 2, article 23, 2005.

[84] B. W. Downs, M. Bagchi, G. V. Subbaraju, M. A. Shara, H. G. Preuss, and D. Bagchi, "Bioefficacy of a novel calcium-potassium salt of (−)-hydroxycitric acid," *Mutation Research*, vol. 579, no. 1-2, pp. 149–162, 2005.

[85] A. C. Sullivan, J. G. Hamilton, O. N. Miller, and V. R. Wheatley, "Inhibition of lipogenesis in rat liver by (−)-hydroxycitrate," *Archives of Biochemistry and Biophysics*, vol. 150, no. 1, pp. 183–190, 1972.

[86] D. Bagchi, G. Trimurtulu, A. V. K. Raju, K. Sengupta, P. B. S. Murthy, and T. V. N. Rao, "Comparative bioavailability of (−)-hydroxycitric acid from oral administration of HCA calcium salt and calcium-potassium double salt in Albino Wistar rats," *Journal of the Federation of American Societies For Experimental Biology*, vol. 24, p. 505, 2010.

[87] M. Asghar, R. Zeyssig, E. Monjok et al., "Hydroxycitric acid (HCA-SX) decreases oxidative stress and insulin resistance and increases brain serotonin levels in obese Zucker rats," *Experimental Biology Meeting*, vol. 20, Article ID A655.4, 2006.

[88] S. Roy, H. Shah, C. Rink et al., "Transcriptome of primary adipocytes from obese women in response to a novel hydroxycitric acid-based dietary supplement," *DNA and Cell Biology*, vol. 26, no. 9, pp. 627–639, 2007.

[89] R. Uauy and E. Díaz, "Consequences of food energy excess and positive energy balance," *Public Health Nutrition*, vol. 8, no. 7 A, pp. 1077–1099, 2005.

[90] M. Shara, S. E. Ohia, T. Yasmin et al., "Dose- and time-dependent effects of a novel (−)-hydroxycitric acid extract on body weight, hepatic and testicular lipid peroxidation, DNA fragmentation and histopathological data over a period of 90 days," *Molecular and Cellular Biochemistry*, vol. 254, no. 1-2, pp. 339–346, 2003.

[91] M. Shara, S. E. Ohia, R. E. Schmidt et al., "Physico-chemical properties of a novel (−)-hydroxycitric acid extract and its effect on body weight, selected organ weights, hepatic lipid

peroxidation and DNA fragmentation, hematology and clinical chemistry, and histopathological changes over a period of 90 days," *Molecular and Cellular Biochemistry*, vol. 260, no. 1, pp. 171–186, 2004.

[92] K. A. Amin, H. H. Kamel, and M. A. Abd Eltawab, "Protective effect of Garcinia against renal oxidative stress and biomarkers induced by high fat and sucrose diet," *Lipids in Health and Disease*, vol. 10, article 6, 2011.

[93] J. A. Watson, M. Fang, and J. M. Lowenstein, "Tricarballylate and hydroxycitrate: substrate and inhibitor of ATP: citrate oxaloacetate lyase," *Archives of Biochemistry and Biophysics*, vol. 135, no. C, pp. 209–217, 1969.

[94] T. A. Berkhout, L. M. Havekes, N. J. Pearce, and P. H. E. Groot, "The effect of (−)-hydroxycitrate on the activity of the low-density-lipoprotein receptor and 3-hydroxy-3-methylglutaryl-CoA reductase levels in the human hepatoma cell line Hep G2," *Biochemical Journal*, vol. 272, no. 1, pp. 181–186, 1990.

[95] H. Chee, D. R. Romsos, and G. A. Leveille, "Influence of (−) hydroxycitrate on lipogenesis in chickens and rats," *Journal of Nutrition*, vol. 107, no. 1, pp. 112–119, 1977.

[96] A. C. Sullivan, J. Triscari, J. G. Hamilton, and O. N. Miller, "Effect of (−)-hydroxycitrate upon the accumulation of lipid in the rat: II. Appetite," *Lipids*, vol. 9, no. 2, pp. 129–134, 1974.

[97] A. C. Sullivan, J. Triscari, and J. G. Hamilton, "Effect of (−)-hydroxycitrate upon the accumulation of lipid in the rat: I. Lipogenesis," *Lipids*, vol. 9, no. 2, pp. 121–128, 1974.

[98] G. D. Lopaschuk, J. R. Ussher, and J. S. Jaswal, "Targeting intermediary metabolism in the hypothalamus as a mechanism to regulate appetite," *Pharmacological Reviews*, vol. 62, no. 2, pp. 237–264, 2010.

[99] N. B. Rederman, A. K. Saha, D. Vavvas, and L. A. Witters, "Malonyl-CoA, fuel sensing, and insulin resistance," *American Journal of Physiology*, vol. 276, pp. E1–E18, 1999.

[100] S. E. Ohia, S. O. Awe, A. M. LeDay, C. A. Opere, and D. Bagchi, "Effect of hydroxycitric acid on serotonin release from isolated rat brain cortex," *Research Communications in Molecular Pathology and Pharmacology*, vol. 109, no. 3-4, pp. 210–216, 2001.

[101] J. McGuirk, R. Muscat, and P. Willner, "Effects of chronically administerd fluoxetine and fenfluramine on food intake, body weight and the behavioural satiety sequence," *Psychopharmacology*, vol. 106, no. 3, pp. 401–407, 1992.

[102] M. Leonhardt, B. Hrupka, and W. Langhans, "Effect of hydroxycitrate on food intake and body weight regain after a period of restrictive feeding in male rats," *Physiology and Behavior*, vol. 74, no. 1-2, pp. 191–196, 2001.

[103] M. R. Greenwood, M. P. Cleary, R. Gruen et al., "Effect of (−)-hydroxycitrate on development of obesity in the Zucker obese rat," *The American journal of physiology*, vol. 240, no. 1, pp. E72–E78, 1981.

[104] A. C. Sullivan and J. Triscari, "Metabolic regulation as a control for lipid disorders. I. Influence of (−)-hydroxycitrate on experimentally induced obesity in the rodent," *American Journal of Clinical Nutrition*, vol. 30, no. 5, pp. 767–776, 1977.

[105] J. Triscari and A. C. Sullivan, "Comparative effects of (−)-hydroxycitrate and (+)-allo hydroxycitrate on acetyl CoA carboxylase and fatty acid and cholesterol synthesis in vivo," *Lipids*, vol. 12, no. 4, pp. 357–363, 1977.

[106] M. Leonhardt, B. Balkan, and W. Langhans, "Effect of hydroxycitrate on respiratory quotient, energy expenditure, and glucose tolerance in male rats after a period of restrictive feeding," *Nutrition*, vol. 20, no. 10, pp. 911–915, 2004.

[107] S. Cheema Dhadli, M. L. Halperin, and C. C. Leznoff, "Inhibition of enzymes which interact with citrate by (−)-hydroxycitrate and 1,2,3 tricarboxybenzene," *European Journal of Biochemistry*, vol. 38, no. 1, pp. 98–102, 1973.

[108] J. M. Lowenstein, "Effect of (−)-hydroxycitrate on fatty acid synthesis by rat liver in vivo," *Journal of Biological Chemistry*, vol. 246, no. 3, pp. 629–632, 1971.

[109] K. Lim, S. Ryu, H. Nho et al., "(−)-Hydroxycitric acid ingestion increases fat utilization during exercise in untrained women," *Journal of Nutritional Science and Vitaminology*, vol. 49, no. 3, pp. 163–167, 2003.

[110] K. Lim, S. Ryu, Y. Ohishi et al., "Short-term (−)-hydroxycitrate ingestion increases fat oxidation during exercise in athletes," *Journal of Nutritional Science and Vitaminology*, vol. 48, no. 2, pp. 128–133, 2002.

[111] J. R. Vasselli, E. Shane, C. N. Boozer, and S. B. Heymsfield, "*Garcinia cambogia* extract inhibits body weight gain via increased Energy Expenditure (EE) in rats," *The FASEB Journal*, vol. 12, no. 4, p. A505, 1998.

[112] V. Leray, H. Dumon, L. Martin et al., "No effect of conjugated linoleic acid or *Garcinia cambogia* on fat-free mass, and energy expenditure in normal cats," *Journal of Nutrition*, vol. 136, no. 7, 2006.

[113] G. Blunden, "Garcinia extract inhibits lipid droplet accumulation without affecting adipose conversion in 3T3-L1 cells," *Phytotherapy Research*, vol. 15, no. 2, pp. 172–173, 2001.

[114] E. D. Rosen, C. J. Walkey, P. Puigserver, and B. M. Spiegelman, "Transcriptional regulation of adipogenesis," *Genes and Development*, vol. 14, no. 11, pp. 1293–1307, 2000.

[115] E. D. Rosen, C. Hsu, X. Wang et al., "C/EBPα induces adipogenesis through PPARγ: a unified pathway," *Genes and Development*, vol. 16, no. 1, pp. 22–26, 2002.

[116] J. B. Kim, H. M. Wright, M. Wright, and B. M. Spiegelman, "ADD1/SREBP1 activates PPARγ through the production of endogenous ligand," *Proceedings of the National Academy of Sciences of the United States of America*, vol. 95, no. 8, pp. 4333–4337, 1998.

[117] S. Dagogo-Jack, "Human leptin regulation and promise in pharmacotherapy," *Current Drug Targets*, vol. 2, no. 2, pp. 181–195, 2001.

[118] H. Staiger, O. Tschritter, J. Machann et al., "Relationship of serum adiponectin and leptin concentrations with body fat distribution in humans," *Obesity Research*, vol. 11, no. 3, pp. 368–372, 2003.

[119] S. T. Nadler, J. P. Stoehr, K. L. Schueler, G. Tanimoto, B. S. Yandell, and A. D. Attie, "The expression of adipogenic genes is decreased in obesity and diabetes mellitus," *Proceedings of the National Academy of Sciences of the United States of America*, vol. 97, no. 21, pp. 11371–11376, 2000.

[120] G. S. Hotamisligil, N. S. Shargill, and B. M. Spiegelman, "Adipose expression of tumor necrosis factor-α: direct role in obesity-linked insulin resistance," *Science*, vol. 259, no. 5091, pp. 87–91, 1993.

[121] J. M. Stephens and P. H. Pekala, "Transcriptional repression of the C/EBP-α and GLUT4 genes in 3T3-L1 adipocytes by tumor necrosis factor-α. Regulation is coordinate and independent of protein synthesis," *The Journal of Biological Chemistry*, vol. 267, no. 19, pp. 13580–13584, 1992.

[122] H. Xing, J. P. Northrop, J. Russell Grove, K. E. Kilpatrick, S. U. Jui-Lan, and G. M. Ringold, "TNFα-mediated inhibition and reversal of adipocyte differentiation is accompanied by

suppressed expression of PPARγ without effects on Pref-1 expression," *Endocrinology*, vol. 138, no. 7, pp. 2776–2783, 1997.

[123] K. Hayamizu, H. Hirakawa, D. Oikawa et al., "Effect of *Garcinia cambogia* extract on serum leptin and insulin in mice," *Fitoterapia*, vol. 74, no. 3, pp. 267–273, 2003.

[124] K. Laubner, T. J. Kieffer, N. T. Lam, X. Niu, F. Jakob, and J. Seufert, "Inhibition of preproinsulin gene expression by leptin induction of suppressor of cytokine signaling 3 in pancreatic β-cells," *Diabetes*, vol. 54, no. 12, pp. 3410–3417, 2005.

[125] R. H. Lustig, "Childhood obesity: behavioral aberration or biochemical drive? Reinterpreting the first law of thermodynamics," *Nature Clinical Practice Endocrinology and Metabolism*, vol. 2, no. 8, pp. 447–458, 2006.

[126] M. H. Pittler and E. Ernst, "Dietary supplements for body-weight reduction: a systematic review," *American Journal of Clinical Nutrition*, vol. 79, no. 4, pp. 529–536, 2004.

[127] V. Badmaev, M. Majeed, A. A. Conte et al., "*Garcinia cambogia* for weight loss [letter]," *Journal of the American Medical Association*, vol. 282, no. 3, pp. 233–235, 1999.

[128] V. Badmaev, M. Majeed, A. A. Conte et al., "*Garcinia cambogia* for weight loss [letter]," *Journal of the American Medical Association*, vol. 282, no. 3, pp. 233–235, 1999.

[129] V. Badmaev, M. Majeed, A. A. Conte et al., "*Garcinia cambogia* for weight loss [letter]," *Journal of the American Medical Association*, vol. 282, no. 3, pp. 233–235, 1999.

[130] J. L. Schaller, "*Garcinia cambogia* for weight loss [letter]," *The journal of the American Medical Association*, vol. 282, no. 3, pp. 234–235, 1999.

[131] I. Onakpoya, S. K. Hung, R. Perry, B. Wider, and E. Ernst, "The use of Garcinia extract (Hydroxycitric Acid) as a weight loss supplement: a systematic review and meta-analysis of randomized clinical trials," *Journal of Obesity*, vol. 2011, Article ID 509038, 9 pages, 2011.

[132] N. S. Deshmukh, M. Bagchi, T. Yasmin, and D. Bagchi, "Safety of a novel calcium/potassium salt of hydroxycitric acid (HCA-SX): I. Two-generation reproduction toxicity study," *Toxicology Mechanisms and Methods*, vol. 18, no. 5, pp. 433–442, 2008.

Hindawi Publishing Corporation
Evidence-Based Complementary and Alternative Medicine
Volume 2013, Article ID 272795, 7 pages
http://dx.doi.org/10.1155/2013/272795

Research Article

Inhibitory Effect of the Hexane Fraction of the Ethanolic Extract of the Fruits of *Pterodon pubescens* Benth in Acute and Chronic Inflammation

Jaqueline Hoscheid,[1] Ciomar Aparecida Bersani-Amado,[2] Bruno Ambrósio da Rocha,[2] Priscila Miyuki Outuki,[1] Maria Angélica Raffaini Cóvas Pereira da Silva,[2] Diego Lacir Froehlich,[3] and Mara Lane Carvalho Cardoso[1]

[1] *Universidade Estadual de Maringá, Centro de Ciências da Saúde, Departamento de Farmácia, Avenida Colombo, 5790 bloco K80. Zona Sete, 87020-900 Maringá, PR, Brazil*
[2] *Universidade Estadual de Maringá, Centro de Ciências da Saúde, Departamento de Farmacologia e Terapêutica, Avenida Colombo, 5790 bloco K68. Zona Sete, 87020-900 Maringá, PR, Brazil*
[3] *Pontifícia Universidade Católica do Paraná-PUCPR, Escola de Ciências Agrárias, Avenida da União, 500. Jardim Coopagro, 85902-532 Toledo, PR, Brazil*

Correspondence should be addressed to Mara Lane Carvalho Cardoso; mlanecc@yahoo.com.br

Received 21 May 2013; Revised 19 June 2013; Accepted 19 June 2013

Academic Editor: Mohamed Eddouks

Fruits of *Pterodon pubescens* Benth have been used traditionally for the treatment of rheumatism, sore throat, and respiratory disorders, and also as anti-inflammatory, analgesic, depurative, tonic, and hypoglycemic agent. The study was aimed at evaluating the anti-inflammatory activity of the hexane fraction of an ethanolic extract of *P. pubescens* fruits. The oil from *P. pubescens* fruits was extracted with ethanol and partitioned with hexane. The anti-inflammatory activity was measured with increasing doses of the hexane fraction (FHPp) by using a carrageenan-induced rat model of pleurisy and a rat model of complete Freund's adjuvant-induced arthritis by using an FHPp dose of 250 mg/kg for 21 days. Treatment with an FHPp resulted in anti-inflammatory activity in both models. The results of biochemical, hematological, and histological analyses indicated a significant decrease in glucose, cholesterol, and triglycerides levels (18.32%, 34.20%, and 41.70%, resp.) and reduction in the numbers of total leukocytes and mononuclear cells. The FHPp dose of 1000 mg/kg induced no changes in behavioral parameters, and no animal died. The results of this study extend the findings of previous reports that have shown that administration of extracts and fractions obtained from species of the genus *Pterodon* exhibits anti-inflammatory activity and lacks toxicity.

1. Introduction

Pterodon pubescens Benth (Leguminosae), commonly known as "faveira," "sucupira," or "sucupira branca," is a tree native to Brazil and is distributed across its central region [1]. The *P. pubescens* fruit is traditionally used in ethnomedicine as an infusion [2], in small doses and at regular time intervals as an anti-inflammatory, analgesic, tonic, depurative [3, 4], and hypoglycemic agent [5].

Active metabolites from species belonging to the genus *Pterodon* are being isolated and their medicinal properties are being investigated. Several studies have shown that oil from the fruit of *P. pubescens* has a significant level of furanoditerpenes, which are directly involved in the pharmacological activities of this fruit [6–9]. The hydroalcoholic extract of the *P. pubescens* fruit when administered orally (gavage) shows antinociceptive properties [10, 11] and anti-inflammatory activity in a mouse model of collagen-induced arthritis [12, 13] without altering hematological, clinical, biochemical, and histopathological parameters [12]. The ethanol extract of the fruit also demonstrates anti-inflammatory activity [7] and suppressive effects on the immune response mediated by T

and B lymphocytes [2]. The goal of our current study was to evaluate the anti-inflammatory activity of the hexane fraction (FHPp) of the ethanol extract obtained from the fruit of *P. pubescens* by using a rat model of pleurisy and a rat model of arthritis induced by complete Freund's adjuvant (CFA).

2. Material and Methods

2.1. Animals. The experimental procedures were approved by the Ethics Committee of the Universidade Estadual de Maringa (protocol number 018/2011). The carrageenan induced pleurisy model was established using male Wistar rats (weight: 200–220 g), and the adjuvant-induced arthritis model was established using male Holtzman rats (weight: 170–200 g); male Swiss mice (weight: 20–30 g) were used for a toxicity study. The animals were housed at 22 ± 2°C under a 12 h light/12 h dark cycle with free access to food and water.

2.2. Collection of the Vegetal Material and Extractive Process. *P. pubescens* Benth fruits were collected from Nossa Senhora do Livramento, M.T., Brazil (15°89′ S; 56°41′ W) in May 2010 and identified by Dr. Germano Guarim Neto from the Herbarium of Federal University of Mato Grosso, and the voucher specimen was deposited in the Herbarium of Maringá State University, under number 20502. The dried fruits (30 g) were extracted with ethanol 99.5% P.A. (600 mL) by turbo extraction and then filtered. The filtrate was partitioned with water:hexane (1 : 1). The organic solvent was evaporated in a vacuum evaporator to yield the hexane fraction (FHPp) as previously described [14].

2.3. Acute Carrageenan-Induced Inflammatory Reaction in the Pleural Cavity of Rats. The test was conducted according to the method described by Vinegar et al. [15]. Groups of rats ($n = 5$ per group) were pretreated by oral gavage with a solution of FHPp (125, 250, and 500 mg/kg) in 2% Tween 80 in water, dexamethasone (0.5 mg/kg) as a standard drug, or a solution of 2% Tween 80 in water as a control. After 1 h, all animals received an intrapleural injection of carrageenan (200 μg/animal). Four hours later, the animals were anesthetized with xylazine (10 mg/kg), the pleural exudate was collected, and its volume was determined. The number of leukocytes that migrated to the exudate was measured using a Neubauer chamber cell counting.

2.4. Induction and Evaluation of Experimental Arthritis. Adjuvant-induced arthritis (AIA) was produced on day 0 by an intradermal injection of 100 μL of a CFA suspension (heat-inactivated *M. tuberculosis* suspended in mineral oil at a concentration of 0.5% w/v) into the left hind paw [16]. The development of AIA was assessed by paw volume changes and appearance of secondary lesions. The volume of the injected and noninjected hind paw was determined by digital plethysmography. The results were expressed as the increase in paw volume relative to the initial volume. Measurements were performed over a 21-day period. The severity of secondary lesions was evaluated using a numerical grading system [17]. Briefly, points were assigned to each of the following events: appearance of nodules in the tail (+1); appearance of nodules in one or both ears (+1 or +2); and appearance of swelling in one or both forelimbs (+1 or +2). The severity of the secondary lesions was graded from 0 to 5, with 0 indicating the absence of lesions. Body weight was assessed daily at 15 h.

In this experiment, the animals ($n = 5$ per group) were divided into 3 treatment groups: (1) animals with arthritis which received only distilled water (AIA control); (2) animals with arthritis which received Tween 80 solution at 2% in distilled water (AIA + Tween); and (3) animals with arthritis which received 250 mg/kg of FHPp suspended in 2% Tween 80 (AIA + FHPp). Treatment was performed daily by oral administration (gavage) for a period of 21 days starting on the day of the intradermal adjuvant injection.

2.5. Subacute Toxicological Evaluation of FHPp

2.5.1. Hematological Examination. An aliquot of blood from the distal end of the rats' tails was collected for the determination of total white blood cell count and white blood cell differentials prior to induction of AIA (day 0) and after 21 days of treatment.

2.5.2. Biochemical Examination. The biochemical analyses for determination of glucose, cholesterol, triglycerides, urea, creatinine, alanine aminotransferase (ALT), and aspartate aminotransferase (AST) levels were performed using blood samples collected with heparin from the abdominal vena cava on treatment day 21. The blood was centrifuged and stored at −4°C until use. The analyses were performed with a spectrophotometer (Bio-BIOPLUS 2000) using biochemical kits (analyzed).

2.5.3. Organ Weights and Histopathological Examination. Animals were killed 21 days after AIA. During necropsy, the weight of several organs (the liver, kidney, spleen, thymus, adrenal gland, and lymph nodes) was determined and expressed as weight (g) of fresh organ/100 g animal body weight.

The livers and kidneys were preserved in a formalin solution for routine histological processing. Then, these were embedded in paraffin, sectioned, and stained with hematoxylin and eosin for histopathological examination according to conventional histological methods.

2.6. Acute Toxicity. For evaluation of toxicity, Swiss mice ($n = 6$) were fasted for 15 h. Each animal was orally administered 1000 mg/kg of the FHPp suspended in 2% Tween 80. During the first 4 h after administration, behavioral parameters (motor activity, convulsions, piloerection, salivation, and sedation) were observed and described according to Malone and Robichaud [18]. Body weight was assessed for a period of 7 days.

2.7. Evaluation of Food Intake and Body Weight of Rats Treated with FHPp. After induction of arthritis by CFA, rats in the treatment group received a solution of 250 mg/kg FHPp in

Table 1: FHPp effect on carrageenan-induced pleurisy.

Group	Exudate volume (mL)	% Edema inhibition	Leukocyte count (cells/mm^3)
Control	0.80 ± 0.02	—	63400 ± 3323
FHPp 125 mg/kg	0.72 ± 0.04	10.0	59277 ± 3068
FHPp 250 mg/kg	0.57 ± 0.03[c]	28.7	51444 ± 3749
FHPp 500 mg/kg	0.59 ± 0.03[b]	26.3	48316 ± 2224[a]
Dexamethasone 0.5 mg/kg	0.20 ± 0.02[c]	75.0	17640 ± 1065[c]

Values expressed in mean ± S.E.M. ($n = 5$). [a]$P < 0.05$; [b]$P < 0.01$; [c]$P < 0.001$ compared to the control group. One-way ANOVA post hoc Tukey test.

Table 2: Effect of FHPp (250 mg/kg) on the severity of secondary injuries induced by CFA.

Day	AIA control	AIA + Tween	AIA + FHPp
11°	1.5	0.5	0.1
12°	4.2	3.5	0.4
13°	4.7	4.0	2.0
14°	4.7	4.2	3.4
15°	5.0	4.7	4.4
16°	5.0	5.0	4.7
17°	5.0	5.0	5.0

2% Tween 80 and distilled water, while control rats received only distilled water. All rats were kept in metabolism cages for 21 days to assess food and water intake and to collect urine. Body weights were evaluated daily.

2.8. Statistical Analysis. Data are presented as means ± standard error of the mean (S.E.M.). Results were statistically analyzed using GraphPad software (GraphPad Software, Inc., San Diego, CA, USA). Student's t-tests for unpaired data (two-tailed) or one-way analysis of variance (ANOVA) followed by post hoc Tukey tests was performed. P values less than 0.05 were considered statistically significant.

3. Results

3.1. Effects of FHPp in the Rat Model of Carrageenan-Induced Pleurisy. In animals treated with vehicle (control group), an intrapleural injection of carrageenan caused accumulation of a pleural exudate and intense recruitment of leukocytes to the inflamed site. Treatment of rats with FHPp at doses of 250 and 500 mg/kg significantly reduced the volume of the inflammatory exudate by 28.7% and 26.6%, respectively. However, only the higher dose (500 mg/kg) caused a significant decrease in the number of leukocytes (Table 1). As expected, animals treated with dexamethasone (0.5 mg/kg) showed no inflammatory cell infiltration.

3.2. Complete Freund's Adjuvant-Induced Arthritis Model

3.2.1. FHPp Effects in the AIA Model. We observed an intense inflammatory reaction in the left hind paw following injection of complete Freund's adjuvant (CFA) on the first day, and the reaction progressively worsened during the following 21 days. An inflammatory response in the noninjected paw (right hind paw) was observed from the tenth day after the induction of AIA and increased gradually until day 21. Treatment of rats with FHPp at a dose of 250 mg/kg did not affect the development of edema in the paw injected with CFA but significantly reduced the edema in the right foot, which was not injected with CFA. Treatment of rats with Tween (used with vehicle) did not affect the inflammatory response in either paw as compared to the control group of AIA rats. The results are shown in Figures 1(a) and 1(b).

As shown in Table 2, treatment with FHPp delayed the onset of the secondary injury that developed starting on the tenth day after the induction of arthritis. In addition, secondary lesions developed less aggressively in the rats treated with FHPp.

Table 3: Effect of FHPp (250 mg/kg) on total and differential circulating leukocytes.

Parameters	Group		
	AIA control	AIA + Tween	AIA + FHPp
Day zero			
TL	11937 ± 323	11950 ± 204	11978 ± 508
MN	9821 ± 328	9890 ± 233	9793 ± 454
PMN	2116 ± 158	2060 ± 132	2185 ± 157
21° day			
TL	51867 ± 3407	45900 ± 1088	37429 ± 2373[a]
MN	42412 ± 1940	36787 ± 370	29681 ± 1884[a]
PMN	9455 ± 1653	9113 ± 973	7748 ± 650

The data are expressed as mean ± S.E.M. ($n = 5$). TL: total leukocyte; MN: mononuclear cells; PMN: polymorphonuclear cells; the determination of the number of cells was performed on day zero (before the injection of CFA in the left hind paw) and on day 21 after induction of arthritis. [a]$P < 0.01$ compared to the AIA control group. One-way ANOVA post hoc Tukey test.

3.2.2. Hematological Examination. Compared to the blood obtained from the control rats, the blood obtained from rats after induction of AIA showed a significant increase in the number of total and differential leukocytes. However, daily treatment with FHPp at a dose of 250 mg/kg significantly reduced the total number of leukocytes and mononuclear cells compared to the corresponding numbers in the controls (Table 3).

3.2.3. Biochemical Analysis. Statistically significant changes were observed in plasma levels of glucose, cholesterol, and triglycerides in AIA rats treated with FHPp compared to the AIA control rats and normal animals.

Compared to the untreated group with arthritis, FHPp-treated rats with arthritis did not show significantly altered levels of creatinine, urea, ALT, or AST. However, ALT and urea levels were significantly different in the 2 groups as compared to the corresponding levels observed in normal Holtzman rats (Table 4).

3.2.4. Relative Weight of Organs and Histological Evaluation. After 21 days of FHPp treatment, there were no significant changes in the relative weight of lymphoid organs (Table 5).

Table 4: Effect of FHPp (250 mg/kg) on biochemical measurements after 21 days of treatment.

Parameters	Groups			
	Normal	AIA control	AIA + Tween	AIA + FHPp
Glucose (mg/dL)	126.8 ± 3.5	124.7 ± 3.7	106.2 ± 5.8	101.8 ± 4.3[a,d]
Total cholesterol (mg/dL)	112.3 ± 3.1	98.0 ± 5.1	88.3 ± 9.9	64.5 ± 3.2[b,e]
Triglycerides (mg/dL)	64.6 ± 5.8	73.5 ± 4.0	51.4 ± 7.2	42.9 ± 4.8[b,c]
Creatinine (mg/dL)	0.62 ± 0.0	0.62 ± 0.0	0.61 ± 0.0	0.63 ± 0.01
Urea (mg/dL)	32.2 ± 1.4	44.0 ± 2.2	43.4 ± 5.4	45.7 ± 3.8[c]
ALT (U/L)	79.4 ± 5.7	37.0 ± 2.7[e]	31.6 ± 0.9[e]	45.3 ± 3.31[e]
AST (U/L)	102.2 ± 2.5	98.1 ± 5.3	110.4 ± 12.2	107.0 ± 2.5

Values expressed in mean ± S.E.M. ($n = 5$). [a]$P < 0.01$; [b]$P < 0.001$ compared to the AIA control group by Tukey's test; [c]$P < 0.05$; [d]$P < 0.01$; [e]$P < 0.001$ compared to the normal group. One-way ANOVA post hoc Tukey test.

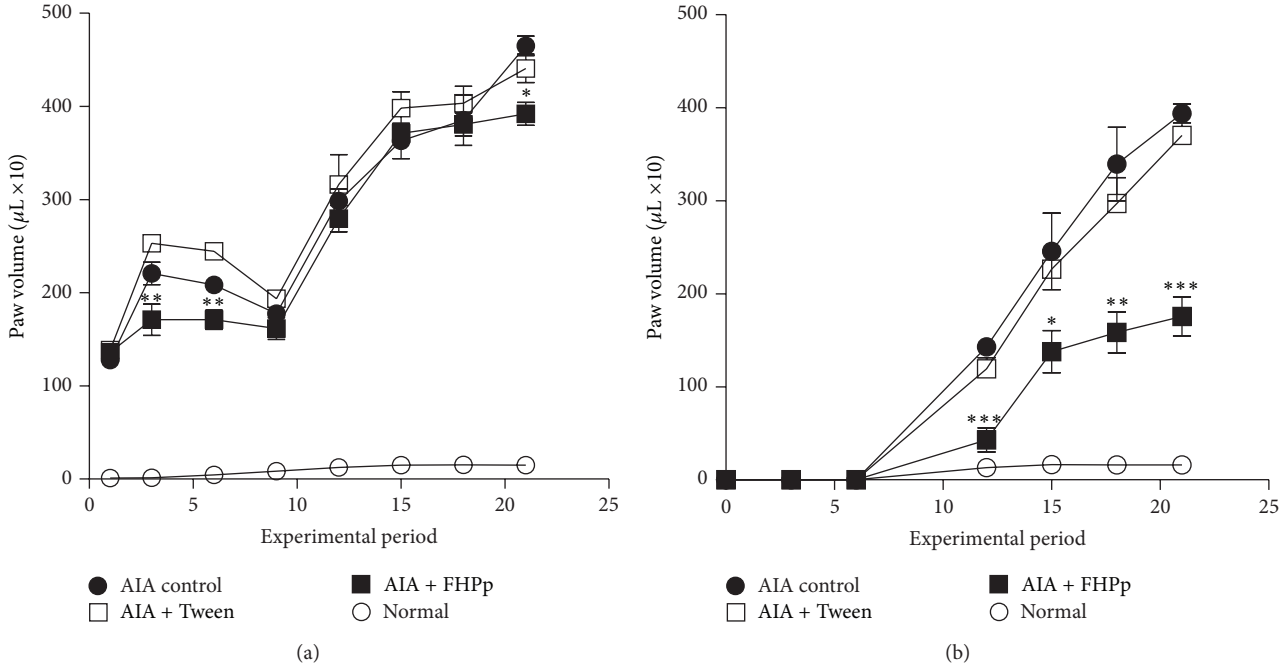

Figure 1: Development of the inflammatory response in the hind paws of rats: (a) left paw injected with complete Freund's adjuvant and (b) right paw, not injected. Each point represents the mean ± S.E.M. ($n = 5$). $^{*}P < 0.05$; $^{**}P < 0.01$; $^{***}P < 0.001$ compared to the AIA control group. One-way ANOVA post hoc Tukey test.

Histological analysis demonstrated the absence of lesions in kidney and liver samples from animals treated with FHPp (Figure 2).

3.2.5. Evaluation of the Toxicity of FHPp. In acute toxicity studies (hippocratic test), treatment with FHPp at doses up to 1000 mg/kg caused no observable changes in behavioral parameters or body weight, and no animal died.

3.2.6. Assessment of Food Intake and Body Weight. The weight of the animals increased progressively until the tenth day, when the systemic manifestations of the disease began, at which time a slight weight loss occurred.

There were no statistically significant changes in water or food intake or in the volume of urine produced between the groups AIA control and AIA + FHPp. However, the group treated daily with 250 mg/kg of FHPp showed significantly less weight gain than the other groups (AIA Control) (Figure 3).

4. Discussion

The present study evaluated the effects of the hexane fraction of the ethanolic extract of *P. pubescens* administered orally in two *in vivo* inflammatory models: carrageenan-induced inflammatory reaction in the pleural cavity and CFA-induced arthritis. The results showed that FHPp treatment induced anti-inflammatory effects in both models.

Our results are consistent with those of Carvalho et al. [6], who evaluated the acute anti-inflammatory activity of the hexane extract of *P. emarginatus* in a carrageenan-induced peritonitis model. They suggested that the activity of the

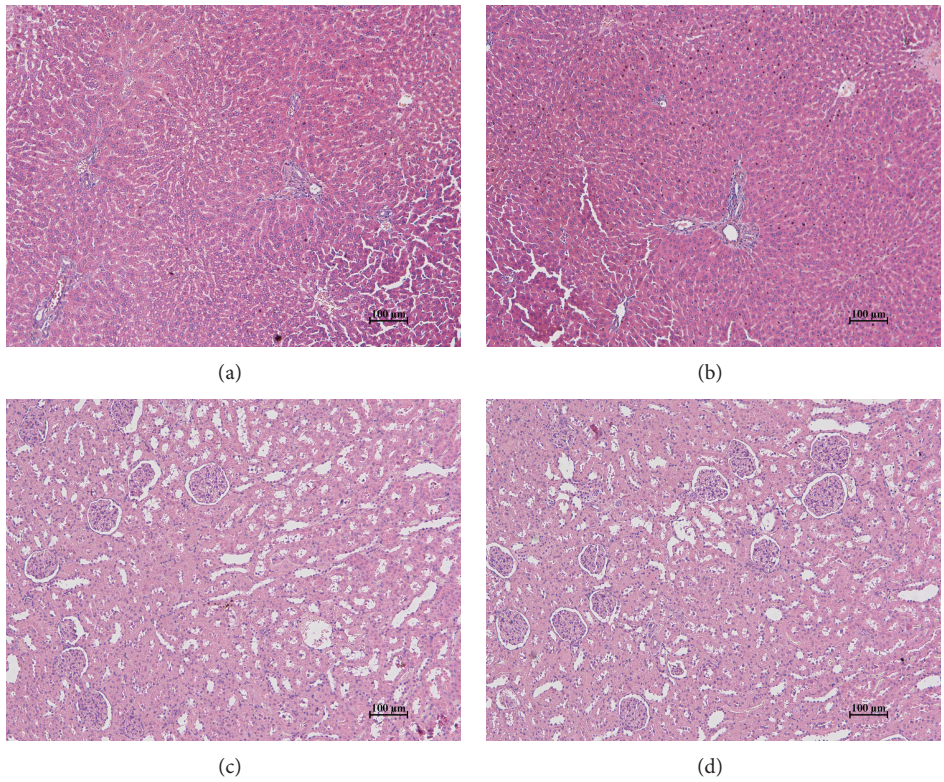

(a) (b) (c) (d)

Figure 2: Livers (portal triad regions) of animals that received intraplantar injection of CFA, treated orally, 21 days, with (a) water or (b) FHPp 250 mg/kg and kidneys (renal glomeruli and tubules) of rats that received intraplantar injection of CFA, treated orally, 21 days, with (c) water or (d) FHPp 250 mg/kg.

Table 5: Effect of FHPp on relative organ weights (g/100 g body weight) in AIA rats.

Organ	Group		
	AIA control	AIA + Tween	AIA + FHPp
Liver	4.331 ± 0.169	3.949 ± 0.125	3.921 ± 0.185
Kidneys	0.466 ± 0.024	0.422 ± 0.008	0.412 ± 0.008
Thymus	0.070 ± 0.003	0.095 ± 0.011	0.072 ± 0.005
Spleen	0.607 ± 0.068	0.560 ± 0.052	0.493 ± 0.044
Left adrenal	0.026 ± 0.003	0.021 ± 0.002	0.022 ± 0.001
Right adrenal	0.020 ± 0.001	0.019 ± 0.002	0.021 ± 0.001
L.I.L.	0.059 ± 0.012	0.047 ± 0.002	0.038 ± 0.004
R.I.L.	0.041 ± 0.001	0.025 ± 0.004	0.036 ± 0.004
L.P.L.	0.035 ± 0.007	0.050 ± 0.005	0.038 ± 0.004
R.P.L.	0.031 ± 0.003	0.050 ± 0.011	0.033 ± 0.004

The data are expressed as mean ± S.E.M. ($n = 5$). L.I.L.: left inguinal lymph node; R.I.L.: right inguinal lymph node; L.P.L.: left popliteal lymph node; R.P.L.: right popliteal lymph node. One-way ANOVA post hoc Tukey test.

extract might be related to inhibition of prostaglandin release and other mediators of the kinin system. Other studies have provided evidence that the ethanol extract of fruit from *P. pubescens* can suppress the humoral and cellular immune system by inhibiting the proliferation of lymphocytes and nitrite production by macrophages, acting as an immunomodulator with potential application in the treatment of patients with inflammatory or autoimmune diseases [2]. Silva et al. [7] demonstrated that the antiedematogenic activity of the alcoholic extract and fractions of *P. pubescens* was due to the compounds identified as geranylgeraniol and farnesol and a complex mixture of furanoditerpenes.

Several diterpenoids have been isolated from the fruits of *Pterodon* species. In a recent study, the diterpene 6α,7β-dihydroxy-vouacapan-17β-oic acid isolated from *P. emarginatus* and administered at a dose 50 mg/kg body weight significantly inhibited inflammation [19]. Thus, there is a high possibility of anti-inflammatory diterpenoids being present in the genus *Pterodon*. Earlier studies by our group have identified the presence of 3 diterpenes in FHPp that may be directly involved in the observed activity: methyl 6α-acetoxy-7β-hydroxyvouacapan-17β-oate, methyl 6α-hydroxy-7β-acetoxyvouacapan-17β-oate, and 14,15-epoxygeranylgeraniol [14].

Arthritis is a chronic, autoimmune inflammation of the joints that is especially exacerbated by the functions of macrophages and lymphocytes, which in turn contributes to the formation of paw edema. Sabino et al. [20] showed that the ethanol extract of *P. pubescens* at doses of up to 8 g/kg could inhibit lymphocyte proliferation and expression of proinflammatory cytokines accompanied by the induction of apoptosis, which consequently caused less leukocyte migration compared to the control group. In our study, the inoculation of CFA was effective in stimulating cell-mediated immunity. Following FHPp treatment, we observed a significant decrease in migration of inflammatory cells, in particular mononuclear cells, which suggested the possible involvement

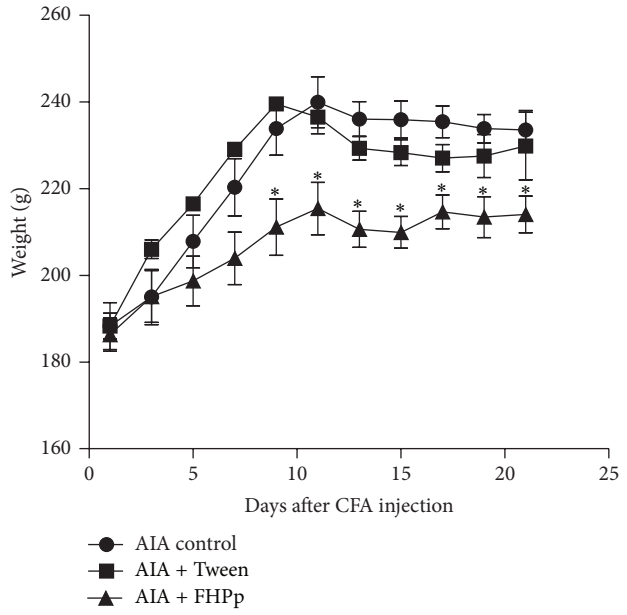

Figure 3: Effect of FHPp (250 mg/kg) on the weight of the arthritic animals. Each point represents the mean ± S.E.M. ($n = 5$). $^{*}P < 0.05$ compared to the AIA control group. One-way ANOVA post-hoc Tukey test.

of the extract on suppression of the immune response and may be related to the inhibition of lymphocyte proliferation and nitrite production by macrophages as suggested by previous studies [2, 13].

Despite the efficacy of existing drugs for the treatment of rheumatoid arthritis, it is important to develop new immunosuppressive drugs that avoid the side effects induced by classical therapy, effects that lead to discontinuation of treatment in a high percentage of patients. Thus, in addition to demonstrating its effectiveness as an anti-inflammatory agent, the elucidation of the toxic effects of FHPp is also important. In order to observe the toxic effects after treatment, biochemical analyses were conducted with blood plasma of animals, and organs were removed and examined for their relative weight. In our study, oral treatment with FHPp caused no apparent changes in results of biochemical analyses or in organ weights, which is consistent with the observations of Pinto Coelho et al. [12] after treatment of mice for 28 days with the hydroalcoholic extract of *P. pubescens*.

We were able to demonstrate statistically significant changes in levels of glucose, cholesterol, and triglycerides. The hypoglycemic activity of the seed oil of *P. emarginatus* has been reported in a study of traditional use of plants involving 17 communities of the Alto Paraguay Bay and Guapore Valley, Mato Grosso [5]. However, it is well known that the effects of reduced levels of glucose, cholesterol and triglycerides, in the genus *Pterodon,* have not been previously reported in animal studies.

We also observed a significant decrease in ALT levels in all groups with AIA compared to healthy animals. Although few studies have addressed this issue, this decrease can be indicative of changes in amino acid metabolism in arthritis [21]. The hepatic activity of ALT decreases up to 65.5% in Holtzman rats with AIA [22]. Ureogenesis and gluconeogenesis are able to interact in a complex way, and it is known that gluconeogenesis from the amino acids alanine and glutamine is accompanied by catabolism by nitrogen. Hence the reactions of nitrogen may be limited by the reaction of gluconeogenesis or vice versa in animals with AIA [21, 23], which explains the changes in ALT and urea levels.

An additional point is that the commonly used dose of FHPp (20 μg/kg) [24] is much lower than the dose used in our study. Although several previous studies have reported the cytotoxicity of some diterpenes from plant materials [25–27], we observed no significant toxic effects, even at high FHPp doses (250 mg/kg), indicating that treatment with doses greater than those commonly used does not cause any side effects. Similar results have been demonstrated by Sabino et al. [20], who observed that the oily fraction extracted from seeds of *P. pubescens* did not induce acute toxicity in healthy rats after oral administration of doses (2, 4, and 8 g/kg) significantly higher than those ingested by humans.

The development of systemic manifestations of AIA involves the appearance of secondary polyarthritis, an increase in lymph node weight, and a decrease in body weight [28]. Because we observed an insignificant increase in the body weight of the arthritis group treated with FHPp, but observed decreased levels of glucose, cholesterol, and triglycerides, the animals were placed in metabolism cages to evaluate whether these effects were the result of metabolic changes or differences in water and food intake. We found no significant differences in food intake between the groups, leading us to believe that FHPp administration may lead to metabolic changes.

The incidences of metabolic disorders such as obesity, insulin resistance, type 2 diabetes, and dyslipidemia have increased dramatically in recent decades. Thus, research aimed at developing new drugs to contain the spread of these metabolic disorders is necessary. An investment in studies on species of the genus *Pterodon* may lead to satisfactory results.

5. Conclusions

The results of this study extend the findings of previous reports that show that administration of extracts and fractions obtained from species of the genus *Pterodon* exhibits anti-inflammatory activity and lacks toxicity. In addition, our study demonstrates for the first time that FHPp decreases plasma levels of glucose, cholesterol, and triglycerides, providing a rational basis for the use of this *P. pubescens* in folk medicine and encouraging the development of new drugs originating from this plant species.

Conflict of Interests

The authors declare that there is no conflict of interests.

Acknowledgments

The authors acknowledge the Fundação Araucária, Coordenação de Aperfeiçoamento de Pessoal de Nível Superior

(CAPES) and Conselho Nacional de Desenvolvimento Científico e Tecnológico (CNPq) for financial support.

References

[1] D. Hansen, M. Haraguchi, and A. Alonso, "Pharmaceutical properties of "sucupira" (*Pterodon* spp)," *Brazilian Journal of Pharmaceutical Sciences*, vol. 46, no. 4, pp. 605–616, 2010.

[2] C. C. Cardoso, A. C. Pinto, P. R. Marques et al., "Suppression of T and B cell responses by *Pterodon pubescens* seeds ethanolic extract," *Pakistan Journal of Biological Sciences*, vol. 11, no. 19, pp. 2308–2313, 2008.

[3] M. F. Agra, K. N. Silva, I. J. L. D. Basílio et al., "Survey of medicinal plants used in the region Northeast of Brazil," *Revista Brasileira De Farmacognosia*, vol. 18, no. 3, pp. 472–508, 2008.

[4] A. M. C. Arriaga, M. A. B. De Castro, E. R. Silveira, and R. Braz-Filho, "Further diterpenoids isolated from *Pterodon polygalaeflorus*," *Journal of the Brazilian Chemical Society*, vol. 11, no. 2, pp. 187–190, 2000.

[5] M. Macedo and A. R. Ferreira, "Plantas hipoglicemiantes utilizadas por comunidades tradicionais na Bacia do Alto Paraguai e Vale do Guaporé, Mato Grosso-Brasil," *Revista Brasileira De Farmacognosia*, vol. 14, pp. 45–47, 2004.

[6] J. C. T. Carvalho, J. A. A. Sertié, M. V. J. Barbosa et al., "Anti-inflammatory activity of the crude extract from the fruits of *Pterodon emarginatus* Vog," *Journal of Ethnopharmacology*, vol. 64, no. 2, pp. 127–133, 1999.

[7] M. C. C. Silva, C. R. M. Gayer, C. S. Lopes et al., "Acute and topic anti-edematogenic fractions isolated from the seeds of *Pterodon pubescens*," *Journal of Pharmacy and Pharmacology*, vol. 56, no. 1, pp. 135–141, 2004.

[8] H. M. Spindola, J. E. de Carvalho, A. L. T. G. Ruiz et al., "Furanoditerpenes from *Pterodon pubescens* benth with selective *in vitro* anticancer activity for prostate cell line," *Journal of the Brazilian Chemical Society*, vol. 20, no. 3, pp. 569–575, 2009.

[9] H. M. Spindola, L. Servat, C. Denny et al., "Antinociceptive effect of geranylgeraniol and 6α,7β-dihydroxyvouacapan-17β-oate methyl ester isolated from *Pterodon pubescens* Benth," *BMC Pharmacology*, vol. 10, article 1, 2010.

[10] L. P. Coelho, P. A. Reis, F. L. De Castro et al., "Antinociceptive properties of ethanolic extract and fractions of *Pterodon pubescens* Benth. seeds," *Journal of Ethnopharmacology*, vol. 98, no. 1-2, pp. 109–116, 2005.

[11] C. Nucci, L. Mazzardo-Martins, J. Stramosk et al., "Oleaginous extract from the fruits *Pterodon pubescens* Benth induces antinociception in animal models of acute and chronic pain," *Journal of Ethnopharmacology*, vol. 143, pp. 170–178, 2012.

[12] M. G. Pinto Coelho, P. R. Marques, C. R. M. Gayer, L. C. A. Vaz, J. F. Nogueira Neto, and K. C. D. C. Sabino, "Subacute toxicity evaluation of a hydroalcoholic extract of *Pterodon pubescens* seeds in mice with collagen-induced arthritis," *Journal of Ethnopharmacology*, vol. 77, no. 2-3, pp. 159–164, 2001.

[13] K. C. C. Sabino, F. A. Castro, J. C. R. Oliveira et al., "Successful treatment of collagen-induced arthritis in mice with a hydroalcohol extract of seeds of *Pterodon pubescens*," *Phytotherapy Research*, vol. 13, pp. 613–615, 1999.

[14] J. Hoscheid, A. Reinas, D. A. G. Cortez et al., "Determination by GC-MS-SIM of furanoditerpenes in *Pterodon pubescens* Benth.: development and validation," *Talanta*, vol. 100, pp. 372–376, 2012.

[15] R. Vinegar, J. F. Truax, J. L. Selph, and F. A. Voelker, "Pathway of onset, development, and decay of carrageenan pleurisy in the rat," *Federation Proceedings*, vol. 41, no. 9, pp. 2588–2595, 1982.

[16] C. M. Pearson and F. D. Wood, "Studies of arthritis and other lesions induced in rats by the injection of mycobacterial adjuvant. VII. Pathologic details of the arthritis and spondylitis," *The American Journal of Pathology*, vol. 42, pp. 73–95, 1963.

[17] M. E. Rosenthale, "A comparative study of the Lewis and Sprague Dawley rat in adjuvant arthritis," *Archives Internationales de Pharmacodynamie et de Therapie*, vol. 188, no. 1, pp. 14–22, 1970.

[18] M. H. Malone and R. C. Robichaud, "A hippocratic screen for pure or crude drug materials," *Lloydia*, vol. 25, no. 4, pp. 320–332, 1962.

[19] C. B. Galceran, J. A. A. Sertie, C. S. Lima, and J. C. T. Carvalho, "Anti-inflammatory and analgesic effects of 6α,7β-dihydroxyvouacapan-17β-oic acid isolated from *Pterodon emarginatus* Vog. fruits," *Inflammopharmacology*, vol. 19, no. 3, pp. 139–143, 2011.

[20] K. C. C. Sabino, C. R. M. Gayer, L. C. A. Vaz, L. R. L. Santos, I. Felzenszwalb, and M. G. P. Coelho, "*In vitro* and *in vivo* toxicological study of the *Pterodon pubescens* seed oil," *Toxicology Letters*, vol. 108, no. 1, pp. 27–35, 1999.

[21] P. Y. Filho, A. Bracht, E. L. Ishii-Iwamoto, S. H. Lousano, L. Bracht, and A. M. Kelmer-Bracht, "The urea cycle in the liver of arthritic rats," *Molecular and Cellular Biochemistry*, vol. 243, no. 1-2, pp. 97–106, 2003.

[22] M. A. Silva, E. L. Ishii-Iwamoto, A. Bracht et al., "Efficiency of combined methotrexate/chloroquine therapy in adjuvant-induced arthritis," *Fundamental and Clinical Pharmacology*, vol. 19, no. 4, pp. 479–489, 2005.

[23] A. Martin-Requero, G. Cipres, C. Gonzalez-Manchon, M. S. Ayuso, and R. Parrilla, "Interrelationships between ureogenesis and gluconeogenesis in perfused rat liver," *Biochimica et Biophysica Acta*, vol. 1158, no. 2, pp. 166–174, 1993.

[24] R. Coimbra, *Notas DE Fitoterapia. Catálogo Dos dados Principais Sobre Plantas Utilizadas Em Medicina E Farmácia*, Silva Araújo, Rio de Janeiro, Brazil, 1st edition, 1942.

[25] R. Croteau, T. M. Kutchan, and N. G. Lewis, "Natural production (secondary metabolites)," in *Biochemistry and Molecular Biology of Plants*, B. Buchanan, W. Gruissem, and R. Jones, Eds., pp. 1250–1318, American Society of Plant Physiologists, Rockville, Md, USA, 2000.

[26] K. Dimas, C. Demetzos, M. Marsellos, R. Sotiriadou, M. Malamas, and D. Kokkinopoulos, "Cytotoxic activity of labdane type diterpenes against human leukemic cell lines *in vitro*," *Planta Medica*, vol. 64, no. 3, pp. 208–211, 1998.

[27] M. Fronza, E. Lamy, S. Günther, B. Heinzmann, S. Laufer, and I. Merfort, "Abietane diterpenes induce cytotoxic effects in human pancreatic cancer cell line MIA PaCa-2 through different modes of action," *Phytochemistry*, vol. 78, pp. 107–119, 2012.

[28] M. G. Torres, F. H. Kwasniewski, L. G. Scaliante et al., "Arthritis induced by adjuvant in spontaneously hypertensive and normotensive rats: endogenous glucocorticoid effects on inflammatory response," *Inflammation*, vol. 32, no. 1, pp. 20–26, 2009.

Hindawi Publishing Corporation
Evidence-Based Complementary and Alternative Medicine
Volume 2013, Article ID 305898, 8 pages
http://dx.doi.org/10.1155/2013/305898

Research Article

Therapeutic Potential of Andrographolide Isolated from the Leaves of *Andrographis paniculata* Nees for Treating Lung Adenocarcinomas

Yu-Tang Tung,[1] Hsiao-Ling Chen,[2] Hsin-Chung Tsai,[1,3] Shang-Hsun Yang,[4] Yi-Chun Chang,[1] and Chuan-Mu Chen[1,5]

[1] *Department of Life Sciences, Agricultural Biotechnology Center, National Chung Hsing University, Taichung 402, Taiwan*
[2] *Department of Bioresources, Da-Yeh University, Changhwa 515, Taiwan*
[3] *Taichung Hospital, Department of Health, Taichung 403, Taiwan*
[4] *Department of Physiology, National Cheng Kung University, Tainan 701, Taiwan*
[5] *Department of Life Sciences, Office of Research and Development, National Chung Hsing University, No. 250, Kuo Kuang Road, Taichung 402, Taiwan*

Correspondence should be addressed to Chuan-Mu Chen; chchen1@dragon.nchu.edu.tw

Received 5 June 2013; Accepted 20 June 2013

Academic Editor: Vincenzo De Feo

Andrographolide is one of the major diterpene lactones found in *Andrographis paniculata* Nees and exhibits remarkable inhibitory effects on various cancers. In this study, the antipulmonary cancer effects of andrographolide were studied in a lung tumor mouse model induced by human vascular endothelial growth factor A_{165} (*hVEGF*-A_{165}). These results demonstrated that andrographolide significantly reduced the expression of hVEGF-A_{165} compared with a mock group in the Clara cells of the lungs. In addition, andrographolide also decreased tumor formation by reducing VEGF, EGFR, Cyclin A, and Cyclin B expression on the transcriptional and translational levels. These results indicated that andrographolide treatment on the overexpression of VEGF can arrest the cell cycle, which induced pulmonary tumors in transgenic mice. In conclusion, the antiangiogenesis and chemotherapeutic potential of andrographolide may provide a cure for pulmonary tumors in the future.

1. Introduction

According to the latest cancer mortality statistics from the People's Health Bureau of Taiwan, pulmonary cancer is ranked as a leading cause of Taiwanese cancer-related deaths [1]. Worldwide, lung cancer has been the most common form of cancer for several decades. Although chemotherapeutic agents for pulmonary tumors have developed, the lung cancer death rate is still high. Thus, many researchers have focused on early tumor detection and more active treatments as the tumor prevention methods [2]. For example, many researchers have discovered useful phytochemicals (compounds found in plants) and phytochemicals derivatives that provide novel anticancer therapies that have been successfully used in the clinic.

Andrographis paniculata Nees, a traditional medicine in Southeastern Asian countries, has been widely used in the clinic as an immunostimulant [3] and for the treatment of the common cold [4], myocardial ischemia [5], pharyngotonsillitis [6], and respiratory tract infections [7]. The major component of *A. paniculata* is andrographolide, which has been used to treat colds, diarrhea, fever, and inflammation, as well as infectious diseases [8]. In addition, the chemopreventive effects against and the inhibitory effects on cancer cell growth of andrographolide have been demonstrated in breast, colon, epidermoid, gastric, liver, leukemia, myeloma, peripheral blood lymphocytes, and prostate cancers [9–12]. The present study is the first to investigate whether andrographolide treatment could inhibit the formation of lung tumor in the hVEGF-A_{165} overexpressing transgenic mice. The airway hyperresponsiveness (AHR) was measured during a five-month treatment of mice with andrographolide. In addition, the pathological histology and the hVEGF

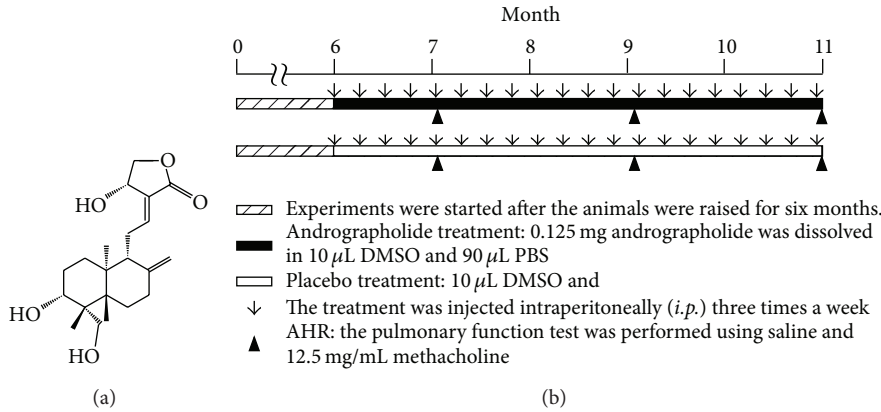

Figure 1: Active component of andrographolide (An) extracted from the leaves of *Andrographis paniculata* Nees and the animal trial timeline. (a) Chemical structure of andrographolide. (b) The schedule of andrographolide treatment. Mice were injected intraperitoneally (*i.p.*) with andrographolide (5 mg/kg body weight) three times a week for 5 months, and mice were sacrificed at 11 months.

immunohistochemistry staining of the lungs of these mice were examined. The related mRNA and protein expression in tumorigenesis and cell cycle regulator makers were also tested to evaluate the mechanism of tumor inhibition by treatment with andrographolide.

2. Materials and Methods

2.1. Production of Lung Tumor Transgenic Mice. We have generated the mccsp-hVegf-A_{165}-sv40 transgenic mice from pronuclear microinjection technique. Homozygous (hVEGF-$A_{165}{}^{+/+}$) or hemizygous (hVEGF-$A_{165}{}^{+/-}$) transgenic mice were identified by genomic DNA PCR. The genomic DNA isolated from the tails of the mice with the following primers: VEGF-94(+): 5′-AAGGAGGAGGGCAGAATCATC-3′ and VEGF-315(−): 5′-GAGGTTTGATCCGCATAATCTG-3′. The exogenic human VEGF-A_{165} protein and mRNA expression levels in homozygous (hVEGF-$A_{165}{}^{+/+}$) or heterozygous (hVEGF-$A_{165}{}^{+/-}$) transgenic mice were also detected by Western blot and RT-PCR.

2.2. Animals. A total of 12 male transgenic mice were given with free access to water and standard laboratory diet at a temperature- and humidity-regulated environment (22 ± 2°C, 65 ± 5% RH) with 12 h dark/light cycle. This study was conducted according to institutional guidelines and approved by the Institutional Animal Care and Utilization Committee of National Chung-Hsing, Taiwan (IACUC no. 96-83). The transgenic mice displaying the hemizygous (hVEGF-$A_{165}{}^{+/-}$) genotype were randomly divided into two groups ($n = 6$) based on their treatment: Tg/Mock (transgenic mice treated with a mock or placebo) and Tg/Andrographolide (transgenic mice treated with andrographolide). Andrographolide (An; Figure 1(a)) was obtained from Sigma Chemical (St. Louis, MO, USA) and dissolved in DMSO. Mice were injected intraperitoneally (*i.p.*) with andrographolide (5 mg/kg body weight) three times a week for 5 months, and mice were sacrificed at 11 months (Figure 1(b)). Pulmonary tissues were collected for pathological histology, immunohistochemistry staining, RNA extraction, and protein extraction according to our previously published protocols [13–15]. All the experiments were repeated twice.

2.3. Measurement of the Airway Hyperresponsiveness (AHR). Bronchial provocation tests that evaluate the AHR in the Tg/Mock and Tg/Andrographolide groups were performed using methacholine. First, the basal pulmonary function was measured; then saline and methacholine at a concentration of 12.5 mg/mL were converted to aerosol using a nebulizer and allowed to be inhaled five times through a Rosenthal-French dosimeter. The pulmonary function was measured 30 times with a portable microspirometer for 3 minutes, and the enhanced pause (penh) values were selected to represent the pulmonary function. The penh, a dimensionless value, represents the proportion of maximal expiratory to maximal inspiratory box pressure signals and the timing of expiration. The AHR was presented as the penh in response to the increasing damage to pulmonary functionality [16].

2.4. Pathological Histology. Pulmonary tissues were fixed in 10% buffered formaldehyde (pH 7.0), embedded with paraffin, sectioned into 3 μm sections, and examined using hematoxylin and eosin (H&E) staining. The hematoxylin and eosin (H&E) staining was described according to our previous reports [17, 18].

2.5. Immunohistochemistry Staining. IHC staining of pulmonary tissues, the VECTASTAIN ABC kit (Universal, Vector, USA) was used. Tissue sections (a thickness of 5 μm) were placed on slides and incubated overnight at 4°C with rabbit anti-hVEGF-A monoclonal primary antibody as previously described [19]. Sections were developed using diaminobenzidine (DAB) as chromogenic substrates and counterstained with hematoxylin [20].

2.6. Real-Time RT-PCR. RNA was extracted from lung tissue using a Trizol reagent (Invitrogen, Carlsbad, CA) in accordance with the manufacturer's instructions. cDNA synthesis

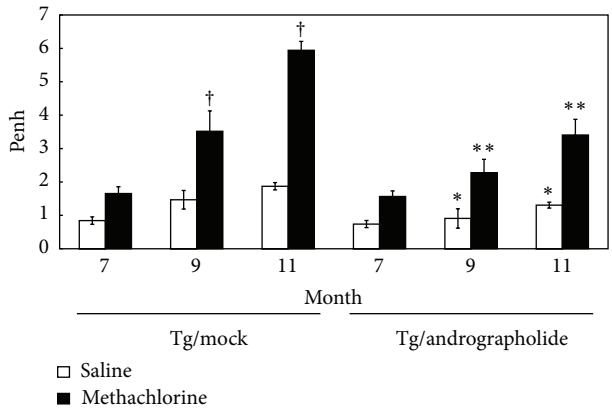

Figure 2: Effects of andrographolide on the airway hyperresponsiveness (AHR) parameters of pulmonary functionality. Data are presented as the means ± SEM ($n = 6$). $^{\dagger}P < 0.01$ Tg/Mock versus Tg/Mock group at 7 months. $^{*}P < 0.05$ Tg/Andrographolide group versus Tg/Mock group in the same month. $^{**}P < 0.01$ Tg/Andrographolide group versus Tg/Mock group in the same month.

reaction was performed by PCR as described for ImProm-IITM reverse transcriptase (Promega, USA). Quantitative real-time RT-PCR (qRT-PCR) was carried out using SYBR Green in a Rotor-Gene 6000. The gene expressions of 14 genes (*vegf*, *kdr*, *nrp-1*, *myc*, *brca-1*, *mmp2*, *mmp9*, *egfr*, *erk2*, *survivin*, *cyclin a*, *cyclin b1*, *cyclin d*, and *cyclin e*) were performed on using cDNA from pulmonary tissue by qRT-PCR [21].

2.7. Western Blotting. The total protein of the pulmonary tissues from each mouse was homogenized in 500 μL of RIPA buffer (5 mM Tris-HCl pH 7.4, 0.15 M NaCl, 1% NP40, 0.25% sodium deoxycholate, 5 mM EDTA, and 1 mM ethylene glycol-bis (2-aminoethyl-ether)-N,N,N,N-tetraacetic acid) and centrifuged at 12,000 ×g for 30 min at 4°C. Protein determination and Western blotting was performed according to the procedure reported [20, 22] with slight modifications. The protein samples (50 μg) were resolved by a 10% SDS-PAGE and electrophoretically transferred to a PVDF membrane. Thus, the membrane was incubated with primary antibody (VEGF-A, EGFR, ERK2, Cyclin A, Cyclin B, or GAPDH) overnight at 4°C and further incubated for 1 h with anti-rabbit IgG antibody conjugated to HRP. The protein expressions were detected by the enhanced chemiluminescence reagents (ECL).

2.8. Statistical Analysis. Statistical significance of differences between treatments was determined by Student's t-test. $P < 0.05$ (*) or $P < 0.01$ (**) were considered to be statistically significant.

3. Results

3.1. Effects of Andrographolide on the Airway Hyperresponsiveness (AHR) Parameters of Pulmonary Functionality. The mccsp-hVegf-A165-sv40 transgenic mice which induces pulmonary tumor [16] was used as a lung cancer animal model for test of andrographolide (An) therapeutic effects. The animal trials timeline was showed in Figure 1(b). Several invasive and noninvasive methods have been used for the evaluation of the airway responsiveness of mice [23]. The AHR, a noninvasive procedure, enables easily and quickly obtained measurements, and it has been an important characteristic of pulmonary function. In this study, the AHR of the andrographolide or mock treatment was measured after 7, 9, and 11 months (Figure 2). The penh values of the Tg/Mock treatment with methacholine were significantly increased from 1.65 (7 months) to 3.52 (9 months), and 5.94 (11 months). However, 5 mg/kg body weight of andrographolide effectively reduced the penh elevation, exhibiting values of 1.57 (7 months), 2.28 (9 months), and 3.41 (11 months). This result revealed that andrographolide dramatically reduced the damage to pulmonary functionality.

Table 1: Lung tumorigenesis frequency of Tg/Mock and Tg/Andrographolide groups in the mouse lung tissues ($n = 6$) using histopathological image analysis.

Variable	Tg/Mock	Tg/Andrographolide
Normal	0 (0%)	2 (33.3%)
Cyst	6 (100%)	4 (66.7%)
Damaged alveoli	4 (66.7%)	2 (33.3%)
Mild emphysematous change	0 (0%)	3 (50%)
Prominent emphysematous change	6 (100%)	1 (16.7%)
Hemosiderin-laden macrophages in alveoli	2 (33.3%)	0 (0%)
Old hemorrhage	6 (100%)	2 (33.3%)
Moderate lymphocytic infiltration	0 (0%)	1 (16.7%)
Marked chronic lymphoid infiltration	6 (100%)	2 (33.3%)
Neoplasm	3 (50%)	1 (16.7%)
Lymphoma	6 (100%)	1 (16.7%)
Adenocarcinoma	5 (83.3%)	2 (33.3%)

3.2. Effect of Andrographolide Treatment on Lung H&E Staining and Pathological Analysis. Figure 3 and Table 1 indicate that transgenic mice (83.3%; 5/6) have found pulmonary tumors; these tumors primarily consisted of neoplasms growth on the periphery of the pulmonary alveolus and adenomas growing on the site near the lung bronchus. In the pulmonary alveoli of the lung bronchi of the transgenic mice, some obvious large-grained pink cells, which represent macrophages, are indicative of an inflammatory response. Furthermore, the group treated with 5 mg/kg andrographolide decreased the neoplasm growing on the periphery of the pulmonary alveolus and the adenomas growing near the site of the lung bronchus (Figures 3(c) and 3(d)). This pathological analysis illustrated that andrographolide has antipulmonary cancer potential (33.3%; 2/6) compared with Tg alone (83.3%; 5/6) and induces anti-inflammatory

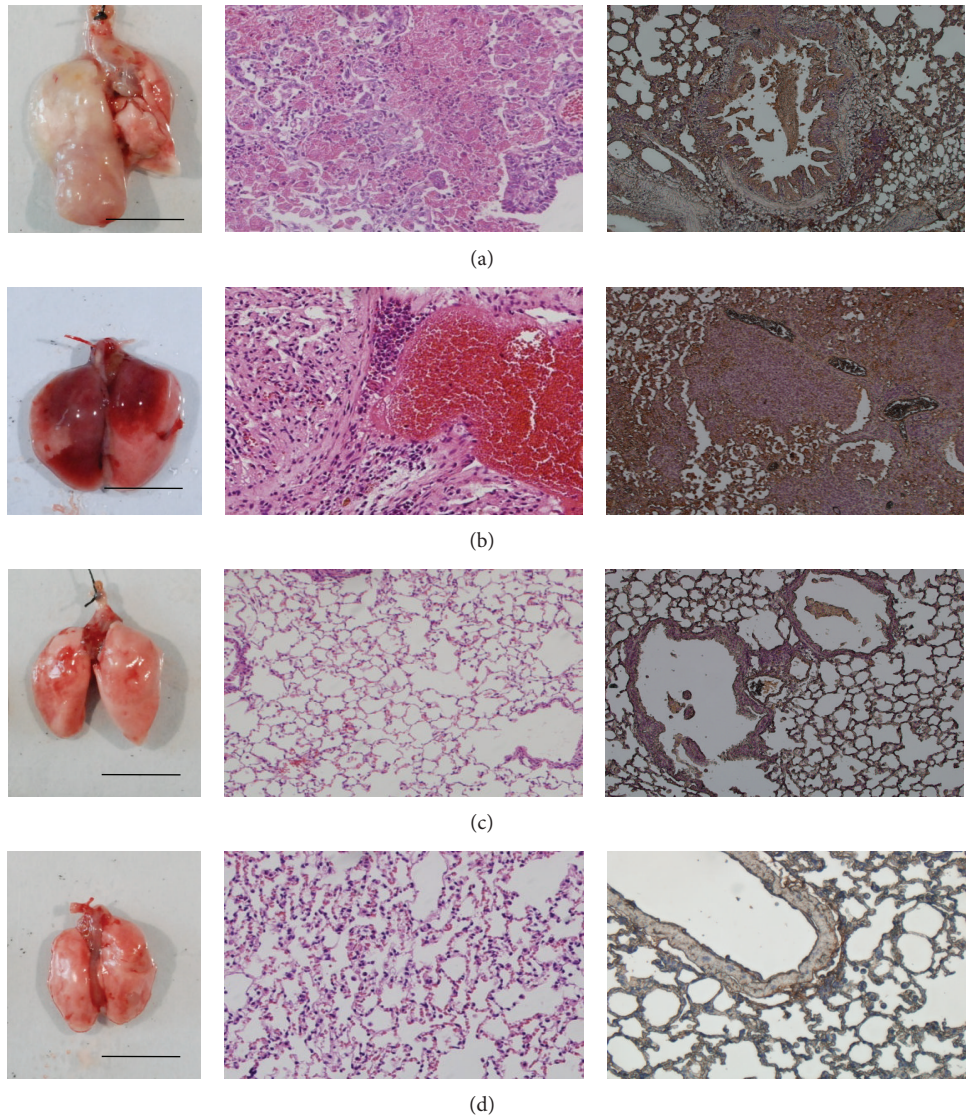

FIGURE 3: The exterior, histopathological slides and immunohistochemical (IHC) staining of the lung tissues of 11-month-old transgenic mice that overexpress hVEGF-A_{165} in the (a, b) Tg/Mock group and (c, d) Tg/Andrographolide group following 5 months of andrographolide treatment.

responses in the lungs of transgenic mice that overexpress hVEGF-A_{165}.

3.3. Effect of Andrographolide Treatment on Immunohistochemistry Staining. Angiogenesis is required for the tumor formation, tumor growth, invasion, and metastasis. VEGF is a principal regulator of vasculogenesis and angiogenesis. Using immunohistochemistry staining (IHC staining), we observed that VEGF was overexpressed in the Clara cells of lung tissues in the transgenic mice (Figures 3(a) and 3(b)) and that the treatment with andrographolide significantly reduced the expression levels of VEGF (Figures 3(c) and 3(d)). These results indicate that transgenic mice treatment with andrographolide can decrease VEGF expression compared with those that were mock treated; thus it may reduce the new blood vessel formation and growth. The anti-VEGF therapy of andrographolide may prevent the previously observed tumor growth, invasion, and metastasis.

3.4. Andrographolide Suppresses the Marker Genes for Tumor Formation. The mRNA levels of *vegf-a165*, *kdr*, *nrp-1*, *myc*, *brca-1*, *mmp2*, *mmp9*, *egfr*, *erk2*, *survivin*, *cyclin a*, *cyclin b1*, *cyclin d,* and *cyclin e* in the Tg/Mock and Tg/Andrographolide groups were evaluated using qRT-PCR (Figure 4). These results demonstrated that treating Tg mice with 5 mg/kg of andrographolide significantly decreased the expression of *vegf-a165*, *kdr*, *nrp-1*, *c-myc*, *egfr*, *erk2*, *surviving*, *cyclin a*, *cyclin b1,* and *cyclin e*. *Kdr* and its coreceptor *nrp-1*, which are the main angiogenic receptors in the vegf pathway, are down-regulated. In addition, both the c-Myc and Ras/MEK/ERK pathways play a vital role in the progression of the G1-cell cycle phase by enhancing cyclins. Thus, in this study *erk2*

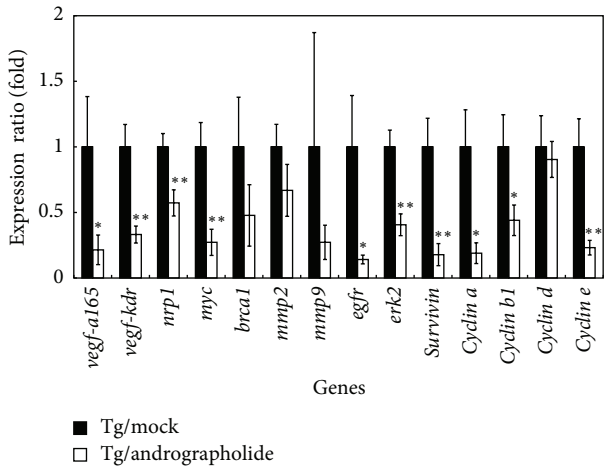

Figure 4: Real-time PCR validations of mRNA expression levels of *vegf*, *kdr*, *nrp-1*, *myc*, *brca-1*, *mmp2*, *mmp9*, *egfr*, *erk2*, *survivin*, *cyclin a*, *cyclin b1*, *cyclin d,* and *cyclin e* in the lung tissues of the Tg/Mock and Tg/Andrographolide groups. β-Actin was used as an internal control. The quantitative mRNA expression levels were measured by qRT-PCR. Data are presented as the means ± SEM ($n = 6$). $^{*}P < 0.05$ versus Tg/Mock group. $^{**}P < 0.01$ versus Tg/Mock group.

and c-myc down-regulation may induce cell cycle G1 arrest. Furthermore, *cyclin a* is essential for *c-myc*-modulated cell-cycle progression.

3.5. Andrographolide Suppresses Cell Cycle Progression Signaling Pathways. VEGF, ERK2, Cyclin A, and Cyclin B were significantly decreased in the Tg/Andrographolide group compared with the Tg/Mock group using Western blot analysis (Figure 5). Andrographolide affects the cell cycle by reducing the levels of Cyclin A and Cyclin B, which regulate the S and G2/M phases, respectively. The andrographolide-induced downregulation of Cyclins A and B may decrease the progression of cells through the S and G2/M phases. This result indicates that the protein expression involved in the S to M phase transition in transgenic mice was inhibited by andrographolide.

4. Discussion

Previous studies have shown that *Andrographis paniculata* possesses potent antiatherosclerotic, anti-inflammatory, antioxidant, hepatoprotective, immunomodulatory, and anticancer effects [24–29]. Andrographolide is one of the major diterpene lactones found in *A. paniculata* and displays potent anticancer and immunomodulatory effects, which may lead to its development as a chemotherapeutic agent [28, 30]. In addition, many researchers have demonstrated that andrographolide displays excellent anticancer effects on breast, colon, epidermoid, gastric, HeLa, liver, leukemia, myeloma, peripheral blood lymphocytes, and prostate cancers [9–12]. Many *in vitro* studies demonstrated that andrographolide promotes apoptosis in cancer cells, suppresses cancer cell proliferation, and induces cell-cycle arrest [12, 31].

The stabilization of HIF-1α mediated the overexpression of VEGF, which has been identified as a common step in the development of carcinomas. Thus, VEGF-inhibitors, which directly or indirectly target the tumor vasculature, have become common in anticancer therapies [32]. In the present study, we use 11-month-old transgenic mice that overexpress a lung-specific hVEGF-A_{165}. These mice contain the mccsp-hVegf-A_{165}-sv40 poly(A) transgene for researching pulmonary tumors and serve as an animal model for researching the regulatory mechanism of andrographolide. We found that these transgenic mice are susceptible to the growth of pulmonary tumors. However, following a 5-month treatment with andrographolide (5 mg/kg b.w. three times a week), these mice exhibited a dramatic decrease in the formation of solid tumors when compared with the mock treatment. The histological examination also indicated that the andrographolide treatment reduced pulmonary tumor formation and inflammation (Figure 3).

Initially, the cancer cells continue to proliferate and thus create a nutrition and oxygen deficiency, which causes significant cell death. The secretion of large quantities of VEGF-A_{165} induces vasculogenesis to provide the rapidly growing tumor with sufficient quantities of nutrients and oxygen [33]. This solid tumor growth is dependent on angiogenesis, and thus the suppression of tumor blood vessels offers a new alternative to prevent and treat cancer. Using IHC staining, we observed that andrographolide reduced the expression of hVEGF-A_{165} to normal levels, specifically in the Clara cells in the lungs of transgenic mice. These results indicate that andrographolide reduced the expression of VEGF in Clara cells when compared with the mock treatment. VEGF is essential for vasculogenesis and angiogenesis during development and tumor progression. In addition, Zhao et al. [34] demonstrated that andrographolide effectively inhibited VEGF expression in prostate cancer. Lin et al. [1] found that the inhibition of PI3 K/Akt signaling by andrographolide significantly suppressed the protein and mRNA levels of HIF-1α, as well as the protein level and transcriptional activation of VEGF in A549 cells. In this study, we further found that treatment with andrographolide in lung tumor animal model effectively reduced the expression of VEGF in tumor tissue; this activity demonstrates that andrographolide may prove a potent antiangiogenic agent for the treatment of pulmonary cancer.

In addition, andrographolide can reduce pulmonary functional damage (Figure 2) and prevent pulmonary cancer formation through elimination of VEGF, ERK2, Cyclin A, and Cyclin B proteins (Figure 5). Andrographolide induced the reduction of Cyclin A and Cyclin B, which likely resulted in the reduced progression through the S and G2/M phases. These results indicated that andrographolide suppressed the protein expression at the transition from the S-phase to the M-phase in transgenic mice. These results also demonstrate that the inhibition of the cell cycle may be a vital pathway that andrographolide affects the transgenic mice that overexpress VEGF. Furthermore, Satyanarayana et al. [12] revealed that andrographolide inhibits cell-cycle arrest in MCF-7 cells by inducing the expression of p27 (the cell-cycle inhibitory protein) and decreasing the expression of cyclin-dependent

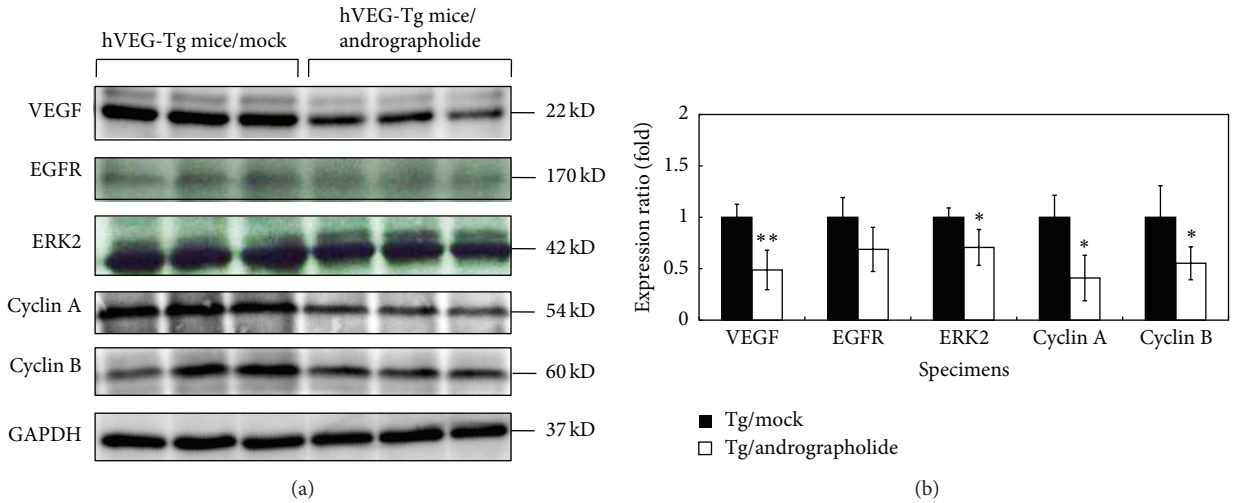

FIGURE 5: Western blot analysis of VEGF-A, EGFR, ERK2, Cyclin A, and Cyclin B protein in the lung tissues of the Tg and Tg/Andrographolide groups. GADPH was used as an internal control. Data are presented as the means ± SEM ($n = 6$). $^{*}P < 0.05$ versus Tg group. $^{**}P < 0.01$ versus Tg group.

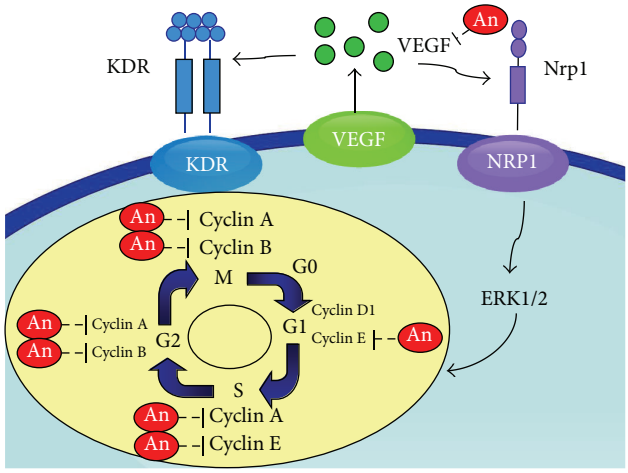

FIGURE 6: Scheme of the andrographolide regulatory pathway. The effects of andrographolide inhibition of lung tumors are hypothesized through a cell-cycle signaling pathway. The diagram shows that andrographolide may inhibit VEGF-A, KDR, Nrp1, ERK2, Cyclin A, and Cyclin B expression.

kinase. Shi et al. [31] also suggested that andrographolide can induce cell-cycle arrest at the G1/S phase by CKI-cyclin-Cdk signaling in Lovo cells. These results revealed that andrographolide can induce cell-cycle arrest in cancer cells. Furthermore, we found that *erk2* downregulation was followed by a downstream decreasing of *c-myc* expression that may induce cell cycle arrest in the G1 phase. Additionally, *cyclin a* is essential for *c-myc*-modulated cell-cycle progression in pulmonary cancer formation. Finally, Tsai et al. [18] found that andrographolide inhibited chemotic migration, which may be due to the inhibition of the ERK1/2 and Akt protein kinase cascades. Here we show a relationship between andrographolide treatment and the transcriptional and translational levels of VEGF, EGFR, ERK2, and Cyclin A (Figure 6).

5. Conclusion

The andrographolide-induced inhibition of VEGF by arresting the cell cycle may be a critical mechanism for preventing pulmonary tumor angiogenesis and metastasis. The inhibition of VEGF by andrographolide may be a useful method for the chemoprevention of pulmonary cancer.

Abbreviations

AHR: Airway hyperresponsiveness
An: Andrographolide
DAB: Diaminobenzidine
H&E: Hematoxylin and eosin
IHC: Immunohistochemistry staining
Penh: The enhanced pause
qRT-PCR: Quantitative real-time RT-PCR
VEGF: Vascular endothelial growth factor.

Acknowledgments

This research was supported in part by the National Science Council Grant NSC-98-2313-B-005-012, the Council of Agriculture Grant COA-97-6.2.1-U1(9), and the Ministry of Education, Taiwan, under the Aiming Top University Plan (ATU-101-S0508). The authors would like to express their gratitude to these entities.

References

[1] H.-H. Lin, C.-W. Tsai, F.-P. Chou et al., "Andrographolide down-regulates hypoxia-inducible factor-1α in human non-small cell lung cancer A549 cells," *Toxicology and Applied Pharmacology*, vol. 250, no. 3, pp. 336–345, 2011.

[2] S.-S. Lin, K.-C. Lai, S.-C. Hsu et al., "Curcumin inhibits the migration and invasion of human A549 lung cancer cells through the inhibition of matrix metalloproteinase-2 and -9 and Vascular Endothelial Growth Factor (VEGF)," *Cancer Letters*, vol. 285, no. 2, pp. 127–133, 2009.

[3] A. Puri, R. Saxena, R. P. Saxena, K. C. Saxena, V. Srivastava, and J. S. Tandon, "Immunostimulant agents from *Andrographis paniculata*," *Journal of Natural Products*, vol. 56, no. 7, pp. 995–999, 1993.

[4] J. Melchior, S. Palm, and G. Wikman, "Controlled clinical study of standardized *Andrographis paniculata* extract in common cold-a pilot trial," *Phytomedicine*, vol. 34, pp. 315–318, 1996.

[5] G. Zhi-ling, Z. Hua-yue, and Z. Xin-hua, "An experimental study of the mechanism of *Andrographis paniculata* nees (APN) in alleviating the Ca2+-overloading in the process of myocardial ischemie reperfusion," *Journal of Tongji Medical University*, vol. 15, no. 4, pp. 205–208, 1995.

[6] V. Thamlikitkul, S. Theerapong, P. Boonroj et al., "Efficacy of *Andrographis paniculata*, nees for pharyngotonsillitis in adults," *Journal of the Medical Association of Thailand*, vol. 74, no. 10, pp. 437–442, 1991.

[7] J. T. Coon and E. Ernst, "*Andrographis paniculata* in the treatment of upper respiratory tract infections: a systematic review of safety and efficacy," *Planta Medica*, vol. 70, no. 4, pp. 293–298, 2004.

[8] Y.-C. Shen, C.-F. Chen, and W.-F. Chiou, "Andrographolide prevents oxygen radical production by human neutrophils: possible mechanism(s) involved in its anti-inflammatory effect," *British Journal of Pharmacology*, vol. 135, no. 2, pp. 399–406, 2002.

[9] Y. Tan, K. Chiow, D. Huang, and S. Wong, "Andrographolide regulates epidermal growth factor receptor and transferrin receptor trafficking in epidermoid carcinoma (A-431) cells: research paper," *British Journal of Pharmacology*, vol. 159, no. 7, pp. 1497–1510, 2010.

[10] C.-G. Jiang, J.-B. Li, F.-R. Liu, T. Wu, M. Yu, and H.-M. Xu, "Andrographolide inhibits the adhesion of gastric cancer cells to endothelial cells by blocking E-selectin expression," *Anticancer Research*, vol. 27, no. 4 B, pp. 2439–2447, 2007.

[11] N. P. Trivedi, U. M. Rawal, and B. P. Patel, "Hepatoprotective effect of andrographolide against hexachlorocyclohexane-induced oxidative injury," *Integrative Cancer Therapies*, vol. 6, no. 3, pp. 271–280, 2007.

[12] C. Satyanarayana, D. S. Deevi, R. Rajagopalan, N. Srinivas, and S. Rajagopal, "DRF 3188 a novel semi-synthetic analog of andrographolide: cellular response to MCF 7 breast cancer cells," *BMC Cancer*, vol. 4, article 26, 2004.

[13] H.-L. Chen, L.-C. Wang, C.-H. Chang et al., "Recombinant porcine lactoferrin expressed in the milk of transgenic mice protects neonatal mice from a lethal challenge with enterovirus type 71," *Vaccine*, vol. 26, no. 7, pp. 891–898, 2008.

[14] C.-J. Shen, W. T. K. Cheng, S.-C. Wu et al., "Differential differences in methylation status of putative imprinted genes among cloned swine genomes," *PLoS ONE*, vol. 7, no. 2, Article ID e32812, 2012.

[15] Y.-J. Chen, C.-Y. Wu, C.-C. Chang, C.-J. Ma, M.-C. Li, and C.-M. Chen, "Nuclear Krüppel-like factor 4 expression is associated with human skin squamous cell carcinoma progression and metastasis," *Cancer Biology & Therapy*, vol. 7, no. 5, pp. 777–782, 2008.

[16] Y.-T. Tung, H.-L. Chen, C.-W. Lai, C.-J. Shen, Y.-W. Lai, and C.-M. Chen, "Curcumin reduces pulmonary tumorigenesis in vascular endothelial growth factor (VEGF)-overexpressing transgenic mice," *Molecular Nutrition and Food Research*, vol. 55, no. 7, pp. 1036–1043, 2011.

[17] H.-L. Chen, Y.-W. Lai, C.-S. Chen et al., "Probiotic *Lactobacillus casei* expressing human lactoferrin elevates antibacterial activity in the gastrointestinal tract," *BioMetals*, vol. 23, no. 3, pp. 543–554, 2010.

[18] T.-C. Tsai, W. Lin, S.-H. Yang et al., "Granzyme G is expressed in the two-cell stage mouse embryo and is required for the maternal-zygotic transition," *BMC Developmental Biology*, vol. 10, article 88, 2010.

[19] C.-M. Chen, C.-M. Hung, C.-C. Yeh et al., "Gingyo-san enhances immunity and potentiates infectious bursal disease vaccination," *Evidence-Based Complementary and Alternative Medicine*, vol. 2011, Article ID 238208, 10 pages, 2011.

[20] C.-C. Yen, C.-Y. Lin, K.-Y. Chong et al., "Lactoferrin as a natural regimen for selective decontamination of the digestive tract: recombinant porcine lactoferrin expressed in the milk of transgenic mice protects neonates from pathogenic challenge in the gastrointestinal tract," *Journal of Infectious Diseases*, vol. 199, no. 4, pp. 590–598, 2009.

[21] J. Y. Chen, H. L. Chen, and J. C. Cheng, "A Chinese herbal medicine, Gexia-Zhuyu Tang (GZT), prevents dimethylnitrosamine-induced liver fibrosis through inhibition of hepatic stellate cells proliferation," *Journal of Ethnopharmacology*, vol. 142, pp. 811–818, 2012.

[22] S.-C. Wu, H.-L. Chen, C.-C. Yen et al., "Recombinant porcine lactoferrin expressed in the milk of transgenic mice enhances offspring growth performance," *Journal of Agricultural and Food Chemistry*, vol. 55, no. 12, pp. 4670–4677, 2007.

[23] V. L. Capelozzi, "Role of immunohistochemistry in the diagnosis of lung cancer," *Jornal Brasileiro de Pneumologia*, vol. 35, no. 4, pp. 375–382, 2009.

[24] H. M. Chang, *Pharmacology and Applications of Chinese Materia Medica*, vol. 2, World Scientific Publishing, Singapore, 1987.

[25] S. S. Handa and A. Sharma, "Hepatoprotective activity of andrographolide against galactosamine and paracetamol intoxication in rats," *Indian Journal of Medical Research Section B*, vol. 92, pp. 284–292, 1990.

[26] R. Ajaya Kumar, K. Sridevi, N. Vijaya Kumar, S. Nanduri, and S. Rajagopal, "Anticancer and immunostimulatory compounds from *Andrographis paniculata*," *Journal of Ethnopharmacology*, vol. 92, no. 2-3, pp. 291–295, 2004.

[27] T. Matsuda, M. Kuroyanagi, S. Sugiyama, K. Umehara, A. Ueno, and K. Nishi, "Cell differentiation-inducing diterpenes from *Andrographis paniculata* NEES," *Chemical and Pharmaceutical Bulletin*, vol. 42, no. 6, pp. 1216–1225, 1994.

[28] S. Rajagopal, R. A. Kumar, D. S. Deevi, C. Satyanarayana, and R. Rajagopalan, "Andrographolide, a potential cancer therapeutic agent isolated from *Andrographis paniculata*," *Journal of Experimental Therapeutics and Oncology*, vol. 3, no. 3, pp. 147–158, 2003.

[29] D. W. Wang and H. Y. Zhao, "Prevention of atherosclerotic arterial stenosis and restenosis after angioplasty with *Andrographis paniculata* nees and fish oil. Experimental studies of effects and mechanisms," *Chinese Medical Journal*, vol. 107, no. 6, pp. 464–470, 1994.

[30] S. R. Jada, A. S. Hamzah, N. H. Lajis, M. S. Saad, M. F. G. Stevens, and J. Stanslas, "Semisynthesis and cytotoxic activities of andrographolide analogues," *Journal of Enzyme Inhibition and Medicinal Chemistry*, vol. 21, no. 2, pp. 145–155, 2006.

[31] M.-D. Shi, H.-H. Lin, Y.-C. Lee, J.-K. Chao, R.-A. Lin, and J.-H. Chen, "Inhibition of cell-cycle progression in human colorectal carcinoma Lovo cells by andrographolide," *Chemico-Biological Interactions*, vol. 174, no. 3, pp. 201–210, 2008.

[32] L. Ellis, H. Hammers, and R. Pili, "Targeting tumor angiogenesis with histone deacetylase inhibitors," *Cancer Letters*, vol. 280, no. 2, pp. 145–153, 2009.

[33] N. Ferrara, "VEGF and the quest for tumour angiogenesis factors," *Nature Reviews Cancer*, vol. 2, no. 10, pp. 795–803, 2002.

[34] F. Zhao, E.-Q. He, L. Wang, and K. Liu, "Anti-tumor activities of andrographolide, a diterpene from *Andrographis paniculata*, by inducing apoptosis and inhibiting VEGF level," *Journal of Asian Natural Products Research*, vol. 10, no. 5-6, pp. 467–473, 2008.

Hindawi Publishing Corporation
Evidence-Based Complementary and Alternative Medicine
Volume 2013, Article ID 502727, 7 pages
http://dx.doi.org/10.1155/2013/502727

Research Article

Effect of Eucalyptus Oil Inhalation on Pain and Inflammatory Responses after Total Knee Replacement: A Randomized Clinical Trial

Yang Suk Jun,[1] Purum Kang,[1] Sun Seek Min,[2] Jeong-Min Lee,[3] Hyo-Keun Kim,[3] and Geun Hee Seol[1]

[1] *Department of Basic Nursing Science, School of Nursing, Korea University, Anam-dong, Seongbuk-gu, Seoul 136-713, Republic of Korea*
[2] *Department of Physiology and Biophysics, School of Medicine, Eulji University, Daejeon 301-746, Republic of Korea*
[3] *KT&G Research Institute, Daejeon 305-805, Republic of Korea*

Correspondence should be addressed to Geun Hee Seol; ghseol@korea.ac.kr

Received 2 April 2013; Revised 7 June 2013; Accepted 7 June 2013

Academic Editor: Vincenzo De Feo

Eucalyptus oil has been reported effective in reducing pain, swelling, and inflammation. This study aimed to investigate the effects of eucalyptus oil inhalation on pain and inflammatory responses after total knee replacement (TKR) surgery. Participants were randomized 1 : 1 to intervention group (eucalyptus inhalation group) or control group (almond oil inhalation group). Patients inhaled eucalyptus or almond oil for 30 min of continuous passive motion (CPM) on 3 consecutive days. Pain on a visual analog scale (VAS), blood pressure, heart rate, C-reactive protein (CRP) concentration, and white blood cell (WBC) count were measured before and after inhalation. Pain VAS on all three days ($P < .001$) and systolic ($P < .05$) and diastolic ($P = .03$) blood pressure on the second day were significantly lower in the group inhaling eucalyptus than that inhaling almond oil. Heart rate, CRP, and WBC, however, did not differ significantly in the two groups. In conclusion, inhalation of eucalyptus oil was effective in decreasing patient's pain and blood pressure following TKR, suggesting that eucalyptus oil inhalation may be a nursing intervention for the relief of pain after TKR.

1. Introduction

Osteoarthritis, the most prevalent musculoskeletal disorder throughout the world, is a common chronic disease that causes pain, restricts activity, and reduces quality of life [1]. Osteoarthritis may occur in all joints, but the knee is the most frequent site [2]. The most common clinical features of osteoarthritis include pain, stiffness, swelling, and inflammation. Surgery may be considered in patients who do not show symptom improvements on nonsurgical treatments, especially when severe pain interferes with daily life [3]. Total knee replacement (TKR) is a surgical procedure in which deformed knee cartilage is resected and replaced by a metal structure filled with polyethylene, resulting in a new joint structure. TKR has been shown to improve the quality of life of patients with severe arthritis by relieving knee pain and increasing knee function [4]. Inflammation by infection after TKR has a negative impact on patient prognosis, with deep infection requiring a second operation [5]. Thus, inflammation control as well as pain management are required for rapid recovery and functionality. Eucalyptus (*Eucalyptus globulus*) oil has been widely used as a folk medicine to treat upper respiratory infections, gastritis, and diabetes [6].

Eucalyptus oil contains α-pinene and 1,8-cineole and acts as an antioxidant, with strong radical scavenging activity [7]. In a mouse model of pain-causing edema in the feet, oral administration of 1,8-cineole, which accounts for 70–90% (w/w) of the contents of eucalyptus oil, suppressed edema formation and reduced inflammation and pain [8]. This effect of 1,8-cineole is due to its inhibition of cytokine secretion by T-lymphocytes [9]. Electromyography has shown that application of eucalyptus oil to a healthy subject had a myorelaxant effect, as well as promoting emotional stability [10]. Moreover, in a rat model of susceptibility to pain from a hot plate, eucalyptus oil was not only analgesic but reduced edema formation and had an anti-inflammatory effect [11].

Although eucalyptus oil has been found to reduce pain and suppress edema and inflammation in animal models, its effects on pain in patients who have undergone TKR have not been determined. We therefore assessed whether eucalyptus oil inhalation could effectively reduce pain and inflammatory responses in patients who have undergone TKR.

2. Materials and Methods

2.1. Study Design and Sample Size. Patients were randomly assigned using table of random numbers to inhalation of eucalyptus oil or almond oil (used as solvent, control) during continuous passive motion (CPM) after TKR, with both investigators and subjects blinded to treatment assignment. Based on an effect size of 0.80, a statistical power of 0.80, and a significance level of 0.05, the minimum number of patients required to compare differences between the experimental and control group was estimated to be 26 patients per group. Twenty-eight subjects were originally assigned to each group, with 52 completing the study, 25 in the experimental and 27 in the control group.

2.2. Participants. Patients diagnosed with osteoarthritis by the same physician and who underwent TKR were invited to participate. All subjects (1) had been prescribed pain medications, including oxycodone hydrochloride, fentanyl, nonsteroidal anti-inflammatory drugs (NASID), and antibiotic pills, (2) had no complications or other inflammatory diseases after surgery, (3) were not being treated with any antidepressant, hormone, or aroma therapy, (4) did not smoke, (5) were conscious and oriented, and (6) had a pain score on a visual analog scale (VAS) >4 before aroma inhalation. The study design and protocol were approved by the Ethical Review Committee of the Korea University Medical Center (Code: ED11285), and all participants provided written informed consent.

2.3. Gas Chromatography-Mass Spectrometry Analysis. Gas chromatography-mass spectrometry (GC-MS) was performed to analyze compositions of eucalyptus oil. GC-MS analysis was performed using an Agilent 7890 gas chromatograph with a 5975 inert mass spectrometer (USA), and analytical capillary column was performed on HP-Innowax (60 m × 0.25 mm i.d., 0.5 μm film thickness, Agilent, USA). Carrier gas was helium and flowrate was 1.0 mL/min. The injector temperature was increased to 280°C. And samples (1.0 μL) were injected at a split ratio of 50 : 1. The column temperature was initially maintained at 50°C (hold for 3 min), ramp to 240°C at 3°C/min, and finally held for 10 min. The ion source and transfer line temperature were set at 230°C and 250°C. The mass spectrometer was operated in the electron impact ionization mode (70 eV).

2.4. Intervention. Eucalyptus oil and almond oil were supplied by Aromarant Co. Ltd. (Rottingen, Germany). Eucalyptus oil was dissolved at a concentration of 3% (v/v) in almond oil. In experimental group, eucalyptus oil (dissolved in almond oil) was placed onto a 4 × 2 inch gauze pad, which was positioned between the nose and philtrum for 30 minutes of CPM on 3 consecutive days, beginning on the third day after surgery. The control group received the same treatment of experimental group except for eucalyptus. Eucalyptus oil and almond oil have a similar color and were packed same-shaped bottles. All experiments were carried out separately. The compounder was the only one who knows which participant affiliated to which group according to the assigned number on bottle. Patients and investigator were not informed about the types and effects of aroma oil.

2.5. Outcome Measurement. Pain was measured using the VAS pain score. It is also used in most studies of anxiety, consists of a horizontal scale, ranging from 0 (no pain) on the left side and 10 (extreme pain) on the right side [12]. Patients were asked to indicate VAS pain score by number at each determination. Blood pressure and heart rate were measured on each day of oil inhalation, before and after CPM, as indicators of the reaction of the autonomic nervous system to pain. Blood pressure was measured in the brachial artery using a Deluxe Aneroid Sphygmomanometer (Mac-check, Japan) after a 10-minute rest in a lying position. Pulse was measured at the radial artery for 1 minute.

In this study, CRP was measured by a Latex Immunoassay with LX-2200 (Eiken Inc., Japan) and WBC was measured by semiconductor flow cytometry with an XE-5000 (Sysmex, Inc., Japan).

2.6. Data Collection. Blood samples were collected before breakfast on the first day of aroma inhalation and on days 4 and 7 for measurements of C-reactive protein (CRP) concentrations and white blood cell (WBC) count. Pain VAS, blood pressure, and heart rate were measured before and after each 30 min inhalation session.

2.7. Statistical Analysis. All statistical analyses were performed using the Statistical Package for the Social Sciences, SPSS 20.0. The demographic and clinical characteristics of the two groups were compared using t-tests, Fisher's exact tests, and Chi-square tests, as appropriate. All data are presented as frequency, percentages, and standard error of the mean (SEM) or standard deviation (SD). Differences in the VAS pain scores before and after aroma inhalation within each group were compared using the Wilcoxon's rank-sum test and paired t-test, and differences between groups were analyzed using Mann-Whitney U-tests and unpaired t-tests.

3. Results

3.1. Compositions of Eucalyptus Oil. A total of 31 compounds were identified (Table 1). The major volatile flavor compounds of eucalyptus oil were 1,8-cienol (61.46%), limonene (13.68%), ρ-cymene (8.55%), γ-terpinene (5.87%), and α-pinene (4.95%).

3.2. Characteristics of the Participants and Test of Homogeneity. Fifty-two individuals were randomized, 25 to the eucalyptus oil and 27 to the almond oil (control) group.

Table 1: Chemical compositions of the eucalyptus oil determined by GC-MS.

RT[a] (min)	KI[b]	Compound	Area %[c]
12.952	1038	α-pinene	4.95
14.513	1075	α-fenchene	0.01
14.897	1084	Camphene	0.03
16.826	1128	β-pinene	0.75
17.571	1144	o-cymene	0.01
19.118	1177	b-myrcene	0.95
19.477	1184	α-phellandrene	1.09
20.221	1199	α-terpinene	0.24
21.447	1227	Limonene	13.68
21.985	1239	1,8-cineole	61.46
22.560	1251	trans-β-ocimene	0.33
23.431	1269	γ-terpinene	5.87
24.619	1293	ρ-cymene	8.55
25.152	1304	α-terpinolen	0.41
25.308	1307	Isoamyl isovalerate	0.04
28.679	1381	o-menthone	0.05
29.771	1403	α-pinene epoxide	0.02
32.286	1461	Dehydro-ρ-cymene	0.02
33.529	1489	cis-Limonene oxide	0.05
36.294	1554	Linalool	0.20
38.286	1600	Fenchyl alcohol	0.07
39.233	1624	4-Terpineol	0.38
41.487	1680	trans-pinocarveol	0.21
42.519	1705	cis-Citral	0.03
42.713	1710	Crypton	0.01
42.883	1715	α-terpineol	0.53
43.115	1721	α-terpinyl acetate	0.01
43.204	1723	Borneol	0.02
44.984	1770	Carvone	0.01
48.033	1852	cis-Carveol	0.02
48.139	1855	trans-Geraniol	0.004

[a]RT: retention time. [b]KI: Kovats indices. [c]Calculated with peak area obtained from GC/MS.

Demographic and disease-associated characteristics were similar in the two groups, including type of surgery, duration of osteoarthritis, and treatments with oral antihypertensive and antidiabetic agents (Table 2). The mean age of the 52 participants was 68.2 years (range, 43–85 years), and most were female. Their average body mass index (BMI) was 26.4 ± 3.1 kg/m^2, and all 52 were overweight/obese (BMI ≥ 25 kg/m^2). Thirty-seven patients (71.2%) underwent a unilateral TKR and 15 (28.9%) underwent a simultaneous, bilateral TKR. The mean durations of osteoarthritis in the eucalyptus and almond oil groups were 8.5 ± 5.7 years and 6.0 ± 5.2 years, respectively. Before aroma inhalation, VAS pain score, systolic blood pressure, diastolic blood pressure, heart rate, CRP, and WBC count were similar in the two groups (Table 3).

3.3. Effects of Eucalyptus Oil on VAS Pain Score. VAS pain scores after aromatherapy on days 1–3 decreased 1.1 ± 0.2, 1.2 ± 0.2, and 1.2 ± 0.2 points, respectively, from the scores before inhalation (Figure 1(a)). In the control group, however, VAS pain scores on days 1–3 increased 0.4 ± 0.2, 0.3 ± 0.2, and 0.1 ± 0.1 points, respectively, from the scores before inhalation. Overall, VAS pain scores were significantly lower in the eucalyptus oil group than in the control group ($P < .001$, Figure 1(a)).

3.4. Effects of Eucalyptus Oil on Heart Rate and Blood Pressure. Relative to pretreatment heart rate, heart rate in the eucalyptus oil group increased 0.3 ± 1.6 beats/min on day 1 of CPM and decreased 1.7±1.7 beats/min and 0.6±1.0 beats/min on days 2 and 3, respectively (Figure 1(b)). The heart rate in the control group, however, showed increases after CPM of 2.1 ± 0.7, 1.5 ± 0.9, and 0.8 ± 0.7 beats/min on days 1–3 of CPM, respectively. Between-group differences in heart rate did not differ significantly.

Systolic blood pressure on days 1–3 decreased 0.8 ± 1.9 mmHg, 4.8 ± 2.2 mmHg, and 2.0 ± 2.0 mmHg, respectively, in the eucalyptus oil group, while increasing 0.4 ± 1.7 mmHg, 3.3 ± 2.2 mmHg, and 1.9 ± 1.6 mmHg, respectively, in the control group (Figure 1(c)). On day 2, SPB was significantly lower in the eucalyptus oil than in the control group ($P < .05$, Figure 1(c)). Similarly, diastolic blood pressure in the eucalyptus oil group decreased 0.4 ± 1.5 mmHg, 0.8 ± 1.5 mmHg, and 0.0 ± 1.2 mmHg, respectively, on days 1–3, while increasing 1.1 ± 1.5 mmHg, 3.7 ± 1.4 mmHg, and 2.6±1.1 mmHg, respectively, in the control group on the same days. Diastolic blood pressure on day 2 was significantly lower in the eucalyptus oil group than in the control group ($P = .03$, Figure 1(d)).

3.5. Effects of Eucalyptus Oil on Inflammatory Responses. Serum CRP concentrations before inhalation and on days 4 and 7 were 7.2 ± 3.9, 53.5 ± 6.8, and 48.8 ± 11.0 mg/L, respectively, in the eucalyptus oil group, and 4.89 ± 2.0, 68.2 ± 8.2, and 46.8 ± 7.7 mg/L, respectively, in the control group (Figure 2(a)). Although CRP concentrations in both groups tended to increase gradually after surgery and then decrease, no between-group significant differences were observed.

WBC counts before inhalation and on days 4 and 7 were 6,513.2 ± 417.0 × $10^3/\mu$L, 7, 062.0 ± 377.9 × $10^3/\mu$L, and 7, 450.0 ± 383.5 × $10^3/\mu$L, respectively, in the eucalyptus oil group, and 6, 793.3 ± 268.8 × $10^3/\mu$L, 7,112.6 ± 336.9 × $10^3/\mu$L, and 7, 970 ± 502.4 × $10^3/\mu$L, respectively, in the control group (Figure 2(b)). None of these differences reached statistical significance.

4. Discussion

Since eucalyptus oil has been reported effective in reducing pain and suppressing inflammation in the various animal models, we tested whether inhalation of eucalyptus oil affected pain, blood pressure, heart rate, CRP concentration, and WBC count following TKR in patients with osteoarthritis.

Pain is an emotion which is quintessentially subjective and personal [13, 14]. To assess patient's subjective pain, we

Table 2: General characteristics of the eucalyptus oil and control groups ($N = 52$).

Characteristics	Total ($n = 52$)	Control ($n = 27$)	Eucalyptus oil ($n = 25$)	t or χ^2	P-value
Age (years)	68.2 (7.6)	67.5 (8.9)	68.9 (6.1)	0.69	.49[a]
Gender					
Female	48 (92.3)	24 (88.9)	24 (96)	0.19	.61[b]
Male	4 (7.7)	3 (11.1)	1 (4.0)		
Surgical classification					
Unilateral	37 (71.2)	18 (66.7)	19 (76.0)	0.19	.66[c]
Bilateral	15 (28.9)	9 (33.3)	6 (24.0)		
BMI (kg/m^2)	26.4 (3.1)	26.1 (3.23)	26.7 (3.0)	−0.68	.50[a]
Education					
≤Elementary	34 (65.4)	16 (59.3)	18 (72.0)	2.17	.37[b]
Middle	5 (9.6)	2 (7.4)	3 (12)		
≥High	13 (25.0)	9 (33.3)	4 (16.0)		
Marital status					
Married	52 (100)	27 (100)	25 (100)		
Employed					
Yes	12 (23.1)	7 (25.9)	5 (20.0)	0.03	.86[c]
No	40 (76.9)	20 (74.1)	20 (80.0)		
Duration of osteoarthritis (years)	7.2 (5.5)	6.0 (5.2)	8.5 (5.7)	−1.67	.11[a]
Hypertension medication					
Yes	38 (73.1)	19 (70.4)	19 (76)	0.02	.89[c]
No	14 (26.9)	8 (29.6)	6 (24)		
Diabetes medication					
Yes	15 (28.9)	8 (29.6)	7 (28)	0.00	1.00[c]
No	37 (71.2)	19 (70.4)	18 (72)		

Data reported as mean (SD) or n (%).
Abbreviations: SD: standard deviation, BMI: body mass index.
[a]t-test.
[b]Fisher's exact test.
[c]Chi-square test.

Table 3: Outcomes in the eucalyptus oil and control groups ($N = 52$).

Variables	Control ($n = 27$)	Eucalyptus oil ($n = 25$)	P-value
VAS (score)	5.0 ± 1.0	5.0 ± 0.0	.44
sBP (mm Hg)	120.0 ± 20.0	120.0 ± 20.0	.31
dBP (mm Hg)	80.0 ± 10.0	80.0 ± 10.0	.93
HR (beats/min)	78.0 ± 8.0	78.0 ± 10.0	.33
CRP (mg/L)	4.9 ± 10.5	7.2 ± 19.3	.59[a]
WBC ($\times 10^3/\mu$L)	6793.3 ± 1396.6	6513.2 ± 2084.9	.57[a]

Abbreviations: VAS: visual analog scale; sBP: systolic blood pressure; dBP: diastolic blood pressure; HR: heart rate; CRP: C-reactive protein; WBC: white blood cell.
Wilcoxon's rank sum test. Data presented as median ± interquartile range.
[a]t-test. Data presented as mean ± standard deviation.

used a VAS measurement tools. We found that inhalation of eucalyptus oil significantly decreased VAS pain scores compared with our control group. The major component of eucalyptus oil is 1,8-cineole, which had a morphine-like effect relieving pain in mice [8]. Another study also found that 1,8-cineole exhibited antinociceptive properties in rats and mice [15]. These findings, taken together with our results, suggest that subjective pain-reducing effects of eucalyptus oil are due, at least in part, to 1,8-cineole.

Serotonin has been considered to have an important role in the control of pain [16]. Activation of serotonin receptor presents on C-fibers has been shown mediating serotonin-induced pronociceptive effects [17]. Recent studies have shown that essential oils act via modulating of the central neurotransmitter system. *Hypericum perforatum* is considered to inhibit the synaptosomal uptake of serotonin [15]. Also, lemon oil reported to have an antixiolytic effects via the suppression of monoamines dopamine and enhancing serotonergic neurons [18]. Therefore pain-relieving effects of eucalyptus oil in the present results should be considered an involvement of serotonergic system. Pain and stress after TKR and during CPM are thought to act on the central and

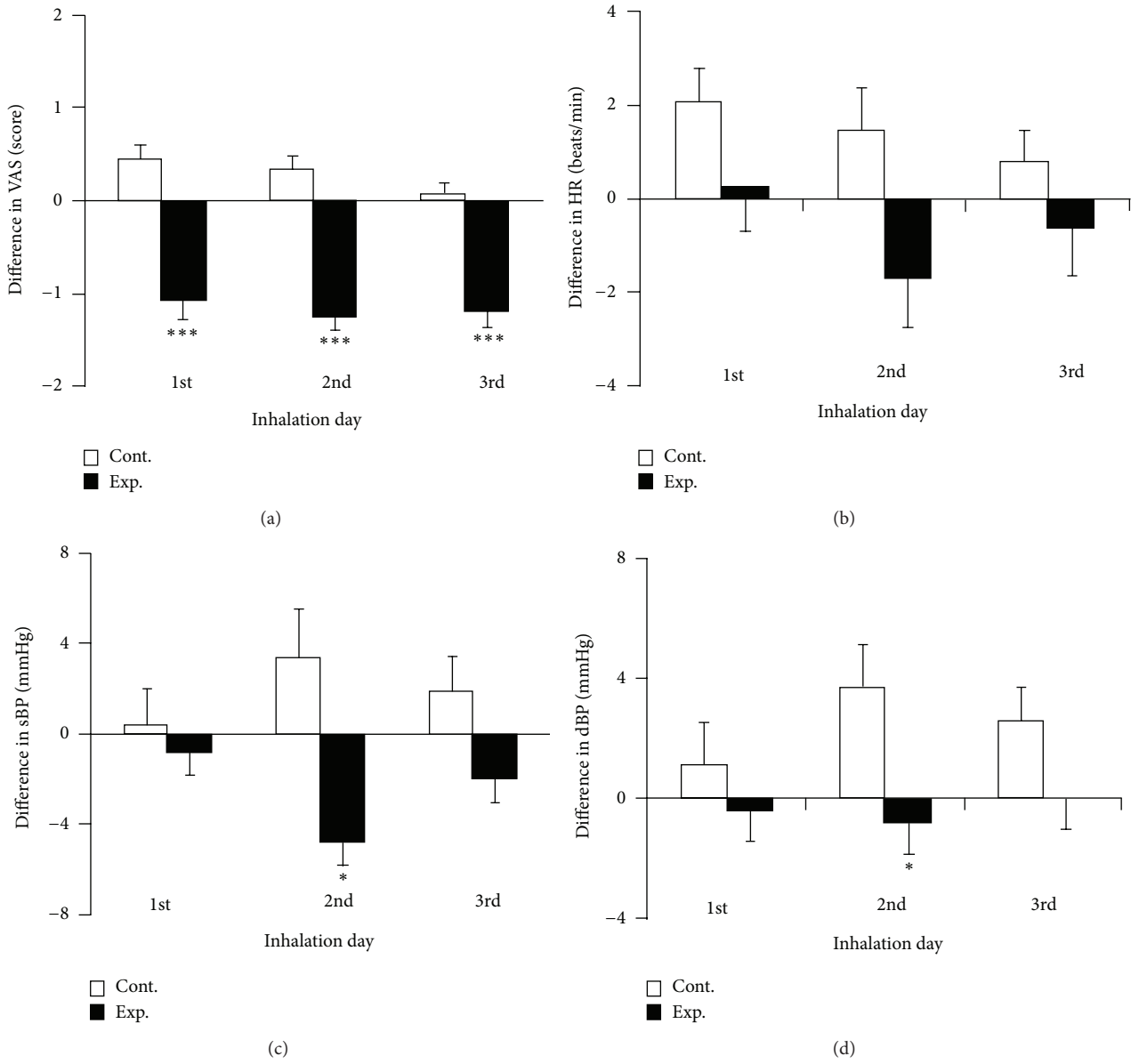

Figure 1: Effects of inhalation on (a) VAS, (b) HR, (c) sBP, and (d) dBP in the eucalyptus oil ($n = 25$) and control (almond oil; $n = 27$) groups. Results are expressed as mean ± SEM. $^{*}P < .05$, $^{***}P < .001$ compared with the control group. Abbreviations: VAS, visual analog scale; HR, heart rate; sBP, systolic blood pressure; dBP, diastolic blood pressure.

sympathetic nervous systems, increasing blood pressure and pulse. In the present study, group treated with eucalyptus oil inhalations showed statistically significant reduction in blood pressure, suggesting that eucalyptus oil could promote relaxation by reducing sympathetic activity while augmenting parasympathetic during CPM after TKR. A possible pathway for this explanation may include the olfactory system. Autonomic nervous system is affected by odorants, thus inhalation of essential oil is direct actions on the autonomic nervous system via olfactory system [19, 20]. Recent study has shown that olfactory stimulation with lavender essential oil and its active component, linalool reduced the sympathetic nerve activity in rats [21]. Therefore, eucalyptus oil also may modulate autonomic responses such as blood pressure via central nervous system and autonomic nervous system. The cardiovascular effects of 1,8-cineole were also investigated in several research. 1,8-cineole decrease blood pressure in normotensive rate and elicited a endothelium-dependent vasorelaxation in rate aorta [22, 23]. Other reports have shown that the administration of 1,8-cineole reduces contractile activity in rat [24]. Thus, there is a possibility that 1,8-cineole contributes to hypotensive effects of eucalyptus essential oil.

Eucalyptus oil has been used to treat influenza infection, owing to its anti-inflammatory and antibacterial effects [25]. Moreover, 1,8-cineole was found to reduce cytokines that

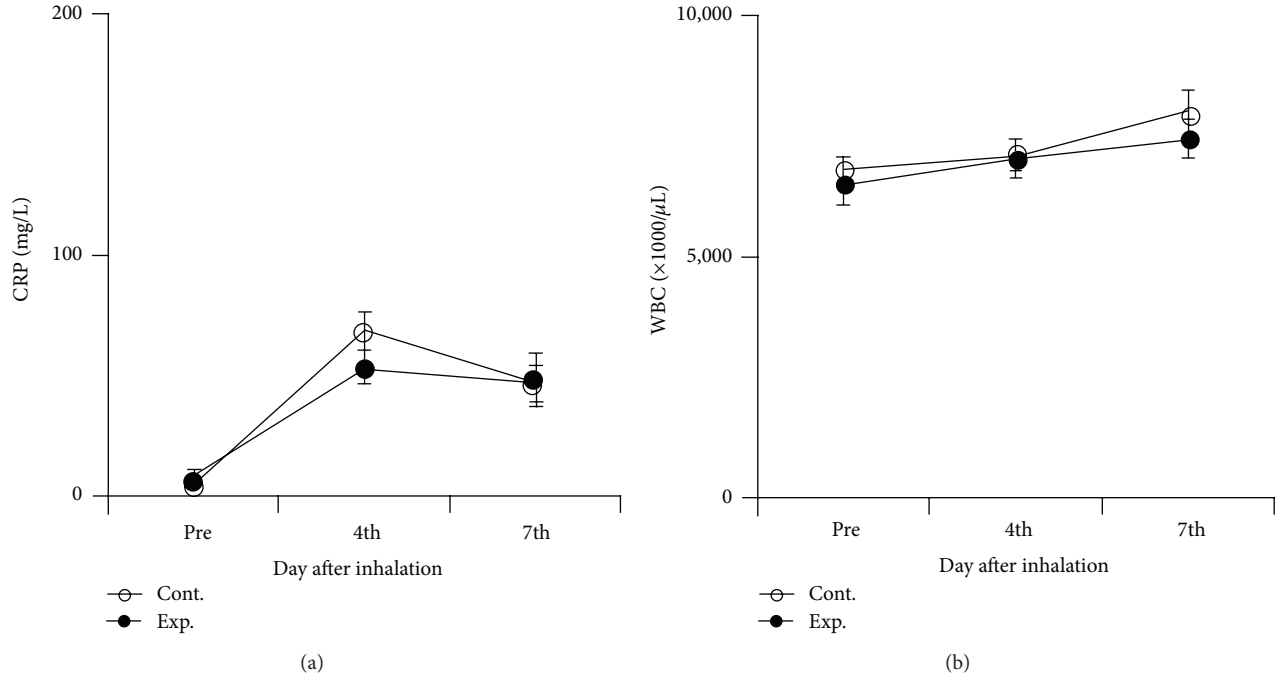

Figure 2: Effects of inhalation on (a) CRP and (b) WBC in the eucalyptus oil ($n = 25$) and control (almond oil; $n = 27$) groups. Values are expressed as mean ± SEM. Abbreviations: CRP, C-reactive protein; WBC, white blood cell.

cause inflammation in guinea pigs [20], and to significantly reduce edema and CRP at sites of inflammation throughout the entire body [26]. These studies prompted us to hypothesize that eucalyptus oil would reduce pain following TKR by lessening inflammatory reactions. However, markers of inflammatory responses, such as CRP concentration and WBC count, did not differ significantly between the our eucalyptus oil and control groups although comparisons before and after inhalation showed that the WBC count tended to be lower in the eucalyptus than in the control group, which may have been due to the time of inspection, the concentration of eucalyptus oil inhaled, and/or its frequency of application.

In summary, this study, which investigated the effects of eucalyptus oil inhalation on patients who underwent TKR, showed that eucalyptus oil inhalation was effective in reducing patient's subjective pain and blood pressure after surgery. These findings suggest that the inhalation of eucalyptus oil might be a valuable nursing intervention for pain relief after TKR.

Conflict of Interests

The authors declare they have no conflict of interests.

Acknowledgments

The first two authors (Yang Suk Jun and Purum Kang) contributed equally to this work. This work was supported by the National Research Foundation of Korea (NRF) Grants funded by the Korea government (MEST) (nos. 2012007145 and 20120004065).

References

[1] F. Salaffi, R. De Angelis, W. Grassi et al., "Prevalence of musculoskeletal conditions in an Italian population sample: results of a regional community-based study. I. The MAPPING study," *Clinical and Experimental Rheumatology*, vol. 23, no. 6, pp. 819–828, 2005.

[2] P. M. Brooks, "Impact of osteoarthritis on individuals and society: how much disability? Social consequences and health economic implications," *Current Opinion in Rheumatology*, vol. 14, no. 5, pp. 573–577, 2002.

[3] M. C. Hochberg, R. D. Altman, K. T. April et al., "American College of Rheumatology 2012 recommendations for the use of nonpharmacologic and pharmacologic therapies in osteoarthritis of the hand, hip, and knee," *Arthritis Care and Research*, vol. 64, no. 4, pp. 465–474, 2012.

[4] A. J. Carr, O. Robertsson, S. Graves et al., "Knee replacement," *The Lancet*, vol. 379, no. 9823, pp. 1331–1340, 2012.

[5] S. C. Lee, J. Y. Yoon, K. A. Jung, C. H. Nam, and S. H. Jung, "Perioperative changes in C-reactive protein levels after unilateral and simultaneous bilateral total knee replacement," *The Journal of the Korean Orthopaedic Association*, vol. 44, no. 4, pp. 442–448, 2009.

[6] H. D. Kumar and S. Laxmidhar, "A review on phytochemical and pharmacological of *Eucalyptus globulus*: a multipurpose tree," *International Journal of Research in Ayurveda & Pharmacy*, vol. 2, no. 5, pp. 1527–1530, 2011.

[7] H. P. Singh, S. Mittal, S. Kaur, D. R. Batish, and R. K. Kohli, "Characterization and antioxidant activity of essential oils from fresh and decaying leaves of *Eucalyptus tereticornis*," *Journal of*

Agricultural and Food Chemistry, vol. 57, no. 15, pp. 6962–6966, 2009.

[8] F. A. Santos and V. S. Rao, "Antiinflammatory and antinociceptive effects of 1,8-cineole a terpenoid oxide present in many plant essential oils," *Phytotherapy Research*, vol. 14, no. 4, pp. 240–244, 2000.

[9] U. R. Juergens, T. Engelen, K. Racké, M. Stöber, A. Gillissen, and H. Vetter, "Inhibitory activity of 1,8-cineol (eucalyptol) on cytokine production in cultured human lymphocytes and monocytes," *Pulmonary Pharmacology and Therapeutics*, vol. 17, no. 5, pp. 281–287, 2004.

[10] H. Gobel, G. Schmidt, and D. Soyka, "Effect of peppermint and eucalyptus oil preparations on neurophysiological and experimental algesimetric headache parameters," *Cephalalgia*, vol. 14, no. 3, pp. 228–234, 1994.

[11] J. Silva, W. Abebe, S. M. Sousa, V. G. Duarte, M. I. L. Machado, and F. J. A. Matos, "Analgesic and anti-inflammatory effects of essential oils of Eucalyptus," *Journal of Ethnopharmacology*, vol. 89, no. 2-3, pp. 277–283, 2003.

[12] M. E. Cline, J. Herman, E. R. Shaw, and R. D. Morton, "Standardization of the visual analogue scale," *Nursing Research*, vol. 41, no. 6, pp. 378–380, 1992.

[13] S. Ogston-Tuck, "A silent epidemic: community nursing and effective pain management," *British Journal of Community Nursing*, vol. 17, no. 11, pp. 512–518, 2012.

[14] M. Osborn and K. Rodham, "Insights into pain: a review of qualitative research," *Reviews in Pain*, vol. 4, no. 1, pp. 2–7, 2010.

[15] C. Liapi, C. Anifantis, I. Chinou, A. P. Kourounakis, S. Theodosopoulos, and P. Galanopoulou, "Antinociceptive properties of 1,8-Cineole and beta-pinene, from the essential oil of *Eucalyptus camaldulensis* leaves, in rodents," *Planta Medica*, vol. 73, no. 12, pp. 1247–1254, 2007.

[16] L. Bardin, "The complex role of serotonin and 5-HT receptors in chronic pain," *Behavioural Pharmacology*, vol. 22, no. 5-6, pp. 390–404, 2011.

[17] C. Sommer, "Serotonin in pain and analgesia: actions in the periphery," *Molecular Neurobiology*, vol. 30, no. 2, pp. 117–125, 2004.

[18] M. Komiya, T. Takeuchi, and E. Harada, "Lemon oil vapor causes an anti-stress effect via modulating the 5-HT and DA activities in mice," *Behavioural Brain Research*, vol. 172, no. 2, pp. 240–249, 2006.

[19] N. Perry and E. Perry, "Aromatherapy in the management of psychiatric disorders: clinical and neuropharmacological perspectives," *CNS Drugs*, vol. 20, no. 4, pp. 257–280, 2006.

[20] V. P. D. Bastos, A. S. Gomes, F. J. B. Lima et al., "Inhaled 1,8-cineole reduces inflammatory parameters in airways of ovalbumin-challenged Guinea pigs," *Basic and Clinical Pharmacology and Toxicology*, vol. 108, no. 1, pp. 34–39, 2011.

[21] J. Shen, A. Niijima, M. Tanida, Y. Horii, K. Maeda, and K. Nagai, "Olfactory stimulation with scent of lavender oil affects autonomic nerves, lipolysis and appetite in rats," *Neuroscience Letters*, vol. 383, no. 1-2, pp. 188–193, 2005.

[22] S. Lahlou, A. F. Figueiredo, P. J. C. Magalhães, and J. H. Leal-Cardoso, "Cardiovascular effects of 1,8-cineole, a terpenoid oxide present in many plant essential oils, in normotensive rats," *Canadian Journal of Physiology and Pharmacology*, vol. 80, no. 12, pp. 1125–1131, 2002.

[23] E. Vigo, A. Cepeda, O. Gualillo, and R. Perez-Fernandez, "In-vitro anti-inflammatory effect of *Eucalyptus globulus* and *Thymus vulgaris*: nitric oxide inhibition in J77RA.1 murine macrophages," *Journal of Pharmacy and Pharmacology*, vol. 56, no. 2, pp. 257–263, 2004.

[24] M. C. M. S. Soares, C. E. N. Damiani, C. M. Moreira, I. Stefanon, and D. V. Vassallo, "Eucalyptol, an essential oil, reduces contractile activity in rat cardiac muscle," *Brazilian Journal of Medical and Biological Research*, vol. 38, no. 3, pp. 453–461, 2005.

[25] A. E. Sadlon and D. W. Lamson, "Immune-modifying and antimicrobial effects of Eucalyptus oil and simple inhalation devices," *Alternative Medicine Review*, vol. 15, no. 1, pp. 33–47, 2010.

[26] W. Kehrl, U. Sonnemann, and U. Dethlefsen, "Therapy for acute nonpurulent rhinosinusitis with cineole: results of a double-blind, randomized, placebo-controlled trial," *Laryngoscope*, vol. 114, no. 4, pp. 738–742, 2004.